

ATM and ATR: Sensing DNA damage

Jun Yang, Zheng-Ping Xu, Yun Huang, Hope E. Hamrick, Penelope J. Duerksen-Hughes, Ying-Nian Yu

Jun Yang, Zheng-Ping Xu, Yun Huang, Ying-Nian Yu, Department of Pathology and Pathophysiology, and Department of Public Health, School of Medicine, Zhejiang University, Hangzhou, 310031, Zhejiang Province, China

Hope E. Hamrick, Department of Psychology, Wellesley College, Wellesley, MA, 02481, U S A

Penelope J. Duerksen-Hughes, Center for Molecular Biology and Gene Therapy, School of Medicine, Loma Linda University, Loma Linda, CA 92354, U S A

Supported by National Key Basic Research and Development Program No. 2002CB512901, China; National Natural Science Foundation No. 30300277, China; the Initial Funds for Returned Overseas Chinese Scholar from Zhejiang University and Ministry of Education, China

Correspondence to: Dr. Ying-Nian Yu, Department of Pathology and Pathophysiology, School of Medicine, Zhejiang University, 353 Yanan Road, Hangzhou, 310031, Zhejiang Province, China. ynyu@hznc.com

Telephone: +86-571-8721 7149 **Fax:** +86-571-8721 7149

Received: 2003-07-17 **Accepted:** 2003-08-18

Abstract

Cellular response to genotoxic stress is a very complex process, and it usually starts with the "sensing" or "detection" of the DNA damage, followed by a series of events that include signal transduction and activation of transcription factors. The activated transcription factors induce expressions of many genes which are involved in cellular functions such as DNA repair, cell cycle arrest, and cell death. There have been extensive studies from multiple disciplines exploring the mechanisms of cellular genotoxic responses, which have resulted in the identification of many cellular components involved in this process, including the mitogen-activated protein kinases (MAPKs) cascade. Although the initial activation of protein kinase cascade is not fully understood, human protein kinases ATM (ataxia-telangiectasia, mutated) and ATR (ATM and Rad3-related) are emerging as potential sensors of DNA damage. Current progresses in ATM/ATR research and related signaling pathways are discussed in this review, in an effort to facilitate a better understanding of genotoxic stress response.

Yang J, Xu ZP, Huang Y, Hamrick HE, Duerksen-Hughes PJ, Yu YN. ATM and ATR: Sensing DNA damage. *World J Gastroenterol* 2004; 10(2): 155-160

<http://www.wjgnet.com/1007-9327/10/155.asp>

INTRODUCTION

Cellular response to genotoxic stress is a very complex process. However, it can be "simply" envisioned as a signal transduction cascade in which DNA lesions act as the initial signal that is detected by sensors and passed down through transducers. Eventually the effectors receive the signal and execute various cellular functions (Figure 1). Much knowledge has been gained over the years concerning the signal transducers, and a large group of serine-threonine protein kinases, namely the mitogen-activated protein kinases (MAPKs), along with their upstream kinases, have been shown to play prominent roles in cellular

genotoxic responses^[1]. Three major classes of MAPKs, i.e., extracellular signal-regulated kinase (ERK), c-Jun N-terminal kinase/stress-activated protein kinase (JNK/SAPK), and p38 (also known as SAPK2, RK, CSBP, or Mxi2), could all be activated by various genotoxic stresses^[1-7]. Although the precise mechanism has not been fully understood, it is known that damage to cellular DNA somehow leads to the activation of a group of serine-threonine kinases called MAPK kinase kinases (MAPKKK, or MEKK, MEK kinase), which phosphorylate the downstream dual-specificity kinases called MAPK kinases (MAPKK, or MEK, MAPK/ERK kinase). These MAPKKs then phosphorylate the threonine and tyrosine residues in MAPKs. This three-component module could be assembled together by scaffold proteins that ensure the efficiency and specificity of each individual MAPK pathway^[8-10]. The activated MAPKs then translocate to the nucleus and phosphorylate scores of target proteins, including many transcription factors. Among these transcription factors is the tumor suppressor p53 protein, which plays such an important role in the genotoxic stress response that has earned the reputation as the "universal sensor for genotoxic stress"^[2,11,12].

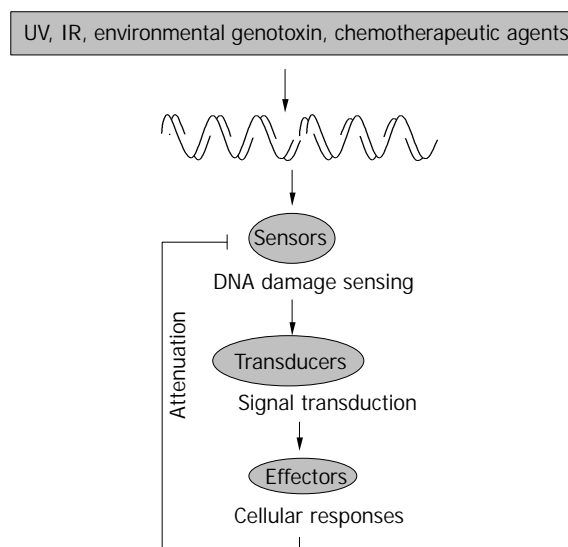


Figure 1 A general schematic representation of cellular responses to genotoxic stress. Ultraviolet (UV), ionizing radiation (IR), and various chemicals can induce DNA damage, such as double strand breaks (DSBs), which can be detected by "sensors". This generates some signal that can be transduced by the transducers to effector molecules. Finally, there is the presence of an attenuation mechanism to control the cellular response to genotoxic stress.

Although studies on MAPKs have provided a lot useful information about signal transducers, the initial sensors for DNA damage remain to be identified. Recently, it has been proposed that some multi-protein complexes that are involved in DNA maintenance or repair, such as the Rad family member Rad1, 9, 17, 26, and Hus1, might function as DNA damage sensors^[13-18]. Members of the phosphatidylinositol 3-kinase (PI-3) superfamily, which are activated at the very early stages of DNA damage response, could also serve as sensors, as

well as initiators, of the ensuing cellular genotoxic stress response, including ATM and ATR in humans^[19]. Although these proteins share the PI-3-like kinase domain, they could not function as lipid kinases, but rather as serine-threonine protein kinases^[14,20-25].

ATM AND ATR

Biochemistry of ATM and ATR

One distinguishing characteristic of the PI-3 family members is their unusually large size, which ranges from around 300 kDa to over 500 kDa. ATM is a 3 056 amino acid (aa) protein while ATR is a 2 644 aa protein, and both have a C-terminal catalytic domain (-300 aa) which is flanked by two loosely conserved domains. Although it has not been known how exactly these two kinases sense the DNA damage, it is clear that both kinases can be activated by DNA damage. However, it has been found that ATM responds primarily to double-strand breaks induced by ionizing irradiation (IR), while ATR also reacts to UV or stalled replication forks^[13,14,26-29].

Activation of ATM and ATR

Several mechanisms have been proposed for the activation of ATM and ATR by DNA damage: a) direct activation through interaction with damaged DNA, b) indirect activation through interaction with DNA repair or maintenance proteins, or c) a combination of both^[30]. Existing experimental data support the third mechanism, that they are activated both through interactions with DNA and members of the repair complexes. For example, ATM could bind directly to DNA. Furthermore, pre-treatment of DNA-cellulose matrix with IR or restriction enzymes could stimulate ATM binding, suggesting that ATM binds to DNA ends^[31,32]. ATR could also bind to DNA, with a higher affinity to UV-damaged than undamaged DNA. In addition, damaged DNA could stimulate the kinase activity of ATR to a significantly higher level than undamaged DNA^[33,34]. ATM and ATR also interact with many proteins that co-localize at the site of DNA damage. For example, ATM as a part of a super protein complex called BRCA1-associated genome surveillance complex (BASC), is involved in the recognition and repair of aberrant DNA structures. It has been found this complex contains several other proteins such as breast cancer gene 1 (BRCA1), mismatch-repair protein hRad50, and BLM helicase^[35]. ATM could bind to histone deacetylase HDAC1 both *in vitro* and *in vivo*, and the extent of this association was increased after exposure of MRC5CV1 human fibroblasts to IR^[36]. ATR was also able to bind to Rad17^[37] and BRCA1^[38], and associated with components of the nucleosome remodeling and deacetylating (NRD) complex such as chromodomain-helicase-DNA-binding protein 4 (CHD4) and histone-deacetylase-2 (HDAC2)^[39]. All these data support the model that multiple checkpoint protein complexes localize at the sites of DNA damage independently and interact to trigger the checkpoint-signaling cascade.

Interaction with c-Abl

c-Abl, a non-receptor tyrosine kinase that is ubiquitously expressed and localized in both nucleus and cytoplasm, could be up-regulated following exposure to IR or genotoxic chemicals such as cisplatin, methyl methane sulfonate (MMS), mitomycin-C, hydrogen peroxide, but not UV^[3,40-42]. IR-induced activation of c-Abl has been shown to require the involvement of ATM in some cases, with ATM phosphorylating serine residue 465 located within the kinase domain of c-Abl^[43-45]. However, other studies found that c-Abl was not essential for ATM function in chromosomal maintenance, suggesting that c-Abl and ATM are at least partially independent^[46].

An important effect which has been found following the activation of c-Abl, is the induction of cell cycle arrest in a p53-dependent manner, with the possible involvement of Rb, but not p21^{Cip1}^[47,48]. c-Abl could directly interact with and phosphorylate p53, and regulate the level of p53 by preventing its nuclear export and ubiquitination-dependent degradation^[49,50]. It could also induce apoptosis in response to DNA damage^[51,52], although this activity involved collaboration with p73 more than p53^[53-55]. c-Abl binds to p73 through its Src-homology (SH3) domain to phosphorylate p73 at tyrosine residues, which in turn activates p73-dependent apoptosis pathway.

Regulation of the tumor suppressor p53 protein

Since p53 is such an important mediator in cellular response to genotoxic stress, it is no wonder that ATM/ATR can regulate p53 activity at multiple levels (Figure 2). The most straightforward way to manage p53 is through direct interaction, e.g., phosphorylation of p53. Both ATM and ATR have been shown to phosphorylate p53 protein at serine 15 to enhance its transactivating activity^[56-59]. ATM is also required for dephosphorylation of Ser 376, which can create a binding site for 14-3-3 protein. The association of p53 and 14-3-3 could increase the affinity of p53 for its specific DNA sequence, therefore enhancing its transcriptional activity^[60]. Other sites that could be phosphorylated by ATM on p53 include Ser 6, 9, 46, and Thr 18, which may be important for the apoptotic activity of p53 (Ser 46) or may enhance the acetylation of p53 (Ser 6, 9, Thr18)^[61]. In addition, ATM/ATR could regulate p53 through the action of other kinases. For example, ATM-activated c-Abl could phosphorylate p53 at Ser 20, which is important for the stabilization of p53 since this modification interferes with the binding between p53 and its regulator murine double minute 2 (Mdm2)^[49,62]. ATM-activated Chk2 could also phosphorylate p53 protein at Ser 20 and possibly at other sites, leading to the activation of p53^[63-65]. Furthermore, ATM has been found able to bind and phosphorylate Mdm2 and HDM2 (the human homologue of Mdm2), thus inhibiting p53 degradation and promoting its accumulation in cells^[66-68].

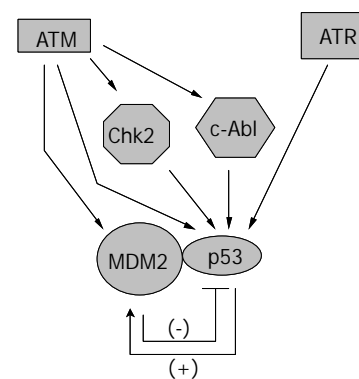


Figure 2 Regulation of p53 protein by ATM and ATR. ATM and ATR can influence the activity of p53 directly through phosphorylation or indirectly through the action of other kinases. Furthermore, ATM can regulate p53 through phosphorylation of Mdm2 molecule, the negative regulator of p53, which can be up-regulated by p53.

Activation of MAPKs

Accumulative data support the notion that the activation of MAPKs in response to genotoxic stress is ATM/ATR dependent. For example, DNA damaging stimuli, including etoposide (ETOP), adriamycin (ADR), IR, and UV could activate ERK1/2 in primary (MEF and IMR90), immortalized (NIH3T3) and transformed (MCF-7) cells. It has further been shown that ERK activation in response to ETOP could be

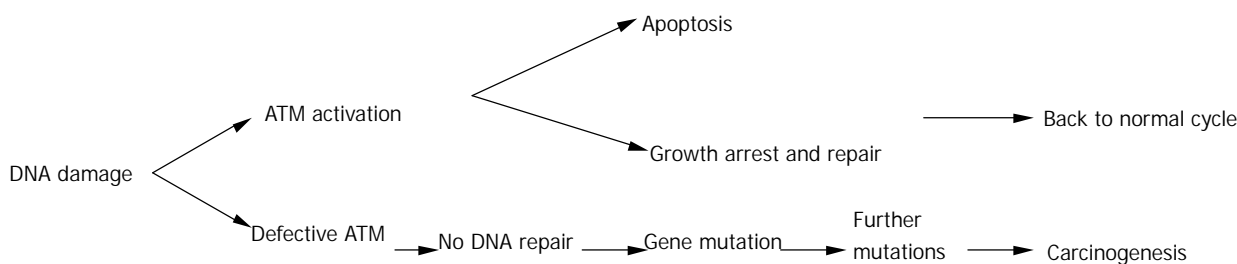


Figure 3 The relationship between ATM and carcinogenesis.

abolished in ATM^{-/-} fibroblasts (GM05823) independently of p53^[69]. UVA (320–400 nm) triggered ATM-dependent p53 phosphorylation and JNK activation that resulted in apoptosis, while ATR was required for UVC (200–290 nm)-mediated p53 phosphorylation and JNK activation^[70]. In addition, activation of ATM by gamma irradiation could lead to the activation of MKK6 and p38 γ isoform, and that activation of both MKK6 and p38 γ was essential for the proper regulation of G2 checkpoint in mammalian cells^[71].

Although the link between ATM/ATR and MAPKs has been established, it is still not clear how ATM/ATR activates MAPKs. In general, MAPK pathways are activated by extracellular signals or signals generated in the cytoplasm, and then the activated MAPKs transduce the specific “messages” to the nucleus. However, in response to genotoxic stress, the signal seems to flow from the nucleus to the cytoplasm to activate MAPKs. In this case, c-Abl kinase may provide an explanation. It has been found that c-Abl can activate p38 through MKK6^[72–74], and JNK by translocating from nucleus to cytoplasm to phosphorylate hematopoietic progenitor kinase (HPK1), an upstream kinase of JNK^[75]. Therefore, c-Abl may fulfill a role as the message carrier to transduce signals between subcellular locations. This may further explain why in response to genotoxic stress the activation of p38 was rather late (- 1 h) and prolonged^[71], while the cytokine activation of p38 was rapid and transient (maximum around 30–60 min)^[76].

In addition to their ability to activate MAPKs, ATM/ATR may also regulate these kinases through their negative regulators, the dual specificity of phosphatase MAPK and phosphatase family (MKP). One member of the MKP family, MKP-5, is known to dephosphorylate and inactivate the stress-activated JNK and p38. The phosphorylation-dephosphorylation cycle of JNK and p38 stimulated by radiomimetic chemical neocarzinostatin (NCS), which can induce double strand breaks (DSBs), could be attenuated in A-T cells^[77], further emphasizing the role of ATM as a master regulator in the cellular response to genotoxic stress.

Mutations in ATM in association with cancer

Homozygous mutations in the ATM gene can cause human genetic disorder ataxia-telangiectasia (A-T), which is characterized by cerebellar degeneration, immunodeficiency, cancer predisposition, and acute sensitivity to IR. The affected individual has been found to be prone to develop T cell prolymphocytic leukemia, B cell chronic lymphocytic leukemia, as well as sporadic colon cancer with microsatellite instability^[78]. ATM-deficient mice also showed a striking predisposition to lymphoid malignancies, particularly thymic lymphomas, to which they succumbed before the age of 1 year. However, much of the literature on ATM mutations and cancer was not about A-T patients, but was, instead, on heterozygous carriers of A-T mutations. For example, recent studies have found an unusually high occurrence of breast cancer in the relatives of A-T patients, and that loss of heterozygosity of ATM occurred frequently during the early stages of breast cancer development^[79].

Furthermore, heterozygous mice were more sensitive to radiation-induced cataracts than their wild-type counterparts^[80]. Spring *et al.*, established a knock-in mouse mutant in which an inframe deletion was previously found to cause A-T in humans was induced. Mice homozygous for this mutation could produce small amounts of inactive ATM and usually showed the hallmarks of the *Atm*-knockout phenotype. Notably, mice heterozygous for this mutation were predisposed to various cancers, unlike the animals that carry a single knockout allele that does not produce any protein^[81]. Therefore, ATM heterozygotes in human population might also be more radiosensitive, and have a higher risk for cancer^[82](Figure 3).

No human disease has been found to link to defects in ATR, although it was found that defects in ATR led to embryonic lethality in mice, suggesting that ATR is essential for development of ATR^[83,84]. Nonetheless, it is known that over-expressing the inactive form of ATR had a dominant negative effect, causing increased sensitivity to DNA damaging stimuli and failure to activate cell cycle checkpoints in response to IR^[28,85]. Finally, over-expressing active ATR could restore S phase checkpoint defect in A-T cells, suggesting that ATM and ATR may complement each other in the cellular genotoxic stress response^[85].

Down-regulation of ATM and ATR

Once the sensors detect DNA damage and initiate the signaling pathway, and the biological consequences (including DNA repair, cell cycle arrest, and apoptosis) take effect, the signals need to be inactivated or attenuated. The regulation of some downstream components in the cellular genotoxic stress response has been rather clearly defined, and usually involves a negative feedback mechanism. One such example is the p53-Mdm2 regulation loop. In this loop p53 could activate the expression of Mdm2, and Mdm2 could mediate the rapid degradation of p53 through the ubiquitin pathway^[62]. MAPKs have a similar feedback regulation mechanism with MKPs. MAPKs could induce the expression of MKPs, and MKPs then could interact with specific MAPKs to deactivate them through dephosphorylation^[1]. On the other hand, the mechanisms for the regulation of ATM and ATR, remain obscure, although some recent studies have significantly advanced our understanding.

In contrast to the vast volume of reports about the activation of ATM under genotoxic stress, very few studies have been conducted to evaluate how ATM was inactivated. The results from these studies so far all pointed toward inactivation of ATM through Caspase-mediated cleavage during apoptosis^[86–88]. This same mechanism has also been shown to regulate many other proteins involved in apoptosis, including serine/threonine protein kinase C δ (PKC δ), Mdm2, PARP, replication factor C, 70 kDa U1snRNP, fodrin and lamins^[87]. It was reported that during apoptosis induced by c-Myc or DNA-damaging agents (such as etoposide or IR), ATM but not ATR, was specifically cleaved by members of the Caspase family. Detailed studies revealed that the Caspase responsible for this

cleavage was either Caspase-3 or -7, but not Caspase-6. This cleavage abrogated the kinase activity of ATM to phosphorylate p53, although the resulting two fragments retained their DNA binding ability and interacted with each other. This finding led to the hypothesis that cleaved ATM protein, without its kinase activity, might act in a trans-dominant-negative fashion to compete with the intact ATM, thus preventing DNA repair and DNA damage signaling through its binding to DNA^[86-88].

Even less information is available regarding the inactivation of ATR. However, the recent identification of an ATR-interacting protein (ATRIP) might provide a lead for future studies^[89]. ATRIP is an 86-kDa protein with a coiled-coil domain near its N-terminal and its expression is regulated by ATR. The deletion of ATR mediated by Cre recombinase could cause the loss of both ATR and ATRIP expression, along with the loss of DNA damage checkpoint responses and cell death. ATRIP could be phosphorylated by ATR and co-localized at intranuclear foci with ATR after DNA damage caused by hydroxyurea (HU), IR, or UV, or inhibition of DNA replication. Conversely, ATRIP could also regulate the expression of ATR, as inhibition of ATRIP expression with small interference RNA (siRNA) would result in decreased ATR protein expression, while ATR mRNA levels would not be affected. Interference with ATRIP function could cause the same loss of G2-M response to DNA damage as that seen in the case of ATR deletion, suggesting that these two proteins work as mutually dependent partners in cell cycle checkpoint pathways^[89].

CONCLUSION

Human cancer is a major health issue for society, causing millions of deaths each year and huge economical losses. Since most of human carcinogens are genotoxins^[90,91], considerable resources have been and are being expended in efforts to understand the mechanism of genotoxin-induced carcinogenesis, thus leading to a better prevention or even the treatment of cancer. Since the sensing of DNA damage is one of the earliest steps in the cellular response to genotoxic stress, identification of these "sensors" is the most prominent challenge. As discussed in this review, ATM and ATR are showing their promise as potential candidates. However, what we should keep in mind is that detection of DNA damage may not be such a simple process, and may require more than just one or two proteins to fulfill this role. Supporting this idea is the finding of "foci" at damaged DNA sites, where many proteins involved in DNA repair and maintenance aggregate. It is more likely that interactions of these proteins, combined with some unidentified factors might function as DNA damage sensors^[92]. Further elucidation of these "foci" will be an exciting area for future research.

REFERENCES

- 1 **Yang J**, Yu Y, Duerksen-Hughes PJ. Protein kinases and their involvement in the cellular responses to genotoxic stress. *Mutat Res* 2003; **543**: 31-58
- 2 **Liu Y**, Guyton KZ, Gorospe M, Xu Q, Lee JC, Holbrook NJ. Differential activation of ERK, JNK/SAPK, and p38/CSBP/RK map kinase family members during the cellular response to arsenite. *Free Radic Biol Med* 1996; **21**: 771-781
- 3 **Liu ZG**, Baskaran R, Lea-Chou ET, Wood LD, Chen Y, Karin M, Wang JY. Three distinct signalling responses by murine fibroblasts to genotoxic stress. *Nature* 1996; **384**: 273-276
- 4 **Sanchez-Prieto R**, Rojas JM, Taya Y, Gutkind JS. A role for the p38 mitogen-activated protein kinase pathway in the transcriptional activation of p53 on genotoxic stress by chemotherapeutic agents. *Cancer Res* 2000; **60**: 2464-2472
- 5 **Kharbanda S**, Saxena S, Yoshida K, Pandey P, Kaneki M, Wang Q, Cheng K, Chen YN, Campbell A, Sudha T, Yuan ZM, Narula J, Weichselbaum R, Nalin C, Kufe D. Translocation of SAPK/JNK to mitochondria and interaction with Bcl-x(L) in response to DNA damage. *J Biol Chem* 2000; **275**: 322-327
- 6 **Zhang Y**, Zhong S, Dong Z, Chen N, Bode AM, Ma W, Dong Z. UVA induces Ser381 phosphorylation of p90RSK/MAPKAP-K1 via ERK and JNK pathways. *J Biol Chem* 2001; **276**: 14572-14580
- 7 **She QB**, Chen N, Dong Z. ERKs and p38 kinase phosphorylate p53 protein at serine 15 in response to UV radiation. *J Biol Chem* 2000; **275**: 20444-20449
- 8 **Akechi M**, Ito M, Uemura K, Takamatsu N, Yamashita S, Uchiyama K, Yoshioka K, Shiba T. Expression of JNK cascade scaffold protein JSAP1 in the mouse nervous system. *Neurosci Res* 2001; **39**: 391-400
- 9 **Tawadros T**, Formenton A, Dudler J, Thompson N, Nicod P, Leisinger HJ, Waerber G, Haefliger JA. The scaffold protein IB1/JIP-1 controls the activation of JNK in rat stressed urothelium. *J Cell Sci* 2002; **115**(pt2): 385-393
- 10 **Ito M**, Akechi M, Hirose R, Ichimura M, Takamatsu N, Xu P, Nakabeppu Y, Tadayoshi S, Yamamoto K, Yoshioka K. Isoforms of JSAP1 scaffold protein generated through alternative splicing. *Gene* 2000; **255**: 229-234
- 11 **Yang J**, Duerksen-Hughes P. A new approach to identifying genotoxic carcinogens: p53 induction as an indicator of genotoxic damage. *Carcinogenesis* 1998; **19**: 1117-1125
- 12 **Wahl GM**, Linke SP, Paulson TG, Huang LC. Maintaining genetic stability through TP53 mediated checkpoint control. *Cancer Surv* 1997; **29**: 183-219
- 13 **Lowndes NF**, Murguia JR. Sensing and responding to DNA damage. *Curr Opin Genet Dev* 2000; **10**: 17-25
- 14 **Abraham RT**. Cell cycle checkpoint signaling through the ATM and ATR kinases. *Genes Dev* 2001; **15**: 2177-2196
- 15 **Rouse J**, Jackson SP. Interfaces between the detection, signaling, and repair of DNA damage. *Science* 2002; **297**: 547-551
- 16 **O'Connell MJ**, Walworth NC, Carr AM. The G2-phase DNA-damage checkpoint. *Trends Cell Biol* 2000; **10**: 296-303
- 17 **Green CM**, Erdjument-Bromage H, Tempst P, Lowndes NF. A novel Rad24 checkpoint protein complex closely related to replication factor C. *Curr Biol* 2000; **10**: 39-42
- 18 **Roos-Mattjus P**, Vroman BT, Burtelow MA, Rauen M, Eapen AK, Karnitz LM. Genotoxin-induced Rad9-Hus1-Rad1 (9-1-1) chromatin association is an early checkpoint signaling event. *J Biol Chem* 2002; **277**: 43809-43812
- 19 **Durocher D**, Jackson SP. DNA-PK, ATM and ATR as sensors of DNA damage: variations on a theme? *Curr Opin Cell Biol* 2001; **13**: 225-231
- 20 **Rotman G**, Shiloh Y. ATM: a mediator of multiple responses to genotoxic stress. *Oncogene* 1999; **18**: 6135-6144
- 21 **Chan ED**, Winston BW, Jarpe MB, Wynes MW, Riches DW. Preferential activation of the p46 isoform of JNK/SAPK in mouse macrophages by TNF alpha. *Proc Natl Acad Sci U S A* 1997; **94**: 13169-13174
- 22 **Bao S**, Tibbetts RS, Brumbaugh KM, Fang Y, Richardson DA, Ali A, Chen SM, Abraham RT, Wang XF. ATR/ATM-mediated phosphorylation of human Rad17 is required for genotoxic stress responses. *Nature* 2001; **411**: 969-974
- 23 **Plumb MA**, Smith GC, Cunniffe SM, Jackson SP, O'Neil P. DNA-PK activation by ionizing radiation-induced DNA single-strand breaks. *Int J Radiat Biol* 1999; **75**: 553-561
- 24 **Jackson SP**. DNA-dependent protein kinase. *Int J Biochem Cell Biol* 1997; **29**: 935-938
- 25 **Gately DP**, Hittle JC, Chan GK, Yen TJ. Characterization of ATM expression, localization, and associated DNA-dependent protein kinase activity. *Mol Biol Cell* 1998; **9**: 2361-2374
- 26 **Pandita TK**, Lieberman HB, Lim DS, Dhar S, Zheng W, Taya Y, Kastan MB. Ionizing radiation activates the ATM kinase throughout the cell cycle. *Oncogene* 2000; **19**: 1386-1391
- 27 **Andegeko Y**, Moyal L, Mittelman L, Tsarfaty I, Shiloh Y, Rotman G. Nuclear retention of ATM at sites of DNA double strand breaks. *J Biol Chem* 2001; **276**: 38224-38230
- 28 **Wright JA**, Keegan KS, Herendeen DR, Bentley NJ, Carr AM, Hoekstra MF, Concannon P. Protein kinase mutants of human ATR increase sensitivity to UV and ionizing radiation and abrogate cell cycle checkpoint control. *Proc Natl Acad Sci U S A* 1998; **95**: 7445-7450

- 29 **Hekmat-Nejad M**, You Z, Yee MC, Newport JW, Cimprich KA. Xenopus ATR is a replication-dependent chromatin-binding protein required for the DNA replication checkpoint. *Curr Biol* 2000; **10**: 1565-1573
- 30 **Wahl GM**, Carr AM. The evolution of diverse biological responses to DNA damage: insights from yeast and p53. *Nature Cell Biol* 2001; **3**: E227-E286
- 31 **Suzuki K**, Kodama S, Watanabe M. Recruitment of ATM protein to double strand DNA irradiated with ionizing radiation. *J Biol Chem* 1999; **274**: 25571-25575
- 32 **Smith GC**, Cary RB, Lakin ND, Hann BC, Teo SH, Chen DJ, Jackson SP. Purification and DNA binding properties of the ataxia-telangiectasia gene product ATM. *Proc Natl Acad Sci U S A* 1999; **96**: 11134-11139
- 33 **Guo Z**, Kumagai A, Wang SX, Dunphy WG. Requirement for Atr in phosphorylation of Chk1 and cell cycle regulation in response to DNA replication blocks and UV-damaged DNA in *Xenopus* egg extracts. *Genes Dev* 2000; **14**: 2745-2756
- 34 **Unsal-Kacmaz K**, Makhov AM, Griffith JD, Sancar A. Preferential binding of ATR protein to UV-damaged DNA. *Proc Natl Acad Sci U S A* 2002; **99**: 6673-6678
- 35 **Wang Y**, Cortez D, Yazdi P, Neff N, Elledge SJ, Qin J. BASC, a super complex of BRCA1-associated proteins involved in the recognition and repair of aberrant DNA structures. *Genes Dev* 2000; **14**: 927-939
- 36 **Kim GD**, Choi YH, Dimtchev A, Jeong SJ, Dritschilo A, Jung M. Sensing of ionizing radiation-induced DNA damage by ATM through interaction with histone deacetylase. *J Biol Chem* 1999; **274**: 31127-31130
- 37 **Zou L**, Cortez D, Elledge SJ. Regulation of ATR substrate selection by Rad17-dependent loading of Rad9 complexes onto chromatin. *Genes Dev* 2002; **16**: 198-208
- 38 **Tibbetts RS**, Cortez D, Brumbaugh KM, Scully R, Livingston D, Elledge SJ, Abraham RT. Functional interactions between BRCA1 and the checkpoint kinase ATR during genotoxic stress. *Genes Dev* 2000; **14**: 2989-3002
- 39 **Schmidt DR**, Schreiber SL. Molecular association between ATR and two components of the nucleosome remodeling and deacetylating complex, HDAC2 and CHD4. *Biochemistry* 1999; **38**: 14711-14717
- 40 **Wang JY**. Cellular responses to DNA damage. *Curr Opin Cell Biol* 1998; **10**: 240-247
- 41 **Wen ST**, Van Etten RA. The PAG gene product, a stress-induced protein with antioxidant properties, is an Abl SH3-binding protein and a physiological inhibitor of c-Abl tyrosine kinase activity. *Genes Dev* 1997; **11**: 2456-2467
- 42 **Kharbanda S**, Ren R, Pandey P, Shafman TD, Feller SM, Weichselbaum RR, Kufe DW. Activation of the c-Abl tyrosine kinase in the stress response to DNA-damaging agents. *Nature* 1995; **376**: 785-788
- 43 **Shafman T**, Khanna KK, Kedar P, Spring K, Kozlov S, Yen T, Hobson K, Gatei M, Zhang N, Watters D, Egerton M, Shiloh Y, Kharbanda S, Kufe D, Lavin MF. Interaction between ATM protein and c-Abl in response to DNA damage. *Nature* 1997; **387**: 520-523
- 44 **Baskaran R**, Wood LD, Whitaker LL, Canman CE, Morgan SE, Xu Y, Barlow C, Baltimore D, Wynshaw-Boris A, Kastan MB, Wang JY. Ataxia telangiectasia mutant protein activates c-Abl tyrosine kinase in response to ionizing radiation. *Nature* 1997; **387**: 516-519
- 45 **Shangary S**, Brown KD, Adamson AW, Edmonson S, Ng B, Pandita TK, Yalowich J, Taccioli GE, Baskaran R. Regulation of DNA-dependent protein kinase activity by ionizing radiation-activated Abl kinase is an ATM-dependent process. *J Biol Chem* 2000; **275**: 30163-30168
- 46 **Takao N**, Mori R, Kato H, Shinohara A, Yamamoto K. c-Abl tyrosine kinase is not essential for ataxia telangiectasia mutated functions in chromosomal maintenance. *J Biol Chem* 2000; **275**: 725-728
- 47 **Yuan ZM**, Huang Y, Whang Y, Sawyers C, Weichselbaum R, Kharbanda S, Kufe D. Role for c-Abl tyrosine kinase in growth arrest response to DNA damage. *Nature* 1996; **382**: 272-274
- 48 **Wen ST**, Jackson PK, van Etten RA. The cytosolic function of c-Abl is controlled by multiple nuclear localization signals and requires the p53 and Rb tumor suppressor gene products. *EMBO J* 1996; **15**: 1583-1595
- 49 **Sionov RV**, Moallem E, Berger M, Kazaz A, Gerlitz O, Ben-Neriah Y, Oren M, Haupt Y. C-Abl neutralizes the inhibitory effect of Mdm2 on p53. *J Biol Chem* 1999; **274**: 8371-8374
- 50 **Sionov RV**, Coen S, Goldberg Z, Berger M, Bercovich B, Ben-Neriah Y, Ciechanover A, Haupt Y. C-Abl regulates p53 levels under normal and stress conditions by preventing its nuclear export and ubiquitination. *Mol Cell Biol* 2001; **21**: 5869-5878
- 51 **Huang Y**, Yuan ZM, Ishiko T, Nakada S, Utsugisawa T, Kato T, Kharbanda S, Kufe DW. Pro-apoptotic effect of the c-Abl tyrosine kinase in the cellular response to 1-beta-D-arabinofuranosylcytosine. *Oncogene* 1997; **15**: 1947-1952
- 52 **Yuan ZM**, Huang Y, Ishiko T, Kharbanda S, Weichselbaum R, Kufe D. Regulation of DNA damage-induced apoptosis by the c-Abl tyrosine kinase. *Proc Natl Acad Sci U S A* 1997; **94**: 1437-1440
- 53 **Shaul Y**. C-Abl: activation and nuclear targets. *Cell Death Differ* 2000; **7**: 10-16
- 54 **Gong JG**, Costanzo A, Yang HQ, Melino G, Kaelin WG Jr, Levrero M, Wang JY. The tyrosine kinase c-Abl regulates p73 in apoptotic response to cisplatin-induced DNA damage. *Nature* 1999; **399**: 806-809
- 55 **Agami R**, Blandino G, Oren M, Shaul Y. Interaction of c-Abl and p73alpha and their collaboration to induce apoptosis. *Nature* 1999; **399**: 809-813
- 56 **Canman CE**, Lim DS, Cimprich KA, Taya Y, Tamai K, Sakaguchi K, Appella E, Kastan MB, Siliciano JD. Activation of the ATM kinase by ionizing radiation and phosphorylation of p53. *Science* 1998; **281**: 1677-1679
- 57 **Banin S**, Moyal L, Shieh S, Taya Y, Anderson CW, Chessa L, Smorodinsky NI, Prives C, Reiss Y, Shiloh Y, Ziv Y. Enhanced phosphorylation of p53 by ATM in response to DNA damage. *Science* 1998; **281**: 1674-1677
- 58 **Nakagawa K**, Taya Y, Tamai K, Yamaizumi M. Requirement of ATM in phosphorylation of the human p53 protein at serine 15 following DNA double-strand breaks. *Mol Cell Biol* 1999; **19**: 2828-2834
- 59 **Tibbetts RS**, Brumbaugh KM, Williams JM, Sarkaria JN, Cliby WA, Shieh SY, Taya Y, Prives C, Abraham RT. A role for ATR in the DNA damage-induced phosphorylation of p53. *Genes Dev* 1999; **13**: 152-157
- 60 **Waterman MJ**, Stavridi ES, Waterman JL, Halazonetis TD. ATM-dependent activation of p53 involves dephosphorylation and association with 14-3-3 proteins. *Nat Genet* 1998; **19**: 175-178
- 61 **Saito S**, Goodarzi AA, Higashimoto Y, Noda Y, Lees-Miller SP, Appella E, Anderson CW. ATM mediates phosphorylation at multiple p53 sites, including Ser(46), in response to ionizing radiation. *J Biol Chem* 2002; **277**: 12491-12494
- 62 **Alarcon-Vargas D**, Ronai Z. p53-Mdm2—the affair that never ends. *Carcinogenesis* 2002; **23**: 541-547
- 63 **Hirao A**, Kong YY, Matsuoka S, Wakeham A, Ruland J, Yoshida H, Liu D, Elledge SJ, Mak TW. DNA damage-induced activation of p53 by the checkpoint kinase Chk2. *Science* 2000; **287**: 1824-1827
- 64 **Chehab NH**, Malikzay A, Appel M, Halazonetis TD. Chk2/hCds1 functions as a DNA damage checkpoint in G₁ by stabilizing p53. *Genes Dev* 2000; **14**: 278-288
- 65 **Chehab NH**, Malikzay A, Stavridi ES, Halazonetis TD. Phosphorylation of Ser-20 mediates stabilization of human p53 in response to DNA damage. *Proc Natl Acad Sci U S A* 1999; **96**: 13777-13782
- 66 **Khosravi R**, Maya R, Gottlieb T, Oren M, Shiloh Y, Shkedy D. Rapid ATM-dependent phosphorylation of MDM2 precedes p53 accumulation in response to DNA damage. *Proc Natl Acad Sci U S A* 1999; **96**: 14973-14977
- 67 **de Toledo SM**, Azzam EI, Dahlberg WK, Gooding TB, Little JB. ATM complexes with HDM2 and promotes its rapid phosphorylation in a p53-independent manner in normal and tumor human cells exposed to ionizing radiation. *Oncogene* 2000; **19**: 6185-6193
- 68 **Maya R**, Balass M, Kim ST, Shkedy D, Leal JF, Shifman O, Moas M, Buschmann T, Ronai Z, Shiloh Y, Kastan MB, Katzir E, Oren M. ATM-dependent phosphorylation of Mdm2 on serine 395: role in p53 activation by DNA damage. *Genes Dev* 2001; **15**: 1067-1077
- 69 **Tang D**, Wu D, Hirao A, Lahti JM, Liu L, Mazza B, Kidd VJ, Mak TW, Ingram AJ. ERK activation mediates cell cycle arrest and apoptosis after DNA damage independently of p53. *J Biol Chem*

- 2002; **277**: 12710-12717
- 70 **Zhang Y**, Ma WY, Kaji A, Bode AM, Dong Z. Requirement of ATM in UVA-induced signaling and apoptosis. *J Biol Chem* 2002; **277**: 3124-3131
- 71 **Wang X**, McGowan CH, Zhao M, He L, Downey JS, Fearn C, Wang Y, Huang S, Han J. Involvement of the MKK6-p38 γ cascade in γ -radiation-induced cell cycle arrest. *Mol Cell Biol* 2000; **20**: 4543-4552
- 72 **Sanchez-Prieto R**, Sanchez-Arevalo VJ, Servitja JM, Gutkind JS. Regulation of p73 by c-Abl through the p38 MAP kinase pathway. *Oncogene* 2002; **21**: 974-979
- 73 **Pandey P**, Raingeaud J, Kaneki M, Weichselbaum R, Davis RJ, Kufe D, Kharbanda S. Activation of p38 mitogen-activated protein kinase by c-Abl-dependent and -independent mechanisms. *J Biol Chem* 1996; **271**: 23775-23779
- 74 **Cong F**, Goff SP. C-Abl-induced apoptosis, but not cell cycle arrest, requires mitogen-activated protein kinase kinase 6 activation. *Proc Natl Acad Sci U S A* 1999; **96**: 13819-13824
- 75 **Ito Y**, Pandey P, Sathyanarayana P, Ling P, Rana A, Weichselbaum R, Tan TH, Kufe D, Kharbanda S. Interaction of hematopoietic progenitor kinase 1 and c-Abl tyrosine kinase in response to genotoxic stress. *J Biol Chem* 2001; **276**: 18130-18138
- 76 **Liu RY**, Fan C, Liu G, Olashaw NE, Zuckerman KS. Activation of p38 mitogen-activated protein kinase is required for tumor necrosis factor- α -supported proliferation of leukemia and lymphoma cell lines. *J Biol Chem* 2000; **275**: 21086-21093
- 77 **Bar-Shira A**, Rashi-Elkeles S, Zlochover L, Moyal L, Smorodinsky NI, Seger R, Shiloh Y. ATM-dependent activation of the gene encoding MAP kinase phosphatase 5 by radiomimetic DNA damage. *Oncogene* 2002; **21**: 849-855
- 78 **Ejima Y**, Yang L, Sasaki MS. Aberrant splicing of the ATM gene associated with shortening of the intronic mononucleotide tract in human colon tumor cell lines: a novel mutation target of microsatellite instability. *Int J Cancer* 2000; **86**: 262-268
- 79 **Shen CY**, Yu JC, Lo YL, Kuo CH, Yue CT, Jou YS, Huang CS, Lung JC, Wu CW. Genome-wide search for loss of heterozygosity using laser capture microdissected tissue of breast carcinoma: an implication for mutator phenotype and breast cancer pathogenesis. *Cancer Res* 2000; **60**: 3884-3892
- 80 **Worgul BV**, Smilenov L, Brenner DJ, Junk A, Zhou W, Hall EJ. Atm heterozygous mice are more sensitive to radiation-induced cataracts than are their wild-type counterparts. *Proc Natl Acad Sci U S A* 2002; **99**: 9836-9839
- 81 **Spring K**, Ahangari F, Scott SP, Waring P, Purdie DM, Chen PC, Hourigan K, Ramsay J, McKinnon PJ, Swift M, Lavin MF. Mice heterozygous for mutation in Atm, the gene involved in ataxia-telangiectasia, have heightened susceptibility to cancer. *Nat Genet* 2002; **32**: 185-190
- 82 **Concannon P**. ATM heterozygosity and cancer risk. *Nat Genet* 2002; **32**: 89-90
- 83 **Brown EJ**, Baltimore D. ATR disruption leads to chromosomal fragmentation and early embryonic lethality. *Genes Dev* 2000; **14**: 397-402
- 84 **de Klein A**, Muijtjens M, van Os R, Verhoeven Y, Smit B, Carr AM, Lehmann AR, Hoeijmakers JH. Targeted disruption of the cell-cycle checkpoint gene ATR leads to early embryonic lethality in mice. *Curr Biol* 2000; **10**: 479-482
- 85 **Cliby WA**, Roberts CJ, Cimprich KA, Stringer CM, Lamb JR, Schreiber SL, Friend SH. Overexpression of a kinase-inactive ATR protein causes sensitivity to DNA-damaging agents and defects in cell cycle checkpoints. *EMBO J* 1998; **17**: 159-169
- 86 **Smith GC**, d'Adda di Fagagna F, Lakin ND, Jackson SP. Cleavage and inactivation of ATM during apoptosis. *Mol Cell Biol* 1999; **19**: 6076-6084
- 87 **Hotti A**, Jarvinen K, Siivola P, Holtta E. Caspases and mitochondria in c-Myc-induced apoptosis: identification of ATM as a new target of caspases. *Oncogene* 2000; **19**: 2354-2362
- 88 **Tong X**, Liu B, Dong Y, Sun Z. Cleavage of ATM during radiation-induced apoptosis: caspase-3-like apoptotic protease as a candidate. *Int J Radiat Biol* 2000; **76**: 1387-1395
- 89 **Cortez D**, Guntuku S, Qin J, Elledge SJ. ATR and ATRIP: partners in checkpoint signaling. *Science* 2001; **294**: 1713-1716
- 90 **Williams GM**, Weisburger JH. Chemical Carcinogenesis. New York, NY, Pergamon Press 1991
- 91 **Smart RC**. Carcinogenesis. Norwalk, CT, Appleton Lange 1994
- 92 **Yang J**, Yu Y, Hamrick HE, Duerksen-Hughes PJ. ATM, ATR, and DNA-PK: initiators of the cellular genotoxic stress responses. *Carcinogenesis* 2003; **24**: 1571-1580

Edited by Zhu LH and Wang XL

Effect of staurosporine on cycle human gastric cancer cell

Min-Wen Ha, Ke-Zuo Hou, Yun-Peng Liu, Yuan Yuan

Min-Wen Ha, Yuan Yuan, Cancer Institute of the First Affiliated Hospital of China Medical University, Shenyang 110001, Liaoning Province, China

Ke-Zuo Hou, Yun-Peng Liu, Department of Oncology of the First Affiliated Hospital of China Medical University, Shenyang 110001, Liaoning Province, China

Supported by The China State Key Basic Research Program, No. G1998051203

Correspondence to: Professor Yuan Yuan, Cancer Institute of the First Affiliated Hospital of China Medical University, 155 Northern Nanjing Street, Heping District, Shenyang 110001, Liaoning Province, China. yyuan@mail.cmu.edu.cn

Telephone: +86-24-23256666 **Fax:** +86-24-22703576

Received: 2003-06-05 **Accepted:** 2003-07-24

Abstract

AIM: To study the effect of staurosporine (ST) on the cell cycle of human gastric cancer cell lines MGC803 and SGC7901.

METHODS: Cell proliferation was evaluated by trypan blue dye exclusion method. Apoptotic morphology was observed under a transmission electron microscope. Changes of cell cycle and apoptotic peaks of cells were determined by flow cytometry. Expression of *p21^{WAF1}* gene was examined using immunohistochemistry and RT-PCR.

RESULTS: The growth of MGC803 and SGC7901 cells was inhibited by ST. The inhibitory concentrations against 50% cells (IC_{50}) at 24 h and 48 h were 54 ng/ml and 23 ng/ml for MGC803, and 61 ng/ml and 37 ng/ml for SGC7901. Typical apoptotic bodies and apoptotic peaks were observed 24 h after cells were treated with ST at a concentration of 200 ng/ml. The percentage of cells at G_0/G_1 phase was decreased and that of cells at G_2/M was increased significantly in the group treated with ST at the concentrations of 40 ng/ml, 60 ng/ml, 100 ng/ml for 24 h, compared with the control group ($P < 0.01$). The expression levels of *p21^{WAF1}* gene in both MGC803 and SGC7901 cells were markedly up-regulated after treatment with ST.

CONCLUSION: ST can cause arrest of gastric cancer cells at G_2/M phase, which may be one of the mechanisms that inhibit cell proliferation and cause apoptosis in these cells. Effect of ST on cells at G_2/M phase may be attributed to the up-regulation of *p21^{WAF1}* gene.

Ha MW, Hou KZ, Liu YP, Yuan Y. Effect of staurosporine on cycle human gastric cancer cell. *World J Gastroenterol* 2004; 10(2): 161-166

<http://www.wjgnet.com/1007-9327/10/161.asp>

INTRODUCTION

Protein kinase C (PKC) isoforms are serine/threonine kinases involved in signal transduction pathways that govern a wide range of physiological processes including differentiation, proliferation, gene expression, membrane transport and

organization of cytoskeletal and extracellular matrix proteins^[1]. PKC isoforms are often overexpressed in disease states such as cancer. The important role they play in the processes relevant to neoplastic transformation, carcinogenesis and tumor cell invasion renders PKC a potentially suitable target for anticancer therapy^[2].

Staurosporine (ST), a microbial alkaloid (indolocarbazole produced by *Streptomyces sp.*), has been shown to be a potent inhibitor of a wide range of protein kinases, including different serine/threonine and tyrosine protein kinases, which acts by competing with the ATP-binding region of the kinase catalytic domain^[3]. Staurosporine has been reported to exert various pharmacological actions involving protein kinase C both *in vivo* and *in vitro*, such as diminishing thrombin enhanced procoagulant activity, reducing carbachol-induced insulin secretion^[4-7]. PKC function is altered in some neoplasias, and this dysfunction has been related to uncontrolled proliferation^[8,9].

Completion of the cell cycle requires the coordination of a variety of macromolecular syntheses, assemblies, and movements^[10]. Coordination of the timing and order of these processes are achieved by a regulatory system that responds to checkpoints at major transitions in the cycle. Two key checkpoints are at the G_1/S and G_2/M phase transitions. G_1 and G_2 cyclins, the cyclin-dependent kinases and cycle kinase inhibitors (CKI) are responsible for controlling the transitions. Here, we investigated the effect of the potent phospholipid/ Ca^{2+} -dependent kinase (PKC) inhibitor, ST, on cell cycle of human gastric cancer cell lines, MGC803 and SGC7901.

MATERIALS AND METHODS

Cell lines and cell culture

Human gastric mucinous adenocarcinoma cell line, MGC803, was obtained from Department of Immunity, China Medical University and human gastric carcinoma metastatic lymph node cell line, SGC7901, was obtained from Laboratory of Oncology, the First Affiliated Hospital of China Medical University. The derived cell lines were grown in RPMI 1640 medium supplemented with 10% heat-inactivated fetal calf serum, 50 U/ml penicillin and 50 μ g/ml streptomycin. The cells were maintained at 37 °C in a humidified atmosphere containing 5% CO_2 . Viability of the cells used in these experiments was consistently more than 95% when evaluated by the trypan blue exclusion method. Staurosporine was purchased from Sigma Company (St. Louis, USA).

Analysis of cell viability

Effect of ST on cell growth and viability was measured by directly counting the number of cells by means of trypan blue dye exclusion. Cells at a density of 2.5×10^5 /ml were seeded onto 24-well plates, and then treated with ST at different concentrations for 24 and 48 h. Control cells were also cultured at the same time. Cell proliferation and inhibition curves were drawn, and the inhibitory concentration against 50% cells (IC_{50}) was determined.

Cell morphological analysis with transmission electron microscope

Transmission electronic microscope was employed to observe

the effect of ST on cell apoptosis. Cells (1×10^6) were collected after being treated with ST at 200 ng/ml for 24 h, washed twice with PBS solution, centrifuged for 5 min at 1 500 rpm, then fixed in 2% glutaraldehyde at 4 °C for 72 h, then placed in 1% phosphotungstic acid. The cells were desiccated with gradients, and embedded with EPON-812. Ultrathin sections were prepared and observed after double staining with uranium and plumbum under a transmission electron microscope. Each experiment was repeated four times. At the same time, the cells without treatment with ST were used as a control group.

Cell cycle analysis

Flow cytometry was employed to determine the DNA content and the apoptotic peaks of the cells. The cells were seeded on 100 mm-dishes and grown in RPMI-1640 supplemented with 10% FCS. After treated with ST at the concentrations of 40 ng/ml, 60 ng/ml, 100 ng/ml, 200 ng/ml, 500 ng/ml for 24 h respectively, the cells were harvested, trypsinized, washed with D-PBS, fixed by adding slowly 2 ml of cold 70% ethanol into the tube and then stored at 4 °C. After fixation, the cells were washed, centrifuged, and resuspended in 0.05 mg/ml propidium iodide (Fluka Co, MILWAUKEE, USA), 100 units/ml RNase (Fluka Co, MILWAUKEE, USA) in PBS. The sample was incubated at room temperature for 30 min, and analyzed on a FACSCalibur (BD PharMingen, FRANKLIN Lakes, USA). Cell cycle data originally obtained with Cell Quest software (BD PharMingen, FRANKLIN Lakes, USA) were re-analyzed using MODFIT software (Verity Software House, Topsham, USA). At the same time negative controls were constructed.

Immunohistochemistry

p21 protein was detected by immunohistochemistry using specific monoclonal antibody (Maxin Co, Fuzhou, China). After treated with ST at the concentrations 40 ng/ml, 60 ng/ml, 100 ng/ml for 24 h, respectively, the cells were harvested. At the same time the negative controls were constructed. The cells were smeared on a slide with cell smear centrifugal apparatus, and stained using conventional S-P immunohistochemical method. Color was developed with DAB reagent and counterstained with hematoxylin. The cells were observed under a light microscope. The cells clearly showing brown color in their nuclei and plasma were considered to be positive for p21 protein.

Semiquantitative reverse transcription-PCR

The expression of p21 mRNA was determined by RT-PCR. After treated with ST at the concentration of 60 ng/ml, the cells were harvested. At the same time the negative controls were constructed. The cells were washed, and total RNA was extracted with the Qiagen RNA isolation kit (GIBCO Co., New York, USA). Aliquots containing 5 µg/ml of RNA from each treatment were used for the first-strand cDNA synthesis (TaKaRa Co., Dalian, China). In each reaction, 100 µl solution containing 3 µM of random hexamers, 25 mM Tris-HCl, 37 mM KCl, 1.5 mM MgCl₂, 10 mM DTT, 0.25 mM dNTP, 40 units of RNasin, an RNase inhibitor, 50 U/ml Super Taq DNA polymerase, and 200 units of reverse transcriptase was used. The annealing mixture was incubated at room temperature for 15 min, and then incubated in a water bath at 41 °C for 60 min. The reverse transcriptase enzyme was inactivated by heating the solution to 95 °C for 5 min. PCR was then carried out using the Perkin-Elmer PCR reaction kit and primers. The PCR was performed using a thermocycler for 30 cycles consisting of denaturation at 94 °C for 1 min, annealing at 57 °C for 1 min, and extension at 72 °C for 2 min. The PCR products were separated on 2% agarose gel. The primers used for PCR

were as follow: p21 sense (5' -GGG GAC AGC AGA GGA AGA C-3'), p21 antisense (5' -CGG CGT TTG GAG TGG TAG A-3'); β-actin sense (5' -GAT TGC CTC AGG ACA TTT CTG- 3'), β-actin antisense (5' -GAT TGC TCA GGA CAT TTC TG-3'). Gene primers were synthesized by Beijing Oake Company (Beijing, China).

Statistical analysis

Student's *t*-test was used to compare the difference between control and ST treated groups. Data of cell growth were presented as $\bar{x} \pm s$. A *P* value less than 0.05 was considered statistically significant.

RESULTS

ST inhibited proliferation of MGC803 and SGC7901 cells in a time-dependent and concentration-dependent manner

In this study, the exponentially grown MGC803 and SGC7901 cells were treated with 40 ng/ml, 60 ng/ml, 100 ng/ml ST, respectively, and the cell proliferation was measured 24 and 48 h after ST addition. Figures 1 and 2 show the cell proliferation curves at various ST concentrations. The inhibition of proliferation of MGC803 and SGC7901 cells by ST was clearly observed in a time-dependent and concentration-dependent manner. The IC₅₀ was 54 ng/ml and 23 ng/ml for MGC803 and 61 ng/ml and 37 ng/ml for SGC7901 at 24 and 48 h.

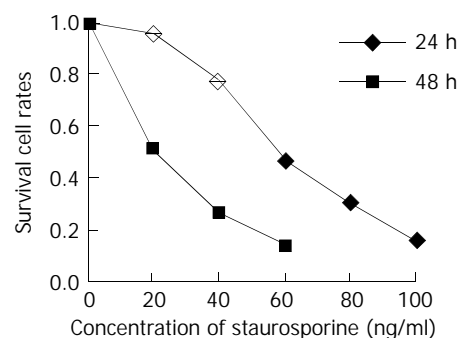


Figure 1 Inhibition of staurosporine on MGC-803 cell proliferation.

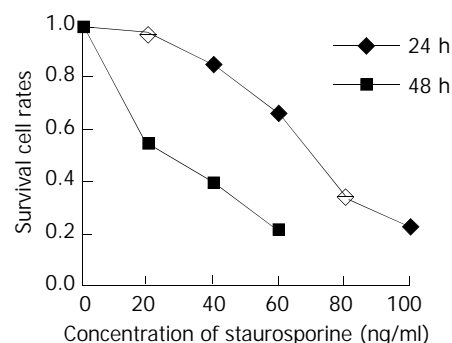


Figure 2 Inhibition of staurosporine on SGC-7901 cell proliferation.

Morphological observation of ST treatment effects

Cell morphological changes were observed under a transmission electron microscope after treatment with ST at the concentration of 200 ng/ml for 24 h. The ultrastructural appearances showed the typical changes in the cell morphology, including blebbing of the plasma membrane, chromatin condensation and formation of apoptotic bodies. Figure 3 shows the morphological changes of MGC803 and SGC7901 cells under a electron microscope after treatment with ST.

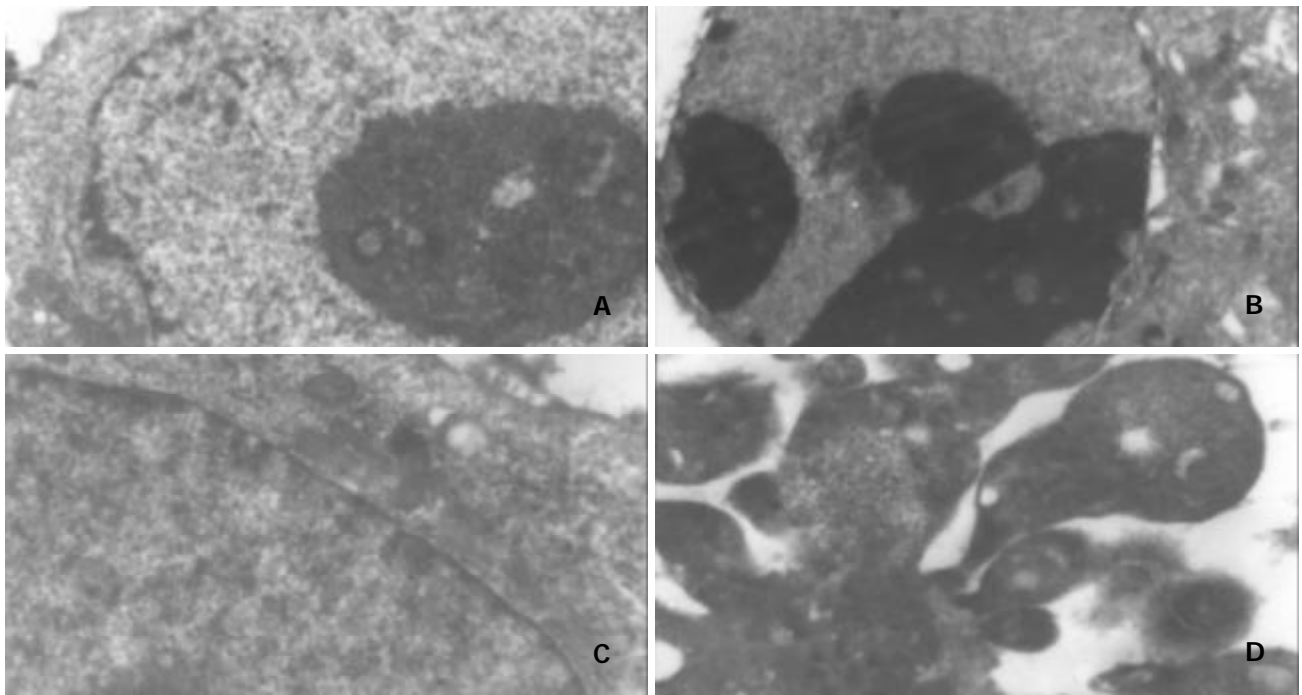


Figure 3 Morphological changes in MGC803 and SGC7901 cells under electron microscope after treatment with ST (200 ng/ml), $\times 5000$. A: MGC803 control cells, B: 200 ng/ml ST-induced MGC803 cells, C: SGC7901 control cells, D: 200 ng/ml ST-induced SGC7901 cells. Note: chromatin condensation and formation of apoptotic bodies.

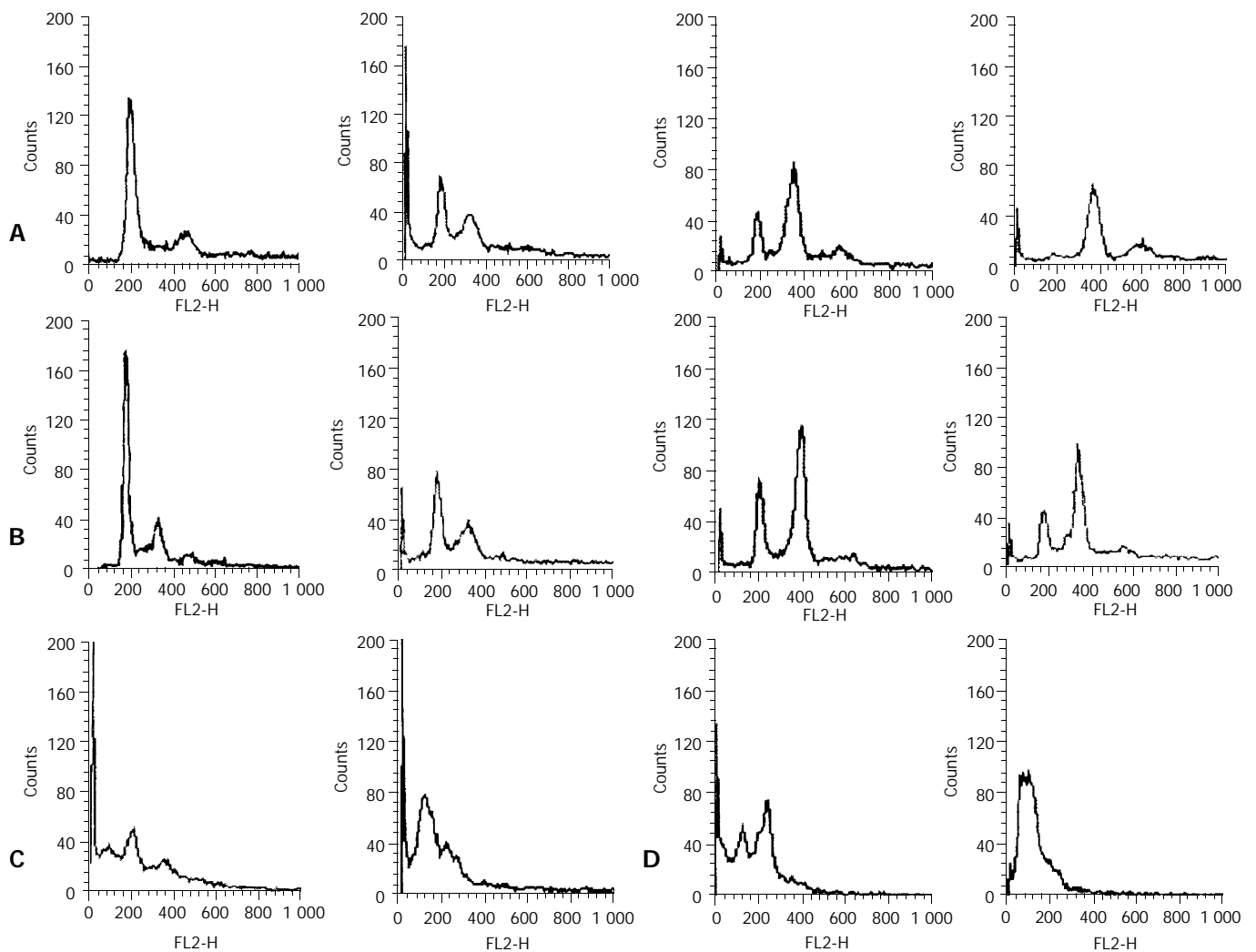


Figure 4 Effect of ST on cell cycle of human gastric cancer cells. A: Changes of cell cycle in MGC803 cells after ST-treatment for 24h, B: Changes of cell cycle in SGC7901 cells after ST-treatment for 24 h, C: ST-induced apoptosis in MGC-803 cells, D: ST-induced apoptosis in SGC-7901 cells.

Table 1 Effect of ST on cell cycle of MGC803 and SGC7901 cells ($\bar{x}\pm s$)

	MGC803				SGC7901			
	G ₀ /G ₁ (%)	S(%)	G ₂ /M(%)	AI	G ₀ /G ₁ (%)	S(%)	G ₂ /M(%)	AI
Control	54.3±3.1	15.2±0.6	13.5±0.2	3.1±0.2	52.5±4.4	10.1±0.6	13.5±2.2	2.8±0.2
40 ng/ml	23.6±1.8 ^a	13.9±1.1	22.6±4.0 ^a	3.8±0.9	27.1±1.4 ^a	12.4±0.1	21.9±2.6 ^a	3.3±0.3
60 ng/ml	11.6±0.7 ^a	12.6±2.8	35.5±0.4 ^a	4.0±0.3	17.0±3.4 ^a	13.4±2.0	39.5±4.9 ^a	3.7±0.6
100 ng/ml	3.3±0.2 ^a	10.9±1.7	36.8±5.5 ^a	5.2±0.4	13.7±0.7 ^a	12.7±0.9	38.4±3.1 ^a	4.4±1.1

AI, apoptotic incidence; ^a $P<0.01$ vs Control.

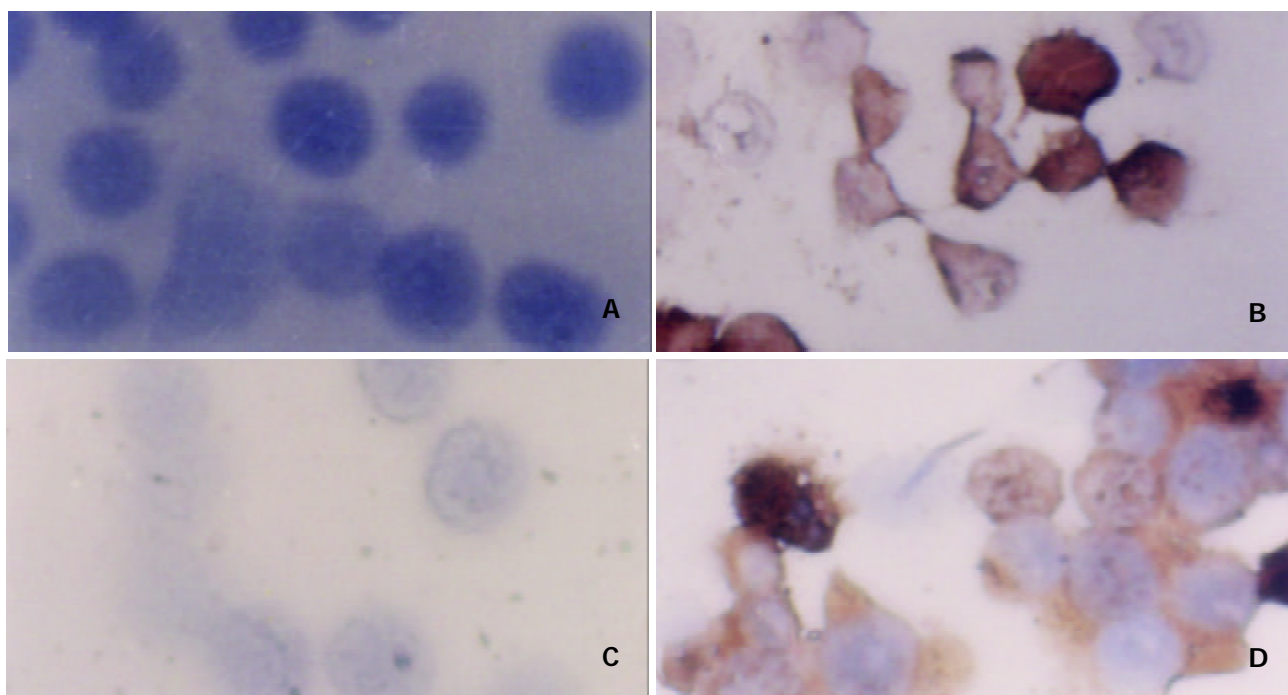


Figure 5 Expression of p21 protein in MGC803 and SGC7901 cells after ST-treatment as determined by immunohistochemistry (SP×400). A: MGC803 control cells, B: MGC803 cells treated with 60 ng/ml ST, C: SGC7901 control cells, D: SGC7901 cells treated with 60 ng/ml ST.

ST induced MGC803 and SGC7901 cells G₂/M phase arrest

The effects of ST on cell cycle progression, population distribution and apoptotic incidence in MGC803 and SGC7901 cells were determined using flow cytometry. ST-induced effects were detected by comparing the cell cycle profiles between ST treated and untreated cells. Notably, the cells demonstrated significant G₂/M arrest 24 h after ST treatment ($P<0.01$), in comparison to untreated cells. Interestingly, the S phase population was also increased, but to a lesser extent as compared with untreated cells. The percentage of cells in the S, G₁, and G₂/M phases are shown in Table 1. Apoptotic peaks were observed and cell apoptotic incidence was determined 24 h after treatment with ST at the concentrations of 200 ng/ml and 500 ng/ml. The apoptotic incidence increased to 50.2% and 89.6% in MGC803 cells, and 34.6% and 80.7% in SGC7901 cells after ST treatment. Figure 4 shows ST-induced apoptosis in MGC803 and SGC7901 cells.

ST resulted in an increase of p21 expression

The effect of ST on p21 protein levels was determined by immunohistochemistry analysis. Normally, p21 was not expressed in MGC803 and SGC7901 cells. However, p21 was significantly expressed, the positive rates were 19.3%, 26.6%, 31.8% in MGC803 cells, and 20.5%, 24.2%, 30.3% in SGC7901 cells after treatment with ST at the concentration 40 ng/ml, 60 ng/ml, 100 ng/ml for 24 h. Figure 5 shows the

levels of p21 expression in MGC803 and SGC7901 cells by immunohistochemistry.

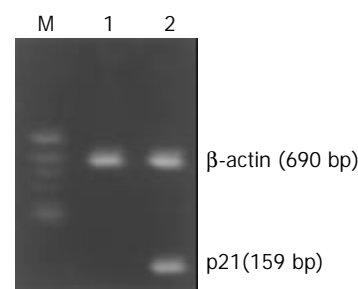


Figure 6 Effect of ST treatment on p21^{WAF1} mRNA expression in MGC803 cells. M: DNA Marks, 1: control cells, 2: cells treated with 60 ng/ml ST.

ST upregulated p21^{WAF1} expression

Normally, p21^{WAF1} mRNA was almost not expressed in MGC803 and SGC7901 cells when detected by RT-PCR. However, treatment with ST at the concentration of 60 ng/ml induced the upregulation of p21^{WAF1} mRNA in MGC803 and SGC7901 cells. Figures 6 and 7 show that p21^{WAF1} mRNA expression was upregulated in MGC803 and SGC7901 cells after treatment with ST.

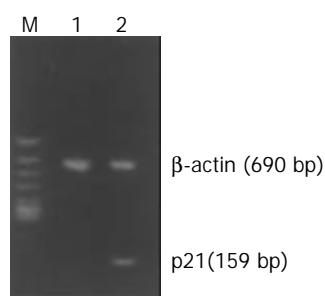


Figure 7 Effect of ST treatment on p21^{WAF1} mRNA expression in SGC7901 cells. M: DNA Marks, 1: control cells, 2: cells treated with 60 ng/ml ST.

DISCUSSION

Cancer cells have been found to be different from normal cells in many important characteristics, including loss of differentiation and decrease of apoptosis^[11,12]. These differences did not arise simply from uncontrolled cellular growth but rather from a process of cellular evolution^[13-15]. Cell cycle plays an important role in the modulation of tumor cell growth, and attention has been paid to preventing unlimited proliferation of tumor cells by cell cycle control^[16].

Twenty years ago, staurosporine (ST) was isolated from bacteria and identified as a potent inhibitor of PKC activity^[17-19]. In this study, the proliferation of human gastric cell lines, MGC803 and SGC7901, was significantly inhibited in a time- and concentration-dependent manner and classical apoptosis (sub-diploid peak on flow cytometry, and typical morphological changes) was observed after treated with ST. ST also blocked the G₂/M phase of the cell cycle. In order to examine the distribution of DNA content, the cells treated with ST were detected using flow cytometry. The first peak (2C C=haploid DNA content) was produced by the cell population in G₁ phase, the second (4C) was produced by the cells in G₂/M phase with or without cells in G₁ phase at a higher DNA ploidy (tetraploidy, G_{1t}), and the third (8C) was produced by cells in G₂ phase at a higher DNA ploidy (tetraploidy, G_{2t}). The results presented in this study indicated that the cells were blocked in G₂/M phase. These results lead to the suggestion that, ST can make damaged cells stagnate at G₂/M phase of cell cycle, and inhibit proliferation of cells, allowing them to repair the damage. If this happens, cells will reenter the cycle, otherwise, they will undergo apoptosis or death. More importantly, ST affects the selectively on G₂/M phase of these cells and participates in the regulation of the cell cycle, and thus the blocking effect of ST on cells in G₂/M phase might be the mechanism of its antitumor effect. These observations may provide some useful information that ST can be used as an antitumor agent.

The present study was undertaken to delineate the mechanism of ST effect on the G₂/M phase arrest of cells, and techniques including immunohistochemistry and RT-PCR were used to detect the expression of p21^{WAF1} protein and gene. Our results revealed that p21^{WAF1} expression was low in MGC803 and SGC7901 cells. However, ST significantly increased the expression of p21 in MGC803 and SGC7901 cells. Cell cycle events, including microtubule dynamics, membrane organization and DNA synthesis, were tightly controlled, and specific changes were induced at particular points in the eukaryotic cell cycle during cell proliferation^[20,21]. Negative controls on cell cycle progression were exerted during development, differentiation, senescence, and cell death. These negative controls might play an important role in preventing tumorigenesis. p21^{WAF1}, the pioneer member of p21 family of cyclin-CDK inhibitor class of proteins, has been implicated as a growth arrest mediator in cell terminal differentiation and

apoptosis^[22]. Regulation of cell cycle progression is orchestrated by a family of CDKs, which can be negatively regulated by CDK inhibitors, such as p21^{WAF1}. p21^{WAF1} is a downstream effector of p53 that mediates both G₁ and G₂/M phase arrest. Mechanistically, the p21^{WAF1}-mediated arrest of the G₂/M cell cycle transition has been suggested to include a p21^{WAF1}-CDK2 and p21^{WAF1}-PCNA protein interaction^[23,24]. p21 is the strongest kinase inhibitor, and has been found to inhibit the CDK4/6-cyclinD complex when overexpressed, leading to growth arrest and, under some conditions, to apoptosis^[25-27]. Although our knowledge on cell cycle checkpoints is still limited, it is clear that many such control points existed within the cell cycle and that they played a major role in maintaining the integrity of the genome^[28,29]. At least two checkpoints could detect DNA damage, one at the G₁-S transition and another at the G₂-M transition^[30-32]. ST up-regulates p21^{WAF1}, which then affects cell growth by repressing G₂/M phase, probably through interaction with cyclin-CDK complex. However, this hypothesis needs to be further investigated.

In conclusion, the present study demonstrates that ST can effectively inhibit the proliferation of human gastric cancer MGC803 and SGC7901 cells, induces apoptosis, blocks these cells in G₂/M phase, and up-regulates the p21^{WAF1} expression. This study provides some experimental data for the use of ST in the treatment of gastric carcinoma.

REFERENCES

- 1 **Caponigro F**, French RC, Kaye SB. Protein Kinase C: a worthwhile target for anticancer drugs? *Anticancer Drugs* 1997; **8**: 26-33
- 2 **Aiello LP**, Bursell SE, Clermont A, Duh E, Ishii H, Takagi C, Mori F, Ciulla TA, Ways K, Jirousek M, Smith LE, King GL. Vascular endothelial growth factor-induced retinal permeability is mediated by protein kinase C *in vivo* and suppressed by an orally effective beta-isoform-selective inhibitor. *Diabetes* 1997; **46**: 1473-1480
- 3 **Toledo LM**, Lydon NB, Elbaum D. The structure-based design of ATP-site directed protein kinase inhibitors. *Curr Med Chem* 1999; **6**: 775-805
- 4 **Zaugg K**, Rocha S, Resch H, Hegyi I, Oehler C, Glanzmann C, Fabbro D, Bodis S, Pruschy M. Differential p53-dependent mechanism of radiosensitization *in vitro* and *in vivo* by the protein kinase C-specific inhibitor PKC412. *Cancer Res* 2001; **61**: 732-738
- 5 **Gescher A**. Analogs of staurosporine: potential anticancer drugs? *Gen Pharmacol* 1998; **31**: 721-728
- 6 **Xia M**, Xue SB, Xu CS. Shedding of TNFR1 in regenerative liver can be induced with TNF alpha and PMA. *World J Gastroenterol* 2002; **8**: 1129-1133
- 7 **Li MS**, Li PF, He SP, Du GG, Li G. The promoting molecular mechanism of alpha-fetoprotein on the growth of human hepatoma Bel7402 cell line. *World J Gastroenterol* 2002; **8**: 469-475
- 8 **Ouyang GL**, Li QF, Peng XX, Liu QR, Hong SG. Effects of tachyplesin on proliferation and differentiation of human hepatocellular carcinoma SMMC-7721 cells. *World J Gastroenterol* 2002; **8**: 1053-1058
- 9 **Han Y**, Han ZY, Zhou XM, Shi R, Zheng Y, Shi YQ, Miao JY, Pan BR, Fan DM. Expression and function of classical protein kinase C isoenzymes in gastric cancer cell line and its drug-resistant sublines. *World J Gastroenterol* 2002; **8**: 441-445
- 10 **Gescher A**. Staurosporine analogues - pharmacological toys or useful antitumor agents? *Crit Rev Oncol Hematol* 2000; **34**: 127-135
- 11 **Chen B**, He L, Savell VH, Jenkins JJ, Parham DM. Inhibition of the interferon- γ /signal transducers and activators of transcription (STAT) pathway by hypermethylation at a STAT-binding site in the p21^{WAF1} promoter region. *Cancer Res* 2000; **60**: 3290-3298
- 12 **Zeng YX**, el-Deiry WS. Regulation of p21^{WAF1}/CIP1 expression by p53-independent pathways. *Oncogene* 1996; **12**: 1557-1564
- 13 **Wu Q**, Kirschmeier P, Hockenberry T, Yang TY, Brassard DL, Wang L, McClanahan T, Black S, Rizzi G, Musco ML, Mirza A, Liu S. Transcriptional regulation during p21^{WAF1}/CIP1 induced apoptosis in human ovarian cancer cells. *J Biol Chem* 2002; **277**: 36329-36337

- 14 **Kovalsky O**, Lung FD, Roller PP, Fornace AJ Jr. Oligomerization of human Gadd45a Protein. *J Biol Chem* 2001; **276**: 39330-39339
- 15 **Mihalik R**, Uher F, Pocsik EE, Berczi L, Benczur M, Kopper L. Detection of drug-induced apoptosis by flow cytometry after alkaline extraction of ethanol fixed cells. *Pathol Oncol Res* 1996; **2**: 78-83
- 16 **Heerdts BG**, Houston MA, Mariadason JM, Augenlicht LH. Dissociation of staurosporine-induced apoptosis from G2-M arrest in SW620 human colonic carcinoma cells: initiation of the apoptotic cascade is associated with elevation of the mitochondrial membrane potential (delta psi). *Cancer Res* 2000; **60**: 6704-6713
- 17 **Salvioli S**, Dobrucki J, Moretti L, Troiano L, Fernandez MG, Pinti M, Pedrazzi J, Franceschi C, Cossarizza A. Mitochondrial heterogeneity during staurosporine-induced apoptosis in HL60 cells: analysis at the single cell and single organelle level. *Cytometry* 2000; **40**: 189-197
- 18 **He SW**, Shen KQ, He YJ, Xie B, Zhao YM. Regulatory effect and mechanism of gastrin and its antagonists on colorectal carcinoma. *World J Gastroenterol* 1999; **5**: 408-416
- 19 **Bernard B**, Fest T, Pretet JL, Mougin C. Staurosporine-induced apoptosis of HPV positive and negative human cervical cancer cells from different points in the cell cycle. *Cell Death Differ* 2001; **8**: 234-244
- 20 **Stokke T**, Smedshammer L, Jonassen TS, Blomhoff HK, Skarstad K, Steen HB. Uncoupling of the order of the S and M phases: effects of staurosporine on human cell cycle kinases. *Cell Prolif* 1997; **30**: 197-218
- 21 **Zeng ZC**, Jiang GL, Wang GM, Tang ZY, Curran WJ, Iliakis G. DNA-PKcs subunits in radiosensitization by hyperthermia on hepatocellular carcinoma hepG2 cell line. *World J Gastroenterol* 2002; **8**: 797-803
- 22 **Bertrand R**, Solary E, O' Connor P, Kohn KW, Pommier Y. Induction of a common pathway of apoptosis by staurosporine. *Exp Cell Res* 1994; **211**: 314-321
- 23 **Fang JY**, Lu YY. Effects of histone acetylation and DNA methylation on p21(WAF1) regulation. *World J Gastroenterol* 2002; **8**: 400-405
- 24 **Wartenberg M**, Fischer K, Hescheler J, Sauer H. Modulation of intrinsic P-glycoprotein expression in multicellular prostate tumor spheroids by cell cycle inhibitors. *Biochim Biophys Acta* 2002; **1589**: 49-62
- 25 **Yuste VJ**, Sanchez-Lopez I, Sole C, Encinas M, Bayascas JR, Boix J, Comella JX. The prevention of the staurosporine-induced apoptosis by Bcl-X(L), but not by Bcl-2 or caspase inhibitors, allows the extensive differentiation of human neuroblastoma cells. *J Neurochem* 2002; **80**: 126-139
- 26 **Shimizu T**, Takahashi N, Tachibana K, Takeda K. Complex regulation of CDK2 and G1 arrest during neuronal differentiation of human prostatic cancer TSU-Prl cells by staurosporine. *Anticancer Res* 2001; **21**: 893-898
- 27 **Narita Y**, Asai A, Kuchino Y, Kirino T. Actinomycin D and staurosporine, potent apoptosis inducers *in vitro*, are potentially effective chemotherapeutic agents against glioblastoma multiforme. *Cancer Chemother Pharmacol* 2000; **45**: 149-156
- 28 **Chen X**, Lowe M, Herliczek T, Hall MJ, Danes C, Lawrence DA, Keyomarsi K. Protection of normal proliferating cells against chemotherapy by staurosporine-mediated, selective, and reversible G(1) arrest. *J Natl Cancer Inst* 2000; **92**: 1999-2008
- 29 **Sausville EA**, Johnson J, Alley M, Zaharevitz D, Senderowicz AM. Inhibition of CDKs as a therapeutic modality. *Ann N Y Acad Sci* 2000; **910**: 207-221
- 30 **Shchepina LA**, Popova EN, Pletjushkina OY, Chernyak BV. Respiration and mitochondrial membrane potential are not required for apoptosis and anti-apoptotic action of Bcl-2 in HeLa cells. *Biochemistry* 2002; **67**: 222-226
- 31 **Swe M**, Sit KH. Staurosporine induces telophase arrest and apoptosis blocking mitosis exit in human Chang liver cells. *Biochem Biophys Res Commun* 1997; **236**: 594-598
- 32 **Stepczynska A**, Lauber K, Engels IH, Janssen O, Kabelitz D, Wesselborg S, Schulze-Osthoff K. Staurosporine and conventional anticancer drugs induce overlapping, yet distinct pathways of apoptosis and caspase activation. *Oncogene* 2001; **20**: 1193-1202

Edited by Xia HHX and Wang XL

Inhibition of β -ionone on SGC-7901 cell proliferation and upregulation of metalloproteinases-1 and -2 expression

Jia-Ren Liu, Bao-Feng Yang, Bing-Qing Chen, Yan-Mei Yang, Hong-Wei Dong, You-Qiang Song

Jia-Ren Liu, Bing-Qing Chen, Yan-Mei Yang, Hong-Wei Dong, Public Health College, Harbin Medical University, Harbin 150001, Heilongjiang Province, China

Bao-Feng Yang, Department of Pharmacology, Harbin Medical University, Harbin 150086, Heilongjiang Province, China

You-Qiang Song, Department of Biochemistry and the Genome Research Centre, The University of Hong Kong, Hong Kong, China

Supported by the National Natural Science Foundation of China, No. 30200229 and the Youth Foundation of Harbin Medical University, China

Correspondence to: Dr. Jia-Ren Liu, Public Health College, Harbin Medical University, 199 Dongdazhi Street, Nangang District, Harbin 150001, Heilongjiang Province, China. jiarl@ems.hrbmu.edu.cn

Telephone: +86-451-3641309 **Fax:** +86-451-3648617

Received: 2003-03-04 **Accepted:** 2003-04-01

Abstract

AIM: To observe the effect of β -ionone on the proliferation of human gastric adenocarcinoma cell line SGC-7901 and the inhibition of metalloproteinase.

METHODS: Using growth inhibition, Zymograms assays and reverse transcription-polymerase-chain reaction (RT-PCR), we examined cell growth rates, activities of matrix metalloproteinases-2 (MMP-2) and -9 (MMP-9), and expression of metalloproteinases-1 (TIMP-1) and -2 (TIMP-2) in SGC-7901 cells after the treatment with β -ionone for 24 h and 48 h, respectively.

RESULTS: β -ionone had an inhibitory effect on the growth of SGC-7901 cells. Eight days after the treatment with β -ionone at concentrations of 25, 50, 100 and 200 $\mu\text{mol/L}$, the inhibition rates were 25.9%, 28.2%, 74.4% and 90.1%, respectively. The IC_{50} value of β -ionone for SGC-7901 cells was estimated to be 89 $\mu\text{mol/L}$. The effects of β -ionone on MMP-2 and MMP-9 activities in SGC-7901 cells were not observed. However, the levels of TIMP-1 and TIMP-2 transcripts were elevated in cells treated with β -ionone in a dose-dependent manner.

CONCLUSION: β -ionone can inhibit the proliferation of SGC-7901 cells, upregulate the expression of TIMP-1 and TIMP-2 expression, and may influence metastasis of cancer.

Liu JR, Yang BF, Chen BQ, Yang YM, Dong HW, Song YQ. Inhibition of β -ionone on SGC-7901 cell proliferation and upregulation of metalloproteinases-1 and -2 expression. *World J Gastroenterol* 2004; 10(2): 167-171

<http://www.wjgnet.com/1007-9327/10/167.asp>

INTRODUCTION

Epidemiological data showed that regular consumption of fruits and vegetables was associated with a reduced risk of chronic diseases such as cancer and cardiovascular diseases^[1-4]. Isoprenoid is an important group of nutritious elements found in fruits,

vegetables and cereal grains, giving rise to about 22 000 secondary products during its metabolism in these plants. It has been found that these compounds shared a common precursor, mevalonic acid^[14]. Isoprenoids have been shown to suppress chemically-induced carcinogenesis^[5-10] and the growth of cancer cells^[11-13]. β -ionone, an end-ring analog of β -carotenoid, represents a subclass of cyclic isoprenoids and has been demonstrated to have an anticancer effect^[15]. β -ionone was effective in chemoprevention of 7,12-dimethylben[a]anthracene-induced mammary carcinogenesis in SD rats, with its tumor multiplicity reduced by 45%^[16]. It has also been found to be associated with growth inhibition of melanoma and breast cancer cells as well as metastasis of tumor cells^[17-20]. However, the exact mechanisms remain to be clarified, and the effect of β -ionone on gastric cancer cells is unknown.

Chemoprevention has been an approach to treat advanced cancers^[21-25]. Gastric cancer is one of the most common malignancies in China and in other parts of the world^[26-34]. Understanding the mechanisms of the possible inhibitory effect of β -ionone on proliferation of gastric adenocarcinoma cells could provide a way to prevent this disease. Therefore, in this study, we studied the effect of β -ionone on the proliferation of human gastric adenocarcinoma cell line SGC-7901 and on the regulative factors of tissue metalloproteinases and investigated the underlying mechanism.

MATERIALS AND METHODS

Cell culture

Human gastric adenocarcinoma cell line SGC-7901, provided by Beijing Cancer Research Institute, was grown in RPMI 1640 medium (Gibco BRL, Life Technologies Inc, Gaithersburg, MD, USA), supplemented with 100 ml/L calf serum, 100×10^3 U/L penicillin and 100 mg/L streptomycin at 37 °C in a humidified atmosphere containing 5% CO_2 .

IC50 and cell growth assessment

β -ionone (purity >95%) (Sigma, USA) was dissolved in absolute ethanol and further diluted to the concentrations of 25, 50, 100 and 200 $\mu\text{mol/L}$, respectively.

The SGC-7901 cells were seeded into six 24-well plates (Nuc, Denmark) with 2×10^4 cells/well after 24 h culture. Twenty-four hour later, the medium was replaced with the media supplemented with at different concentrations of β -ionone. In the next 8 days, the cells were treated with a trypsin-EDTA solution at 37 °C for 2 minutes and harvested from 3 wells per day for each plate. The cells were pelleted by a short spin at 1 000 g and resuspended in phosphate-buffered saline (PBS). Typan blue exclusion test was used to count viable cells by a hemocytometer. The number of cells at 24 h was deducted from the final cell counts to provide an estimate of the net increase. The β -ionone concentration required to inhibit the net increase in the 48 h cell count by 50% (IC_{50}) was measured by plotting data obtained from three or more times. The means were obtained on each of the eight days and used to draw a cell growth curve. The inhibitory rate (IR) was calculated according to the formula: $\text{IR} (\%) = (\text{total number of cells in}$

negative control - number of cells in test group)/total number of cells in negative control $\times 100\%$.

Zymograms assay for activities of gelatinase

Although many kinds of proteinase are involved in tumor metastasis, members of the matrix metalloproteinase (MMPs, gelatinase) and TIMP families, play a pivotal role in these events. MMPs are a group of zinc-dependent endopeptidase molecules that have the potential to degrade proteins of the extracellular matrix. MMP activity was under regulation at several levels, including activation of the MMP zymogens and specific inhibition by the tissue inhibitors of metalloproteinase (TIMPs)^[54]. We determined the activities of gelatinase in SGC-7901 cells treated with β -ionone.

The SGC-7901 cells were seeded in 100 ml bottles, each containing 5×10^6 cells. After incubation for 24 h, the medium was replaced with 400 μ L of serum-free medium supplemented with β -ionone at different concentrations for 24 h and 48 h. The serum-free media were loaded onto a 100 g/L SDS-polyacrylamide gel co-polymerized with 1 g/L gelatin (Amresco Corp, USA) and separated under a non-denaturing condition for 3-4 h. Then, the gels were incubated in 25 g/L Triton X-100 (Sigma, USA) for 1 h and subsequently in a substrate buffer (50 μ mol/L Tris, pH 7.5, containing 10 mmol/L CaCl_2 , 200 mmol/L NaCl and 1 μ mol/L ZnCl_2) for 12 to 16 h at 37 $^\circ\text{C}$. Finally, the gels were stained in a solution containing 1 g/L Coomassie blue R250, 450 g/L methanol and 100 g/L acetic acid, and the gelatinolytic activity was indicated by bands in a blue background.

RT-PCR

Tissue inhibitor of TIMP-1 and TIMP-2 were related to several tumorigenic processes in lung, stomach, and mammary gland^[56]. We examined the expression of TIMP-1 and TIMP-2 in SGC-7901 cells exposed to different concentrations of β -ionone.

SGC-7901 cells (5×10^6) were incubated at different concentrations of β -ionone for 24 h and 48 h, the total cellular RNA was isolated. Concentrations and purity of total RNA were determined. RT-PCR was performed following the manufacturer's instructions (Takara Biotech, Dalian, China). Total RNA (5 μ g) and AMV reverse transcriptase XL were used to synthesize cDNA. Twenty-five μ L PCR mixture containing 4 μ L of RT reaction product, 2.5 U *Taq* DNA polymerase and 20 pmol primers, was heated for 5 min at 94 $^\circ\text{C}$ for pre-denaturation, and then subjected to 35 PCR cycles, denaturation at 94 $^\circ\text{C}$ for 30 s, annealing at 60 $^\circ\text{C}$ for 30 s for and extension at 72 $^\circ\text{C}$ for 45 s, in a PTC-100 thermocycler (MJ Research, USA). TIMP-1 and TIMP-2 genes were amplified with specific primers, with the gene for β -actin as an internal control (Table 1). The amplified products were resolved in a 20 g/L agarose gel containing ethidium bromide, and visualized under ultraviolet light. The density and area of each band were analyzed using the ChemiImagerTM 4 000 digital system (Alpha Innotech Corp, USA).

Table 1 Primer sequences and size of TIMP-1 and TIMP-2 in expected PCR products for RT-PCR

Genes	Primer sequences	Product size (bp)
TIMP-1	Sense: 5'-CTGTTGGCTGTGAGGAATGCACAG-3'	106
	Antisense: 5'-TTCAGAGCCTTGGAGGAGCTGGTC-3'	
TIMP-2	Sense: 5'-AGACGTAGTGATCGGGCCA-3'	490
	Antisense: 5'-GTACCACGC GAAGAACCT-3'	
β -actin	Sense: 5'-AAGGATTCCTATGTGGGC-3'	532
	Antisense: 5'-CATCTCTTGCTCGAAGTC-3'	

Statistical analysis

Student's *t* test was used for analysis of data. $P < 0.05$ was considered statistically significant.

RESULTS

Cell growth inhibition of β -ionone

The inhibitory effect of β -ionone on the growth of SGC-7901 cells was shown in Figure 1. Growth of the cells in the media containing 200 μ mol/L and 100 μ mol/L β -ionone was markedly slower than that of the negative control within 8 d ($P < 0.01$). The change was less obvious the cells treated with 50 μ mol/L and 25 μ mol/L of β -ionone. The inhibitory rates were 25.9%, 28.2%, 74.4% and 90.1%, respectively. The IC_{50} of β -ionone was 89 μ mol/L.

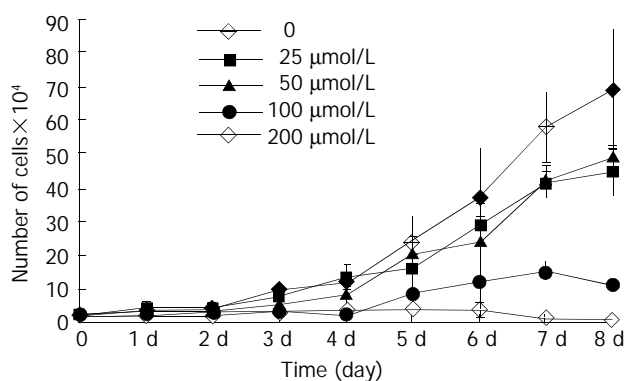


Figure 1 Proliferation kinetics of SGC-7901 cells treated at various concentrations of β -ionone.

Expression of type IV collagenases

The effects of β -ionone on type IV collagenase activities (97kD for MMP-9 and 72kD for MMP-2) in SGC-7901 cells were presented in Figure 2. In the serum-free supernatants of SGC-7901 cells preincubated in the media supplemented with various concentrations of β -ionone, the activities of type IV collagenases (both MMP-9 and MMP-2) were not different in comparison with the negative control. No effect of β -ionone on the activities of type IV collagenases in SGC-7901 cells was shown.

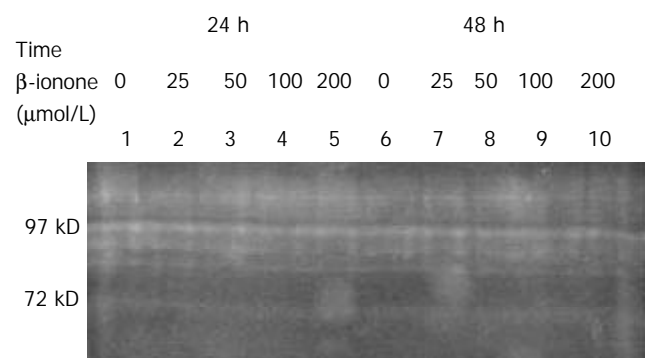


Figure 2 Effect of β -ionone on gelatinase/type IV collagenase secretion (97kD for MMP-9 and 72kD for MMP-2) in SGC-7901 cells.

Levels of TIMP-1 and TIMP-2 mRNA in SGC-7901 cells

As shown in Figures 3 and 4, the levels of TIMP-1 and TIMP-2 transcripts in SGC-7901 cells were gradually elevated with increase of the β -ionone concentration, indicating an upregulation effect of β -ionone on the expression of TIMP-1 and TIMP-2 in SGC-7901 cells.

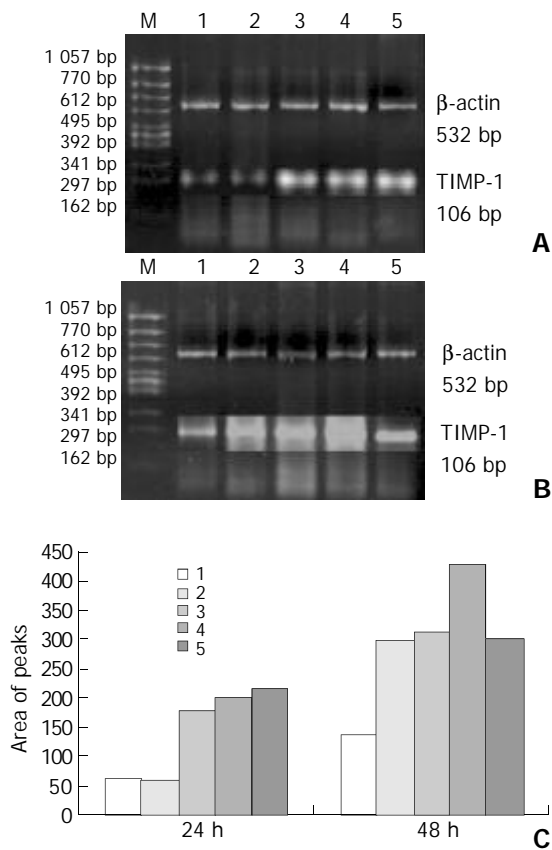


Figure 3 RT-PCR result: expression of TIMP-1 mRNA in SGC-7901 cells treated by β -ionone for 24 h (A) and 48 h (B). C: area of peaks; Lanes 1-5: 0, 25, 50, 100 and 200 μ mol/L of β -ionone; M: molecular weight markers.

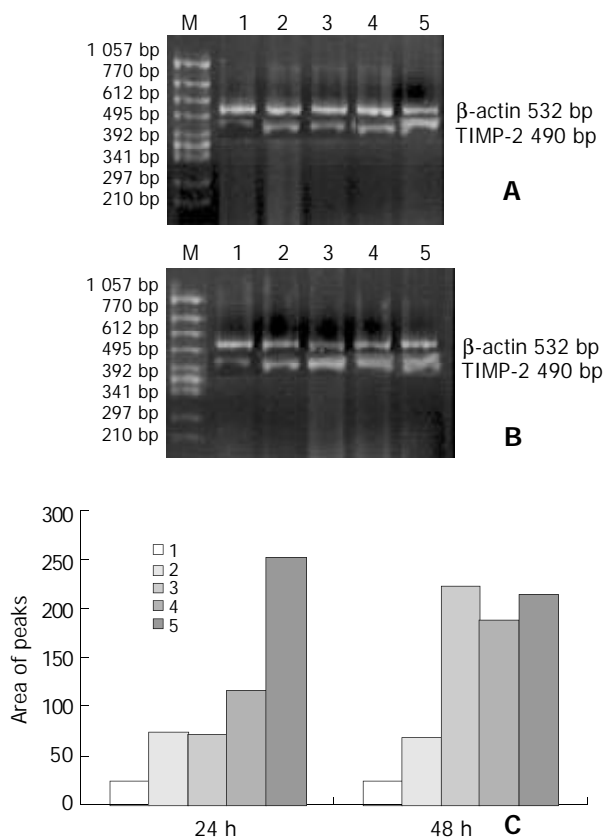


Figure 4 RT-PCR results showing expression of TIMP-2 mRNA in SGC-7901 cells treated by β -ionone for 24 h (A) and 48 h (B). C: chart of area of peaks; Lanes 1-5: 0, 25, 50, 100 and 200 μ mol/L of β -ionone; M: molecular weight markers.

DISCUSSION

Interactions between cells and extracellular matrix (ECM) were critical for many cellular functions including division, migration, differentiation, and apoptosis^[35]. In different mature normal tissues, ECM is specified by its structures and compositions to maintain tissue homeostasis and cellular quiescence. It has been found that remodeling of the ECM occurred during embryonic development and certain normal pathological processes such as wound-healing^[36,37]. However, restructuring of the ECM has also been implicated in the pathogenesis of various human diseases including impaired wound-healing and fibrosis^[38], rheumatoid arthritis^[39], restenosis following balloon angioplasty^[40], atherosclerosis^[41], tumor development, invasion and metastasis^[35,42].

Tumor invasion is a complex biological process, during which tumor cells detach from the primary tumor and infiltrate the surrounding tissues. This process has been found to require loss of cell contacts between tumor cells, active cell migration, adhesion to ECM and proteolytic degradation of the ECM^[43,44]. Different molecules including cadherins, integrins, proteases, and growth factors were implicated in the regulation of invasion of tumor cells^[44].

A major group of enzymes responsible for ECM degradation in cancer tissue has been found to be the MMP family, including collagenases, gelatinase, and stromelysins^[45-49]. Collagenases can cleave fibrillar collagens at neutral conditions and play an important role in matrix remodeling. The largest sub-family of the MMPs is membrane-type (MT). MT-MMPs play a dual role in cell surface proteolysis. They can cleave a variety of extracellular components, and activate some secreted MMPs. Evidence has suggested that proteolytic activities at cell surface could promote cell invasion^[50]. MMP-2, a 72-kDa type IV collagenase, is a cell surface-associated type I collagen-degrading MMP, which was found to designate gelatinase A^[51]. Its overexpression has been observed in different types of tumors, and it was believed to be involved in tumor metastasis, primary tumor growth and angiogenesis^[52]. MMP-2 is also regarded as a type IV collagenase involved in cell invasion across basement membrane. Thus, serum and tissue MMP profiles have been used as prognostic factors in certain types of malignant tumors including gastric and breast cancers^[53]. MMP-9, a 97-kDa type IV collagenase also designating gelatinase B, was found to be associated with tumor invasion as well, its expression has been proven to be correlated with the differentiation grade of some malignancies^[54]. In the present study, we did not find any effect of β -ionone on MMP-9 and MMP-2 activities in SGC-7901 cells. The growth inhibition on SGC-7901 cells appeared to be independence of the type IV collagenase activity.

TIMPs (TIMP-1, -2, -3 and -4) have been found to be the key regulators of MMP activity and ECM degradation^[60]. The MMP inhibitors, TIMP-1 and TIMP-2 have been associated to several tumorigenic processes including development, invasion and metastasis of bronchial cancer^[55-59]. Recent transgenic animal studies have demonstrated that alteration of the MMP/TIMP balance *in vivo* in favor of TIMP-1 activity could block neoplastic proliferation in the SV40 T antigen-induced murine hepatocellular carcinoma^[61]. Active MT1-MMP was found to bind to amino-terminal domain of TIMP-2^[62], whereas an interaction between the carboxyl-terminal domains of TIMP-2 and pro-MMP-2 was also described^[63]. TIMP-2 might prevent SH2-protein-tyrosine phosphatase-1 (SHP-1) dissociation from immunoprecipitable epidermal growth factor receptor complex and a selective increase in total SHP-1 activity^[64]. Our results showed that β -ionone might increase the expression of TIMP-1 and TIMP-2 in SGC-7901 cells. Clearly, further studies are needed to elucidate whether β -ionone inhibits metastasis of the cancer cells.

In summary, β -ionone can inhibit SGC-7901 cell growth

and proliferation and has an effect on upregulating TIMP-1 and TIMP-2 expression in SGC-7901 cells. It seems to be related to potential tumor metastasis in SGC-7901 cells induced by β -ionone. However, the mechanism of the inhibitory effect of β -ionone inhibits cell proliferation remains to be clarified.

ACKNOWLEDGEMENT

We thank Dr. Dong-Yan Jin for his critically reading and revising of the manuscript.

REFERENCES

- 1 **Michaud DS**, Pietinen P, Taylor PR, Virtanen M, Virtamo J, Albanes D. Intakes of fruits and vegetables, carotenoids and vitamins A, E, C in relation to the risk of bladder cancer in the ATBC cohort study. *Br J Cancer* 2002; **87**: 960-965
- 2 **Ito LS**, Inoue M, Tajima K, Yamamura Y, Kodera Y, Hirose K, Takezaki T, Hamajima N, Kuroishi T, Tominaga S. Dietary factors and the risk of gastric cancer among Japanese women. A comparison between the differentiated and non-differentiated subtypes. *Ann Epidemiol* 2003; **13**: 24-31
- 3 **Willett WC**. Balancing life-style and genomics research for disease prevention. *Science* 2002; **296**: 695-698
- 4 **Block G**, Patterson B, Subar A. Fruit, vegetables, and cancer prevention: a review of the epidemiological evidence. *Nutr Cancer* 1992; **18**: 1-29
- 5 **Elson CE**. Suppression of mevalonate pathway activities by dietary isoprenoids: protective roles in cancer and cardiovascular disease. *J Nutr* 1995; **125**: 1666-1672
- 6 **Elson CE**, Yu SG. The chemoprevention of cancer by mevalonate-derived constituents of fruits and vegetables. *J Nutr* 1994; **124**: 607-614
- 7 **Huang C**, Huang Y, Li J, Hu W, Aziz R, Tang MS, Sun N, Cassady J, Stoner GD. Inhibition of benzo(a)pyrene diol-epoxide-induced transactivation of activated protein 1 and nuclear factor kappaB by black raspberry extracts. *Cancer Res* 2002; **62**: 6857-6863
- 8 **Serafini M**, Bellocco R, Wolk A, Ekstrom AM. Total antioxidant potential of fruit and vegetables and risk of gastric cancer. *Gastroenterology* 2002; **123**: 985-991
- 9 **Pandey M**, Shukla VK. Diet and gallbladder cancer: a case-control study. *Eur J Cancer Prev* 2002; **11**: 365-368
- 10 **Devasena T**, Menon VP. Enhancement of circulatory antioxidants by fenugreek during 1,2-dimethylhydrazine-induced rat colon carcinogenesis. *J Biochem Mol Biol Biophys* 2002; **6**: 289-292
- 11 **Agarwal C**, Singh RP, Agarwal R. Grape seed extract induces apoptotic death of human prostate carcinoma DU145 cells via caspases activation accompanied by dissipation of mitochondrial membrane potential and cytochrome c release. *Carcinogenesis* 2002; **23**: 1869-1876
- 12 **Ohyama K**, Akaike T, Hirobe C, Yamakawa T. Cytotoxicity and apoptotic Inducibility of vitex agnus-castus fruit extract in cultured human normal and cancer cells and effect on growth. *Biol Pharm Bull* 2003; **26**: 10-18
- 13 **Dietrich M**, Block G, Norkus EP, Hudes M, Traber MG, Cross CE, Packer L. Smoking and exposure to environmental tobacco smoke decrease some plasma antioxidants and increase gamma-tocopherol *in vivo* after adjustment for dietary antioxidant intakes. *Am J Clin Nutr* 2003; **77**: 160-166
- 14 **Bach TJ**. Some new aspects of isoprenoid biosynthesis in plants—a review. *Lipids* 1995; **30**: 191-202
- 15 **Mo H**, Elson CE. Apoptosis and cell-cycle arrest in human and murine tumor cells are initiated by isoprenoids. *J Nutr* 1999; **129**: 804-813
- 16 **Yu SG**, Anderson PJ, Elson CE. Efficacy of β -ionone in the chemoprevention of rat mammary carcinogenesis. *J Agric Food Chem* 1995; **43**: 2144-2147
- 17 **He L**, Mo H, Hadisusilo S, Qureshi AA, Elson CE. Isoprenoids suppress the growth of murine B16 melanomas *in vitro* and *in vivo*. *J Nutr* 1997; **127**: 668-674
- 18 **Nangia MP**, Hogan V, Honjo Y, Baccarini S, Tait L, Bresalier R, Raz A. Inhibition of human cancer cell growth and metastasis in nude mice by oral intake of modified citrus pectin. *J Natl Cancer Inst* 2002; **94**: 1854-1862
- 19 **Kimura Y**, Taniguchi M, Baba K. Antitumor and antimetastatic effects on liver of triterpenoid fractions of *Ganoderma lucidum*: mechanism of action and isolation of an active substance. *Anti-cancer Res* 2002; **22**: 3309-3318
- 20 **Dabrosin C**, Chen J, Wang L, Thompson LU. Flaxseed inhibits metastasis and decreases extracellular vascular endothelial growth factor in human breast cancer xenografts. *Cancer Lett* 2002; **185**: 31-37
- 21 **Tovey FI**, Hobsley M. Post-gastrectomy patients need to be followed up for 20-30 years. *World J Gastroenterol* 2000; **6**: 45-48
- 22 **Morgner A**, Miehke S, Stolte M, Neubauer A, Alpen B, Thiede C, Klann H, Hierlmeier FX, Ell C, Ehninger G, Bayerdörffer E. Development of early gastric cancer 4 and 5 years after complete remission of *Helicobacter pylori*-associated gastric low-grade marginal zone B-cell lymphoma of MALT type. *World J Gastroenterol* 2001; **7**: 248-253
- 23 **Niu WX**, Qin XY, Liu H, Wang CP. Clinicopathological analysis of patients with gastric cancer in 1200 cases. *World J Gastroenterol* 2001; **7**: 281-284
- 24 **Deng DJ**. Progress of gastric cancer etiology: N-nitrosamides in the 1990s. *World J Gastroenterol* 2000; **6**: 613-618
- 25 **Wang X**, Liu FK, Li X, Li JS, Xu GX. Inhibitory effect of endostatin expressed by human liver carcinoma SMMC7721 on endothelial cell proliferation *in vitro*. *World J Gastroenterol* 2002; **8**: 253-257
- 26 **Cao WX**, Ou JM, Fei XF, Zhu ZG, Yin HR, Yan M, Lin YZ. Methionine-dependence and combination chemotherapy on human gastric cancer cells *in vitro*. *World J Gastroenterol* 2002; **8**: 230-232
- 27 **Liu JR**, Chen BQ, Yang YM, Wang XL, Xue YB, Zheng YM, Liu RH. Effect of apoptosis on gastric adenocarcinoma cell line SGC-7901 induced by *cis*-9, *trans*-11-conjugated linoleic acid. *World J Gastroenterol* 2002; **8**: 999-1004
- 28 **Li Y**, Lu YY. Applying a highly specific and reproducible cDNA RDA method to clone garlic up-regulated genes in human gastric cancer cells. *World J Gastroenterol* 2002; **8**: 213-216
- 29 **Sun ZJ**, Pan CE, Liu HS, Wang GJ. Anti-hepatoma activity of resveratrol *in vitro*. *World J Gastroenterol* 2002; **8**: 79-81
- 30 **Liu JR**, Li BX, Chen BQ, Han XH, Xue YB, Yang YM, Zheng YM, Liu RH. Effect of *cis*-9, *trans*-11-conjugated linoleic acid on cell cycle of gastric adenocarcinoma cell line (SGC-7901). *World J Gastroenterol* 2002; **8**: 224-229
- 31 **Wang X**, Lan M, Shi YQ, Lu J, ZhongYX, Wu HP, Zai HH, Ding J, Wu KC, Pan BR, Jin JP, Fan DM. Differential display of vincristine-resistance-related genes in gastric cancer SGC-7901 cells. *World J Gastroenterol* 2002; **8**: 54-59
- 32 **Gao F**, Yi J, Shi GY, Li H, Shi XG, Tang XM. The sensitivity of digestive tract tumor cells to As_2O_3 is associated with the inherent cellular level of reactive oxygen species. *World J Gastroenterol* 2002; **8**: 36-39
- 33 **Chen BQ**, Xue YB, Liu JR, Yang YM, Zheng YM, Wang XL, Liu RH. Inhibition of conjugated linoleic acid on mouse forestomach neoplasia induced by benzo(a)pyrene and chemopreventive mechanisms. *World J Gastroenterol* 2003; **9**: 44-49
- 34 **Wu K**, Li Y, Zhao Y, Shan YJ, Xia W, Yu WP, Zhao L. Roles of Fas signaling pathway in vitamin E succinate-induced apoptosis in human gastric cancer SGC-7901 cells. *World J Gastroenterol* 2002; **8**: 982-986
- 35 **Lukashev ME**, Werb Z. ECM signalling: orchestrating cell behaviour and misbehaviour. *Trends Cell Biol* 1998; **8**: 437-441
- 36 **Werb Z**, Chin JR. Extracellular matrix remodeling during morphogenesis. *Ann NY Acad Sci* 1998; **857**: 110-118
- 37 **Raghow R**. The role of extracellular matrix in postinflammatory wound healing and fibrosis. *FASEB J* 1994; **8**: 823-831
- 38 **Friedman S**. Seminars in medicine of the Beth Israel Hospital, Boston. The cellular basis of hepatic fibrosis. Mechanisms and treatment strategies. *N Engl J Med* 1993; **328**: 1828-1835
- 39 **Cawston T**. Matrix metalloproteinases and TIMPs: properties and implications for the rheumatic diseases. *Mol Med Today* 1998; **4**: 130-137
- 40 **Batchelor WB**, Robinson R, Strauss BH. The extracellular matrix in balloon arterial injury: a novel target for restenosis prevention. *Prog Cardiovasc Dis* 1998; **41**: 35-49
- 41 **Newby AC**, Zaltsman AB. Fibrous cap formation or destruction—the critical importance of vascular smooth muscle cell proliferation, migration and matrix formation. *Cardiovasc Res* 1999; **41**: 345-360
- 42 **Stenlicht MD**, Lochter A, Sympon CJ, Huey B, Rougier JP, Gray JW, Pindel D, Bissell MJ, Werb Z. The stromal proteinase MMP3/

- stromelysin-1 promotes mammary carcinogenesis. *Cell* 1999; **98**: 137-146
- 43 **Mareel MM**, Van Roy FM, Bracke ME. How and when do tumor cells metastasize? *Crit Rev Oncog* 1993; **4**: 559-594
- 44 **Engers R**, Gabbert HE. Mechanisms of tumor metastasis: cell biological aspects and clinical implications. *J Cancer Res Clin Oncol* 2000; **126**: 682-692
- 45 **Nagase H**, Woessner JF Jr. Matrix metalloproteinases. *J Biol Chem* 1999; **274**: 21491-21494
- 46 **Birkedal-Hansen H**, Moore WG, Bodden MK, Windsor LJ, Birkedal-Hansen B, DeCarlo A, Engler JA. Matrix metalloproteinases: a review. *Crit Rev Oral Biol Med* 1993; **4**: 197-250
- 47 **Stetler-Stevenson WG**. Matrix metalloproteinases in angiogenesis: a moving target for therapeutic intervention. *J Clin Invest* 1999; **103**: 1237-1241
- 48 **Nelson AR**, Fingleton B, Rothenberg ML, Matrisian LM. Matrix metalloproteinases: biologic activity and clinical implications. *J Clin Oncol* 2000; **18**: 1135-1149
- 49 **Onodera S**, Nishihira J, Koyama KI, Yoshida K, Tanaka S, Minami A. Macrophage Migration Inhibitory Factor Up-regulates Matrix Metalloproteinase-9 and -13 in Rat Osteoblasts. *J Biol Chem* 2002; **277**: 7865-7874
- 50 **Murphy G**, Gavrilovic J. Proteolysis and cell migration: creating a path? *Curr Opin Cell Biol* 1999; **11**: 614-621
- 51 **Zhuge Y**, Xu J. Rac1 Mediates Type I Collagen-dependent MMP-2 Activation. *J Biol Chem* 2001; **276**: 16248-16256
- 52 **Sato H**, Seiki M. Membrane-type matrix metalloproteinases (MT-MMPs) in tumor metastasis. *J Biochem* 1996; **119**: 209-215
- 53 **McCawley LJ**, Matrisian LM. Matrix metalloproteinases: multifunctional contributors to tumor progression. *Mol Med Today* 2000; **6**: 149-156
- 54 **Rao JS**, Yamamoto M, Mohaman S, Gokaslan ZL, Fuller GN, Stetler-Stevenson WG, Rao VH, Liotta LA, Nicolson GL, Sawaya RE. Expression and localization of 92 kDa type IV collagenase/gelatinase B (MMP-9) in human gliomas. *Clin Exp Metastasis* 1996; **14**: 12-18
- 55 **Brand K**. Cancer gene therapy with tissue inhibitors of metalloproteinases (TIMPs). *Curr Gene Ther* 2002; **2**: 255-271
- 56 **Jiang Y**, Goldberg ID, Shi YE. Complex roles of tissue inhibitors of metalloproteinases in cancer. *Oncogene* 2002; **21**: 2245-2252
- 57 **Chang C**, Werb Z. The many faces of metalloproteases: cell growth, invasion, angiogenesis and metastasis. *Trends Cell Biol* 2001; **11**: 37-43
- 58 **Giannelli G**, Antonaci S. Gelatinases and their inhibitors in tumor metastasis: from biological research to medical applications. *Histol Histopathol* 2002; **17**: 339-345
- 59 **Chung AS**, Yoon SO, Park SJ, Yun CH. Roles of matrix metalloproteinases in tumor metastasis and angiogenesis. *J Biochem Mol Biol* 2003; **36**: 128-137
- 60 **Gomez DE**, Alonso DF, Yoshiji H, Thorgeirsson UP. Tissue inhibitors of metalloproteinases: structure, regulation and biological functions. *Eur J Cell Biol* 1997; **74**: 111-122
- 61 **Martin DC**, Sanchez-Sweatman OH, Ho AT, Inderdeo DS, Tsao MS, Khokha R. Transgenic TIMP-1 inhibits simian virus 40 T antigen-induced hepatocarcinogenesis by impairment of hepatocellular proliferation and tumor angiogenesis. *Lab Invest* 1999; **79**: 225-234
- 62 **Zucker S**, Drews M, Conner C, Foda HD, DeClerck YA, Langley KE, Bahou WF, Docherty AJ, Cao J. Tissue inhibitor of metalloproteinase-2 (TIMP-2) binds to the catalytic domain of the cell surface receptor, membrane type 1-matrix metalloproteinase 1 (MT1-MMP). *J Biol Chem* 1998; **273**: 1216-1222
- 63 **Overall CM**, Tam E, McQuibban GA, Morrison C, Wallon UM, Bigg HF, King AE, Roberts CR. Domain interactions in the gelatinase A.TIMP-2.MT1-MMP activation complex. The ectodomain of the 44-kDa form of membrane type-1 matrix metalloproteinase does not modulate gelatinase A activation. *J Biol Chem* 2000; **275**: 39497-39506
- 64 **Hoegy SE**, Oh HR, Corcoran ML, Stetler-Stevenson WG. Tissue Inhibitor of Metalloproteinases-2 (TIMP-2) Suppresses TKR-Growth Factor Signaling Independent of Metalloproteinase Inhibition. *J Biol Chem* 2001; **276**: 3203-3214

Edited by Ren SY and Wang XL

Correlation of thymidylate synthase, thymidine phosphorylase and dihydropyrimidine dehydrogenase with sensitivity of gastrointestinal cancer cells to 5-fluorouracil and 5-fluoro-2'-deoxyuridine

Tao Ma, Zheng-Gang Zhu, Yu-Bao Ji, Yi Zhang, Ying-Yan Yu, Bing-Ya Liu, Hao-Ran Yin, Yan-Zhen Lin

Tao Ma, Zheng-Gang Zhu, Yu-Bao Ji, Yi Zhang, Ying-Yan Yu, Bing-Ya Liu, Hao-Ran Yin, Yan-Zhen Lin, Shanghai Institute of Digestive Surgery, Ruijin Hospital, Shanghai Second Medical University, Shanghai 200025, China

Correspondence to: Dr. Zheng-Gang Zhu, Shanghai Institute of Digestive Surgery, Ruijin Hospital, Shanghai Second Medical University, Shanghai 200025, China. digsurg@online.sh.cn

Telephone: +86-21-64373909 **Fax:** +86-21-64373909

Received: 2003-08-06 **Accepted:** 2003-08-28

Abstract

AIM: To determine the expression levels of three metabolic enzymes of fluoropyrimidines: thymidylate synthase (TS), thymidine phosphorylase (TP) and dihydropyrimidine dehydrogenase (DPD) in seven human gastrointestinal cancer cell lines, and to compare the enzyme levels with the sensitivity to 5-fluorouracil (5-FU) and 5-fluoro-2'-deoxyuridine (FdUrd).

METHODS: TS, TP and DPD mRNA levels were assessed by semi-quantitative RT-PCR, TP and DPD protein contents were measured by ELISA. Fifty percent inhibitory concentrations of growth (IC50), representing the sensitivity to drugs, were determined by MTT assay.

RESULTS: IC50 values ranged from 1.28 to 12.26 μ M for 5-FU, and from 5.02 to 24.21 μ M for FdUrd, respectively. Cell lines with lower DPD mRNA and protein levels tended to be more sensitive to 5-FU ($P < 0.05$), but neither TS nor TP correlated with 5-FU IC50 ($P > 0.05$). Only TS mRNA level was sharply related with FdUrd sensitivity ($P < 0.05$), but TP and DPD were not ($P > 0.05$). A correlation was found between mRNA and protein levels of DPD ($P < 0.05$), but not TP ($P < 0.05$).

CONCLUSION: DPD and TS enzyme levels may be useful indicators in predicting the antitumor activity of 5-FU or FdUrd, respectively.

Ma T, Zhu ZG, Ji YB, Zhang Y, Yu YY, Liu BY, Yin HR, Lin YZ. Correlation of thymidylate synthase, thymidine phosphorylase and dihydropyrimidine dehydrogenase with sensitivity of gastrointestinal cancer cells to 5-fluorouracil and 5-fluoro-2'-deoxyuridine. *World J Gastroenterol* 2004; 10(2): 172-176 <http://www.wjgnet.com/1007-9327/10/172.asp>

INTRODUCTION

The antimetabolite, 5-fluorouracil (5-FU), remains to be widely prescribed in the treatment of gastrointestinal carcinoma. Although it was originally synthesized 46 years ago, and the deoxyribonucleoside derivative of 5-FU, 5-fluoro-2'-deoxyuridine (FdUrd) is also applied in clinics through regional administration^[1-3].

The response rate of gastrointestinal carcinoma to 5-FU as a single agent, however, is only 10%-30%, and differs greatly among patients^[1,4]. So it is imperative to identify some indexes which could be applied to predict the efficacy of 5-FU in clinical settings. As a pyrimidine analog, 5-FU is metabolized *in vivo* similarly to uracil, and exerts its antitumor effects through anabolism, which is determined by the rate of catabolism. Thus, the expression level of genes coding for key enzymes in the metabolism within tumor cells may play a pivotal role in the sensitivity and efficacy of 5-FU^[1,4,5].

The primary biochemical mechanism responsible for cytotoxicity of 5-FU and FdUrd is the formation of 5-fluorouridine monophosphate (FdUMP), which can bind tightly to and inhibit thymidylate synthase (TS) in the presence of 5, 10-methylene tetrahydrofolate (CH_2FH_4). TS catalyzes the reductive methylation of deoxyuridine-5'-monophosphate (dUMP) to deoxythymidine-5'-monophosphate (dTMP), which is the only pathway for *de novo* synthesis of dTMP, so the inhibition of TS by FdUMP disrupts intracellular nucleotide pools necessary for DNA synthesis^[1,3]. As the main target of fluoropyrimidines, the expression level of TS is assumed to influence the response of chemotherapy, although the amount of TS is not unanimously recognized as a determinant factor of 5-FU sensitivity^[6-8].

Thymidine phosphorylase (TP) is known to be elevated in tumors compared with surrounding normal tissue. When 5-FU is administered, it is anabolized to FdUMP by TP present in the tumor, and FdUrd can be converted to 5-FU by TP^[9-11]. TP levels might affect the sensitivity of 5-FU, the transfection of TP cDNA into cancer cells increased their sensitivity to 5-FU^[12]. The expression of TP was reported to be useful for predicting the efficacy and survival of fluoropyrimidine chemotherapy^[13,14], but this tendency was not confirmed in a recent clinical trial of colorectal carcinoma^[15]. The relationship between TP and the sensitivity of fluoropyrimidines needs to be further explored.

In contrast to anabolism of 5-FU, much less attention has been focused on its catabolism. In human, dihydropyrimidine dehydrogenase (DPD) is the initial and rate-limiting enzyme of 5-FU catabolism, 85% of an administered dose of 5-FU is degraded to inactive metabolites by DPD, with only 1-3% of the drug anabolized. While anabolism is essential for the antitumor activity of 5-FU, catabolism by indirectly controlling the availability of 5-FU for anabolism is a critical determinant of 5-FU cytotoxicity^[4,5,16,17]. Several studies have shown a great interindividual difference in DPD activity, and suggested that DPD activity could be used as a predictive marker of 5-FU response^[18-20].

We measured the expression levels of TS, DPD and TP on a panel of seven gastrointestinal cancer cell lines to probe the correlation between TS/DPD/TP and 5-FU or FdUrd sensitivity.

MATERIALS AND METHODS

Chemicals

5-FU was kindly provided by Faulding Pharmaceuticals Co,

FdUrd and MTT were obtained from Sigma-Aldrich Chemicals Co.

Cell culture

Seven cancer cell lines of human origin were adopted, including four gastric carcinoma cells (MKN45, SGC7901, MKN28 and AGS) and three colorectal carcinoma cells (SW1116, Lovo and HCT-8). Cells were routinely cultured in RPMI-1640 media (Gibco BRL), supplemented with 10% heat-inactivated fetal bovine serum (Gibco BRL), 100 u/ml penicillin and 100 ug/ml streptomycin in a humidified incubator at 37 °C with an atmosphere containing 5% CO₂.

Evaluation of 5-FU and FdUrd-induced cytotoxicity by MTT assay

Cells were dispersed into 96-well microtitration plates, and the initial cell density was 5 000-10 000 cells per well, so that the cells were in a Log growth phase. Twenty-four hours after plating, the cells were exposed to a series of 10-fold dilutions of 5-FU or FdUrd (10⁻²-10⁻⁹M) for 72 hours. Each concentration was performed in quadruplicate, the percentage of growth inhibition was assessed by MTT assay, and determined according to the following equation: $[1-(T-T_0)/(C-T_0)] \times 100\%$, where T is the absorbance of the experimental wells after 72 h of 5-FU or FdUrd exposure, and T₀ is that of background control with the same drug concentrations, C is that of cell control wells (without drug) after 72 h incubation. The 5-FU or FdUrd concentrations causing a 50% growth inhibition as compared to cell controls (IC₅₀) were calculated by modified Kärbers method^[21]: $IC_{50} = 10^{i-1} [X_k - i(\sum P - 0.5)]$, in which X_k represents logarithm of the highest drug concentration, i is that of ratio of adjacent concentration, $\sum P$ equals the sum of the percentage of growth inhibition at various concentrations, and 0.5 is a constant of experience. All experiments were repeated 4 times, from which we reported the mean and standard deviation of IC₅₀.

Semi-quantification of TS/DPD/TP mRNA by RT-PCR

Total RNA from seven gastrointestinal cancer cell lines was extracted using TRIzol (Gibco BRL) and quantified by UV spectrophotometry. First-strand cDNA was synthesized from 1 µg of total RNA with oligo (dT)₁₅ primer and avian myeloblastosis virus reverse transcriptase using an RT-PCR kit (Promega) following the conditions of the manufacturer. PCR primers were designed based on the sequences of human TS/DPD/TP and GAPDH mRNA (internal standard), and the specificity of all primers was confirmed by DNA sequencing of the PCR products amplified with them (Table 1).

Table 1 Primers for TS, DPD, TP and GAPDH amplification

mRNA	Bases	Sequences (5' → 3')	Product size (bp)
TS	613-632	accaaccctgacgacagaag	405
	998-1017	atcgaggattgtacccttcaa	
DPD	1325-1344	tgctcggacagagcaaatg	400
	1705-1724	cttcaatccggccatttcta	
TP	390-408	aggagacctggctgctgac	402
	772-791	tgagaatggaggctgtgatg	
GAPDH	109-127	gaaggtgaaggtcggagtc	226
	315-334	gaagatggtgatgggatttc	

TS/DPD/TP was co-amplified with GAPDH in 50 µl of PCR mixture containing 4 µg of cDNA template, 2.5 mM MgCl₂, 5 µl 10×buffer, 0.4 mM dNTP, 2.5 u Taq polymerase (Promega), 12.5pmol of each sense and anti-sense primer. The PCR profile of TS consisted of an initial 4 min denaturation at

95 °C, followed by 25 PCR cycles (at 94 °C for 1 min, at 60 °C for 30 s, and at 72 °C for 1 min) and a final 7 min extension (33 cycles of amplification for DPD and 35 cycles for TP). The PCR products were separated by ethidium bromide-stained 2% agarose gel electrophoresis, the images were scanned and analyzed by densitometry using Fluro-s™ image software (Bio-Rad). The relative amount of mRNA was calculated by determining the product intensity ratio of TS/DPD/TP to GAPDH within the linear amplification range of PCR, and four separate experiments were repeated.

Protein contents of TP and DPD

Cell lines in a Log growth phase were harvested and washed twice by phosphate buffered saline (PBS, pH 7.4). After the last wash, cell pellets were resuspended in 500 µl PBS and lysed by a sonifier (pulses, 10 min), then the lysates were centrifuged at 13 000×g for 15 min, and the supernatants were carefully collected, the protein concentration of which were determined using a BCA protein assay reagent kit (Pierce).

The protein contents of DPD and TP in cell lines were determined by sandwich ELISA (Roche), according to the manufacturer's instructions. Enzyme levels were expressed as U/mg protein, where one U of TP is an amount equivalent to 1 µg 5-FU generated in an hour, and one U of DPD is an amount equivalent to catabolizing 1pmol of 5-FU per minute.

Determination of population doubling time

As described before^[22], 1-2×10⁵ cells were cultured in a 25 ml flask containing 2.5 ml of RPMI-1640, and the number of cells per flask was counted every 24 hours for 7 days. When the cells were in a Log growth phase, the population doubling time (dt) was determined by the following formula: $dt = 1 \lg 2 / g (C_t/C_0) \times t$, where t means the time between cell counts C_t and C₀, C₀ is the initial count, and C_t is the count after time t.

Statistics

Linear regression analysis and paired *t*-test were performed by SPSS software, *P*<0.05 was regarded as statistically significant.

RESULTS

Sensitivity of cell lines to 5-FU and FdUrd

Table 2 shows the parameters of interest for the whole cell line panel. After 72-hour drug exposure, the chemosensitivity of cell lines presented a marked difference, with IC₅₀ values ranged from 1.28 to 12.26µM for 5-FU (9.57-fold), and from 5.02 to 24.21µM (4.83-fold) for FdUrd, respectively. The IC₅₀ value of 5-FU was 2.8-fold lower than that of FdUrd (*P*<0.01), and there was no significant correlation between IC₅₀ values of these two drugs among seven gastrointestinal cancer cell lines (*P*>0.05).

TS mRNA levels

TS mRNA was highly expressed in the seven cell lines, and the TS:GAPDH product intensity ratio varied from 0.84 to 2.69 (Figure 1A, Table 2). TS mRNA expression was significantly correlated with the sensitivity of cell lines to FdUrd (*r*=0.81, *P*=0.028), where low TS mRNA levels were associated with the high sensitivity to FdUrd (Figure 2), but the sensitivity to 5-FU was not influenced by TS mRNA levels.

DPD mRNA and protein levels

DPD mRNA expression was measurable in all cell lines but HCT-8 (Figure 1B). Although cDNA of DPD was amplified by PCR with 8 more cycles, DPD mRNA expression was much lower than TS expression, as shown in Table 2. DPD protein content, representing enzyme activity, ranged from 1.16 to

Table 2 Sensitivity to 5-FU or FdUrd and enzyme levels for cell lines

Cell line	IC50 ^a		TS mRNA ^b	DPD		TP		Doubling time (hours)
	5-FU	FdUrd		mRNA ^b	protein ^c	mRNA ^b	protein ^c	
MKN45	12.26±2.13	16.85±2.28	1.13±0.22	0.57±0.17	10.13	0.72±0.13	5.11	22.9
SGC7901	8.97±1.55	12.45±1.46	1.04±0.17	0.50±0.09	9.13	0.59±0.06	1.78	25.8
MKN28	3.44±0.36	5.02±1.32	0.84±0.21	0.36±0.12	4.57	0.70±0.12	0.55	20.5
AGS	2.77±0.58	19.31±1.85	1.27±0.23	0.35±0.08	4.95	0.67±0.20	3.835	29.5
SW1116	5.45±0.47	24.21±3.26	2.69±0.36	0.47±0.11	5.99	0.57±0.11	2.60	22.2
Lovo	4.86±0.92	14.41±0.96	1.19±0.12	0.31±0.05	1.83	0.70±0.08	0.04	33.9
HCT-8	1.28±0.43	17.62±1.84	1.54±0.31	ND ^d	1.16	0.10±0.06	0.67	28.1

a: values of IC50 ($\bar{x}\pm s$), b: TS/DPD/TP mRNA levels, expressed as TS/DPD/TP:GAPDH product intensity ratio ($\bar{x}\pm s$), c: DPD/TP protein levels, in U/mg protein, d: not detectable.

10.13 U/mg protein (8.73-fold), and there was a statistically significant correlation between mRNA and protein level of DPD ($r=0.88$, $P=0.009$, Figure 3A).

Linear regression analysis showed that both mRNA ($r=0.82$, $P=0.025$) and protein level of DPD ($r=0.88$, $P=0.009$) were significantly correlated to the sensitivity to 5-FU (Figure 4). The greater the enzyme level was, the higher the IC50 of 5-FU. The most sensitive cell line (HCT-8) exhibited the lowest DPD mRNA and protein level, and the most resistant cell line (MKN45) had the greatest DPD mRNA and protein level. But the correlation between mRNA or protein level of DPD and the IC50 of FdUrd was not found ($P>0.05$).

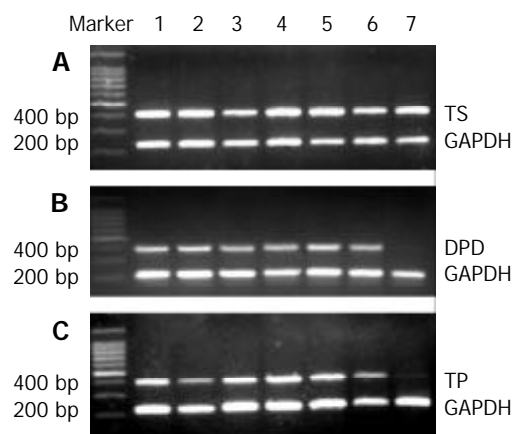


Figure 1 mRNA expression of seven gastrointestinal cancer cell lines by RT-PCR. (A) the bands of TS and GAPDH; (B) the bands of DPD and GAPDH; (C) the bands of TP and GAPDH (1-MKN45; 2-SGC7901; 3-MKN28; 4-AGS; 5-SW1116; 6-Lovo; 7-HCT-8). The relative amount of mRNA was expressed as the intensity ratio of TS/DPD/TP to GAPDH RT-PCR products, as showed in Table 2.

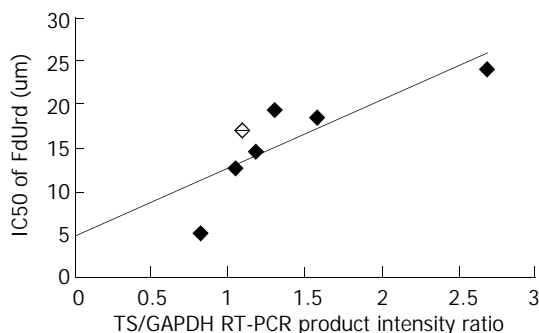


Figure 2 Linear regression for the sensitivity to FdUrd as a function of TS mRNA level (FdUrd-IC50=7.89TS mRNA+4.77, $r=0.81$, $P=0.028$). Scatter plot shows the correlation between TS mRNA levels and IC50 of FdUrd.

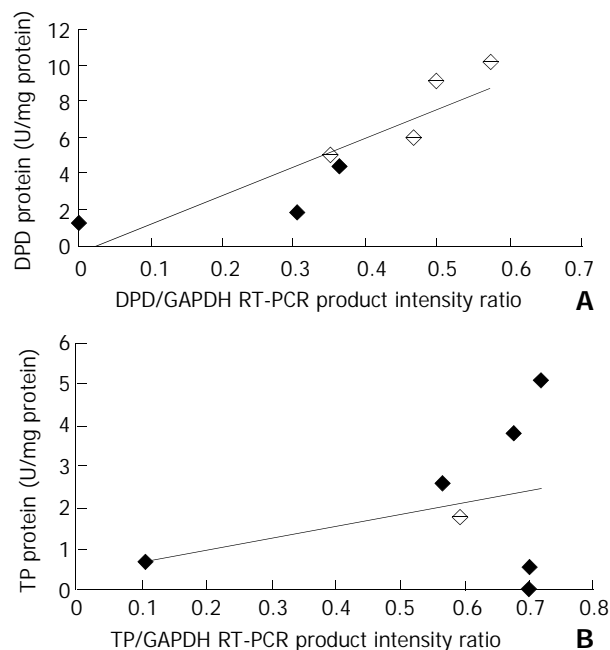


Figure 3 (A) Correlation between mRNA and protein level of DPD ($r=0.88$, $P=0.009$); (B) Correlation between mRNA and protein level of TP ($r=0.33$, $P=0.466$).

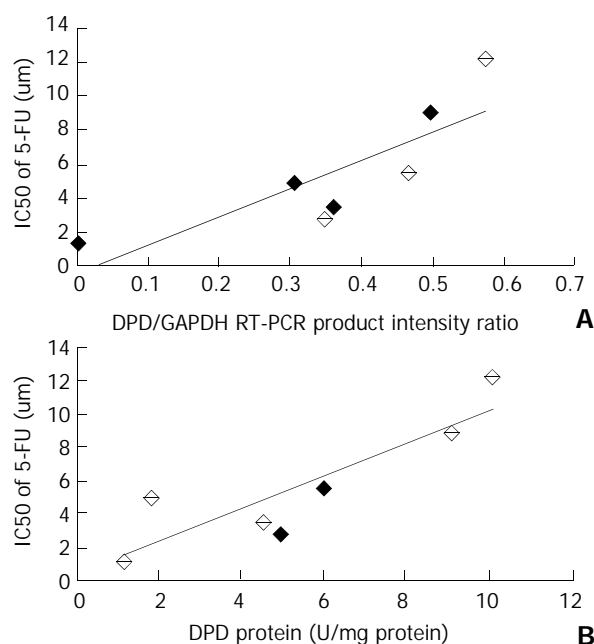


Figure 4 (A) Linear regression for the sensitivity to 5-FU as a function of DPD mRNA level (5-FU-IC50=16.77DPD mRNA-0.54, $r=0.82$, $P=0.025$). (B) Linear regression for the sensitivity to

5-FU as a function of of DPD protein level (5-FU-IC₅₀=1.00DPD protein+0.20, $r=0.88$, $P=0.009$). Scatter plot shows the correlation between DPD mRNA or protein levels and IC₅₀ of 5-FU.

TP mRNA and protein levels

Both mRNA and protein of TP had lower expression levels compared to TS or DPD (Figure 1C, Table 2). Figure 3B shows no correlation between TP/GAPDH RT-PCR product intensity ratio and TP protein level ($r=0.33$, $P=0.466$). Although it was expected that mRNA and protein level of TP would predict the sensitivity to 5-FU or FdUrd, no significant correlation was shown ($P>0.05$).

Doubling time of cell lines

The cell doubling time ranged from 20.5 (MKN28) to 33.9 hours (Lovo), and no correlation was demonstrated between the doubling time and IC₅₀ of 5-FU or FdUrd. Cell doubling time did not correlate with either TS/DPD/TP mRNA or protein levels ($P>0.05$).

DISCUSSION

There is a high prevalence of gastrointestinal cancer, including gastric and colorectal cancer in China, but most of the diagnoses are established at advanced stages, when chemotherapy is regarded as one of the main treatments. At present, 5-FU has been considered as the principal component of chemotherapy regimen for gastrointestinal cancer in both advanced disease and the adjuvant setting^[2,23], and FdUrd is also available commercially for chemotherapy, especially for intraarterial and intracavitary infusion. But the response of gastrointestinal cancer to fluoropyrimidines was still unsatisfactory and their efficacy varied greatly among individuals, so how to enhance the chemotherapeutic response of 5-FU has become a very interesting subject^[24,25]. The identification of predictive markers of chemosensitivity through pharmacogenomics means could clarify which subset of patients might benefit, and enable clinicians to design individualized chemotherapy regimens^[26].

It has been demonstrated in our study that the sensitivity of seven gastrointestinal cancer cell lines to 5-FU corresponded to DPD mRNA or DPD protein levels linearly. The cancer cells with lower DPD levels were more sensitive to 5-FU, and DPD mRNA was even undetectable in the most sensitive cell line HCT-8. But no correlation between TS or TP levels and sensitivity to 5-FU was found in the present study, in view of the known relevance of TS or TP as a determinant of response of 5-FU in some preclinical and clinical studies^[6,7,27], therefore the results obtained from the study of seven cancer cell lines must be interpreted scrupulously.

The low expression levels of TP could partly explain our finding, besides inhibition of TS activity through anabolism to FdUMP by TP catalyzation. 5-FU exerted its antitumor activity by converting to FdUTP and FUTP for incorporating into DNA and RNA, respectively^[1], thereby interfering with their normal structure and function, so there was no correlation between TS or TP levels and 5-FU sensitivity. On the other hand, Nita *et al.*^[28] also observed DPD expression and predicted 5-FU sensitivity in colorectal cancer cell lines. Etienne *et al.*^[29] confirmed this association in tumor biopsy tissues from the patients of head and neck cancers, but no relationship was demonstrated between TS activity and 5-FU response, either. Our findings, similar to these results, suggested that most of 5-FU within insensitive tumor cells was quickly catabolized by a higher DPD level, which regulated the amount of 5-FU available for anabolism, thereby affecting its cytotoxicity. In addition, these results suggested that DPD inhibitors, such as eniluracil^[30], uracil^[31], 5-chloro-2,4-dihydroxypyrimidine (CDHP)^[32], and BOF-A2^[33], might be used as a novel type of biochemical

modulators for elevating the antitumor activity of 5-FU.

It has been indicated in our work that TS may contribute greatly to the sensitivity of FdUrd, and the higher the TS mRNA levels, the higher the IC₅₀ of FdUrd. Because both TP mRNA and protein levels of this panel of cell lines were rather low, and only little amount of FdUrd could be converted to 5-FU, the suppression of TS through conversion to FdUMP was the principal mechanism of action of FdUrd^[1,10,11]. Therefore TS may serve as a predictive marker of FdUrd. Given the metabolic characteristics of FdUrd, it is comprehensible that there was no correlation between TP or DPD levels and FdUrd sensitivity.

Grem *et al.*^[8] found cell doubling time was a potentially important variable in drug sensitivity, and cell lines with faster doubling times tended to have higher TS activities, but we did not observe the similar trend. In their study, the cytotoxicity was determined by MTT assay after 48 hours of drug exposure, whilst we did it after 72 hours by the same protocol. Since the cell doubling time, ranging from 20.5 to 33.9 hours, was relatively shorter in our study than Grem's, the influence of doubling time on fluoropyrimidines seemed to be much weaker.

We used semi-quantitative RT-PCR and ELISA to determine DPD/TP mRNA and protein level, respectively, and found a statistically significant correlation between mRNA level and protein content of DPD. Compared to traditional radioisotopic enzyme activity assay^[34], RT-PCR and ELISA were less laborious, less expensive, and more feasible in most laboratories. In general, even small amounts (≤ 100 mg) of tissues were enough for them, and the correlation between DPD activity and mRNA or protein levels has been already confirmed in several preclinical and clinical trials^[18,35-38]. But there was no such a correlation in TP, a close look showed three cell lines had extremely low TP protein contents, and even TP enzyme level of MKN45, the highest one, was only 5.11 U/mg protein. A recent clinical trial disclosed that the range of TP level in primary colorectal cancer was 13.8-196.0 U/mg protein^[36], which might explain this apparent discrepancy between mRNA and protein level. Griffiths also pointed out by immunohistochemistry that the predominant cells positive for TP were macrophages and other stroma cells within tumor tissues, and the activation of fluoropyrimidines in human might rely on the paracrine of TP by these stroma cells, but not tumor cells^[10]. As the low expression of TP could directly influence the sensitivity of these seven cell lines to fluoropyrimidines, the role of TP in gastrointestinal cancer cells sensitive to 5-FU and FdUrd needs to be more deeply explored.

In summary, we found that DPD and TS were potential indicators in predicting tumor sensitivity to 5-FU and FdUrd. However, the conclusions were drawn from the limited *in vitro* experiment. This study was merely a first step toward the goal of individualized fluoropyrimidine chemotherapy for gastrointestinal cancers. Controlled, prospective clinical trials are required to confirm our results and to establish the advantage of pre-treatment tumor biopsy for TS/DPD screening, which permits a more rational decision on whether to proceed a fluoropyrimidine-based therapy as first-line treatment. So patients who are unlikely to respond may spare unnecessary toxicity and can be treated with alternative drugs such as CPT-11, oxaliplatin, or with potent biochemical modulators of fluoropyrimidine.

REFERENCES

- 1 **Grem JL.** 5-Fluoropyrimidines. in: Chabner BA, Longo DL eds. *Cancer Chemotherapy and Biotherapy* 3rd ed. Philadelphia: Lippincott Raven 2001: 186-264
- 2 **Ren G, Cai R, Chen Q.** The update advance in chemotherapy of gastric cancer. *Shijie Huaren Xiaohua Zazhi* 2002; **10**: 83-85
- 3 **Nakagawa H, Maeda N, Tsuzuki T, Suzuki T, Hirayama A, Miyahara E, Wada K.** Intracavitary chemotherapy with 5-fluoro-

- 2'-deoxyuridine (FdUrd) in malignant brain tumors. *Jpn J Clin Oncol* 2001; **31**: 251-258
- 4 **Diasio RB**, Johnson MR. The role of pharmacogenetics and pharmacogenomics in cancer chemotherapy with 5-fluorouracil. *Pharmacology* 2000; **61**: 199-203
 - 5 **Diasio RB**. Improving fluorouracil chemotherapy with novel orally administered fluoropyrimidines. *Drugs* 1999; **58**(Suppl 3): 119-126
 - 6 **Van Triest B**, Peters GJ. Thymidylate synthase: a target for combination therapy and determinant of chemotherapeutic response in colorectal cancer. *Oncology* 1999; **57**: 179-194
 - 7 **Leichman CG**, Lenz HJ, Leichman L, Danenberg K, Baranda J, Groshen S, Boswell W, Metzger R, Tan M, Danenberg PV. Quantitation of intratumoral thymidylate synthase expression predicts for disseminated colorectal cancer response and resistance to protracted-infusion fluorouracil and weekly leucovorin. *J Clin Oncol* 1997; **15**: 3223-3229
 - 8 **Grem JL**, Danenberg KD, Behan K, Parr A, Young L, Danenberg PV, Nguyen D, Drake J, Monks A, Allegra CJ. Thymidine kinase, thymidylate synthase, and dihydropyrimidine dehydrogenase profiles of cell lines of the National Cancer Institute's Anticancer Drug Screen. *Clin Cancer Res* 2001; **7**: 999-1009
 - 9 **Ikeguchi M**, Makino M, Kaibara N. Thymidine phosphorylase and dihydropyrimidine dehydrogenase activity in colorectal carcinoma and patients prognosis. *Langenbecks Arch Surg* 2002; **387**:240-245
 - 10 **Griffiths L**, Stratford IJ. Platelet-derived endothelial cell growth factor thymidine phosphorylase in tumour growth and response to therapy. *Br J Cancer* 1997; **76**: 689-693
 - 11 **Creaven PJ**, Rustum YM, Petrelli NJ, Meropol NJ, Raghavan D, Rodriguez-Bigas M, Levine EG, Frank C, Udvary-Nagy S, Proefrock A. Phase I and pharmacokinetic evaluation of floxuridine /leucovorin given on the Roswell Park weekly regimen. *Cancer Chemother Pharmacol* 1994; **34**: 261-265
 - 12 **Marchetti S**, Chazal M, Dubreuil A, Fischel JL, Etienne MC, Milano G. Impact of thymidine phosphorylase surexpression on fluoropyrimidine activity and on tumour angiogenesis. *Br J Cancer* 2001; **85**: 439-445
 - 13 **Mader RM**, Sieder AE, Braun J, Rizovski B, Kalipciyan M, Mueller MW, Jakesz R, Rainer H, Steger GG. Transcription and activity of 5-fluorouracil converting enzymes in fluoropyrimidine resistance in colon cancer *in vitro*. *Biochem Pharmacol* 1997; **54**: 1233-1242
 - 14 **Saito H**, Tsujitani S, Oka S, Kondo A, Ikeguchi M, Maeta M, Kaibara N. The expression of thymidine phosphorylase correlates with angiogenesis and the efficacy of chemotherapy using fluorouracil derivatives in advanced gastric carcinoma. *Br J Cancer* 1999; **81**: 484-489
 - 15 **Metzger R**, Danenberg K, Leichman CG, Salonga D, Schwartz EL, Wadler S, Lenz HJ, Groshen S, Leichman L, Danenberg PV. High basal level gene expression of thymidine phosphorylase (platelet-derived endothelial cell growth factor) in colorectal tumors is associated with nonresponse to 5-fluorouracil. *Clin Cancer Res* 1998; **4**: 2371-2376
 - 16 **Fischel JL**, Etienne MC, Spector T, Formento P, Renee N, Milano G. Dihydropyrimidine dehydrogenase: a tumoral target for fluorouracil modulation. *Clin Cancer Res* 1995; **1**: 991-996
 - 17 **Mattison LK**, Soong R, Diasio RB. Implications of dihydropyrimidine dehydrogenase on 5-fluorouracil pharmacogenetics and pharmacogenomics. *Pharmacogenomics* 2002; **3**: 485-492
 - 18 **Tanaka-Nozaki M**, Onda M, Tanaka N, Kato S. Variations in 5-fluorouracil concentrations of colorectal tissues as compared with dihydropyrimidine dehydrogenase(DPD) enzyme activities and DPD messenger RNA levels. *Clin Cancer Res* 2001; **7**: 2783-2787
 - 19 **Ishikawa Y**, Kubota T, Otani Y, Watanabe M, Teramoto T, Kumai K, Takechi T, Okabe H, Fukushima M, Kitajima M. Dihydropyrimidine dehydrogenase and messenger RNA levels in gastric cancer: possible predictor for sensitivity to 5-fluorouracil. *Jpn J Cancer Res* 2000; **91**: 105-112
 - 20 **Milano G**, McLeod HL. Can dihydropyrimidine dehydrogenase impact 5-fluorouracil-based treatment? *Eur J Cancer* 2000; **36**: 37-42
 - 21 **Liu GF**. Median effective dose. in: Jiang ZJ eds. Medical statistics. 1sted. Beijing: People's Medical Publishing House 1997: 136-153
 - 22 **Feng RH**, Zhu ZG, Li JF, Liu BY, Yan M, Yin HR, Lin YZ. Inhibition of human telomerase in MKN-45 cell line by antisense hTR expression vector induces cell apoptosis and growth arrest. *World J Gastroenterol* 2002; **8**: 436-440
 - 23 **Hu JK**, Chen ZX, Zhou ZG, Zhang B, Tian J, Chen JP, Wang L, Wang CH, Chen HY, Li YP. Intravenous chemotherapy for resected gastric cancer: meta-analysis of randomized controlled trials. *World J Gastroenterol* 2002; **8**: 1023-1028
 - 24 **Shi YQ**, Xiao B, Miao JY, Zhao YQ, You H, Fan DM. Construction of eukaryotic expression vector pBK-fas and MDR reversal test of drug-resistant gastric cancer cells. *Shijie Huaren Xiaohua Zazhi* 1999; **7**: 309-312
 - 25 **Xiao B**, Shi YQ, Zhao YQ, You H, Wang ZY, Liu XL, Yin F, Qiao TD, Fan DM. Transduction of fas gene or bcl-2 antisense RNA sensitizes cultured drug resistant gastric cancer cells to chemotherapeutic drugs. *Huaren Xiaohua Zazhi* 1998; **6**: 675-679
 - 26 **McLeod HL**, Evans WE. Pharmacogenomics: unlocking the human genome for better drug therapy. *Annu Rev Pharmacol Toxicol* 2001; **41**: 101-121
 - 27 **Wong NA**, Brett L, Stewart M, Leitch A, Longley DB, Dunlop MG, Johnston PG, Lessells AM, Jodrell DI. Nuclear thymidylate synthase expression, p53 expression and 5FU response in colorectal carcinoma. *Br J Cancer* 2001; **85**: 1937-1943
 - 28 **Nita ME**, Tominaga O, Nagawa H, Tsuruo T, Muto T. Dihydropyrimidine dehydrogenase but not thymidylate synthase expression is associated with resistance to 5-fluorouracil in colorectal cancer. *Hepatogastroenterology* 1998; **45**: 2117-2122
 - 29 **Etienne MC**, Cheradame S, Fischel JL, Formento P, Dassonville O, Renee N, Schneider M, Thyss A, Demard F, Milano G. Response to fluorouracil therapy in cancer patients: the role of tumoral dihydropyrimidine dehydrogenase activity. *J Clin Oncol* 1995; **13**: 1663-1670
 - 30 **Mani S**, Hochster H, Beck T, Chevlen EM, O'Rourke MA, Weaver CH, Bell WN, White R, McGuirt C, Levin J, Hohneker J, Schilsky RL, Lokich J. Multicenter phase I study to evaluate a 28-day regimen of oral fluorouracil plus eniluracil in the treatment of patients with previously untreated metastatic colorectal cancer. *J Clin Oncol* 2000; **18**: 2894-2901
 - 31 **Colevas AD**, Amrein PC, Gomolin H, Barton JJ, Read RR, Adak S, Benner S, Costello R, Posner MR. A phase II study of combined oral uracil and ftorafur with leucovorin for patients with squamous cell carcinoma of the head and neck. *Cancer* 2001; **92**: 326-331
 - 32 **Takechi T**, Fujioka A, Matsushima E, Fukushima M. Enhancement of the antitumour activity of 5-fluorouracil(5-FU) by inhibiting dihydropyrimidine dehydrogenase activity(DPD) using 5-chloro-2,4-dihydroxypyridine(CDHP) in human tumour cells. *Eur J Cancer* 2002; **38**: 1271-1277
 - 33 **Sugimachi K**, Maehara Y. A phase II trial of a new 5-fluorouracil derivative, BOF-A2 (Emitofur), for patients with advanced gastric cancer. *Surg Today* 2000; **30**: 1067-1072
 - 34 **Johnson MR**, Yan J, Shao L, Albin N, Diasio RB. Semi-automated radioassay for determination of dihydropyrimidine dehydrogenase (DPD) activity. Screening cancer patients for DPD deficiency, a condition associated with 5-fluorouracil toxicity. *J Chromatogr B Biomed Sci Appl* 1997; **696**: 183-191
 - 35 **Hiroyasu S**, Shiraishi M, Samura H, Tokashiki H, Shimoji H, Isa T, Muto Y. Clinical relevance of the concentrations of both pyrimidine nucleoside phosphorylase(PyNPase) and dihydropyrimidine dehydrogenase (DPD) in colorectal cancer. *Jpn J Clin Oncol* 2001; **31**: 65-68
 - 36 **Nishimura G**, Terada I, Kobayashi T, Ninomiya I, Kitagawa H, Fushida S, Fujimura T, Kayahara M, Shimizu K, Ohta T, Miwa K. Thymidine phosphorylase and dihydropyrimidine dehydrogenase levels in primary colorectal cancer show a relationship to clinical effects of 5'-deoxy-5-fluorouridine as adjuvant chemotherapy. *Oncol Rep* 2002; **9**: 479-482
 - 37 **Hoque MO**, Kawamata H, Nakashiro KI, Omotehara F, Shinagawa Y, Hino S, Begum NM, Uchida D, Yoshida H, Sato M, Fujimori T. Dihydropyrimidine dehydrogenase mRNA level correlates with the response to 5-fluorouracil-based chemio-immuno-radiation therapy in human oral squamous cell cancer. *Int J Oncol* 2001; **19**: 953-958
 - 38 **Johnson SJ**, Ridge SA, Cassidy J, McLeod HL. Regulation of dihydropyrimidine dehydrogenase in colorectal cancer. *Clin Cancer Res* 1999; **5**: 2566-2570

Expression of NF- κ B and human telomerase reverse transcriptase in gastric cancer and precancerous lesions

Wei Wang, He-Sheng Luo, Bao-Ping Yu

Wei Wang, He-Sheng Luo, Bao-Ping Yu, Department of Gastroenterology, Renmin Hospital of Wuhan University, Wuhan 430060, Hubei Province, China

Correspondence to: Professor He-Sheng Luo, Department of Gastroenterology, Renmin Hospital of Wuhan University, Wuhan 430060, Hubei Province, China. luotang@public.wh.hb.cn

Telephone: +86-27-88041911-2134

Received: 2003-06-16 **Accepted:** 2003-07-24

Abstract

AIM: To investigate the expression of NF- κ Bp65 protein and human telomerase reverse transcriptase (hTERT) and their correlation in gastric cancer and precancerous lesions.

METHODS: Forty-one patients with primary gastric cancer, 15 with dysplasia, 23 intestinal metaplasia and 10 with normal gastric mucosa were included in this study. Expression of NF- κ Bp65 protein, hTERT mRNA and protein were determined by immunohistochemistry and *in situ* hybridization.

RESULTS: The rate of p65 expression in normal gastric mucosa, intestinal metaplasia, dysplasia and carcinoma was 0%, 34.78%, 53.33% and 60.98%, respectively, while the rate of hTERT mRNA expression was 10.00%, 39.13%, 66.67% and 85.37% and the rate of hTERT protein expression was 0%, 30.43%, 60.00% and 78.05%, respectively. All the three parameters were significantly increased in dysplasia and carcinoma compared to normal mucosa, while the expression levels were also significantly higher in carcinoma than in intestinal metaplasia ($P < 0.05$). In gastric cancer tissues, nuclear staining rates of p65 and hTERT protein were both significantly associated with the degree of differentiation, lymph node metastasis, clinical stage and invasion depth ($P < 0.05$). However, hTERT mRNA expression was only significantly associated with clinical stage. There was a positive correlation between p65 and hTERT mRNA ($r_s = 0.661-0.752$, $P < 0.01$), and between hTERT protein and hTERT mRNA ($r_s = 0.609-0.750$, $P < 0.01$).

CONCLUSION: NF- κ Bp65 and hTERT expressions are upregulated at the early stage of gastric carcinogenesis. NF- κ B activation may contribute to hTERT expression and thereby enhance telomerase activity, which represents an important step in carcinogenesis progress.

Wang W, Luo HS, Yu BP. Expression of NF- κ B and human telomerase reverse transcriptase in gastric cancer and precancerous lesions. *World J Gastroenterol* 2004; 10(2): 177-181
<http://www.wjgnet.com/1007-9327/10/177.asp>

INTRODUCTION

NF- κ B is a family of dimeric transcription factors that play a critical role in host defense by regulating the expression of immune and inflammatory genes^[1-3]. The most common dimer is RelA (p65)/NF- κ B1 (p50) heterodimer. In resting cells, NF-

κ B is localized in the cytoplasm, which is noncovalently associated with the cytoplasmic inhibitory protein I κ B. Upon stimulation with a variety of pathogenic inducers such as viruses, mitogens, bacteria, agents providing oxygen radicals, and inflammatory cytokines, I κ B is phosphorylated, ubiquitinated, and degraded in the cytoplasm, and the NF- κ B complex migrates into the nucleus and binds to DNA recognition sites in the regulatory regions of target genes^[4]. Recently, there were several reports on the role of NF- κ B gene products in cell proliferation, transformation, and tumor development^[5-9]. Recent studies have also indicated that NF- κ B is constitutively activated in several tumors^[10-13]. However, the biological significance of NF- κ B activation remains unclear in gastric carcinogenesis although gastric cancer is one of the most aggressive forms of cancer.

Telomerase is a key enzyme that catalyzes the synthesis of telomere DNA participating in cell immortalization through stabilization of chromosomal structure^[14]. Telomerase is expressed in germ tissues as well as in majority of human tumors, including gastrointestinal carcinomas, but is low and difficult to detect in somatic cells generally^[15-19]. So it may be a useful molecular marker for cancer diagnosis and therapeutic strategies. Human telomerase reverse transcriptase (hTERT) has been identified as a putative catalytic subunit of human telomerase^[20]. Recent reconstitution experiments, both *in vitro* and *in vivo*, also strongly suggest that hTERT is the major determinant of human telomerase activity^[21,22]. Overexpression of hTERT in cancer cells is thought to contribute to tumor development and angiogenesis^[23-25]. However, the mechanism by which hTERT is overexpressed in cancer cells remains unclear. There are evidences that hTERT expression may be regulated by the highly inducible NF- κ B transcription factor^[26]. So it is interesting to investigate the relation between NF- κ B and hTERT at cellular level.

We undertook the present study to determine whether NF- κ B was constitutively activated in precancerous and cancerous tissues of the stomach, to examine whether expression of hTERT gene correlated with NF- κ B activation, and to evaluate the relationship between clinicopathological features and NF- κ B activation as well as hTERT gene expression.

MATERIALS AND METHODS

Tissue samples

Gastric tissues were obtained by surgical resection from 89 patients: 10 with normal gastric mucosa, 23 with intestinal metaplasia, 15 with dysplasia and 41 with gastric cancer. Patients with gastric cancer were admitted to Renmin Hospital of Wuhan University from February to December in 2000, and had not been treated with chemotherapy or radiation therapy before operation. Histological examinations were performed, according to the criteria of the Japanese Gastric Cancer Association^[27]. All specimens were fixed in 10 % buffered neutral formalin and embedded in paraffin. Serial tissue sections (4.5 μ m thick) were placed on glass slides coated with 3-aminopropyltriethoxysilane (Sigma, USA), and then used in the following experiments.

Immunohistochemistry for NF- κ B p65 and hTERT proteins

Immunostaining was performed as described previously with slight modification^[28]. Briefly, slides were treated overnight at 4 °C with either anti-p65 mAb (4 μ g/ml) or anti-hTERT polyclonal antibody (3 μ g/ml). Both antibodies were from Santa Cruz Biotechnology (USA). Then, slides were incubated with secondary antibody by using a streptavidin-peroxidase kit (Maixin-Bio, Fujian). Finally, the antigen sites were visualized by incubating with diaminobendizine (DAB) solution (Zhongshan Biotechnical Co, Beijing), and the nuclei were weakly counterstained with Mayer's hematoxylin (Maixin-Bio, Fujian). The specificity of immunostaining was determined by replacement of the primary antibody with PBS. Positive reaction was detected as nuclear stain presenting in brown-yellow color. Slides positively stained were further stratified from 1+ to 3+ based on the overall intensity and percentage of the stained tumor cells, with an estimated scale of <25% cell positive =1+, 25% to 50% =2+, and >50% =3+. Staining was defined as negative if positive cells were <5%.

In situ hybridization for hTERT mRNA

hTERT mRNA ISH detection kit and antisense polyoligonucleotide probe (digoxin-labeled) were purchased from Boster Biological Technology Ltd. (Wuhan). In brief, deparaffinized sections were incubated with 3% hydrogen peroxide for 30 min and then with 1 μ g/ml pepsin for 15 min. The prehybridization was performed at 37 °C for 2 h, and the hybridization was conducted in a 42 °C water bath for 18 h with each section covered with a soil coverslip. After thorough washing, tissue sections were preblocked for 20 min with blocking solution. Then, rabbit anti-digoxin antibody was added for 60 min at 37 °C. After washed in PBS, the sections were visualized according to the manufacturer's instructions. A negative control was prepared by using a hybridization solution without the probe. A positive reaction was detected as plasmatic stain presenting in brown-yellow color. Slides positively stained were further stratified from 1+ to 3+ as described above.

Statistics

Statistical analysis was performed using chi-squared test, Fisher's exact test, and spearman rank test. A *P* value <0.05 (one-sided) was accepted as statistically significant.

RESULTS

Staining of NF- κ Bp65 protein, hTERT mRNA and protein

P65 immunostaining was significantly enhanced both in cytoplasm and in nuclei of the tumor cells in comparison to that in normal epithelial cells (Figure 1). Since nuclear staining, which indicated nuclear transportation of p65, was considered as a marker of NF- κ B activation, we only counted the number of nuclear stained cells and took them into calculation of the percentage of positively stained cells. Similarly, hTERT protein was mainly localized in the nuclei of tumor cells, and only a small number of cells showed a positive reaction in the cytoplasm (Figure 2). Stromal cells such as endothelial cells and smooth muscle cells (except lymphocytes) showed no reaction for hTERT. Weak staining of p65 and hTERT proteins was observed in some epithelial cells in the lower two-thirds of the glands of nonneoplastic mucosa.

In situ hybridization

Revealed that hTERT mRNA was significantly enhanced in the cytoplasm of tumor cells (Figure 3). Only a few signals were seen in nonneoplastic cells, which were slightly increased in the replicating basal layer, and in intestinal metaplastic cells as well as in activated lymphocytes, while the surface epithelia were negative (Figure 4).

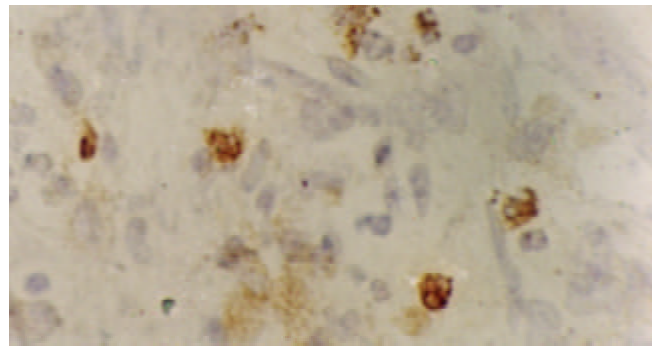


Figure 1 Immunohistochemical detection of NF- κ Bp65 protein in gastric carcinoma showing cytoplasmic and nuclear staining SP \times 400.

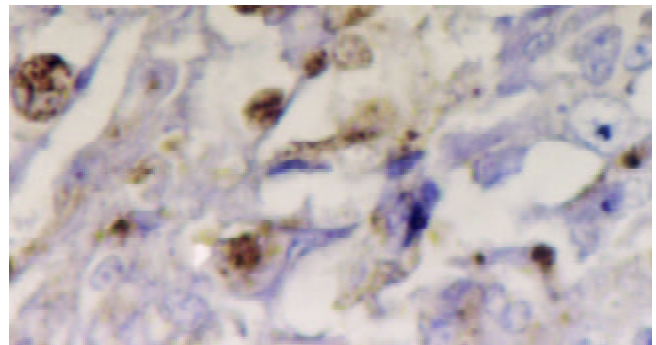


Figure 2 Immunohistochemical detection of hTERT protein in poorly differentiated gastric carcinoma. A positive reaction was shown in the nuclei of cancer cells. SP \times 400.

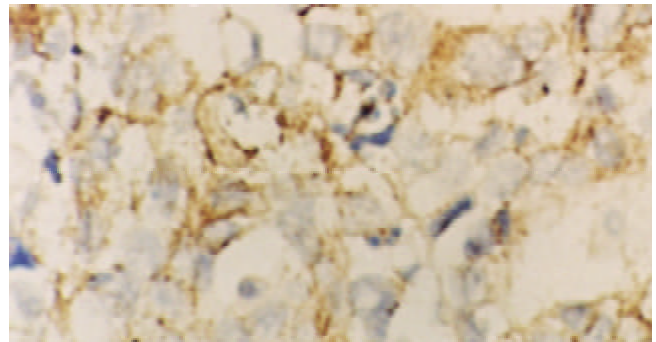


Figure 3 Detection of hTERT mRNA in a mucinous adenocarcinoma. Most tumor cells displayed strong signals that were localized in the cytoplasm. ISH \times 400.

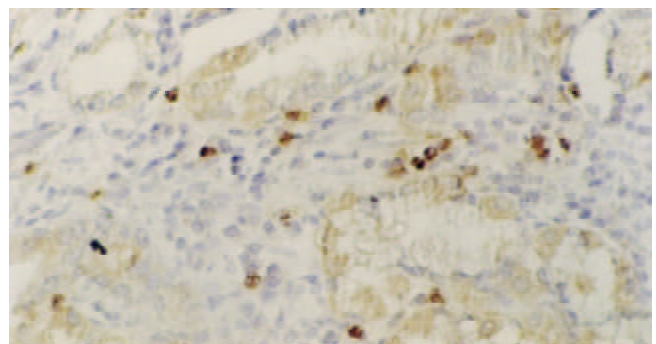


Figure 4 Detection of hTERT mRNA in intestinal metaplasia. The reaction was localized in the cytoplasm of intestinal metaplastic cells, activated lymphocytes, as well as replicating cells in basal layer, while the surface epithelia were negative. ISH \times 100.

Table 1 Expression of NF- κ Bp65 protein, hTERT mRNA and protein in precancerous lesions and gastric cancer

Lesion	Cases	NF- κ Bp65				hTERT mRNA				hTERT protein			
		+	++	+++	Total (%)	+	++	+++	Total (%)	+	++	+++	Total (%)
Normal	10	0	0	0	0 (0)	1	0	0	1 (10.00)	0	0	0	0 (0)
Intestinal metaplasia	23	7	1	0	8 (34.78) ^b	6	3	0	9 (39.13) ^b	5	2	0	7 (30.43) ^b
Dysplasia	15	7	1	0	8 (53.33) ^a	7	3	0	10 (66.67) ^a	7	2	0	9 (60.00) ^a
Cancer	41	7	14	4	25 (60.98) ^a	6	20	9	35 (85.37) ^a	6	20	6	32 (78.05) ^a

^a $P < 0.05$, vs normal mucosa group; ^b $P < 0.01$, vs cancer group.

Expression of NF- κ Bp65 protein, hTERT mRNA and protein

Expression of p65 protein, hTERT mRNA and protein in gastric precancerous and cancerous tissues was increased compared with normal mucosa (Table 1). The nuclear staining rates of p65 (active form) were higher in gastric cancer than in intestinal metaplasia ($P < 0.05$), or normal mucosa ($P < 0.05$). The rates were also significantly higher in dysplasia than in normal mucosa. Similarly, expression of hTERT mRNA and protein was increased in precancerous and cancerous tissues (Table 1).

The relations between clinicopathological features and expression of p65 and hTERT in the 41 patients with gastric carcinoma were further analyzed (Table 2). Nuclear staining rates of p65 and hTERT proteins were both significantly associated with the degree of differentiation, lymph node metastasis, clinical stage and the depth of invasion ($P < 0.01-0.05$). Furthermore, the nuclear staining of p65 was significantly higher in tumors ≥ 5 cm than in those < 5 cm. With respect to expression of hTERT mRNA, we found that carcinomas at advanced stage showed a significantly higher level than those at early stage. However, there was no significant association between expression of hTERT mRNA and other clinicopathological features.

Table 2 Correlation between expression of NF- κ Bp65 protein, hTERT mRNA and protein and clinicopathological features

Factor	Cases	NF- κ B p65 (%)	hTERT mRNA (%)	hTERT protein (%)
Gender				
Male	30	16 (53.33)	24 (80.00)	24 (80.00)
Female	11	9 (81.82)	11 (100.00)	8 (72.73)
Age (years)				
< 60	24	14 (58.33)	21 (87.50)	20 (83.33)
≥ 60	17	11 (64.71)	14 (82.35)	12 (70.59)
Histology (type)				
Intestinal	16	7 (43.75)	12 (75.00)	10 (62.50)
Diffuse	25	18 (72.00)	23 (92.00)	22 (88.00)
Differentiation				
Well	13	3 (23.08) ^b	9 (69.23)	7 (53.85) ^a
Poor	28	22 (78.57)	26 (92.86)	25 (89.29)
Lymph node metastasis				
Negative	16	4 (25.00) ^b	12 (75.00)	9 (56.25) ^a
Positive	25	21 (84.00)	23 (92.00)	23 (92.00)
Stage				
Early	12	2 (16.67) ^b	7 (58.33) ^b	5 (41.67) ^b
Advanced	29	23 (79.31)	28 (96.55)	27 (93.10)
Tumor size (cm)				
< 5	19	6 (31.58) ^b	14 (73.68)	13 (68.42)
≥ 5	22	19 (86.36)	21 (95.45)	19 (86.36)
Depth of invasion				
m, sm	10	2 (20.00) ^a	6 (60.00)	4 (40.00) ^a
ms, ss	17	11 (64.71)	16 (94.12)	15 (88.24)
se, si	14	12 (85.71)	13 (92.86)	13 (92.86)

^a $P < 0.05$, ^b $P < 0.01$, From comparison in each group of clinicopathologic feature by chi-square test or Fisher's exact test. m: mucosa,

sm: submucosa, mp: muscularis propria, ss: subserosa, se: invasion to serosa, si: invasion to other organ. Tumor size was defined as the largest size in extension on the gastric mucosa.

Correlation between NF- κ B activation and expression of hTERT

There was a positive correlation between NF- κ B activation and hTERT mRNA expression in patients with intestinal metaplasia ($r_s = 0.665$), dysplasia ($r_s = 0.661$) and gastric cancer ($r_s = 0.752$). Similarly, hTERT mRNA expression was also positively correlated with hTERT protein in these three groups ($P < 0.05$), with the r_s values of 0.609, 0.750 and 0.730, respectively.

DISCUSSION

The present study reported the detection of NF- κ B activation and hTERT gene expression, as well as their correlation, in cancerous and precancerous tissues of stomach.

NF- κ B, an important transcription factor, consists of dimeric complexes. We used immunohistochemistry to detect NF- κ B activation. The polyclonal antibody we used, could bind to the active and inactive forms of p65, one of NF- κ B subunits, as shown in a previous study^[29]. We only quantified the nuclear staining (active form) to evaluate NF- κ B activation. With such an analysis, nuclear translocation of p65 could be estimated at single-cell level. We found that active NF- κ B was not only in the nuclei of tumor cells but also in the nuclei of infiltrating inflammatory cells, especially lymphocytes, which was accordant with the role of NF- κ B involved in immune and inflammatory responses^[30,31]. Isomoto *et al*^[32] also reported that in *Helicobacter pylori*-associated gastritis, activated NF- κ B was expressed in macrophages, vascular endothelial cells and B lymphocytes in addition to epithelial cells, which might be involved in the inflammation process.

Using *in situ* hybridization and immunohistochemistry methods, we detected the expression of hTERT at both RNA and protein levels. Importantly, the *in situ* detection enabled us to differentiate whether telomerase activity was due to proliferative normal cells or lymphocytes. Therefore immunohistochemical detection of hTERT might be a novel tool for the diagnosis of gastric cancer^[33]. In this study, we demonstrated that, besides tumor cells, hTERT mRNA and protein were also expressed, albeit weakly in normal gastric fundic mucosa. These epithelial cells were terminally differentiated. It is possible that low levels of hTERT expression might be the characteristics of physically regenerating tissues containing stem cells, and hTERT-positive cells might be competent for regeneration if severe mucosal damage occurred^[28]. Although the level of hTERT mRNA correlated significantly with that of hTERT protein in our study, their expression levels were not always coincident in precancerous and cancerous lesions. It is likely that post-translational modifications, such as phosphorylation by akt kinase, might be involved in hTERT expression^[28,34].

The present study revealed that NF- κ Bp65 nuclear staining rates were higher in cancer tissues, followed by dysplasia,

intestinal metaplasia and normal mucosa. This is the first report on NF- κ Bp65 detection in gastric precancerous tissues. As to the expression of hTERT gene, previous studies revealed that carcinomas could express hTERT more frequently than noncancerous tissues^[25,35-38]. Our findings support these results. The present study indicated that NF- κ B and telomerase were both activated in precancerous lesions, suggesting that NF- κ B activation and increased hTERT gene expression emerge at the early stage of gastric carcinogenesis, and that they may be the prerequisites for malignant transformation. Therefore, NF- κ B and telomerase might be potentially important targets for the development of anti-tumor therapies for gastric carcinoma^[15,39,40].

Sasaki *et al*^[29] reported that NF- κ B activation was positively correlated with tumor size, lymphatic invasion, depth of invasion and peritoneal metastasis. Besides that, our study also revealed significantly positive correlations between nuclear staining of NF- κ B p65 and differentiation degree and clinical stage. Therefore, NF- κ B activation might be associated with tumor growth, invasion and metastasis.

It has been reported that hTERT expression might be downstream of NF- κ B activation^[26,41]. Yin *et al*^[26] found a potential NF- κ B binding site at 350 base pairs upstream from the translational start site of mouse TERT promoters and NF- κ B was found to contribute to the activation of TERT expression. In addition, Akiyama *et al*^[41] showed that NF- κ B interacted directly with hTERT protein in multiple myeloma cells. In the present study we examined the relationship between nuclear staining of NF- κ Bp65 and hTERT mRNA at the cellular level by immunohistochemistry and *in situ* hybridization. We observed that both p65 and hTERT mRNA were overexpressed in gastric cancer with the positive staining rates of 60.98% and 85.37%, respectively. In fact, most specimens showing a high p65 level also showed high hTERT mRNA expression and *vice versa*. Furthermore, the expression of p65 and hTERT mRNA showed a significant correlation in cancerous and precancerous tissues (intestinal metaplasia and dysplasia). And in nonneoplastic mucosa, the positive staining of p65 and hTERT mRNA were detected simultaneously in proliferative glands and activated lymphocytes. All of these suggested that NF- κ Bp65 cooperated with hTERT in gastric carcinogenesis. We speculate that NF- κ Bp65 may induce hTERT promoter activity and upregulate telomerase activity and contribute to the aggressiveness of gastric carcinoma.

However, our study was limited by the high specificity of p65 mAb for the p65 subunit, and thus we could not evaluate other NF- κ B dimers. The relationship between other NF- κ B subunits and gastric cancer needs further studies.

In conclusion, we demonstrated the presence of activated NF- κ Bp65 and increased hTERT expression in gastric cancerous and precancerous tissues. The levels of p65 and hTERT expression were higher in gastric cancer than in normal mucosa, and NF- κ B activation was associated with tumor growth, invasion and metastasis. Our findings suggest that NF- κ Bp65 cooperates with hTERT in gastric carcinogenesis.

REFERENCES

- Bauerle PA, Baltimore D. NF-kappa B: ten years after. *Cell* 1996; **87**: 13-20
- Jia CK, Zheng SS, Li QY, Zhang AB. Immunotolerance of liver allotransplantation induced by intrathymic inoculation of donor soluble liver specific antigen. *World J Gastroenterol* 2003; **9**: 759-764
- Gong JP, Liu CA, Wu CX, Li SW, Shi YJ, Li XH. Nuclear factor kB activity in patients with acute severe cholangitis. *World J Gastroenterol* 2002; **8**: 346-349
- Thanos D, Maniatis T. NF-kappa B: a lesson in family values. *Cell* 1995; **80**: 529-532
- Pahl HL. Activators and target genes of Rel/NF-kappaB transcription factors. *Oncogene* 1999; **18**: 6853-6866
- de Martin R, Schmid JA, Hofer-Warbinek R. The NF-KappaB/Rel family of transcription factors in oncogenic transformation and apoptosis. *Mutat Res* 1999; **437**: 231-243
- Li HL, Chen DD, Li XH, Zhang HW, Lu YQ, Ye CL, Ren XD. Changes of NF-kB, p53, Bcl-2 and caspase in apoptosis induced by JTE-522 in human gastric adenocarcinoma cell line AGS cells: role of reactive oxygen species. *World J Gastroenterol* 2002; **8**: 431-435
- La Rosa FA, Pierce JW, Sonenshein GE. Differential regulation of the c-myc oncogene promoter by the NF-kappa B rel family of transcription factors. *Mol Cell Biol* 1994; **14**: 1039-1044
- Sonenshein GE. Rel/NF-kappa B transcription factors and the control of apoptosis. *Semin Cancer Biol* 1997; **8**: 113-119
- Zhu JW, Yu BM, Ji YB, Zheng MH, Li DH. Upregulation of vascular endothelial growth factor by hydrogen peroxide in human colon cancer. *World J Gastroenterol* 2002; **8**: 153-157
- Wang W, Abbruzzese JL, Evans DB, Larry L, Cleary KR, Chiao PJ. The nuclear factor-kappa B RelA transcription factor is constitutively activated in human pancreatic adenocarcinoma cells. *Clin Cancer Res* 1999; **5**: 119-127
- Sovak MA, Bellas RE, Kim DW, Zanieski GJ, Rogers AE, Traish AM, Sonenshein GE. Aberrant nuclear factor-kappaB/Rel expression and the pathogenesis of breast cancer. *J Clin Invest* 1997; **100**: 2952-2960
- Guo SP, Wang WL, Zhai YQ, Zhao YL. Expression of nuclear factor-kappa B in hepatocellular carcinoma and its relation with the X protein of hepatitis B virus. *World J Gastroenterol* 2001; **7**: 340-344
- Blackburn EH. Telomerases. *Annu Rev Biochem* 1992; **61**: 113-129
- Burger AM, Bibby MC, Double JA. Telomerase activity in normal and malignant mammalian tissues: feasibility of telomerase as a target for cancer chemotherapy. *Br J Cancer* 1997; **75**: 516-522
- Lu JP, Mao JQ, Li MS, Lu SL, Hu XQ, Zhu SN, Nomura S. *In situ* detection of TGF betas, TGF beta receptor II mRNA and telomerase activity in rat cholangiocarcinogenesis. *World J Gastroenterol* 2003; **9**: 590-594
- Liao C, Zhao MJ, Zhao J, Song H, Pineau P, Marchio A, Dejean A, Tiollais P, Wang HY, Li TP. Mutation analysis of novel human liver-related putative tumor suppressor gene in hepatocellular carcinoma. *World J Gastroenterol* 2003; **9**: 89-93
- Shen ZY, Xu LY, Chen MH, Shen J, Cai WJ, Zeng Y. Progressive transformation of immortalized esophageal epithelial cells. *World J Gastroenterol* 2002; **8**: 976-981
- Feng RH, Zhu ZG, Li JF, Liu BY, Yan M, Yin HR, Lin YZ. Inhibition of human telomerase in MKN-45 cell line by antisense hTR expression vector induces cell apoptosis and growth arrest. *World J Gastroenterol* 2002; **8**: 436-440
- Meyerson M, Counter CM, Eaton EN, Ellisen LW, Steiner P, Caddle SD, Ziaugra L, Beijersbergen RL, Davidoff MJ, Liu Q, Bacchetti S, Haber DA, Weinberg RA. hEST2, the putative human telomerase catalytic subunit gene, is up-regulated in tumor cells and during immortalization. *Cell* 1997; **90**: 785-795
- Weinrich SL, Pruzan R, Ma L, Ouellette M, Tesmer VM, Holt SE, Bodnar AG, Lichtsteiner S, Kim NW, Trager JB, Taylor RD, Carlos R, Andrews WH, Wright WE, Shay JW, Harley CB, Morin GB. Reconstitution of human telomerase with the template RNA component hTR and the catalytic protein subunit hTERT. *Nat Genet* 1997; **17**: 498-502
- Nakayama J, Tahara H, Tahara E, Saito M, Ito K, Nakamura H, Nakanishi T, Tahara E, Ide T, Ishikawa F. Telomerase activation by hTERT in human normal fibroblasts and hepatocellular carcinomas. *Nat Genet* 1998; **18**: 65-68
- Shao JC, Wu JF, Wang DB, Qin R, Zhang H. Relationship between the expression of human telomerase reverse transcriptase gene and cell cycle regulators in gastric cancer and its significance. *World J Gastroenterol* 2003; **9**: 427-431
- Pallini R, Pierconti F, Falchetti ML, D' Arcangelo D, Fernandez E, Maira G, D' Ambrosio E, Larocca LM. Evidence for telomerase involvement in the angiogenesis of astrocytic tumors: expression of human telomerase reverse transcriptase messenger RNA by vascular endothelial cells. *J Neurosurg* 2001; **94**: 961-971
- Kumaki F, Kawai T, Hiroi S, Shinomiya N, Ozeki Y, Ferrans VJ, Torikata C. Telomerase activity and expression of human

- telomerase RNA component and human telomerase reverse transcriptase in lung carcinomas. *Hum Pathol* 2001; **32**: 188-195
- 26 **Yin L**, Hubbard AK, Giardina C. NF-kappa B regulates transcription of the mouse telomerase catalytic subunit. *J Biol Chem* 2000; **275**: 36671-36675
- 27 **Japanese Gastric Cancer Association**. Japanese Classification of Gastric Carcinoma - 2nd English Edition -. *Gastric Cancer* 1998; **1**: 10-24
- 28 **Yasui W**, Tahara E, Tahara H, Fujimoto J, Naka K, Nakayama J, Ishikawa F, Ide T, Tahara E. Immunohistochemical detection of human telomerase reverse transcriptase in normal mucosa and precancerous lesions of the stomach. *Jpn J Cancer Res* 1999; **90**:589-595
- 29 **Sasaki N**, Morisaki T, Hashizume K, Yao T, Tsuneyoshi M, Noshiro H, Nakamura K, Yamanaka T, Uchiyama A, Tanaka M, Katano M. Nuclear factor-kappaB p65 (RelA) transcription factor is constitutively activated in human gastric carcinoma tissue. *Clin Cancer Res* 2001; **7**: 4136-4142
- 30 **Cong B**, Li SJ, Yao YX, Zhu GJ, Ling YL. Effect of cholecystokinin octapeptide on tumor necrosis factor α transcription and nuclear factor-kappaB activity induced by lipopolysaccharide in rat pulmonary interstitial macrophages. *World J Gastroenterol* 2002; **8**: 718-723
- 31 **Meng AH**, Ling YL, Zhang XP, Zhang JL. Anti-inflammatory effect of cholecystokinin and its signal transduction mechanism in endotoxic shock rat. *World J Gastroenterol* 2002; **8**: 712-717
- 32 **Isomoto H**, Mizuta Y, Miyazaki M, Takeshima F, Omagari K, Murase K, Nishiyama T, Inoue K, Murata I, Kohno S. Implication of NF-kappaB in *Helicobacter pylori*-associated gastritis. *Am J Gastroenterol* 2000; **95**: 2768-2776
- 33 **Yasui W**, Tahara H, Tahara E, Fujimoto J, Nakayama J, Ishikawa F, Ide T, Tahara E. Expression of telomerase catalytic component, telomerase reverse transcriptase, in human gastric carcinomas. *Jpn J Cancer Res* 1998; **89**: 1099-1103
- 34 **Kang SS**, Kwon T, Kwon DY, Do SI. Akt protein kinase enhances human telomerase activity through phosphorylation of telomerase reverse transcriptase subunit. *J Biol Chem* 1999; **274**: 13085-13090
- 35 **Lan J**, Xiong YY, Lin YX, Wang BC, Gong LL, Xu HS, Guo GS. *Helicobacter pylori* infection generated gastric cancer through p53-Rb tumor-suppressor system mutation and telomerase reactivation. *World J Gastroenterol* 2003; **9**: 54-58
- 36 **Yao XX**, Yin L, Sun ZC. The expression of hTERT mRNA and cellular immunity in gastric cancer and precancerosis. *World J Gastroenterol* 2002; **8**: 586-590
- 37 **Kammori M**, Kanauchi H, Nakamura K, Kawahara M, Weber TK, Mafune K, Kaminishi M, Takubo K. Demonstration of human telomerase reverse transcriptase in human colorectal carcinomas by *in situ* hybridization. *Int J Oncol* 2002; **20**: 15-21
- 38 **Jong HS**, Park YI, Kim S, Sohn JH, Kang SH, Song SH, Bang YJ, Kim NK. Up-regulation of human telomerase catalytic subunit during gastric carcinogenesis. *Cancer* 1999; **86**: 559-565
- 39 **Ueda M**, Kokura S, Imamoto E, Naito Y, Handa O, Takagi T, Yoshida N, Yoshikawa T. Blocking of NF-kappaB activation enhances the tumor necrosis factor alpha-induced apoptosis of a human gastric cancer cell line. *Cancer Lett* 2003; **193**: 177-182
- 40 **Akari H**, Bour S, Kao S, Adachi A, Strebler K. The human immunodeficiency virus type 1 accessory protein Vpu induces apoptosis by suppressing the nuclear factor kappaB-dependent expression of antiapoptotic factors. *J Exp Med* 2001; **194**: 1299-1311
- 41 **Akiyama M**, Hideshima T, Hayashi T, Tai YT, Mitsiades CS, Mitsiades N, Chauhan D, Richardson P, Munshi NC, Anderson KC. Nuclear factor-kappaB p65 mediates tumor necrosis factor alpha-induced nuclear translocation of telomerase reverse transcriptase protein. *Cancer Res* 2003; **63**: 18-21

Edited by Xia HHX and Wang XL

Correlation of tumor-positive ratio and number of perigastric lymph nodes with prognosis of gastric carcinoma in surgically-treated patients

Yong-Bin Ding, Guo-Yu Chen, Jian-Guo Xia, Xi-Wei Zang, Hong-Yu Yang, Li Yang, Yue-Xian Liu

Yong-Bin Ding, Guo-Yu Chen, Jian-Guo Xia, Xi-Wei Zang, Hong-Yu Yang, Li Yang, Department of General Surgery, First Affiliated Hospital of Nanjing Medical University, Nanjing 210029, Jiangsu Province, China

Yue-Xian Liu, Nanjing University of Traditional Chinese Medicine, Nanjing 210029, Jiangsu Province, China

Correspondence to: Yong-Bin Ding, Department of General Surgery, First Affiliated Hospital of Nanjing Medical University, Nanjing 210029, Jiangsu Province, China. njdyb@sina.com

Telephone: +86-25-86563750

Received: 2003-03-04 **Accepted:** 2003-04-19

Abstract

AIM: To evaluate the tumor-positive ratio and number of perigastric lymph nodes as prognostic factors of gastric carcinoma in surgically-treated patients.

METHODS: The postoperative survival of 169 patients with gastric cancer who were performed D₂ curative gastrectomy was analyzed with regard to its lymph node metastasis ratio and number. Meanwhile correlation of tumor-positive ratio and number of perigastric lymph nodes with pathological parameters of these patients was studied.

RESULTS: The overall 5-year survival rate of all the patients studied was 29.6%. The 5-year cumulative survival rate in patients with 1%-20% and more than 20% of tumor-positive lymph nodes was 70.6% and 12.0% respectively, and 46.6% and 17.4% in those with 1-5 and more than 5 of tumor-positive lymph nodes respectively, which were significantly decreased with the increment of involved lymph nodes assessed by either numbers or ratio ($P < 0.05$). Multiple stepwise regression analysis showed that both the positive ratio and number of tumor-involved lymph nodes were sensitive prognostic factors in these surgically-treated patients, which were also significantly correlated with tumor size and depth of submucosal invasion ($P < 0.05$).

CONCLUSION: Tumor-positive ratio and number of perigastric lymph nodes are associated with cancer progression and five-year survival rate, and may serve as valuable prognostic factors of gastric cancer in surgically-treated patients.

Ding YB, Chen GY, Xia JG, Zang XW, Yang HY, Yang L, Liu YX. Correlation of tumor-positive ratio and number of perigastric lymph nodes with prognosis of gastric carcinoma in surgically-treated patients. *World J Gastroenterol* 2004; 10(2): 182-185 <http://www.wjgnet.com/1007-9327/10/182.asp>

INTRODUCTION

It has been well recognized that lymph node metastasis in patients with gastric cancer is one of the important prognostic factors^[1-4]. In 1997, the International Union Contrele Cancer

(UICC) and American Joint Commission for Cancer (AJCC) redefined metastatic status of lymph node on the basis of the involved node number rather than its location, in which pN1 was defined as 1-6 local lymph nodes being involved, pN2 as 7-15 local lymph nodes being involved and pN3 as more than 15 local lymph nodes being involved^[5-7]. Some reports strongly suggested that this classification was more sensitive with a higher reproducibility in the prognostic evaluation of gastric cancer patients than that assessed by the metastatic locations of lymph node^[8,9]. However, In China there are few reports concerning the correlation of local lymph node metastatic ratio and number with the prognosis of gastric cancer patients, which was the motivation for us to initiate the present study of such cases in the Chinese population.

MATERIALS AND METHODS

Patients and materials

Between January 1995 and November 1997, 304 patients with primary gastric cancer were performed D₂ radical gastrectomy in the Department of General Surgery, First Affiliated Hospital of Nanjing Medical University. Of them, 121 male and 48 female cases aging from 32 to 78 years (mean, 58.4 years) were found to have lymph node metastasis, and analyzed in the present study, with a following-up time from 0 to 61 months postoperation.

Methods

The status of lymph nodes was assessed according to the staging system formulated by UICC/AJCC in 1997. Of the 169 patients with positive lymph nodes, 32 were found to have remote lymphatic metastasis such as that in the retropancreatic, mesenteric and paraortic regions. The total number of resected lymph nodes was 10 223 (mean: 34.1, range: 11-122), the median number of examined lymph nodes was 26 (mean: 31.1, range: 12 to 91) for all 304 patients, the median number of involved regional lymph nodes was 5.0 (mean: 7.1, range: 1 to 42). Lymph node metastasis ratio was defined as the number of metastatic lymph nodes to the total number of resected ones.

To elucidate the prognostic significance of metastatic lymph nodes, the clinical and histopathological records of these 169 patients were analyzed. The relationships of 5-year survival rate with sex, age, tumor location, histopathological grading, macroscopic type, lymph node resection and depth of tumor invasion were determined. Tumor location, macroscopic type, and lymph node resection were graded according to the Japanese classification of gastric carcinoma proposed by Japanese Gastric Carcinoma Association (JGCA). Histopathological grading was defined according to the fifth edition of TNM classification. Following-up information was obtained from routine clinical examinations.

Statistical analysis

Statistical analysis was carried out using SPSS 10.0 for Windows. The 5-year survival rate of those performed using D₂ radical gastrectomy was analyzed by cox's proportional

hazard models. The log rank test was used to compare the survival data between groups. Comparison between qualitative results for the PN categories and clinical or histopathological parameters was performed using the χ^2 test. Independent predictors of postoperation survival were identified by logistic regression analysis. Kaplan-Meier curves were used to demonstrate survival distribution.

RESULTS

Among the 304 patients, 169(55.6%) had lymph node metastasis. The 5-year survival rate was 29.6% for the node-positive patients, and was 91.2% for the node-negative patients. The cancer -specific 5-year survival rate of patients with lymph node metastasis was significantly lower than that of those without lymph node metastasis ($P<0.05$).

Correlation between lymph node metastatic ratio and 5-year survival rate

The patients were divided into two groups by the ratio of metastatic lymph node number to the total number of resected lymph nodes. The 5-year survival rate of 51 patients with metastatic lymph nodes less than 20% was 70.6%(36 cases), while that of 118 patients with 21% or more was 12% (14 cases). A significant difference was noted between the two groups ($P<0.05$, Table 1). As the ratio of lymph node metastasis increased, the 5-year survival rate decreased (Figure 1).

Table 1 Correlation between lymph node metastatic ratio and survival years

Ratio of positive lymph nodes	n	Survival years					P
		1	2	3	4	5	
<20%	51	51	49	45	39	36	<0.05
>21%	118	104	87	66	43	14 ^a	

^a $P<0.05$ vs the group with lymph node metastatic ratio less than 20%.

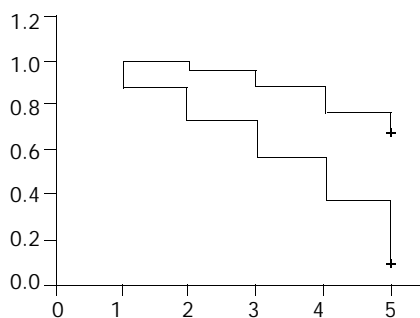


Figure 1 Negative correlation between survival years and ratio of metastatic lymph nodes in patients with gastric cancer. +: patients with metastatic ratio of lymph node less than 20%; -: patients with metastatic ratio of lymph node more than 21%.

Relation between lymph node metastasis number and 5-year survival rate

There was no significant difference in the outcome of patients with 1, 2, 3, 4 or 5 positive nodes, but there was a sharp decrease in survival rate when the sixth node was involved (Table 1), So the patients were divided into two groups according to the lymph node metastatic number. Group A having less than 5 and group B having more than 6. The 5-year survival rate of 71 patients with less than 5 metastatic lymph nodes was 46.6%(33 cases), and the 5-year survival rate of 98 patients with more than 6 metastatic lymph nodes was 17.4% (17 cases).

A sharp decrease in survival was seen between two groups ($P<0.05$, Table 2). The 5-year survival rate decreased as the number of lymph node metastases increased (Figure 2).

Table 2 Correlation between lymph node metastatic number and survival years

Number of positive lymph node	n	Survival years					P
		1	2	3	4	5	
1	9	9	9	8	6	5	
2	20	20	19	18	15	10	0.908
3	12	12	12	10	9	5	1.0
4	11	11	9	8	6	5	0.79
5	19	17	16	14	11	8	0.704
6	41	36	30	22	11	10	0.009
7	20	18	16	13	9	5	0.555
8	16	14	11	9	7	3	0.698
≥9	21	18	13	9	8	3	0.688
1-5	71	69	66	58	47	33	
>5	98	86	70	53	35	17	0.00072 ^a

^a $P<0.05$, vs the group with lymph node metastatic number more than 5.

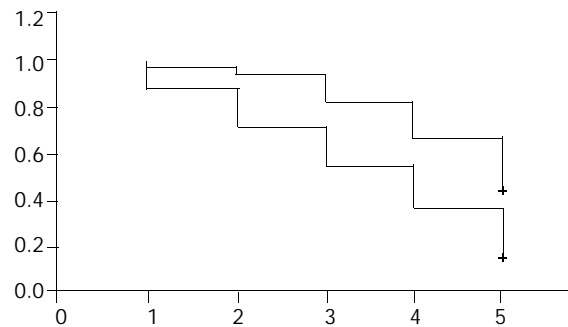


Figure 2 Negative correlations between survival years and number of metastatic lymph nodes in patients with gastric cancer. +: patients with metastatic number of lymph nodes less than 5; -: patients with metastatic number of lymph nodes more than 6.

Correlation between positive ratio of lymph node metastasis and tumor characteristics

As shown in Table 3, lymph node metastatic ratio was positively correlated to tumor size, depth of invasion. No significant difference was found between lymph node metastatic ratio and tumor location.

Table 3 Correlation between lymph node metastatic ratio and tumor characteristics

Pathological characteristics	Lymph node <20% metastatic ratio	>21%	P
Size of tumor			
<4 cm	42	43	
≥4 cm	9	74 ^a	0.48
location			
Lower third	5	8	
Middle third	22	47	
Upper third	24	63	<0.001
Depth of invasion			
Mucosa and submucosa	12	9	
Muscle and subserosa	16	6	
Serosa	23	103 ^b	<0.001

^a $P<0.05$, ^b $P<0.05$ vs the group with lymph node metastatic ratio less than 20%.

Correlation between number of positive lymph nodes and tumor characteristics

As shown in Table 4, tumors with one to five involved lymph nodes compared with those with six or more involved lymph nodes were significantly characterized by size, depth of invasion, there was no significant difference between the number of involved lymph nodes and tumor location.

Table 4 Correlation between number of involved lymph nodes and tumor characteristics

Pathological characteristics	Number of positive lymph nodes 1-5	>5	P
Size of tumor			
<4 cm	51	34	
≥4 cm	20	64 ^a	0.48
location			
Lower third	7	6	
Middle third	31	38	
Upper third	33	54	<0.05
Depth of invasion			
Mucosa and submucosa	20	1	
Muscle and subserosa	18	4	
Serosa	33	93 ^b	<0.05

^aP<0.05, ^bP<0.05 vs the group with lymph node metastatic number more than 5.

DISCUSSION

Gastric carcinoma, one of the most common human malignant tumors, is as the first leading cause of gastrointestinal cancer-related mortality. Over 50% of patients with gastric cancer operated in China had lymph node metastasis, which resulted in poor prognosis of these patients^[10-13]. As yet, lymph node status has been considered as the major determinant of gastric cancer recurrence for patients undergoing a curative gastrectomy^[14-16]. However, some authors suggested that the prognostic assessment of these patients by counting the number of positive lymph nodes related to tumor locations was too complicated to be used in routine practice. A simple and easy system for lymph node staging has been considered to be urgently needed^[14-16].

In the present study, we observed the effect of metastatic lymph node number on the survival years of gastric cancer patients. The result showed that the five-year survival rate in patients with 0, 1-5 and more than 5 tumor-positive lymph nodes was 91.2%, 46.6% and 17.4% respectively, indicating that considerable differences in the five-year survival rate existed between the patients. However, There was no significant difference observed between the outcomes of patients with 1, 2, 3, 4 and 5 tumor-positive lymph nodes. Thus it is more reasonable to classify gastric cancer patients with criteria of tumor-positive node numbers rather than tumor-positive nodes. Similar results have been revealed in a previous report by Wu *et al.* They divided the gastric cancer patients into two groups according to the number of involved lymph nodes, and found that the number of positive nodes rather than lymph node involvement was suitable for the classification of nodal stages in gastric cancer^[8,17,18].

Lymph node metastatic ratio, namely the number of metastatic lymph nodes to the total number of resected lymph nodes, has also been found to be an important prognostic factor^[19-22]. We observed that the 5-year survival rate in patients with the metastatic lymph node ratio of 0, 1-20% and more than 21%, was 91.2%, 70.6% and 12% respectively. Similar results have been shown by Kwon and his colleagues that the

metastatic ratio of lymph nodes was one of the main factors in determining the five-year survival rate of gastric cancer patients. Furthermore, the lymph node metastatic ratio has also been found to be more objective and reliable than the metastatic number in the prognosticating outcomes of these patients, because the former could effectively eliminate the influence of variance in resected lymph number on the prognosis of gastric cancer patients^[23-27].

It is generally accepted the depth of cancer invasion is an other important prognostic indicator in gastric cancer. Yasuda *et al* showed that the metastatic rate of lymph nodes was correlated with the depth of submucosal invasion in early stage of gastric carcinoma^[28,29], which was in accordance with our present results. We found that the number and ratio of metastatic lymph nodes were positively related with the depth of cancer invasion and tumor size in gastric cancer cases.

In conclusion, gastric cancer patients with 5 or more positive lymph nodes and 20% or more of positive lymph node metastasis associated with a poor prognosis. The positive number and ratio of lymph node metastasis are simple and useful indicators in evaluating the surgical results of patients with gastric cancer^[19,30,31].

REFERENCES

- 1 **Manfe AZ**, Segalina P, Maffei Faccioli A. Prognostic factors in gastric cancer. Our experience and review of the literature. *Minerva Chir* 2000; **55**: 299-305
- 2 **Takagane A**, Terashima M, Abe K, Araya M, Irinoda T, Yonezawa H, Nakaya T, Inaba T, Oyama K, Fujiwara H, Saito K. Evaluation of the ratio of lymph node metastasis as a prognostic factor in patients with gastric cancer. *Gastric Cancer* 1999; **2**: 122-128
- 3 **Yokota T**, Kunii Y, Teshima S, Yamada Y, Saito T, Takahashi M, Kikuchi S, Yamauchi H. Significant prognostic factors in patients with early gastric cancer. *Int Surg* 2000; **85**: 286-290
- 4 **Ding YB**, Chen GY, Xia JG, Zang XW, Yang HY, Yang L. Association of VCAM-1 Overexpression with oncogenesis, tumor angiogenesis and metastasis of gastric carcinoma. *World J Gastroenterol* 2003; **9**: 1409-1414
- 5 **Jahne J**. Lymphadenectomy in gastric carcinoma? *Zentralbl Chir* 2002; **127**: 550-553
- 6 **Hayashi H**, Ochiai T, Suzuki T, Shimada H, Hori S, Takeda A, Miyazawa Y. Superiority of a new UICC-TNM staging system for gastric carcinoma. *Surgery* 2000; **127**: 129-135
- 7 **Omejc M**, Juvan R, Jelenc F, Repse S. Lymph node metastases in gastric cancer: correlation between new and old UICC TNM classification. *Int Surg* 2001; **86**: 14-19
- 8 **Wu CW**, Hsieh MC, Lo SS, Shen KH, Lui WY, P'eng FK. Comparison of the UICC/AJCC 1992 and 1997 pN categories for gastric cancer patients after surgery. *Hepatogastroenterology* 2001; **48**: 279-284
- 9 **Katai H**, Yoshimura K, Maruyama K, Sasako M, Sano T. Evaluation of the New International Union Against Cancer TNM staging for gastric carcinoma. *Cancer* 2000; **88**: 1796-1800
- 10 **Abe N**, Watanabe T, Suzuki K, Machida H, Toda H, Nakaya Y, Masaki T, Mori T, Sugiyama M, Atomi Y. Risk factors predictive of lymph node metastasis in depressed early gastric cancer. *Am J Surg* 2002; **183**: 168-172
- 11 **Yamaguchi T**, Sano T, Katai H, Sasako M, Maruyama K. Node-positive mucosal gastric cancer: a follow-up study. *Jpn J Clin Oncol* 2001; **31**: 153-156
- 12 **de Manzoni G**, Verlato G, di Leo A, Guglielmi A, Laterza E, Ricci F, Cordiano C. Perigastric lymph node metastases in gastric cancer: comparison of different staging systems. *Gastric Cancer* 1999; **2**: 201-205
- 13 **Chen CY**, Wu CW, Lo SS, Hsieh MC, Lui WY, Shen KH. Peritoneal carcinomatosis and lymph node metastasis are prognostic indicators in patients with Borrmann type IV gastric carcinoma. *Hepatogastroenterology* 2002; **49**: 874-877
- 14 **Pan W**, Ishii H, Ebihara Y, Gobe G. Prognostic use of growth characteristics of early gastric cancer and expression patterns of apoptotic, cell proliferation, and cell adhesion proteins. *J Surg*

- Oncol* 2003; **82**: 104-110
- 15 **Nakamura K**, Morisaki T, Sugitani A, Ogawa T, Uchiyama A, Kinukawa N, Tanaka M. An early gastric carcinoma treatment strategy based on analysis of lymph node metastasis. *Cancer* 1999; **85**: 1500-1505
 - 16 **Kodera Y**, Yamamura Y, Shimizu Y, Torii A, Hirai T, Yasui K, Morimoto T, Kato T, Kito T. Lymph node status assessment for gastric carcinoma: is the number of metastatic lymph nodes really practical as a parameter for N categories in the TNM Classification? *Tumor Node Metastasis. J Surg Oncol* 1998; **69**: 15-20
 - 17 **Shimada S**, Yagi Y, Honmyo U, Shiomori K, Yoshida N, Ogawa M. Involvement of three or more lymph nodes predicts poor prognosis in submucosal gastric carcinoma. *Gastric Cancer* 2001; **4**: 54-59
 - 18 **Bouvier AM**, Haas O, Piard F, Roignot P, Bonithon-Kopp C, Faivre J. How many nodes must be examined to accurately stage gastric carcinomas? Results from a population based study. *Cancer* 2002; **94**: 2862-2866
 - 19 **Inoue K**, Nakane Y, Iiyama H, Sato M, Kanbara T, Nakai K, Okumura S, Yamamichi K, Hioki K. The superiority of ratio-based lymph node staging in gastric carcinoma. *Ann Surg Oncol* 2002; **9**: 27-34
 - 20 **Yasuda K**, Shiraishi N, Suematsu T, Yamaguchi K, Adachi Y, Kitano S. Rate of detection of lymph node metastasis is correlated with the depth of submucosal invasion in early stage gastric carcinoma. *Cancer* 1999; **85**: 2119-2123
 - 21 **Bando E**, Yonemura Y, Taniguchi K, Fushida S, Fujimura T, Miwa K. Outcome of ratio of lymph node metastasis in gastric carcinoma. *Ann Surg Oncol* 2002; **9**: 775-784
 - 22 **Hyung WJ**, Noh SH, Yoo CH, Huh JH, Shin DW, Lah KH, Lee JH, Choi SH, Min JS. Prognostic significance of metastatic lymph node ratio in T3 gastric cancer. *World J Surg* 2002; **26**: 323-329
 - 23 **Yin T**, Ji XL, Shen MS. Relationship between lymph node sinuses with blood and lymphatic metastasis of gastric cancer. *World J Gastroenterol* 2003; **9**: 40-43
 - 24 **Lee E**, Chae Y, Kim I, Choi J, Yeom B, Leong AS. Prognostic relevance of immunohistochemically detected lymph node micrometastasis in patients with gastric carcinoma. *Cancer* 2002; **94**: 2867-2873
 - 25 **Choi HJ**, Kim YK, Kim YH, Kim SS, Hong SH. Occurrence and prognostic implications of micrometastases in lymph nodes from patients with submucosal gastric carcinoma. *Ann Surg Oncol* 2002; **9**: 13-19
 - 26 **Tsujitani S**, Kaibara N. Clinical significance of molecular biological detection of micrometastases in gastric carcinoma. *Nippon Geka Gakkai Zasshi* 2001; **102**: 741-744
 - 27 **Fukagawa T**, Sasako M, Mann GB, Sano T, Katai H, Maruyama K, Nakanishi Y, Shimoda T. Immunohistochemically detected micrometastases of the lymph nodes in patients with gastric carcinoma. *Cancer* 2001; **92**: 753-760
 - 28 **Monig SP**, Zirbes TK, Schroder W, Baldus SE, Lindemann DG, Dienes HP, Holscher AH. Staging of gastric cancer: correlation of lymph node size and metastatic infiltration. *Am J Roentgenol* 1999; **173**: 365-367
 - 29 **Saiura A**, Umekita N, Inoue S, Maeshiro T, Miyamoto S, Matsui Y, Asakage M, Kitamura M. Clinicopathological features and outcome of hepatic resection for liver metastasis from gastric cancer. *Hepatogastroenterology* 2002; **49**: 1062-1065
 - 30 **Yoshizumi Y**, Matuyama T, Koike H, Aiko S, Sugiura Y, Maehara T. Long-term survival after gastric cancer and liver and paraaortic lymph node metastases: report of a case. *Surg Today* 2001; **31**: 159-162
 - 31 **Kologlu M**, Kama NA, Reis E, Doganay M, Atli M, Dolapci M. A prognostic score for gastric cancer. *Am J Surg* 2000; **179**: 521-526

Edited by Zhu L and Wang XL

Construction of a targeting Adenoviral vector carrying AFP promoter for expressing EGFP gene in AFP producing hepatocarcinoma cell

Yu-Jun Shi, Jian-Ping Gong, Chang-An Liu, Xu-Hong Li, Ying Mei, Can Mi, Yan-Ying Huo

Yu-Jun Shi, Jian-Ping Gong, Chang-An Liu, Xu-Hong Li, Ying Mei, Department of General Surgery, the Second College of Clinical Medicine and the Second Affiliated Hospital of Chongqing University of Medical Sciences, Chongqing 400010, China

Can Mi, Department of Pathology, Basic Medical College, Chongqing University of Medical Sciences, Chongqing 400016, China

Yan-Ying Huo, Institute for Radiology, Military Academy of Medical Sciences, Beijing 100850, China

Supported by the Key Program of Medical Science Foundation of Chongqing Public Health Bureau, [2001] 01-1-018

Correspondence to: Professor Chang-An Liu, Department of General Surgery, the Second College of Clinical Medicine and the Second Affiliated Hospital of Chongqing University of Medical Science, Chongqing 400010, China. shiyujun1128@hotmail.com

Telephone: +86-23-63848842

Received: 2003-08-11 **Accepted:** 2003-10-23

Abstract

AIM: To construct a recombinant adenoviral vector carrying AFP promoter and EGFP gene for specific expression of EGFP gene in AFP producing hepatocellular carcinoma (HCC) HepG2 cells.

METHODS: Based on the Adeno-X™ expression system, the human immediate early cytomegalovirus promoter (P_{CMV IE}) was removed from the plasmid, *pshuttle*, and replaced by a 0.3 kb α -fetoprotein (AFP) promoter that was synthesized by polymerase chain reaction (PCR). The enhanced green fluorescent protein (EGFP) gene was inserted into the multi-clone site (MCS), and then the recombinant adenovirus vector carrying the 0.3 kb AFP promoter and EGFP gene was constructed. Cells of a normal liver cell line (LO2), a hepatocarcinoma cell line (HepG2) and a cervical cancer cell line (HeLa) were transfected with the adenovirus. Northern blot and fluorescence microscopy were used to detect the expression of the EGFP gene at mRNA or protein level in three different cell lines.

RESULTS: The 0.3 kb AFP promoter was synthesized through PCR from the human genome. The AFP promoter and EGFP gene were directly inserted into the plasmid *pshuttle* as confirmed by restriction digestion and DNA sequencing. Northern blot showed that EGFP gene was markedly transcribed in HepG2 cells, but only slightly in LO2 and HeLa cells. In addition, strong green fluorescence was observed in HepG2 cells under a fluorescence microscopy, but fluorescence was very weak LO2 and HeLa cells.

CONCLUSION: Under control of the 0.3 kb human AFP promoter, the recombinant adenovirus vector carrying EGFP gene can be specially expressed in AFP-producing HepG2 cells. Therefore, this adenovirus system can be used as a novel, potent and specific tool for gene-targeting therapy for the AFP positive primary hepatocellular carcinoma.

Shi YJ, Gong JP, Liu CA, Li XH, Mei Y, Mi C, Huo YY. Construction of a targeting Adenoviral vector carrying AFP promoter for

expressing EGFP gene in AFP producing hepatocarcinoma cell. *World J Gastroenterol* 2004; 10(2): 186-189

<http://www.wjgnet.com/1007-9327/10/186.asp>

INTRODUCTION

In recent years, research in tumor gene therapy has made great progress in laboratory. However, there is an urgent need for gene therapy in clinical practice. Recombinant adenovirus is one of the most popular and promising tools for gene therapy^[1,2]. But how to construct a proper recombinant adenovirus vector carrying the interested gene that is specifically expressed only in target tumor cells has become the bottle neck which restricts the application of the vector in clinical gene therapy for tumors^[3,4]. The aim of this study was to construct a recombinant adenovirus vector carrying a 0.3 kb AFP promoter, and to investigate the expression of enhanced green fluorescent protein (EGFP) gene that was inserted into the vector in AFP positive hepatocarcinoma cells.

MATERIALS AND METHODS

Reagents

EX Taq DNA polymerase, T4 ligase, DNA isolation and purification kit were purchased from Promega (USA), restriction endonucleases and the DNA marker from Takara Biotechnology, Dalian (China), Lipofectamin™ 2000 from Invitrogen (USA), and RPMI 1640 medium and fetal calf serum from Hyclone (USA).

Cell lines

Hepatocarcinoma cell line, HepG2, was a gift from Professor Wei-Xue Tang, Department of Pathophysiology, Chongqing University of Medical Sciences. A normal hepatocyte cell line, LO2, and human cervical cancer cell line, HeLa, were preserved in our laboratory. Low-passage HEK 293 cells were obtained from the Institute for Cytobiology, Chinese Academy of Sciences, Shanghai. All cells were cultured in RPMI-1640 medium containing 10% fetal calf serum at 37 °C in saturated humidified air with 5% CO₂. The cells were subcultured once every three days.

Vectors

Adenovirus vector Adeno-X™ expression system and *pEGFP-C1* were purchased from Clontech Corporation (USA).

Polymerase chain reaction (PCR)

PCR was employed to amplify human AFP promoter and EGFP gene from HepG2 cell genomic DNA and *pEGFP-C1*, respectively. Specific primers for AFP promoter were as follows: 5' -GCG CTA GCA TTC TGT AGT TTG AGG AG-3' (sense), 5' -ATG GGC CCA TTG GCA GTG GTG GAA-3' (antisense). *NheI* and *ApaI* sites were introduced into the sense and antisense primer, respectively, as underlined. Specific primers for EGFP gene were as follows: 5' -AAG GGC CCT TTA GTG AAC CGT CAG AT-3' (sense), 5' -GCCTTA AGT

TAT CTA GAT CCG GTG GAT-3' (antisense). *ApaI* and *AflIII* sites were introduced into the sense and antisense primer, respectively.

To remove the p_{CMVIE} from the *pshuttle*, PCR was used to amplify the 99-744 region of *pshuttle*, and specific primers were as follows: 5' -AGC CAG TAT CTG CTC CCT GCT TGT G-3' (sense), 5' -ATG CTA GCG GTG CCA AAA CAA ACT CCC A-3' (antisense). *NheI* site was introduced into the antisense primer.

PCR was performed in a total volume of 50 μ l consisting of 1 μ M each primer, 200 μ M each dNTP, 5 μ l 10 \times polymerase reaction buffer, 1.25U EX taq DNA polymerase and 1 μ l DNA template. The samples were heated to 94 $^{\circ}$ C for 5 min followed by amplification for 30 cycles at 94 $^{\circ}$ C for 30 s, 55 $^{\circ}$ C for 30 s, and 72 $^{\circ}$ C for 50 s. After the last cycle, a final extension step was at 72 $^{\circ}$ C for 7 min. Then 5 μ l of each product was analyzed by 1% agarose gel (containing 0.5 μ g/ml EB) electrophoresis. PCR products were purified from the agarose gel using DNA purification kit.

Construction of the adenoviral vector

pshuttle and the PCR products of 99-744 region were both doubly digested with *MluI* and *NheI*, and the digested products were ligated with T4 ligase. *MluI* site was 256, and the *NheI* was 921 in *pshuttle*. The 256-921 region of the *pshuttle* was removed from the plasmid, and replaced by the region of 256-744, then the 744-921 region containing the p_{CMVIE} was removed from *pshuttle*. Thus, a new plasmid p_{CMV}^{-} was constructed.

Subsequently, the p_{CMV}^{-} and *AFP* PCR products were doubly digested with *NheI* and *ApaI*. The 0.3 kb *AFP* promoter was inserted into the p_{CMV}^{-} , which was called *pAFP*. Then the p_{CMVIE} was replaced by the *AFP* promoter.

To insert the *EGFP* gene into the *pAFP*, both the *pAFP* and *EGFP* PCR products were doubly digested with *ApaI* and *AflIII*. The digested products were ligated to construct *pAFP-EGFP*.

The newly constructed plasmid *pAFP-EGFP* was then doubly digested with *PI-SceI/Ceu I* (New England Biolabs, UK), and the purified product was ligated with Adeno-X genome DNA. It was amplified in *E. coli DH5a*. The HEK293 cells were transfected with recombinant adenovirus which was linearized with *PacI*, as described in the manual. In brief, the HEK293 cells were cultured in a 60 mm plate, and 10 μ l *Pac I*-digested Adeno-X DNA was added in the culture medium when the cells were 50-70% confluent, then the cells were transfected with Lipofectamin and incubated for another week. For virus collection, the cells were lysed with three consecutive freeze-thaw cycles, and the virus was collected from supernatant. The titer of the virus was about 1×10^7 pfu/ml, which was determined with end-point dilution assay.

Northern blot analysis

HepG2, LO2 and HeLa cells were cultured in 6-well plates, and the medium was removed after 24 h, followed by addition of adenovirus at multiplicity of infection (M.O.I) of 100 plaque-forming units (pfu)/cell, and fresh culture medium was added 4 h later. After 48 h of normal culture, total RNA was extracted from the cells for Northern blot. In brief, 10 μ g total RNA of each sample was added to 10 g \cdot L $^{-1}$ formaldehyde denatured agarose gel, and electrophoresis was performed. mRNA was transferred onto the nitrocellular (NC) membranes by capillary blot, and exposed to 254 nm ultraviolet for 1 min ($600 \times 100 \mu$ J \cdot cm $^{-1}$) to fix mRNA. The NC membranes were pre-hybridized for 3 h at 42 $^{\circ}$ C. The cDNA probes were labeled by a random primer method. The probes were added and hybridized at 42 $^{\circ}$ C for 20 h. Then the membranes were washed,

dried and used for X-ray film autoradiography at -70 $^{\circ}$ C in a black box for 48 h. The relative amount of *EGFP* cDNA was semi-quantified from relative optical density of the band, using a Bio-image analysis system (Bio-Rad Doc Gel 2000, USA).

Fluorescence microscopy

The cells were cultured and transfected with the recombinant adenovirus as described above. Fluorescent images were captured at 490 nm using a Nikon Eclipse E1000 microscope.

RESULTS

PCR amplification and DNA sequencing of *AFP* promoter

Electrophoretic results of PCR product of the human 0.3 kb *AFP* promoter are shown in Figure 1. The sequence of the promoter was described as below:

```
gcgctagcat tctgtagttt gaggagaata ttgttatat ttgcaaaata aaataagttt
NheI -229
gcaagttttt tttttctgcc ccaaagagct ctgtgctct gaacataaaa tacaataaac
GRE
cgctctgctg taattattg gcaaatgtcc cattttcaac ctaaggaaat accataaagt
HNF-1
aacagatata ccaacaaaag gttactagtt aacaggcatt gctgaaaag agtataaaaag
HNF-1
aattcageca tgattttcca tattgtgcttc caccactgcc aatgggccc a
+25 Apa I
```

The *AFP* promoter region of -229 to 25 was indicated with italics; GRE: glucocorticoid response element; HNF-1: hepatocyte nuclear factor; *tata*: TATA Box.

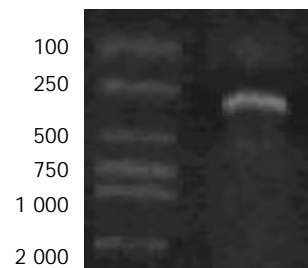


Figure 1 Human 0.3 kb *AFP* promoter.

Enzyme digestion analysis of the recombinant *pshuttle*

The plasmid *pshuttle* and the 99-744 region of the PCR product were both doubly digested with *MluI* and *NheI* (Figure 2). A 670 bp fragment was released from *pshuttle*, and replaced by a 490 bp fragment that was digested from the PCR product. The p_{CMVIE} was removed from the *pshuttle*.

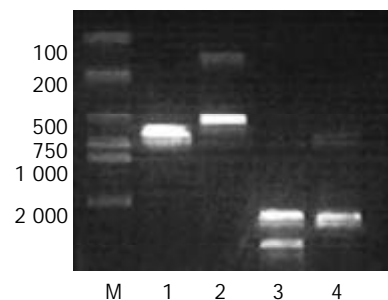


Figure 2 Plasmid *pshuttle* and PCR product doubly-digested with *MluI/NheI*. M: marker, 1: the PCR product of 99-744 region of *pshuttle*, 2: the product of PCR doubly digested with *MluI/NheI*, 3: *pshuttle*, 4: doubly-digested *pshuttle* with *MluI/NheI*, a 670 bp fragment was released from *pshuttle*.

Specific expression of EGFP gene in HepG2 cells

As shown in Figure 3, strong expression of *EGFP* mRNA was observed in HepG2 cells but was weak in AFP negative LO2 and HeLa cells, only 38% and 17% of that in HepG2 cells, respectively.

Under fluorescence microscopy, green fluorescence indicating expression of EGFP was strong in HepG2 cells (Figure 4A) but very weak in LO2 (Figure 4B) and invisible in HeLa cells.

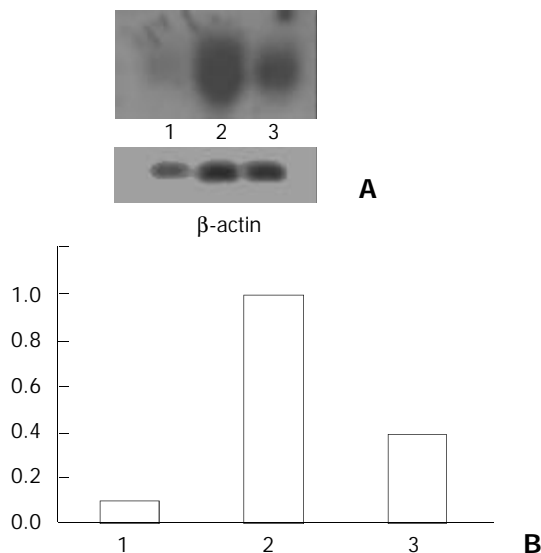


Figure 3 A: Transcription levels of *EGFP* shown by Northern blot in three different cell lines, B: Transcription levels of *EGFP* gene detected by semi-quantity analysis in three cell lines. Lane 1, HeLa cell; lane 2, HepG2 cell; lane 3, LO2 cell.

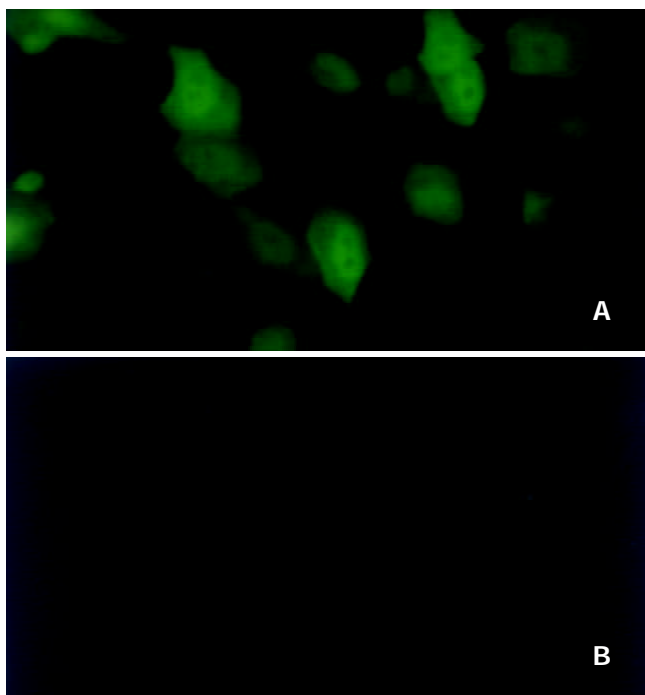


Figure 4 Expression of *EGFP* mRNA in HepG2 cells (A) and LO2 cells (B) $\times 200$.

DISCUSSION

Hepatocellular carcinoma (HCC) is one of the most common malignancies worldwide. All the treatment strategies used today had a poor outcome^[5-7]. Gene therapy might be a promising

way^[8,9]. Gene transfer into specific tissues or cell types is a key technique in the development of gene therapy. A tissue-specific promoter has been found to be potentially valuable for the study of specific gene function and for gene therapy^[10-14], as it permitted a linked cytotoxic or any other gene to be expressed specifically in target cells^[15-17]. The AFP could be re-expressed in the majority of hepatocellular carcinomas^[18,19], and thus utility of the *AFP* promoter for gene therapy against HCC might be a rational approach^[20-22].

Adenoviral gene transfer is one of the most reliable methods for introducing genes into almost all types of mammalian cells and for expressing the genes at high levels since many cells receive multiple copies of the recombinant genome. Gene therapy using replication-competent adenovirus that selectively propagates in tumor cells might be an effective treatment for cancer^[23,24]. We developed an adenovirus carrying an *AFP* promoter, thus the replication of the target gene was restricted specifically in AFP-producing HCC^[25]. The full length *AFP* promoter was 5.1 kb^[26,27], previous studies have shown that the 0.3 kb of the *AFP* promoter had an enough activity to stimulate *AFP* transcription containing a glucocorticoid response element and two binding sites of hepatocyte nuclear factor (HNF)-1, a hepatocyte-specific transcriptional factor, and a TATA box, but no typical CCAAT sequence^[28,29].

In this study, primers containing specific enzyme-cutting sites were designed to amplify the 0.3 kb *AFP* promoter from human genome, and the 0.3 kb sequence was cloned into the plasmid *pshuttle* to replace the primary *CMV* promoter. *EGFP* gene as a target gene was inserted into the downstream of *AFP* promoter. Then AFP expressing hepatocarcinoma cells (HepG2), AFP negative normal hepatocytes (LO2) and HeLa cells were transfected with the recombinant adenovirus. Northern blot showed that *EGFP* gene was dramatically transcribed in HepG2 cells, however, in LO2 and HeLa cells, the transcription was very weak. Under fluorescent microscopy, green fluorescence was strong in HepG2 cells, but very weak in the other two cell lines. Therefore, this recombinant adenovirus carrying the 0.3 kb *AFP* promoter can be used as a proper vector to express the interested gene in AFP expressing hepatocarcinoma cells or tissues.

It has been reported that the promoter activity of 0.3 kb *AFP* promoter was limited for transcription of downstream genes^[30,31]. For this reason, several enhancers have been inserted into the upstream of the promoter in order to upgrade its activity^[32-35]. In our study, the original enhancer in *pshuttle* was reserved, which might contribute to the satisfactory transcription of the downstream gene using the 0.3 kb promoter.

REFERENCES

- 1 **Alemay R**, Lai S, Lou YC, Jan HY, Fang X, Zhang WW. Complementary adenoviral vectors for oncolysis. *Cancer Gene Ther* 1999; **6**: 21-25
- 2 **Kanai F**. Transcriptional targeted gene therapy for hepatocellular carcinoma by adenovirus vector. *Mol Biotechnol* 2001; **18**: 243-250
- 3 **Murayama Y**, Tadakuma T, Kunitomi M, Kumai K, Tsutsui K, Yasuda T, Kitajima M. Cell-specific expression of the diphtheria toxin A-chain coding sequence under the control of the upstream region of the human alpha-fetoprotein gene. *J Surg Oncol* 1999; **70**: 145-149
- 4 **Bui LA**, Butterfield LH, Kim JY, Ribas A, Seu P, Lau R, Glaspy JA, McBride WH, Economou JS. *In vivo* therapy of hepatocellular carcinoma with a tumor-specific adenoviral vector expressing interleukin-2. *Hum Gene Ther* 1997; **8**: 2173-2182
- 5 **Tang ZY**. Hepatocellular carcinoma—cause, treatment and metastasis. *World J Gastroenterol* 2001; **7**: 445-454
- 6 **Di Maio M**, De Maio E, Perrone F, Pignata S, Daniele B. Hepatocellular carcinoma: systemic treatments. *J Clin Gastroenterol* 2002; **35**(5 Suppl 2): S109-114

- 7 **Lin DY**, Lin SM, Liaw YF. Non-surgical treatment of hepatocellular carcinoma. *J Gastroenterol Hepatol* 1997; **12**: S319-328
- 8 **Raper SE**, Wilson JM. Gene therapy for human liver disease. *Prog Liver Dis* 1995; **13**: 201-230
- 9 **Huang TG**, Savontaus MJ, Shinozaki K, Sauter BV, Woo SL. Telomerase-dependent oncolytic adenovirus for cancer treatment. *Gene Ther* 2003; **10**: 1241-1247
- 10 **Sato Y**, Tanaka K, Lee G, Kanegae Y, Sakai Y, Kaneko S, Nakabayashi H, Tamaoki T, Saito I. Enhanced and specific gene expression via tissue-specific production of Cre recombinase using adenovirus vector. *Biochem Biophys Res Commun* 1998; **244**: 455-462
- 11 **Igarashi T**, Suzuki S, Takahashi M, Tamaoki T, Shimada T. A novel strategy of cell targeting based on tissue-specific expression of the ecotropic retrovirus receptor gene. *Hum Gene Ther* 1998; **9**: 2691-2698
- 12 **Dachs GU**, Dougherty GJ, Stratford IJ, Chaplin DJ. Targeting gene therapy to cancer: a review. *Oncol Res* 1997; **9**: 313-325
- 13 **Kanai F**, Lan KH, Shiratori Y, Tanaka T, Ohashi M, Okudaira T, Yoshida Y, Wakimoto H, Hamada H, Nakabayashi H, Tamaoki T, Omata M. *In vivo* gene therapy for alpha-fetoprotein-producing hepatocellular carcinoma by adenovirus-mediated transfer of cytosine deaminase gene. *Cancer Res* 1997; **57**: 461-465
- 14 **Xu GW**, Sun ZT, Forrester K, Wang XW, Coursen J, Harris CC. Tissue-specific growth suppression and chemosensitivity promotion in human hepatocellular carcinoma cells by retroviral-mediated transfer of the wild-type p53 gene. *Hepatology* 1996; **24**: 1264-1268
- 15 **Hanke P**, Serwe M, Dombrowski F, Sauerbruch T, Caselmann WH. DNA vaccination with AFP-encoding plasmid DNA prevents growth of subcutaneous AFP-expressing tumors and does not interfere with liver regeneration in mice. *Cancer Gene Ther* 2002; **9**: 346-355
- 16 **Vollmer CM Jr**, Eilber FC, Butterfield LH, Ribas A, Dissette VB, Koh A, Montejo LD, Lee MC, Andrews KJ, McBride WH, Glaspy JA, Economou JS. Alpha-fetoprotein-specific genetic immunotherapy for hepatocellular carcinoma. *Cancer Res* 1999; **59**: 3064-3067
- 17 **Wang XW**, Xu B. Several new targets of antitumor agents. *Zhongguo Yaoli Xuebao* 1997; **18**: 289-292
- 18 **Johnson PJ**. Role of alpha-fetoprotein in the diagnosis and management of hepatocellular carcinoma. *J Gastroenterol Hepatol* 1999; **14**(Suppl): S32-36
- 19 **Chen XP**, Zhao H, Zhao XP. Alternation of AFP-mRNA level detected in blood circulation during liver resection for HCC and its significance. *World J Gastroenterol* 2002; **8**: 818-821
- 20 **Lu SY**, Sui YF, Li ZS, Pan CE, Ye J, Wang WY. Construction of a regulable gene therapy vector targeting for hepatocellular carcinoma. *World J Gastroenterol* 2003; **9**: 688-691
- 21 **Wills KN**, Huang WM, Harris MP, Macherer T, Maneval DC, Gregory RJ. Gene therapy for hepatocellular carcinoma: chemosensitivity conferred by adenovirus-mediated transfer of the HSV-1 thymidine kinase gene. *Cancer Gene Ther* 1995; **2**: 191-197
- 22 **Barajas M**, Mazzolini G, Genove G, Bilbao R, Narvaiza I, Schmitz V, Sangro B, Melero I, Qian C, Prieto J. Gene therapy of orthotopic hepatocellular carcinoma in rats using adenovirus coding for interleukin12. *Hepatology* 2001; **33**: 52-61
- 23 **Ferry N**. Gene therapy of primary cancers of the liver: hopes and realities. *Bull Cancer* 1997; **84**: 431-434
- 24 **Kaneko S**, Hallenbeck P, Kotani T, Nakabayashi H, McGarrity G, Tamaoki T, Anderson WF, Chiang YL. Adenovirus-mediated gene therapy of hepatocellular carcinoma using cancer-specific gene expression. *Cancer Res* 1995; **55**: 5283-5287
- 25 **Ohashi M**, Kanai F, Tateishi K, Taniguchi H, Marignani PA, Yoshida Y, Shiratori Y, Hamada H, Omata M. Target gene therapy for alpha-fetoprotein-producing hepatocellular carcinoma by E1B55k-attenuated adenovirus. *Biochem Biophys Res Commun* 2001; **282**: 529-535
- 26 **Nakabayashi H**, Hashimoto T, Miyao Y, Tjong KK, Chan J, Tamaoki T. A position-dependent silencer plays a major role in repressing alpha-fetoprotein expression in human hepatoma. *Mol Cell Biol* 1991; **11**: 5885-5893
- 27 **Kaneko S**, Tamaoki T. Gene therapy vectors harboring AFP regulatory sequences. Preparation of an adenoviral vector. *Mol Biotechnol* 2001; **19**: 323-330
- 28 **Tamaoki T**. Human alpha-fetoprotein transcriptional regulatory sequences. Application to gene therapy. *Adv Exp Med Biol* 2000; **465**: 47-56
- 29 **Ido A**, Nakata K, Kato Y, Nakao K, Murata K, Fujita M, Ishii N, Tamaoki T, Shiku H, Nagataki S. Gene therapy for hepatoma cells using a retrovirus vector carrying herpes simplex virus thymidine kinase gene under the control of human alpha-fetoprotein gene promoter. *Cancer Res* 1995; **55**: 3105-3109
- 30 **Bilbao R**, Gerolami R, Bralet MP, Qian C, Tran PL, Tennant B, Prieto J, Brechet C. Transduction efficacy, antitumoral effect, and toxicity of adenovirus-mediated herpes simplex virus thymidine kinase/ganciclovir therapy of hepatocellular carcinoma: the woodchuck animal model. *Cancer Gene Ther* 2000; **7**: 657-662
- 31 **Ohguchi S**, Nakatsukasa H, Higashi T, Ashida K, Nouse K, Ishizaki M, Hino N, Kobayashi Y, Uematsu S, Tsuji T. Expression of alpha-fetoprotein and albumin genes in human hepatocellular carcinomas: limitations in the application of the genes for targeting human hepatocellular carcinoma in gene therapy. *Hepatology* 1998; **27**: 599-607
- 32 **Cao G**, Kuriyama S, Tsujinoue H, Chen Q, Mitoro A, Qi Z. A novel approach for inducing enhanced and selective transgene expression in hepatocellular-carcinoma cells. *Int J Cancer* 2000; **87**: 247-252
- 33 **Ido A**, Uto H, Moriuchi A, Nagata K, Onaga Y, Onaga M, Hori T, Hirono S, Hayashi K, Tamaoki T, Tsubouchi H. Gene therapy targeting for hepatocellular carcinoma: selective and enhanced suicide gene expression regulated by a hypoxia-inducible enhancer linked to a human alpha-fetoprotein promoter. *Cancer Res* 2001; **61**: 3016-3021
- 34 **Ishikawa H**, Nakata K, Mawatari F, Ueki T, Tsuruta S, Ido A, Nakao K, Kato Y, Ishii N, Eguchi K. Utilization of variant-type of human alpha-fetoprotein promoter in gene therapy targeting for hepatocellular carcinoma. *Gene Ther* 1999; **6**: 465-470
- 35 **Cao G**, Kuriyama S, Gao J, Nakatani T, Chen Q, Yoshiji H, Zhao L, Kojima H, Dong Y, Fukui H, Hou J. Gene therapy for hepatocellular carcinoma based on tumour-selective suicide gene expression using the alpha-fetoprotein (AFP) enhancer and a housekeeping gene promoter. *Eur J Cancer* 2001; **37**: 140-147

Effects of p53 on apoptosis and proliferation of hepatocellular carcinoma cells treated with transcatheter arterial chemoembolization

En-Hua Xiao, Jing-Qing Li, Jie-Fu Huang

En-Hua Xiao, Department of Radiology, the Second Xiangya Hospital, Central South University, Changsha 410011, Hunan Province, China

Jin-Qing Li, Jie-Fu Huang, Liver Cancer Research Center, Sun Yat-Sen University of Medical Sciences, Guangzhou 510060, Guangdong Province, China

Supported by the National Natural Science Foundation of China, No. 30070235

Correspondence to: Dr. En-Hua Xiao, Department of Radiology, the Second Xiangya Hospital, Central South University, Changsha 410011, Hunan Province, China. xiaogdk@sohu.com

Telephone: +86-731-5550355

Received: 2003-06-05 **Accepted:** 2003-07-30

Abstract

AIM: To evaluate the effects of p53 on apoptosis and proliferation of hepatocellular carcinoma (HCC) cells treated with transcatheter arterial chemoembolization (TACE).

METHODS: A total of 136 patients with HCC received TACE and other management before surgery were divided into TACE group and non-TACE group. TACE group included 79 patients who had 1-5 courses of TACE before surgery, of them, 11 patients had 1-4 courses of chemotherapy (group A), 33 patients had 1-5 courses of chemotherapy combined with iodized oil (group B), 23 patients had 1-3 courses of chemotherapy, iodized oil and gelatin sponge (group C), 12 patients had 1-3 courses of chemotherapy combined with iodized oil, ethanol and gelatin sponge (group D). Non-TACE group included the remaining 57 patients who had surgery only. The extent of apoptosis was analyzed by transferase mediated dUTP nick end labeling (TUNEL) staining. The expressions of p53, Bcl-2, Bax, Ki-67 and PCNA protein were detected by immunohistochemical method.

RESULTS: P53 protein expressions in trabecular and clear cells in HCC specimens were significantly lower than that in pseudoglandular, solid, poorly differentiated or undifferentiated and sclerosis HCC ($P < 0.05$). Expression of p53 protein in HCC cells increased with the increase of pathological grades ($P < 0.05$), and correlated positively with expressions of Ki-67 and PCNA protein, and negatively with Bcl-2 to Bax protein expression rate and AI ($P < 0.05$). Expression of p53 protein was significantly higher in group A than in groups B, C, D and the non-TACE group, and was higher in group B than in groups C and D, and lower in group D than in the non-TACE group ($P < 0.05$).

CONCLUSION: Expression of p53 protein can enhance proliferation of HCC cells and suppress apoptosis of HCC cells after TACE.

Xiao EH, Li JQ, Huang JF. Effects of p53 on apoptosis and proliferation of hepatocellular carcinoma cells treated with transcatheter arterial chemoembolization. *World J Gastroenterol* 2004; 10(2): 190-194

<http://www.wjgnet.com/1007-9327/10/190.asp>

INTRODUCTION

Hepatocellular carcinoma (HCC) is one of the most common malignancies. Surgical resection has been recognized as the most effective method for the treatment of HCC^[1,2], but it is only indicated for small number of HCC patients. Transcatheter arterial chemoembolization (TACE) has become one of the most popular and effective palliative methods for HCC. Various mixtures of anticancer drugs, Lipiodol and gelatin sponge have been used as TACE agents. There have been a few reports on comparison of the efficacy of different TACE regimens on HCC patients^[3].

Cellular homeostasis in tissue depends on the balance between apoptosis and cell proliferation. Wild-type p53 protein inhibits the growth of tumor by arrest of cell proliferation and induction of apoptosis^[4]. Bcl-2 and Bax protein are important regulators of apoptosis^[5]. Bcl-2 proteins can prolong cell survival by suppressing apoptosis, and Bax proteins can enhance apoptosis^[6]. PCNA and Ki-67 protein are useful markers for proliferative activity^[7]. PCNA functions as a cofactor of DNA-polymerase and an important mark for evaluating the proliferation of colon cancer^[8], gastric adenocarcinoma^[9], *H pylori* associated gastric epithelial lesions^[10], lung cancer^[11], ovarian cancer^[12], large intestine polyps^[13] and HCC^[14,15].

As far as we know, the effect of p53 on apoptosis and proliferation of HCC cells treated with different TACE regimens has not been investigated yet. In particular, it is unclear whether p53 can affect apoptosis and proliferation of HCC cells treated with TACE by modulating the expressions of Bcl-2, Bax, PCNA and Ki-67 proteins. In the present study, we examined the effects of p53 on apoptosis and proliferation of HCC cells treated with TACE alone or in combination with others.

MATERIALS AND METHODS

Patients

From February 1992 to February 2001, 136 patients with HCC were referred to our hospital for surgery, including 122 men and 14 women with a mean age of 45 years (range 20 to 70 years). Preoperative ultrasound (US), computed tomography (CT), magnetic resonance (MRI), digital subtraction angiography (DSA) and plasma AFP levels were used to diagnose the conditions and the diagnosis was finally confirmed with pathological biopsy.

Surgical procedure

The patients were divided into TACE or non-TACE group. In TACE group, 79 patients underwent 1-5 courses chemoembolization prior to liver resection. Of them, 11 patients had 1-4 courses of chemotherapy only (group A), 33 patients had 1-5 courses of chemotherapy combined with iodized oil (group B), 23 patients had 1-3 courses of chemotherapy, iodized oil and gelatin sponge (group C), 12 patients had 1-3 courses of chemotherapy combined with iodized oil, ethanol and gelatin - sponge (group D). Considering the course of TACE, 50 patients underwent one course, 19 patients underwent two courses, 10 patients underwent three or more courses. The interval from the last TACE to the surgery was 52.8 ± 12.2 days ($\bar{x} \pm s$), 25 patients had

1 month or less, 29 patients had 2 months or less, 16 patients had 3 months or less, 9 patients had over 3 months. In non-TACE group, 57 patients had surgery without preoperative TACE. The types of hepatectomy were dependent on the location of tumor, the severity of concomitant hepatic cirrhosis and preoperative hepatic function.

TUNNEL staining

Transferase-mediated dUTP nick end labeling (TUNEL) staining was used to examine apoptosis. Positive control slides were treated with DNase-1 and negative controls were stained in the absence of terminal deoxynucleotidyl transferase enzyme. Dark brown nuclei with nuclear condensation in stained cells were considered as TUNEL positive. Apoptotic index was the ratio of the number of positively stained tumor cells to the total number of tumor cells.

Immunohistochemical method

The formalin-fixed, paraffin-embedded specimens were examined immunohistochemically using respective antibodies to p53 M7001 (dilution:1:100), Bcl-2 MO887(dilution:1:60), Bax A3533 (dilution:1:200), Ki-67 M7187(dilution:1:50) and PCNA M0879 (dilution:1:200) (LSAB kit Dako). Positive controls were selected cases known to be positive for the primary antibody, such as laryngeal carcinoma or normal lymph nodes. Negative controls were stained with a nonspecific Ig G (normal rabbit Ig G) and Tris-buffered saline. Brown-yellow staining in nuclei of cancer was found in p53, Ki-67 and PCNA positive cells, while brown-yellow staining in cytoplasm and/or cell membrane was observed in Bcl-2 and Bax positive cells. All slides were reviewed and scored by two independent observers in blind. A few cases with discrepant scoring were reevaluated to reach a final agreement.

Statistical analysis

Data were expressed as $\bar{x} \pm s$ and analyzed by means of SPSS 10.0 software package (SPSS, Chicago, IL, USA, 1999). The Student *t* test, the Crosstabs (chi-square and Fisher's exact probability test), K independent samples and Pearson rank correlation coefficient test were used to test the correlation between parameters. A *P* value <0.05 was considered statistically significant.

RESULTS

P53 expression in different histopathologic types

P53 protein expression in trabecular and clear cells of HCC was significantly lower than that in pseudoglandar, solid, poorly differentiated or undifferentiated and sclerosis HCC (*P*<0.05, Table 1).

Table 1 P53 protein expression of different types of HCC

Groups	Histological types					
	Trabecular	Pseudoglandar	Solid	Clear cell	Poorly differentiated	Sclerosis
Non-TACE	63.66±19.96	72.29±12.47	70.83±24.45	68.27±19.22	74.79±16.18	72.11±0.00
TACE	56.90±17.12	72.35±13.70	74.93±8.76	62.15±11.78	73.66±8.54	
<i>P</i>	>0.05	>0.05	>0.05	>0.05	>0.05	

Table 3 Correlation p53 expression with Ki-67, PCNA, Bax, Bcl-2 and AI

		Ki-67	PCNA	bcl-2	bax	bcl-2/bax	AI
Non-TCAE group	P53	PC 0.454 ^a	0.331 ^a	-0.141	0.054	-0.375 ^a	-0.198
TACE group	p53	PC 0.553 ^a	0.577 ^a	0.007	-0.142	0.001	-0.459 ^a

^aCorrelation is significant at the 0.05 level (2-tailed), PC: Pearson correlation.

P53 expression in different pathological grades

Pathological grades were divided into four groups. Expression of p53 protein in HCC cells increased as the increase of pathological grade in non-TACE or TACE group (*P*<0.05). P53 protein expression in grade II specimens in TACE group was significantly lower than that in non-TACE group (*P*<0.05, Table 2).

Table 2 Expressions of proteins in different grades of HCC

Treat groups	I	II	III	IV
Non-TACE	60.99±30.58	67.22±15.53	72.98±20.60	93.47±0.00
TACE	32.59±11.68	60.02±14.67	74.69±8.65	82.64±1.11
<i>P</i>	>0.05	<0.05	>0.05	>0.05

P53 expression in HCC cells

Expression of p53 protein in HCC cells was 69.37±18.81% in the non-TACE group, 65.09±15.71% in TACE group, 75.34±5.36% in group A, 69.34±12.59% in group B, 60.94±17.24% in group C, and was 53.41±18.13% in group D. Expression of p53 protein was significantly higher in group A than in groups B, C, D and non-TACE group, and was higher in group B than in groups C and D, and lower in group D than in non-TACE group (*P*<0.05, Figures 1-4).

Correlation between courses of TACE and p53 protein expression

Expression of p53 protein in HCC cells was 69.37±18.81% in non-TACE group, 65.76±13.96% in one-course of TACE group, 64.09±19.81% in two-courses of TACE group, and 65.19±17.80% in three or more courses of TACE group. No statistical difference was found among groups (*P*>0.05).

Correlation between interval of TACE and p53 protein expression

Considering the interval from the last TACE to the operation, expression of p53 protein was 69.37±18.81% in non-TACE group, 63.54±13.72% in TACE group with an interval ≤1 month, 61.17±18.32% in TACE group with a 1-2 months interval, 70.87±15.06% in TACE group with a 2-3 months interval, and 73.67±5.87% in TACE group with an interval >3 months. P53 protein expression was significantly lower in patients with an interval ≤2 months than that in patients with an interval >3 months (*P*<0.05).

Correlation of p53 expression with Ki-67, PCNA, Bax, Bcl-2 protein expressions and AI

In non-TCAE group, p53 expression (69.37±18.81%) had a positive correlation with expressions of Ki-67 protein

($44.43 \pm 20.70\%$, $P < 0.05$), PCNA ($62.92 \pm 17.21\%$, $P < 0.05$), and Bax ($44.29 \pm 23.73\%$, $P > 0.05$), and a negative correlation with the ratio of Bcl-2 to Bax (0.48 ± 0.64 , $P < 0.05$), AI (5.71 ± 1.38 , $P > 0.05$) and Bcl-2 ($12.72 \pm 4.92\%$, $P > 0.05$) (Table 3).

In TACE group, expression of p53 protein ($65.09 \pm 15.71\%$) had a positive correlation with expression of Ki-67 ($40.24 \pm 16.59\%$, $P < 0.05$), PCNA ($59.95 \pm 17.75\%$, $P < 0.05$), and Bcl-2 ($7.47 \pm 6.41\%$, $P > 0.05$), Bcl-2 to Bax ratio (0.21 ± 0.29 , $P > 0.05$), and a negative correlation with AI ($14.69 \pm 6.29\%$, $P < 0.05$) and Bax ($54.59 \pm 23.63\%$, $P > 0.05$) (Table 3).

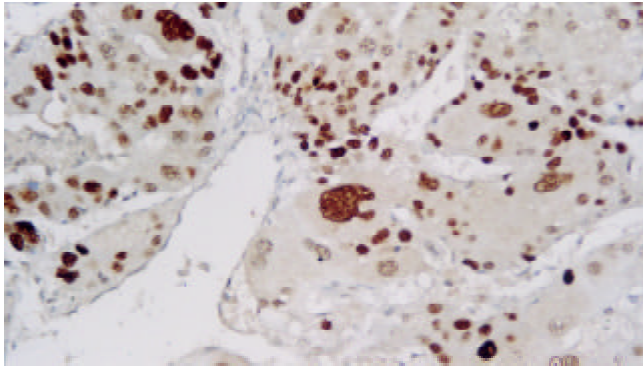


Figure 1 P53 immunostaining cells in one representative HCC specimen in non-TACE group (Dako Envision, peroxidase method $\times 200$).

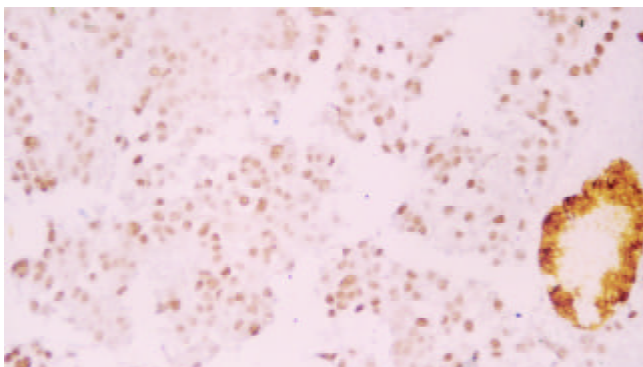


Figure 2 P53 staining cells in HCC in group B (Dako Envision, peroxidase method $\times 200$).

DISCUSSION

HCC is one of the most common malignant neoplasms. Most HCC patients are treated palliatively to improve the resectable rate and prolong survival. The best therapeutic method for HCC with tumor thrombi in portal vein (PVTT) has been regional hepatic TACE treatment after hepatic resection with removal of tumor thrombi^[16]. TACE has become one of the most common and effective palliative approaches. The prognosis of patients treated with TACE was dependent on both the effect of TACE and tumor factors^[17].

To our knowledge, few data regarding the molecular mechanism of TACE treatment for HCC are available, the current study is the first report to describe the correlations between p53 expression and different TACE regimens.

Our study showed that the frequency of p53 expression was higher in group A than in group B, non-TACE group and TACE group, the lowest in group C and D ($P < 0.05$). Our previous study showed that multidrug resistant gene product-Pgp protein was significantly increased in chemotherapy group alone^[18], suggesting that p53 expression increased after chemotherapy with the development of chemoresistance. p53 status might be an important determinant of tumor response to

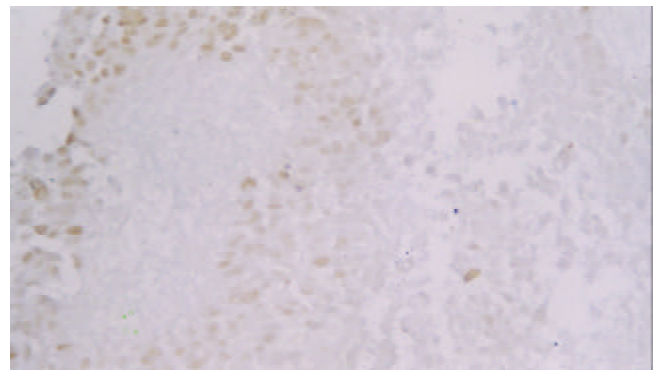


Figure 3 P53 staining cells in HCC in group D (Dako Envision, peroxidase method $\times 200$).

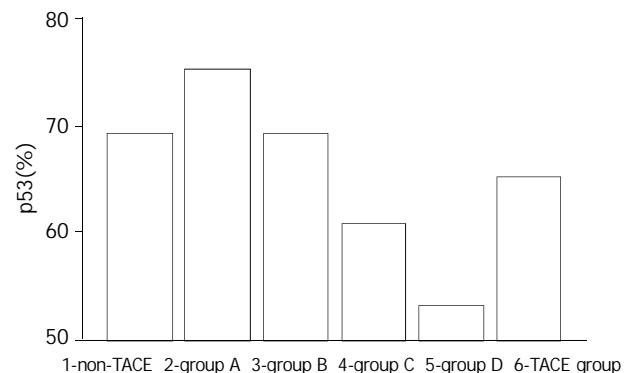


Figure 4 P53 expressions in different groups.

chemotherapy. Tumors with P53 (-) expression might respond to chemotherapy. Inversely, chemotherapy was not effective in patients with P53 (+) expression^[19]. This study demonstrated that p53 protein expression had no significant difference between the TACE and non-TACE groups^[20].

The reverse correlation between AI and p53 protein expression of HCC cells was found in both TACE and non-TACE groups in this study. Most p53 protein measured was the mutant-type. AI was significantly positively correlated with wild-type p53 which enhanced apoptosis by activating proapoptotic Bax and by down-regulating antiapoptotic Bcl-2^[21].

The current study demonstrated that p53 expression was positively related to Ki-67 and PCNA protein expression in the non-TACE and TACE groups, suggesting that the mutated p53 protein could enhance the growth of HCC. Our previous study showed both PCNA and p53 expressions had a significantly parallel correlation, the overexpression of mutated p53 resulted in cancer immortalization, high tumor recurrence risk, more aggressive growth and poor survival^[22] and Kieser *et al* found that a mutated p53 gene could provide an advantage for tumor proliferation^[23]. Igarashi *et al* reported that expression of p53 protein like Ki-67 labeling index was a useful indicator for high proliferative activity^[24]. A mutated p53 gene provided an advantage for tumor proliferation not only by allowing escape from apoptosis, but also by leading to formation of a vascular-rich microenvironment^[25]. However, it has been known that wild-type p53 could inhibit the expression of PCNA^[26].

Wild-type p53 is a positive transcriptional activator for human Bax gene and a negative transcriptional activator for human Bcl-2 gene. The activation of p53 pathway could lead to the down-regulation of Bcl-2 and up-regulation of Bax^[27]. The current study demonstrated that p53 protein expression was positively related to Bax expression, and negatively to Bcl-2 expression in the non-TACE group. Bcl-2 expression had an inverse correlation with mutant p53, and wild-type p53

and majority of mutant p53 proteins could down-regulate Bcl-2 expression and up-regulate Bax expression *in vitro* and *in vivo*^[28]. Moreover, Bcl-2 and p53 could cooperate in regulating pathogenetic pathways in the processes of tumor invasion and metastasis^[29].

The current study demonstrated that p53 protein expression was negatively related to Bax expression, and positively to Bcl-2 expression in the TACE group, which was in accordance with the previous report that Bax expression was significantly increased in tumors with wild-type p53 gene after chemotherapy but did not increase in tumors with mutant p53 gene^[21].

This study demonstrated that discrepancy of P53 existed in different types of HCC. P53 protein expression was significantly lower in trabecular and clear cells of HCC than that in solid and poorly differentiated or undifferentiated HCC, in both non-TACE and TACE groups, Zhao *et al* reported that p53 gene mutation varied in histological types and the mutated rate was 10.5% in trabecular cells, 37.5% in pseudoglandular cells, 60.0% in solid cells and 33.3% in sclerosis ($P < 0.05$)^[30]. Our previous study showed that trabecular and clear cells were more sensitive to TACE than solid, poorly or undifferentiated, and small cells of HCC^[31]. Wang *et al* also found that the clear cells of HCC were more sensitive to TAE than small cells of HCC and poorly differentiated or undifferentiated HCCs^[32]. Yamashita *et al* found that most HCCs responded to TACE well^[33]. These suggest that p53 protein expression would influence the effects of TACE on HCC. Further study is needed to clarify the correlation between p53 protein expression and tumor necrosis and patient survival.

This study also demonstrated that P53 protein expression increased as grades increased in both non-TACE and TACE groups ($P < 0.05$), which was inconsistent with the study of Zhao *et al*^[30].

P53 protein expression of grade II HCC was significantly lower in TACE group than in non-TACE group, suggesting that influences of the molecular markers were very complicated and discrepancy in therapeutic effect of TACE on different histopathological types of HCC was existed. It would be the best choice to use TACE in an individualized mode.

The best interval of treatment for repeated TACE or second stage resection is controversial. In this study, we found that p53 protein expression of HCC cells was significantly lower in the group with a 2 months or less interval than in the group with an over 3 month treatment interval ($P < 0.05$). We found that the best interval between treatment with TACE or second stage resection was 2-3 months.

In conclusion, discrepancy of histological types and pathological grades in p53 protein expression is existed in HCC. P53 protein expression can enhance proliferation of HCC cells and suppress apoptosis of HCC cells after TACE. P53 protein expression would influence effects of TACE on HCC. We need further study to clarify the correlation between p53 protein expression, tumor necrosis and patient survival.

REFERENCES

- Parks RW**, Garden OJ. Liver resection for cancer. *World J Gastroenterol* 2001; **7**: 766-771
- Tang ZY**. Hepatocellular Carcinoma-Cause, Treatment and Metastasis. *World J Gastroenterol* 2001; **7**: 445-454
- Ueno K**, Miyazono N, Inoue H, Nishida H, Kanetsuki I, Nakajo M. Transcatheter arterial chemoembolization therapy using iodized oil for patients with unresectable hepatocellular carcinoma: evaluation of three kinds of regimens and analysis of prognostic factors. *Cancer* 2000; **88**: 1574-1581
- Xie X**, Clausen OP, De Angelis P, Boysen M. The prognostic value of spontaneous apoptosis, Bax, Bcl-2, and p53 in oral squamous cell carcinoma of the tongue. *Cancer* 1999; **86**: 913-920
- Oltvai ZN**, Milliman CL, Korsmeyer SJ. Bcl-2 heterodimerizes *in vivo* with a conserved homolog, Bax, that accelerates programmed cell death. *Cell* 1993; **74**: 609-619
- Xu HY**, Yang YL, Guan XL, Song G, Jiang AM, Shi LJ. Expression of regulating gene and apoptosis index in primary liver cancer. *World J Gastroenterol* 2000; **6**: 721-724
- Perry A**, Jenkins RB, O' Fallon JR, Schaefer PL, Kimmel DM, Mahoney MR, Scheithauer BW, Smith SM, Hill EM, Sebo TJ, Levitt R, Krook J, Tschetter LK, Morton RF, Buckner JC. Clinicopathologic study of 85 similarly treated patients with anaplastic astrocytic tumors: An analysis of DNA content (ploidy), cellular proliferation, and p53 expression. *Cancer* 1999; **86**: 672-683
- Kanazawa Y**, Onda M, Tanaka N, Seya. Proliferation cell nuclear antigen and p53 protein expression in submucosal invasive colorectal carcinoma. *J Nippon Medical School* 2000; **67**: 242-249
- Elpek GO**, Gelen T, Aksoy NH, Karpuzoglu T, Keles N. Microvessel count, proliferating cell nuclear antigen and Ki-67 indices in gastric adenocarcinoma. *Pathol Oncol Res* 2000; **6**: 59-64
- Zhang Z**, Yuan Y, Gao H, Dong M, Wang L, Gong YH. Apoptosis, proliferation and p53 gene expression of *H pylori* associated gastric epithelial lesions. *World J Gastroenterol* 2001; **7**: 779-782
- Fukuse T**, Hirata T, Naiki H, Hitomi S, Wada H. Expression of proliferating cell nuclear antigen and CD44 variant isoforms in the primary and metastatic sites of nonsmall cell lung carcinoma with intrapulmonary metastases. *Cancer* 1999; **86**: 1174-1181
- Wu X**, Zhang Z, Cai S. Proliferating cell nuclear antigen(PCNA) in ovarian carcinoma and its relation to lymph node metastasis and prognosis. *Zhonghua Zhongliu Zazhi* 1998; **20**: 68-70
- Luo YQ**, Ma LS, Zhao YL, Wu KC, Pan BR, Zhang XY. Expression of proliferating cell nuclear antigen in polyps from large intestine. *World J Gastroenterol* 1999; **5**: 160-164
- Wu WY**, Xu Q, Shi LC, Zhang WB. Inhibitory effects of *Curcuma aromatica* oil on proliferation of hepatoma in mice. *World J Gastroenterol* 2000; **6**: 216-219
- Lin GY**, Chen ZL, Lu CM, Li Y, Ping XJ, Huang R. Immunohistochemical study on p53, H-rasp21, c-erbB-2 protein and PCNA expression in HCC tissues of Han and minority ethnic patients. *World J Gastroenterol* 2000; **6**: 234-238
- Fan J**, Wu ZQ, Tang ZY, Zhou J, Qiu SJ, Ma ZC, Zhou XD, Ye SL. Multimodality treatment in hepatocellular carcinoma patients with tumor thrombi in portal vein. *World J Gastroenterol* 2001; **7**: 28-32
- Rose DM**, Chapman WC, Brockenbrough AT, Wright JK, Rose AT, Meranze S, Mazer M, Blair T, Blanke CD, Debelak JP, Pinson CW. Transcatheter arterial chemoembolization as primary treatment for hepatocellular carcinoma. *Am J Surg* 1999; **177**: 405-410
- Xiao EH**, Hu GD, Liu PC, Hu DY, Liu SC, Hao CY. The effect of different interventional treatment on P-glycoprotein in different histopathological types of primary hepatocellular carcinoma. *Zhonghua Fangshexue Zazhi* 1999; **33**: 150-152
- Okumura H**, Natsugoe S, Nakashima S, Matsumoto M, Sakita H, Nakano S, Kusano C, Baba M, Takao S, Furukawa T, Akiyama SI, Aikou T. Apoptosis and cell proliferation in esophageal squamous cell carcinoma treated by chemotherapy. *Cancer Lett* 2000; **158**: 211-216
- Huang JF**, He XS, Lin XJ. Effect of preoperative transcatheter arterial chemoembolization on tumor cell activity in hepatocellular carcinoma. *Chin Med J* 2000; **113**: 446-448
- Sato S**, Kigawa J, Minagawa Y, Okada M, Shimada M, Takahashi M, Kamazawa S, Terakawa N. Chemosensitivity and p53-dependent apoptosis in epithelial ovarian carcinoma. *Cancer* 1999; **86**: 1307-1313
- Li JQ**, Zhang CQ, Feng KT. PCNA, p53 protein and prognosis in primary liver cancer. *China Natl J New Gastroenterol* 1996; **2**: 220-222
- Kieser A**, Weich HA, Brander G, Marme D, Kolch W. Mutant p53 potentiates protein kinase C induction of vascular endothelial growth factor expression. *Oncogene* 1994; **9**: 963-969
- Igarashi N**, Takahashi M, Ohkubo H, Omata K, Iida R, Fujimoto S. Predictive value of Ki-67, p53 protein, and DNA content in the diagnosis of gastric carcinoma. *Cancer* 1999; **86**: 1449-1454
- Matsuura T**, Fukuda Y, Fujitaka T, Nishisaka T, Sakatani T, Ito

- H. Preoperative treatment with Tegafur Suppositories enhances apoptosis and reduces the intratumoral microvessel density of human colorectal carcinoma. *Cancer* 2000; **88**: 1007-1015
- 26 **Deb S**, Jackson CT, Subler MA, Martin DW. Modulation of cellular and viral promoters by mutant human p53 proteins found in tumor cells. *J Virol* 1992; **66**: 6164-6170
- 27 **Miyashita T**, Krajewski S, Krajewska M, Wang HG, Lin HK, Liebermann DA, Hoffman B, Reed JC. Tumor suppressor p53 is a regulator of bcl-2 and bax gene expression *in vitro* and *in vivo*. *Oncogene* 1994; **9**: 1799-1805
- 28 **Ioachim E**, Malamou-Mitsi V, Kamina SA, Goussia AC, Agnantis NJ. Immunohistochemical expression of Bcl-2 protein in breast lesions: Correlation with Bax, p53, Rb, C-erbB-2, EGFR and proliferation indices. *Anticancer Res* 2000; **20**: 4221-4226
- 29 **Giatromanolaki A**, Stathopoulos GP, Tsiobanou E, Papadimitriou C, Georgoulas V, Gatter KC, Harris AL, Koukourakis MI. Combined role of tumor angiogenesis, bcl-2, and p53 expression in the prognosis of patients with colorectal carcinoma. *Cancer* 1999; **86**: 1421-1430
- 30 **Zhao P**, Yang GH, Mao X. A molecular pathological study of p53 gene in hepatocellular carcinoma. *Zhonghua Binglixue Zazhi* 1993; **22**: 16-18
- 31 **Xiao EH**, Hu GD, Li JQ, Zhang YQ, Chen MS, Guo YP, Lin XG, Li SP, Shi M. The effect of transcatheter arterial chemoembolization on the different histopathological types of hepatocellular carcinoma. *Zhonghua Gandanwaikexue Zazhi* 2001; **7**: 411-414
- 32 **Wang YP**, Zhang JS, Gao YA. Therapeutic efficacy of transcatheter arterial embolization of primary hepatocellular carcinoma: discrepancy in different histopathological types of HCC. *Zhonghua Fangshexue Zazhi* 1997; **31**: 586-591
- 33 **Yamashita Y**, Matsukawa T, Arakawa A, Hatanaka Y, Urata J, Takahashi M. Us-guided liver biopsy: Predicting the effect of interventional treatment of hepatocellular carcinoma. *Radiology* 1995; **196**: 799-804

Edited by Ren SY and Wang XL

Expression of co-stimulator 4-1BB molecule in hepatocellular carcinoma and adjacent non-tumor liver tissue, and its possible role in tumor immunity

Yun-Le Wan, Shu-Sen Zheng, Zhi-Cheng Zhao, Min-Wei Li, Chang-Ku Jia, Hao Zhang

Yun-Le Wan, Shu-Sen Zheng, Zhi-Cheng Zhao, Min-Wei Li, Chang-Ku Jia, Hao Zhang, Key Laboratory of Combined Multi-organ Transplantation, Ministry of Public Health, Department of Hepatobiliary and Pancreatic Surgery, First Affiliated Hospital, School of Medicine, Zhejiang University, Hangzhou 310000, Zhejiang Province, China

Correspondence to: Dr. Yun-Le Wan, Department of Hepatobiliary and Pancreatic Surgery, First Affiliated Hospital, School of Medicine, Zhejiang University, Hangzhou 310000, Zhejiang Province, China. wanyl036@sina.com

Telephone: +86-571-87236570 **Fax:** +86-571-87236570

Received: 2003-06-05 **Accepted:** 2003-08-16

Abstract

AIM: To investigate the expression of 4-1BB molecule in hepatocellular carcinoma (HCC) and its adjacent tissues.

METHODS: Reverse transcription-polymerase chain reaction (RT-PCR) was used to determine the gene expression of 4-1BB in hepatocarcinoma and its adjacent tissues, and peripheral blood mononuclear cells (PBMCs) from both HCC and health control groups. Flow cytometry was used to analyse the phenotypes of T cell subsets from the blood of HCC patients and healthy volunteers, and further to determine whether 4-1BB molecules were also expressed on the surface of CD4⁺ and CD8⁺ T cells. The localization of 4-1BB proteins on tumor infiltrating T cells was determined by direct immunofluorescence cytochemical staining and detected by confocal microscopy.

RESULTS: 4-1BB mRNA, which was not detectable in normal liver, was found in 19 liver tissues adjacent to tumor edge (<1.0 cm). Low expression of 4-1BB mRNA was shown in 8 tumor tissues and 6 liver tissues located within 1 to 5 cm away from tumor edge. In PBMCs, 4-1BB mRNA was almost not detected. Percentage of CD4⁺, CD8⁺ and CD3⁺/CD25⁺ T cells, as well as ratio of CD4 to CD8 revealed no difference between groups ($P>0.05$, respectively), while a significant lower percentage of CD3⁺ T cell was found in HCC group as compared to healthy control group ($P<0.05$). However, 4-1BB molecules were almost not found on the surface of CD4⁺ and CD8⁺ T cells in HCC and healthy control group. Double-staining of 4-1BB⁺/CD4⁺ and 4-1BB⁺/CD8⁺ immunofluorescence on tumor infiltrating T cells was detected in 13 liver tissues adjacent to tumor edge (<1.0 cm) by confocal microscopy.

CONCLUSION: Although HCC may escape from immune attack by weak immunogenicity or downregulated expression of MHC-1 molecules on the tumor cell surface, tumor infiltrating T cells can be activated via other costimulatory signal pathways to exert a limited antitumor effect on local microenvironment. The present study also implicates that modulating 4-1BB/4-1BBL costimulatory pathway may be an effective immunotherapy strateg to augment the host response.

Wan YL, Zheng SS, Zhao ZC, Li MW, Jia CK, Zhang H. Expression of co-stimulator 4-1BB molecule in hepatocellular carcinoma and adjacent non-tumor liver tissue, and its possible role in tumor immunity. *World J Gastroenterol* 2004; 10(2): 195-199

<http://www.wjgnet.com/1007-9327/10/195.asp>

INTRODUCTION

Hepatocellular carcinoma (HCC) has a very poor prognosis owing to its high malignancy, and it ranks second cause of cancer death in China^[1]. Curative tumour resection or orthotopic liver transplantation (LTx) seems to be an optimal treatment. Nevertheless, the recurrence rate remains high both after tumour resection and LTx^[2-10]. Chemotherapy and embolisation are at best palliative with few impacts on survival^[3]. Recently, immunotherapy has been used with some success for such tumours as melanoma^[11-14] and renal-cell carcinoma^[15,16] that are associated with an inflammatory or immune response. However, like most solid tumours, HCC has long been considered poorly immunogenic and substantially refractory to immunotherapy. Since a better prognosis of HCC attributes to the anti-tumor effect induced by cellular immunity of infiltrating CD8⁺ and CD4⁺ T lymphocytes^[17], these tumor infiltrating lymphocytes (TILs) might be in an activated status and play a limited immune protection in microenvironment.

The 4-1BB receptor, a recently identified molecule of tumor necrosis factor- receptor (TNFR) superfamily, is a type I membrane protein expressed on activated cytolytic and helper T cells^[18,19], as well as NK cells^[20]. The ligand for 4-1BB receptor is a 4-1BB ligand (4-1BBL), which is expressed on APCs including B cells, macrophages, and dendritic cells^[21,22]. Ligation of 4-1BB with 4-1BB ligand plays an important role in sustaining T cells activation, amplifying cytotoxic T lymphocyte (CTL) response, as well as inducing IL-2 production in the complete absence of a signal through CD28 molecule^[22,23]. A recent research demonstrated that immunomodulatory gene therapy with 4-1BB ligand could induce long-term remission of liver metastases in a mouse model and augment CTL response against tumor^[24]. The present study was to detect whether 4-1BB molecules were expressed on infiltrating CD4⁺ and CD8⁺ T cells in HCC and its adjacent tissues, and to illustrate the role of 4-1BB/4-1BBL pathway in tumor immunity.

MATERIALS AND METHODS

Patients

Nineteen patients with HCC confirmed by histopathologic examination were selected. Among them, 14 were male and 5 female aged from 28 to 68 years (average, 49.67±13.04 years). Three liver specimens from mismatched cadaver donor and 22 healthy peripheral blood specimens from Blood Center of Zhejiang Province were served as controls.

Reagents

Fluorescein isothiocyanate (FITC) -conjugated mouse

monoclonal antibodies (mAbs) specific for human surface antigens including anti-CD4 (IgG1k clone RPA-T4), anti-CD8 (IgG1k clone RPA-T8), anti-CD3 (IgG1k clone UCHT1), phycoerythrin (PE)-conjugated anti-CD25 (IgG1k clone M-A251), anti-4-1BB (IgG1k clone 4B4-1), and FITL or PE-conjugated mouse IgG1k (clone MOPC-21) as isotype controls were purchased from Becton Dickinson, San Jose, CA. RevertAid™ M-MuLV reverse transcriptase and Taq DNA polymerase were obtained from Promega, USA.

Peripheral blood mononuclear cell preparation

In order to isolate PBMCs, 5 ml heparinized blood was diluted 1:1 with PBS containing 0.6% Na₃-citrate and layered over a 5 ml Ficoll cushion. After centrifugation (20 min, 700×g), the interface containing PBMCs was collected and washed twice with PBS. This precipitate contained approximately 25% monocytes and 75% lymphocytes.

Reverse transcriptase-polymerase chain reaction (RT-PCR)

Semi-quantitative assessment of 4-1BB mRNA expression was performed using RT-PCR on a PTC-200 DNA engine (MJ Research, USA). Briefly, total RNA was prepared from PBMCs and liver tissues using TRIZOL (Gibco BRL Life Technologies, Breda, the Netherlands). cDNA was synthesized with 2 µg of total RNA template using the superscript pre-amplification system (Promega, USA) and random primers in a final volume of 20 µl. The cDNA used as template was checked in respect to human β₂-MG amplification. The following primers (Shanghai Sangon, China) were used: β₂-MG sense primer: 5' -CCAGCAGAGAATGGAAAGTC-3', β₂-MG antisense primer: 5' -GATGCTGCTTACATGTCTCG-3', 4-1BB sense primer: 5' -TCAGGACCAGGAAGGAGTGT-3', 4-1BB antisense primer: 5' -AACGGAGCGTGAGGAAGAAC-3'. Using these primers, fragments of 240 bp, and 414 bp were expected to result from amplification of β₂-MG and 4-1BB cDNAs, respectively. PCR reactions contained 20 pmol of each primer for 4-1BB, 2.5 u of Taq polymerase, 1 µl of 25 mM dNTPs, 1.2 µl of 25 mM MgCl₂ and 10×PCR buffer in a final volume of 25 µl. For β₂-MG amplification, 1 µl of each primer at a 1:8 diluted concentration to 4-1BB primers was used for the reaction. PCR products (8 µl) were analyzed on 1.5% agarose gel containing ethidium bromide using Kodak DNA analyser (Gibco BRL) with Kodak digital science 1S 2.0 software. The expression level of 4-1BB mRNA was described as the ratio of 4-1BB/β₂-MG×100.

Flow cytometric analysis

One hundred microliters of heparinized peripheral blood were incubated with monoclonal antibody at room temperature in dark for 15 min to 30 min according to the manufacturer's instructions. Another 100 µl of heparinized peripheral blood incubated with FITL or PE-conjugated mouse IgG1k (clone MOPC-21) was used as negative isotype control. Erythrocytes were lysed in turn with ImmunoPrep A, B, and C haemolytic solution on Coulter Q-Prep (Beckman-coulter). Alignment was checked using immunocheck beads (Beckman-coulter). All results were obtained using EPICS® XL FACScan (Beckman-coulter) with system™ software.

Direct immunofluorescence histochemical staining protocol

Tissues were stored at -70 °C until use. Four µm-thick frozen sections (on poly-L-lysine coated slides) were fixed in acetone for 10 min at 4 °C. The sections were blocked in phosphate buffered saline (PBS) and 1% bovine serum albumin (BSA) for 1 h, followed by incubation with FITC and PE labeled antibodies or conjugated isotype matched control antibodies for 16 h at 4 °C. After extensively washed (overnight), stained sections were covered in PBS and kept in dark at 4 °C.

Confocal microscopy

LEICA TCS-SP confocal microscope (Germany) was equipped with argon lasers and Leica inverted research biological microscope with an oil immersion objective lens of ×40 (NA1.30). The sections processed for immunocytochemistry were viewed under LEICA TCS-SP confocal microscope. After standard fluorescence observations, 4-1BB and CD4 or CD8 localization on TIL was automatically scanned by laser emitted at 488 nm and imaged by using PowerScanner physiology software. FITC and PE fluorescence emissions were captured through grating at 530/30-nm and 605/30-nm respectively.

Statistical analysis

Data were expressed as mean±SD. Statistical analysis was performed using one-way ANOVA with SPSS 10.0 software. Kruskal-Wallis H test and Student's *t* test were also used for the nonparametric and parametric data analysis between two groups, respectively. A *P* value ≤ 0.05 was considered significant.

RESULTS

Expression of 4-1BB mRNA in tumor tissues but almost not in PBMCs

4-1BB mRNA was not detectable in normal liver, but was detected in all 19 liver tissues adjacent to tumor edge (<1.0 cm). Low expression of 4-1BB mRNA was shown in 8 tumor tissues and 6 liver tissues located within 1 to 5 cm away from tumor edge. However, in PBMCs, 4-1BB mRNA expression was not detected in samples from 18 healthy controls (81.82%, 18/22) and 13 patients with HCC (68.42%, 13/19). Very low expression of 4-1BB mRNA was detected in another 4 healthy volunteers and 6 patients with HCC. However, the median level of 4-1BB mRNA expression from PBMCs in each group was 0 (*P*>0.05) (Figures 1, 2).

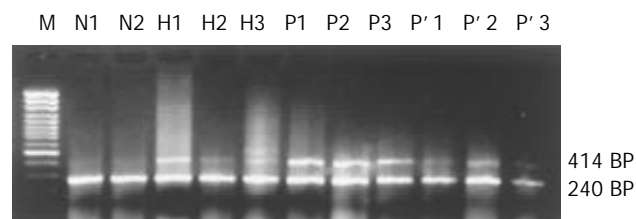


Figure 1 Representative RT-PCR results of 4-1BB mRNA expression in normal liver, and HCC tissues as well as its adjacent tissues. (M, GeneRuler™ 100 bp DNA Ladder Plus; N, normal liver; H, HCC tissues; P, adjacent tissues to HCC (<1 cm), P': liver tissues located within 1 to 5 cm away from tumor edge)

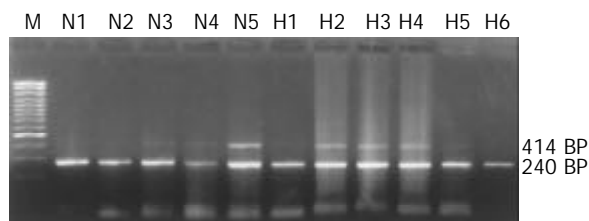


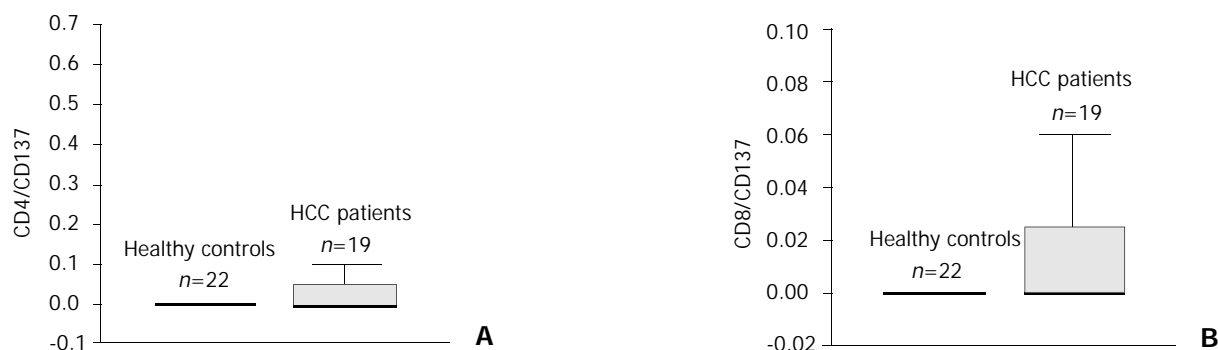
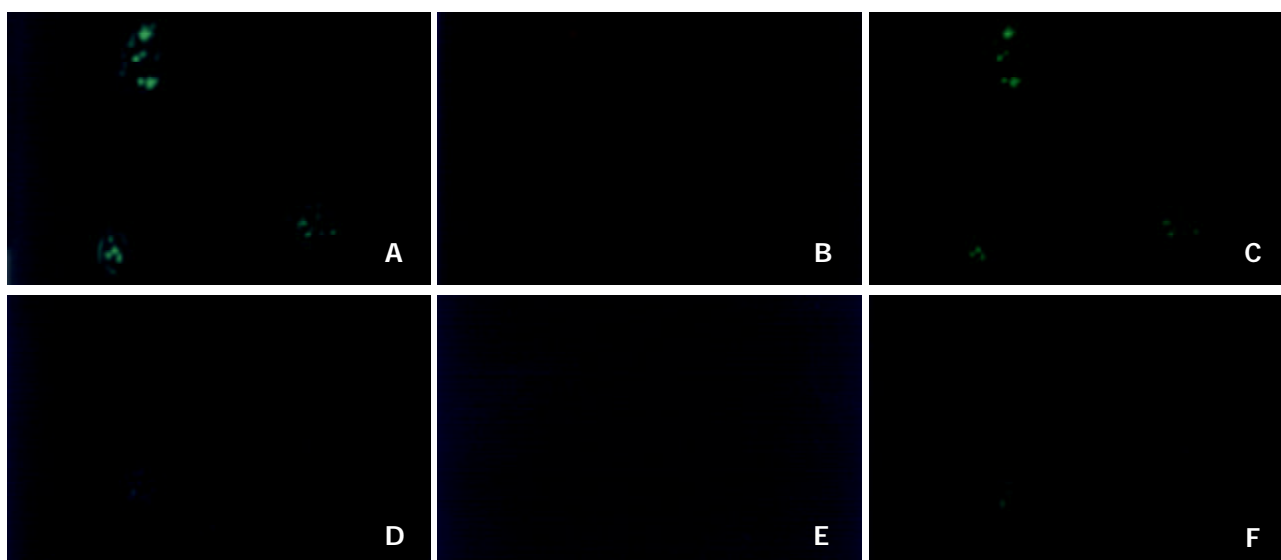
Figure 2 Representative RT-PCR results of 4-1BB mRNA expression in PBMCs (M, GeneRuler™ 100 bp DNA Ladder Plus; N, healthy control; H, HCC group).

Almost no detection of 4-1BB molecules on CD4⁺ or CD8⁺ T cells in PBMCs

In order to analyze T cell phenotypes, and determine whether 4-1BB molecules expressed on T cells from PBMCs, flow

Table 1 Analysis of T cells phenotypes of PBMCs from healthy controls and HCC patients (Mean±SD)

Groups	<i>n</i>	CD4	CD8	CD3	CD3/CD25	CD4/CD8
Normal control	22	34.74±6.19	28.70±5.11	66.56±10.24	1.22±0.13	1.20±0.18
HCC	19	31.40±4.70	25.83±3.98	61.30±4.61	1.22±0.12	1.26±0.17
<i>P</i> value		0.058	0.051	0.038	0.918	0.279

**Figure 3** Comparison of 4-1BB molecules on CD4⁺ or CD8⁺ PBMCs between healthy controls and HCC patients.**Figure 4** Confocal laser micrographs of TILs in HCC adjacent tissues processed for the immunocytochemical detection of 4-1BB and CD4 or CD8 molecules. (A and D, FITC immunofluorescence for CD4 and CD8 molecules respectively; B and E, PE immunofluorescence for 4-1BB molecules; C and F, automatically synthetic micrographs by computer soft for A and B, and D and E, respectively).

cytometric analysis was used. The results are shown in Table 1. Percentages of CD4⁺, CD8⁺ T cells and CD3⁺CD25⁺ T cells, as well as the ratio of CD4 to CD8 had no significant differences between the groups ($P>0.05$). However, a significantly higher percentage of CD3⁺ T cells was found in healthy control group as compared to HCC group ($P<0.05$). 4-1BB molecules were almost not found on the surface of CD4⁺ and CD8⁺ T cells in HCC and healthy control group. The percentage of 4-1BB⁺/CD4⁺ or CD8⁺ T cells in two groups was not more than 0.1%, and the median value in each group was 0 ($P=0.406$ for 4-1BB⁺/CD4⁺, $P=0.209$ for 4-1BB⁺/CD8⁺, respectively). (Table 1, Figure 3).

Co-localization of 4-1BB and CD4 or CD8 on TILs

To determine whether TILs were the same clones as T lymphocytes from peripheral blood, confocal laser microscopy was used to detect 4-1BB expressions on TILs. As expected, we did not find any PE conjugated 4-1BB and FITC conjugated CD4 or CD8 fluorescence located within 3 normal liver tissues. However, co-localization of 4-1BB⁺/CD4⁺ or CD8⁺ on TIL was visualized by confocal laser microscopy in 3 tumor tissues and

1 liver tissue located within 1 to 5 cm away from tumor edge, as well as 13 tumor adjacent tissues within 1 cm. (Figure 4).

DISCUSSION

It seems that a better prognosis of HCC could attribute to the anti-tumor effect induced by cellular immunity of infiltrating CD8⁺ and CD4⁺ T lymphocytes^[17]. However, like most solid tumours, HCC has long been considered poorly immunogenic. Tumor cells were capable of delivering antigen-specific signals to T cells clone, but could not deliver costimulatory signals, e.g., a B7/CD28 interaction^[25-27], necessary for full T cell activation, could lead to the evasion of immune surveillance by malignant cells^[28]. Moreover, evidences have demonstrated that TILs can down-regulate the expression of CD28 molecules, but still could retain a limited immune protection in local tumor microenvironment^[27]. Therefore, other molecules may involve in sustaining T cells activation and amplifying cytotoxic T lymphocytes response.

In this study, we found that 4-1BB mRNA transcripts were

not detectable in normal liver, but were detected in all 19 liver tissues adjacent to tumor edge (<1.0 cm). In some tumor and liver tissues located within 1 to 5 cm away from tumor edge, low expression of 4-1BB mRNA was also detected. Since 4-1BB molecules were mainly expressed on activated T lymphocytes^[18,19], 4-1BB transcripts might derive from TILs. To identify this hypothesis, direct immunofluorescence staining of 4-1BB and CD4 or CD8 on TILs was examined by confocal microscope. Co-localization of 4-1BB⁺/CD4⁺ or CD8⁺ fluorescence located on TILs was visualized by confocal microscopy in tumor and liver tissue within 1 to 5 cm away from tumor edge, as well as tumor adjacent tissues within 1 cm. Previous researches reported that interaction of 4-1BB with 4-1BB ligand played an important role in sustaining T cells activation, amplifying cytotoxic T lymphocyte (CTL) response, as well as inducing IL-2 production in the complete absence of a signal through CD28 molecule^[22,23]. A recent report indicated that under the condition of repeated Ag-stimulation, down-regulated expression of CD28 molecule on activated T cells could lead to activation-induced cell death (AICD)^[29], while very few 4-1BB molecules might supply sufficient costimulatory signals to sustain T cells activation, and inhibit AICD^[30,31]. In fact, accumulative evidence has confirmed that 4-1BB/4-1BB ligand pathway plays a role in transplant immunity^[32-34] and autoimmune disease^[35-37]. Therefore, the present study may provide an important clue that 4-1BB molecules are also involved in the process of infiltrating CD4⁺ and CD8⁺ T cells activation, at least partly, and that modulating 4-1BB/4-1BB ligand pathway might augment CTL response against tumor^[24,38-40].

However, even if these infiltrating lymphocytes are functionally activated via 4-1BB signals or the others, and are truly specific for tumor cells, why they could not inhibit the tumour growth? This phenomenon was inexplicable. Cytotoxic T cells propagated from biopsies showed a specific killing of the tumor cells *in vitro*, confirming that the complex microenvironment inside the tumor tissue was not able to provide the optimal condition for TILs to fully exert their functions in inhibiting tumor growth, or even to induce apoptosis of TILs through Fas/Fas ligand system^[41,42].

To explore if the TILs were the same clones as T lymphocytes from peripheral blood, we analyzed the phenotypes of peripheral blood lymphocytes, and examined 4-1BB molecules and its mRNA transcripts by flow cytometry and RT-PCR respectively. To our surprise, we failed to detect 4-1BB mRNA in peripheral blood lymphocytes and 4-1BB molecules on peripheral CD4⁺ or CD8⁺ T cells from HCC patients. But our results confirmed that a significantly lower percentage of CD3⁺ T cells was found in HCC group as compared to healthy control group, which was coincided with other research data^[43]. Since the phenotype and function of lymphocytes collected from the peripheral blood were not the same as those of lymphocytes from tumor draining regional lymph nodes and tumor tissues, we found that 4-1BB molecules were existed in infiltrating CD4⁺ and CD8⁺ T cells but not in peripheral blood lymphocytes. Therefore, we may conclude that TILs and peripheral blood lymphocytes are not the same clones^[43-45].

In summary, we examined 4-1BB molecules expression in infiltrating T cells in HCC specimens, indicating that tumor infiltrating T cells can be activated via other costimulatory signals, e.g., 4-1BB, and exert a limited antitumor protection in local microenvironment. The present study also implicates that modulating 4-1BB/4-1BBL costimulatory pathway may be an effective immunotherapy strategy to augment the host response.

REFERENCES

- 1 **Tang ZY**, Yu YQ, Zhou XD, Ma ZC, Wu ZQ. Progress and prospects in hepatocellular carcinoma surgery. *Ann Chir* 1998; **52**: 558-563
- 2 **Zhao WH**, Ma ZM, Zhou XR, Feng YZ, Fang BS. Prediction of recurrence and prognosis in patients with hepatocellular carcinoma after resection by use of CLIP score. *World J Gastroenterol* 2002; **8**: 237-242
- 3 **Qin LX**, Tang ZY. The prognostic significance of clinical and pathological features in hepatocellular carcinoma. *World J Gastroenterol* 2002; **8**: 193-199
- 4 **Kanematsu T**, Furui J, Yanaga K, Okudaira S, Shimada M, Shirabe K. A 16-year experience in performing hepatic resection in 303 patients with hepatocellular carcinoma: 1985-2000. *Surgery* 2002; **131**(Suppl 1): S153-158
- 5 **Chiappa A**, Zbar AP, Audisio RA, Leone BE, Biella F, Staudacher C. Factors affecting survival and long-term outcome in the cirrhotic patient undergoing hepatic resection for hepatocellular carcinoma. *Eur J Surg Oncol* 2000; **26**: 387-392
- 6 **Ouchi K**, Sugawara T, Fujiya T, Kamiyama Y, Kakugawa Y, Mikuni J, Yamanami H, Nakagawa K. Prediction of recurrence and extratumor spread of hepatocellular carcinoma following resection. *J Surg Oncol* 2000; **75**: 241-245
- 7 **Otto G**, Heuschen U, Hofmann WJ, Krumm G, Hinz U, Herfarth C. Survival and recurrence after liver transplantation versus liver resection for hepatocellular carcinoma: a retrospective analysis. *Ann Surg* 1998; **227**: 424-432
- 8 **Philosophe B**, Greig PD, Hemming AW, Cattral MS, Wanless I, Rasul I, Baxter N, Taylor BR, Langer B. Surgical management of hepatocellular carcinoma: resection or transplantation? *J Gastrointest Surg* 1998; **2**: 21-27
- 9 **Margarit C**, Charco R, Hidalgo E, Allende H, Castells L, Bilbao I. Liver transplantation for malignant diseases: selection and pattern of recurrence. *World J Surg* 2002; **26**: 257-263
- 10 **Hemming AW**, Cattral MS, Reed AI, Van Der Werf WJ, Greig PD, Howard RJ. Liver transplantation for hepatocellular carcinoma. *Ann Surg* 2001; **233**: 652-659
- 11 **Lucas ML**, Heller L, Coppola D, Heller R. IL-12 plasmid delivery by *in vivo* electroporation for the successful treatment of established subcutaneous B16.F10 melanoma. *Mol Ther* 2002; **5**: 668-675
- 12 **Hsueh EC**, Essner R, Foshag LJ, Ollila DW, Gammon G, O' Day SJ, Boasberg PD, Stern SL, Ye X, Morton DL. Prolonged survival after complete resection of disseminated melanoma and active immunotherapy with a therapeutic cancer vaccine. *J Clin Oncol* 2002; **20**: 4549-4554
- 13 **Dreno B**, Nguyen JM, Khammari A, Pandolfino MC, Tessier MH, Bercegeay S, Cassidanius A, Lemarre P, Billaudel S, Labarriere N, Jotereau F. Randomized trial of adoptive transfer of melanoma tumor-infiltrating lymphocytes as adjuvant therapy for stage III melanoma. *Cancer Immunol Immunother* 2002; **51**: 539-546
- 14 **Labarriere N**, Pandolfino MC, Gervois N, Khammari A, Tessier MH, Dreno B, Jotereau F. Therapeutic efficacy of melanoma-reactive TIL injected in stage III melanoma patients. *Cancer Immunol Immunother* 2002; **51**: 532-538
- 15 **Mickisch GH**, Garin A, van Poppel H, de Prijck L, Sylvester R. Radical nephrectomy plus interferon-alfa-based immunotherapy compared with interferon alfa alone in metastatic renal-cell carcinoma: a randomised trial. *Lancet* 2001; **358**: 966-970
- 16 **Stadler WM**, Kuzel T, Dumas M, Vogelzang NJ. Multicenter phase II trial of interleukin-2, interferon-alpha, and 13-cis-retinoic acid in patients with metastatic renal-cell carcinoma. *J Clin Oncol* 1998; **16**: 1820-1825
- 17 **Wada Y**, Nakashima O, Kutami R, Yamamoto O, Kojiro M. Clinicopathological study on hepatocellular carcinoma with lymphocytic infiltration. *Hepatology* 1998; **27**: 407-414
- 18 **Kwon BS**, Weissman SM. cDNA sequences of two inducible T-cell genes. *Proc Natl Acad Sci U S A* 1989; **86**: 1963-1967
- 19 **Pollok KE**, Kim YJ, Zhou Z, Hurtado J, Kim KK, Pickard RT, Kwon BS. Inducible T cell antigen 4-1BB. Analysis of expression and function. *J Immunol* 1993; **150**: 771-781
- 20 **Melero I**, Johnston JV, Shufford WW, Mittler RS, Chen L. NK1.1 cells express 4-1BB (CDw137) costimulatory molecule and are required for tumor immunity elicited by anti-4-1BB monoclonal antibodies. *Cell Immunol* 1998; **190**: 167-172
- 21 **Pollok KE**, Kim YJ, Hurtado J, Zhou Z, Kim KK, Kwon BS. 4-1BB T-cell antigen binds to mature B cells and macrophages, and

- costimulates anti- μ -primed splenic B cells. *Eur J Immunol* 1994; **24**: 367-374
- 22 **DeBenedette MA**, Shahinian A, Mak TW, Watts TH. Costimulation of CD28- T lymphocytes by 4-1BB ligand. *J Immunol* 1997; **158**: 551-559
- 23 **Chu NR**, DeBenedette MA, Stiernholm BJ, Barber BH, Watts TH. Role of IL-12 and 4-1BB ligand in cytokine production by CD28⁺ and CD28⁻ T cells. *J Immunol* 1997; **158**: 3081-3089
- 24 **Martinet O**, Ermekova V, Qiao JQ, Sauter B, Mandeli J, Chen L, Chen SH. Immunomodulatory gene therapy with interleukin 12 and 4-1BB ligand: long- term remission of liver metastases in a mouse model. *J Natl Cancer Inst* 2000; **92**: 931-936
- 25 **Tatsumi T**, Takehara T, Katayama K, Mochizuki K, Yamamoto M, Kanto T, Sasaki Y, Kasahara A, Hayashi N. Expression of costimulatory molecules B7-1 (CD80) and B7-2 (CD86) on human hepatocellular carcinoma. *Hepatology* 1997; **25**: 1108-1114
- 26 **Qiu YR**, Yang CL, Chen LB, Wang Q. Analysis of CD8⁺ and CD8⁻CD28⁻ cell subsets in patients with hepatocellular carcinoma. *Diyi Junyi Daxue Xuebao* 2002; **22**: 72-73
- 27 **Tang KF**, Chan SH, Loh KS, Chong SM, Wang D, Yeoh KH, Hu H. Increased production of interferon-gamma by tumour infiltrating T lymphocytes in nasopharyngeal carcinoma: indicative of an activated status. *Cancer Lett* 1999; **140**: 93-98
- 28 **Chavan SS**, Chiplunkar SV. Immunophenotypes and cytotoxic functions of lymphocytes in patients with hepatocellular carcinoma. *Tumori* 1997; **83**: 762-767
- 29 **Kim YJ**, Kim SH, Mantel P, Kwon BS. Human 4-1BB regulates CD28 co-stimulation to promote Th1 cell responses. *Eur J Immunol* 1998; **28**: 881-890
- 30 **DeBenedette MA**, Chu NR, Pollok KE, Hurtado J, Wade WF, Kwon BS, Watts TH. Role of 4-1BB ligand in costimulation of T lymphocyte growth and its upregulation on M12 B lymphomas by cAMP. *J Exp Med* 1995; **181**: 985-992
- 31 **Hurtado JC**, Kim YJ, Kwon BS. Signals through 4-1BB are costimulatory to previously activated splenic T cells and inhibit activation-induced cell death. *J Immunol* 1997; **158**: 2600-2609
- 32 **Blazar BR**, Kwon BS, Panoskaltis-Mortari A, Kwak KB, Peschon JJ, Taylor PA. Ligation of 4-1BB (CDw137) regulates graft-versus-host disease, graft-versus-leukemia, and graft rejection in allogeneic bone marrow transplant recipients. *J Immunol* 2001; **166**: 3174-3183
- 33 **DeBenedette MA**, Wen T, Bachmann MF, Ohashi PS, Barber BH, Stocking KL, Peschon JJ, Watts TH. Analysis of 4-1BB ligand (4-1BBL)-deficient mice and of mice lacking both 4-1BBL and CD28 reveals a role for 4-1BBL in skin allograft rejection and in the cytotoxic T cell response to influenza virus. *J Immunol* 1999; **163**: 4833-4841
- 34 **Tan JT**, Ha J, Cho HR, Tucker-Burden C, Hendrix RC, Mittler RS, Pearson TC, Larsen CP. Analysis of expression and function of the costimulatory molecule 4-1BB in alloimmune responses. *Transplantation* 2000; **70**: 175-183
- 35 **Sun Y**, Lin X, Chen HM, Wu Q, Subudhi SK, Chen L, Fu YX. Administration of agonistic anti-4-1BB monoclonal antibody leads to the amelioration of experimental autoimmune encephalomyelitis. *J Immunol* 2002; **168**: 1457-1465
- 36 **Michel J**, Langstein J, Hofstadter F, Schwarz H. A soluble form of CD137 (ILA/4-1BB), a member of the TNF receptor family, is released by activated lymphocytes and is detectable in sera of patients with rheumatoid arthritis. *Eur J Immunol* 1998; **28**: 290-295
- 37 **Sharief MK**. Heightened intrathecal release of soluble CD137 in patients with multiple sclerosis. *Eur J Neurol* 2002; **9**: 49-54
- 38 **Giuntoli RL 2nd**, Lu J, Kobayashi H, Kennedy R, Celis E. Direct costimulation of tumor-reactive CTL by helper T cells potentiate their proliferation, survival, and effector function. *Clin Cancer Res* 2002; **8**: 922-931
- 39 **Ye Z**, Hellstrom I, Hayden-Ledbetter M, Dahlin A, Ledbetter JA, Hellstrom KE. Gene therapy for cancer using single-chain Fv fragments specific for 4-1BB. *Nat Med* 2002; **8**: 343-348
- 40 **Martinet O**, Divino CM, Zang Y, Gan Y, Mandeli J, Thung S, Pan PY, Chen SH. T cell activation with systemic agonistic antibody versus local 4-1BB ligand gene delivery combined with interleukin-12 eradicate liver metastases of breast cancer. *Gene Ther* 2002; **9**: 786-792
- 41 **Bennett MW**, O'Connell J, O' Sullivan GC, Brady C, Roche D, Collins JK, Shanahan F. The Fas counterattack in vivo: apoptotic depletion of tumor-infiltrating lymphocytes associated with Fas ligand expression by human esophageal carcinoma. *J Immunol* 1998; **160**: 5669-5675
- 42 **Bodey B**, Bodey B Jr, Siegel SE, Kaiser HE. Immunocytochemical detection of leukocyte-associated and apoptosis-related antigen expression in childhood brain tumors. *Crit Rev Oncol Hematol* 2001; **39**: 3-16
- 43 **Santin AD**, Ravaggi A, Bellone S, Pecorelli S, Cannon M, Parham GP, Hermonat PL. Tumor-infiltrating lymphocytes contain higher numbers of type 1 cytokine expressors and DR⁺ T cells compared with lymphocytes from tumor draining lymph nodes and peripheral blood in patients with cancer of the uterine cervix. *Gynecol Oncol* 2001; **81**: 424-432
- 44 **Echchakir H**, Dorothee G, Vergnon I, Menez J, Chouaib S, Mami-Chouaib F. Cytotoxic T lymphocytes directed against a tumor-specific mutated antigen display similar HLA tetramer binding but distinct functional avidity and tissue distribution. *Proc Natl Acad Sci U S A* 2002; **99**: 9358-9363
- 45 **Santin AD**, Hermonat PL, Ravaggi A, Bellone S, Roman JJ, Smith CV, Pecorelli S, Radominska-Pandya A, Cannon MJ, Parham GP. Phenotypic and functional analysis of tumor-infiltrating lymphocytes compared with tumor-associated lymphocytes from ascitic fluid and peripheral blood lymphocytes in patients with advanced ovarian cancer. *Gynecol Obstet Invest* 2001; **51**: 254-261

Edited by Zhang JZ and Wang XL

Antitumor immunopreventive effect in mice induced by DNA vaccine encoding a fusion protein of α -fetoprotein and CTLA4

Geng Tian, Ji-Lin Yi, Ping Xiong

Geng Tian, Ji-Lin Yi, Department of General Surgery, Tongji Hospital, Tongji Medical College, Huazhong University of Science and Technology, Wuhan 430030, Hubei Province, China

Ping Xiong, Department of Immunology, Tongji Medical College, Huazhong University of Science and Technology, Wuhan 430030, Hubei Province, China

Correspondence to: Geng Tian, Department of General Surgery, Tongji Hospital, Tongji Medical College, Huazhong University of Science and Technology, Wuhan 430030, Hubei Province, China. geng_tian707@hotmail.com

Telephone: +86-27-83663402

Received: 2003-07-12 **Accepted:** 2003-07-30

Abstract

AIM: To develop a tumor DNA vaccine encoding a fusion protein of murine AFP and CTLA4, and to study its ability to induce specific CTL response and its protective effect against AFP-producing tumor.

METHODS: Murine α -fetoprotein (mAFP) gene was cloned from total RNA of Hepa1-6 cells by RT-PCR. A DNA vaccine was constructed by fusion murine α -fetoprotein gene and extramembrane domain of murine CTLA4 gene. The DNA vaccine was identified by restriction enzyme analysis, sequencing and expression. EL-4 (mAFP) was developed by stable transfection of EL-4 cells with pmAFP. The frequency of cells producing IFN- γ in splenocytes harvested from the immunized mice was measured by ELISPOT. Mice immunized with DNA vaccine were inoculated with EL-4 (mAFP) cells in back to observe the protective effect of immunization on tumor. On the other hand, blood samples were collected from the immunized mice to check the functions of liver and kidney.

RESULTS: 1.8 kb mAFP cDNA was cloned from total RNA of Hepa1-6 cells by RT-PCR. The DNA vaccine encoding a fusion protein of mAFP-CTLA4 was constructed and confirmed by restriction enzyme analysis, sequencing and expression. The expression of mAFP mRNA in EL-4 (mAFP) was confirmed by RT-PCR. The ELISPOT results showed that the number of IFN- γ -producing cells in pmAFP-CTLA4 group was significantly higher than that in pmAFP, pcDNA3.1 and PBS group. The tumor volume in pmAFP-CTLA4 group was significantly smaller than that in pmAFP, pcDNA3.1 and PBS group, respectively. The hepatic and kidney functions in each group were not altered.

CONCLUSION: AFP-CTLA4 DNA vaccine can stimulate potent specific CTL responses and has distinctive antitumor effect on AFP-producing tumor. The vaccine has no impact on the function of mouse liver and kidney.

Tian G, Yi JL, Xiong P. Antitumor immunopreventive effect in mice induced by DNA vaccine encoding a fusion protein of α -fetoprotein and CTLA4. *World J Gastroenterol* 2004; 10 (2): 200-204

<http://www.wjgnet.com/1007-9327/10/200.asp>

INTRODUCTION

Hepatocellular carcinoma (HCC) is a major cause of cancer death with more than 1.2 million global annual incidences. The incidence of HCC has been increasing rapidly in both Asian and Western countries because of the global pandemic of hepatitis B and C infections^[1]. Surgery and liver transplantation are the only effective treatments, but most HCC patients are not eligible due to the advanced stage of disease or poor hepatic function concomitant with cirrhosis^[2-8]. It is important to develop novel therapies for HCC, and some genes and immunotherapeutic strategies for HCC are under investigation.

Understanding of antigen processing and presentation by antigen-presenting cells, as well as the conditions of induction of T-cell immunity, has spawned the discipline of genetic immunotherapy. DNA-based immunization can induce strong cellular immune responses to a variety of antigens, including tumor antigens, such as antigens associated with malignant melanoma^[9-11], ovarian carcinoma^[12], breast cancer^[13,14], small-cell lung cancer^[15], neuroblastoma^[16] and prostate carcinoma^[17].

Two major obstacles in developing rational strategies in tumor immunotherapy are identification of suitable target tumor antigens and effective process and presentation by professional antigen-presenting cells to induce T cell immunity.

Recent studies on the immunodominant epitopes of AFP have provided a solution to the obstacle of HCC immunotherapy. The majority of human HCCs overexpress the oncofetal antigen AFP, M_r 70 000 glycoprotein. AFP is produced at fetal liver at high levels, and transcriptionally repressed at birth and is present thereafter at low serum levels throughout life^[18]. Butterfield *et al*^[19-21] found recently that 4 peptides of human AFP processed and presented in the context of HLA-A0201, could be recognized by the human T cell repertoire, and could be used to generate AFP-specific CTL in human T cell cultures and HLA-A0201/ K^b -transgenic mice. It was also found that the murine immune system could generate T-cell responses to this oncofetal antigen^[22-24]. AFP can serve as an effective tumor-specific antigen but its immunogenicity is weak^[19-25].

Cytotoxic T-lymphocyte antigen 4 (CTLA4) is a glycoprotein expressed on activated T cells. It has a strong binding affinity to both B7-1 (CD80) and B7-2 (CD86) molecules^[26], which are primarily expressed on APCs. CTLA4 is a homodimer, but dimerization of CTLA4 is not required for B7 binding^[27]. CTLA4-Ig has been used as an immunosuppressive drug in animal models of transplantation and autoimmune diseases^[28,29].

In the present study, we investigated whether the immunogenicity of mouse AFP could be improved by targeting to APCs through B7-1 and B7-2 molecules. We constructed a plasmid DNA encoding mAFP and the extramembrane domain of mouse CTLA4 and found this DNA vaccine could stimulate potent specific CTL responses and had distinctive antitumor effect on AFP-producing tumor.

MATERIALS AND METHODS

Cell lines and plasmids

Hepa 1-6 (murine HCC) and EL-4 (murine lymphoma) cell lines were gifts from Dr Wang Hao (The Second Military

Medical University, Shanghai, China). CHO cells were provided by China Center for Type Culture Collection (Wuhan, China). The plasmid pmCTLA4-Ig encoding murine CTLA4-Ig was kindly provided by Professor Wang DW (Tongji Medical College, Huazhong University of Science and Technology, Hubei, China). Eukaryotic expression vector pcDNA3.1/myc-His was from Invitrogen Company.

Main reagents

TRIzol was a product of Gibco Company. RT-PCR kit was purchased from TaKaRa Biotechnology Company. Lipofectamine 2000 was a product of Invitrogen Company. Goat anti-AFP polyclonal antibody was purchased from Sant Cruz Company. Biotinylated rabbit anti-CTLA4 polyclonal antibody was purchased from PepraTech Company. Primers were synthesized by the Shanghai Bioasia Biocompany. ECL Western blotting detection reagents were products of Pharmacia Company. Murine IFN- γ ELISPOT kit was a product of Diaclone Company.

Construction of Plasmids

The 1.8 kb mAFP cDNA was cloned from total RNA of Hepa1-6 cells by RT-PCR. Total RNA was isolated from Hepa1-6 cells by the TRIzol method. RT-PCR primers were designed to include the entire mAFP coding region, including the signal sequence. The primers used were 5' -CTCAGGAATTCGCC ATGAAGTGGATCACAC-3' and 5' -CTCTGCTCTAGATT ACTCGAGAACGCCCAAAGCATCACG-3'. The 1.8 kb mAFP cDNA PCR product was cloned into pcDNA3.1/myc-His to construct the plasmid pmAFP. The plasmid pmCTLA4-Ig was used as a temple to get the extramembrane domain of CTLA4 through PCR. To construct the mAFP-mCTLA4 fusion protein expression vector, we used overlap PCR to add a GGGGSGGGGS peptide linker upstream of the extramembrane domain of mouse CTLA4 gene. The forward primer 5' -TATGGCGGGGCTCGATGGAAGCCATAC AGGTG-3' and the reverse primer 5' -CTCTCTCTAGATC AAGAATCCGGGCATGGT-3' were used in the first round PCR on the mouse CTLA4-Ig gene. The PCR product was used as a template to perform a second round PCR using the same reverse primer and a second forward primer 5' -TTATATTCTC GAGGGAGGCGGGGCTCGGGAGGCGGGGCTCGATGG-3'. The 5' side of the first forward primer and the 3' side of the second forward primer were overlapped for 17 nucleotides. The N terminal of extramembrane domain of CTLA4 with linker was fused in frame with the C terminal of mAFP in pmAFP to construct the mAFP-mCTLA4 fusion protein expression plasmid pmAFP-CTLA4. The recombinant vector was identified by restriction enzyme analysis and sequencing.

Western blot

Lipofectamine 2000 was used for transient transfection of CHO cells according to the manufacturer's instructions. Proteins were separated on SDS-PAGE, and transferred onto a nitrocellulose membrane by semidry electroblotting. Proteins were stained with goat anti-AFP polyclonal antibody or biotinylated rabbit anti-CTLA4 polyclonal antibody, followed by anti-goat IgG-HRP or HRP-avidin. The blot was developed with ECL Western blotting detection reagents.

Stable transfection of EL-4 cells with plasmids pmAFP

EL-4 (mAFP) was developed by stable transfection of EL-4 cells with pmAFP by Lipofectamine 2000 according to the manufacturer's instructions. Transfectants were selected and maintained with G418 (0.3 mg/ml) in RPMI1640 complete media. The expression of mAFP mRNA in EL-4(mAFP) was assessed by RT-PCR.

Immunization and ELISPOT assay

Twenty-four female C57BL/6 mice were divided into pmAFP-CTLA4 group, pmAFP group, pcDNA3.1 group and PBS group, each group had 6 mice. For each mouse, 100 μ g plasmid was administered in the left anterior tibialis muscle on day 0 and day 14, respectively. On day 28 of study, all mice were killed. The splenic lymphocytes were separated for ELISPOT and the blood was drawn for examination of the functions of liver and kidney. The splenocytes were restimulated *in vitro* by EL-4(mAFP) as reported^[22]. In brief, splenocytes were cultured with irradiated EL-4 (mAFP) cells containing 10 unit/ml human IL-2 for 48 h at 37 °C. The anti-IFN- γ antibody coated ELISPOT plate was incubated with restimulated cells at 37 °C for 24 h.

Protective effect of DNA vaccine against tumor

Another 24 C57BL female mice were grouped and immunized as above. Two weeks after the last immunization, all mice were injected by 2×10^5 EL-4 (mAFP) on the back subcutaneously. Tumor mass was assessed two times weekly as the follow formula: $4/3\pi r^3$ (r = radius).

Examination of functions of liver and kidney

The serum ALT and creatinine were measured with ALT assay kit and creatinine assay kit, respectively.

Statistical analysis

Software SPSS 10.0 was employed to process the data. The *t* test was used for statistical analysis. $P < 0.05$ was considered significant.

RESULTS

Plasmids construction

The 1.8 kb mAFP cDNA was isolated from murine HCC cell line Hepa1-6 by RT-PCR and subcloned into pcDNA3.1 to construct plasmid pmAFP. We cloned the extracellular domain of mouse CTLA4 from plasmid pmCTLA4-Ig, and added a flexible linker (GGGGSGGGGS) before CTLA4 by overlap PCR. The N terminal of extramembrane domain of CTLA4 with linker was fused in frame with the C terminal of mAFP in pmAFP to construct the mAFP-mCTLA4 fusion protein expression plasmid pmAFP-CTLA4. Correct orientation of the ligations was determined by restriction enzyme analysis (Figure 1). Sequencing analysis showed that the reading frame was correct.

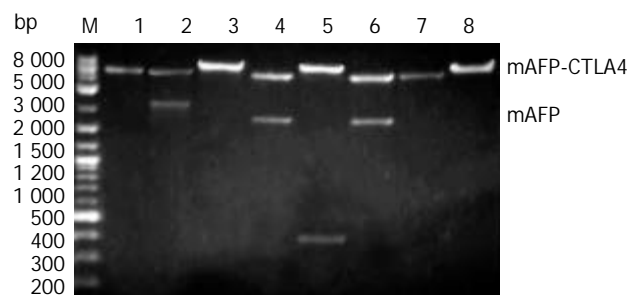


Figure 1 Identification of pmAFP and pmAFP-CTLA4 with restriction enzyme analysis. M: DNA marker, Lane 1: pcDNA3.1/EcoRI, Lane 2: pmAFP-CTLA4/EcoRI+XbaI, Lane 3: pmAFP-CTLA4/EcoRI, Lane 4: pmAFP-CTLA4/EcoRI+XhoI, Lane 5: pmAFP-CTLA4/XhoI+XbaI, Lane 6: pmAFP/EcoRI+XbaI, Lane 7: pcDNA3.1/EcoRI, Lane 8: pmAFP/EcoRI.

Western blot

Expression of plasmids pmAFP and pmAFP-CTLA4 in transient transfection of CHO cells was analyzed with Western blotting, the expected two protein bands (-70 and -84 kDa)

were shown (Figure 2). The expression of mAFP mRNA in EL-4(mAFP) was confirmed by RT-PCR(data not shown).

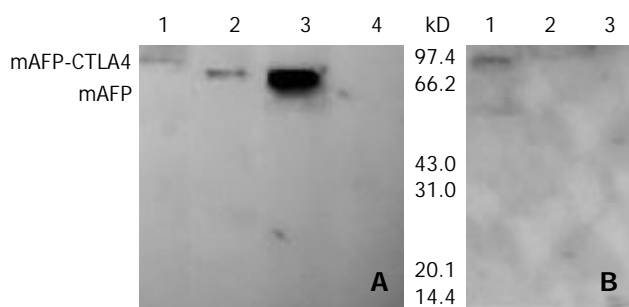


Figure 2 Detection of protein expression of plasmids by Western blotting. A: the blot was probed with anti-AFP. Lane 1: CHO/pmAFP-CTLA, Lane 2: CHO/pmAFP, Lane 3: Hepa 1-6, Lane 4: CHO/pcDNA3.1, B: the blot was probed with anti-CTLA4. Lane 1: CHO/pmAFP-CTLA, Lane 2: CHO/pmAFP, Lane 3: CHO/pcDNA3.1.

ELISPOT assay

ELISPOT results showed the number of IFN- γ -producing cells in pmAFP-CTLA4 group was significantly higher than that in pmAFP group ($P<0.01$), pcDNA3.1 group ($P<0.01$) and PBS group ($P<0.01$) (Figure 3).

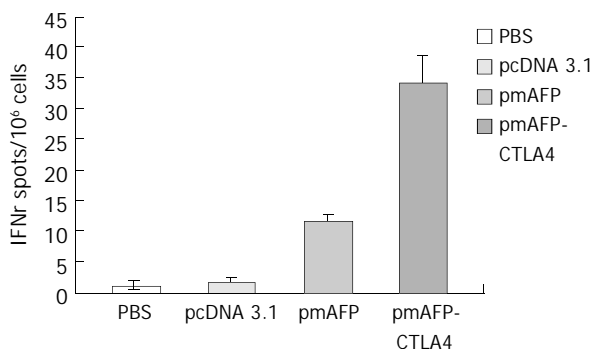


Figure 3 Number of IFN- γ -producing cells in 4 different groups.

Protective effect of DNA vaccine against tumor

The tumor growth in pmAFP-CTLA4 group was slower than that in other groups. Twenty two days after tumor challenge, the tumor volume of pmAFP-CTLA4 group was significantly smaller than that in pmAFP group ($P<0.01$), pcDNA3.1 group ($P<0.01$) and PBS group ($P<0.01$) (Figure 4).

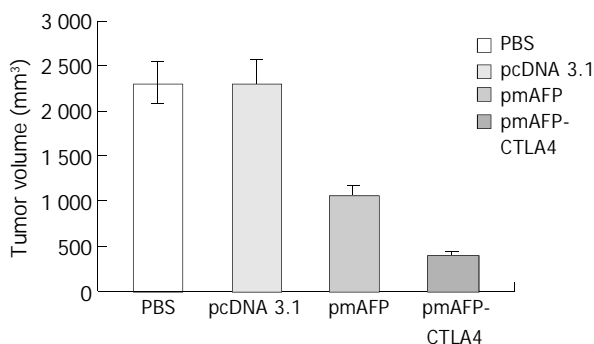


Figure 4 Comparison of tumor masses in 4 groups on 22 days following tumor challenge.

Functions of liver and kidney

The serum level of ALT and creatinine in each group was

unchanged (Table 1), suggesting that the immunization had no impact on the function of liver and kidney.

Table 1 Serum level of ALT and creatinine after immunization with DNA vaccine

Groups	<i>n</i>	ALT/U·mL ⁻¹ ($\bar{x}\pm s$)	Creatinine/ μ mol·L ⁻¹ ($\bar{x}\pm s$)
PBS	6	51.1 \pm 1.7	119.4 \pm 6.9
pcDNA3.1	6	50.9 \pm 1.5	116.6 \pm 9.7
pmAFP	6	51.6 \pm 2.5	116.4 \pm 6.0
pmAFP-CTLA4	6	52.5 \pm 3.2	118.6 \pm 11.5

DISCUSSION

Many tumors express tumor-associated or tumor-specific antigens but do not elicit an efficient immune response. Various experimental strategies have been explored to enhance the immunogenicity of tumor vaccines. Targeting immunogens to APCs with Abs against class MHC^[30,31], Fc γ R^[30], 33D1^[31], or surface Ig^[32] could substantially increase Ab responses. Antigens could be presented to APCs more efficiently by conjugating with Fc γ R^[33], IP10^[34], MCP-3^[34], L-selectin^[35] and CTLA4^[35,36], and lead to significant antitumor immunity^[34,36]. A DNA vaccine that can express carcinoembryonic Ag (CEA), AFP, and CD40 ligand trimer fusion protein, could break peripheral T cell tolerance against CEA and achieve effective tumor-protective immunity against murine colon carcinoma in CEA-transgenic mice^[37].

HCC is a highly malignant tumor with a poor prognosis and few therapeutic options. AFP is a HCC-associated Ag but can not elicit efficient immune response. Some experimental strategies have been explored to enhance the immunogenicity of HCC vaccines based on AFP. Previous experiments of AFP-specific genetic immunotherapy for HCC included AFP plasmid immunization, AFP-transduced DCs immunization and AFP plasmid prime-AFP adenovirus boost immunization. Plasmid AFP immunization resulted in detectable but low levels of AFP-specific T-cell responses and poorly reproducible protective immunity^[22-25]. DCs engineered to express murine AFP demonstrated a powerful ability to generate AFP-specific T-cell responses and protective immunity in mice^[22,23]. However, the need for costly cell culture procedures precluded their wide availability for clinical use, and minor variation in the culture technique or antigen loading might yield sub optimal, even tolerating vaccines^[38,39]. AFP plasmid prime-AFP adenovirus boost immunization could generate significant AFP-specific T-cell responses and protective immunity in mice^[23]. But this method at least has two steps. In the present study, we tested a novel strategy for inducing anti-HCC immunity by specifically targeting APCs with a DNA vaccine encoding both AFP and CTLA4 in mice. We found that the vaccine elicited strong AFP-specific T-cell responses and had distinctive preventive effect on AFP-producing tumor.

We attributed the successful α -fetoprotein specific T cell responses in mice to the CTLA4 moiety targets APCs for efficient receptor-mediated uptake and processing of mAFP. CTLA4 could likely provide such a strong adjuvant activity due to its strong binding affinity to B7 molecules on APCs. CTLA4 could bind to both B7-1 and B7-2 with a 20- to 50-fold higher affinity than CD28^[40]. A CTLA4-Ig fusion protein composed of CTLA4 and IgG Fc was 4-fold high of that in draining lymph nodes, levels of nontargeted protein within 2-24 hours administration^[41]. Monomeric CTLA4 also has binding activity for B7-1 and B7-2, though its binding activity is low when compared with dimeric CTLA4.

CTLA4-Ig has been used as an immunosuppressive drug in animal models of transplantation and autoimmune

diseases^[28,29]. Our current study showed the enhanced immunogenicity of mAFP-CTLA4. CTLA4 had 20 to 50-fold higher affinity to both B7-1 and B7-2 than CD28. The immune suppression mediated by CTLA4-Ig was likely through its inhibition of CD28-B7 interactions, which provide an important positive signal for T-cell proliferation and cytokine release^[42]. The different immunomodulating effects of CTLA4 might be caused by varied doses of CTLA4 administered. In previous studies, to achieve maximal immune suppression, 50-500 µg CTLA4-Ig was applied before and after transplantation for several consecutive days. But when fusion protein Id-CTLA4 was used as vaccine in another experiment, only twice administration of 0.1-50 µg Id-CTLA4 was sufficient enough to elicit strong immune response to Id^[36]. Vaccination with DNA encoding CTLA4-Ig provided an additional evidence that CTLA4-Ig at low levels could increase both Ab and T-cell proliferation responses^[35,43].

In summary, the result suggests that a DNA vaccine encoding AFP and CTLA4 can elicit strong AFP-specific T-cell responses and has distinctive antitumor effect on AFP-producing tumor.

REFERENCES

- Schafer DF**, Sorrell MF. Hepatocellular carcinoma. *Lancet* 1999; **353**: 1253-1257
- Tang ZY**. Hepatocellular carcinoma—cause, treatment and metastasis. *World J Gastroenterol* 2001; **7**: 445-454
- Qin LX**, Tang ZY. The prognostic significance of clinical and pathological I features in hepatocellular carcinoma. *World J Gastroenterol* 2002; **8**: 193-199
- Zhang G**, Long M, Wu ZZ, Yu WQ. Mechanical properties of hepatocellular carcinoma cells. *World J Gastroenterol* 2002; **8**: 243-246
- Tang ZY**, Sun FX, Tian J, Ye SL, Liu YK, Liu KD, Xue Q, Chen J, Xia JL, Qin LX, Sun HC, Wang L, Zhou J, Li Y, Ma ZC, Zhou XD, Wu ZQ, Lin ZY, Yang BH. Metastatic human hepatocellular carcinoma models in nude mice and cell line with metastatic potential. *World J Gastroenterol* 2001; **7**: 597-601
- Zheng WW**, Zhou KR, Chen ZW, Shen JZ, Chen CZ, Zhang SJ. Characterization of focal hepatic lesions with SPIO-enhanced MRI. *World J Gastroenterol* 2002; **8**: 82-86
- Fu JM**, Yu XF, Shao YF. Telomerase and primary liver cancer. *Shijie Huaren Xiaohua Zazhi* 2000; **8**: 461-463
- Su YH**, Zhu SN, Lu SL, Gu YH. HCV genotypes expression in hepatocellular carcinoma by reverse transcription *in situ* polymerase chain reaction. *Shijie Huaren Xiaohua Zazhi* 2000; **8**: 874-878
- Mendiratta SK**, Thai G, Eslahi NK, Thull NM, Matar M, Bronte V, Pericle F. Therapeutic tumor immunity induced by polyimmunization with melanoma antigens gp100 and TRP-2. *Cancer Res* 2001; **61**: 859-862
- Wagner SN**, Wagner C, Luhrs P, Weimann TK, Kutil R, Goos M, Stinge G, Schneeberger A. Intracutaneous genetic immunization with autologous melanoma-associated antigen Pmel17/gp100 induces T cell-mediated tumor protection *in vivo*. *J Invest Dermatol* 2000; **115**: 1082-1087
- Park JH**, Kim CJ, Lee JH, Shin SH, Chung GH, Jang YS. Effective immunotherapy of cancer by DNA vaccination. *Mol Cells* 1999; **9**: 384-391
- Neglia F**, Orengo AM, Cilli M, Meazza R, Tomassetti A, Canevari S, Melani C, Colombo MP, Ferrini S. DNA vaccination against the ovarian carcinoma-associated antigen folate receptor- α (Fr α) induces cytotoxic T lymphocyte and antibody responses in mice. *Cancer Gene Ther* 1999; **6**: 349-357
- Pupa SM**, Invernizzi AM, Forti S, Di Carlo E, Musiani P, Nanni P, Lollini PL, Meazza R, Ferrini S, Menard S. Prevention of spontaneous neu-expressing mammary tumor development in mice transgenic for rat proto-neu by DNA vaccination. *Gene Ther* 2001; **8**: 75-79
- Lachman LB**, Rao XM, Kremer RH, Ozpolat B, Kiriakova G, Price JE. DNA vaccination against neu reduces breast cancer incidence and metastasis in mice. *Cancer Gene Ther* 2001; **8**: 259-268
- Ohwada A**, Nagaoka I, Takahashi F, Tominaga S, Fukuchi Y. DNA vaccination against HuD antigen elicits antitumor activity in a small-cell lung cancer murine model. *Am J Respir Cell Mol Biol* 1999; **21**: 37-43
- Lode HN**, Pertl U, Xiang R, Gaedicke G, Reisfeld RA. Tyrosine hydroxylase-based DNA vaccination is effective against murine neuroblastoma. *Med Pediatr Oncol* 2000; **35**: 641-646
- Kim JJ**, Yang JS, Dang K, Manson KH, Weiner DB. Engineering enhancement of immune responses to DNA-based vaccines in a prostate cancer model in rhesus macaques through the use of cytokine gene adjuvants. *Clin Cancer Res* 2001; **7**: 882s-889s
- Deutsch HF**. Chemistry and biology of α -fetoprotein. *Adv Cancer Res* 1991; **56**: 253-311
- Butterfield LH**, Koh A, Meng W, Vollmer CM, Ribas A, Dissette VB, Lee E, Glaspy JA, McBride WH, Economou JS. Generation of human T cell responses to an HLA-A2.1-restricted peptide epitope from α Fetoprotein. *Cancer Res* 1999; **59**: 3134-3142
- Butterfield LH**, Meng WS, Koh A, Vollmer CM, Ribas A, Dissette VB, Faull K, Glaspy JA, McBride WH, Economou JS. T cell responses to HLA-A*0201-restricted peptides derived from α -fetoprotein. *J Immunol* 2001; **166**: 5300-5308
- Meng WS**, Butterfield LH, Ribas A, Heller JB, Dissette VB, Glaspy JA, McBride WH, Economou JS. Fine specificity analysis of an HLA-A2.1-restricted immunodominant T cell epitope derived from human alpha-fetoprotein. *Mol Immunol* 2000; **37**: 943-950
- Vollmer CM Jr**, Eilber FC, Butterfield LH, Ribas A, Dissette VB, Koh A, Montejó L, Andrews K, McBride WH, Glaspy JA, Economou JS. α fetoprotein-specific immunotherapy for hepatocellular carcinoma. *Cancer Res* 1999; **59**: 3064-3067
- Meng WS**, Butterfield LH, Ribas A, Dissette VB, Heller JB, Miranda GA, Glaspy JA, McBride WH, Economou JS. α -fetoprotein-specific tumor immunity induced by plasmid prime-adenovirus boost genetic vaccination. *Cancer Res* 2001; **61**: 8782-8786
- Grimm CF**, Ortman D, Mohr L, Michalak S, Krohne TU, Meckel S, Eisele S, Encke J, Blum HE, Geissler M. Mouse α -fetoprotein-specific DNA-based immunotherapy of hepatocellular carcinoma leads to tumor regression in mice. *Gastroenterology* 2000; **119**: 1104-1112
- Bei R**, Budillon A, Reale MG, Capuano G, Pomponi D, Budillon G, Frati L, Muraro R. Cryptic epitopes on α -fetoprotein induce spontaneous immune responses in hepatocellular carcinoma, liver cirrhosis, and chronic hepatitis patients. *Cancer Res* 1999; **59**: 5471-5474
- Linsley PS**, Ledbetter JA. The role of the CD28 receptor during T cell responses to antigen. *Annu Rev Immunol* 1993; **11**: 191-212
- Linsley PS**, Nadler SG, Bajorath J, Peach R, Leung HT, Rogers J, Bradshaw J, Stebbins M, Leytze G, Brady W, Malacko AR, Marquardt H, Shaw SY. Binding stoichiometry of the cytotoxic T lymphocyte-associated molecule-4. *J Biol Chem* 1995; **270**: 15417-15424
- Lin H**, Bolling SF, Linsley PS. Long-term acceptance of major histocompatibility complex mismatched cardiac allografts induced by CTLA4Ig plus donor-specific transfusion. *J Exp Med* 1993; **178**: 1801-1806
- Frinck BK**, Linsley PS, Wofsy D. Treatment of murine lupus with CTLA4Ig. *Science* 1994; **265**: 1225-1227
- Snider DP**, Kaubisch A, Segal DM. Enhanced antigen immunogenicity induced by bispecific antibodies. *J Exp Med* 1990; **171**: 1957-1963
- Carayanniotis G**, Skea DL, Luscher MA, Barber BH. Adjuvant-independent immunization by immunotargeting antigens to MHC and non-MHC determinants *in vivo*. *Mol Immunol* 1991; **28**: 261-267
- Kawamura H**, Berzofsky JA. Enhancement of antigenic potency *in vitro* and immunogenicity *in vivo* by coupling the antigen to anti-immunoglobulin. *J Immunol* 1986; **136**: 58-65
- Gosselin EJ**, Wardwell K, Gosselin DR, Alter N, Fisher JL, Guyre PM. Enhanced antigen presentation using human Fc gamma receptor (monocyte/macrophage)-specific immunogens. *J Immunol* 1992; **149**: 3477-3481
- Biragyn A**, Tani K, Grimm MC, Weeks S, Kwak LW. Genetic fusion of chemokines to a self tumor antigen induces protective, T-cell dependent antitumor immunity. *Nat Biotechnol* 1999; **17**: 253-258

- 35 **Boyle JS**, Brady JL, Lew AM. Enhanced responses to a DNA vaccine encoding a fusion antigen that is directed to sites of immune induction. *Nature* 1998; **392**: 408-411
- 36 **Huang TH**, Wu PY, Lee CN, Huang HI, Hsieh SL, Kung J, Tao MH. Enhanced antitumor immunity by fusion of CTLA4 to a self tumor antigen. *Blood* 2000; **96**: 3663-3670
- 37 **Xiang R**, Primus FJ, Ruehlmann JM, Niethammer AG, Silletti S, Lode HN, Dolman CS, Gillies SD, Reisfeld RA. A dual-function DNA vaccine encoding carcinoembryonic antigen and CD40 ligand trimer induces T cell-mediated protective immunity against colon cancer in carcinoembryonic antigen-transgenic mice. *J Immunol* 2001; **167**: 4560-4565
- 38 **Steinman RM**, Turley S, Mellman I, Inaba K. The induction of tolerance by dendritic cells that have captured apoptotic cells. *J Exp Med* 2000; **191**: 411-416
- 39 **Chakraborty A**, Li L, Chakraborty NG, Mukherji B. Stimulatory and inhibitory differentiation of human myeloid dendritic cells. *Clin Immunol* 2000; **94**: 88-98
- 40 **Linsley PS**, Greene JL, Brady W, Bajorath J, Ledbetter JA, Peach R. Human B7-1 (CD80) and B7-2 (CD86) bind with similar avidities but distinct kinetics to CD28 and CTLA4 receptors. *Immunity* 1994; **1**: 793-801
- 41 **Deliyannis G**, Boyle JS, Brady JL, Brown LE, Lew AM. A fusion DNA vaccine that targets antigen-presenting cells increases protection from viral challenge. *Proc Natl Acad Sci U S A* 2000; **97**: 6676-6680
- 42 **Lenschow DJ**, Walunas TL, Bluestone JA. CD28/B7 system of T cell costimulation. *Annu Rev Immunol* 1996; **14**: 233-258
- 43 **Chaplin PJ**, De Rose R, Boyle JS, McWaters P, Kelly J, Tennent JM, Lew AM, Scheerlinck JP. Targeting improves the efficacy of a DNA vaccine against *Corynebacterium pseudotuberculosis* in sheep. *Infect Immun* 1999; **67**: 6434-6438

Edited by Ren SY and Wang XL

Enhancement of osteopontin expression in HepG2 cells by epidermal growth factor via phosphatidylinositol 3-kinase signaling pathway

Guo-Xin Zhang, Zhi-Quan Zhao, Hong-Di Wang, Bo Hao

Guo-Xin Zhang, Zhi-Quan Zhao, Hong-Di Wang, Bo Hao, Department of Gastroenterology, the First Affiliated Hospital, Nanjing Medical University, Nanjing 210029, Jiangsu Province, China

Correspondence to: Dr. Guo-Xin Zhang, 300 Guangzhou Road, Department of Gastroenterology, the First Affiliated Hospital, Nanjing Medical University, Nanjing 210029, Jiangsu Province, China. guoxinz2002@yahoo.com

Telephone: +86-25-3718836 **Fax:** +86-25-3724440

Received: 2003-06-21 **Accepted:** 2003-08-16

Abstract

AIM: Osteopontin (OPN) is a phosphorylated glycoprotein with diverse functions including cancer development, progression and metastasis. It is unclear how osteopontin is regulated in HepG2 cells. The aim of this study was to investigate the effect of epidermal growth factor on the expression of osteopontin in HepG2 cells, and to explore the signal transduction pathway mediated this expression.

METHODS: Osteopontin expression was detected by RNAase protection assay and Western blot. Wortmannin, a specific inhibitor of PI3K, was used to see if PI3K signal transduction was involved in the induction of osteopontin gene expression.

RESULTS: HepG2 cells constitutively expressed low levels of osteopontin. Treatment with epidermal growth factor increased osteopontin mRNA and protein level in a dose- and time-dependent manner. Application of wortmannin caused a dramatic reduction of epidermal growth factor-induced osteopontin expression.

CONCLUSION: Osteopontin gene expression can be induced by treatment of HepG2 cells with epidermal growth factor. Epidermal growth factor may regulate osteopontin gene expression through PI3K signaling pathway. Several potential targets in the pathway can be manipulated to block the synthesis of osteopontin and inhibit liver cancer metastasis.

Zhang GX, Zhao ZQ, Wang HD, Hao B. Enhancement of osteopontin expression in HepG2 cells by epidermal growth factor via phosphatidylinositol 3-kinase signaling pathway. *World J Gastroenterol* 2004; 10(2): 205-208

<http://www.wjgnet.com/1007-9327/10/205.asp>

INTRODUCTION

Osteopontin (OPN) is a secreted arginine-glycine-aspartate (RGD)-containing phosphoprotein with cell adhesive and chemotactic properties *in vitro* and *in vivo*^[1-3]. It is closely associated with infiltrating macrophages in tumors and can directly stimulate macrophage migration, which has made it a key target as a molecule likely to be important in mediating tumor metastasis^[4]. It has been shown that osteopontin is up-regulated in many kinds of cancer, including hepatocellular

carcinoma^[5,6], breast cancer^[7-9], prostate cancer^[10,11], ovarian cancer^[12,13], brain cancer^[14,15] and lung cancer^[16]. Elevated osteopontin transcription often correlates with increased metastatic potential of cancers.

Epidermal growth factor (EGF) receptor (EGFR) is a member of the ErbB family of ligand-activated tyrosine kinase receptors, which play a central role in the proliferation, differentiation, and/or oncogenesis of epithelial cells, neural cells, and fibroblasts^[17,18]. It has been reported that EGF can induce osteopontin expression of breast cancer cells^[19], rat kidney epithelial cells^[20] and HL60 cells^[21], and the induction of osteopontin may involve in signaling pathway related to PKC and tyrosine kinase^[22]. The mechanism responsible for osteopontin up-regulation in HCC is unknown, but may involve induction by specific cytokines. We have investigated this hypothesis by testing the effects of epidermal growth factor on osteopontin regulation in hepatocellular carcinoma cell line, HepG2. Using RNase protection assay, Western blot, we found that HepG2 cells constitutively expressed low levels of osteopontin mRNA and protein. EGF is a potent inducer of osteopontin mRNA and protein in HepG2 cells. Wortmannin, a specific PI3-K inhibitor, blocks the EGF-induced OPN expression. Our study suggests that OPN expression induced by EGF is dependent on PI3-K signaling pathway in HepG2 cells.

MATERIALS AND METHODS

Cell line and culture

HepG2 cell line was obtained from Cell Biology Institute (Shanghai, China). Cells were cultured in DMEM (Gibco BRL) containing 10% fetal calf serum (Hyclone).

Induction of growth factor signaling

Cells were plated at 1×10^5 per well in 6-well plates, and were grown overnight. Next morning, the cultures were washed twice with PBS and maintained in serum-free medium (containing 0.05% BSA) for 24 hours. The cells were then stimulated with the indicated amounts of EGF (Sigma) for the indicated time frames before harvesting and analysis.

To assess signal transduction molecules involved in the induction of osteopontin gene expression, the PI3-Kinase inhibitor wortmannin (Calbiochem) was added to the cells. The cells were pretreated with respective inhibitors or vehicle (DMSO) alone for half an hour and then treated in combination with EGF for 8 hours. Preliminary dose-response experiments had defined the concentrations of 100nM wortmannin to be effective and non-toxic.

DNA constructs and *in vitro* transcription

Plasmid pGEM-OPN containing osteopontin fragments was constructed in our laboratory. A 486bp of OPN fragment was obtained by reverse transcription-PCR from plasmid pBlueScript-OPN containing full length human osteopontin (a kind gift from Dr. Chambers, Canada) using the sense primer 5' -ATGGATCCGATGACACTGATGATTCTCAC-3' and

antisense primer 5'-GCGAATTCGAATTCACGGCTGACAAA-3'. The resultant BamHI-EcoRI cDNA fragment was ligated into the vector pGEM, and confirmed by direct sequencing.

To make RNA probes for OPN and β -actin (a linearized plasmid containing β -actin fragment included in the kit), *in vitro* transcription was performed with a commercial kit (Ambion), according to the user's instructions.

RNA isolation and RNase protection assay

Total RNA was isolated using the RNeasy Mini kit (QIAGEN GmbH, Germany). RNase protection assay was performed with a commercial kit (Ambion). $\alpha^{32}\text{P}$ -UTP labeled probes were mixed with sample RNA and co-precipitated. Hybridization was proceeded for 10 minutes at 68 °C, followed by digestion with RNase A-T1 for 30 minutes at 37 °C, and separation of hybridized RNA on 5% acrylamide and 8M urea gels. The gels were dried on filter paper for 40 minutes at 80 °C, and exposed to X-ray film. The autoradiographs were scanned using an AlphaImager 2200 spot densitometer (Alpha Innotech Corporation), and the integrated densities of areas were recorded.

Western blot

Cultured cells were lysed in RIPA buffer (50 mM Tris-HCL pH 7.5, 150 mM NaCl, 1% NP-40, 0.5% Na-deoxycholate,

0.1% sodium dodecyl sulfate). Cell lysates were denatured at 100 °C for 5 minutes, and equal amounts of protein were loaded onto 10% SDS-polyacrylamide gels. The separated proteins were transferred to PVDF membranes (ROCHE) and probed with antibodies to osteopontin (Calbiochem). Membranes were stripped and re-probed with antibodies to tubulin as an internal control.

RESULTS

OPN expression in HepG2 cells induced by EGF-treatment

In order to examine the regulators of osteopontin expression in hepatocellular carcinoma cells, HepG2 cells were incubated in serum-free medium and then treated with epidermal growth factor that had been implicated in HCC. As shown in Figures 1 and 2, HepG2 cells constitutively expressed low levels of osteopontin, stimulation of the cells with EGF increased osteopontin mRNA expression as well as protein level in a dose-dependent and time-dependent manner. To quantitate this finding, densitometry of osteopontin mRNA levels was recorded (Figure 1B and Figure 2B). Osteopontin expression was elevated after treatment with EGF within a 8-hour period, expression levels were further increased at 16 hours and 24 hours following treatment.

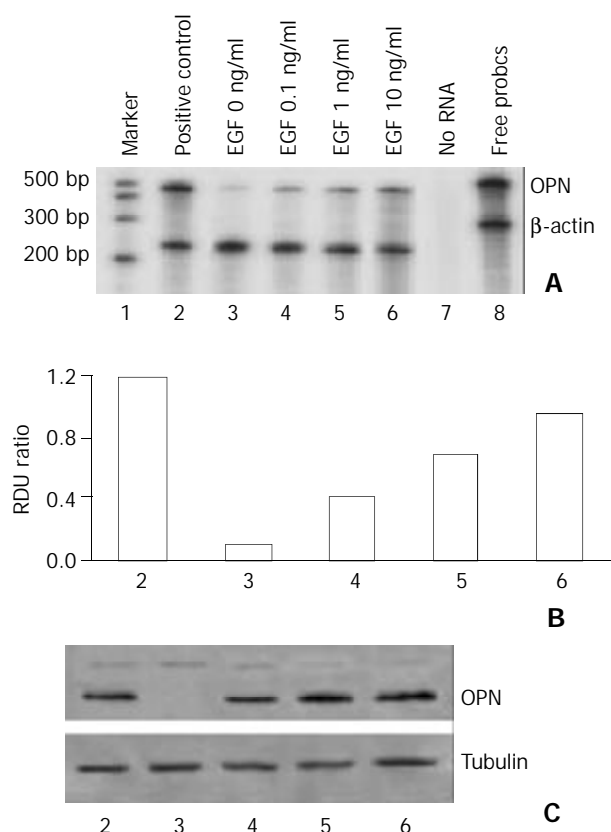


Figure 1 Dose-dependent effect of EGF on osteopontin expression in HepG2 cells. 1×10^5 cells were plated in 6-well plates. Next morning, cell cultures (near 80% confluent) were incubated in serum-free medium for 24 hours. The cells were stimulated dose-dependently by epidermal growth factor. Positive control denotes cells in normal growth medium containing 10% fetal calf serum. A. Osteopontin mRNA level was analyzed by RNase protection assay on total RNA using a 486 base-pair probe and controlling the loading with a probe for β -actin. B. Quantitation of osteopontin mRNA levels is shown in (A). RDU ratio reflects relative density units of osteopontin mRNA divided by β -actin mRNA. C. The results from RNase protection assay were confirmed by Western blot of osteopontin protein. Tubulin was served as loading control.

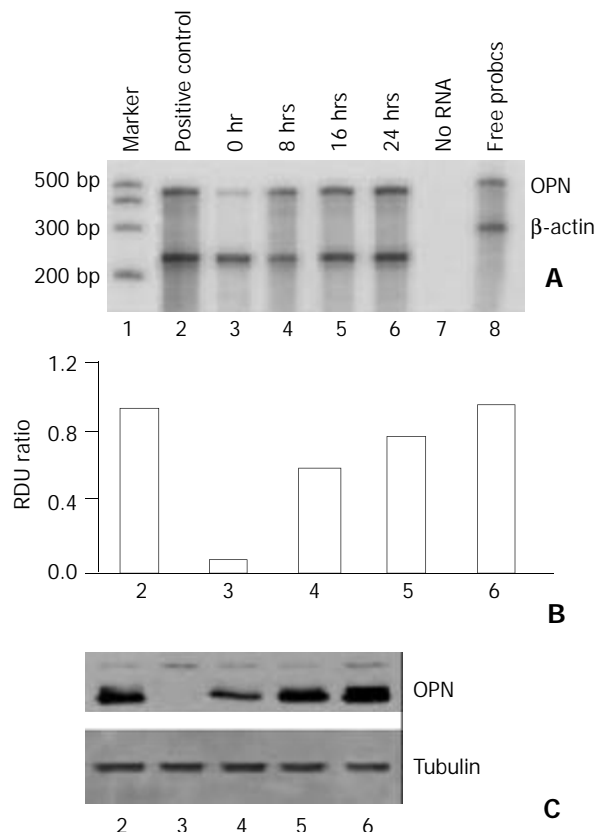


Figure 2 Time course showing effect of EGF on osteopontin expression in HepG2 cells. 1×10^5 cells were plated in 6-well plates. Next morning, cell cultures (near 80% confluent) were incubated in serum-free medium for 24 hours. The cells were stimulated time-dependently by 10 ng/ml EGF. Positive control denotes cells in normal growth medium containing 10% fetal calf serum. A. Osteopontin gene expression was analyzed by RNase protection assay on total RNA using a 486 base pair probe and standardized by comparison to β -actin. B. Quantitation of osteopontin mRNA levels is shown in (A). RDU ratio reflects relative density units of osteopontin mRNA divided by β -actin mRNA. C. Western blot of osteopontin protein by cell lysates confirmed the results from RNase protection assay. Tubulin was served as loading control.

Interference of EGF-induced osteopontin gene expression in HepG2 cells with inhibition of PI3-kinase

We analyzed the involvement of EGF signaling pathway in the induction of osteopontin gene expression. Addition of the PI3-kinase inhibitor wortmannin blocked EGF-mediated increase of osteopontin mRNA levels in HepG2 cells (Figure 3). It should be mentioned that wortmannin only partially reversed EGF-induced osteopontin expression, suggesting that other pathways related to EGF might involve the induction of osteopontin expression.

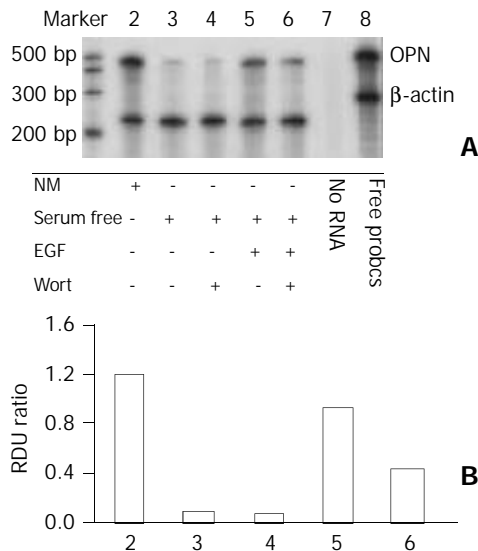


Figure 3 Phosphatidylinositol 3-kinase pathway dependent of osteopontin expression in HepG2 cells. The PI3-kinase inhibitor wortmannin was used to assess EGF-dependent signal transduction leading to osteopontin gene expression. 1×10^5 cells were plated in 6-well plates. Next morning, cell cultures (near 80% confluent) were incubated in serum-free medium for 24 hours. 100 nM wortmannin was added to the cells 30 minutes before incubation in the presence or absence of 10 ng/ml EGF. A. Osteopontin mRNA level was analyzed by RNase protection assay on total RNA using a 486 base-pair probe and controlling the loading with a probe for β -actin. B. Quantitation of osteopontin mRNA levels is shown in (A). RDU ratio reflects relative density units of osteopontin mRNA divided by β -actin mRNA.

DISCUSSION

Hepatocellular carcinoma (HCC) is one of the most malignant tumors in the world^[23]. In China, at least 100 000 new cases occur every year, and the estimated number of HCC-related deaths exceeds 110 000 per year. Recent studies indicate that the incidence of HCC in the US and UK has increased substantially over the last two decades^[24,25]. Although remarkable advances in surgery have improved the prognosis of HCC patients, the high rate of intra-hepatic recurrence and metastasis remains a major challenge in HCC therapy^[26,27]. Recently, it has been reported metastasis genes or metastasis-associated genes are involved in the migration and dissemination of cancers through certain signaling pathway^[28,29]. Therefore, if the signal transduction pathway that regulates the expression of metastasis genes could be defined, some candidate targets via the pathway can be used to block the malignancy-promoting effects of metastasis genes, which will be useful for therapeutic intervention, including controlling the recurrence and metastasis of HCC.

Cytokine osteopontin, one of the metastatic genes, has been found in a number of tumors^[5-16], and to be essential for the dissemination of various cancers^[30]. Transfection of the cells

with anti-sense OPN RNA reduced the malignancy of the cells and caused the decrease of tumorigenesis^[31], while transfection with osteopontin increased their malignant phenotype^[32]. Osteopontin was up-regulated in hepatocellular carcinoma and the increase of OPN expression was correlated with the metastatic ability of HCC and invasiveness of liver tumor-derived cell lines *in vitro*^[5,6]. In the present study, we found that HepG2 cells constitutively expressed low levels of osteopontin, and EGF induced osteopontin expression in a dose- and time- dependent manner in the cell line. The concentration of EGF in the cells was very low. The induction of osteopontin was prominent at 0.1 ng/ml EGF concentration in our study, while the concentration of EGF was high up to 100 ng/ml in the literature^[19,33]. The difference can be caused by many kinds of reasons, one of them may be that the different cells have different response to EGF. To our knowledge, this is the first study to demonstrate that EGF can cause the induction of osteopontin mRNA and protein levels in liver cancer cells. In other cell lines, the up-regulation of osteopontin by EGF was confirmed by overwhelming number of studies, including in kidney epithelial cells^[33] and osteoblasts^[22].

We then investigated the mechanism of osteopontin regulation by EGF in HepG2 cells. Using wortmannin, a specific inhibitor of PI3K, we found that EGF-induced osteopontin expression was significantly down-regulated. It suggested that the induction of osteopontin by EGF was dependent on PI3K signal transduction pathway in HepG2 cells. On the other hand, our results showed that wortmannin could not totally block EGF-induced osteopontin expression in HepG2 cells, suggesting that other pathways associated with EGF and its receptor may involve in the osteopontin induction.

A conclusion may be drawn from the study that EGF/PI3K signal pathway can regulate the expression of osteopontin in hepatocellular carcinoma cell line, HepG2. Several candidate targets via this pathway can be used for therapeutic intervention of HCC.

ACKNOWLEDGEMENTS

We thank Dr. Chambers for generously supplying the osteopontin construct.

REFERENCES

- 1 **Oldberg A**, Franzen A, Heinegard D. Cloning and sequence analysis of rat bone sialoprotein (osteopontin) cDNA reveals an Arg-Gly-Asp cell-binding sequence. *Proc Natl Acad Sci U S A* 1986; **83**: 8819-8823
- 2 **Nasu K**, Ishida T, Setoguchi M, Higuchi Y, Akizuki S, Yamamoto S. Expression of wild-type and mutated rabbit osteopontin in *Escherichia coli* and their effects on adhesion and migration of P388D1 cells. *Biochem J* 1995; **307**(Pt 1): 257-265
- 3 **Weber GF**, Ashkar S, Glimcher MJ, Cantor H. Receptor-ligand interaction between CD44 and osteopontin (Eta-1). *Science* 1996; **271**: 509-512
- 4 **Singh RP**, Patarca R, Schwartz J, Singh P, Cantor H. Definition of a specific interaction between the early T lymphocyte activation 1 (Eta-1) protein and murine macrophages *in vitro* and its effect upon macrophages *in vivo*. *J Exp Med* 1990; **171**: 1931-1942
- 5 **Gotoh M**, Sakamoto M, Kanetaka K, Chuuma M, Hirohashi S. Overexpression of osteopontin in hepatocellular carcinoma. *Pathol Int* 2002; **52**: 19-24
- 6 **Ye QH**, Qin LX, Forgues M, He P, Kim JW, Peng AC, Simon R, Li Y, Robles AI, Chen Y, Ma ZC, Wu ZQ, Ye SL, Liu YK, Tang ZY, Wang XW. Predicting hepatitis B virus-positive metastatic hepatocellular carcinomas using gene expression profiling and supervised machine learning. *Nat Med* 2003; **9**: 416-423
- 7 **Urquidí V**, Sloan D, Kawai K, Agarwal D, Woodman AC, Tarin D, Goodison S. Contrasting expression of thrombospondin-1 and osteopontin correlates with absence or presence of metastatic phenotype in an isogenic model of spontaneous human breast

- cancer metastasis. *Clin Cancer Res* 2002; **8**: 61-74
- 8 **Reinholz MM**, Iturria SJ, Ingle JN, Roche PC. Differential gene expression of TGF-beta family members and osteopontin in breast tumor tissue: analysis by real-time quantitative PCR. *Breast Cancer Res Treat* 2002; **74**: 255-269
- 9 **Tuck AB**, Chambers AF. The role of osteopontin in breast cancer: clinical and experimental studies. *J Mammary Gland Biol Neoplasia* 2001; **6**: 419-429
- 10 **Tozawa K**, Yamada Y, Kawai N, Okamura T, Ueda K, Kohri K. Osteopontin expression in prostate cancer and benign prostatic hyperplasia. *Urol Int* 1999; **62**: 155-158
- 11 **Angelucci A**, Festuccia C, D'Andrea G, Teti A, Bologna M. Osteopontin modulates prostate carcinoma invasive capacity through RGD-dependent upregulation of plasminogen activators. *Biol Chem* 2002; **383**: 229-234
- 12 **Kim JH**, Skates SJ, Uede T, Wong Kk KK, Schorge JO, Feltmate CM, Berkowitz RS, Cramer DW, Mok SC. Osteopontin as a potential diagnostic biomarker for ovarian cancer. *JAMA* 2002; **287**: 1671-1679
- 13 **Tiniakos DG**, Yu H, Liapis H. Osteopontin expression in ovarian carcinomas and tumors of low malignant potential (LMP). *Hum Pathol* 1998; **29**: 1250-1254
- 14 **Weber GF**, Ashkar S. Molecular mechanisms of tumor dissemination in primary and metastatic brain cancers. *Brain Res Bull* 2000; **53**: 421-424
- 15 **Ding Q**, Stewart J Jr, Prince CW, Chang PL, Trikha M, Han X, Grammer JR, Gladson CL. Promotion of malignant astrocytoma cell migration by osteopontin expressed in the normal brain: differences in integrin signaling during cell adhesion to osteopontin versus vitronectin. *Cancer Res* 2002; **62**: 5336-5343
- 16 **Zhang J**, Takahashi K, Takahashi F, Shimizu K, Ohshita F, Kameda Y, Maeda K, Nishio K, Fukuchi Y. Differential osteopontin expression in lung cancer. *Cancer Lett* 2001; **171**: 215-222
- 17 **Walker F**, Kato A, Gonez LJ, Hibbs ML, Pouliot N, Levitzki A, Burgess AW. Activation of the ras/mitogen-activated protein kinase pathway by kinase-defective epidermal growth factor receptors results in cell survival but not proliferation. *Mol Cell Biol* 1998; **18**: 7192-7204
- 18 **Zhang K**, Sun J, Liu N, Wen D, Chang D, Thomason A, Yoshinaga SK. Transformation of NIH 3T3 cells by HER3 or HER4 receptors requires the presence of HER1 or HER2. *J Biol Chem* 1996; **271**: 3884-3890
- 19 **Zhang G**, He B, Weber GF. Growth factor signaling induces metastasis genes in transformed cells: molecular connection between akt kinase and osteopontin in breast cancer. *Mol Cell Biol* 2003; **23**: 6507-6519
- 20 **Malyankar UM**, Almeida M, Johnson RJ, Pichler RH, Giachelli CM. Osteopontin regulation in cultured rat renal epithelial cells. *Kidney Int* 1997; **51**: 1766-1773
- 21 **Atkins KB**, Simpson RU, Somerman MJ. Stimulation of osteopontin mRNA expression in HL-60 cells is independent of differentiation. *Arch Biochem Biophys* 1997; **343**: 157-163
- 22 **Chackalaparampil I**, Peri A, Nemir M, Mckee MD, Lin PH, Mukherjee BB, Mukherjee AB. Cells *in vivo* and *in vitro* from osteopetrotic mice homozygous for c-src disruption show suppression of synthesis of osteopontin, a multifunctional extracellular matrix protein. *Oncogene* 1996; **12**: 1457-1467
- 23 **Bosch FX**, Ribes J, Borrás J. Epidemiology of primary liver cancer. *Semin Liver Dis* 1999; **19**: 271-285
- 24 **El-Serag HB**, Mason AC. Rising incidence of hepatocellular carcinoma in the United States. *N Engl J Med* 1999; **340**: 745-750
- 25 **Taylor-Robinson SD**, Foster GR, Arora S, Hargreaves S, Thomas HC. Increase in primary liver cancer in the UK, 1979-94. *Lancet* 1997; **350**: 1142-1143
- 26 **Yuki K**, Hirohashi S, Sakamoto M, Kanai T, Shimosato Y. Growth and spread of hepatocellular carcinoma: A review of 240 consecutive autopsy cases. *Cancer* 1990; **66**: 2174-2179
- 27 **Genda T**, Sakamoto M, Ichida T, Asakura H, Kojiro M, Narumiya S, Hirohashi S. Cell motility mediated by rho and Rho-associated protein kinase plays a critical role in intrahepatic metastasis of human hepatocellular carcinoma. *Hepatology* 1999; **30**: 1027-1036
- 28 **Weber GF**. The metastasis gene osteopontin: a candidate target for cancer therapy. *Biochim Biophys Acta* 2001; **1552**: 61-85
- 29 **Oates AJ**, Barraclough R, Rudland PS. The identification of osteopontin as a metastasis-related gene product in a rodent mammary tumor model. *Oncogene* 1996; **13**: 97-104
- 30 **Denhardt DT**, Mistretta D, Chambers AF, Krishna S, Porter JF, Raghuram S, Rittling SR. Transcriptional regulation of osteopontin and the metastatic phenotype: evidence for a Ras-activated enhancer in the human OPN promoter. *Clin Exp Metastasis* 2003; **20**: 77-84
- 31 **Denhardt DT**, Guo X. Osteopontin: a protein with diverse functions. *FASEB J* 1993; **7**: 1475-1482
- 32 **Laverdure GR**, Banerjee D, Chackalaparampil I, Mukherjee BB. Epidermal and transforming growth factors modulate secretion of a 69 kDa phosphoprotein in normal rat kidney fibroblasts. *FEBS Lett* 1987; **222**: 261-265
- 33 **Pianetti S**, Arsura M, Romieu-Mourez R, Coffey RJ, Sonenshein GE. Her-2/neu overexpression induces NF-kappaB via a PI3-kinase/Akt pathway involving calpain-mediated degradation of I-kappaB-alpha that can be inhibited by the tumor suppressor PTEN. *Oncogene* 2001; **20**: 1287-1299

Edited by Zhang JZ and Wang XL

Genetic detection of Chinese hereditary nonpolyposis colorectal cancer

Long Cui, Hei-Ying Jin, Hui-Yu Cheng, Yu-Di Yan, Rong-Gui Meng, De-Hong Yu

Long Cui, Hei-Ying Jin, Hui-Yu Cheng, Rong-Gui Meng, De-Hong Yu, Department of Colorectal Surgery, Changhai Hospital, The Second Military Medical University, Shanghai 200433, China
Yu-Di Yan, Department of Colorectal Surgery, Gansu People's Hospital, Lanzhou 730000, Gansu Province, China

Supported by the National Natural Science Foundation of China, No. 30170927

Correspondence to: Dr. Long Cui, Department of Colorectal Surgery, Changhai Hospital, The Second Military Medical University, 174 Changhai Road, Shanghai 200433, China. cui-longdr@yahoo.com

Telephone: +86-21-25072073 **Fax:** +86-21-65492727

Received: 2003-06-04 **Accepted:** 2003-07-30

Abstract

AIM: To explore the germline mutations of the two main DNA mismatch repair genes (*hMSH2* and *hMLH1*) between patients with hereditary non-polyposis colorectal cancer (HNPCC) and suspected (atypical) HNPCC.

METHODS: Genomic DNA was extracted from the peripheral blood of the index patient of each family, and germline mutations of *hMSH2* and *hMLH1* genes were detected by PCR-single strand conformation polymorphism (PCR-SSCP) and DNA sequencing techniques.

RESULTS: For PCR-SSCP analysis, 67% (4/6) abnormal exons mobility in typical group and 33% (2/6) abnormal exons mobility in atypical group were recognized. In direct DNA sequencing, 50% (3/6) mutation of MMR genes in typical group and 33% (2/6) mutation of MMR genes in atypical group were found, and 4/6 (66.67%) and 1/6 (16.67%) mutations of *hMSH2* and *hMLH1* were identified in typical HNPCC and atypical HNPCC, respectively.

CONCLUSION: Mutation detection of the patients is of benefit to the analysis of HNPCC and, PCR-SSCP is an effective strategy to detect the mutations of HNPCC equivalent to direct DNA sequence. It seems that there exist more complicated genetic alterations in Chinese HNPCC patients than in Western countries.

Cui L, Jin HL, Cheng HY, Yan YD, Meng RG, Yu DH. Genetic detection of Chinese hereditary nonpolyposis colorectal cancer. *World J Gastroenterol* 2004; 10(2): 209-213

<http://www.wjgnet.com/1007-9327/10/209.asp>

INTRODUCTION

Hereditary nonpolyposis colorectal cancer (HNPCC) is characterized by early onset of colorectal cancer, location of tumors in the proximal colon, and an increased risk of neoplasms of extracolonic organs, including endometrium, stomach, urothelium, small intestine, and ovary^[1-6]. The International Collaborative Group on HNPCC (ICG-HNPCC) proposed a set of clinical diagnostic criteria (Amsterdam Criteria I) for HNPCC in 1990 and has revised them recently

(Amsterdam Criteria II) to provide a uniformity in collaborative studies^[7,8]. According to these criteria, there should have at least three patients in two consecutive generations who had colorectal cancer or the other extracolonic malignancies including endometrial cancer, small bowel cancer, cancer of the ureter and cancer of the renal pelvis. One of them should be a first-degree relative of the other two, one cancer should be diagnosed before age 50, and familial adenomatous polyposis (FAP) should be excluded. In Asia, on the other hand, the Japan Research Society for Cancer of the Colon and Rectum developed the clinical criteria (Japanese criteria) for HNPCC in 1991^[9]. According to these criteria, at least two relatives in at least two successive generations should have colorectal cancer, and one of them should be a first-degree relative of the other, also, we called them atypical HNPCC.

Nevertheless, according to those criteria above, all families that are diagnosed as having HNPCC are identified on the basis of a family history of colorectal or other certain malignancies. Sometimes the accuracy and reliability of the family history provided by patients themselves and their relatives or recorded by physicians are questionable, as there is much variability for the family history. Therefore, the requirements for establishing objective strategies to identify this disease are imperative. In the last decade, the progress in genetic study that DNA mismatch repair genes have been identified as being mutated in HNPCC including *hMSH2*, *hMLH1*, *hPMS1*, *hPMS2*, and *hMSH6* makes it possible to identify the cohort of patients through genetic test. Totally, these genes are now believed to account for about 50%-70% of all families with HNPCC and over 90% of the identified mutations focused on the two genes, *hMSH2* and *hMLH1*^[10-18]. There are many studies about the procedures of genetic testing of HNPCC, such as microsatellite instability (MSI), PCR-SSCP, immunohistochemistry (IHC) and direct DNA sequencing^[19-24]. However, much knowledge and a higher grade of technical development are required, before this strategy becomes applicable to the general population.

It has no doubt that there is a large population of HNPCC in China^[25,26]. Unfortunately, there have been few reports about clinical and genetic characteristics of HNPCC^[27]. In this study, six HNPCC families and six atypical HNPCC families were enrolled and, the germline mutations of *hMSH2* and *hMLH1* in the index patients from each family were investigated.

MATERIALS AND METHODS

Subjects

The project was approved by the Institutional Review Board and informed consent was obtained from each participant before the procedures were carried out. Personal and family cancer history was obtained from the proband and participating relatives, and cancer diagnosis and deaths were confirmed by review of medical records, pathological reports or death certificates. Families were identified by the Amsterdam or Japanese criteria for HNPCC. Patients and families were classified as the HNPCC group according to the Amsterdam criteria, suspected HNPCC group according to the Japanese criteria and control group without any family history.

Genetic testing

Preparation of peripheral blood samples and DNA amplification Genetic analysis was performed on a blood specimen from the proband in each family. Specimens were collected and immediately frozen in liquid nitrogen. DNA was extracted from blood specimens using the Wizard genomic purification kit (Qiagen, Shanghai) according to the manufacturer's instructions. Each of the exons from hMSH2 and hMLH1 genes was amplified by polymerase chain reaction (PCR). Next, the samples were heat-treated at 95 °C for 5 minutes to inactivate the enzyme, and used as the template DNA. All DNA amplification was performed in a 50 µl volume containing 100 ng template DNA, 10⁻³ M Tris-HCl (pH 8.9), 50⁻³M KCl, 2.5 mM MgCl₂, 0.2⁻³M of each dNTP, 10 pmol each primer, and 1U Taq polymerase was subjected to 35 PCR cycles (5 mins at 94 °C, 40 s at 94 °C, 60 s at 55 °C, and 40 s at 72 °C). Oligonucleotide sequences were designed from the sequences published in Genbank.

PCR-SSCP analysis and direct sequencing

Single-strand conformation polymorphism (SSCP) The technique of single-strand conformational polymorphism (SSCP) was used to identify mutations in the mismatch repair genes^[28,29]. Each exon of *hMSH2* and *hMLH1* was amplified specifically using PCR (details of oligonucleotide sequences and conditions are available from the authors). PCR products were electrophoresed on 10% non-denaturing polyacrylamide gels with an acrylamide: bisacrylamide ratio of 30:0.8 at 70volt for 12 h at room temperature. DNA was detected by silver staining according to the methods described by others. Those single stranded DNAs that took up an altered conformation appeared as aberrantly migrating bands on the electrophoresis gel.

Direct sequencing

The nucleotide sequence of PCR products showing an abnormal mobility on SSCP was determined by direct sequencing. The PCR products were purified with 1.5% low melted point agarose, and then performed using automated DNA

sequencer. Sequence alterations with an allele frequency of at least 5% were considered as normal variants (polymorphisms) and not reported.

Statistical analysis

The genetic differences of the typical HNPCC groups and the suspected HNPCC groups were analyzed for statistical significance using the chi square test. $P < 0.05$ was considered statistically significant.

RESULTS

Results of genetic testing

Characterization of the variants of PCR-SSCP and DNA sequencing analysis found in the 12 families/individuals in the study is presented in Table 1. A total of seven abnormal motilities were identified in PCR-SSCP including five in typical group and two in atypical group (part of PCR-SSCP analysis is shown in Figure 1). DNA sequencing found 6/7 (85.7%) abnormal motilities of PCR-SSCP, which were proven to be pathogenic germline mutations of *hMSH2* and *hMLH1*. The other abnormal mobility, an "A" insertion in *hMLH1* intron 10 occurred in the C10-1 patient, was proven to be polymorphism.

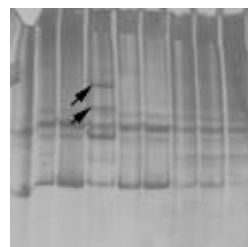


Figure 1 Results of PCR-SSCP in C13 family (*hMSH2*-exon11). Arrow shows the abnormal mobility.

Totally, five patients were found to harbor MMR gene mutations in the direct DNA sequencing. Three of six (50%)

Table 1 Characterization of variants in PCR-SSCP and sequence detection

Family	Abnormal mobility	DNA change	Mutation	Group
C4-1	<i>hMLH1</i> exon18 <i>hMSH2</i> exon15	T insert in 2 081 C insert in 2 469 G insert in 2 471	Frameshift Frameshift Frameshift	Typical HNPCC
C13-1	<i>hMSH2</i> exon11	T insert in 1 760 A→C missense in 1 688	Frameshift Tyr563Ser	Typical HNPCC
C11-1	<i>hMSH2</i> exon13	T to A missense in 2 091	Cys697	Typical HNPCC
C1-1	<i>hMLH1</i> exon11	A insert in 934	Terminator Condon Frameshift	Atypical HNPCC
C8-2	<i>hMLH1</i> exon12	C to G missense in 1 198 C to G missense in 1 261 C insert in 1 364 and 1 372	Leu400Val Val421Leu Frameshift	Atypical HNPCC
C10-1	<i>hMLH1</i> intron10	-	Polymorphism	Typical HNPCC

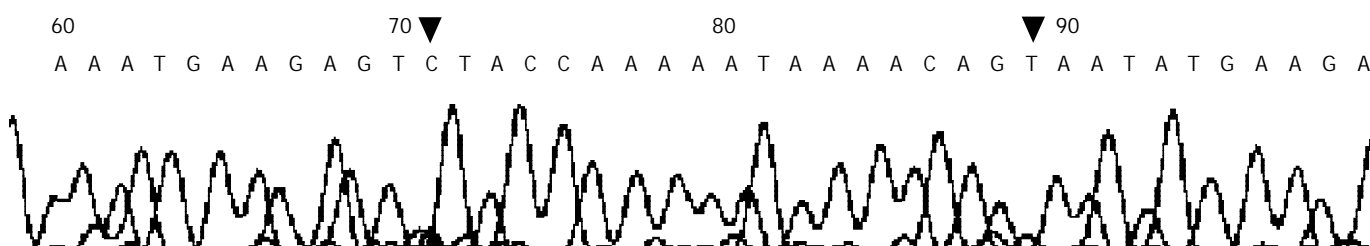


Figure 2 Results of direct sequencing of exon 11 of *hMSH2* in C13 family (A to C substitution in 1 688 and T insertion in 1 760).

patients with HNPCC and 2/6 (33%) patients with suspected HNPCC were found to harbor mutations. However, we found the mutations were complicated as the total number of mutations was more than five and all the mutations we found were novel and of unknown pathogenicity (part of sequence analysis is shown in Figure 2).

In typical HNPCC, the germline mutation of *hMLH1* and *hMSH2* was detected in 3 of 6 HNPCC families. Seven novel mutations were found in 3 exons of *hMSH2* and 1 exon of *hMLH1*, two mutations were detected at 11 exons of *hMSH2* in C13 family, one was the frame shift mutation resulted from an insertion of "T" at 1 760 so that a terminate cordon appeared ahead, the other was "A to C" missense mutation at 1 688 leading to Tyr-Ser substitution. A "T to A" substitution at 2 091 of exon 13 of *hMSH2* in C11 family resulted in a terminate cordon at 697. The mutations in C4 family were worthy of specific comment, as the mutation occurred in *hMLH1* as well as *hMSH2*, there was a frame shift mutation resulted from an insertion of T at 2 081 of exon 18 of *hMLH1*, there were "C, G" inserts at 2 469, 2 471 respectively. However, all families without germline *hMSH2* and *hMLH1* mutations were combined with extracolonic tumors.

In atypical HNPCC, only the germline mutation of *hMLH1* was detected in 2 of 6 HNPCC families, one was the frame shift mutation in exon 11 resulted from an insertion of "A" at 934 in C13 family. In C8 family, the mutation occurred at four locations, one was "C to G" missense mutation at 1 198 leading to Leu400Val substitution, one was "C to G" missense mutation at 1 261 leading to Val421Leu substitution and the other two shift mutations occurred at 1 364 and 1 372 resulted from the A insertion at the two locations respectively. The detailed results of sequencing are shown in Table 2.

Table 2 Comparison of two kinds of HNPCC with PCR-SSCP and sequencing

	Typical HNPCC (n=6)	Atypical HNPCC (n=6)	P
PCR-SSCP	4 (67%)	2 (33%)	0.269
Sequencing	3 (50%)	2 (33%)	0.575

DISCUSSION

To date, HNPCC is defined either by the so-called Amsterdam I+II criteria or by detection of a mutation in one of the mismatch repair genes. Once the positive mutation is identified, predictive testing of family members at risk is available. Screening recommendations for clinically identified families, mutation carriers, and their unaffected relatives at risk must be defined for clinical management^[30].

Recently, Watson *et al.*^[31] published their results about that carrier risk status changes resulted from mutation testing in hereditary non-polyposis colorectal cancer and hereditary breast-ovarian cancer. They concluded that mutation testing could raise the accuracy of carrier risk assessments, and lower the number of persons at high carrier risk. The most common risk assessment change resulted from DNA testing was a change from those at risk to non-carriers. To the extent that these persons were aware of their carrier risk and were obtaining heightened cancer surveillance test, this could be expected to lead to a reduced emotional toll and a reduced pressure on limited medical resources.

A better understanding of the molecular basis of hereditary colorectal cancer syndromes such as hereditary nonpolyposis colorectal cancer syndrome (HNPCC) and familial adenomatous polyposis (FAP) would have profound consequences for both the diagnosis and (prophylactic) treatment of (pre)malignant neoplastic lesions^[32] Clinically, when we see a patient with

colorectal cancer with a family history of suspected HNPCC, we need to work out our surgical strategies for this patient, the same as we do for the patients with HNPCC, in whom colonoscopy surveillance or prophylaxis surgeries such as subtotal colectomy are needed. One of the evidences of special surgical treatment has been found to be genetic detection^[33,34]. Since HNPCC is resulted from the dysfunction of mismatch repair genes and some reports indicated that mutation of *hMSH2* and *hMLH1* accounted for 40%-70% HNPCC^[35-39], we decided to detect the germline mutation of *hMSH2* and *hMLH1* in this study. In PCR-SSCP analysis of genomic DNA of 12 probands, we identified seven abnormal mobilities, five in typical HNPCC and two in suspected HNPCC and six of them were testified to be mutations by DNA sequencing. When we compared the genetic investigation of two groups we studied, we also concluded that there were no statistical differences in the results of both PCR-SSCP and direct sequence.

We also found that the mutations occurred both in typical HNPCC group and in atypical HNPCC group. Beck *et al.* found germline HNPCC mutations in six families in which none fulfilled the Amsterdam criteria. They highlighted that if germline mutations of the mismatch repair genes were common in families with features of HNPCC, but not fulfilling the Amsterdam criteria, then it was very important that all such families were also referred to cancer clinics for assessment and possible genetic testing^[40]. It was suggested that many suspected HNPCC patients might not be recognized and might be excluded from genetic counseling^[41,42].

Upon reviewing the literature and checking the variants registried in the ICG-HNPCC mutation database (<http://www.nfdht.nl>), we found that all the mutations were novel. It is rarely reported that there exist multiple mutations in the same exons. However, it seemed to be common in our analysis, two mutations were found at 11 exons of *hMSH2* in C13 family and C8 family. The mutation occurred at four locations, one was "C to G" missense mutation at 1 198 leading to Leu400Val substitution, one was "C to G" missense mutation at 1 261 leading to Val421Leu substitution and the other two shift mutations occurred at 1 364 and 1 372 resulted from the A insertion at the two locations, respectively. Furthermore, it is the first report that the mutation occurred in both *hMLH1* and *hMSH2* in C4 family.

Several techniques for genetic detection of HNPCC have been developed including MSI, immunohistochemistry, SSCP, denaturing gradient gel electrophoresis (DGGE) and sequencing. SSCP was considered inefficient in detecting mutations^[43,44] and was expected to miss approximately 20% of point and frameshift mutations. Furthermore, it was unable to detect the whole exon deletions, which occurred in some HNPCC families^[45]. We chose SSCP first because it was relatively simple, quick and cheap, and did not require special apparatus. In our study, 12 abnormal bands found in SSCP were proven to represent 11 mutations (91.7%). We found it was a practical procedure for the genetic screening of HNPCC.

Given the limitations of current techniques, direct PCR product sequencing analysis is more efficient for detecting mutations, but it is laborious, more expensive in term of reagents and data analysis time and not 100% efficient. It is much more acceptable clinically to take the screening techniques, such as SSCP, first and use sequencing to analyze the details of the mutation. Recently, some studies demonstrated that large genomic rearrangements accounted for 10%-20% of all *hMSH2* mutations, and a lower proportion of all *hMLH1* mutations. Nakagawa^[46] used the multiplex ligation-dependent probe amplification (MLPA) method to screen *hMSH2* and *hMLH1* deletions in 70 patients whose colorectal or endometrial tumors were MSI positive, yet no mutation was found by genomic exon-by-exon sequencing of *hMSH2*, *hMLH1*, and *hMSH6*. They

identified five candidates with four different hMSH2 deletions and one candidate with an hMLH1 deletion.

In summary, our study demonstrates that the Amsterdam criteria are important but inappropriate for the establishment of diagnosis, some atypical families not fulfilling all the Amsterdam criteria probably possess the similar genetic alterations. We conclude that the mutation detection of patients is of benefit to the analysis of HNPCC and, PCR-SSCP is as effective as direct DNA sequence in detecting the mutations of HNPCC. Furthermore, it seems that there exist more complicated genetic alterations in Chinese HNPCC patients than in Western countries.

However, there are also some cases without any mutation, further investigations should be carried out such as detection of other mismatch repair genes as well as detection of gene methylation of hMLH1.

REFERENCES

- Lynch HT, Lynch JF. Hereditary nonpolyposis colorectal cancer. *Semin Surg Oncol* 2000; **18**: 305-313
- Vasen HF, Watson P, Mecklin JP, Jass JR, Green JS, Nomizu T, Muller H, Lynch HT. The epidemiology of endometrial cancer in hereditary nonpolyposis colorectal cancer. *Anticancer Res* 1994; **14**(4B): 1675-1678
- Jass JR. Pathology of hereditary nonpolyposis colorectal cancer. *Ann N Y Acad Sci* 2000; **910**: 62-73; 73-74
- Vasen HF, Sanders EA, Taal BG, Nagengast FM, Griffioen G, Menko FH, Kleibeuker JH, Houwing-Duistermaat JJ, Meera Khan P. The risk of brain tumours in hereditary non-polyposis colorectal cancer (HNPCC). *Int J Cancer* 1996; **65**: 422-425
- Song YM, Zheng S. Analysis for phenotype of HNPCC in China. *World J Gastroenterol* 2002; **8**: 837-840
- Dunlop MG, Farrington SM, Carothers AD, Wyllie AH, Sharp L, Burn J, Liu B, Kinzler KW, Vogelstein B. Cancer risk associated with germline DNA mismatch repair gene mutations. *Hum Mol Genet* 1997; **6**: 105-110
- Vasen HF, Mecklin JP, Khan PM, Lynch HT. The International Collaborative Group on HNPCC. *Anticancer Res* 1994; **14**(4B): 1661-1664
- Vasen HF, Watson P, Mecklin JP, Lynch HT. New clinical criteria for hereditary nonpolyposis colorectal cancer (HNPCC, Lynch syndrome) proposed by the International Collaborative group on HNPCC. *Gastroenterology* 1999; **116**: 1453-1456
- Fujita S, Moriya Y, Sugihara K, Akasu T, Ushio K. Prognosis of hereditary nonpolyposis colorectal cancer (HNPCC) and the role of Japanese Criteria for HNPCC. *Jpn J Oncol* 1996; **26**: 351-355
- Lynch HT, Lynch JF. The Lynch Syndrome: Melding natural history and molecular genetics to genetic counseling and cancer control. *Cancer Control* 1996; **3**: 13-19
- Peltomaki P, Aaltonen L, Sistonen P, Pylkkanen L, Mecklin J-P, Jarvinen H, Green JS, Jass JR, Weber JL, Leach FS, Petersen GM, Hamilton SR, de la Chapelle A, Vogelstein B. Genetic mapping of a locus predisposing to human colorectal cancer. *Science* 1993; **260**: 810-812
- Leach FS, Nicolaides NC, Papadopoulos N, Liu B, Jen J, Parsons R, Peltomaki P, Sistonen P, Aaltonen LA, Nystrom-Lahti M, Guan XY, Zhang J, Metzler PS, Yu JW, Kao FT, Chen DJ, Cersosoletti KM, Fournier REK, Todd S, Lewis T, Leach RJ, Naylor SL, Weissbach J, Mecklin JP, Jarvinen H, Petersen GM, Hamilton SR, Green J, Jass J, Watson P, Lynch HT, Trent JM, de la Chapelle A, Kinzler KW, Vogelstein B. Mutations of a mutS homolog in hereditary nonpolyposis colorectal cancer. *Cell* 1993; **75**: 1215-1225
- Fishel R, Lescoe MK, Rao MR, Copeland NG, Jenkins NA, Garber J, Kane M, Kolodner R. The human mutator gene homolog MSH2 and its association with hereditary nonpolyposis colon cancer. *Cell* 1993; **75**: 1027-1038
- Nicolaides NC, Papadopoulos N, Liu B, Wei YF, Carter KC, Ruben SM, Rosen CA, Haseltine WA, Fleischmann RD, Fraser CM, Adams MD, Venter JC, Dunlop MG, Hamilton SR, Petersen GM, de la Chapelle A, Vogelstein B, Kinzler KW. Mutations of two PMS homologs in hereditary nonpolyposis colon cancer. *Nature* 1994; **371**: 75-80
- Nystrom-Lahti M, Parsons R, Sistonen P, Pylkkanen L, Aaltonen LA, Leach FS, Hamilton SR, Watson P, Bronson E, Fusaro R. Mismatch repair genes on chromosomes 2p and 3p account for a major share of hereditary nonpolyposis colorectal cancer families evaluable by linkage. *Am J Hum Genet* 1994; **55**: 659-665
- Papadopoulos N, Nicolaides NC, Wei YF, Ruben SM, Carter KC, Rosen CA, Haseltine WA, Fleischmann RD, Fraser CM, Adams MD. Mutation of a mutL homolog in hereditary colon cancer. *Science* 1994; **263**: 1625-1629
- Bronner CE, Baker SM, Morrison PT, Warren G, Smith LG, Lescoe MK, Kane M, Earabino C, Lipford J, Lindblom A. Mutation in the DNA mismatch repair gene homologue hMLH1 is associated with hereditary non-polyposis colon cancer. *Nature* 1994; **368**: 258-261
- Peltomaki P, de la Chapelle A. Mutations predisposing to hereditary nonpolyposis colorectal cancer. *Adv Cancer Res* 1997; **71**: 93-119
- Wijnen J, Vasen H, Khan PM, Menko FH, van der Klift H, van Leeuwen C, van den Broek M, van Leeuwen-Cornelisse I, Nagengast F, Meijers-Heijboer A. Seven new mutations in hMSH2, an HNPCC gene, identified by denaturing gradient-gel electrophoresis. *Am J Hum Genet* 1995; **56**: 1060-1066
- Ikenaga M, Tomita N, Sekimoto M, Ohue M, Yamamoto H, Miyake Y, Mishima H, Nishisho I, Kikkawa N, Monden M. Use of microsatellite analysis in young patients with colorectal cancer to identify those with hereditary nonpolyposis colorectal cancer. *J Surg Oncol* 2002; **79**: 157-165
- Merkelbach-Bruse S, Kose S, Losen I, Bosserhoff AK, Buettner R. High throughput genetic screening for the detection of hereditary non-polyposis colon cancer (HNPCC) using capillary electrophoresis. *Comb Chem High Throughput Screen* 2000; **3**: 519-524
- Holinski-Feder E, Muller-Koch Y, Friedl W, Moeslein G, Keller G, Plaschke J, Ballhausen W, Gross M, Baldwin-Jedele K, Jungck M, Mangold E, Vogelsang H, Schackert HK, Lohse P, Murken J, Meitinger T. DHPCL mutation analysis of the hereditary nonpolyposis colon cancer (HNPCC) genes hMLH1 and hMSH2. *J Biochem Biophys Methods* 2001; **47**: 21-32
- Kurzawski G, Safranow K, Suchy J, Chlubek D, Scott RJ, Lubinski J. Mutation analysis of MLH1 and MSH2 genes performed by denaturing high-performance liquid chromatography. *J Biochem Biophys Methods* 2002; **51**: 89-100
- Wahlberg SS, Schmeits J, Thomas G, Loda M, Garber J, Syngal S, Kolodner RD, Fox E. Evaluation of microsatellite instability and immunohistochemistry for the prediction of germ-line MSH2 and MLH1 mutations in hereditary nonpolyposis colon cancer families. *Cancer Res* 2002; **62**: 3485-3492
- Cai SJ, Xu Y, Cai GX, Lian P, Guan ZQ, Mo SJ, Sun MH, Cai Q, Shi DR. Clinical characteristics and diagnosis of patients with hereditary nonpolyposis colorectal cancer. *World J Gastroenterol* 2003; **9**: 284-287
- Cai Q, Sun MH, Lu HF, Zhang TM, Mo SJ, Xu Y, Cai SJ, Zhu XZ, Shi DR. Clinicopathological and molecular genetic analysis of 4 typical Chinese HNPCC families. *World J Gastroenterol* 2001; **7**: 805-810
- Beck NE, Tomlinson IP, Homfray T, Frayling I, Hodgson SV, Harocopos C, Bodmer WF. Use of SSCP analysis to identify germline mutations in HNPCC families fulfilling the Amsterdam criteria. *Hum Genet* 1997; **99**: 219-224
- Viel A, Genuardi M, Capozzi E, Leonardi F, Bellacosa A, Paravatou-Petsotas M, Pomponi MG, Fornasari M, Percesepe A, Roncucci L, Tamassia MG, Benatti P, Ponz de Leon M, Valenti A, Covino M, Anti M, Foletto M, Boiocchi M, Neri G. Characterization of MSH2 and MLH1 mutations in Italian families with hereditary nonpolyposis colorectal cancer. *Genes Chromosomes Cancer* 1997; **18**: 8-18
- Moslein G. Clinical implications of molecular diagnosis in hereditary nonpolyposis colorectal cancer. *Recent Results Cancer Res* 2003; **162**: 73-78
- Watson P, Narod SA, Fodde R, Wagner A, Lynch JF, Tinley ST, Snyder CL, Coronel SA, Riley B, Kinarsky Y, Lynch HT. Carrier risk status changes resulting from mutation testing in hereditary non-polyposis colorectal cancer and hereditary breast-ovarian cancer. *J Med Genet* 2003; **40**: 591-596

- 31 **Church JM.** Prophylactic colectomy in patients with hereditary nonpolyposis colorectal cancer. *Ann Med* 1996; **28**: 479-482
- 32 **Hanna NN, Mentzer RM Jr.** Molecular genetics and management strategies in hereditary cancer syndromes. *J Ky Med Assoc* 2003; **101**: 100-107
- 33 **Lynch HT, Watson P, Shaw TG, Lynch JF, Harty AE, Franklin BA, Kapler CR, Tinley ST, Liu B, Lerman C.** Clinical impact of molecular genetic diagnosis, genetic counseling, and management of hereditary cancer. Part II: Hereditary nonpolyposis colorectal carcinoma as a model. *Cancer* 1999; **86**(11 Suppl): 2457-2463
- 34 **Boland CR.** Molecular genetics of hereditary nonpolyposis colorectal cancer. *Ann N Y Acad Sci* 2000; **910**: 50-61
- 35 **Jacob S, Praz F.** DNA mismatch repair defects: role in colorectal carcinogenesis. *Biochimie* 2002; **84**: 27-47
- 36 **Bocker T, Ruschoff J, Fishel R.** Molecular diagnostics of cancer predisposition: hereditary non-polyposis colorectal carcinoma and mismatch repair defects. *Biochim Biophys Acta* 1999; **1423**: 1-10
- 37 **Planck M, Koul A, Fernebro E, Borg A, Kristoffersson U, Olsson H, Wenngren E, Mangell P, Nilbert M.** hMLH1, hMSH2 and hMSH6 mutations in hereditary non-polyposis colorectal cancer families from southern Sweden. *Int J Cancer* 1999; **83**: 197-202
- 38 **Kruger S, Plaschke J, Jeske B, Gorgens H, Pistorius SR, Bier A, Kreuz FR, Theissig F, Aust DE, Saeger HD, Schackert HK.** Identification of six novel MSH2 and MLH1 germline mutations in HNPCC. *Hum Mutat* 2003; **21**: 445-446
- 39 **Beck NE, Tomlinson IP, Homfray T, Hodgson SV, Harocopus CJ, Bodmer WF.** Genetic testing is important in families with a history suggestive of hereditary non-polyposis colorectal cancer even if the Amsterdam criteria are not fulfilled. *Br J Surg* 1997; **84**: 233-237
- 40 **Wang Q, Desseigne F, Lasset C, Saurin JC, Navarro C, Yagci T, Keser I, Bagci H, Luleci G, Gelen T, Chayvialle JA, Puisieux A, Ozturk M.** Prevalence of germline mutations of hMLH1, hMSH2, hPMS1, hPMS2, and hMSH6 genes in 75 French kindreds with nonpolyposis colorectal cancer. *Hum Genet* 1999; **105**: 79-85
- 41 **Wagner A, Hendriks Y, Meijers-Heijboer EJ, de Leeuw WJ, Morreau H, Hofstra R, Tops C, Bik E, Brocker-Vriends AH, van Der Meer C, Lindhout D, Vasen HF, Breuning MH, Cornelisse CJ, van Krimpen C, Niermeijer MF, Zwinderman AH, Wijnen J, Fodde R.** Atypical HNPCC owing to MSH6 germline mutations: analysis of a large Dutch pedigree. *J Med Genet* 2001; **38**: 318-322
- 42 **Moslein G, Pistorius S, Saeger HD, Schackert HK.** Preventive surgery for colon cancer in familial adenomatous polyposis and hereditary nonpolyposis colorectal cancer syndrome. *Langenbecks Arch Surg* 2003; **388**: 9-16
- 43 **Syngal S, Fox EA, Eng C, Kolodner RD, Garber JE.** Sensitivity and specificity of clinical criteria for hereditary non-polyposis colorectal cancer associated mutations in MSH2 and MLH1. *J Med Genet* 2000; **37**: 641-645
- 44 **Liu B, Parsons R, Papadopoulos N, Nicolaidis NC, Lynch HT, Watson P, Jass JR, Dunlop M, Wyllie A, Peltomaki P, de la Chapelle A, Hamilton SR, Vogelstein B, Kinzler KW.** Analysis of mismatch repair genes in hereditary non-polyposis colorectal cancer patients. *Nat Med* 1996; **2**: 169-174
- 45 **Nakagawa H, Hampel H, Chapelle Ad Ade L.** Identification and characterization of genomic rearrangements of MSH2 and MLH1 in Lynch syndrome (HNPCC) by novel techniques. *Hum Mutat* 2003; **22**: 258

Edited by Ma JY and Wang XL

Expression of estrogen receptor β in human colorectal cancer

Li-Qun Xie, Jie-Ping Yu, He-Sheng Luo

Li-Qun Xie, Jie-Ping Yu, He-Sheng Luo, Department of Gastroenterology Renmin Hospital, Wuhan University, Wuhan 430060, Hubei Province, China

Correspondence to: Jie-Ping Yu, Department of Gastroenterology, Renmin Hospital, Wuhan University, 283 Jie-Fang Road, Wuhan 430060, Hubei Province, China. xieliquan1966@sohu.com

Received: 2003-05-13 **Accepted:** 2003-06-07

Abstract

AIM: To determine the expression of estrogen receptor (ER) β in Chinese colorectal carcinoma (CRC) patients.

METHODS: ER β expression in CRC was investigated by immunohistochemical staining of formalin-fixed, paraffin-embedded tissue sections from 40 CRCs, 10 colonic adenomas, and 10 normal colon mucosa biopsies. The percentage of positive cells was recorded, mRNA expression of ER α and ER β in 12 CRC tissues and paired normal colon tissues were detected by RT-PCR.

RESULTS: Positive ER immunoreactivity was present in part of normal epithelium of biopsy (2/10), adenomas (3/10), and the sections of CRC tissue, most of them were nuclear positive. In CRCs, nuclear ER β immunoreactivity was detected in over 10% of the cancer cells in 57.5% of the cases and was always associated with cytoplasmic immunoreactivity. There was no statistical significance between ER β positive and negative groups in regard to depth of invasion and nodal metastases. Of the 12 CRC tissues and paired normal colon tissues, the expression rate of ER α mRNA in CRC tissue and corresponding normal colon tissue was 25% and 16.6%, respectively. ER β mRNA was expressed in 83.3% CRC tissue and 91.7% paired normal colon tissue, respectively. There was no significant difference in ER β mRNA level between CRC tissues and paired normal colon tissues.

CONCLUSION: A large number of CRCs are positive for ER β , which can also be detected in normal colonic epithelia. There is a different localization of ER β immunoreactivity among normal colon mucosae, adenomas and CRCs. ER α and ER β mRNA can be detected both in CRC tissue and in corresponding normal colon tissue. A post-transcriptional mechanism may account for the decrease of ER β protein expression in CRC tissues.

Xie LQ, Yu JP, Luo HS. Expression of estrogen receptor β in human colorectal cancer. *World J Gastroenterol* 2004; 10(2): 214-217
<http://www.wjgnet.com/1007-9327/10/214.asp>

INTRODUCTION

Epidemiological data have shown that the risk of colorectal cancer is reduced among postmenopausal hormone users, compared with those who have never used these hormones. Animal models showed that male rats had a higher risk developing colon cancer compared with their female counterparts when exposed to dimethylhydrazine, an experimental carcinogen. The results indicated that 17 β -

oestradiol (E₂) treatment could significantly reduce the frequency of dimethylhydrazine-induced large intestinal tumors in rats^[1-3]. These evidences suggest that estrogen maybe involved in the growth of colonic tumors. Estrogen receptor locates at the cellular nuclei of target tissues, estrogen molecules diffuse into cytoplasm, and bind to estrogen receptors, then modulate gene expression by interaction with promoter response elements or other transcription factors. The estrogen receptor discovered in 1986 is named ER α , and another ER subtype identified in 1997 is called ER β . ER β protein contains 485 amino acids, with a molecular weight of 54.2 Kda. The DNA binding domain (DBD) contains a two-zinc finger structure which plays an important role in receptor dimerization and in binding of receptors to specific DNA sequence. The DBDs of ER α and ER β are highly homologous^[4]. Up to now, several ER β isoforms have been identified such as ER β 1, ER β 2, ER β 3, ER β 4, ER β 5, *etc*^[5]. However, the physiological significance of these ER β isoforms is still unknown. Meanwhile, published data about the expression of ER α and ER β in colon cancer tissues were often controversial^[6-20]. Therefore it is reasonable to reevaluate ER status and hormonal modulation of cell growth in colon cancer. In this study, immunohistochemistry and reverse transcription-polymerase chain reaction (RT-PCR) techniques were used to explore the precise mechanism of hormonal modulation of colon cancer.

MATERIALS AND METHODS

Patients and tissues

The study was performed in tissue sections of CRC from 40 patients who underwent surgical resection of colorectal cancer in the Department of Surgery of Renmin Hospital, Wuhan University from June 1998 to December 2000. The age of the patients ranged from 38 to 78 years (average age 65 years). Ten sections of colonic adenoma were studied, and 10 sections of normal colonic mucosa biopsy were used as control. Information about depth of invasion and nodal metastases was obtained from a review of the pathology reports. Fresh tumor tissues and corresponding normal colon tissue were obtained from 12 patients who underwent surgical resection of colon cancer in the Department of Surgery of Affiliated Hospital of Wujing Medical College and Tianjin First Central Hospital from June 2001 to December 2002. The patients were comprised of 8 men and 4 women aged 49-79 years (mean 63.3 years). The tumorous and paired normal tissues were divided into two parts. One part was fixed in 10% formalin, embedded in paraffin and stained with hematoxylin-eosin for pathological diagnosis. The other part was frozen in liquid nitrogen and stored at -80 °C until RNA was extracted. ER α and ER β mRNA were detected by RT-PCR.

Immunohistochemistry

Rabbit anti-rat or human ER β polyclonal antibody was purchased from Santa Cruz, USA. S-P kit and DAB kit were purchased from Fuzhou Maixin Biotechnology Company.

Formalin-fixed and paraffin-embedded tissue sections from 40 CRCs, 10 colonic adenomas, and 10 normal colonic mucosa biopsies were immunostained by SP technique with the following procedures. The slides were washed in 0.01 M phosphate-buffered saline (PBS). Endogenous peroxidase was

blocked by 0.3% H₂O₂ for 25 minutes, followed by incubation in normal goat serum for 15 minutes at room temperature. Then the slides were incubated with a 1:75 dilution of the primary ER β polyclonal antibody for 2 hours at room temperature. After that the slides were washed with a reagent (biotinylated anti-immunoglobulin) for 20 minutes at room temperature. After rinsed in PBS, the slides were incubated with the peroxidase-conjugated streptavidin label for 20 minutes at room temperature, and incubated with diaminobenzidine and H₂O₂ for 5 minutes. Finally the sections were counterstained with hematoxylin.

RT-PCR amplification

Total RNA was isolated with TRIZOL reagent (Life Technologies, USA), and quantified by spectrometry (λ 260 nm). Only those RNA preparations with 260/280>1.7 were used in this study.

Reverse transcription was performed using a reverse transcription system (revertaid™ first strand cDNA synthesis kit, MBI). RT of RNA was performed in a final volume of 20 μ l containing 5 \times first strand buffer (containing 1 mM Tris-HCl, pH8.3, 1.5 mM KCl and 60 μ M MgCl₂), 25 μ M dNTP mixture, 200 pM random primer, 100 units of Moloney murine leukemia virus reverse transcriptase, 2 μ g total RNA. Then DEPC treated water was added to 20 μ l. RT reaction procedure was as follows: at 70 °C for 1 min \rightarrow at 37 °C for 5 min \rightarrow at 42 °C for 60 min \rightarrow at 98 °C for 5 min. ER α , ER β and β -actin were amplified using several pairs of appropriate oligonucleotide primers as follows: ER α (530 bp): (sense)5' -ATGTGGGAGAGGAT GAGG AG-3', (antisense) 5' -AACCGAGATGATGTAGCCAGCAGC-3'. ER β (256 bp): (sense) 5' -TAGG GTCCATGGCCAGTTAT-3', (antisense) 5' -GGGAGCCACACT TC ACCAT-3'. β -actin (control) (540 bp): (sense) 5' -GTGGG GCGCC CCAGG CAC CA-3', (antisense) 5' -CTTCC TTAAT GTCAC GCACG ATTTC-3' (Figure 1).

PCR was performed in a final volume of 50 μ l containing 4 μ l 10 \times pc buffer, 2.5 U recombinant Taq DNA polymerase (Taraka, Japan), 0.1 mM MgCl₂, 100 μ M dNTP mixture, and 50 pM of each primer. PCR was performed for 40 cycles (denaturation at 94 °C for 1 min, annealing at 55 °C for 1 min, and extension at 72 °C for 1.5 min). The PCR condition for inter control β -actin was 35 cycles (denaturation at 94 °C for 45 seconds, annealing at 60 °C for 45 seconds, and extension at 72 °C for 45 seconds). The PCR products were separated by electrophoresis on a 2% agarose gel and visualized by ethidium bromide staining and UV illumination.

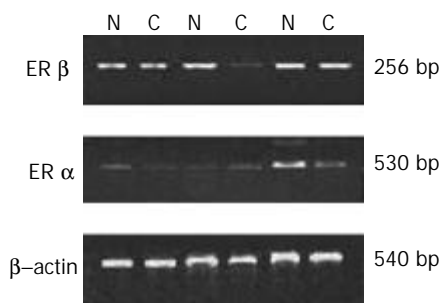


Figure 1 mRNA expression of ER α and ER β in paired representative tissues from cancer and adjacent normal mucosa. C: cancer, N: normal mucosa. RT-PCR result of β -actin was used to show equal loading.

Statistical analysis

The association between expression of ER α and ER β , the significance of ER α and ER β in groups dichotomized according to clinical and histopathologic characteristics of the patients were compared and assessed by Chi-square test and Student's *t*-test. A *P* value <0.05 was considered significant.

RESULTS

Expression of ER α and ER β protein

Using immunoperoxidase technique, ER β immunoreactivity was detected in or near the nuclei of normal colonic mucosa in the same sections of carcinoma. ER immunoreactivity was present in some of normal epithelia (2/10), and adenomas (3/10). Nuclear immunoreactivity was consistently found in part of normal colonic mucosa, and in all areas of the crypt epithelium, and most abundant at the bottom (Figures 2A,2B). One section of rectal tubular adenocarcinoma showed strong positive nuclear and cytoplasmic staining of ER β (Figure 2C). A few stromal cells, smooth muscle cells and vascular endothelial cells were also positive (Figure 2D). In CRCs, nuclear ER β immunoreactivity was associated with cytoplasmic immunoreactivity. Some sections showed only cytoplasmic staining of ER β (Figure 2E), Positive ER β was detected in more than 10% of the cancer cells in 57.5% of the CRC cases (Figure 3).

Three of the 12 randomly selected cases stained with anti-ER α antibody showed positive. None of the 10 normal colonic mucosa biopsies was stained positive with anti-ER α antibody. There were no statistically significant differences between positive and negative ER β groups in regard to the depth of invasion, and nodal metastases (Tables 1-2).

Table 1 Expression of ER β and ER α in CRCs, colonic adenomas and normal colonic mucosa

Group	<i>n</i>	ER α positive (%)	<i>n</i>	ER β positive (%)
Normal colon mucosa	10	0 (0%)	10	2 (20%)
CRCs	12	3 (25%)	40	23 (57.5%)
Colonic adenoma			10	3 (30%)

Table 2 Clinicopathological characteristics of patients with CRCs and their association with ER β expression

Category	<i>n</i>	ER β negativity	ER β positivity(%)	<i>P</i> value
Age (years)				>0.05
<50	4	2	2 (50.0)	
\geq 50	36	15	21 (58.3)	
Sex				>0.05
Male	23	9	14 (60.9)	
Female	17	8	9 (52.9)	
Lymph node metastasis				>0.05
0	18	7	11 (61.1)	
\geq 1	22	10	12 (54.5)	
Duke's type				>0.05
A	15	5	10 (66.7)	
B	10	3	7 (70.0)	
C	7	3	4 (57.1)	
D	3	1	2 (66.7)	
Histological grading				>0.05
Well-differentiated	15	5	10 (66.7)	
Moderately-differentiated	15	7	8 (53.3)	
Poorly-differentiated	10	5	5 (50.5)	

Table 3 Expression of ER α mRNA in CRC tissue and adjacent normal mucosa tissue

Tissue type	<i>n</i>	+	Positive rate (%)
CRCs	12	3	25%
Normal tissue	12	2	16.6%

Table 4 Expression of ER β mRNA in CRC tissue and adjacent normal mucosa tissue

Tissue type	<i>n</i>	+	Expression rate (%)	Level of ER β mRNA	<i>P</i>
CRCs	12	10	83.3%	91.15 \pm 3.56	>0.05
Normal tissue	12	11	91.7%	95.38 \pm 2.79	

ER α and ER β mRNA expression

Table 3 and Table 4 show that the expression of ER α mRNA in CRC tissue and corresponding normal colon tissue was 25% and 16.6%, respectively. ER β mRNA was predominantly expressed in CRC tissue and paired normal colon tissue, the positive rate was 83.3% and 91.7%, respectively. There was no statistically significant difference.

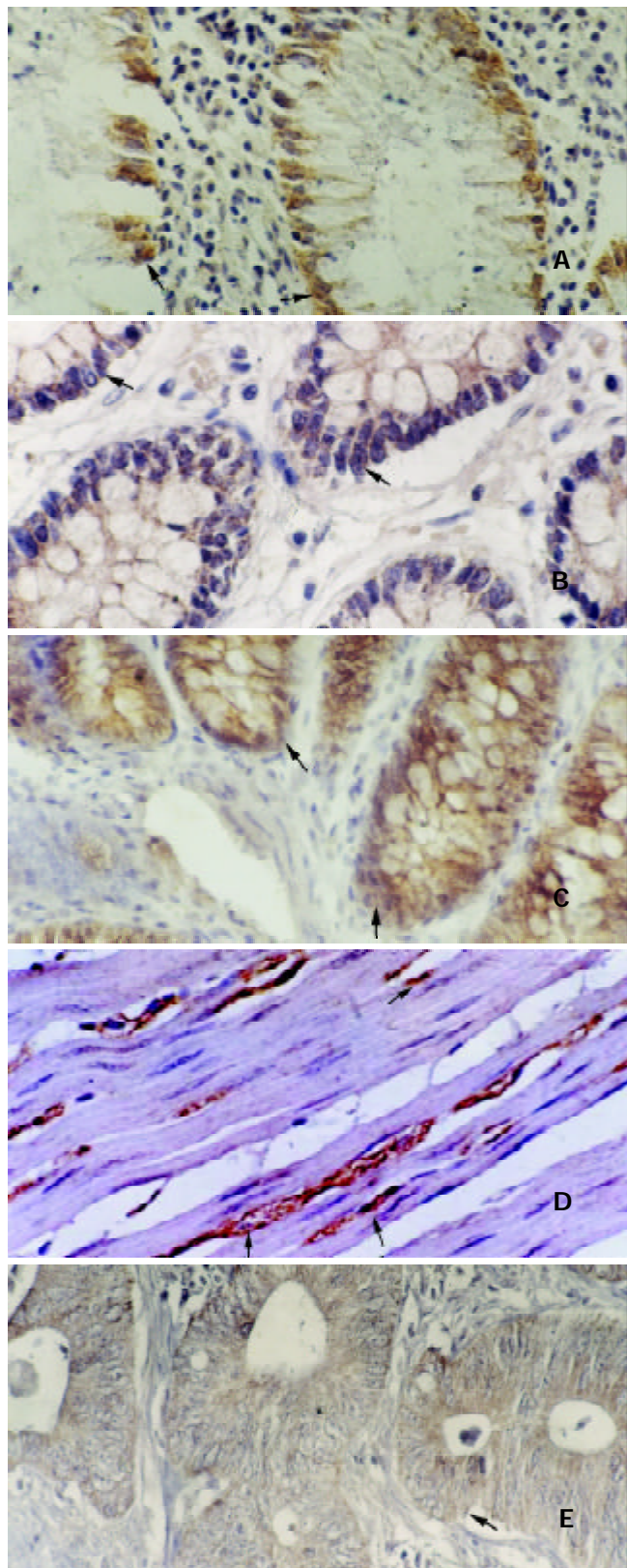


Figure 2 Immunohistochemical staining of ER β in CRC and normal colonic mucosa. A: shows the ER β positive epithelium. $\times 200$. B: shows the ER β positive crypt cell. $\times 200$. C: shows the nuclear

and cytoplasmic staining in rectal tubular adenocarcinoma. $\times 200$. D: shows the ER β positive smooth muscle cell and stromal cell. $\times 400$. E shows diffuse cytoplasmic staining in CRC. $\times 400$.

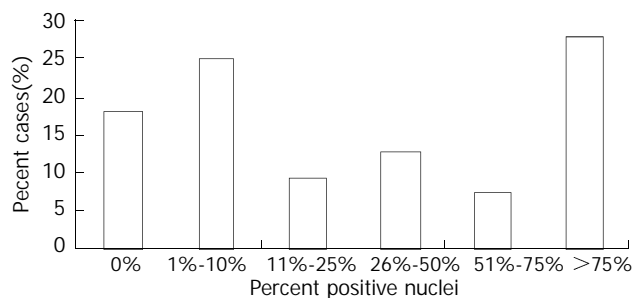


Figure 3 Extent of nuclear ER- β immunoreactivity in 40 cases of CRC.

DISCUSSION

Several epidemiologic studies have shown that colon cancer might be influenced by steroid hormones^[1-3], and estrogen use might be associated with a low risk of colon cancer^[21-27]. Some experimental results indicated that estrogen had a trophic effect on colon cancer^[11,11-12]. However, the effect of estrogen on colon cancer is controversial according to some reports. For example, Qiu *et al*^[28] reported that estradiol could induce apoptosis in colo205, a colon cancer cell line expressing only ER β . The question is whether ER expresses in normal colon mucosa or CRC. Earlier studies using biochemical ER-binding assay concluded that there was no ER in human colon. A more recent study concluded that ER was present in normal human colon and CRC tissues. Several immunohistochemical studies from China or Japan have shown that ER was present in normal human colon and CRC tissues^[12-18]. Similarly, our immunohistochemical study using ER antibodies (clone number 1D5), which are specific for ER α , showed that ER α was present in normal colon mucosa and CRC. However, the expression rate of ER α was about 20-40%, which was lower than that of ER β .

In 1997, the second type of ER (ER β) was cloned, and recent studies indicated ER β was distributed in human tissues^[5]. Several basic studies have shown that different distribution and regulatory mechanism of these two types of ER played different roles^[29,30]. ER β expression in normal colonic epithelium, especially at the bottom portion of colonic crypts, suggests that estrogens may play an important role in the growth and regeneration of normal colonic mucosa. ER β expression in a large number of CRCs indicates that estrogens may exert effects on these cancers, which may have significant implications for the treatment and prevention of CRC.

According to some published reports, ER α was also present in gastric or colon cancer^[11-18]. Our results support this conclusion. However, the positive rate of ER α in CRC was less than that of ER β in CRC. Some research results indicated that ER α and ER β could interact with the fos/jun transcription factor complex on AP1 sites to stimulate gene expression. However, they had opposite effects in the presence of estradiol. In the presence of ER α , estradiol functioned as an agonist in the AP1 pathway. In contrast, in the presence of ER β , tamoxifen and raloxifene behaved as fully competent agonists in the AP1 pathway, while estradiol acted as an antagonist, inhibiting the activity of both tamoxifen and raloxifene^[29,30]. It is the presence of two ERs that explains the conflicting experimental results. We deduced that estradiol might have trophic effects via combining with ER α . However, estradiol could inhibit tumour growth by combining with ER β .

In this study, we found no significant correlation between ER β expression and clinicopathologic features, including

Duke's types, lymph node metastasis and differentiation. Because of the relatively small sample size in this study, a study using a larger sampled study is necessary to further investigate the relationship between ER β expression and clinicopathologic characteristics and survival of colorectal cancer patients.

Our RT-PCR results showed that ER α and ER β mRNA were both expressed in CRC, semiquantitative RT-PCR revealed there was no statistical significance in ER β mRNA level between CRC tissue and paired normal colon tissue. Our immunohistochemical results showed that some sections were only cytoplasmically stained. Foley *et al*^[33] reported that Western blot analysis revealed very low levels of ER α protein in tumor and normal colon tissue. However, malignant colon tissue showed a selective loss of ER β protein expression when compared to normal colon tissue in the same patient. A post-transcriptional mechanism may account for the decrease of ER β protein expression in CRC tissue. Another reason is the different expressions of ER β isoforms in CRC. There are at least 5 different ER β isoforms, which show different amino acid sequences at the COOH terminus and are differently expressed in tumor cell lines^[31-35]. Campbell-Thompson *et al*^[35] and Witte *et al*^[36] showed that ER β was the predominant ER subtype between human colon and that the decreased levels of ER β 1 and ER β 2 mRNA were associated with colonic tumorigenesis in females. Their data suggest that there is a change in the relative expression of ER β isoforms. Therefore, It is possible that the cytoplasmic immunoreactivity in CRC tissue is caused by one of the overexpressed ER β subtypes. Further study should determine not only whether there are different ER β isoform expressions between normal colon and CRC, but also whether different isoforms are associated with different responses to estrogens and antiestrogens.

REFERENCES

- Singh S**, Langman MJ. Oestrogen and colonic epithelial cell growth. *Gut* 1995; **37**: 737-739
- Di Leo A**, Messa C, Cavallini A, Linsalata M. Estrogens and colorectal cancer. *Curr Drug Targets Immune Endocr Metabol Disord* 2001; **1**: 1-12
- Al-Azzawi F**, Wahab M. Estrogen and colon cancer: current issues. *Climacteric* 2002; **5**: 3-14
- Dardes RC**, Jordan VC. Novel Agents to modulate oestrogen action. *Br Med Bull* 2000; **56**: 773-786
- Enmark E**, Peltö-Huikko M, Grandien K, Lagercrantz S, Lagercrantz J, Fried G, Nordenskjöld M, Gustafsson JA. Human estrogen receptor β -gene structure, chromosomal localization, and expression pattern. *J Clin Endocrinol Metab* 1997; **82**: 4258-4265
- Leygue E**, Dotzlaw H, Watson PH, Murphy LC. Expression of estrogen receptor beta 1, beta2, and beta5 messenger RNAs in human breast tissue. *Cancer Res* 1999; **59**: 1175-1179
- Tong D**, Schuster E, Seifert M, Czerwenka K, Leodolte S, Zeillinger R. Expression of estrogen receptor beta isoforms in human breast cancer tissues and cell lines. *Breast Cancer Res Treat* 2002; **71**: 249-255
- Poola I**, Abraham J, Baldwin K. Identification of ten exon deleted ERbeta mRNAs in human ovary, breast, uterus and bone tissues: alternate splicing pattern of estrogen receptor beta mRNA is distinct from that of estrogen receptor alpha. *FEBS Lett* 2002; **516**: 133-138
- Shiau AK**, Barstad D, Radek JT, Meyers MJ, Nettles KW, Katzenellenbogen BS, Katzenellenbogen JA, Agard DA, Greene GL. Structural characterization of a subtype-selective ligand reveals a novel mode of estrogen receptor antagonism. *Nat Struct Biol* 2002; **9**: 359-364
- Yi P**, Driscoll MD, Huang J, Bhagat S, Hilf R, Bambara RA, Muyan M. The effects of estrogen-responsive element- and ligand-induced structural changes on the recruitment of cofactors and transcriptional responses by ER alpha and ER beta. *Mol Endocrinol* 2002; **16**: 674-693
- Sciascia C**, Olivero G, Comandone A, Festa T, Fiori MG, Enrichens F. Estrogen receptors in colorectal adenocarcinomas and in other large bowel diseases. *Int J Biol Markers* 1990; **5**: 38-42
- Slattery ML**, Samowitz WS, Holden JA. Estrogen and progesterone receptors in colon tumors. *Am J Clin Pathol* 2000; **113**: 364-368
- Oshima CT**, Wonraht DR, Catarino RM, Mattos D, Forones NM. Estrogen and progesterone receptors in gastric and colorectal cancer. *Hepatogastroenterology* 1999; **46**: 3155-3158
- Zhang ZS**, Zhang YL. Progress in research of colorectal cancer in China. *Shijie Huaren Xiaohua Zazhi* 2001; **9**: 489-494
- Qin ZK**, Lian JY, Wan DS, Hou JH, Lin HL. Expression and Prognostic Values of p21 Protein and Estrogen Receptor in Colorectal Cancers. *Ai zheng* 2001; **20**: 77-78
- Jiang YA**, Zhang YY, Luo HS, Xing SF. Mast cell density and the context of clinicopathological parameters and expression of p185, estrogen receptor, and proliferating cell nuclear antigen in gastric carcinoma. *World J Gastroenterol* 2002; **8**: 1005-1008
- Zhao XH**, Gu SZ, Liu SX, Pan BR. Expression of estrogen receptor and estrogen receptor messenger RNA in gastric carcinoma tissues. *World J Gastroenterol* 2003; **9**: 665-669
- Gao MX**, Zhang NZ, Ji CX. Estrogen receptor and PCNA in gastric carcinomas. *Shijie Huaren Xiaohua Zazhi* 2000; **8**: 1117-1120
- Xie LQ**, Yu JP, Luo HS. Estrogen receptor beta expression in Chinese colorectal adenocarcinoma. *Shijie Huaren Xiaohua Zazhi* 2002; **10**: 774-778
- Konstantinopoulos PA**, Kominea A, Vandoros G, Sykiotis GP, Andricopoulos P, Varakis I, Sotiropoulou-Bonikou G, Papavassiliou AG. Oestrogen receptor beta (ERbeta) is abundantly expressed in normal colonic mucosa, but declines in colon adenocarcinoma paralleling the tumour's dedifferentiation. *Eur J Cancer* 2003; **39**: 1251-1258
- Grodstein F**, Newcomb PA, Stampfer MJ. Postmenopausal Hormone therapy and the risk of colorectal cancer: A review and meta-analysis. *Am J Med* 1999; **106**: 574-582
- Moghissi KS**. Hormone replacement therapy for menopausal women. *Compr Ther* 2000; **26**: 197-202
- Gambacciani M**, Monteleone P, Sacco A, Genazzani AR. Hormone replacement therapy and endometrial, ovarian and colorectal cancer. *Best Pract Res Clin Endocrinol Metab* 2003; **17**: 139-147
- Burkman RT**. Reproductive hormones and cancer: ovarian and colon cancer. *Obstet Gynecol Clin North Am* 2002; **29**: 527-540
- Giovannucci E**. Obesity, gender, and colon cancer. *Gut* 2002; **51**: 147
- Adlercreutz H**. Phyto-oestrogens and cancer. *Lancet Oncol* 2002; **3**: 364-373
- Barrett-Connor E**, Stuenkel CA. Hormone replacement therapy (HRT)—risks and benefits. *Int J Epidemiol* 2001; **30**: 423-426
- Qiu Y**, Waters CE, Lewis AE, Langman MJ, Eggo MC. Oestrogen-induced apoptosis in colonocytes expressing oestrogen receptor beta. *J Endocrinol* 2002; **174**: 369-377
- Ing NH**, Spencer TE, Bazer FW. Estrogen enhances endometrial estrogen receptor gene expression by a posttranscriptional mechanism in the ovariectomized ewe. *Biol Reprod* 1996; **54**: 591-599
- Yeap BB**, Krueger RG, Leedman PJ. Differential posttranscriptional regulation of androgen receptor gene expression by androgen in prostate and breast cancer cells. *Endocrinology* 1999; **140**: 3282-3291
- Fiorelli G**, Picariello L, Martinetti V, Tonelli F, Brandi ML. Functional estrogen receptor beta in colon cancer cells. *Biochem Biophys Res Commun* 1999; **261**: 521-527
- Arai N**, Strom A, Rafter JJ, Gustafsson JA. Estrogen receptor beta mRNA in colon cancer cells: growth effects of estrogen and genistein. *Biochem Biophys Res Commun* 2000; **270**: 425-431
- Foley EF**, Jazaeri AA, Shupnik MA, Jazaeri O, Rice LW. Selective loss of estrogen receptor beta in malignant human colon. *Cancer Res* 2000; **60**: 245-248
- Vladusic EA**, Hornby AE, Guerra-Vladusic FK, Lakins J, Lupu R. Expression and regulation of estrogen receptor beta in human breast tumors and cell lines. *Oncol Rep* 2000; **7**: 157-167
- Campbell-Thompson M**, Lynch II, Bhardwaj B. Expression of estrogen receptor (ER) subtypes and ER beta isoforms in colon cancer. *Cancer Res* 2001; **61**: 632-640
- Witte D**, Chirala M, Younes M, Li Y, Younes M. Estrogen receptor beta is expressed in human colorectal adenocarcinoma. *Hum Pathol* 2001; **32**: 940-944

Ethylene diamine tetraacetic acid induced colonic crypt cell hyperproliferation in rats

Qing-Yong Ma, Kate E Williamson, Brian J Rowlands

Qing-Yong Ma, Department of Surgery, First Hospital of Xi'an Jiaotong University, Xi'an 710061, Shaanxi Province, China

Kate E Williamson, Department of Pathology, Institute of Clinical Science, The Queen's University of Belfast, Belfast, UK

Brian J Rowlands, Department of Surgery, School of medical and Surgical Sciences, University of Nottingham, Nottingham, NG7 2UH, UK

Supported by DHSS of Northern Ireland

Correspondence to: Professor Qing-Yong Ma, Department of Surgery, First Hospital of Xi'an Jiaotong University, Xi'an 710061, Shaanxi Province, China. qyma0@163.com

Telephone: +86-29-85324009

Received: 2003-06-05 **Accepted:** 2003-08-16

Abstract

AIM: To investigate the effect of ethylene diamine tetraacetic acid (EDTA) on proliferation of rat colonic cells.

METHODS: EDTA was administered into Wistar rats, carcinogenesis induced by 1,2-dimethylhydrazine (DMH) in rats was studied with immunohistochemistry.

RESULTS: Marked regional differences in cell proliferation were found in all groups. In EDTA-treated animals, total labelling indexes in both proximal (10.00 ± 0.44 vs 7.20 ± 0.45) and distal (11.05 ± 0.45 vs 8.65 ± 0.34) colon and proliferative zone size (21.67 ± 1.13 vs 16.75 ± 1.45 , 27.73 ± 1.46 vs 21.74 ± 1.07) were significantly higher than that in normal controls ($P < 0.05$) and lower than that in DMH group (10.00 ± 0.44 vs 11.54 ± 0.45 , 11.05 ± 0.45 vs 13.13 ± 0.46 , 21.67 ± 1.13 vs 35.52 ± 1.58 , 27.73 ± 1.46 vs 39.61 ± 1.32 , $P < 0.05$). Cumulative frequency distributions showed a shift of the EDTA distal curve to the right ($P < 0.05$) while the EDTA proximal curve did not change compared to normal controls. Despite the changes of proliferative parameters, tumours did not develop in EDTA treated animals.

CONCLUSION: Hyperproliferation appears to be more easily induced by EDTA in distal colon than in proximal colon. Hyperproliferation may need to exceed a threshold to develop colonic tumours. EDTA may work as a co-factor in colonic tumorigenesis.

Ma QY, Williamson KE, Rowlands BJ. Ethylene diamine tetraacetic acid induced colonic crypt cell hyperproliferation in rats. *World J Gastroenterol* 2004; 10(2): 218-222

<http://www.wjgnet.com/1007-9327/10/218.asp>

INTRODUCTION

Colonic epithelial hyperproliferation has been considered as a high risk factor in both human and animal colonic cancer models^[1-19]. Evidence from animal studies has shown that experimental colonic tumours induced by procarcinogen 1, 2-dimethylhydrazine (DMH) are of epithelial origin with a similar histology, morphology and anatomy to human colonic

neoplasms^[2,3,20,21]. Furthermore, prior to the development of colonic cancer, injections of DMH could result in increased colonic crypt cellularity, colonic crypt cell proliferation and colonic crypt proliferative zone^[22,23]. This procarcinogen thus provides an adequate model for kinetic and therapeutic studies of the colorectal cancer.

It is important to compare cell proliferation in the distal and proximal colon. As in normal rats, the location of stem cells and the direction of colonocyte migration differ in these two regions^[24]. In addition, differences in the incidence, morphology and clinical behaviour of colonic carcinoma in the proximal and distal colon have been reported^[25,26].

EDTA is widely used as a vehicle solution in chemical-induced colorectal carcinogenesis. However, little is known about the nature of its effect on cell proliferation. *In vitro*, EDTA could inhibit cell proliferation^[27,29] and DNA synthesis^[30]. Inhibition on cell growth is not associated with EDTA's chelational stability^[28]. *In vivo*, EDTA has been shown to stimulate cell proliferation in a neural crest tumour model^[31]. In the present study BrdUrd *in vivo* cell labelling was employed to determine crypt cell proliferation patterns in proximal and distal rat colons from normal, EDTA and DMH-induced colon cancer animals.

MATERIALS AND METHODS

Animals and treatment

Forty eight male Wistar rats (weighing 180-220 g) were divided equally into DMH group and EDTA group. Three animals were housed in each cage in a containment isolator with negative pressure to protect experimenters against the effects of the carcinogen. A specific colonic procarcinogen 1, 2-dimethylhydrazine (DMH, Aldric, Poole, Dorset) at a dosage of 20 mg/kg body weight was administered subcutaneously to the animals weekly for 20 weeks. DMH was dissolved in 1 mM EDTA (BDH Ltd, Poole, Dorset), and adjusted to pH 6.5 with 10% sodium hydroxide (BDH Ltd, Poole, Dorset) immediately before injection. Animals in EDTA group were given weekly subcutaneous injection of EDTA for 20 weeks, and sacrificed 2 weeks after the last injection. In addition, six normal rats were used as controls for BrdUrd immunohistochemistry.

In vivo BrdUrd labelling and tissue sampling

Eighteen rats (6 per group) from normal controls, EDTA-treated group and DMH-treated group were used for a crypt cell proliferation study. Fifteen minutes before removal of the colon, the anaesthetised animals had a peritoneal injection with 50 mg/kg body weight of 2% BrdUrd (Sigma B-5002) between 9 and 11 a.m. to avoid diurnal variation. The colon was removed and rinsed with tap water. Following excision of the caecum and rectum, the remaining colon was divided into proximal and distal halves. A 1-2 cm segment of each end of the proximal and distal colon was discarded. After fixation in 70% ethanol for 4 hours the segments were rolled prior to processing and embedding in paraffin wax.

BrdUrd immunohistochemistry

Several 3 μ m thick sections were cut and placed on poly-L-

lysine coated slides. The slides were dewaxed before DNA was denatured in 1M HCl at 37 °C for 12 minutes. After rinsed in phosphate buffered saline (PBS, pH 7.1) the sections were incubated with 30 µl of mouse anti-BrdUrd monoclonal antibody (M 744 Dako, Bucks, England) diluted 1:50 in PBS with 0.05% Tween 20 (PBST) with added normal rat serum diluted 1:25 for 60 minutes at room temperature. After a further rinsing in PBS the sections were incubated with biotinylated rabbit anti-mouse F(ab')₂ antibody (E 413 Dako, Bucks, England) at a dilution of 1:200 in PBST with added rat serum for 30 minutes at room temperature. The slides were again rinsed in PBS and then incubated with streptavidin-biotin peroxidase complex (K 377 Dako, Bucks, England) for 30 minutes at room temperature. Finally the reaction product was visualised using diaminobenzidine hydrochloride (DAB) (Sigma, Dorset, England) primed with 100 µl of 30% H₂O₂ (diluted 1:20 with distilled water) for approximately 5 minutes. After DAB was washed off with distilled water the sections were lightly counterstained in Harris haematoxylin before dehydration and mounting in DPX.

Counting and scoring criteria

Only complete well-orientated longitudinally sectioned crypts which extended from the luminal surface into the muscularis mucosae and contained at least 30 cells per hemicrypt were used for analysis. To facilitate scoring each crypt was divided at the base into 2 crypt columns (hemicrypts). Starting at the base of the hemicrypt, cells were numbered up to the luminal surface of the colon to determine the number of cells per hemicrypt. Crypts were then divided into 5 compartments each containing the same number of cells. The number and the position of BrdUrd-labelled cells in the hemicrypt were recorded. The proliferative zone, which was expressed as a percentage, was obtained by calculating the difference between the highest and lowest labelled cells in each hemicrypt and dividing this figure by the total number of cells in the hemicrypt. Labelling index (LI) was determined for the whole hemicrypt, for each compartment and for the proliferative zone as follows, $\text{equation} = (\frac{\text{the number of labelled cells}}{\text{the number of total cells}}) \times 100$. Each hemicrypt was then normalised to a notional 100 cell positions. The frequency of BrdUrd positive cells in each of the 100 normalised positions was recorded.

Statistical analysis

Mean and standard error of the mean were calculated where appropriate. Since the sample size for crypt cell proliferation was more than 100 except in one group (normal proximal colon group in which the sample size was 78) and all groups appeared to have normal distribution, a two sided Student's *t* test was used to identify the differences between individual variables. Kolmogorov-Smirnov 2 sample test^[16] was used to compare the BrdUrd cumulative labelling frequency curves with reference to the presence of EDTA or DMH treatment and the site of origin of the sample from the colon. Results were considered as significant when $P < 0.05$. Statistics were analysed running the SPSS package for Windows.

RESULTS

Characterisation of tumours

All animals survived to the time when they were sacrificed. In the EDTA control animals no macroscopical changes were observed in the mucosa of large intestine after 20 weeks of treatment. However, in the DMH group a total of 66 tumours were found in 23 animals (96%) and 1 rat was tumour free. Most of the tumours (73%) were located in the distal colon. Microscopically, the tumours were either adenoma or

adenocarcinoma. Most rats had one or more types of lesions, indicating that the response to DMH was heterogeneous. The number and distribution of both adenoma and adenocarcinoma are summarised in Table 1.

Table 1 Characterisation of colorectal tumours

Location	Adenoma	Carcinoma	Total (%)
Caecum	0	1	1 (1.5)
Proximal	2	6	8 (12.1)
Flexure	4	4	8 (12.1)
Distal	12	36	48 (72.7)
Rectum	0	1	1 (1.5)
Total	18	48	66

Differences between proximal and distal colon

The number of cells per hemicrypt in the proximal colon was significantly higher than that in the distal colon in all respective groups ($P < 0.05$, Table 2). Although the number of labelled cells per hemicrypt was similar in the proximal and distal colon in all groups, the total LI was significantly higher in distal colon compared to proximal colon both in normal control group ($P < 0.05$) and in DMH treated animals ($P < 0.05$). In EDTA treated group, the total LI in the distal colon was higher than that in the proximal colon with no statistical significance ($P = 0.11$). The size of the proliferative zone was higher in distal colon than that in proximal colon in all groups ($P < 0.05$) while the LI in proliferative zone did not significantly change. In the normal controls, BrdUrd labelled cells in the proximal colon were located predominantly in compartments 2 and 3 (88.4%), whereas the labelled cells in the distal colon were mostly in compartments 1 and 2 (85.3%). In compartment 1, the LI was significantly higher in the distal colon than in the proximal colon ($P < 0.05$), while in compartment 3 the LI was significantly lower in the distal colon than in the proximal colon ($P < 0.05$). None of the labelled cells appeared in compartment 5. When the cumulative labelling distribution curves of the proximal and distal colon of normal rats were compared, the distal colon showed a significant shift to the left ($P < 0.05$, Figure 1).

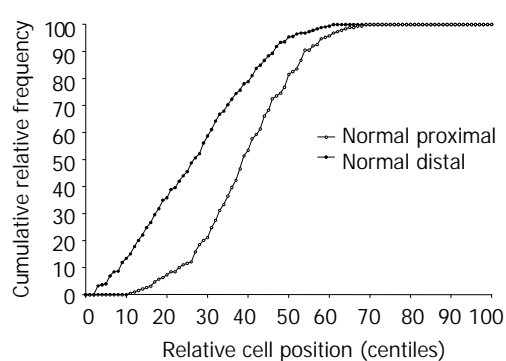


Figure 1 Different patterns of cumulative labelling distributions in proximal and distal rat colons of normal controls. The curve was significantly shifted to the right when the proximal colon was compared to the distal colon.

Effect of EDTA

In EDTA-treated animals, the number of cells per hemicrypt, labelled cells per hemicrypt and total LI were all significantly increased in both the proximal and distal colons when compared to normal controls. In addition, the size of proliferative zone in EDTA treated animals was significantly higher in both proximal and distal colons than in normal controls. However, the LI in proliferative zone was not changed. In the proximal colon, the increase in LI was limited

to compartment 3 while in the distal colon the increase in LI was extended from compartment 2 to compartment 4. When compared to the normal controls cumulative frequency distributions of the EDTA distal curve shifted to the right ($P < 0.05$, Figure 2) but the EDTA proximal curve did not change ($P > 0.05$, Figure 3).

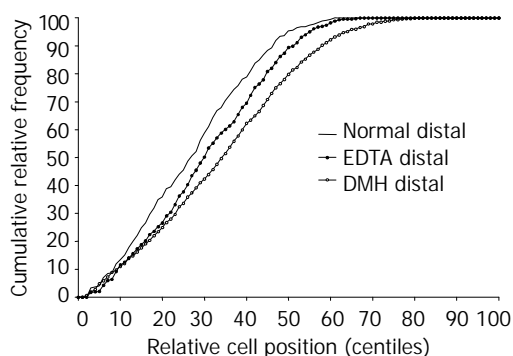


Figure 2 Cumulative labelling distribution in normal, EDTA and DMH treated distal rat colons, respectively. The curve was significantly shifted to the right in EDTA distal colon compared to normal distal colons. The curve was further shifted to the right in DMH distal colon compared to either normal or EDTA distal colon.

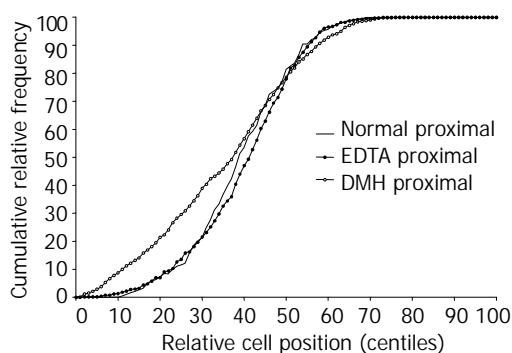


Figure 3 Cumulative labelling distribution in normal, EDTA and DMH treated proximal rat colons. The curve of EDTA

treated proximal rat colon did not change compared to the normal proximal curve. Whereas the curve of DMH treated proximal rat colon was initially significantly shifted to the left and then at higher centiles shifted to the right.

Effect of DMH treatment

DMH treatment significantly increased the number of cells per hemicrypt in both proximal and distal colons in comparison with either normal controls or EDTA treated animals. The number of labelled cells per hemicrypt and total LI were also significantly increased following DMH injections in both proximal and distal colons. Additionally, DMH increased the size of the proliferative zone in both proximal and distal colonic crypts. However, the LI of proliferative zone was reduced because of the increased denominator (Table 2). In the proximal colon the increase in LI was in compartments 1, 3 and 4, whereas in the distal colon the increase in LI in DMH rats was most marked in compartments 2, 3 and 4. The extent of LI in compartment 3 in the distal colon was significantly greater than that in the proximal colon ($P < 0.05$). Further analysis of the cumulative labelling distributions showed a shift of the DMH distal curve to the 81st centile which was to the right of the plateau of the normal distal colon located at the 61st centile ($P < 0.05$) and EDTA distal colon located at the 67th centile ($P < 0.05$, Figure 2). In contrast, the cumulative labelling distribution curve in DMH proximal colon demonstrated a shift to the left in the lower crypt cell positions and then shifted to the right high up the crypt compared with normal ($P < 0.05$) and EDTA ($P < 0.05$) proximal cumulative frequency curves (Figure 3).

DISCUSSION

This study supported the findings that adenoma and adenocarcinoma of intestine could be obtained, using DMH or its metabolites in Wistar rats^[20,32,33]. Another advantage of DMH and its metabolites is the specificity for the large bowel. The incidences of cancer at small intestine and extra-intestine were very low^[34]. In our study the vast majority of colon tumours occurred distally and were mainly polypoid neoplasms or adenocarcinomas. The types of the proximal colon tumours were reported to be variable histopathologically, dominated

Table 2 Features of proliferative colonic crypt cells in 6 groups

Group	LC	CPC	TLI	LI 1	LI 2	LI 3	LI 4	PZone	LIPZ
NP(76)	2.49±0.16	34.45±0.39	7.20±0.45	3.11±0.11	18.78±1.64	13.21±1.50	0.90±0.39	16.75±1.45	59.43±3.39
ND(198)	2.74±0.11	31.45±0.2	8.65±0.34	17.33±1.06	19.54±1.21	6.38±0.76	0.00	21.74±1.07	55.13±2.17
EP(134)	3.71±0.16	37.68±0.27	10.00±0.44	3.36±0.62	19.46±1.41	24.45±1.55	1.67±0.43	21.67±1.13	55.87±2.22
ED(130)	3.58±0.15	32.55±0.21	11.05±0.47	14.76±1.33	23.74±1.66	15.49±1.29	0.9±0.31	27.73±1.46	51.68±2.43
DP(138)	5.7±0.24	49.09±0.65	11.54±0.45	12.87±1.11	21.72±1.41	19.72±1.21	3.47±0.62	35.52±1.58	39.84±1.77
DD(182)	5.67±0.23	42.68±0.53	13.13±0.46	18.23±1.08	24.86±1.31	18.83±1.19	3.43±0.6	39.61±1.32	38.89±1.50
<i>P</i> Values									
ND:NP	0.21	0.000	0.019	0.000	0.731	0.000	0.000	0.011	0.3
ED:EP	0.571	0.000	0.107	0.000	0.05	0.000	0.151	0.001	0.203
DD:DP	0.94	0.000	0.017	0.003	0.107	0.604	0.966	0.047	0.682
ND:ED	0.000	0.000	0.000	0.131	0.037	0.000	0.000	0.001	0.3
ND:DD	0.000	0.000	0.000	0.556	0.003	0.000	0.000	0.000	0.000
ED:DD	0.000	0.000	0.002	0.043	0.593	0.062	0.001	0.000	0.000
NP:EP	0.000	0.000	0.000	0.798	0.765	0.000	0.237	0.009	0.365
NP:DP	0.000	0.000	0.000	0.000	0.195	0.001	0.004	0.000	0.000
EP:DP	0.000	0.000	0.016	0.000	0.259	0.017	0.019	0.000	0.000

Values represented as $\bar{x} \pm S_x$, NP(76): Normal proximal, 76 hemi-crypts were counted, ND: Normal distal, EP: EDTA proximal, ED: EDTA distal, DP: DMH proximal, DD: DMH distal, LC: Labelled cells per hemi-crypt, CPC: Cells per hemi-crypt, TLI: Total labelling index, LI1: Labelling index of compartment 1, Pzone: Proliferative zone size, LIPZ: Labelling index of proliferative zone Size.

with the mucinous type of adenocarcinoma^[35]. The different responses of bowel segments to DMH, and the reasons for the predilection of colonic neoplasia to distal colon as well as the differences in morphological type of tumours between the proximal and distal colon are not fully understood. However it is known that the structure and function of intestinal mucosa differed significantly between humans^[36] and experimental animals^[37-39]. An understanding of these inherent regional differences may be pivotal in study of the mechanisms of colonic tumorigenesis.

Significant regional differences in the distribution of BrdUrd-labelled cells in proximal and distal rat colon were demonstrated in this study. The differences in distribution of proliferative cells between proximal and distal colons were previously shown with ³H-thymidine autoradiography and immunohistochemistry. ³H-thymidine LI and proliferative zone size were reported to be significantly greater distally than proximally^[40]. In the distal colon PCNA expression was strictly confined to the lower third of the crypt, whereas in the proximal colon it was located in the mid-crypt^[23].

Sunter noted that the peak LI in the proximal colon was located in the middle third of the crypt while the peak of LI in the distal colon was located in the lower third near the base of the crypt^[41]. These findings, together with ours, tended to support the theory of crypt cell origin and colonocyte migration given by Sato and Ahnen^[24]. After a double labelling with ³H-thymidine and BrdUrd, Sato and Ahnen investigated the location of stem cells and the direction of colonocyte migration in normal rat colonic crypt, and reported that distal stem cells were located in the crypt base while proximal stem cells in the mid-crypt, thus postulating that colonocytes migrated up toward the luminal surface in the distal colon in contrast to the bidirectional migration, i.e. up toward the luminal surface and down toward the crypt base in the proximal colon.

Our results showed that after EDTA treatment, the number of proliferative colonic crypt cells was significantly increased in the distal and proximal colon. The LI in the proliferative zone in the EDTA animals did not increase which could be attributable to the concomitant increase of the zone size. In the EDTA treated animals, LIs in all compartments in the distal colon increased except the LI in compartment 1, a significant increase of LI in the proximal colon was found in compartment 3 only. This was corroborated by the cumulative labelling distribution curves. In comparison with normal control, the distal curve shifted toward to the right, but the proximal curve did not change. The fact that the proximal curve did not shift might be important. If hyperproliferation preceded tumour formation and was a cause of tumor formation, then these findings indicated that the distal colon was more susceptible. EDTA did not induce colorectal tumours after administration for 20 weeks, but prolonged EDTA treatment might induce tumours. Another hypothesis is that hyperproliferation in EDTA animals is a co-factor in DMH-induced colonic tumour formation.

DMH treatment further increased colonic crypt cell proliferation. Although DMH treatment increased the LI in both the proximal and distal colon, the cumulative labelling distribution was markedly shifted to the right in the distal colon whereas the proximal curve shifted to the left (*i.e.* downwards in the crypt). The distribution of DMH-induced colorectal cancer resembled human colorectal carcinoma^[42-44]. We found that when the total colon was exposed to the procarcinogen DMH, 73% of tumours occurred distally and only 12% proximally.

Further investigation is required to understand the differences of tumour distribution, and their relationship to the proliferation of different crypt cells and differentiation patterns in the proximal and distal colon. It has been shown that in the proximal colon, mucous cells were predominant in the lower third of the crypt, whereas columnar cells in the

upper third^[45]. In contrast, crypts of the distal colon contained only a small number of mucous cells in basal positions. The undifferentiated cells or the cells with the lowest level of differentiation (presumptive stem cells) were the vacuolated cells located near or at the base of crypt^[46]. The progeny of the vacuolated cells migrated upward to differentiate into columnar cells and downward to differentiate into mucous cells^[47].

In this study we observed a great number of cells in the crypt in the proximal colon than in the distal colon, which was in contrary to published data^[39,40]. This disparity might be due to different criteria for recoding the overlapping nuclei, selecting crypts or ascertaining the top of the crypt. In this study longitudinally well-oriented crypts were selected and all visible nuclei were counted.

EDTA increased crypt cell proliferation but all of the increased parameters were significantly lower than those in the DMH group. The number of crypt cells in hyperproliferation induced by a carcinogen might reach or exceed a limited value (threshold) before colonic tumours developed. While proliferative crypt cells that did not exceed this threshold as in the EDTA animals, might act as a promoting agent to stimulate tumour growth. In conclusion, EDTA's effect of increasing crypt cell proliferation may be a co-factor in this model.

ACKNOWLEDGEMENT

We thank Dr. Hin LY for his statistical advice and Dr. Hamilton PW for his critical suggestions.

REFERENCES

- Huang ZH**, Fan YF, Xia H, Feng HM, Tang FX. Effects of TNP-470 on proliferation and apoptosis in human colon cancer xenografts in nude mice. *World J Gastroenterol* 2003; **9**: 281-283
- Ma QY**, Williamson KE, Rowlands BJ. Variability of cell proliferation in the proximal and distal colon of normal rats and rats with dimethylhydrazine induced carcinogenesis. *World J Gastroenterol* 2002; **8**: 847-852
- Ma QY**, Williamson KE, O'rouke D, Rowlands BJ. The effects of l-arginine on crypt cell hyperproliferation in colorectal cancer. *J Surg Res* 1999; **81**: 181-188
- Chen XX**, Lai MD, Zhang YL, Huang Q. Less cytotoxicity to combination therapy of 5-fluorouracil and cisplatin than 5-fluorouracil alone in human colon cancer cell lines. *World J Gastroenterol* 2002; **8**: 841-846
- Li J**, Guo WJ, Yang QY. Effects of ursolic acid and oleanolic acid on human colon carcinoma cell line HCT15. *World J Gastroenterol* 2002; **8**: 493-495
- Jia XD**, Han C. Chemoprevention of tea on colorectal cancer induced by dimethylhydrazine in Wistar rats. *World J Gastroenterol* 2000; **6**: 699-703
- Chapkin RS**, Lupton JR. Colonic cell proliferation and apoptosis in rodent species. Modulation by diet. *Adv Exp Med Biol* 1999; **470**: 105-118
- Mills SJ**, Mathers JC, Chapman PD, Burn J, Gunn A. Colonic crypt cell proliferation state assessed by whole crypt microdissection in sporadic neoplasia and familial adenomatous polyposis. *Gut* 2001; **48**: 41-46
- Ochsenkuhn T**, Bayerdorffer E, Meining A, Schinkel M, Thiede C, Nussler V, Sackmann M, Hatz R, Neubauer A, Paumgartner G. Colonic mucosal proliferation is related to serum deoxycholic acid levels. *Cancer* 1999; **85**: 1664-1669
- Akedo I**, Ishikawa H, Ioka T, Kaji I, Narahara H, Ishiguro S, Suzuki T, Otani T. Evaluation of epithelial cell proliferation rate in normal-appearing colonic mucosa as a high-risk marker for colorectal cancer. *Cancer Epidemiol Biomarkers Prev* 2001; **10**: 925-930
- Barnes CJ**, Hardman WE, Cameron IL. Presence of well-differentiated distal, but not poorly differentiated proximal, rat colon carcinomas is correlated with increased cell proliferation in and lengthening of colon crypts. *Int J Cancer* 1999; **80**: 68-71
- Wong WM**, Wright NA. Cell proliferation in gastrointestinal mucosa. *J Clin Pathol* 1999; **52**: 321-333

- 13 **Kozoni V**, Tsioulis G, Shiff S, Rigas B. The effect of lithocholic acid on proliferation and apoptosis during the early stages of colon carcinogenesis: differential effect on apoptosis in the presence of a colon carcinogen. *Carcinogenesis* 2000; **21**: 999-1005
- 14 **Lipkin M**, Blattner WE, Fraumeni JF Jr, Lynch HT, Deschner E, Winawer S. Tritiated thymidine (fp, fh) labelling distribution as a marker for hereditary predisposition to colon cancer. *Cancer Res* 1983; **43**: 1899-1904
- 15 **Lipkin M**, Blattner WE, Gardner EJ, Burt RW, Lynch H, Deschner E, Winawer S, Fraumeni JF Jr. Classification and risk assessment of individuals with familial polyposis, Gardner's syndrome, and familial non-polyposis colon cancer from [³H]-thymidine labelling patterns in colonic epithelial cells. *Cancer Res* 1984; **44**: 4201-4207
- 16 **Wilson RG**, Smith AN, Bird CC. Immunohistochemical detection of abnormal cell proliferation in colonic mucosa of subjects with polyps. *J Clin Pathol* 1990; **43**: 744-747
- 17 **Roncucci L**, Pedroni M, Vaccina F, Benatti P, Marzona L, De Pol A. Aberrant crypt foci in colorectal carcinogenesis. Cell and crypt dynamics. *Cell Prolif* 2000; **33**: 1-18
- 18 **Terpstra OT**, van Blankenstein M, Dees J, Eilers GAM. Abnormal pattern of cell proliferation in the entire colonic mucosa of patients with colon adenoma or cancer. *Gastroenterology* 1987; **92**: 704-708
- 19 **Yamada K**, Yoshitke K, Sato M, Ahnen DJ. Proliferating cell nuclear antigen expression in normal, preneoplastic colonic epithelium of the rat. *Gastroenterology* 1992; **103**: 160-167
- 20 **Ma QY**, Hoper M, Anderson N, Rowlands BJ. Effect of supplemental L-arginine in a chemical-induced model of colorectal cancer. *World J Surg* 1996; 1087-1091
- 21 **Maskens AP**. Histogenesis and growth pattern of 1,2-dimethylhydrazine induced rat colon adenocarcinoma. *Cancer Res* 1976; **36**: 1585-1592
- 22 **Richards TC**. Early changes in the dynamics of crypt cell populations in mouse colon following administration of 1,2-dimethylhydrazine. *Cancer Res* 1977; **37**: 1680-1685
- 23 **Heitman DW**, Grubbs BG, Heitman TO, Cameron IL. Effects of 1,2-dimethylhydrazine treatment and feeding regimen on rat colonic epithelial cell proliferation. *Cancer Res* 1983; **43**: 1153-1162
- 24 **Sato M**, Ahnen D. Regional variability of colonocyte growth and differentiation in the rat. *Anat Record* 1992; **233**: 409-414
- 25 **Freeman HJ**, Kim YS, Kim YS. Glycoprotein metabolism in normal proximal and distal rat colon and changes associated with 1, 2-dimethylhydrazine induced colonic neoplasia. *Cancer Res* 1978; **38**: 3385-3390
- 26 **Greene FL**. Distribution of colorectal neoplasm. A left to right shift of polyps and cancer. *Am Surg* 1983; **49**: 62-65
- 27 **Krishnamurti C**, Saryan LA, Petering DH. Effects of ethylenediaminetetracetic acid and 1, 10-phenanthroline on cell proliferation and DNA synthesis of Ehrlich ascites cells. *Cancer Res* 1980; **40**: 4092-4099
- 28 **Skehan P**. Nonchelational cell growth inhibition by EDTA. *Life Science* 1986; **39**: 1787-1793
- 29 **Grummt F**, Weinmann-Dorsch C, Schneider-Schaulies J, Lux A. Zinc as a second messenger of mitogenic induction: effects of diadenosine tetrphosphate (Ap₄A) and DNA synthesis. *Exp Cell Res* 1986; **163**: 191-200
- 30 **Rubin H**. Inhibition of DNA synthesis in animal cells by ethylene diamine tetraacetate, and its reversal by zinc. *Proc Natl Acad Sci* 1972; **69**: 713-716
- 31 **Nozue AT**. Effect of EDTA in newborn mice with special reference to neural crest cells. *Anatomischer Anzeiger* 1988; **166**: 209-217
- 32 **Pozharisski K**. Morphology and morphogenesis of experimental epithelial tumors of the intestine. *JNCI* 1975; **54**: 1115-1135
- 33 **Sunter JP**, Appleton DR, Wright NA, Watson AJ. Kinetics of changes in the crypts of the jejunal mucosa of dimethylhydrazine-treated rats. *Br J Cancer* 1978; **37**: 662-672
- 34 **Martin MS**, Martin F, Michiels R, Bastien H, Justrabo E, Bordes M, Viry B. An experimental model for cancer of the colon and rectum. Intestinal carcinoma induced in the rat by 1,2-dimethylhydrazine. *Digestion* 1973; **8**: 22-34
- 35 **Ward JM**, Yamamoto RS, Brown CA. Pathology of intestinal neoplasm and other lesions in rats exposed to azoxymethane. *JNCI* 1973; **51**: 1029-1039
- 36 **Filipe MI**, Branfoot AC. Abnormal pattern of mucus secretion in apparently normal mucosa of large intestine with carcinoma. *Cancer* 1974; **34**: 282-290
- 37 **Reid PE**, Culling CFA, Dunn WL, Ramey CW, Clay MG. Differences in chemical composition between the epithelial glycoproteins of the upper and lower halves of rat colon. *Can J Biochem* 1975; **53**: 1328-1332
- 38 **Freeman HJ**, Kim Y, Kim YS. Glycoprotein metabolism in normal proximal and distal rat colon and changes associated with 1, 2-dimethylhydrazine-induced colonic neoplasia. *Cancer Res* 1978; **38**: 3385-3390
- 39 **Mian N**, Cowen DM, Nutman CA. Glycosidases heterogeneity among dimethylhydrazine induced rat colonic tumours. *Br J Cancer* 1974; **30**: 231-237
- 40 **McGarrity TJ**, Perffer LP, Colony PC. Cellular proliferation in proximal and distal rat colon during 1,2-dimethylhydrazine-induced carcinogenesis. *Gastroenterology* 1988; **95**: 343-348
- 41 **Sunter JP**, Watson AJ, Wright NA, Appleton DR. Cell proliferation at different sites along the length of the rat colon. *Virchows Arch B Cell Path* 1979; **32**: 75-87
- 42 **Rodgers AE**, Nauss KM. Rodent model for carcinoma of the colon. *Dig Dis Sci* 1985; **30**: 87S-102S
- 43 **Shamsuddin AK**, Trump BF. Colon Epithelium: II. *In vivo* studies of colon carcinogenesis. Light microscopic, histochemical, and ultrastructural studies of histogenesis of azoxymethane-induced colon carcinogenesis in Fischer 344 rats. *JNCI* 1981; **66**: 389-401
- 44 **Sunter JP**, Hull DL, Appleton DR, Watson AJ. Cell proliferation of colonic neoplasms in dimethylhydrazine-treated rats. *Br J Cancer* 1980; **42**: 95-102
- 45 **Shamsuddin AK**, Trump BF. Colon Epithelium: I. Light microscopic, histochemical, and ultrastructural features of normal colon epithelium of male Fischer 344 rats. *JNCI* 1981; **66**: 375-388
- 46 **Nabeyama A**. Presence of cells combining features of two different cell types in the colonic crypt and pyloric glands of the mouse. *Am J Anat* 1975; **142**: 471-484
- 47 **Chang WWL**, Leblond CP. Renewal of the epithelium in the descending colon of the mouse. I. Presence of three cell populations: vacuolated-columnar, mucous and argentaffin. *Am J Anat* 1971; **131**: 73-99

Low grade gastric MALTOMA: Treatment strategies based on 10 year follow-up

Sang Kil Lee, Yong Chan Lee, Jae Bock Chung, Chae Yoon Chon, Young Myoung Moon, Jin Kyung Kang, In-Suh Park, Chang Ok Suh, Woo Ik Yang

Sang Kil Lee, Yong Chan Lee, Jae Bock Chung, Chae Yoon Chon, Young Myoung Moon, Jin Kyung Kang, Division of Gastroenterology, Department of Internal Medicine, Yonsei University College of Medicine, Seoul, South Korea

In-Suh Park, Department of Internal Medicine, NHIC Ilsan Hospital, Ilsan, South Korea

Chang Ok Suh, Department of Radiation Oncology, Yonsei University College of Medicine, Seoul, South Korea

Woo Ik Yang, Department of Pathology, Yonsei University College of Medicine, Seoul, South Korea

Correspondence to: Dr. Jae Bock Chung, Division of Gastroenterology, Department of Internal Medicine, Yonsei University College of Medicine, 134 Shinchon-dong, Seodaemun-gu, Seoul, South Korea. jbchung@yumc.yonsei.ac.kr

Telephone: +82-2-361-5410 **Fax:** +82-2-393-6884

Received: 2003-07-17 **Accepted:** 2003-09-24

Abstract

AIM: To deduce strategic guideline of gastric mucosa associated lymphoid tissue lymphoma (MALTOMA) by evaluating the long-term outcome of patients in respect to various treatment modalities.

METHODS: A total of 55 patients with MALTOMA from May 1992 to August 2002 were retrospectively reviewed.

RESULTS: Complete remission was obtained in 24 (82.8%) of 29 patients treated with anti *Helicobacter pylori* (*H pylori*) regimen only. The duration to reach complete remission was 12 months (85 percentile, 2-33 months). Five patients showed complete remission with radiation therapy (26-86 months). Two of them were *H pylori* treatment failure cases.

CONCLUSION: *H pylori* eradication is an effective primary treatment option for low grade MALTOMA and radiation therapy could be considered in patients with no evidence of *H pylori* infection or who do not respond to *H pylori* eradication therapy 12 months after successful eradication.

Lee SK, Lee YC, Chung JB, Chon CY, Moon YM, Kang JK, Park IS, Suh CO, Yang WI. Low grade gastric MALTOMA: Treatment strategies based on 10 year follow-up. *World J Gastroenterol* 2004; 10(2): 223-226

<http://www.wjgnet.com/1007-9327/10/223.asp>

INTRODUCTION

In 1983, Isaacson and Wright introduced the term MALTOMA to characterize primary low grade gastric B-cell lymphoma and immunoproliferative small-intestinal disease^[1]. Subsequently, the definition of MALTOMA was extended to include several other extranodal low grade B-cell lymphomas, with a similar histology to Peyer's patches, including those of the salivary gland, lung, and thyroid, but gastric form is the most common and best characterized MALTOMA^[2].

Low grade MALTOMA is composed of small cells with dense nuclear chromatin and a low proliferation fraction; the converse is true for diffuse large B cell lymphoma. Low grade gastric MALTOMA is a neoplasia with a very indolent course and an excellent prognosis. It has a tendency to remain localized to the gastric wall and seldom involve lymph nodes and bone marrow.

In the past, primary low grade gastric MALTOMA was treated with surgery in the same way as adenocarcinoma. This often necessitated a total gastrectomy due to the multi-focal or diffuse nature of gastric lymphomas. Since the introduction of *H pylori* concept, the association of this bacterium with chronic active gastritis, peptic ulcer and gastric cancer has been demonstrated^[3-5]. Furthermore, *H pylori* is suggested to be associated with low-grade gastric MALTOMA. It was proposed that low grade gastric MALTOMA was formed by the immune response to *H pylori* infection in the gastric mucosa^[6,7]. The discovery of a causal role for *H pylori* in the development of gastric marginal zone lymphoma of the MALT type has dramatically altered the therapeutic approach to patients with early stage disease^[8,9]. According to recent data, durable complete remissions might be achieved in up to 80% of patients with early stage MALTOMA following eradication of the bacteria^[9]. In the patients who failed to respond to *H pylori* eradication or had low grade gastric MALTOMA without *H pylori* infection, radiotherapy, chemotherapy or surgery has been tried.

However, the long-term follow-up result of *H pylori* eradication on low grade MALT lymphoma has been seldom reported. Furthermore, a clear-cut time is difficult to define the failure to *H pylori* eradication therapy and currently there has been no standard guideline to assess the result of eradication therapy. Also the time interval to perform endoscopic examination to evaluate histologic and morphologic remission is unclear. Consequently, a suitable strategic guideline to decide subsequent treatment option when one fails has not been well proposed. We aimed to evaluate the long-term outcome of patients with low grade gastric MALTOMA in respect to various treatment modalities. We also tried to deduce suitable strategic guideline to treat low grade gastric MALTOMA.

MATERIALS AND METHODS

Patients

We retrospectively studied 55 patients of primary low grade gastric MALTOMA aged 23 to 74 years from May 1992 to August 2002. All the patients were pathologically confirmed as low grade gastric MALTOMA. The diagnosis of low grade gastric MALTOMA was made according to the criteria of Isaacson^[10] and scoring system of Wotherspoon *et al*^[11]. The initial staging procedures included a complete physical examination, chest roentgenogram, bone marrow examination, abdominal CT scan and endoscopic ultrasonography (EUS).

Methods

We evaluated the patients' initial presenting symptoms and the status of *H pylori* infection. *H pylori* infection was diagnosed by rapid urease test (CLOTM, Delta West, Bentley,

Western Austria), and/or histologic examination. *H pylori* status was considered positive if any of the two tests was positive. Endoscopic findings included the shape, size, location and number of lesions. Gross phenotype was classified according to the endoscopic features into seven types: 1) gastritis: only mucosal color change, 2) granular: small nodules on the lesion, 3) ulcerative: one or more ulceration, 4) ulceroinfiltrative: one or more ulceration with surrounding mucosal infiltration, 5) depressed: depressed or EGC IIc like lesion, 6) protruding: elevated or polypoid, and 7) mixed, and then was categorized into diffuse and localized type according to the pattern of distribution.

RESULTS

Clinical and endoscopic features of patients

The male to female ratio was 1:1.3. The mean age of the patients was 47.8 years (23-74). All but three of the patients were symptomatic at presentation: The main symptoms were abdominal pain (56.4%), indigestion (23.6%), epigastric discomfort (12.7%) and vomiting (1%). A total of 48 (48/53, 90.5%) met the case definition for *H pylori* positivity (Table 1). When each test was considered individually, *H pylori* infection was detected by histology and rapid urease test in 42 (87.5%) and 39 (81.3%) patients, respectively. Initial endoscopic findings are summarized in Table 2.

Table 1 Clinical features of patients and *H pylori* state (n=55)

Age (years)	47.8±11.3 (23-74)	
Sex	Male:Female=24:31	
<i>H pylori</i> status ^a	Positive	48 (90.5%)
	Negative	5 (9.5%)

^aExcluding two cases of unknown *H pylori* status.

Table 2 Endoscopic findings and location of low grade MALTOMA (n=55)

Location	No. of cases (%)	Findings	No. of cases (%)
Body only	21 (38.2)	Ulcerative	15 (27.3)
Antrum only	11 (20.0)	Mixed	15 (27.3)
Antrum & body	20 (36.4)	Ulceroinfiltrative	10 (18.2)
Fundus/Cardia	3 (5.4)	Depressed	6 (10.9)
		Gastritis	5 (9.1)
		Protruding	3 (5.5)
		Granular	1 (1.8)

Treatment modalities and outcomes

Treatment modalities included *H pylori* eradication, surgery, radiotherapy and combination therapy (Table 3). A total of twenty nine patients were treated with *H pylori* eradication therapy (omeprazole + amoxicillin + metronidazole or clarithromycin for 2 weeks). All but one was positive in urease test or histologic examination for *H pylori*. Endoscopic ultrasonography was done before *H pylori* eradication and cases with lymph node metastasis or involvement beyond the submucosal layer were excluded. For determination of the response, two months after the end of eradication therapy, biopsy specimens were collected from the multiple sites including the lesion for histologic examination. One additional specimen was obtained for rapid urease test. For the remission failure case, a repeat endoscopy was performed every two to three months until complete remission was achieved. In cases with complete remission, endoscopic examination and biopsy were performed every 6-12 months. Overall *H pylori* eradication rate was 96.4% (27/28). Complete remission of

low grade MALTOMA was achieved in 24 out of 29 cases (82.8%). The median time to get complete remission was 4 months (2-33) (Table 3). In terms of histologic remission of the low grade gastric MALTOMA, the mucosal lesions changed to atrophic or endoscopically normal appearance (Figure 1). There were five treatment failures to *H pylori* eradication therapy. Radiation treatment was given in two patients who failed to respond to anti *H pylori* treatment after 6 months and 9 months of follow-up, respectively. One underwent operation. They all had complete remission in the subsequent follow-up. The remaining two patients were recommended to receive other treatment with persistence of localized MALTOMA.

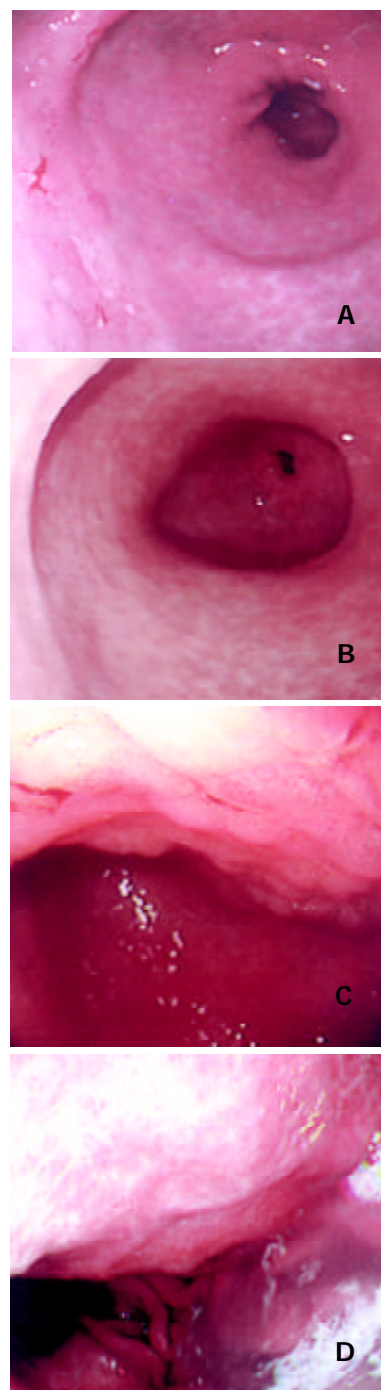


Figure 1 A: A case with irregular ulceration on the anterior wall of antrum before eradication. B: 3 months after *H pylori* eradication therapy, ulceration was disappeared. C: A case with mucosal nodularities on the posterior wall of the upper body before eradication. D: 2 months after *H pylori* eradication therapy, the lesion was replaced by atrophic mucosa.

Sixteen patients underwent surgery, including 11 total gastrectomies and 5 subtotal gastrectomies (Table 3). Most of them were treated by surgery because they were suspected to have lymph node metastasis or infiltration beyond the submucosal layer in endoscopic ultrasonographic examination. Among the sixteen patients, 4 patients showed lymph node metastasis. Three patients received additional radiation therapy or chemotherapy after surgery because of lymph node metastasis or perigastric fat infiltration of low grade gastric MALTOMA.

Five patients received radiation therapy. These cases included two patients with *H pylori* negativity, two patients with failure to *H pylori* eradication, and one case with recurrence in remnant stomach after surgery (Table 3). The median radiation dose was 30.6 Gy (range 30-39) with a daily fraction of 1.5-1.8 Gy.

The comparative study among different endoscopic types of low grade MALT lymphoma patients who showed failure to eradication treatment disclosed no significant correlation. However, the lesion of localized mass type showed the tendency to higher treatment failure (Table 4).

Table 3 Initial treatments and outcomes of low grade MALTOMA

	<i>H pylori</i> eradication (n=29)	Surgery (n=16)	Radiotherapy (n=5)
Complete remission (%)	24 (82.8%)	16 (100%)	5 (100%)
Failure (%)	5 (17.2%)	0	0
Recurrence (%)	1 (4.2%)	1	0
Median follow-up (months)	24 (2-74)	46.5 (12-120)	35.5 (26-86)
Time to get CR in 85 percentile of patients (interval) (months)	12 (2-33)		

CR: Complete remission.

Table 4 Failures of *H pylori* eradication treatment according to endoscopic findings

Endoscopic types	Treatment cases	Failure cases (% ^a)
Diffuse	13	1 (17.7) ^b
Gastritis	2	0 (0)
Granular	1	0 (0)
Mixed	10	1 (10.0)
Localized	16	4 (25.0) ^a
Ulcerative	8	2 (25.0)
Ulceroinfiltrative	3	1 (33.3)
Depressed	4	0 (0)
Protruding	1	1 (100.0)
Total	29	5 (17.2)

^aFailure rate of each endoscopic type, ^b $P > 0.05$ by χ^2 test.

DISCUSSION

The relationship between *H pylori* and low grade gastric MALTOMA is strong, and therefore treatment strategies are aimed at *H pylori* eradication in early stages. Recently, durable complete remissions have been supposed to achieve in up to 80% of patients with early stage MALTOMA following eradication of the bacteria^[9]. In the largest MALTOMA study to date, 120 patients with early stage low grade gastric MALTOMA were treated with *H pylori* eradication therapy and followed^[12]. After mean follow-up period of 48 months, 81% of patients were in complete remission. Relapse after complete remission occurred in less than 10% of cases, and whether this was always caused by *H pylori* reinfection has been unknown^[13-24]. Follow-up is essential in patients with

MALTOMA treated with *H pylori* eradication therapy. Endoscopic follow-up with biopsy for histology and *H pylori*, and EUS at least yearly after remission was recommended^[12,25]. Because some residual cells lay dormant after clinical and histological remission was achieved, some investigators insisted that molecular studies should be included in addition to histologic study^[20]. At present, histologic study is considered as the gold standard.

Because eradication therapy is never 100% successful, it is also important to choose the most suitable additional treatment for treatment failure. MALTOMA that were not *H pylori* positive or did not respond to eradication therapy could be treated with surgery, radiation, or chemotherapy. Radical gastrectomy has 5- and 10-yr survival rates of 90% and 70%, but lead to significant morbidity^[26]. Monotherapy with alkylating agents was tried in MALTOMA patients who did not respond to *H pylori* eradication therapy. In this study, remission could be achieved with chlorambucil in only 58% of the nonresponding patients to *H pylori* eradication therapy^[25].

Our results showed 82.8% of remission induction in low grade gastric MALTOMA by *H pylori* eradication alone with a single relapse. About 50% of patients with low grade gastric MALTOMA showed complete remission by 4 months after *H pylori* eradication. However, delayed response by up to 33 months occurred in one case. Overall, complete remission was achieved within 12 months in 85 percentile. We propose that it is necessary to wait for 12 months after initial eradication therapy of *H pylori* to define the time for *H pylori* eradication failure, because relapse is relatively rare after 12 months and nearby all the cases would have complete remission by 12 months. In addition, other treatment modalities could be used 12 months after initial *H pylori* eradication therapy, such as radiation therapy, surgery or chemotherapy.

A recent series from the memorial Sloan-Kettering Cancer Center and Yonsei Cancer Center reported a 100% complete remission rate with radiation alone. Especially, radiation therapy was chosen in the management of low grade gastric MALTOMA in patients with no evidence of *H pylori* infection or who showed no response to *H pylori* eradication therapy^[27,28]. In our study, complete remission was obtained in all the patients after various treatment modalities. All the patients who received radiotherapy tolerated the treatment well and completed the treatment course without significant acute or delayed toxicities. Radiation therapy was superior to surgery or chemotherapy because it had significant advantages of gastric preservation and lower morbidity.

Our results provide further supports to the recommendation by Issacson and Spencer that eradication of *H pylori* is harmless and inexpensive and should be the first-line treatment for localized low grade gastric MALTOMA. If no response is observed by 12 months after eradication therapy, radiotherapy should be considered.

Several investigators evaluated endoscopic appearance of primary gastric lymphoma^[29,30]. In low grade lymphoma, endoscopic findings were often interpreted as a benign condition, in contrast to high grade lymphoma, for which carcinoma was the most frequently suspected diagnosis. Our results were consistent with previous reports that low grade gastric MALTOMA was found at a relatively high frequency (94.6%) in the middle third of the stomach^[31]. The most frequent endoscopic appearance of gastric lymphoma was ulceration, while the finding of polypoid lesions or other forms (as gastritis or erosions) had a lower frequency^[32]. Also in this study, the majority of the endoscopic features of low grade gastric MALTOMA was superficial, such as shallow ulceration or mixed type, and was multiple rather than single. But these cases also exhibited variegated pictures. In terms of the result of *H pylori* eradication therapy, we did not see any correlation

with the endoscopic findings. It might be due to the small number of cases of *H pylori* eradication failure and complexity of endoscopic findings of low grade MALTOMA. However, the lesion of localized mass type showed the tendency to higher treatment failure (Table 4). Nevertheless, if we consider the fact that high grade lymphoma is often accompanied with deep ulceration or protruding mass in the stomach, our results might be valuable on the presumption that mixed type MALTOMA might exist which was responsible for the treatment failure.

REFERENCES

- 1 **Isaacson P**, Wright DH. Malignant lymphoma of mucosa-associated lymphoid tissue. A distinctive type of B-cell lymphoma. *Cancer* 1983; **52**: 1410-1416
- 2 **Zhou Q**, Xu TR, Fan QH, Zhen ZX. Clinicopathologic study of primary intestinal B cell malignant lymphoma. *World J Gastroenterol* 1999; **5**: 538-540
- 3 **Marshall BJ**, Warren JR. Unidentified curved bacilli in the stomach of patients with gastritis and peptic ulceration. *Lancet* 1984; **16**: 1311-1315
- 4 **NIH Consensus conference**. *Helicobacter pylori* in peptic ulcer disease. NIH Consensus Development Panel on *Helicobacter pylori* in Peptic Ulcer Disease. *JAMA* 1994; **272**: 65-69
- 5 **Parsonnet J**, Friedman GD, Vandersteen DP, Chang Y, Vogelstein JH, Orentreich N, Sibley RK. *Helicobacter pylori* infection and the risk of gastric carcinoma. *N Engl J Med* 1991; **325**: 1127-1131
- 6 **Wyatt JL**, Rathbone BJ. Immune response of the gastric mucosa to *Campylobacter pylori*. *Scand J Gastroenterol Suppl* 1988; **142**: 44-49
- 7 **Stolte M**, Eidt S. Lymphoid follicles in antral mucosa: immune response to *Campylobacter pylori*? *J Clin Pathol* 1989; **42**: 1269-1271
- 8 **Isaacson PG**. Gastric MALT lymphoma: from concept to cure. *Ann Oncol* 1999; **10**: 637-645
- 9 **Neubauer A**, Thiede C, Morgner A, Alpen B, Ritter M, Neubauer B, Wundisch T, Ehninger G, Stolte M, Bayerdorffer E. Cure of *Helicobacter pylori* infection and duration of remission of low-grade gastric mucosa-associated lymphoid tissue lymphoma. *J Natl Cancer Inst* 1997; **89**: 1350-1355
- 10 **Isaacson PG**. Gastrointestinal lymphoma. *Hum pathol* 1994; **25**: 1020-1029
- 11 **Wotherspoon AC**, Doglioni C, Diss TC, Pan L, Moschini A, de Boni M, Isaacson PG. Regression of primary low-grade B-cell gastric lymphoma of mucosa-associated lymphoid tissue type after eradication of *Helicobacter pylori*. *Lancet* 1993; **342**: 575-577
- 12 **Stolte M**, Bayerdorffer E, Morgner A, Alpen B, Wundisch T, Thiede C, Neubauer A. *Helicobacter* and gastric MALT lymphoma. *Gut* 2002; **50**: 19-24
- 13 **Isaacson PG**, Diss TC, Wotherspoon AC, Barbazza R, De Boni M, Doglioni C. Long-term follow-up of gastric MALT lymphoma treated by eradication of *H pylori* with antibodies. *Gastroenterology* 1999; **117**: 750-751
- 14 **Du MQ**, Isaacson PG. Gastric MALT lymphoma: from aetiology to treatment. *Lancet Oncol* 2002; **3**: 97-104
- 15 **Roggero E**, Zucca E, Pinotti G, Pascarella A, Capella C, Savio A, Pedrinis E, Paterlini A, Venco A, Cavalli F. Eradication of *Helicobacter pylori* infection in primary low-grade gastric lymphoma of mucosa-associated lymphoid tissue. *Ann Intern Med* 1995; **122**: 767-769
- 16 **Savio A**, Franzin G, Wotherspoon AC, Zamboni G, Negrini R, Buffoli F, Diss TC, Pan L, Isaacson PG. Diagnosis and posttreatment follow-up of *Helicobacter pylori*-positive gastric lymphoma of mucosa-associated lymphoid tissue: histology, polymerase chain reaction, or both? *Blood* 1996; **87**: 1255-1260
- 17 **Sackmann M**, Morgner A, Rudolph B, Neubauer A, Thiede C, Schulz H, Kraemer W, Boersch G, Rohde P, Seifert E, Stolte M, Bayerdorffer E. Regression of gastric MALT lymphoma after eradication of *Helicobacter pylori* is predicted by endosonographic staging. MALT Lymphoma Study Group. *Gastroenterology* 1997; **113**: 1087-1090
- 18 **Montalban C**, Manzanal A, Boixeda D, Redondo C, Alvarez I, Calleja JL, Bellas C. *Helicobacter pylori* eradication for the treatment of low-grade gastric MALT lymphoma: follow-up together with sequential molecular studies. *Ann Oncol* 1997; **8**(Suppl 2): 37-39
- 19 **Papa A**, Cammarota G, Tursi A, Gasbarrini A, Gasbarrini G. *Helicobacter pylori* eradication and remission of low-grade gastric mucosa-associated lymphoid tissue lymphoma: a long-term follow-up study. *J Clin Gastroenterol* 2000; **31**: 169-171
- 20 **Montalban C**, Santon A, Boixeda D, Redondo C, Alvarez I, Calleja JL, de Argila CM, Bellas C. Treatment of low grade gastric mucosa-associated lymphoid tissue lymphoma in stage I with *Helicobacter pylori* eradication. Long-term results after sequential histologic and molecular follow-up. *Haematologica* 2001; **86**: 609-617
- 21 **Ruskone-Fourmestraux A**, Lavergne A, Aegerter PH, Megraud F, Palazzo L, de Mascarel A, Molina T, Rambaud JL. Predictive factors for regression of gastric MALT lymphoma after anti-*Helicobacter pylori* treatment. *Gut* 2001; **48**: 297-303
- 22 **Steinbach G**, Ford R, Globber G, Sample D, Hagemester FB, Lynch PM, McLaughlin PW, Rodriguez MA, Romaguera JE, Sarris AH, Younes A, Luthra R, Manning JT, Johnson CM, Lahoti S, Shen Y, Lee JE, Winn RJ, Genta RM, Graham DY, Cabanillas FF. Antibiotic treatment of gastric lymphoma of mucosa-associated lymphoid tissue: An uncontrolled trial. *Ann Intern Med* 1999; **131**: 88-95
- 23 **Nakamura S**, Matsumoto T, Suekane H, Takeshita M, Hizawa K, Kawasaki M, Yao T, Tsuneyoshi M, Iida M, Fujishima M. Predictive value of endoscopic ultrasonography for regression of gastric low grade and high grade MALT lymphomas after eradication of *Helicobacter pylori*. *Gut* 2001; **48**: 454-460
- 24 **Cheng H**, Wang J, Zhang CS, Yan PS, Zhang XH, Hu PZ, Ma FC. Clinicopathologic study of mucosa-associated lymphoid tissue lymphoma in gastroscopic biopsy. *World J Gastroenterol* 2003; **9**: 1270-1272
- 25 **Levy M**, Copie-Bergman C, Traulle C, Lavergne-Slove A, Brousse N, Flejou JF, de Mascarel A, Hemery F, Gaulard P, Delchier JC. Conservative treatment of primary gastric low-grade B-cell lymphoma of mucosa-associated lymphoid tissue: predictive factors of response and outcome. *Am J Gastroenterol* 2002; **97**: 292-297
- 26 **Radaszkiewicz T**, Dragosics B, Bauer P. Gastrointestinal malignant lymphomas of the mucosa-associated lymphoid tissue: factors relevant to prognosis. *Gastroenterology* 1992; **102**: 1628-1638
- 27 **Park HC**, Park W, Hahn JS, Kim CB, Lee YC, Noh JK, Suh CO. Low grade MALT lymphoma of the stomach: treatment outcome with radiotherapy alone. *Yonsei Med J* 2002; **43**: 601-606
- 28 **Schechter NR**, Portlock CS, Yahalom J. Treatment of mucosa-associated lymphoid tissue lymphoma of the stomach with radiation alone. *J Clin Oncol* 1998; **16**: 1916-1921
- 29 **Taal BG**, den Hartog Jager FC, Burgers JM, van Heerde P, Tio TL. Primary non-Hodgkin's lymphoma of the stomach: Changing aspects and therapeutic choices. *Eur J Cancer Clin Oncol* 1989; **25**: 439-450
- 30 **Seifert E**, Schulte F, Weismuller J, de Mas CR, Stolte M. Endoscopic and bioptic diagnosis of malignant non-Hodgkin's lymphoma of the stomach. *Endoscopy* 1993; **25**: 497-501
- 31 **Hiyama T**, Haruma K, Kitadai Y, Masuda H, Miyamoto M, Ito M, Kamada T, Tanaka S, Uemura N, Yoshihara M, Sumii K, Shimamoto F, Chayama K. Clinicopathological features of gastric mucosa-associated lymphoid tissue lymphoma: a comparison with diffuse large B-cell lymphoma without a mucosa-associated lymphoid tissue lymphoma component. *J Gastroenterol Hepatol* 2001; **16**: 734-739
- 32 **Isaacson PG**. Recent developments in our understanding of gastric lymphomas. *Am J Surg Pathol* 1996; **20**(Suppl): S1-7

Effect of *Helicobacter pylori* infection on expressions of Bcl-2 family members in gastric adenocarcinoma

Hao Zhang, Dian-Chun Fang, Rong-Quan Wang, Shi-Ming Yang, Hai-Feng Liu, Yuan-Hui Luo

Hao Zhang, Dian-Chun Fang, Rong-Quan Wang, Shi-Ming Yang, Hai-Feng Liu, Yuan-Hui Luo, Department of Gastroenterology of Southwest Hospital, Third Military Medical University, Chongqing 400038, China

Supported by the National Natural Science Foundation of China, No.30070043, and the Key Programs of the Military Medical and Health Foundation during the 10th Five-Year Plan Period, No.01Z075

Correspondence to: Professor Dian-Chun Fang, Department of Gastroenterology of Southwest Hospital, Chongqing 400038, China. fangdianchun@hotmail.com

Telephone: +86-23-68754124

Received: 2003-07-12 **Accepted:** 2003-08-16

Abstract

AIM: To investigate the effect of *Helicobacter pylori* (*H pylori*) infection on the expressions of Bcl-2 family members in gastric adenocarcinoma.

METHODS: Gastric adenocarcinoma and resection margin tissues of 95 patients were studied. Semi-quantitative RT-PCR was used to measure Bid, Bax and Bcl-2 mRNA expressions.

RESULTS: Expressions of Bid and Bax in gastric adenocarcinoma tissues without *H pylori* infection, with *cagA*⁻ *H pylori* infection and *cagA*⁺ *H pylori* infection increased significantly in turn (Bid, 0.304, 0.422 and 0.855 respectively, $P < 0.05$; Bax, 0.309, 0.650 and 0.979 respectively, $P < 0.05$). Bcl-2 mRNA levels increased significantly in gastric adenocarcinoma tissues with *cagA*⁻ *H pylori* infection and *cagA*⁺ *H pylori* infection, compared with those without *H pylori* infection (0.696 and 0.849 vs 0.411, $P < 0.05$). Expressions of Bid, Bax and Bcl-2 in resection margin tissues without *H pylori* infection, with *cagA*⁻ *H pylori* infection and *cagA*⁺ *H pylori* infection increased significantly in turn (Bid, 0.377, 0.686 and 0.939 respectively, $P < 0.05$; Bax, 0.353, 0.645 and 1.001 respectively, $P < 0.05$; Bcl-2, 0.371, 0.487 and 0.619 respectively, $P < 0.05$). In *H pylori* negative specimens, expressions of Bid and Bax correlated negatively with that of Bcl-2 respectively in adenocarcinoma tissues (Bid vs Bcl-2, $r = -0.409$, $P < 0.05$; Bax vs Bcl-2, $r = -0.451$, $P < 0.05$). In *H pylori* positive specimens, expressions of Bid and Bax did not correlate with that of Bcl-2 in adenocarcinoma tissues (Bid vs Bcl-2, $r = 0.187$, $P > 0.05$; Bax vs Bcl-2, $r = 0.201$, $P > 0.05$), but correlated positively with that of Bcl-2 respectively in resection margin tissues (Bid vs Bcl-2, $r = 0.331$, $P < 0.05$; Bax vs Bcl-2, $r = 0.295$, $P < 0.05$).

CONCLUSION: *H pylori* may enhance Bid, Bax and Bcl-2 mRNA levels and cause deregulation of these apoptosis-associated genes expressions, which may play a role during development of gastric adenocarcinoma induced by *H pylori*.

Zhang H, Fang DC, Wang RQ, Yang SM, Liu HF, Luo YH. Effect of *Helicobacter pylori* infection on expressions of Bcl-2 family members in gastric adenocarcinoma. *World J Gastroenterol* 2004; 10(2): 227-230

<http://www.wjgnet.com/1007-9327/10/227.asp>

INTRODUCTION

Helicobacter pylori (*H pylori*) infection is the most common chronic infection in humans and is the major cause of gastritis worldwide. This infection is also accepted as the etiological factor of the majority of peptic ulcers. It has been implicated as a significant contributing factor in the development of gastric malignancy, both gastric MALT lymphoma and gastric adenocarcinoma^[1-14], and *H pylori* was classified as a group 1 carcinogen for gastric cancer in 1994 by the WHO and International Agency for Research on Cancer (IARC)^[15]. The role of *H pylori* infection in the gastric carcinogenesis is not clear. It might be involved in imbalance between apoptosis and proliferation^[16-33]. Bcl-2 family members have been closely related to apoptosis, which could either promote cell survival (Bcl-2, Bcl-x_L, A1, Mcl-1, and Bcl-w) or promote cell death (Bax, Bak, Bcl-x_S, Bad, Bid, Bik, Bim, Hrk, Bok)^[34-36]. In the present study, we investigated the effect of *H pylori* infection on the expressions of Bcl-2 family members in gastric adenocarcinoma and resection margin tissues.

MATERIALS AND METHODS

Tissue specimens

Specimens of gastric adenocarcinoma of 95 patients (72 males and 23 females, age range 31 to 84 years, mean 56 years), who had undergone resection surgical at the Southwest Hospital in Chongqing and had not taken anti-*H pylori* drugs before operation, were collected from 2001 to 2002. Gastric adenocarcinoma tissues were examined microscopically. Resection margin tissues were also examined to verify that they did not contain malignant cells. The histological diagnosis was confirmed by a professional pathologist. The remaining specimens were snap-frozen and stored at -80 °C until assayed. Warthin-Starry silver staining and polymerase chain reaction (PCR) analysis for *H pylori* urease gene A (*ureA*) were performed to detect *H pylori* infection. PCR analysis for *H pylori cagA* gene was performed to verify *cagA*⁺ *H pylori* infection. Fifty-eight patients whose both Warthin-Starry staining and PCR for *ureA* showed positive results were diagnosed as suffering from *H pylori* infection and 37 were *cagA*⁺ *H pylori*.

RT-PCR analysis of Bid, Bax and Bcl-2 mRNA

According to references^[37,38], primers were designed for β -actin (GenBank accession No.BC013380), 5' -GTG GGG CGC CCC AGG CAC CA-3' (sense) and 5' -CTC CTT AAT GTC ACG CAC GAT TTC-3' (antisense), 540 bp product; for Bid (GenBank accession No.AF087891), 5' -ATG GAC TGT TGA GGT CAA CAA C-3' (sense) and 5' -TCA GTC CAT CCC ATT TCT GGC T-3' (antisense), 588 bp product; for Bax (GenBank accession No.AY217036), 5' -ACC AAG AAG CTG AGC GAG TGT C-3' (sense) and 5' -ACA AAG ATG GTC ACG GTC TGC C-3' (antisense), 332 bp product; and for Bcl-2 (GenBank accession No.M13994), 5' -TGC ACC TGA CGC CCT TCA C-3' (sense), 5' -AGA CAG CCA GGA GAA ATC AAA CAG-3' (antisense), 293 bp product.

Total RNA was prepared from gastric adenocarcinoma

tissues and resection margin tissues by using TriPure isolation reagent (Roche) according to the manufacturer's protocol. Reverse transcription (RT) was performed for first-strand cDNA by using 2 µg of total RNA and 1 µl of oligo(dT)18 primer in the presence of 5 unit AMV reverse transcriptase (Promega), 20 unit RNase inhibitor, 0.5 mmol/L of each dNTP and 1×buffer in 20 µl for 60 min at 42 °C. Then 2 µl reverse transcription products were used for PCR. In a total of 20 µl reactive mixture, 5 pmol/L sense primer and 5 pmol/L antisense primer, 0.25 mmol/L of each dNTP, 1×reaction buffer and 1.5 unit Taq polymerase were mixed. The reaction was run for 33 cycles, and each consisted of denaturation at 94 °C for 60 s, annealing at 58 °C for 60 s, extension at 72 °C for 60 s and final extension prolonged for 7 min at 72 °C. PCR-amplified products (8 µl each) were analyzed on 1.5% agarose gels after ethidium bromide staining. Expression levels of Bid, Bax and Bcl-2 were quantitated using Quantity One quantitation software (Bio-Rad Laboratories) and were reported to be normalized to β-actin levels.

Statistical analysis

All data were presented as means ± standard error. Differences in means were examined by ANOVA, and correlations were analyzed by using Spearman's rank correlation coefficient (SPSS 10.0 for Windows). A *P* value < 0.05 was considered significant.

RESULTS

Effect of *H pylori* on expressions of Bid, Bax and Bcl-2 mRNA

In gastric adenocarcinoma tissues, expressions of Bid and Bax mRNA in *H pylori* negative group, *cagA*⁻ *H pylori* infection group and *cagA*⁺ *H pylori* infection group increased in an ascending pattern, respectively (*P* < 0.05). Expression of Bcl-2 in *H pylori* negative group was significantly lower than that in *H pylori* infection group (*P* < 0.05). Levels of Bcl-2 mRNA between *cagA*⁻ *H pylori* infection group and *cagA*⁺ *H pylori* infection group did not show any significant difference.

In resection margin tissues, expressions of Bid, Bax and Bcl-2 mRNA in *H pylori* negative group, *cagA*⁻ *H pylori* infection group and *cagA*⁺ *H pylori* infection group increased in turn (*P* < 0.05) (Figure 1, Tables 1-3).

Table 1 Effect of *H pylori* infection on expression of Bid

	Adenocarcinoma	Resection margin
<i>H pylori</i> (-)	0.304±0.113	0.377±0.119
<i>H pylori</i> (+) <i>cagA</i> (-)	0.422±0.149 ^a	0.686±0.285 ^a
<i>H pylori</i> (+) <i>cagA</i> (+)	0.855±0.305 ^{ac}	0.939±0.383 ^{ac}

^a*P* < 0.05, vs *H pylori* negative group, ^c*P* < 0.05, vs *cagA*⁻ *H pylori* infection group.

Table 2 Effect of *H pylori* infection on expression of Bax

	Adenocarcinoma	Resection margin
<i>H pylori</i> (-)	0.309±0.123	0.353±0.139
<i>H pylori</i> (+) <i>cagA</i> (-)	0.650±0.393 ^a	0.645±0.327 ^a
<i>H pylori</i> (+) <i>cagA</i> (+)	0.979±0.375 ^{ac}	1.001±0.361 ^{ac}

^a*P* < 0.05, vs *H pylori* negative group, ^c*P* < 0.05, vs *cagA*⁻ *H pylori* infection group.

Table 3 Effect of *H pylori* infection on expression of Bcl-2

	Adenocarcinoma	Resection margin
<i>H pylori</i> (-)	0.411±0.132	0.371±0.153
<i>H pylori</i> (+) <i>cagA</i> (-)	0.696±0.318 ^a	0.487±0.241 ^a
<i>H pylori</i> (+) <i>cagA</i> (+)	0.849±0.352 ^a	0.619±0.243 ^{ac}

^a*P* < 0.05, vs *H pylori* negative group, ^c*P* < 0.05, vs *cagA*⁻ *H pylori* infection group.

Correlation among levels of Bid, Bax and Bcl-2 mRNA

In *H pylori* negative group, levels of Bid and Bax mRNA correlated negatively with that of Bcl-2 in gastric adenocarcinoma tissues (Bid vs Bcl-2, *r* = -0.409, *P* < 0.05; Bax vs Bcl-2, *r* = -0.451, *P* < 0.05). In *H pylori* positive group, expressions of Bid and Bax did not correlate with that of Bcl-2 in adenocarcinoma tissues (Bid vs Bcl-2, *r* = 0.187, *P* > 0.05; Bax vs Bcl-2, *r* = 0.201, *P* > 0.05), but correlated positively with that of Bcl-2 respectively in resection margin tissues (Bid vs Bcl-2, *r* = 0.331, *P* < 0.05; Bax vs Bcl-2, *r* = 0.295, *P* < 0.05).

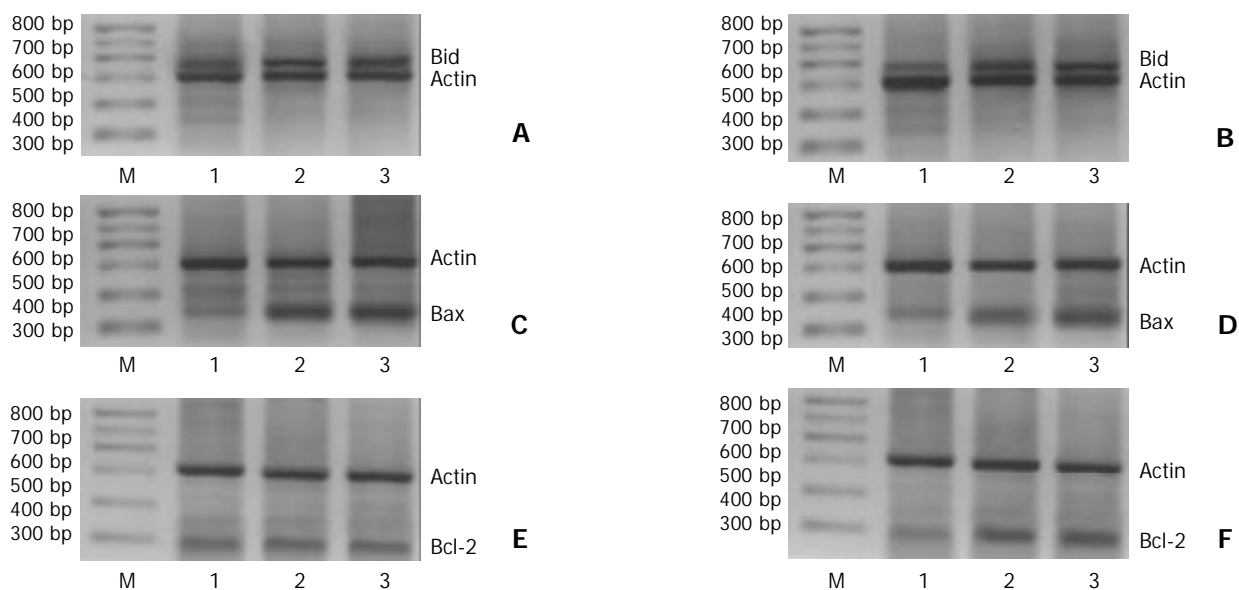


Figure 1 Effect of *H pylori* infection on mRNA expressions of Bcl-2 family members in gastric adenocarcinoma and resection margin tissues. A: Expression of Bid in gastric adenocarcinoma, B: Expression of Bid in resection margin, C: Expression of Bax in gastric adenocarcinoma, D: Expression of Bax in resection margin, E: Expression of Bcl-2 in gastric adenocarcinoma, F: Expression of Bcl-2 in resection margin, 1: *H pylori* negative group, 2: *cagA*⁻ *H pylori* group, 3: *cagA*⁺ *H pylori* group.

DISCUSSION

Bid, Bax and Bcl-2 are representative members of Bcl-2 family. Bid and Bax are pro-apoptosis members. Bcl-2 is an anti-apoptosis member. In the mechanism of regulating apoptosis, Bid as a BH3 domain protein, is one of the initiators to apoptosis and Bax is the key member. Either Bid or Bcl-2 must rely on Bax to induce or inhibit apoptosis^[39-43].

Studies have shown that *H pylori* infection could induce Fas antigen (Fas Ag) expression in gastric epithelial cells^[44]. In addition, *H pylori* infection was also associated with increased mucosal inflammatory cytokines, including TNF- α ^[45] and IFN- γ ^[46]. The cytokines generated during the immune response to *H pylori* also increased expression of Fas Ag in gastric cell lines^[47]. Fas Ag, after binding specifically to its ligand (Fas L), trimerizes and activates Caspase-8. Activation of Caspase-8 could result in the cleavage of cytosolic Bid to truncate tBID, which could translocate to mitochondria and initiate apoptosis^[48]. Shibayama et al^[31] found that *H pylori* infection induced the activation of Caspase-8 and the expression of Bid in human gastric epithelial cells, and inhibition of Caspase-8 suppressed the expression of Bid. In the present study, we found that *H pylori* infection upregulated expression of Bid mRNA in both gastric adenocarcinoma and resection margin tissues. That might be due to the upregulation of Fas and the activation of Caspase-8.

Bax is a cytosolic protein and translocates from the cytosol to the mitochondria for integration into the membrane following a proapoptotic stimulus. This action then results in cytochrome C release and initiates apoptosis. We have previously demonstrated that *H pylori* infection could promote Bax protein expression in chronic gastritis and premalignant lesions. Expression of Bax correlated positively with apoptotic index. The apoptotic index in Bax expression positive group in intestinal metaplasia, gastric dysplasia and gastric carcinoma was significantly higher than that in Bax negative group. In the present study, we found *H pylori* infection also increased levels of Bax mRNA in both gastric adenocarcinoma and resection margin tissues, and the effect was stronger in CagA⁺ *H pylori* group than cagA⁻ *H pylori* group. These results showed *H pylori* infection might promote apoptosis in gastric adenocarcinoma and its resection margin tissues.

Bcl-2 is an important anti-apoptosis protein. We found that Bcl-2 mRNA levels in *H pylori* negative group in gastric adenocarcinoma tissues were lower than in *H pylori* positive group. In resection margin tissues, Bcl-2 mRNA levels in *H pylori* negative group, cagA⁻ *H pylori* infection group and cagA⁺ *H pylori* infection group respectively increased in turn, suggesting that *H pylori* might promote expression of Bcl-2 in both gastric adenocarcinoma and resection margin tissues.

Although *H pylori* could promote expressions of Bid, Bax and Bcl-2, the correlations among them are still unclear. In the present study, it showed that levels of Bid and Bax mRNA were correlated negatively with that of Bcl-2 in gastric adenocarcinoma tissues without *H pylori* infection. This result is correspondent with the findings that apoptosis decreases in tumor tissues. In *H pylori* positive group, levels of Bid, Bax and Bcl-2 mRNA in gastric adenocarcinoma all increased. Besides, levels of Bid, Bax, and Bcl-2 did not correlate with each other. In the resection margin tissues, levels of Bid and Bax mRNA were correlated positively with that of Bcl-2. These results indicated that although *H pylori* could promote expressions of Bid, Bax and Bcl-2, it might play a different role in the development of gastric adenocarcinoma. In benign gastric lesions, *H pylori* infection might mainly upregulate expressions of pro-apoptotic genes such as Bid and Bax, and this effect might be stronger than its upregulatory effect on Bcl-2, which is consistent with the phenomena that *H pylori* infection increases apoptosis in atrophic gastritis and gastric

ulcer. During development of gastric adenocarcinoma, upregulatory effect of *H pylori* on anti-apoptotic genes, for example Bcl-2, might increase gradually and counteract pro-apoptosis effect of Bid and Bax, which may induce or worsen deregulation of apoptosis-associated genes expressions during the course of the formation of gastric adenocarcinoma.

Recently, it was found that not only excessive proliferation played an important role in gastric adenocarcinoma, but also reduction of apoptosis contributed to the carcinogenesis of gastric mucosa. The abnormal expressions of Bid, Bax and Bcl-2 induced by *H pylori* might result in inhibition of apoptosis, which may play an important role during development of gastric adenocarcinoma induced by *H pylori*^[49]. The detailed mechanism still remains to be studied.

REFERENCES

- 1 Jones RG, Trowbridge DB, Go MF. *Helicobacter pylori* infection in peptic ulcer disease and gastric malignancy. *Front Biosci* 2001; **6**: E213-226
- 2 Parsonnet J, Hansen S, Rodriguez L, Gelb AB, Warnke RA, Jellum E, Orentreich N, Vogelstein JH, Friedman GD. *Helicobacter pylori* infection and gastric lymphoma. *N Engl J Med* 1994; **330**: 1267-1271
- 3 Huang JQ, Sridhar S, Chen Y, Hunt RH. Meta-analysis of the relationship between *Helicobacter pylori* seropositivity and gastric cancer. *Gastroenterology* 1998; **114**: 1169-1179
- 4 Matsukura N. Relation between *Helicobacter pylori* and diseases: knowledge for clinician. *J Nippon Med Sch* 2002; **69**: 200-204
- 5 Miwa H, Go MF, Sato N. *H pylori* and gastric cancer: the Asian enigma. *Am J Gastroenterol* 2002; **97**: 1106-1112
- 6 Lan J, Xiong YY, Lin YX, Wang BC, Gong LL, Xu HS, Guo GS. *Helicobacter pylori* infection generated gastric cancer through p53-Rb tumor-suppressor system mutation and telomerase reactivation. *World J Gastroenterol* 2003; **9**: 54-58
- 7 Gao HJ, Yu LZ, Bai JF, Peng YS, Sun G, Zhao HL, Miu K, Lü XZ, Zhang XY, Zhao ZQ. Multiple genetic alterations and behavior of cellular biology in gastric cancer and other gastric mucosal lesions: *H pylori* infection, histological types and staging. *World J Gastroenterol* 2000; **6**: 848-854
- 8 Wang RT, Wang T, Chen K, Wang JY, Zhang JP, Lin SR, Zhu YM, Zhang WM, Cao YX, Zhu CW, Yu H, Cong YJ, Zheng S, Wu BQ. *Helicobacter pylori* infection and gastric cancer: evidence from a retrospective cohort study and nested case-control study in China. *World J Gastroenterol* 2002; **8**: 1103-1107
- 9 Xue FB, Xu YY, Wan Y, Pan BR, Ren J, Fan DM. Association of *H pylori* infection with gastric carcinoma: a Meta analysis. *World J Gastroenterol* 2001; **7**: 801-804
- 10 Cai L, Yu SZ, Zhang ZF. *Helicobacter pylori* infection and risk of gastric cancer in Changle County, Fujian Province, China. *World J Gastroenterol* 2000; **6**: 374-376
- 11 Zhang ZW, Farthing MJ. Molecular mechanisms of *H pylori* associated gastric carcinogenesis. *World J Gastroenterol* 1999; **5**: 369-374
- 12 Hu GY, Yu BP, Dong WG, Li MQ, Yu JP, Luo HS, Rang ZX. Expression of TFF2 and *Helicobacter pylori* infection in carcinogenesis of gastric mucosa. *World J Gastroenterol* 2003; **9**: 910-914
- 13 Yang YL, Xu B, Song YG, Zhang WD. Overexpression of c-fos in *Helicobacter pylori*-induced gastric precancerosis of Mongolian gerbil. *World J Gastroenterol* 2003; **9**: 521-524
- 14 Guo XL, Wang LE, Du SY, Fan CL, Li L, Wang P, Yuan Y. Association of cyclooxygenase-2 expression with Hp-cagA infection in gastric cancer. *World J Gastroenterol* 2003; **9**: 246-249
- 15 Schistosomes, liver flukes and *Helicobacter pylori*. IARC working Group on the Evaluation of Carcinogenic Risks to Humans. Lyon, 7-14 June 1994. *IARC Monogr Eval Carcinog Risks Hum* 1994; **61**: 1-241
- 16 Jang TJ, Kim JR. Proliferation and apoptosis in gastric epithelial cells of patients infected with *Helicobacter pylori*. *J Gastroenterol* 2000; **35**: 265-271
- 17 Chan AO, Wong BC, Lam SK. Gastric cancer: past, present and future. *Can J Gastroenterol* 2001; **15**: 469-474
- 18 Liu HF, Liu WW, Fang DC, Men RP. Expression and significance of proapoptotic gene Bax in gastric carcinoma. *World J Gastroenterol* 1999; **5**: 15-17

- 19 **Liu HF**, Liu WW, Fang DC, Liu FX, He GY. Clinical significance of Fas antigen expression in gastric carcinoma. *World J Gastroenterol* 1999; **5**: 90-91
- 20 **Maeda S**, Yoshida H, Mitsuno Hirata Y, Ogura K, Shiratori Y, Omata M. Analysis of apoptotic and antiapoptotic signalling pathways induced by *Helicobacter pylori*. *Gut* 2002; **50**: 771-778
- 21 **Wu YL**, Sun B, Zhang XJ, Wang SN, He HY, Qiao MM, Zhong J, Xu JY. Growth inhibition and apoptosis induction of Sulindac on Human gastric cancer cells. *World J Gastroenterol* 2001; **7**: 796-800
- 22 **Hamajima N**, Matuo K, Watanabe Y, Suzuki T, Nakamura T, Matsuura A, Yamao K, Ohashi K, Tominaga S. A pilot study to evaluate stomach cancer risk reduction by *Helicobacter pylori* eradication. *Am J Gastroenterol* 2002; **97**: 764-765
- 23 **Kodama M**, Fujioka T, Kodama R, Takahashi K, Kubota T, Murakami K, Nasu M. p53 expression in gastric mucosa with *Helicobacter pylori* infection. *J Gastroenterol Hepatol* 1998; **13**: 215-219
- 24 **Zhu GH**, Yang XL, Lai KC, Ching CK, Wong BC, Yuen ST, Ho J, Lam SK. Nonsteroidal antiinflammatory drugs could reverse *Helicobacter pylori*-induced apoptosis and proliferation in gastric epithelial cells. *Dig Dis Sci* 1998; **43**: 1957-1963
- 25 **Kohda K**, Tanaka K, Aiba Y, Yasuda M, Miwa T, Koga Y. Role of apoptosis induced by *Helicobacter pylori* infection in the development of duodenal ulcer. *Gut* 1999; **44**: 456-462
- 26 **Konturek PC**, Pierzchalski P, Konturek SJ, Meixner H, Faller G, Kirchner T, Hahn EG. *Helicobacter pylori* induces apoptosis in gastric mucosa through an upregulation of Bax expression in humans. *Scand J Gastroenterol* 1999; **34**: 375-383
- 27 **Fan X**, Crowe SE, Behar S, Gunasena H, Ye G, Haeberle H, Van Houten N, Gourley WK, Ernst PB, Reyes VE. The effect of class II major histocompatibility complex expression on adherence of *Helicobacter pylori* and induction of apoptosis in gastric epithelial cells: a mechanism for T helper cell type 1-mediated damage. *J Exp Med* 1998; **187**: 1659-1669
- 28 **Anti M**, Armuzzi A, Iascone E, Valenti A, Lippi ME, Covino M, Vecchio FM, Pierconti F, Buzzi A, Pignataro G, Bonvicini F, Gasbarrini G. Epithelial-cell apoptosis and proliferation in *Helicobacter pylori*-related chronic gastritis. *Ital J Gastroenterol Hepatol* 1998; **30**: 153-159
- 29 **Watanabe S**, Takagi A, Koga Y, Kamiya S, Miwa T. *Helicobacter pylori* induces apoptosis in gastric epithelial cells through inducible nitric oxide. *J Gastroenterol Hepatol* 2000; **15**: 168-174
- 30 **Takagi A**, Watanabe S, Igarashi M, Koike J, Hasumi K, Deguchi R, Koga Y, Miwa T. The effect of *Helicobacter pylori* on cell proliferation and apoptosis in gastric epithelial cell lines. *Aliment Pharmacol Ther* 2000; **14**(Suppl 1): 188-192
- 31 **Shibayama K**, Doi Y, Shibata N, Yagi T, Nada T, Inuma Y, Arakawa Y. Apoptotic signaling pathway activated by *Helicobacter pylori* infection and increase of apoptosis-inducing activity under serum-starved conditions. *Infect Immun* 2001; **69**: 3181-3189
- 32 **Igarashi M**, Kitada Y, Yoshiyama H, Takagi A, Miwa T, Koga Y. Ammonia as an accelerator of tumor necrosis factor alpha-induced apoptosis of gastric epithelial cells in *Helicobacter pylori* infection. *Infect Immun* 2001; **69**: 816-821
- 33 **Xia HH**, Talley NJ. Apoptosis in gastric epithelium induced by *Helicobacter pylori* infection: implications in gastric carcinogenesis. *Am J Gastroenterol* 2001; **96**: 16-26
- 34 **Puthalakath H**, Strasser A. Keeping killers on a tight leash: transcriptional and post-translational control of the pro-apoptotic activity of BH3-only proteins. *Cell Death Differ* 2002; **9**: 505-512
- 35 **Adams JM**, Cory S. The Bcl-2 protein family: arbiters of cell survival. *Science* 1998; **281**: 1322-1326
- 36 **Gross A**, McDonnell JM, Korsmeyer SJ. BCL-2 family members and the mitochondria in apoptosis. *Genes Dev* 1999; **13**: 1899-1911
- 37 **Lee EH**, Wan XH, Song J, Kang JJ, Cho JW, Seo KY, Lee JH. Lens epithelial cell death and reduction of anti-apoptotic protein Bcl-2 in human anterior polar cataracts. *Mol Vis* 2002; **8**: 235-240
- 38 **Tafani M**, Karpinich NO, Hurster KA, Pastorino JG, Schneider T, Russo MA, Farber JL. Cytochrome c release upon Fas receptor activation depends on translocation of full-length bid and the induction of the mitochondrial permeability transition. *J Biol Chem* 2002; **277**: 10073-10082
- 39 **Zong WX**, Lindsten T, Ross AJ, MacGregor GR, Thompson CB. BH3-only proteins that bind pro-survival Bcl-2 family members fail to induce apoptosis in the absence of Bax and Bak. *Genes Dev* 2001; **15**: 1481-1486
- 40 **Letai A**, Bassik MC, Walensky LD, Sorcinelli MD, Weiler S, Korsmeyer SJ. Distinct BH3 domains either sensitize or activate mitochondrial apoptosis, serving as prototype cancer therapeutics. *Cancer Cell* 2002; **2**: 183-192
- 41 **Theodorakis P**, Lomonosova E, Chinnadurai G. Critical requirement of BAX for manifestation of apoptosis induced by multiple stimuli in human epithelial cancer cells. *Cancer Res* 2002; **62**: 3373-3376
- 42 **Cheng EH**, Wei MC, Weiler S, Flavell RA, Mak TW, Lindsten T, Korsmeyer SJ. BCL-2, BCL-X(L) sequester BH3 domain-only molecules preventing BAX- and BAK-mediated mitochondrial apoptosis. *Mol Cell* 2001; **8**: 705-711
- 43 **Shangary S**, Johnson DE. Peptides derived from BH3 domains of Bcl-2 family members: a comparative analysis of inhibition of Bcl-2, Bcl-x(L) and Bax oligomerization, induction of cytochrome c release, and activation of cell death. *Biochemistry* 2002; **41**: 9485-9495
- 44 **Houghton J**, Macera-Bloch LS, Harrison L, Kim KH, Korah RM. Tumor necrosis factor alpha and interleukin 1beta up-regulate gastric mucosal Fas antigen expression in *Helicobacter pylori* infection. *Infect Immun* 2000; **68**: 1189-1195
- 45 **D'Elia MM**, Manghetti M, De Carli M, Costa F, Baldari CT, Burrioni D, Telford JL, Romagnani S, Del Prete G. T helper 1 effector cells specific for *Helicobacter pylori* in the gastric antrum of patients with peptic ulcer disease. *J Immunol* 1997; **158**: 962-967
- 46 **Harris PR**, Mobley HL, Perez-Perez GI, Blaser MJ, Smith PD. *Helicobacter pylori* urease is a potent stimulus of mononuclear phagocyte activation and inflammatory cytokine production. *Gastroenterology* 1996; **111**: 419-425
- 47 **Houghton J**, Korah RM, Condon MR, Kim KH. Apoptosis in *Helicobacter pylori*-associated gastric and duodenal ulcer disease is mediated via the Fas antigen pathway. *Dig Dis Sci* 1999; **44**: 465-478
- 48 **Wei MC**, Lindsten T, Mootha VK, Weiler S, Gross A, Ashiya M, Thompson CB, Korsmeyer SJ. tBID, a membrane-targeted death ligand, oligomerizes BAK to release cytochrome c. *Genes Dev* 2000; **14**: 2060-2071
- 49 **Konturek PC**, Konturek SJ, Pierzchalski P, Bielanski W, Duda A, Marlicz K, Starzynska T, Hahn EG. Cancerogenesis in *Helicobacter pylori* infected stomach—role of growth factors, apoptosis and cyclooxygenases. *Med Sci Monit* 2001; **7**: 1092-1107

Chinese literature associated with diagnosis of *Helicobacter pylori*

Yi Wan, Yong-Yong Xu, Jian-Hui Jiang, Fan-Shu Kong, Fu-Bo Xue, Yu-Xiang Bai, Bo-Rong Pan, Jun Ren, Dai-Ming Fan

Yi Wan, Yong-Yong Xu, Jian-Hui Jiang, Fu-Bo Xue, Yu-Xiang Bai, Department of Health Statistics, Fourth Military Medical University, Xi'an 710032, Shaanxi Province, China

Fan-Shu Kong, Department of Postgraduate, Fourth Military Medical University, Xi'an 710032, Shaanxi Province, China

Bo-Rong Pan, Jun Ren, Department of Oncology of Xijing Hospital, Fourth Military Medical University, Xi'an 710032, Shaanxi Province, China

Dai-Ming Fan, Department of Gastroenterology of Xijing Hospital, Fourth Military Medical University, Xi'an 710032, Shaanxi Province, China

Supported by the National Natural Science Foundation of China, No. 30024002 and the University Key Teachers Fund of Ministry of Education of China, No. 2000-65

Correspondence to: Dai-Ming Fan, Department of Gastroenterology of Xijing Hospital, Fourth Military Medical University, Xi'an 710032, Shaanxi Province, China. fandaim@fmmu.edu.cn

Telephone: +86-29-3375221 **Fax:** +86-29-2539041

Received: 2003-06-16 **Accepted:** 2003-08-28

Abstract

AIM: To synthetically analyze and probe into the diagnosis of *H pylori* infection, we followed the principles of evidence-based medicine.

METHODS: A total of 22 papers of prevalence survey and case-control studies were selected for studying about diadynamic methods. Using meta-analysis, we analyzed the different diadynamic methods of *H pylori* in China.

RESULTS: Through meta-analysis, among the five diadynamic methods, the accuracy of polymerase chain reaction (PCR) was the highest (98.47%) and PCR was the most sensitive method (*Sp*: 99.03%).

CONCLUSION: Among the five diadynamic methods, the accuracy of PCR is the highest and PCR is the most sensitive method to diagnose the infection of *H pylori*.

Wan Y, Xu YY, Jiang JH, Kong FS, Xue FB, Bai YX, Pan BR, Ren J, Fan DM. Chinese literature associated with diagnosis of *Helicobacter pylori*. *World J Gastroenterol* 2004; 10(2): 231-233 <http://www.wjgnet.com/1007-9327/10/231.asp>

INTRODUCTION

Since *Helicobacter pylori* (*H pylori*) was first isolated in 1982,

the association of *H pylori* and related diseases has become the hot spot of gastroenterological studies. The distribution of *H pylori* infection is worldwide, and the prevalence rate of *H pylori* among populations is very high. With the deepening of *H pylori* researches, studies about *H pylori*, which aimed at effectively controlling the infection, were of great significance in preventing and curing the chronic stomach troubles. Because of the independence of each study and limit to the region and sample source, a great majority of studies did not have enough evidence and totally unanimous conclusion, which influenced the reliability of the conclusion. However, meta-analysis method could appraise and analyze synthetically the results of study with the same research purpose^[1], thus improving the efficiency of statistics, solving the problem with inconsistent results of studies, and making the conclusion of study more reliable. Therefore, we used meta-analysis to analyze synthetically the results of studies associated with *H pylori* diagnosis so as to express them more accurately.

MATERIALS AND METHODS

Literature selection and data

A Chinese biology and medicine database (CBM) search of non-review articles since 1995 was performed with the MeSH headings "*Helicobacter pylori*", "diagnosis", "polymerase chain reaction", "enzyme-linked immunosorbent assay" and "urea enzymes test".

Standard of selection The research objects were the population who could possibly suffer from *H pylori*, and the results of study had intact statistics.

***H pylori*-positive result judgment** *H pylori* cultivation was positive or one or two of the followings were positive: *H pylori* morphology (smear, histology or immunohistochemistry), urea enzyme test (RUT, ¹³C or ¹⁴C-urea breath test), PCR detection, serologic test (ELISA or immunoblotting test, etc.).

Standard of rejection The sample size was too small for statistical study, children less than one year old who possibly carried mother's antibody, studies without definite detection of *H pylori* or strict quality control.

Study on diadynamic methods of *H pylori* The literature search result were classified as follows. Twenty-two reports^[2-23] appraised synthetically according to 5 commonly used clinical diagnostic methods, the evaluation targets included sensitivity (*Se*), specificity (*Sp*) and accuracy (π). Bibliographic retrieval results of ¹³C-urea breath test, ¹⁴C-urea breath test, ELISA, RUT and PCR are shown in Tables 1-5.

Table 1 Related literature of ¹³C-urea breath test

Study No. (i)	<i>H pylori</i> positive		<i>H pylori</i> negative		<i>Se</i> (%)	<i>Sp</i> (%)	π (%)	<i>PV</i> (%)	<i>PV</i> ₊ (%)
	a	c	b	d					
1	36	0	0	24	100	98.50	99.40	100	100
2	148	5	0	165	96.70	100	98.41	97.06	100
3	13	0	1	23	100	95.83	97.41	100	92.86
4	39	3	0	10	92.86	100	94.23	76.92	100
5	42	0	0	10	100	96.97	99.42	100	100
6	52	2	3	13	96.30	81.25	92.86	94.55	86.67
7	47	1	0	32	97.92	100	98.75	97.14	100
8	147	3	0	3	98	90.70	97.86	96.10	95.30
9	74	3	0	49	96	100	97.56	94.23	100

Table 2 Related literature of ¹⁴C-urea breath test

Study No. (i)	<i>H pylori</i> positive		<i>H pylori</i> negative		Se (%)	Sp (%)	π (%)	PV. (%)	PV ₊ (%)
	a	c	b	d					
1	81	2	2	52	97.06	96.12	96.69	95.12	97.06
2	52	5	0	23	91.23	100	93.73	82.14	100
3	51	1	2	16	97.36	88.89	95.47	97.36	96.23
4	56	3	1	59	94.92	98.33	96.61	95.16	98.25
5	83	0	3	75	100	96.15	98.35	100	96.51
6	78	5	2	76	93.98	97.44	95.65	93.83	97.50
7	79	4	2	76	95.18	97.44	96.27	95	97.53

Table 3 Related literature of ELISA

Study No. (i)	<i>H pylori</i> positive		<i>H pylori</i> negative		Se (%)	Sp (%)	π (%)	PV. (%)	PV ₊ (%)
	a	c	b	d					
1	85	11	2	38	88.54	95	90.41	77.55	97.70
2	55	2	2	26	96.49	92.86	95.25	92.86	96.49
3	38	6	2	13	86.36	86.67	86.44	68.42	95
4	43	1	1	14	97.37	93.33	96.34	93.33	97.73
5	37	7	4	11	84.09	73.33	81.35	61.11	90.24
6	64	2	2	15	96.97	88.23	95.18	88.24	96.97
7	44	0	3	12	100	80	94.92	100	93.62

Table 4 Related literature of RUT

Study No. (i)	<i>H pylori</i> positive		<i>H pylori</i> negative		Se (%)	Sp (%)	π (%)	PV. (%)	PV ₊ (%)
	a	c	b	d					
1	34	2	0	24	94.44	100	96.64	92.31	100
2	32	10	0	10	76.19	100	80.77	50	100
3	38	4	1	9	89.74	90.91	89.97	69.23	97.44
4	30	2	2	17	93.75	89.47	92.16	89.74	93.75
5	55	4	7	53	93.22	88.33	90.73	92.98	88.71
6	62	4	4	13	93.94	76.47	90.36	76.47	93.94
7	46	8	4	12	85.52	75	83.12	60	92
8	151	50	11	47	75.12	81.03	76.35	48.45	93.21
9	171	30	7	51	85.07	87.93	85.84	62.96	96.07
10	72	15	0	63	82.76	100	90.02	80.77	100
11	227	22	6	29	91.16	82.86	90.05	56.86	97.42
12	73	14	0	63	83.91	100	90.66	81.82	100
13	58	7	1	30	89.23	96.77	91.65	81.08	98.31
14	34	0	7	28	100	80	89.86	100	82.93
15	64	15	3	13	81.01	81.25	81.05	46.43	95.52

Table 5 Related literature of PCR

Study No. (i)	<i>H pylori</i> positive		<i>H pylori</i> negative		Se (%)	Sp (%)	π (%)	PV. (%)	PV ₊ (%)
	a	c	b	d					
1	178	0	0	98	100	100	100	100	100
2	32	0	5	14	100	73.68	90.19	100	86.49
3	34	0	1	34	100	97.14	98.53	100	97.14
4	34	2	1	34	94.44	97.14	95.73	94.44	97.14
5	149	0	0	10	100	100	100	100	100
6	77	2	2	14	97.47	87.50	95.82	87.50	97.47

Methods

In the statistical analysis of data, Meta-analysis method with a fixed effect model and a random effect model was used to reach an integrated conclusion^[24-26].

RESULTS

Among the five diadynamic methods, the accuracy of PCR was the highest and PCR was the most sensitive method, specificity of ¹³C-urea breath test was the highest, the sensitivity and accuracy of RUT were the lowest, specificity of ELISA

was the lowest (Table 6).

Table 6 Synthetic evaluation of five diadynamic methods

Diadynamic methods	Se (%)	Sp (%)	π (%)
¹³ C-urea breath test	99.34	95.09	97.78
¹⁴ C-urea breath test	97.56	94.96	96.40
ELISA	93.96	81.78	90.09
PCR	98.25	99.03	98.47
RUT	95.58	71.19	87.02

DISCUSSION

This study used bibliographic retrieval to collect the relevant materials of *H pylori* infection, and meta-analysis, including combination of statistics in many studies by weight and equalized test, to analyze the diagnosis of *H pylori* infection.

The five diadynamic methods of *H pylori* infection all had a high sensitivity, specificity and accuracy, among which PCR was most sensitive and accurate. ¹³C-urea breath test was the most specific. As an ideal diadynamic method, it should have the following advantages: a high sensitivity and specificity, minimal incursions into or no damage to patients, simple and convenient in manipulation, less sophisticated technique or equipment, low cost and easy acceptance by patients. However, in fact, it is difficult for one diadynamic method to possess all these qualities. Above all, among the five diadynamic methods of *H pylori* infection, ELISA is the most convenient, which has the lowest cost and damage, therefore, serological positivity can merely explain the situation of whether patients have been infected or being infected. ¹³C-urea breath test has no harm, and can provide the whole infection information of stomach, which is relatively ideal, but it is difficult to popularize for the need of equipments and high expense. Although ¹⁴C-urea breath test can be done by well-equipped hospital and has lower cost than ¹³C-urea breath test, it has some radioactivity risk. RUT belongs to indirect test, whose intensity is determined by bacterial density of biopsy specimen. PCR is more sensitive than other methods. PCR can also detect *H pylori*, which cannot be detected by other methods, and at present it has been widely used in detection of various kinds of clinical specimens^[27]. So which diadynamic methods would be adopted in clinical detection must be determined according to the specific situation and different requirements^[28-32].

H pylori infection is common and study of *H pylori* infection involves a wide extent. A large number of researches and works on this aspect have been done in China, and have achieved a great progress, although some problems were found in these studies such as flaw in experimental design, scattered data, deficiency of objective and reliable conclusion. Therefore, many aspects of *H pylori* infection are still to be studied to obtain accurate and consummate results.

REFERENCES

- Schweitzer IL**, Dun AEG, Peters RL, Spears RL. Viral hepatitis B in neonates and infants. *Am J Med* 1973; **55**: 762-771
- Zhu RM**, Lu YK, Wang L. Analysis on antibodies of *Helicobacter pylori* in serum and saliva. *Zhonghua Xiaohua Zazhi* 1997; **17**: 342-344
- Xie Y**, Wang CW, Zhu JQ, Zhang KH. IgA to *Helicobacter pylori* in gastric juice and its clinical significance. *Zhonghua Weishengwuxue He Mianyixue Zazhi* 1997; **17**: 430-432
- Lu YK**, Xu GM, Zhou ZQ, Zhang HF. Purification of the specific antigens of *Helicobacter pylori* for semiquantitative serodiagnosis. *Dier Junyi Daxue Xuebao* 1997; **18**: 449-451
- Chen JP**, Xu CP, Cheng SJ, Xu QW, Liu FX, Wang ZH, Fuang DC, Guao PH. Microdose capsule-based ¹⁴C-urea breath test for the diagnosis of *Helicobacter pylori* infection. *Disan Junyi Daxue Xuebao* 1997; **19**: 317-320
- Qu HT**, Fang ZH, Liu Y, Yang XL. A modified PCR assay for detection of *Helicobacter pylori* in gastric biopsy specimens. *Zhonghua Xiaohua Neijing Zazhi* 1997; **14**: 207-210
- Xu CP**, Xu H, Cheng SJ, Xu QW, Liu FX, Wang ZH. ¹⁴C-urea breath test in the diagnosis of *Helicobacter pylori* infection in the stomach. *Zhonghua Neike Zazhi* 1995; **34**: 239-242
- Zhang WQ**, You JF, Hu B, Xiang ZQ, Xu CD. Reliability of ¹³C-urea breath test in detection of *Helicobacter pylori* infections in children. *Zhonghua Erke Zazhi* 1999; **37**: 484-485
- Kang HZ**, Ma JZ, Shu MJ, Cha JZ, Li BB, Wu YL, Xiang ZQ. ¹³C-urea breath test for the diagnosis of *Helicobacter pylori* infection in pediatric patients. *Linchuang Erke Zazhi* 1999; **17**: 137-140
- Li ZJ**, Zou WM, Jiang T. Evaluation of Salivary anti-*Hp* IgG detection in the diagnosis of *Helicobacter pylori* infection. *Linchuang Neike Zazhi* 1999; **16**: 88-89
- Peng H**, Pan GZ, Cao SZ, Zhao RG. The significance of detection of *Helicobacter pylori* in saliva. *Zhonghua Neike Zazhi* 1999; **38**: 171-173
- Wu LJ**, Zhang WJ, Zhang H, Deng GG. Comparison of three rapid diagnosis of *Helicobacter pylori* infection. *Disan Junyi Daxue Xuebao* 1999; **21**: 301-302
- Shu HJ**, Ge ZZ, Xiang ZQ, Liu Y, Ren WP, Xiao SD. Evaluation of detecting methods of *Helicobacter pylori* infection-histology, serology, ¹³Curea breath test, and Rapid urease tests. *Zhonghua Xiaohua Zazhi* 1998; **18**: 260-262
- Wu SM**, Shi Y, Liu WZ, Zhang DZ, Xiao SD, Xiang ZQ. Reliability of ¹³C-urea breath test (UBT) in detection of *Helicobacter pylori* infection. *Zhonghua Xiaohua Zazhi* 1998; **18**: 263-264
- Wang WH**, Hu FL, Jia BQ, Wang HH. Detection of *Helicobacter pylori* from gastric mucosa by using polymerase chain reaction. *Xin Xiaohuabingxue Zazhi* 1997; **5**: 11-12
- Zhang DR**, Hu GH, Wu F, Xiao SD, Yuan JM, Xiang ZQ. ¹⁴C-urea breath test in diagnosing *Helicobacter pylori* infection. *Shanghai Yixue* 1996; **19**: 373-375
- Huang QD**, Zheng PF, Cheng L, Cheng JX, Zhao L. Evaluation of trace of ¹⁴C-urea breath test in diagnosing *Helicobacter pylori* infection. *Linchuang Neike Zazhi* 1999; **16**: 80-81
- Zhang XY**, Xu SF, Yuan JP, Zhang HJ, Zhao ZQ. Parallel detection of *Helicobacter pylori* infection. *Zhonghua Xiaohua Neijing Zazhi* 1998; **15**: 166-167
- Jiang K**, Pan GZ, Wen SH, Yang XO, Bei L, Jiang J, Zhang CX. Evaluation of diagnostic methods of *Helicobacter pylori* infection. *Zhongguo Shiyong Neike Zazhi* 1998; **18**: 33-34
- Zhang WQ**, You JK, Lu YM, Yao PY, Cao LF, Ying CM, Xiang ZQ, Xiu CD. Comparison of rapid diagnosis of *Helicobacter pylori* infection in pediatric patients. *Linchuang Erke Zazhi* 1999; **17**: 140-141
- Su YQ**, Li CQ. Low dosage ¹³C-urea breath test in detection of *Helicobacter pylori* infection. *Zhongguo Neijing Zazhi* 1996; **2**: 39-41
- Zhu RM**, Lu YK, Wang L. Detection of antibodies of *Helicobacter pylori* in saliva. *Zhonghua Neike Zazhi* 1997; **36**: 469-470
- Zhao R**, Lin SR. Detection of *Helicobacter pylori* from gastric juices by using polymerase chain reaction. *Zhonghua Neike Zazhi* 1998; **37**: 701-702
- Li LS**. Principle and Method for Study in Clinical medicine, Practical Clinical Epidemiology. 1sted. Xi'an. *Shaanxi Kexue Jishu Chubanshe* 2000: 357-372
- Guo ZC**. Yixue Tongjixue. 1sted. Beijing. *Renmin Junyi Chubanshe* 1999: 152-154
- Zhao N**, Yu SZ. The relationship of smoking and lung cancer in china: a Meta analysis. *Zhonghua Liuxingbingxue Zazhi* 1993; **14**: 350-353
- Guo MX**, Xu HJ, Zhao SL, Xiao HM, Hong FZ. Clinical significance of PCR in *Helicobacter pylori* DNA detection in human gastric disorders. *China Natl J New Gastroenterol* 1997; **2**: 98-100
- Liu YB**, Su LY. ¹⁴C-urea breath test to diagnosis *Helicobacter pylori*. *Xuzou Yixueyuan Xuebao* 1998; **18**: 118-119
- Yuan MB**, Liu XF. Laboratory diagnosis of *Helicobacter pylori*. *Yishi Jinxu Zazhi* 2002; **25**: 3-5
- Yan Y**, Qian LS, Wang WF. Research on of rapid diagnosis of *Helicobacter pylori*. *Fudan Xuebao* 2002; **29**: 410-413
- Lin H**, Zheng DZ, Ye HQ, Wei L, Wang QG, Tang FK. Comparison of five detection methods for *Helicobacter pylori*. *Haixia Yufang Yixue Zazhi* 2001; **7**: 38-39
- Li XB**, Liu WZ, Ge ZZ, Ran ZH, Chen XY, Xiu WW, Xiao SD. Evaluate of normal diagnosis of *Helicobacter pylori*. *Zhonghua Xiaohua Zazhi* 2002; **22**: 691-693

Stable expression of human cytochrome P450 2D6*10 in HepG2 cells

Jian Zhuge, Ying-Nian Yu, Xiao-Dan Wu

Jian Zhuge, Ying-Nian Yu, Department of Pathology and Pathophysiology, School of Medicine, Zhejiang University, Hangzhou 310031, Zhejiang Province, China

Xiao-Dan Wu, Center of Analysis, Zhejiang University, Hangzhou 310031, Zhejiang Province, China

Supported by National Natural Science Foundation of China, No. 39770868 and Natural Science Foundation of Zhejiang Province, No. 397490

Correspondence to: Professor Ying-Nian Yu, Department of Pathology and Pathophysiology, School of Medicine, Zhejiang University, Hangzhou 310031, Zhejiang Province, China. ynyu@mail.hz.zj.cn
Telephone: +86-571-87217149 **Fax:** +86-571-87217149

Received: 2003-06-26 **Accepted:** 2003-08-16

Abstract

AIM: Over 90% of drugs are metabolized by the cytochrome P-450 (CYP) family of liver isoenzymes. The most important enzymes are CYP1A2, 3A4, 2C9/19, 2D6 and 2E1. Although CYP2D6 accounts for <2% of the total CYP liver enzyme content, it mediates metabolism in almost 25% of drugs. In order to study its enzymatic activity for drug metabolism, its cDNA was cloned and a HepG2 cell line stably expressing CYP2D6 was established.

METHODS: Human *CYP2D6* cDNA was amplified with reverse transcription-polymerase chain reaction (RT-PCR) from total RNA extracted from human liver tissue and cloned into pGEM-T vector. cDNA segment was identified by DNA sequencing and subcloned into a mammalian expression vector pREP9. A cell line was established by transfecting the recombinant plasmid of pREP9-CYP2D6 to hepatoma HepG2 cells. Expression of mRNA was validated by RT-PCR. Enzyme activity of catalyzing dextromethorphan *O*-demethylation in postmitochondrial supernatant (S9) fraction of the cells was determined by high performance liquid chromatography (HPLC).

RESULTS: The cloned cDNA had 4 base differences, e.g. 100 C→T, 336 T→C, 408 C→G and 1 457 G→C, which resulted in P34S, and S486T amino acid substitutions, and two samesense mutations were 112 F and 136 V compared with that reported by Kimura *et al* (GenBank accession number: M33388). P34S and S486T amino acid substitutions were the characteristics of *CYP2D6*10* allele. The relative activity of S9 fraction of HepG2-CYP2D6*10 metabolized dextromethorphan *O*-demethylation was found to be 2.31 ± 0.19 nmol·min⁻¹·mg⁻¹ S9 protein ($n=3$), but was undetectable in parental HepG2 cells.

CONCLUSION: cDNA of human *CYP2D6*10* can be successfully cloned. A cell line, HepG2-CYP2D6*10, expressing CYP2D6*10 mRNA and having metabolic activity, has been established.

Zhuge J, Yu YN, Wu XD. Stable expression of human cytochrome P450 2D6*10 in HepG2 cells. *World J Gastroenterol* 2004; 10 (2): 234-237

<http://www.wjgnet.com/1007-9327/10/234.asp>

INTRODUCTION

Over 90% of drugs are metabolized by the cytochrome P-450 (CYP) family of liver isoenzymes^[1]. The most important enzymes are CYP1A2, 3A4, 2C9/19, 2D6 and 2E1. Although CYP2D6 accounts for <2% of the total CYP liver enzyme content, it mediates metabolism in almost 25% of drugs. Among these are many antipsychotics and antidepressants, beta-blockers, antiarrhythmic agents and opiates^[2,3]. *CYP2D6* exhibits extensive polymorphism. Over 40 *CYP2D6* allelic variants have been discovered^[4] (<http://www.imm.ki.se/CYPalleles/cyp2d6.htm>).

Human CYP1A1^[5], CYP2B6^[5], CYP2A6^[6], CYP3A4^[7], CYP2C9^[8], CYP2C18^[9] and a phase II metabolism enzyme UDP-glucuronosyltransferase, UGT1A9^[10] have been stably expressed in Chinese hamster lung CHL cells in our laboratory. Among the human hepatic cell lines, HepG2 is derived from a human liver tumor and characterized by many xenobiotic-metabolizing activities as compared to fibroblasts. Therefore, HepG2 cell is useful in the prediction of the metabolism and cytotoxicity of chemicals in human liver^[11]. But it does not produce a significant amount of CYP^[12,13]. Yoshitomi *et al*^[14] have established stable expression of a series of human CYP subtypes, e.g. CYP1A1, CYP1A2, CYP2A6, CYP2B6, CYP2C8, CYP2C9, CYP2C19, CYP2D6, CYP2E1 and CYP3A4, respectively in the HepG2 cells.

In this study human *CYP2D6*10* cDNA was amplified with reverse transcription-polymerase chain reaction (RT-PCR), and a cell line stably expressing CYP2D6.10 was established.

MATERIALS AND METHODS

Materials

Restriction endonucleases and Moloney murine leukemia virus (M-MuLV) reverse transcriptase were supplied by MBI Fermentas AB, Lithuania. PCR primers, DNA sequence primers, random hexamer primers and dNTPs were synthesized or supplied by Shanghai Sangon Biotechnology Co. Expand fidelity PCR system and NADPH were from Roche Molecular Biochemicals. DNA sequencing kit was purchased from Perkin-Elmer Co. TRIzol reagent, G418, Dulbecco's modified Eagle's medium (DMEM) and newborn bovine calf sera were from Gibco. Diethyl pyrocarbonate (DEPC), dextromethorphan HBr and dextrophan D-tartrate were purchased from Sigma/RBI. T4 DNA ligase and pGEM-T vector system were from Promega. HPLC solvents and other chemicals were all of the highest grade from commercial sources.

Methods

Cloning of human *CYP2D6* cDNA from human liver Total RNA was extracted from a surgical specimen of human liver with TRIzol reagent according to the manufacture's instructions. RT-PCR amplifications using expand fidelity PCR system were described before. Two specific 28-mer oligonucleotide PCR primers were designed according to the cDNA sequence of *CYP2D6* reported by Kimura *et al*^[15] (GenBank accession no.M33388). The sense primer corresponding to base position -12 to 13 was CYP2D6 F1: 5' -

CTCGAGGCAGGTATGGGGCTAGAAG-3', with a restriction site of *Xho* I, and the anti-sense one, corresponding to the base position from 1 503 to 1 530, was CYP2D6 R1: 5' - GGATCCTGAGCAGGCTGGGGACTAGGTA-3', with a restriction site of *Bam*HI. The anticipated PCR products were 1.543 kb in length. PCR was performed at 94 °C for 5 min, then 35 cycles at 94 °C for 60 s, at 62 °C for 60 s, at 72 °C for 2 min, and a final extension at 72 °C for 10 min. An aliquot (10 µL) from PCR was subjected to electrophoresis in a 1% agarose gel stained with ethidium bromide.

Construction of recombinant pGEM-CYP2D6 and sequencing of CYP2D6 cDNA^[8] The PCR products were ligated with pGEM-T vector, and transformed to *E. coli* DH5α. cDNA of *CYP2D6* cloned in pGEM-T was sequenced by dideoxy chain-termination method marked with BigDye with primers of T7, SP6 promoters and two specific primers of 5' - ACCTCATGAATCACGGCAGT-3' (1 088-1 069), and 5' - CCGTGTCCAACAGGAGA-3' (987-1 003). The termination products were dissolved and detected using an automated DNA sequencer (Perkin-Elmer-ABI Prism 310).

Construction of pREP9 based expression plasmid for CYP2D6^[8] *Xho* I/*Bam*HI fragment having the total span of human *CYP2D6* cDNA in pGEM-CYP2D6 was subcloned to a mammalian expression vector pREP9 (Invitrogen). The recombinant was transformed to *E. coli* Top 10, screened by ampicillin resistant and identified by restriction mapping.

Transfection and selection^[8, 16] HepG2 cells were maintained as monolayer cell cultures at 37 °C in DMEM supplemented with 10% new born calf sera. HepG2 cells were transfected with the resultant recombinant plasmid, pREP9-CYP2D6, using a modified calcium phosphate method. A cell line named HepG2-CYP2D6 was established by selecting in the culture medium containing G418.

RT-PCR assay of CYP2D6 mRNA expression in HepG2-CYP2D6 and HepG2 cells Total RNA was prepared from G-418-resistant clones by TRIzol reagent. RT-PCR was performed as described before^[8], using 200 mmol·L⁻¹ of CYP2D6F1 and CYP2D6R1 primers and 200 mmol·L⁻¹ primers of beta-actin as internal control. The sense and anti-sense primers used for PCR amplification of beta-actin (GenBank accession no. NM_001101) are 5' -TCCCTGGAGAAGAGCTACGA-3' (776-795) and 5' -CAAGAAAGGGTGTACGCAAC-3' (1 217-1 237), respectively. PCR was performed at 94 °C for 2 min, then 35 cycles at 94 °C for 30 s, at 62 °C for 30 s, at 72 °C for 90 s, and a final extension at 72 °C for 7 min. The anticipated beta-actin PCR products were 462 bp in length and that of *CYP2D6* were 1 543 bp in length. An aliquot (10 µL) from PCR was subjected to electrophoresis in a 1.2% agarose gel stained with ethidium bromide.

Preparation of postmitochondrial supernant (S9) of HepG2-CYP2D6 The procedure for the preparation of S9 fraction was described before^[8]. The protein in S9 was determined by Lowry's method, with bovine serum albumin as standard.

Dextromethorphan O-demethylation assays^[17-20] *CYP2D6* dextromethorphan *O*-demethylation activity of S9 was determined by reversed phase high performance liquid chromatography (HPLC). Briefly, incubation reactions were performed in 50 mmol·L⁻¹ potassium phosphate buffer (pH7.4), containing 3 mmol·L⁻¹ MgCl₂, 1 mmol·L⁻¹ EDTA, 40 mmol·L⁻¹ dextromethorphan and 200 µg S9 protein in a final volume of 200 µL. Reactions were initiated by addition of 1 mmol·L⁻¹ NADPH and terminated with 30% acetic acid after incubation for 10 min at 37 °C. Protein was precipitated by centrifugation at 10 000 g for 4 min, and the supernatant was stored at -20 °C for analysis. On HPLC analysis, 10 µL of supernatant was injected into a Water HPLC equipped with a Shimadzu RF-535 fluorescence detector. A CLC phenyl column (15 cm×4.5-mm

i.d.) was used to separate the metabolites. The mobile phase consisted of a mixture of 30% acetonitrile, 1% acetic acid, and 0.05% triethylamine in water. The flow rate through the column at 25 °C was 0.75 ml·min⁻¹. The excitation and emission wavelengths of the fluorescence detector were 285 nm and 310 nm, respectively. The rates of product formation were determined from standard curves prepared by adding varying amounts of dextrophan D-tartrate to incubations conducted without NADPH.

RESULTS

Construction of human CYP2D6*10 cDNA recombinants

The pGEM-CYP2D6 recombinant was constructed by inserting human *CYP2D6* cDNA into the pGEM-T vector. Selection and identification of the recombinant were carried out by *Xho* I/*Bam*HI endonuclease digestion, agarose gel electrophoresis (Figure 1) and DNA sequencing. Compared with the cDNA sequence reported by Kimura *et al.*^[15] (GenBank accession no. M33388), differences were found in 100 C→T, 336 T→C, 408 C→G and 1457 G→C, that result in P34S and S486T amino acid substitutions, and two samesense mutations of 112 F and 136 V.

The *Xho* I/*Bam*HI fragment (1.543 kb) containing the complete *CYP2D6* cDNA was subcloned into the *Xho* I/*Bam*HI site of mammalian expression vector pREP9. Selection and identification of the recombinant were carried out by *Xho* I/*Bam*HI endonuclease digestion and agarose gel electrophoresis (Figure 1). The resulting plasmid was designated as pREP9-CYP2D6 and contained the entire coding region, along with 11 bp of the 5' and 35 bp of the 3' untranslated region of *CYP2D6* cDNA, respectively.

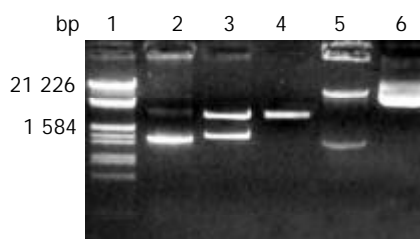


Figure 1 Electrophoresis identification of pGEM-CYP2D6 and pREP9-CYP2D6 recombinants. Lane 1: Marker (λ /*Eco*R I and *Hind* III), 2: PCR products of *CYP2D6* (1.543 kb), 3: Recombinant of pGEM-CYP2D6 digested by *Xho* I and *Bam*HI, 4: pGEM-T vector (3 kb), 5: Recombinant of pREP9-CYP2D6 digested by *Xho* I and *Bam*HI, 6: pREP9 vector (10.5 kb).

Establishment of cell line HepG2-CYP2D6

HepG2 cells were transfected with pREP9-CYP2D6, and selected with G418. The surviving clones were subcultured and the cell line termed HepG2-CYP2D6 was established.

RT-PCR assay of CYP2D6 mRNA expression in HepG2-CYP2D6 cells

CYP2D6 mRNA expression in HepG2-CYP2D6 cells was detected by RT-PCR with CYP2D6F1 and CYP2D6R1 primers. It was easily to identify a 1.5 kb band from HepG2-CYP2D6 cells, but not from HepG2 cells (Figure 2).

Dextromethorphan O-demethylation activity in HepG2-CYP2D6 cells

The dextromethorphan *O*-demethylation activity in S9 of HepG2-CYP2D6 cells was assayed by reverse HPLC. A typical elution profile of metabolites in supernatant was shown (Figure 3). The retention times for dextrophan and dextromethorphan

were 6.5 min and 16.8 min, respectively. The CYP2D6 enzyme activity towards dextromethorphan *O*-demethylation was found to be $2.31 \pm 0.19 \text{ nmol} \cdot \text{min}^{-1} \cdot \text{mg}^{-1}$ S9 protein ($n=3$), but was undetectable in parent HepG2 cells.

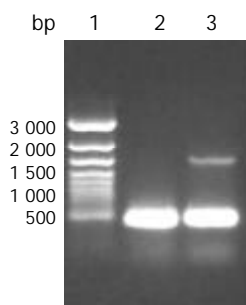


Figure 2 Identification of CYP2D6 mRNA expression in HepG2-CYP2D6 and HepG2 cells by RT-PCR with beta-actin as internal control. Lane 1: 1 kb ladder marker, 2: RT-PCR products of HepG2 cells showing a 462 bp of beta-actin, 3: RT-PCR products of HepG2-CYP2D6 cells showing a 462 bp of beta-actin and 1.5 kb of CYP2D6.

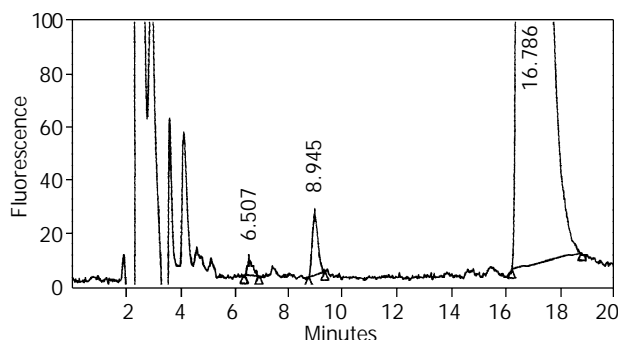


Figure 3 Representative chromatograms of metabolites in supernatant. 10 μL of supernatant was injected into a Water HPLC equipped with a Shimadzu RF-535 fluorescence detector. A CLC phenyl column (15 $\text{cm} \times 4.5\text{-mm}$ i.d.) was used to separate the metabolites. The mobile phase consisted of a mixture of 30% acetonitrile, 1% acetic acid, and 0.05% triethylamine in water. The flow rate through the column at 25 $^{\circ}\text{C}$ was 0.75 $\text{ml} \cdot \text{min}^{-1}$. The excitation and emission wavelengths of the fluorescence detector were 285 nm and 310 nm, respectively. The retention times for dextrophan and dextromethorphan were 6.5 min and 16.8 min, respectively. The retention time of an unidentified metabolite was 8.9 min.

DISCUSSION

The gene encoding CYP2D6 enzyme is localized on chromosome 22. Three major mutant alleles, termed *CYP2D6**3, 4, and 5, associated with the poor metabolizer (PM) phenotype, were found early on in Caucasians^[3]. *CYP2D6* gene has turned out to be extremely polymorphic with 44 alleles described to 10-Nov-2003 (<http://www.imm.ki.se/CYPalleles/cyp2d6.htm>). Three fairly population specific alleles have been found with *CYP2D6**4 in Caucasians, *10 in Asians and *17 in Africans^[3]. The *CYP2D6**10 allele with 100 C \rightarrow T and 1457 G \rightarrow C, can result in P34S and S486T amino acids substitute and an unstable enzyme with decreased catalytic activity. This allele occurred from 38% to 70% in Asian population^[4]. The most frequent allele in Chinese was *CYP2D6**10 allele with a frequency of about 51.3%^[21], it was 57.2% in Guangdong Chinese population^[22], 41.17% in Hong Kong Chinese population^[23]. The *CYP2D6* cDNA we cloned has the characteristics of *CYP2D6**10 allele with 2 amino acid substitutions of P34S and S486T.

Ramamoorthy *et al*^[24] have compared CYP2D6.10 with CYP2D6.1 *in vitro* in a baculovirus expression system using various substrates, such as dextromethorphan, *P*-methoxyamphetamine, 1-methyl-4-phenyl-1, 2, 3, 6-tetrahydropyridine and (+/-)-3, 4-methylenedioxymethamphetamine, the ratio of intrinsic clearance ($V_{\text{max}}/K_{\text{m}}$) of CYP2D6.1 to CYP2D6.10 was 50, 34, 22 and 123, respectively.

Yu *et al*^[25] reported that the purified CYP2D6.10 enzyme prepared from *in vitro* and to a high homogeneity was reconstituted with lipid and cytochrome P450 reductase, and exhibited an estimated enzyme efficiency (as $V_{\text{max}}/K_{\text{m}}$) 50-fold lower for dextromethorphan *O*-demethylation and 100-fold lower for fluoxetine *N*-demethylation when compared with CYP2D6.1, whereas no measurable catalytic activity was observed for this variant toward codeine.

The intrinsic clearances ($V_{\text{max}}/K_{\text{m}}$) in reconstituted microsomes expressing CYP2D6.10 were reduced by 135-fold with (+/-)-3, 4-methylenedioxymethamphetamine and by 164-fold with dextromethorphan compared with that of wild-type CYP2D6.1^[26].

Bufuralol 1'-hydroxylase activity in microsomes of yeast expressing CYP2D6.10 was rapidly decreased by heat treatment, supporting the idea that the thermal stability of the enzyme was reduced by amino acid replacement. Thermal instability together with the reduced intrinsic clearance of CYP2D6.10 is one of the causes responsible for the known fact that Orientals show lower metabolic activities than Caucasians for drugs metabolized mainly by CYP2D6^[27].

Subjects homozygous for *CYP2D6**10 had higher total areas under the plasma concentration-time curve, lower apparent oral clearances, and longer mean plasma half-life of nortriptyline than subjects in the *CYP2D6**1/*1 and the heterozygous groups^[28].

The plasma haloperidol concentration/dose ratio was significantly higher in older subjects (at least 50 years old) than in younger subjects with non-*2D6**10 homozygous genotypes, but not for those with *2D6**10 homozygous genotype^[29]. No significant differences in plasma concentration of fluvoxamine divided by daily dose of fluvoxamine per body weight ratio were found between subjects with no, one or two *CYP2D6**10 alleles in Japanese subjects^[30].

Cai *et al*^[31] found that patients with homozygous mutant of *CYP2D6**10 not only had a plasma concentration at peak (C_{max}) of propafenone two times as high as those of wild-type genotype, but also showed a two-fold higher inhibitory rate of ventricular premature contractions compared with those with homozygous *CYP2D6**1.

Venlafaxine, a new antidepressant, is metabolized mainly by CYP2D6 to an active metabolite, *O*-desmethylvenlafaxine. C_{max} and areas under the plasma concentration-time curve of venlafaxine were 184% and 484% higher in the *CYP2D6**10/*10 subjects than in the *CYP2D6**1/*1 subjects^[32].

Bufuralol 1'-hydroxylation has been commonly used by pharmaceutical industry to study *in vitro* drug interactions for CYP2D6^[33]. Dextromethorphan has been a widely used probe drug for human CYP2D6 activity both *in vitro* and *in vivo*^[34]. In humans, dextromethorphan is metabolized to dextrophan, 3-methoxymorphinan and 3-hydroxymorphinan. CYP2D6 contributes at least 80% to the formation of dextrophan, and CYP3A4 contributes more than 90% to the formation of 3-hydroxymorphinan. Dextromethorphan as a marker for monitoring both CYP2D6 and CYP3A activities has been found to be practical in human liver microsomal preparation^[35].

The expression of CYP2D6*10 mRNA was validated by RT-PCR. The dextromethorphan *O*-demethylation of HepG2-CYP2D6*10 was $2.31 \pm 0.19 \text{ nmol} \cdot \text{min}^{-1} \cdot \text{mg}^{-1}$ S9 protein, which was higher than baculovirus expressed CYP2D6 ($1.3420 \pm 0.1466 \text{ nmol} \cdot \text{min}^{-1} \cdot \text{mg}^{-1}$ protein) and human liver

microsome 0.17 to 0.30 nmol·min⁻¹·mg⁻¹ protein^[36]. This cell line is a useful tool for further studies of the function and biochemical mechanism of CYP2D6.10 enzyme.

REFERENCES

- Danielson PB.** The cytochrome P450 superfamily: biochemistry, evolution and drug metabolism in humans. *Curr Drug Metab* 2002; **3**: 561-597
- Anzenbacher P,** Anzenbacherova E. Cytochromes P450 and metabolism of xenobiotics. *Cell Mol Life Sci* 2001; **58**: 737-747
- Bertilsson L,** Dahl ML, Dalen P, Al-Shurbaji A. Molecular genetics of CYP2D6: clinical relevance with focus on psychotropic drugs. *Br J Clin Pharmacol* 2002; **53**: 111-122
- Bradford LD.** CYP2D6 allele frequency in European Caucasians, Asians, Africans and their descendants. *Pharmacogenomics* 2002; **3**: 229-243
- Wu J,** Dong H, Cai Z, Yu Y. Stable expression of human cytochrome CYP2B6 and CYP1A1 in Chinese hamster CHL cells: their use in micronucleus assays. *Chin Med Sci J* 1997; **12**: 148-155
- Yan L,** Yu Y, Zhuge J, Xie HY. Cloning of human cytochrome P450 2A6 cDNA and its expression in mammalian cells. *Zhongguo Yaolixue Yu Dulixue Zazhi* 2000; **14**: 31-35
- Chen Q,** Wu J, Yu Y. Establishment of transgenic cell line CHL-3A4 and its metabolic activation. *Zhonghua Yufang Yixue Zazhi* 1998; **32**: 281-284
- Zhuce J,** Yu YN, Li X, Qian YL. Cloning of cytochrome P-450 2C9 cDNA from human liver and its expression in CHL cells. *World J Gastroenterol* 2002; **8**: 318-322
- Zhuce J,** Yu YN, Qian YL, Li X. Establishment of a transgenic cell line stably expressing human cytochrome P450 2C18 and identification of a CYP2C18 clone with exon 5 missing. *World J Gastroenterol* 2002; **8**: 888-892
- Li X,** Yu YN, Zhu GJ, Qian YL. Cloning of UGT1A9 cDNA from liver tissues and its expression in CHL cells. *World J Gastroenterol* 2001; **7**: 841-845
- Rueff J,** Chiapella C, Chipman JK, Darroudi F, Silva ID, Duvergeran Bogaert M, Fonti E, Glatt HR, Isern P, Laires A, Leonard A, Llagostera M, Mossesso P, Natarajan AT, Palitti F, Rodrigues AS, Schinoppi A, Turchi G, Werle-Schneider G. Development and validation of alternative metabolic systems for mutagenicity testing in short-term assays. *Mutat Res* 1996; **353**: 151-176
- Rodriguez-Antona C,** Donato MT, Boobis A, Edwards RJ, Watts PS, Castell JV, Gomez-Lechon MJ. Cytochrome P450 expression in human hepatocytes and hepatoma cell lines: molecular mechanisms that determine lower expression in cultured cells. *Xenobiotica* 2002; **32**: 505-520
- Jover R,** Bort R, Gomez-Lechon MJ, Castell JV. Cytochrome P450 regulation by hepatocyte nuclear factor 4 in human hepatocytes: a study using adenovirus-mediated antisense targeting. *Hepatology* 2001; **33**: 668-675
- Yoshitomi S,** Ikemoto K, Takahashi J, Miki H, Namba M, Asahi S. Establishment of the transformants expressing human cytochrome P450 subtypes in HepG2, and their applications on drug metabolism and toxicology. *Toxicol In Vitro* 2001; **15**: 245-256
- Kimura S,** Umeno M, Skoda RC, Meyer UA, Gonzalez FJ. The human debrisoquine 4-hydroxylase (CYP2D) locus: sequence and identification of the polymorphic CYP2D6 gene, a related gene, and a pseudogene. *Am J Hum Genet* 1989; **45**: 889-904
- Sambrook J,** Fritsch EF, Maniatis T. Molecular Cloning, A Laboratory Manual, 2nd ed. New York: Cold Spring Harbor Laboratory Press 1989: 6.28-6.29
- Kronbach T,** Mathys D, Umeno M, Gonzalez FJ, Meyer UA. Oxidation of midazolam and triazolam by human liver cytochrome P450III A4. *Mol Pharmacol* 1989; **36**: 89-96
- Palamanda JR,** Casciano CN, Norton LA, Clement RP, Favreau LV, Lin C, Nomeir AA. Mechanism-based inactivation of CYP2D6 by 5-fluoro-2-[4-[(2-phenyl-1H-imidazol-5-yl)methyl]-1-piperazinyl]pyrimidine. *Drug Metab Dispos* 2001; **29**: 863-867
- Yu A,** Dong H, Lang D, Haining RL. Characterization of dextromethorphan O- and N-demethylation catalyzed by highly purified recombinant human CYP2D6. *Drug Metab Dispos* 2001; **29**: 1362-1365
- Barecki ME,** Casciano CN, Johnson WW, Clement RP. *In vitro* characterization of the inhibition profile of loratadine, desloratadine, and 3-OH-desloratadine for five human cytochrome P-450 enzymes. *Drug Metab Dispos* 2001; **29**: 1173-1175
- Ji L,** Pan S, Marti-Jaun J, Hanseler E, Rentsch K, Hersberger M. Single-step assays to analyze CYP2D6 gene polymorphisms in Asians: allele frequencies and a novel *14B allele in mainland Chinese. *Clin Chem* 2002; **48**: 983-988
- Gao Y,** Zhang Q. Polymorphisms of the GSTM1 and CYP2D6 genes associated with susceptibility to lung cancer in Chinese. *Mutat Res* 1999; **444**: 441-449
- Garcia-Barcelo M,** Chow LY, Chiu HF, Wing YK, Lee DT, Lam KL, Waye MM. Genetic analysis of the CYP2D6 locus in a Hong Kong Chinese population. *Clin Chem* 2000; **46**: 18-23
- Ramamoorthy Y,** Tyndale RF, Sellers EM. Cytochrome P450 2D6.1 and cytochrome P450 2D6.10 differ in catalytic activity for multiple substrates. *Pharmacogenetics* 2001; **11**: 477-487
- Yu A,** Kneller BM, Rettie AE, Haining RL. Expression, purification, biochemical characterization, and comparative function of human cytochrome P450 2D6.1, 2D6.2, 2D6.10, and 2D6.17 allelic isoforms. *J Pharmacol Exp Ther* 2002; **303**: 1291-1300
- Ramamoorthy Y,** Yu AM, Suh N, Haining RL, Tyndale RF, Sellers EM. Reduced (+/-)-3,4-methylenedioxymethamphetamine ("Ecstasy") metabolism with cytochrome P450 2D6 inhibitors and pharmacogenetic variants *in vitro*. *Biochem Pharmacol* 2002; **63**: 2111-2119
- Nakamura K,** Ariyoshi N, Yokoi T, Ohgiya S, Chida M, Nagashima K, Inoue K, Kodama T, Shimada N, Kamataki T. CYP2D6.10 present in human liver microsomes shows low catalytic activity and thermal stability. *Biochem Biophys Res Commun* 2002; **293**: 969-973
- Yue QY,** Zhong ZH, Tybring G, Dalen P, Dahl ML, Bertilsson L, Sjoqvist F. Pharmacokinetics of nortriptyline and its 10-hydroxy metabolite in Chinese subjects of different CYP2D6 genotypes. *Clin Pharmacol Ther* 1998; **64**: 384-390
- Ohara K,** Tanabu S, Ishibashi K, Ikemoto K, Yoshida K, Shibuya H. Effects of age and the CYP2D6*10 allele on the plasma haloperidol concentration/dose ratio. *Prog Neuropsychopharmacol Biol Psychiatry* 2003; **27**: 347-350
- Ohara K,** Tanabu S, Ishibashi K, Ikemoto K, Yoshida K, Shibuya H. CYP2D6*10 alleles do not determine plasma fluvoxamine concentration/dose ratio in Japanese subjects. *Eur J Clin Pharmacol* 2003; **58**: 659-661
- Cai WM,** Xu J, Chen B, Zhang FM, Huang YZ, Zhang YD. Effect of CYP2D6*10 genotype on propafenone pharmacodynamics in Chinese patients with ventricular arrhythmia. *Acta Pharmacol Sin* 2002; **23**: 1040-1044
- Fukuda T,** Yamamoto I, Nishida Y, Zhou Q, Ohno M, Takada K, Azuma J. Effect of the CYP2D6*10 genotype on venlafaxine pharmacokinetics in healthy adult volunteers. *Br J Clin Pharmacol* 1999; **47**: 450-453
- Yuan R,** Madani S, Wei XX, Reynolds K, Huang SM. Evaluation of cytochrome p450 probe substrates commonly used by the pharmaceutical industry to study *in vitro* drug interactions. *Drug Metab Dispos* 2002; **30**: 1311-1319
- Streetman DS,** Bertino JS Jr, Nafziger AN. Phenotyping of drug-metabolizing enzymes in adults: a review of *in vivo* cytochrome P450 phenotyping probes. *Pharmacogenetics* 2000; **10**: 187-216
- Yu A,** Haining RL. Comparative contribution to dextromethorphan metabolism by cytochrome P450 isoforms *in vitro*: can dextromethorphan be used as a dual probe for both CYP2D6 and CYP3A activities? *Drug Metab Dispos* 2001; **29**: 1514-1520
- Abdel-Rahman SM,** Marcucci K, Boge T, Gotschall RR, Kearns GL, Leeder JS. Potent inhibition of cytochrome P-450 2D6-mediated dextromethorphan O-demethylation by terbinafine. *Drug Metab Dispos* 1999; **27**: 770-775

Dynamic changes of capillarization and peri-sinusoid fibrosis in alcoholic liver diseases

Guang-Fu Xu, Xin-Yue Wang, Gui-Ling Ge, Peng-Tao Li, Xu Jia, De-Lu Tian, Liang-Duo Jiang, Jin-Xiang Yang

Guang-Fu Xu, Xin-Yue Wang, De-Lu Tian, Liang-Duo Jiang, Jin-Xiang Yang, Digestive Department of the Affiliated Dongzhimen Hospital, Beijing University of Traditional Chinese Medicine, Beijing 100700, China

Gui-Ling Ge, Central Electronic Microscope Examination Studio of Beijing University of TCM, Beijing 100029, China

Peng-Tao Li, Xu Jia, Basic Medical College of Beijing University of TCM, Beijing 100029, China

Correspondence to: Dr. Guang-Fu Xu, Digestive Department of the Affiliated Dongzhimen Hospital, Beijing University of TCM, Beijing 100700, China. guangfuxu@hotmail.com

Telephone: +86-10-84290755

Received: 2003-05-12 **Accepted:** 2003-06-07

Abstract

AIM: To investigate the dynamic changes of capillarization and peri-sinusoid fibrosis in an alcoholic liver disease model induced by a new method.

METHODS: Male SD rats were randomly divided into 6 groups, namely normal, 4 d, 2 w, 4 w, 9 w and 11 w groups. The animals were fed with a mixture of alcohol for designated days and then decollated, and their livers were harvested to examine the pathological changes of hepatocytes, hepatic stellate cells, sinusoidal endothelial cells, sinusoid, peri-sinusoid. The generation of three kinds of extra cellular matrix was also observed.

RESULTS: The injury of hepatocytes became severer as modeling going on. Under electronic microscope, fatty vesicles and swollen mitochondria in hepatocytes, activated hepatic stellate cells with fibrils could be seen near or around it. Fenestrae of sinusoidal endothelial cells were decreased or disappeared, sinusoidal basement was formed. Under light microscopy typical peri-sinusoid fibrosis, gridding-like fibrosis, broaden portal areas, hepatocyte's fatty and balloon denaturation, iron sediment, dot necrosis, congregated lymphatic cells and leukocytes were observed. Type I collagen showed an increasing trend as modeling going on, slightly recovered when modeling stopped for 2 weeks. Meanwhile, type IV collagen decreased rapidly when modeling began and recovered after modeling stopped for 2 weeks. Laminin increased as soon as modeling began and did not recover when modeling stopped for 2 weeks.

CONCLUSION: The pathological changes of the model were similar to that of human ALD, but mild in degree. It had typical peri-sinusoid fibrosis, however, capillarization seemed to be instable. It may be related with the reduction of type IV collagen in the basement of sinusoid during modeling.

Xu GF, Wang XY, Ge GL, Li PT, Jia X, Tian DL, Jiang LD, Yang JX. Dynamic changes of capillarization and peri-sinusoid fibrosis in alcoholic liver diseases. *World J Gastroenterol* 2004; 10 (2): 238-243

<http://www.wjgnet.com/1007-9327/10/238.asp>

INTRODUCTION

In China alcoholic liver disease patients have been on the rise. Acetaldehyde and hydroxy free radicals oxidized from alcohol can injure hepatocytes and activate lipid peroxidation. Hydroxy free radicals are able to activate phagocytes to secrete cytokines and activate hepatic stellate cells (HSC). The activation of HSC leads to the production of various components of extracellular matrix (ECM). Researchers have reported that peri-sinusoid fibrosis, capillarization, gridding-like fibrosis, bridging fibrosis and even cirrhosis are most typical morphological changes in alcoholic consumers for more than 10 or even 20 years. But mild and/or moderate drinkers may not experience such severe damages of the liver. Among the ECM produced during fibrosis, types I and IV collagen and laminin are closely related to the formation of capillarization and peri-sinusoid fibrosis. The Tsukamoto-French model has been used to investigate ALD, but it is expensive and complicated. Many researchers like to make use of the gavage model because of its simplicity and convenience, but there are many inconsistent reports about the content of alcohol ingested, the time of modeling, *etc.* In order to probe into the mechanism of ALD and find a more suitable model, we investigated the dynamic changes of capillarization and peri-sinusoid fibrosis, the contents of types I and IV collagen and laminin, *etc.* in male SD rats during modeling so as to explore whether it was acceptable.

MATERIALS AND METHODS

Materials

Male SD rats, weighing 150±5g, were purchased from Beijing Vital River Company. Corn oil was from Carrefour Supermarket. Xanthan gum and maltose were from Beijing Chemical Agent Company. Edible alcohol was from Beijing General Alcohol Brewing Company. Carbonyl iron and pirazole were from Sigma, USA. First antibody to type I collagen, type IV collagen and laminin were from Antibody Diagnostic Inc, ADI, USA. PV-6001 Kits were from Power Vision, USA. ZLI-9030 and ZLI9001 were from Beijing Zhongshan Company.

Methods

Fifty-six rats were divided into normal(6), 4 d(8), 2 w(8), 4 w(10), 9 w(12), 11 w(12) groups.

ALD model was induced by intragastric infusion of a mixture made of alcohol (5 g/d·kg), pirazole (30 mg/d·kg), corn oil (3 ml/d·kg), carbonyl iron (35 mg/d·kg, which was decreased to 15 mg after 4 w), a little xanthan gum and maltose once a day for 5 days consecutively, with 2 days off per week, until 9 w. The rats were fed with normal diet and water *ad libitum*.

The rats were executed at the end of 4 d, 2 w, 4 w, 9 w and 11 w, respectively. Harvested livers were split and fixed for electron microscopy, hematoxylin and eosin, and Masson complex staining. A portion was snap frozen for biochemical and molecular analysis. Histological analysis of each liver was undertaken. Further sections were cut from each liver, deparaffinized and subjected to amylopin antigen retrieval before being immunostained with primary antigen and second envision agents for types I and IV collagen and laminin. Semi-quantitative computation of types I and IV collagen and laminin

was done by the image analyzing system MIS-2000, which was from 3Y Company, USA. The slides for electron microscopic examination were made according to routine protocol, sub-cellular morphology was investigated and photographed under JEM-1200EX (80KV).

Statistics

SPSS Version 10.0 was used. All values were expressed as mean ±SD. One-way ANOVA was used to determine the

significance of differences among the six groups. $P < 0.05$ was considered statistically significant.

RESULTS

HE staining

Normal hepatocytes in neat plates, had big and round nuclei, with a clear profile. Hepatocytes in Four d group became swollen and turbid, or balloon denatured. Sinus stricture was

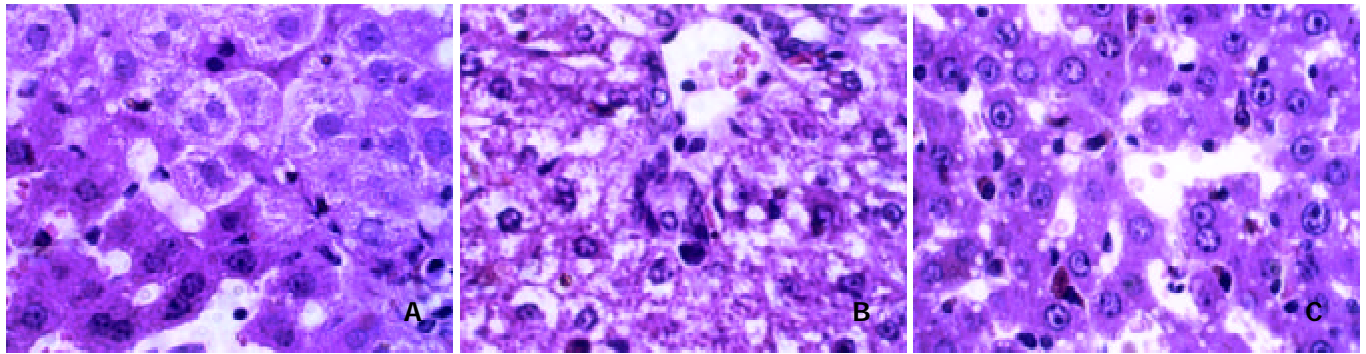


Figure 1 Changes of hepatocytes after HE staining. A: normal HE, B: 4 d HE, C: 4 w HE.

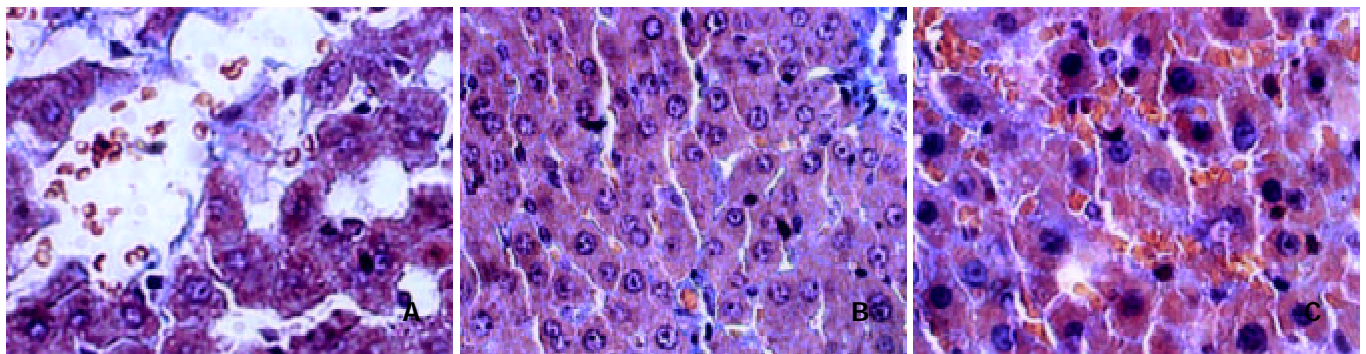


Figure 2 Changes of hepatocytes after Masson staining. A: normal Masson, B: 4 w Masson, C: 11 w Masson

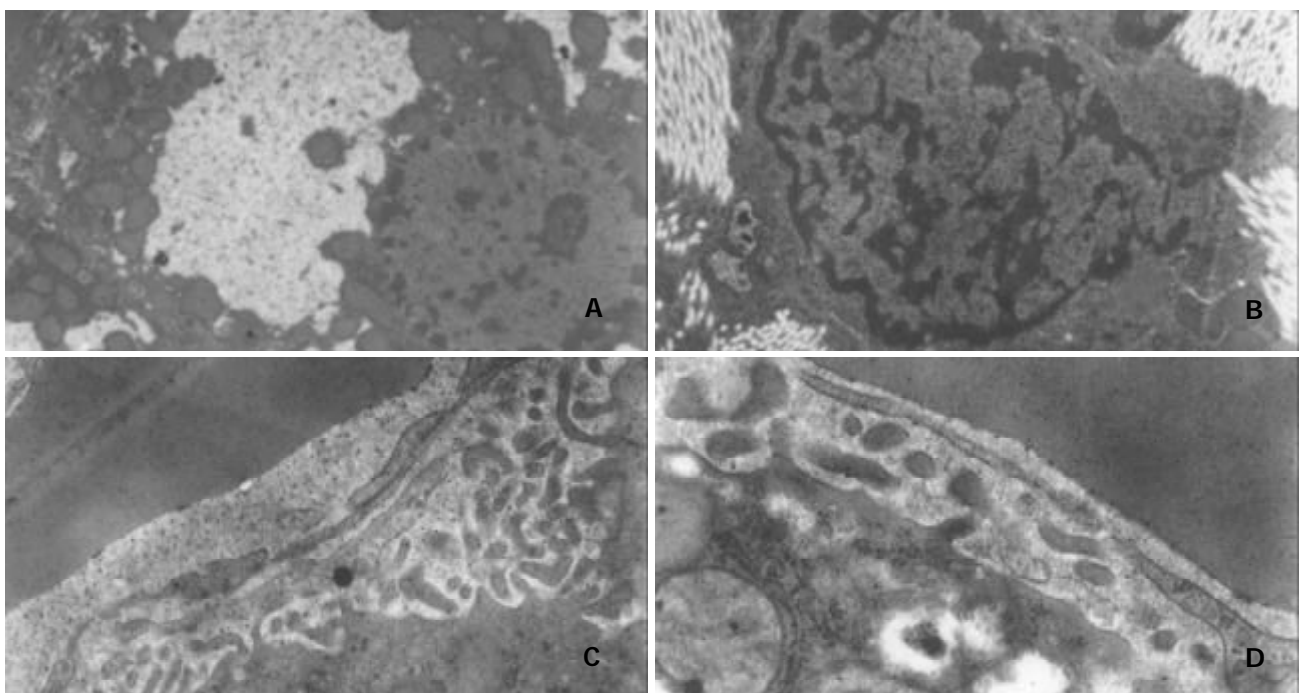


Figure 3 Changes of hepatocytes observed by electron microscopy. A: fatty vesicle in hepatocytes, B: activated HSC and fibril, C: sinusoidal endothelium and basement, D: endothelium, less fenestrae.

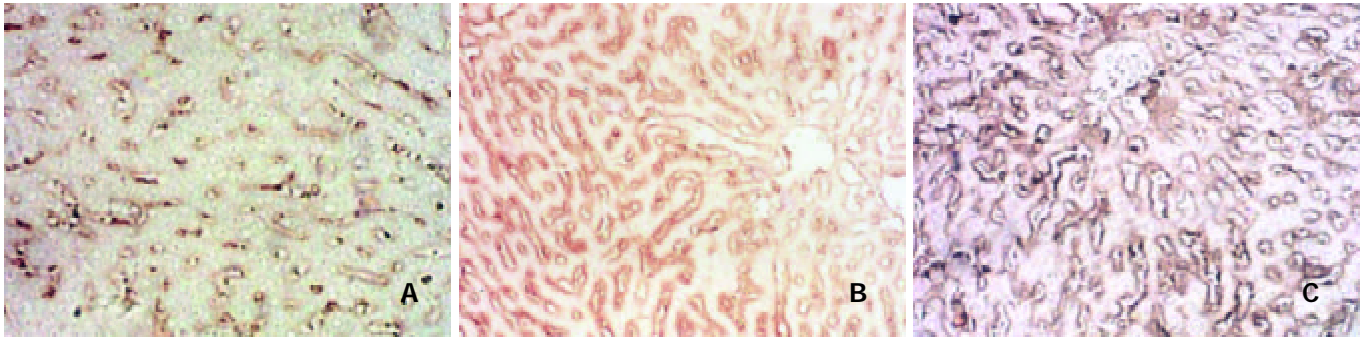


Figure 4 Changes of type I collagen after immunohistochemical staining. A: col-I Normal group, B: Col-I in 4 w group, C: Col-I in 9 w group.

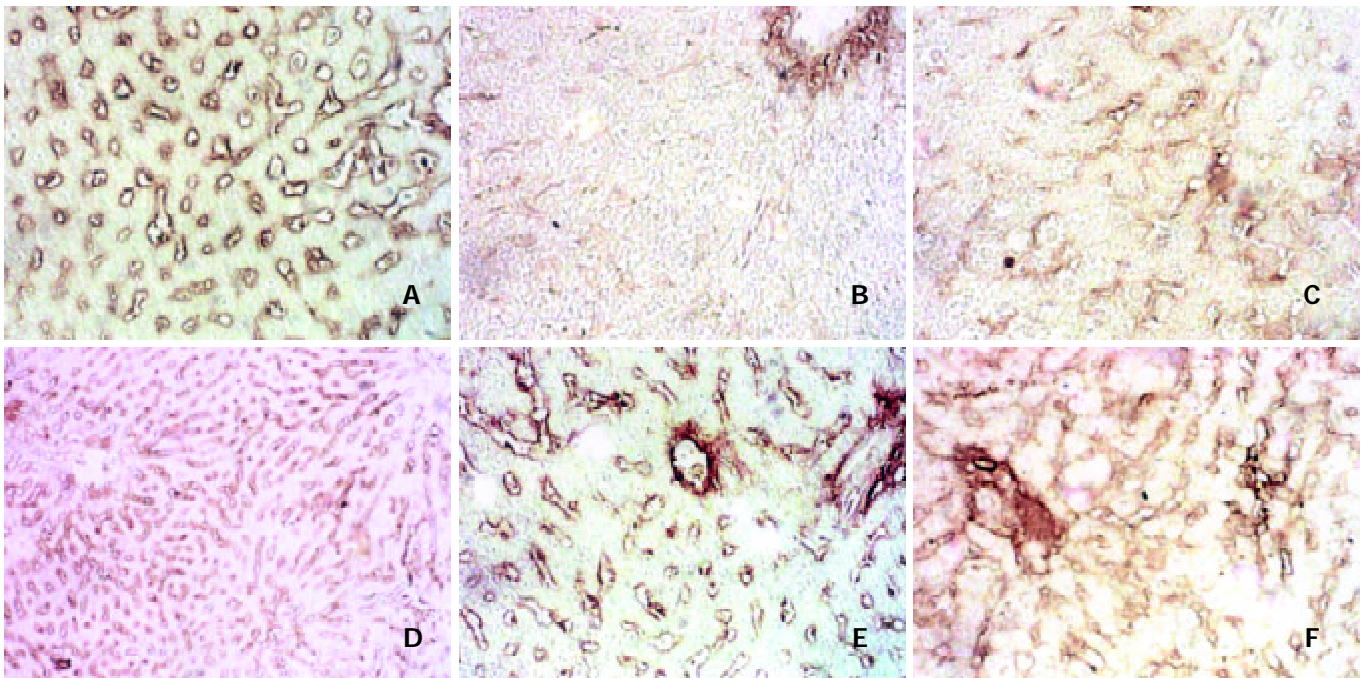


Figure 5 Changes of type IV collagen after immunohistochemical staining. A: col-IV Normal group, B: Col-IV in 4 d group, C: Col-IV in 2 w group, D: Col-IV in 4 w group, E: Col-IV in 9 w group, F: Col-IV in 11 w group.

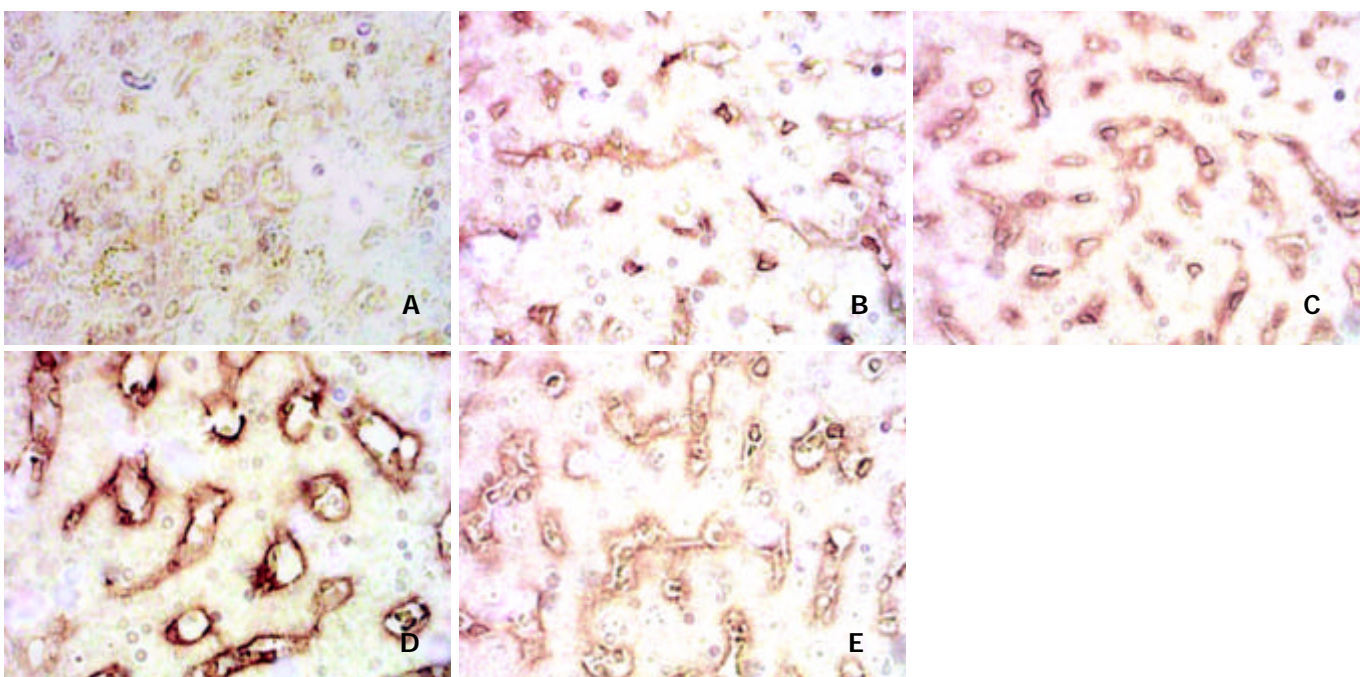


Figure 6 Changes of laminin after immunohistochemical staining. A: laminin Normal group, B: Laminin in 4 d group, C: Laminin in 4 w group, D: Laminin in 9 w group, E: Laminin in 11 w group.

evident. Hepatocytes in 2 w group showed bridging balloon denaturation at around-lobules and portal area, dot necrosis and congregating inflammatory cells could be seen. Four w group exhibited evident hepatocytes coagulation necrosis, mesenchymal cells hyperplasia, broadened portal area with fibrosis. In the Nine w group Mallory body and widespread fatty vesicle denaturation in hepatocytes, piecemeal necrosis, congregating inflammatory cells and fibrosis could be seen. Eleven w group had denatured hepatocytes and a little necrosis, hepatic stellate cells showed dark nuclei (Figure 1. A, B, C)

HE-masson staining

Normal group showed very light stain of the basement of central veins of lobules, Which was mildly evident in blood vessels at the portal area. Four d group showed more evident stain of central vein basement, parts of the hepatocytes were surrounded by gridding-like stains. Two w group showed more gridding-like stains. In 4 w group almost all hepatocytes were surrounded by gridding-like fibrosis and thicker basements of central veins were seen. Thick fibers in portal area bridged with those in hepatic lobules. The fibrotic changes in 9 w group deteriorated. In 11 w group the gridding-like fibrosis slightly ameliorated, but no evident changes were seen in central veins and portal areas (Figure 2. A, B, C).

Electron microscopic examination

Normal hepatocytes had round and clear nuclei, many microvilli extended to touch sinusoidal endothelial cells, or encircle hepatic stellate cells. Its mitochondria presented oval profiles and clear crests. Sinusoidal endothelial cells had many fenestrae and flat nuclei, without obvious basement and fibril underneath. HSC showed tight nuclear chromatin, few in number, and without fibril surrounded by. As modeling going on, the microvilli of hepatocytes became swollen and broken, rough endoplasmic reticulum showed turbulence, mitochondria became swollen and crest broken. The nuclei of sinusoidal endothelial cells became darker and thicker, nuclei chromatin grew crassitude. Fewer fenestrae and basement could be seen under which a large amount of fibrils was found. HSC proliferated actively, with nuclear chromatin turned into crassitude, and lots of fibril surrounded lay (Figure 3. A, B, C, D).

Table 1 Dynamic changes of types I and IV collagen and laminin ($\bar{x}\pm s$)

Group	Type I Collagen	Type IV Collagen	Laminin
Normal	0.2874±0.0224	0.3421±0.0217	0.2263±0.0010
4 d	0.2811±0.0151	0.2907±0.0109 ^a	0.2975±0.0034 ^a
2 w	0.2912±0.0122	0.2463±0.0062 ^a	0.2962±0.0048 ^a
4 w	0.3853±0.0401 ^a	0.3165±0.0049 ^a	0.3336±0.0091 ^a
9 w	0.4262±0.0992 ^a	0.3202±0.0039 ^a	0.3523±0.0108 ^a
11 w	0.3734±0.1239 ^a	0.3249±0.0119	0.3549±0.0120 ^a

^aP<0.05 vs normal.

Immunohistochemical staining

The content of type I collagen grew gradually from Two w and reached the peak in Nine w. After 2 week recovery, it dropped a little in 11 week but was still higher than that of normal rats (Figure 4. A, B, C).

The content of type IV collagen in normal rats was moderate, but it rapidly decreased after the infusion of alcohol mixture, and was sustained at a low level during the course of modeling. However, it recovered in Eleven w (Figure 5. A, B, C, D, E, F).

There were few positive stains of laminin in normal rats, but as soon as the modeling began, its content increased rapidly,

maintaining at high levels during the course, and did not return to normal in 11 w group, but much higher than that of normal rats (Figure 6. A, B, C, D, E, Table 1).

DISCUSSION

The viewpoints^[1-3] that moderate drinking might be beneficial to heart and vascular system or might improve the ability of senior citizens to cognize imply that the disadvantages of alcohol have not been sufficiently recognized. Investigations on pathological changes of mild and moderate drinkers in the liver, especially capillarization and peri-sinusoid fibrosis are not so profound.

Alcohol abuse has become a severe problem in China. The modeling method for the purpose of ALD research is one of the key factors. ALD may be formed in more than 10 or even 20 years, meanwhile have been found many differences due to their various genotypes^[4,5]. As to modeling, pure alcohol intake was difficult in inducing a successful model in a relative short period of time^[6]. Tsukamoto-French model can do so by means of consecutive infusion of alcohol into stomach through a gastric fistula and does not need quite a long time, but it is complicated and expensive. At present the most widely used method of modeling is “gavage” of alcohol^[7,8]. In order to make a model in a relative short period of time, other assisting materials besides alcohol must be added to promote the pathological progress. But the materials added should be of or about the same mechanism as that of alcohol, and the contents of them have to be restrained in order not to overcome alcohol. The core is whether the model has similar pathological changes to ALD and suitable for drug researches, whether it can illustrate the mechanism of treatment so to serve clinic investigation reliably.

The mechanism of ALD has been thought to have a close relation to many factors such as lipid peroxidation^[9], endotoxin^[10-13], acetaldehyde and immunological injuries it induced^[14-16], gender^[17], sediment of iron^[18-25], free radicals^[26], *etc.* Analysis^[27] of alcohol-responsive genes showed that alcohol might injure the liver omnidirectionally, causing not only fatty liver, necrosis and inflammation, hepatocyte apoptosis and hyperhomocysteinemia, but also turbulence in glucose metabolism and DNA damages, *etc.* It has been recognized that the occurrence of fibrosis induced by alcohol or other factors is due to the activation of hepatic stellate cells^[28-41]. All materials added besides alcohol such as iron, polyunsaturated fatty acid and endotoxin during modeling should be designed to strengthen the common mechanism. Our model accepted iron as an additive to promote the course of lipid peroxidation. Corn oil had similar functions. Pirazole could delay the course of alcohol to be cleared from plasmid. Meanwhile we used pirazole to cause or promote blood stasis and flatulence of the intestinal tract, this might be due to its stimulating effect on local mucosa. It needs more evidences to say that pirazole can promote endotoxin absorption. But whether the fibrosis model induced by alcohol and CCl₄ is suitable for ALD research should be under further observation^[42].

Some researchers reported^[43] that capillarization, peri-sinusoid fibrosis and gridding-like fibrosis were typical morphological changes in alcoholic cirrhosis of human beings which are rather different from that of fibrosis or cirrhosis induced by virus infection, yet we do not know whether it would happen in average moderate drinkers, and how the extracellular matrix was involved in changes of types I and IV collagen and laminin. Since there was no unification about the species of rats, the dosage of alcohol and additives used during modeling, we introduced a model established by intragastric infusion of a new mixture of alcohol for 9 weeks consecutively and studied the dynamic changes of types I and IV collagen as

well as laminin, in order to find out whether this model was suitable or not for ALD research^[44,45].

The end products of alcohol in the liver include acetaldehyde and hydroxy free radicals which can injure hepatocytes and activate lipid peroxidation. Phagocytes are susceptible to the course, and would excrete many cytokines such as TNF- α , TGF- β 1, which in turn activate hepatic stellate cells. Activation of HSC is the key event of various kinds of fibrosis. We found in this model, however, as modeling going on, the pathological changes of hepatocytes and fibrosis were gradually deteriorated. The rats in 2 w group were low in spirit with hair standing and diarrhea, the rats in 4 w group became worse and even died. However, because of sustained alcohol intake, after 4 w the rats seemed to get better in spirits and activities, implying that they might develop some mechanisms to adapt to alcohol intake.

In this model we found that the pathological changes of hepatocytes, HSC, endothelia under electronic microscopy, HE stain, HE-masson complex stain were consistent with that of ALD in human beings. Histological analysis showed that the degree of fibrosis was stages I-II^[46,47]. This model may be a good representative of average moderate drinkers who have extensive mild pathological injuries of the liver. Our study may provide some clues for investigation about mild and moderate drinkers in clinic.

Capillarization was a process in which the liver sinusoid became consecutive capillaries with evident basement around. The morphological changes mainly included decreased fenestrae in number or even disappearance in endothelia, and the formation of evident basement^[48-51]. The progression of fibrosis was directly linked to the activation of HSC, and always accompanied by the activation of matrix metalloproteinase2 (MMP-2), without strong expression of the family of tissue inhibitor of matrix metalloproteinases (TIMPs) which was usually observed at the primary stages of fibrosis. Capillarization might not be always stably formed. Our observation demonstrated this might be true, because the content of type IV collagen was low and changed during the modeling, the basement might be mainly composed of laminin. Some of the basements of the liver sinusoid in the rats of 4 w and 9 w groups were not so typical but indeed existed.

The laminin content showed a consecutive high level during the modeling, and did not return to normal even after 2 week recovery. It implied that decomposition of laminin in this model was slightly tough. It deserves further investigation in human ALD. Thus MMP-2's activity alone may not be able to promote the reverse of capillarization.

The content of type I collagen is less than that of type III collagen in normal rats' liver, but it is not so when fibrosis occurs. In normal rats we saw few fibrils near the sinusoid, as modeling going on, many fibrils appeared around sinusoidal endothelial cells. We postulate that type I collagen may take part in this course. Because most researchers believed that type I collagen was not involved in the formation of basement during capillarization. We conclude that the peri-sinusoid fibrosis may be mainly composed of fibrils consisting of type I collagen. Electron microscopic observation showed that peri-sinusoid fibrils were not prone to decomposition after modeling stopped. Immunohistochemical staining observation was consistent with this.

This model had stable alcohol intake during modeling, this ensured less deaths but resulted in moderate pathological changes. If we increase the content of alcohol intake after 4 w and last it for a longer time, or do not reduce the content of iron intake, there may be more severe injuries of the liver such as cirrhosis, but also more dead animals would come forth which may lead to modeling ending in failure. However, the model still needs further improvements.

REFERENCES

- 1 **Laatikainen T**, Manninen L, Poikolainen K, Vartiainen E. Increased mortality related to heavy alcohol intake pattern. *J Epidemiol Community Health* 2003; **57**: 379-384
- 2 **Ambler G**, Royston P, Head J. Non-linear models for the relation between cardiovascular risk factors and intake of wine, beer and spirits. *Stat Med* 2003; **22**: 363-383
- 3 **Zuccala G**, Onder G, Pedone C, Cesari M, Landi F, Bernabei R, Cocchi A. Dose-related impact of alcohol consumption on cognitive function in advanced age: results of a multicenter survey. *Alcohol Clin Exp Res* 2001; **25**: 1743-1748
- 4 **Tadic SD**, Elm MS, Li HS, Van Londen GJ, Subbotin VM, Whitcomb DC, Eagon PK. Sex differences in hepatic gene expression in a rat model of ethanol-induced liver injury. *J Appl Physiol* 2002; **93**: 1057-1068
- 5 **Wang G**, Wang B, Liu C. Relation between activities of hepatic and gastric alcohol dehydrogenases and formation of chronic alcoholic liver diseases. *Zhonghua Ganzangbing Zazhi* 2001; **9**: 265-267
- 6 **Ren C**, Paronetto F, Mak KM, Leo MA, Lieber CS. Cytokeratin 7 staining of hepatocytes predicts progression to more severe fibrosis in alcohol-fed baboons. *J Hepatol* 2003; **38**: 770-775
- 7 **Li J**, French BA, Fu P, Bardag-Gorce F, French SW. Mechanism of the alcohol cyclic pattern: role of catecholamines. *Am J Physiol Gastrointest Liver Physiol* 2003; **285**: G442-448
- 8 **French SW**. Intra-gastric ethanol infusion model for cellular and molecular studies of alcoholic liver disease. *J Biomed Sci* 2001; **8**: 20-27
- 9 **Chen WH**, Liu P, Xu GF, Lu X, Xiong WG, Li FH, Liu CH. Role of lipid peroxidation in liver fibrogenesis induced by dimethylnitrosamine in rats. *Shijie Huaren Xiaohua Zazhi* 2001; **9**: 645-648
- 10 **Murohisa G**, Kobayashi Y, Kawasaki T, Nakamura S, Nakamura H. Involvement of platelet-activating factor in hepatic apoptosis and necrosis in chronic ethanol-fed rats given endotoxin. *Liver* 2002; **22**: 394-403
- 11 **Tamai H**, Horie Y, Kato S, Yokoyama H, Ishii H. Long-term ethanol feeding enhances susceptibility of the liver to orally administered lipopolysaccharides in rats. *Alcohol Clin Exp Res* 2002; **26** (8 Suppl): 75S-80S
- 12 **Keshavarzian A**, Choudhary S, Holmes EW, Yong S, Banan A, Jakate S, Fields JZ. Preventing gut leakiness by oats supplementation ameliorates alcohol-induced liver damage in rats. *J Pharmacol Exp Ther* 2001; **299**: 442-448
- 13 **Mathurin P**, Deng QG, Keshavarzian A, Choudhary S, Holmes EW, Tsukamoto H. Exacerbation of alcoholic liver injury by enteric endotoxin in rats. *Hepatology* 2000; **32**: 1008-1017
- 14 **Jarvelainen HA**, Vakeva A, Lindros KO, Meri S. Activation of complement components and reduced regulator expression in alcohol-induced liver injury in the rat. *Clin Immunol* 2002; **105**: 57-63
- 15 **Shimada S**, Yamauchi M, Takamatsu M, Uetake S, Ohata M, Saito S. Experimental studies on the relationship between immune responses and liver damage induced by ethanol after immunization with homologous acetaldehyde adducts. *Alcohol Clin Exp Res* 2002; **26** (8 Suppl): 86S-90S
- 16 **Searashi Y**, Yamauchi M, Sakamoto K, Ohata M, Asakura T, Ohkawa K. Acetaldehyde-induced growth retardation and micro-heterogeneity of the sugar chain in transferrin synthesized by HepG2 cells. *Alcohol Clin Exp Res* 2002; **26** (8 Suppl): 32S-37S
- 17 **Colantoni A**, Emanuele MA, Kovacs EJ, Villa E, Van Thiel DH. Hepatic estrogen receptors and alcohol intake. *Mol Cell Endocrinol* 2002; **193**: 101-104
- 18 **Boireau A**, Marechal PM, Meunier M, Dubedat P, Moussaoui S. The anti-oxidant ebselen antagonizes the release of the apoptogenic factor cytochrome c induced by Fe2+/citrate in rat liver mitochondria. *Neurosci Lett* 2000; **289**: 95-98
- 19 **Karbownik M**, Reiter RJ, Garcia JJ, Cabrera J, Burkhardt S, Osuna C, Lewinski A. Indole-3-propionic acid, a melatonin-related molecule, protects hepatic microsomal membranes from iron-induced oxidative damage: relevance to cancer reduction. *J Cell Biochem* 2001; **81**: 507-513
- 20 **Schumann K**. Safety aspects of iron in food. *Ann Nutr Metab* 2001; **45**: 91-101
- 21 **Valerio LG Jr**, Petersen DR. Characterization of hepatic iron over-

- load following dietary administration of dicyclopentadienyl iron (Ferrocene) to mice: cellular, biochemical, and molecular aspects. *Exp Mol Pathol* 2000; **68**: 1-12
- 22 **MacDonald GA**, Bridle KR, Ward PJ, Walker NI, Houghlum K, George DK, Smith JL, Powell LW, Crawford DH, Ramm GA. Lipid peroxidation in hepatic steatosis in humans is associated with hepatic fibrosis and occurs predominately in acinar zone 3. *J Gastroenterol Hepatol* 2001; **16**: 599-606
- 23 **Raynard B**, Balian A, Fallik D, Capron F, Bedossa P, Chaput JC, Naveau S. Risk factors of fibrosis in alcohol-induced liver disease. *Hepatology* 2002; **35**: 635-638
- 24 **De Feo TM**, Fargion S, Duca L, Cesana BM, Boncinelli L, Lozza P, Cappellini MD, Fiorelli G. Non-transferrin-bound iron in alcohol abusers. *Alcohol Clin Exp Res* 2001; **25**: 1494-1499
- 25 **Tsukamoto H**. Iron regulation of hepatic macrophage TNF α expression. *Free Radic Biol Med* 2002; **32**: 309-313
- 26 **Kono H**, Bradford BU, Rusyn I, Fujii H, Matsumoto Y, Yin M, Thurman RG. Development of an intragastric enteral model in the mouse: studies of alcohol-induced liver disease using knock-out technology. *J Hepatobiliary Pancreat Surg* 2000; **7**: 395-400
- 27 **Ji C**, Kaplowitz N. Betaine decreases hyperhomocysteinemia, endoplasmic reticulum stress, and liver injury in alcohol-fed mice. *Gastroenterology* 2003; **124**: 1488-1499
- 28 **Friedman SL**. Stellate cell activation in alcoholic fibrosis—an overview. *Alcohol Clin Exp Res* 1999; **23**: 904-910
- 29 **Okuno M**, Sato T, Kitamoto T, Imai S, Kawada N, Suzuki Y, Yoshimura H, Moriwaki H, Onuki K, Masushige S, Muto Y, Friedman SL, Kato S, Kojima S. Increased 9,13-di-cis-retinoic acid in rat hepatic fibrosis: implication for a potential link between retinoid loss and TGF-beta mediated fibrogenesis *in vivo*. *J Hepatol* 1999; **30**: 1073-1080
- 30 **Friedman SL**. Cytokines and fibrogenesis. *Semin Liver Dis* 1999; **19**: 129-140
- 31 **Li D**, Friedman SL. Liver fibrogenesis and the role of hepatic stellate cells: new insights and prospects for therapy. *J Gastroenterol Hepatol* 1999; **14**: 618-633
- 32 **Whalen R**, Rockey DC, Friedman SL, Boyer TD. Activation of rat hepatic stellate cells leads to loss of glutathione S-transferases and their enzymatic activity against products of oxidative stress. *Hepatology* 1999; **30**: 927-933
- 33 **Eng FJ**, Friedman SL. Fibrogenesis I. New insights into hepatic stellate cell activation: the simple becomes complex. *Am J Physiol Gastrointest Liver Physiol* 2000; **279**: G7-G11
- 34 **Boireau A**, Marechal PM, Meunier M, Dubedat P, Moussaoui S. The anti-oxidant ebselen antagonizes the release of the apoptogenic factor cytochrome c induced by Fe $^{2+}$ /citrate in rat liver mitochondria. *Neurosci Lett* 2000; **289**: 95-98
- 35 **Albanis E**, Friedman SL. Hepatic fibrosis. Pathogenesis and principles of therapy. *Clin Liver Dis* 2001; **5**: 315-334
- 36 **Eng FJ**, Friedman SL. Transcriptional regulation in hepatic stellate cells. *Semin Liver Dis* 2001; **21**: 385-395
- 37 **Nieto N**, Friedman SL, Cederbaum AI. Stimulation and proliferation of primary rat hepatic stellate cells by cytochrome P450 2E1-derived reactive oxygen species. *Hepatology* 2002; **35**: 62-73
- 38 **Reeves HL**, Friedman SL. Activation of hepatic stellate cells—a key issue in liver fibrosis. *Front Biosci* 2002; **7**: d808-826
- 39 **Saxena NK**, Ikeda K, Rockey DC, Friedman SL, Anania FA. Leptin in hepatic fibrosis: evidence for increased collagen production in stellate cells and lean littermates of ob/ob mice. *Hepatology* 2002; **35**: 762-771
- 40 **Safadi R**, Friedman SL. Hepatic fibrosis—role of hepatic stellate cell activation. *Med Gen Med* 2002; **4**: 27
- 41 **Albanis E**, Safadi R, Friedman SL. Treatment of hepatic fibrosis: almost there. *Curr Gastroenterol Rep* 2003; **5**: 48-56
- 42 **Chae HB**, Jang LC, Park SM, Son BR, Sung R, Choi JW. An experimental model of hepatic fibrosis induced by alcohol and CCl $_4$: can the lipopolysaccharide prevent liver injury induced by alcohol and CCl $_4$? *Taehan Kan Hakhoe Chi* 2002; **8**: 173-178
- 43 **Zhao JB**, Wang TL, Zhang DM. Morphological study on 40 cases of alcoholic liver disease. *Zhonghua Binglixue Zazhi* 1994; **23**: 14-16
- 44 **Bo AH**, Tian CS, Xue GP, Du JH, Xu YL. Morphology of immune and alcoholic liver diseases in rats. *Shijie Huaren Xiaohua Zazhi* 2001; **9**: 157-160
- 45 **Lin H**, Lü M, Zhang YX, Wang BY, Fu BY. Induction of a rat model of alcoholic liver diseases. *Shijie Huaren Xiaohua Zazhi* 2001; **9**: 24-28
- 46 **Hepatic Fibrosis Research Branch of Chinese Hepatic Diseases Associate**. Some agreements evaluating the diagnosis and curative effects of hepatic fibrosis. *Zhonghua Ganzangbing Zazhi* 2002; **10**: 327-328
- 47 **Infectious, parasitic and hepatic diseases branch of Chinese Medical Association**. Prevention and treatment program for Virus Hepatitis. *Zhonghua Ganzangbing Zazhi* 2000; **8**: 324-329
- 48 **Xu GF**, Tian DL. Progress in capillarization research of hepatic sinusoid. *Zhongguo Zhongxixiyi Jiehe Xiaohua Zazhi* 2002; **10**: 314-316
- 49 **Lu X**, Xu GF, Chen WH, Liu CH, Liu P. The dynamic changes of capillarization during hepatic fibrosis induced by DMN in rats. *Shijie Huaren Xiaohua Zazhi* 2000; **8**: 1415-1416
- 50 **Lu X**, Liu CH, Xu GF, Chen WH, Liu P. Successive observation of laminin and collagen IV on hepatic sinusoid during the formation of the liver fibrosis in rats. *Shijie Huaren Xiaohua Zazhi* 2001; **9**: 260-262
- 51 **Cheng J**. The biology of molecules of extracellular matrix and the relation with clinical diseases. 1st ed, Beijing: *The Publishing Company of Beijing University of Medical Sciences* 1999

Edited by Wang XL and Zhu LH

Preparation and property analysis of a hepatocyte targeting pH-sensitive liposome

Si-Yuan Wen, Xiao-Hong Wang, Li Lin, Wei Guan, Sheng-Qi Wang

Si-Yuan Wen, Xiao-Hong Wang, Li Lin, Wei Guan, Sheng-Qi Wang, Beijing Institute of Radiation Medicine, Beijing 100850, China
Supported by the grants of the State 863 High Technology Project of China, No. 102-08-04-01

Correspondence to: Professor Sheng-Qi Wang, Beijing Institute of Radiation Medicine, No. 27 Taiping Road, Beijing 100850, China. sqwang@nic.bmi.ac.cn

Telephone: +86-10-66932211 **Fax:** +86-10-66932211

Received: 2003-04-02 **Accepted:** 2003-06-04

Abstract

AIM: To develop a hepatocyte targeting pH-sensitive liposome for drug delivery based on active targeting technology mediated by asialoglycoprotein receptors.

METHODS: Four types of targeting molecules with galactose residue were synthesized and mixed with pH-sensitive lipids DC-chol/DOPE to prepare liposome with integrated property of hepatocyte specificity and pH sensitivity. Liposome 18-gal was selected with the best transfection activity through cellular uptake experiment. Property analysis was made through experiments of competitive inhibition of receptors, red blood cell hemolysis, *in vitro* cytotoxicity test by MTS assay and mediation of inhibitory effects of antisense phosphorothioate ODN on gene expression, *etc.*

RESULTS: Liposome 18-gal had the desired properties of hepatocyte specificity, pH sensitivity, low cytotoxicity, and high transfection efficiency.

CONCLUSION: Liposome 18-gal can be further developed as a potential hepatocyte-targeting delivery system.

Wen SY, Wang XH, Lin L, Guan W, Wang SQ. Preparation and property analysis of a hepatocyte targeting pH-sensitive liposome. *World J Gastroenterol* 2004; 10(2): 244-249
<http://www.wjgnet.com/1007-9327/10/244.asp>

INTRODUCTION

Previous studies have suggested a promising future of antisense oligodeoxynucleotide (ODN) in the treatment of viral hepatitis^[1-6]. However, as a polyanionic macromolecule, antisense ODN has two major limitations: poor efficiency of cellular uptake and rapid degradation. The realization of its *in vivo* biological effect is accomplished under the mediation of liposome. In recent years, with the advent of cationic liposome and active targeting technology^[7-10], liposome technology has been widely applied in the transfer of antisense ODNs for its virtues of high transfection efficiency, protection for the entrapped and ease of chemical modification.

The effectiveness of cationic liposome in the mediation of antisense ODN transfer in clinical trials was reported^[11-15], while its deficiency lay in the lack of tissue specificity. To improve the targeting property, active targeting technology based on specific receptor-ligand recognition reaction has been applied.

Hepatocytes exclusively expressed large numbers of high affinity asialoglycoprotein receptors which can recognize the ligand molecules with galactose residues and mediate their endocytosis^[16-20]. In this study, four types of targeting molecules bearing galactose residue were synthesized and mixed with the pH-sensitive lipids DC-chol/DOPE to prepare liposome with integrated property of hepatocyte specificity and pH sensitivity.

MATERIALS AND METHODS

Chemicals and reagents

Chloroformylcholesterol, N,N-dimethylethylenediamine, dioleoylphosphatidylethanol-amine, hydrolytic lactose were purchased from Sigma Chemicals (St. Louis, MO), DC-chol was synthesized according to the published methods^[21]. Enzymes, vectors, luciferase assay system and Celltiter 96@AQ_{ueous} non-radioactive cell proliferation assay test kit were obtained from Promega Corp (Madison, WI). All other reagents were analytically pure.

Plasmid and transgenic cell line HepG2.9706^[22]

pHCV-neo4 was constructed by cloning the complete 5' NCR (non-coding region) and part C region of fusion protein of Chinese HCV genome into pGL3 luciferase reporter vector in which the start codon was deleted without frameshift. In pHCV-neo4, the expression of luciferase gene could be suppressed by blocking the HCV 5' NCR. Transgenic cell strain HepG2.9706 with permanent expression of luciferase gene was constructed by selection of the transfected HepG2 cell with pHCV-neo4 using G418.

Phosphorothioate oligodeoxynucleotide

Phosphorothioate ODN HCV363a (5' GAG-GTT-TAG-GAT-TCG-TGC-TCA-TG 3') is a 23-mer sequence complimentary to part of HCV 5' NCR (noncoding region). HCV363s (5' CAT-GAG-CAC-GAA-TCC-TAA-ACC-TC 3') is the reverse complimentary sequence to HCV363a. NSC (non-specific control: 5' GCA-GAG-GTG-AAA-AAG-TTG-CAT 3') is a random sequence with low homology to HCV5' NCR. The oligonucleotides were synthesized with the automatic DNA synthesizer (390Z, Applied Biosystems, Inc) and purified by HPLC (Micro Pure II reverse phase column).

Synthesis of targeting molecule

Four types of amphiphilic glycolipid molecules (octadecyl galactoside, octadecyl lactoside, cholesteryl galactoside, cholesteryl lactoside) bearing galactose residues were synthesized according to the published method^[23,24] with some modifications. Hydrophilic groups were galactose and lactose, and hydrophobic groups were octadecanol and cholesterol. Structure confirmation was made through element analysis, nuclear magnetic resonance and mass spectrum (data not shown).

Preparation of liposome

Targeting molecule: DC-chol:DOPE (optimum:6:4 molar ratio) was dissolved in the solvent mixture of ethanol/chloroform

(1:1 v/v), evaporated to a thin film in a rotating evaporator, resuspended in the sterile PBS buffer (pH 7.4) and incubated overnight at 4 °C with gentle stirring. The suspension was sonicated in a bath sonicator for 30 minutes and passed through a polycarbonate membrane (pore diameter 0.4 µm) filter for sterility and granular uniformity. The particle size of the liposomes was measured in a dynamic light scattering spectrophotometer (LS-900, Otsuka Electronics, Osaka, Japan). Lipid concentration in stock solution was determined by phosphorus assay.

Plasmid transfection experiment

Cells (HepG2, GLC) were maintained in DMEM supplement with 10% FBS at 37 °C under an atmosphere of 5% CO₂ in air. The cells were seeded onto a 96-well plate at a density of 10⁴/well and cultivated in 0.2 mL DMEM supplemented with 10% FBS. After 24 h, the culture medium was replaced with DMEM containing plasmid DNA/liposome complexes. Five hours later, the incubation medium was replaced again with DMEM supplemented with 10% FBS and incubated for an additional period of 36 h. The cells were then collected and washed with PBS buffer twice, mixed with 30 µL/well cell lysis solution. Ten minutes later, 100 µL/well luciferase substrate buffer was added and the light produced was immediately measured using a luminometer. The activity was indicated as the relative light units per mg protein. The protein content of the cell suspension was determined by a modified Lowry method using BSA as a standard. In the experiment of competitive inhibition of receptors, the galactose/glucose solution was added 5 minutes before plasmid DNA/liposome complexes, and all other procedures were the same. All assays were performed in triplicate.

Red blood cell hemolysis experiment

A series of 0.1 mol/L PBS buffer with gradient pH value (4.0, 5.0, 6.0, 7.0, 8.0) were prepared. Eighty µL 1% (v/v) newly prepared chicken red blood cell suspension and 20 µL plasmid DNA/liposome complexes (1:5 wt/wt, lipid concentration: 0.5 µg/µL) were mixed in 100 µL 0.1M PBS buffer of different pH value. The mixture was shaken at 37 °C, and an aliquot of suspension was taken at the given time periods (10 min, 30 min and 90 min), centrifuged at 1 000×g. Absorbance value of the supernatant was measured at wavelength 540nm in a photometer (Multiscan MS). Controls were set as follows:
Parallel control: 100 µL PBS buffer + 80 µL 1% (v/v) RBC + 20 µL saline;
Negative control: 120 µL saline + 80 µL 1% (v/v) RBC.

In vitro cytotoxicity assay

DNA/liposome (1:5 wt/wt) complexes were diluted with DMEM supplemented with 2% FBS in an index gradient way (index number: 2, initial lipid concentration: 0.5 µg/µL). HepG2 cells were seeded onto a 96-well plate at a density of 10⁴/well and cultivated in 0.2 mL DMEM supplemented with 10% FBS. After 24 h, the culture medium was replaced with DMEM containing DNA/liposome complexes prepared, and cells were incubated for an additional period of 24 h. Cytotoxicity was evaluated by MTS assay according to the instructions of Celltiter 96@AQ_{ueous} non-radioactive cell proliferation assay test kit, and commercially available cationic liposome Lipofectin served as the control.

Delivery of phosphorothioate ODN to HepG2.9706 cells

Phosphorothioate ODNs were dissolved in DMEM at various concentrations (0.2 µmol/L, 0.4 µmol/L and 0.8 µmol/L), alone or in combination with liposome 18-gal (octadecanol-galactoside:DC-chol:DOPE 1:6:4) at a ratio of 1:5 (wt/wt).

The HepG2.9706 cells seeded onto a 24-well plate at a density of 2×10⁴/well were incubated in DMEM supplement with 10% FBS. After 24 h, the culture medium was replaced with DMEM containing phosphorothioate ODNs. Five hours later, the incubation medium was replaced again with DMEM supplemented with 10% FBS and incubated for an additional period of 24 h. Then the activity of luciferase enzyme was determined as in the plasmid transfection experiment.

RESULTS

Analysis of liposomal transfection efficiency and targeting property

Four types of targeting liposomes (denoted as 18-gal, 18-lac, chol-gal and chol-lac respectively) were prepared by mixing glycolipids with DC-chol/DOPE in a molar ratio of 1:6:4, respectively. A fixed amount of (0.4 µg/well) plasmid DNA encoding a luciferase gene was complexed with these liposomes at a ratio of 1:5 (wt/wt). Figure 1 shows the expression of luciferase gene in HepG2 cells (liver cells) and GLC cells (lung cells lacking asialoglycoprotein receptor) treated with the DNA/liposome complexes. The transfection activity of DC-chol/DOPE was similar in the two cell lines, whereas the transfection activity of the targeting liposomes was significantly higher in HepG2 cells than in GLC cells. When compared with the transfection activity of DC-chol/DOPE in HepG2 cells, there was a significant increase in that of 18-gal ($P<0.01$) while a relatively significant decrease in those of 18-lac and chol-lac ($P<0.05$), and no significant difference was observed between those of chol-gal and DC-chol/DOPE ($P>0.05$). In GLC cells, the transfection activity of the targeting liposomes was significantly lower than that of DC-chol/DOPE ($P<0.05$). These results suggested that the addition of poorly soluble and electrically neutral glycoside molecules could impair the transfection activity of DC-chol/DOPE to some extent. However, asialoglycoprotein receptor-mediated internalization induced by targeting molecules with galactose residues could specifically enhance the transfection activity of targeting liposomes in HepG2 cells, especially that of 18-gal.

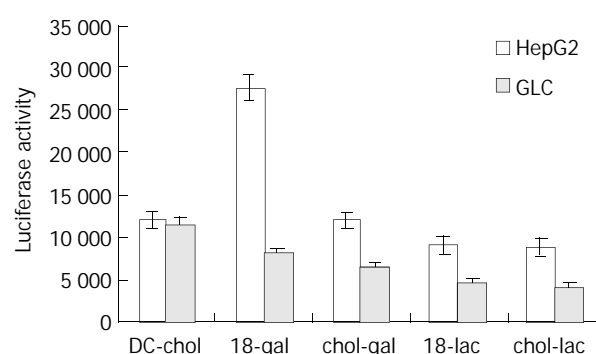


Figure 1 Transfection activity of plasmid DNA/liposome complexes in HepG2 cells and GLC cells. Four types of targeting liposomes (18-gal, 18-lac, chol-gal and chol-lac) were prepared by mixing the targeting molecules with DC-chol/DOPE at a molar ratio of 1:6:4, respectively. A fixed amount (0.4 µg/well) of plasmid DNA was complexed with liposomes at a ratio of 1:5 (wt/wt). Each value represents $\bar{x} \pm s$ ($n=3$).

The following experiments were performed with liposome 18-gal. To optimize the lipid composition, the molar ratio of octadecanol-galactoside to lipid DC-chol/DOPE varied from 0:6:4 to 5:6:4. The liposomal transfection activity showed a bell-shape dependence on the molar percentage of octadecanol-galactoside in liposomal composition. The maximum gene

expression (about 3 times that of DC-chol/DOPE) was observed at the ratio of octadecanol-galactoside:DC-chol:DOPE 1:6:4 (Figure 2). When the molar percentage of octadecanol-galactoside exceeded 20%, the colloidal solution was easy to agglomerate into turbidity, and the liposomal transfection efficiency dropped significantly. Therefore, the maximum molar proportion of octadecanol-galactoside in the liposomal formula should not exceed 20 mol%.

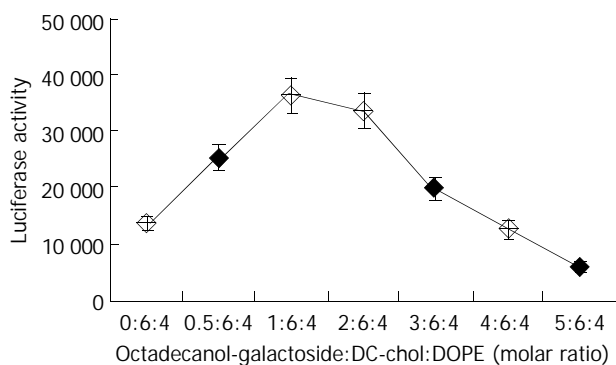


Figure 2 Effect on liposomal transfection activity in HepG2 cells of molar ratio of octadecanol-galactoside (targeting molecules) in liposome composition. The molar ratio of octadecanol-galactoside to lipid DC-chol/DOPE varied from 0:6:4 to 5:6:4. A fixed amount (0.4 $\mu\text{g}/\text{well}$) of plasmid DNA was complexed with liposomes at a ratio of 1:5 (wt/wt). Each value represents $\bar{x} \pm s$ ($n=3$).

A fixed amount of plasmid DNA (0.4 $\mu\text{g}/\text{well}$) was complexed with liposome 18-gal (octadecanol-galactoside:DC-chol:DOPE 1:6:4) in different ratios (1:2.5, 1:5, 1:10, 1:20 wt/wt) to treat HepG2 cells. The greatest gene expression was achieved at the ratio of 1:5-1:10 (Figure 3).

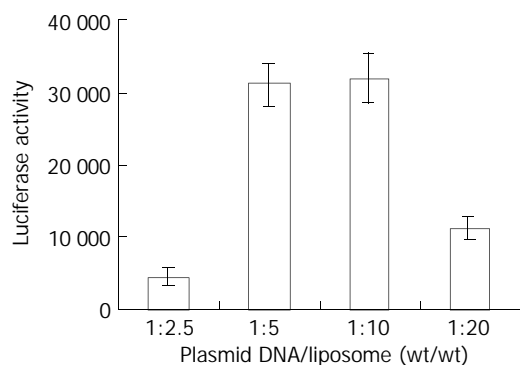


Figure 3 Transfection activity of plasmid DNA/liposome complexes at various ratios (wt/wt) in HepG2 cells. Liposomal composition was octadecanol-galactoside:DC-chol:DOPE 1:6:4 (molar ratio). Plasmid DNA amount was fixed at 0.4 $\mu\text{g}/\text{well}$ in all experiments. Each value represents $\bar{x} \pm s$ ($n=3$).

To investigate whether the cellular uptake of liposome 18-gal in HepG2 cells was partly mediated by asialoglycoprotein receptors, the inhibitory effect of 20 mmol/L galactose solution on the transfection activity of liposome 18-gal of different compositions (the ratio of octadecanol-galactoside to DC-chol/DOPE ranging from 0:6:4 to 2:6:4) was measured. As shown in Figure 4A, the transfection efficiency of liposome 18-gal was significantly inhibited ($P < 0.01$, the mean inhibition rates were 35%, 40% and 46% respectively) in the presence of galactose, but not that of DC-chol/DOPE(6:4). On the other hand, no significant difference was found in the gene expression of DNA/liposome 18-gal complexes in the presence or absence of glucose (Figure 4B).

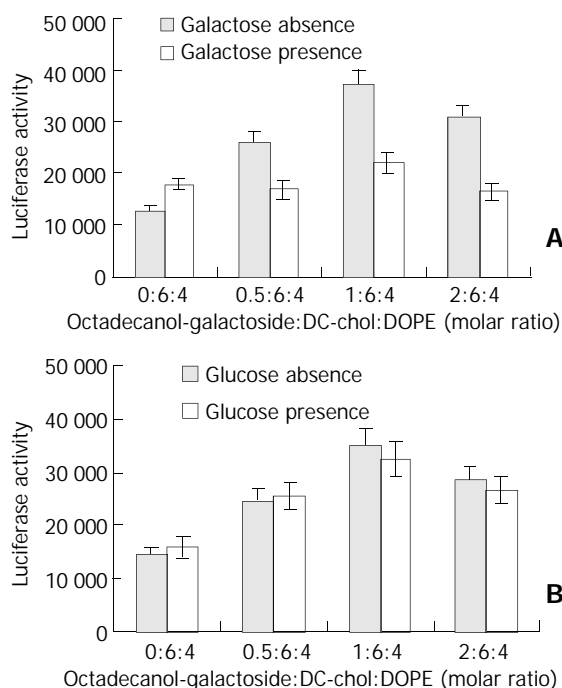


Figure 4 Effect of copresence of 20 mmol/L galactose (A) and glucose (B) on transfection activity of liposomes of different composition in HepG2 cells. Cells were transfected with DNA/liposome complexes in the presence (\square) and absence (\blacksquare) of galactose or glucose. A fixed amount (0.4 $\mu\text{g}/\text{well}$) of plasmid DNA was complexed with liposomes at a ratio of 1:5 (wt/wt). Each value represents $\bar{x} \pm s$ ($n=3$).

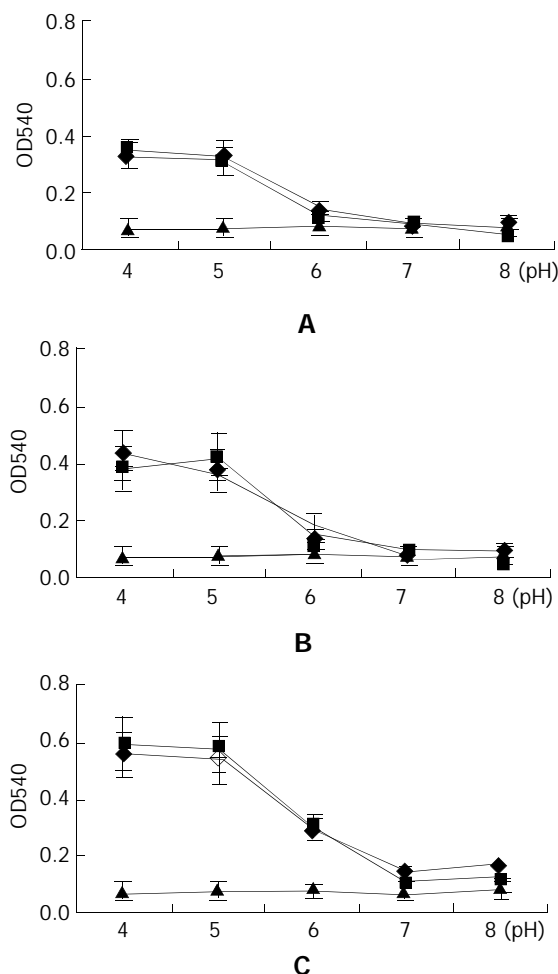


Figure 5 Fusion of plasmid DNA/liposome complexes with chicken hematocyte at various pH values. \blacksquare DC-chol/DOPE

6:4, ◆ octadecanol-galactoside:DC-chol:DOPE 1:6:4, ▲ PBS buffer. Plasmid DNA was complexed with liposomes (lipid concentration: 0.5 $\mu\text{g}/\mu\text{L}$) at a ratio of 1:5 (wt/wt). The release of hemachrome was determined at 10 min (A), 30 min (B) and 90 min (C). Each value represents $\bar{x}\pm s$ ($n=3$).

Characterization of liposomal pH sensitivity

To characterize the liposomal pH sensitivity, plasmid DNA/liposome complexes were mixed with chicken hematocyte in different pH conditions, and release of hemachrome which indicates cell membrane fusion was determined at 10 min, 30 min and 90 min. As shown in Figure 5, there was no difference ($P>0.05$) at the release of hemachrome in the PBS buffer of various pH values. They were close to the negative control (the mean value of negative control: 10 min, 0.076; 30 min, 0.077; 90 min, 0.082). The membrane fusion of red blood cells with DNA/liposome complexes was significantly dependent on the pH value. There was a significant difference between the release amounts of hemachrome in the intervals before and after pH=6 ($P<0.01$).

In vitro cytotoxicity of liposome

The cytotoxicity of liposome 18-gal was tested and compared with that of lipofectin. As shown in Figure 6, within lipid concentrations of 0.5, 0.25, 0.125 and 0.0625 $\mu\text{g}/\mu\text{L}$, the cytotoxicity of lipofectin was significantly higher than that of liposome 18-gal and DC-Chol/DOPE at corresponding concentrations, the latter two only demonstrated certain cytotoxicity at the concentration of 0.5 $\mu\text{g}/\mu\text{L}$ (about 25%). When the concentration that generated 25% cytotoxicity (IC_{25}) was compared, the cytotoxicity of lipofectin was 16 (2^4) times higher than that of the other two liposomes. This results confirmed that DC-Chol/DOPE was a type of cationic liposome with low cytotoxicity, and the addition of octadecanol-galactoside in the liposomal formula did not increase the cytotoxicity.

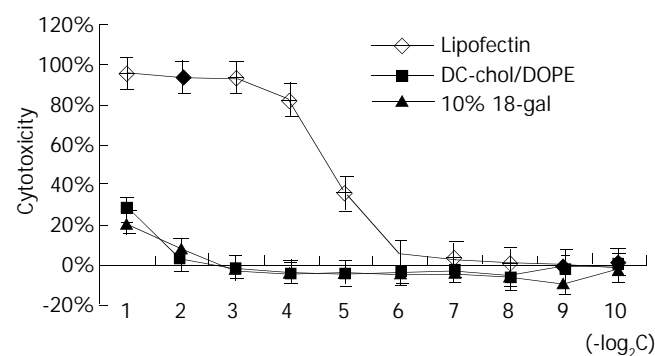


Figure 6 *In vitro* cytotoxicity of cationic liposomes (◆ lipofectin, ■ DC-chol/DOPE 6:4, ▲ octadecanol-galactoside:DC-chol:DOPE 1:6:4). The DNA/liposome (1:5 wt/wt) complexes were diluted with DMEM supplemented with 2% FBS in an index gradient way (initial lipid concentration: 0.5 $\mu\text{g}/\mu\text{L}$). Each value represents $\bar{x}\pm s$ ($n=3$).

Assessment of liposomal activity in mediating phosphorothioate ODNs delivery

HepG2.9706 cells were treated with phosphorothioate ODNs at different concentrations (0.2, 0.4 and 0.8 $\mu\text{mol}/\text{L}$), alone or in combination with liposome 18-gal. As shown in Figure 7, within the range of 0.2-0.8 $\mu\text{mol}/\text{L}$, HCV363a/18-gal complexes had a significantly dose-dependent inhibitory activity on the expression of luciferase gene, and the inhibition rate was 31%, 43% and 54% respectively. HCV363s/18-gal complexes showed stimulating effects on gene expression to some extent. The stimulating effects of sense oligonucleotides on gene expression were also reported by other researchers^[25,26], but

the cause has been unclear. NSC/18-gal complexes had nonspecific inhibitory effects on gene expression of no more than 15%. Treatment with phosphorothioate ODNs alone showed no inhibitory effects on the expression of luciferase gene in HepG2.9706 within the concentration of 0.8 $\mu\text{mol}/\text{L}$.

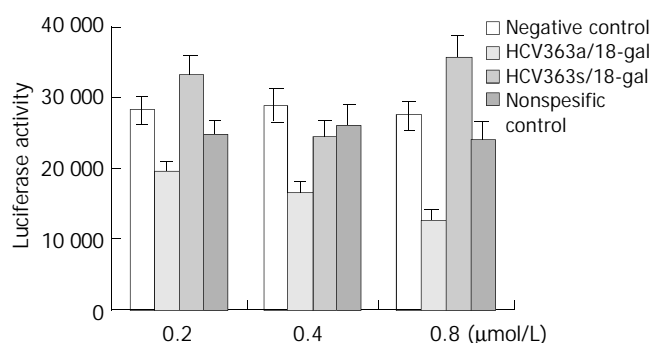


Figure 7 Effects of phosphorothioate ODNs transfected by liposome 18-gal on luciferase gene expression in HepG2.9706 cells. Phosphorothioate ODNs were dissolved in DMEM at various concentrations (0.2 $\mu\text{mol}/\text{L}$, 0.4 $\mu\text{mol}/\text{L}$, 0.8 $\mu\text{mol}/\text{L}$) and complexed with liposome 18-gal (octadecanol-galactoside:DC-chol:DOPE 1:6:4) at a ratio of 1:5 (wt/wt). Each value represents $\bar{x}\pm s$ ($n=3$).

In addition, the effect of administration time on the inhibitory activity of HCV363a/18-gal complexes was also investigated. HepG2.9706 cells were consecutively treated 3 times with HCV363a/18-gal complexes and the activity of luciferase enzyme was determined each time 24h after HCV363a/18-gal complexes were administered. As shown in Figure 8, the inhibitory effects of HCV363a/18-gal complexes increased with the administration time.

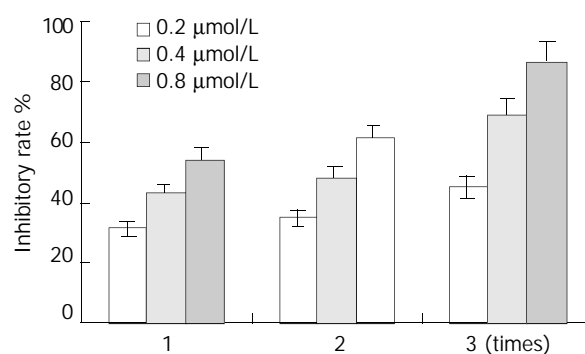


Figure 8 Effect of administration time on inhibitory efficiency of HCV363a in HepG2.9706. Phosphorothioate ODN (HCV363a) was dissolved in DMEM at various concentrations (0.2 $\mu\text{mol}/\text{L}$, 0.4 $\mu\text{mol}/\text{L}$, 0.8 $\mu\text{mol}/\text{L}$) and complexed with liposome 18-gal (octadecanol-galactoside:DC-chol:DOPE 1:6:4) at a ratio of 1:5 (wt/wt). HepG2.9706 cells were consecutively treated 3 times with HCV363a/18-gal complexes and the activity of luciferase enzyme was determined each time 24 h after HCV363a/18-gal complexes was administered. Each value represents $\bar{x}\pm s$ ($n=3$).

DISCUSSION

In the present study, we synthesized targeting molecules with galactose residue and developed a novel formula for a hepatocyte-targeting pH sensitive liposome. Liposome 18-gal was selected with the best transfection activity that was greatly mediated by asialoglycoprotein receptor in HepG2 cells. The hepatocyte specificity of liposome 18-gal was confirmed by the following facts: (1) There was a significant difference

($P < 0.01$) in the transfection efficiencies of DNA/18-gal complexes between HepG2 cells (liver cells) and GLC cells (lung cells lacking asialoglycoprotein receptors). (2) Within a certain proportion (< 20 mol%), the addition of octadecanogalactoside greatly increased the transfection efficiency of DC-chol/DOPE in HepG2 cells (maximum: about 3 folds). This effect was significantly inhibited by galactose but not by glucose. In comparison, the transfection activity of DC-chol/DOPE was similar in the presence or absence of galactose or glucose in HepG2 cells.

In the presence of excessive proportion of targeting molecules (> 20 mol%, molar percentage in liposome composition), the colloidal solution was easy to form turbidity, and the transfection efficiency of prepared liposomes dropped significantly. It was because that a large amount of electrically neutral targeting molecules reduced the positive charge density of cationic liposome. Studies with phospholipid containing liposomes have shown that an increase in a glycolipid or gangliosides greater than 10 mol% resulted in the solubility of liposome into micelles. Due to the potential shielding of the cationic lipid interaction with plasmid DNA by the carbohydrate head group, a heterogeneous population of mixed micelles could be generated at a high molar percent, thus explaining the bell shaped curve for expression. The poor solubility of glycoside molecules in organic solvent also affected the preparation and property of liposome to some extent.

pH-sensitivity is another important property of liposome, which was considered as a mechanism to amass the enclosed antisense ODN at the action site of cytoplasm^[27-29]. In brief, liposome is selectively uptaken by specific cells based on active targeting mechanism. The pH sensitivity inducing the liposomal escape from endosome/lysosome at low pH value makes the entrapped antisense ODN release at cytoplasm to take action. In the present study, the significant dependence on the pH value of membrane fusion of chicken hematocytes with DNA/liposome complexes confirmed the pH sensitivity of the two liposomes, and the similarity of the two liposomes in the membrane fusion experiment strongly indicated the pH-sensitivity of liposome 18-gal as that of DC-chol/DOPE which has been proved to be a pH sensitive liposome^[30].

Transgenic cell strain HepG2.9706 with permanent expression of luciferase gene is a convenient cell model purposely constructed to evaluate the inhibitory effect of antisense ODNs on the HCV 5' NCR. The comparison between the effects on gene expression of phosphorothioate ODNs with or without liposome 18-gal mediation showed that liposome 18-gal was highly efficient in mediating the delivery of phosphorothioate ODNs into HepG2.9706 cells.

In conclusion, the liposome 18-gal prepared in this study has the desired properties of hepatocyte specificity, pH sensitivity, low cytotoxicity, and high transfection efficiency. It can be further developed as a potential hepatocyte-targeting ODN delivery system.

REFERENCES

- Heintges T, Encke J, zu Putlitz J, Wands JR. Inhibition of hepatitis C virus NS3 function by antisense oligodeoxynucleotides and protease inhibitor. *J Med Virol* 2001; **65**: 671-680
- Robaczewska M, Guerret S, Remy JS, Chemin I, Offensperger WB, Chevallier M, Behr JP, Podhajka AJ, Blum HE, Trepo C, Cova L. Inhibition of hepatitis C viral replication by polyethylenimine-based intravenous delivery of antisense phosphodiester oligodeoxynucleotides to the liver. *Gene Ther* 2001; **8**: 874-881
- Alt M, Eisenhardt S, Serwe M, Renz R, Engels JW, Caselmann WH. Comparative inhibitory potential of differently modified antisense oligodeoxynucleotides on hepatitis C virus translation. *Eur J Clin Invest* 1999; **29**: 868-876
- Alt M, Renz R, Hofschneider PH, Caselmann WH. Core specific antisense phosphorothioate oligodeoxynucleotides as potent and specific inhibitors of hepatitis C viral translation. *Arch Virol* 1997; **142**: 589-599
- Alt M, Renz R, Hofschneider PH, Paumgartner G, Caselmann WH. Specific inhibition of hepatitis C viral gene expression by antisense phosphorothioate oligodeoxynucleotides. *Hepatology* 1995; **22**: 707-717
- Liu Y, Chen Z, He N. Inhibition of hepatitis C virus by antisense oligodeoxynucleotide *in vitro*. *Zhonghua Yixue Zazhi* 1997; **77**: 567-570
- Zabner J. Cationic lipids used in gene transfer. *Adv Drug Deliv Rev* 1997; **27**: 17-28
- Kim JK, Choi SH, Kim CO, Park JS, Ahn WS, Kim CK. Enhancement of polyethylene glycol (PEG)-modified cationic liposome-mediated gene deliveries: effects on serum stability and transfection efficiency. *J Pharm Pharmacol* 2003; **55**: 453-460
- Abra RM, Bankert RB, Chen F, Egilmez NK, Huang K, Saville R, Slater JL, Sugano M, Yokota SJ. The next generation of liposome delivery systems: recent experience with tumor-targeted, sterically-stabilized immunoliposomes and active-loading gradients. *J Liposome Res* 2002; **12**: 1-3
- Mastrobattista E, Koning GA, Storm G. Immunoliposomes for the targeted delivery of antitumor drugs. *Adv Drug Deliv Rev* 1999; **40**: 103-127
- Hyde SC, Southern KW, Gileadi U, Fitzjohn EM, Mofford KA, Waddell BE, Gooi HC, Goddard CA, Hannavy K, Smyth SE, Egan JJ, Sorgi FL, Huang L, Cuthbert AW, Evans MJ, Colledge WH, Higgins CF, Webb AK, Gill DR. Repeat administration of DNA/liposomes to the nasal epithelium of patients with cystic fibrosis. *Gene Ther* 2000; **7**: 1156-1165
- Stopeck AT, Jones A, Hersh EM, Thompson JA, Finucane DM, Gutheil JC, Gonzalez R. Phase II study of direct intralesional gene transfer of allovectin-7, an HLA-B7/beta2-microglobulin DNA-liposome complex, in patients with metastatic melanoma. *Clin Cancer Res* 2001; **7**: 2285-2291
- Hortobagyi GN, Ueno NT, Xia W, Zhang S, Wolf JK, Putnam JB, Weiden PL, Willey JS, Carey M, Branham DL, Payne JY, Tucker SD, Bartholomeusz C, Kilbourn RG, De Jager RL, Sneige N, Katz RL, Anklesaria P, Ibrahim NK, Murray JL, Theriault RL, Valero V, Gershenson DM, Bevers MW, Huang L, Lopez-Berestein G, Hung MC. Cationic liposome-mediated E1A gene transfer to human breast and ovarian cancer cells and its biologic effects: a phase I clinical trial. *J Clin Oncol* 2001; **19**: 3422-3433
- Hui KM, Ang PT, Huang L, Tay SK. Phase I study of immunotherapy of cutaneous metastases of human carcinoma using allogeneic and xenogeneic MHC DNA-liposome complexes. *Gene Ther* 1997; **4**: 783-790
- Gill DR, Southern KW, Mofford KA, Seddon T, Huang L, Sorgi F, Thomson A, MacVinish LJ, Ratcliff R, Bilton D, Lane DJ, Littlewood JM, Webb AK, Middleton PG, Colledge WH, Cuthbert AW, Evans MJ, Higgins CF, Hyde SC. A placebo-controlled study of liposome-mediated gene transfer to the nasal epithelium of patients with cystic fibrosis. *Gene Ther* 1997; **4**: 199-209
- Gao S, Chen J, Xu X, Ding Z, Yang YH, Hua Z, Zhang J. Galactosylated low molecular weight chitosan as DNA carrier for hepatocyte-targeting. *Int J Pharm* 2003; **255**: 57-68
- Kunath K, von Harpe A, Fischer D, Kissel T. Galactose-PEI-DNA complexes for targeted gene delivery: degree of substitution affects complex size and transfection efficiency. *J Control Release* 2003; **88**: 159-172
- Yuan L, He S, Guan C, Pang Q. The preparation and study on hepatic targeting tendency of galactosyl-anti-CD3-McAb in mice. *Huaxi Yike Daxue Xuebao* 2001; **32**: 424-426
- Kawakami S, Yamashita F, Nishikawa M, Takakura Y, Hashida M. Asialoglycoprotein receptor-mediated gene transfer using novel galactosylated cationic liposomes. *Biochem Biophys Res Commun* 1998; **252**: 78-83
- Hara T, Kuwasawa H, Aramaki Y, Takada S, Koike K, Ishidate K, Kato H, Tsuchiya S. Effects of fusogenic and DNA-binding amphiphilic compounds on the receptor-mediated gene transfer into hepatic cells by asialofetuin-labeled liposomes. *Biochim Biophys Acta* 1996; **1278**: 51-58

- 21 **Gao X**, Huang L. A novel cationic liposome reagent for efficient transfection of mammalian cells. *Biochem Biophys Res Commun* 1991; **179**: 280-285
- 22 **Wang XH**, Wang SQ, Li MD, Zhu BZ. Establishment of a HCV 5' NCR transgenic cell model. *Bingdu Xuebao* 1998; **14**: 296-301
- 23 **Smits E**, Ernberts FN, Kellogg RM. Reliable method for the synthesis of aryl b-D-glucopyranosides, using boron trifluoride-diethyl ether as catalysts. *J Chem Soc Perkin Trans* 1996; **2873-2877**
- 24 **Lubineu A**, Queneau Y. Aqueous cycloadditions using gluco-organic substrates 1. stereo- chemical course of the reaction. *J Org Chem* 1987; **52**: 1001-1009
- 25 **Wakita T**, Wands JR. Specific inhibition of hepatitis C virus expression by antisense oligodeoxynucleotides. *In vitro* model for selection of target sequence. *J Biol Chem* 1994; **269**: 14205-14210
- 26 **Chen J**, Simon RP, Nagayama T, Zhu R, Loeffert JE, Watkins SC, Graham SH. Suppression of endogenous bcl-2 expression by antisense treatment exacerbates ischemic neuronal death. *J Cereb Blood Flow Metab* 2000; **20**: 1033-1039
- 27 **Venugopalan P**, Jain S, Sankar S, Singh P, Rawat A, Vyas SP. pH-sensitive liposomes: mechanism of triggered release to drug and gene delivery prospects. *Pharmazie* 2002; **57**: 659-671
- 28 **Simoes S**, Slepishkin V, Duzgunes N, Pedroso de Lima MC. On the mechanisms of internalization and intracellular delivery mediated by pH-sensitive liposomes. *Biochim Biophys Acta* 2001; **1515**: 23-37
- 29 **Simoes S**, Slepishkin V, Pires P, Gaspar R, de Lima MP, Duzgunes N. Mechanisms of gene transfer mediated by lipoplexes associated with targeting ligands or pH-sensitive peptides. *Gene Ther* 1999; **6**: 1798-1807
- 30 **Wrobel I**, Collins D. Fusion of cationic liposomes with mammalian cells occurs after endocytosis. *Biochim Biophys Acta* 1995; **1235**: 296-304

Edited by Ma JY and Wang XL

Effects of estradiol on liver estrogen receptor- α and its mRNA expression in hepatic fibrosis in rats

Jun-Wang Xu, Jun Gong, Xin-Ming Chang, Jin-Yan Luo, Lei Dong, Ai Jia, Gui-Ping Xu

Jun-Wang Xu, Xin-Ming Chang, Ai Jia, Gui-Ping Xu, Department of Gastroenterology, First Hospital of Xi'an Jiaotong University, Xi'an 710061, Shaanxi Province, China

Jun Gong, Jin-Yan Luo, Lei Dong, Department of Gastroenterology, Second Hospital of Xi'an Jiaotong University, Xi'an 710031, Shaanxi Province, China

Supported by the Doctorate Foundation of Xi'an Jiaotong University, No.2001-13

Correspondence to: Dr. Jun-Wang Xu, Department of Gastroenterology, First Hospital of Xi'an Jiaotong University, Xi'an 710061, Shaanxi Province, China. xujw@pub.xaonline.com

Telephone: +86-29-85323507 **Fax:** +86-29-85263190

Received: 2003-05-11 **Accepted:** 2003-06-07

(18.7 \pm 3.8, 23.1 \pm 3.7) fibrotic groups (P <0.05).

CONCLUSION: The increase in hepatic ER and mRNA expression may be part of the molecular mechanisms underlying the suppressive effect of estradiol on liver fibrosis induced by CCl₄ administration.

Xu JW, Gong J, Chang XM, Luo JY, Dong L, Jia A, Xu GP. Effects of estradiol on liver estrogen receptor- α and its mRNA expression in hepatic fibrosis in rats. *World J Gastroenterol* 2004; 10(2): 250-254

<http://www.wjgnet.com/1007-9327/10/250.asp>

Abstract

AIM: Estradiol treatment regulates estrogen receptor (ER) level in normal rat liver. However, little information is available concerning the role of estrogen in regulating liver ER in hepatic fibrosis in rats. The present study was conducted to determine whether estradiol treatment in CCl₄-induced liver fibrosis of female and ovariectomized rats altered liver ER α and its mRNA expression, and to investigate the possible mechanisms.

METHODS: Seventy female rats were divided into seven groups with ten rats in each. The ovariectomy groups were initiated with ovariectomies and the sham operation groups were initiated with just sham operations. The CCl₄ toxic fibrosis groups received 400 mL/L CCl₄ subcutaneously at a dose of 2 mL/kg twice weekly. Estrogen groups were treated subcutaneously with estradiol 1 mg/kg, the normal control group and an ovariectomy group received injection of peanut oil vehicle twice weekly. At the end of 8 weeks, all the rats were killed to detect their serum and hepatic indicators, their hepatic collagen content, and liver ER and ER mRNA expression.

RESULTS: Estradiol treatment in both ovariectomy and sham ovariectomy groups reduced liver levels of ALT (from 658 \pm 220 nkat/L to 311 \pm 146 nkat/L and 540 \pm 252 nkat/L to 314 \pm 163 nkat/L, P <0.05) and AST (from 697 \pm 240 nkat/L to 321 \pm 121 nkat/L and 631 \pm 268 nkat/L to 302 \pm 153 nkat/L, P <0.05), increased serum nitric oxide (NO) level (from 53.7 \pm 17.1 μ mol/L to 93.3 \pm 24.2 μ mol/L and 55.3 \pm 23.1 μ mol/L to 87.5 \pm 23.6 μ mol/L, P <0.05) and hepatic nitric oxide synthase (NOS) activity (from 1.73 \pm 0.71 KU/g to 2.49 \pm 1.20 KU/g and 1.65 \pm 0.46 KU/g to 2.68 \pm 1.17 KU/g, P <0.05), diminished the accumulation of hepatic collagen, decreased centrolobular necrotic areas as well as the inflammatory reaction in rats subjected to CCl₄. The positive signal of ER and ER mRNA distributed in parenchymal and non-parenchymal hepatic cells, especially near the hepatic centrolobular and periportal areas. Ovariectomy decreased ER level (from 10.2 \pm 3.2 to 4.3 \pm 1.3) and ER mRNA expression (from 12.8 \pm 2.1 to 10.9 \pm 1.3) significantly (P <0.05). Hepatic ER and ER mRNA concentrations were elevated after treatment with estradiol in both ovariectomy (15.8 \pm 2.4, 20.8 \pm 3.1) and sham ovariectomy

INTRODUCTION

The progression of various forms of chronic liver diseases is more rapid in men than in women. This has been specifically noted in hepatic cirrhosis and hepatocellular carcinoma^[1-3]. The specific mechanisms underlying these clinical findings are unclear. Hepatic fibrosis is a consequence of severe liver damage, which occurs in many chronic liver diseases as a forerunner to cirrhosis. We recently found^[4] that estradiol treatment inhibited the proliferation of hepatic stellate cells, suppressed hepatic collagen content and reduced hepatic type I collagen in fibrotic rats induced by CCl₄ administration, and thus improved liver fibrosis. The mechanisms of the antifibrogenic effect of estradiol have been hypothesized by an indirect way—a hepatocellular membrane protection and a radical scavenging action.

Chronic fibrotic diseases can differ from each other in etiology. But, in terms of pathogenesis, they share some basic common features^[5]. For instance, three serious chronic diseases—atherosclerosis, glomerulosclerosis, and liver fibrosis—have many properties in common. Therefore, factors that affect the development of atherosclerosis or glomerulosclerosis may affect liver fibrosis by similar mechanisms. Studies showed^[6] that estradiol could suppress atherosclerosis and glomerulosclerosis in rats by directly affecting the estrogen receptor (ER) on smooth muscle cells and mesangial cells. The liver is not considered as a kind of classic estrogen-dependent tissue, as are the breast and uterus, but livers in both male and female rats have shown to contain high affinity, low capacity of ER and respond to estrogen by regulating liver function^[7]. Previous data have shown^[4] that tamoxifen, an antiestrogen agent, acts by occupying the estrogen-binding site of the receptor protein, increases fibrogenesis in CCl₄-induced fibrosis of the liver. It was proposed that estrogen might suppress hepatic fibrosis also by a receptor mechanism. In the liver, ER α is the dominant form of ER, while the other subtype, ER β , has not yet been demonstrated^[8]. Hence, only ER α would be further considered in this paper.

Previously published data indicated that 17 β -estradiol treatment could regulate the levels of ER in normal rat liver^[9]. However, little information is available concerning the role of estrogen in the regulation of liver ER in fibrotic rats. The present study was conducted to determine whether estradiol treatment in CCl₄-induced liver fibrosis of female and

ovariectomy rats altered the liver ER and its mRNA expression, and to investigate the possible mechanisms.

MATERIALS AND METHODS

Animals

Seventy female Sprague-Dawley rats (obtained from the Experimental Animal Holding Unit of Shaanxi Province, China), weighing 209 ± 19 g, with an average age of approximately 10 weeks, were housed in a temperature-humidity-controlled environment with 12 h light-dark cycles (lights on from 07:00 AM to 19:00 PM) and had free access to food and water. They were randomly divided into seven groups with ten rats in each. Ovariectomy groups were initiated with a bilateral ovariectomy and sham operation groups were initiated with just a sham operation. For two CCl₄ toxic fibrosis groups, with bilateral ovariectomy (CCl₄+Ovx) and sham operation (CCl₄), 400 mL/L CCl₄ in peanut oil was injected subcutaneously at a dose of 2 mL/kg twice weekly, and the first dosage was doubled. The two estrogen groups, with bilateral ovariectomy (CCl₄+Ovx+E) and sham operation (CCl₄+E), were treated subcutaneously with estradiol (benzoic estradiol) 1 mg/kg twice weekly (The Ninth Pharmaceutical Factory of Shanghai, China). All of the above four groups were fed with a modified high fat diet containing 5 g/kg cholesterol and 200 g/kg pig oil. CCl₄ and estradiol were used 2 weeks after operation. A control ovariectomy treated group (Ovx+E) was just given estradiol 1 mg/kg twice weekly. The normal control group (Control) and an ovariectomy group (Ovx) were given normal food and water, and received injection of peanut oil vehicle twice weekly. At the end of a 8-week experimental period, all the rats were fasted overnight and sacrificed by cervical dislocation after anaesthetised by intramuscular injection of sodium pentobarbital (40 mg/kg). Blood was collected from the animals and serum was analysed. The livers were removed immediately.

Estimation of serum indicators and hepatic nitric oxide synthase

Activities of serum aspartate aminotransferase (AST) and alanine aminotransferase (ALT) were assayed by a 917-Hitachi automatic analyzer. Serum nitric oxide (NO) and hepatic nitric oxide synthase (NOS) were measured following the instructions of the reagent kit (purchased from Jiancheng Medical Institute, Nanjing, China).

Histopathological study

Liver tissues excised from each rat were fixed in 100 mL/L neutral formalin, embedded in paraffin, and stained with hematoxylin-eosin (HE) and Masson's trichrome. Evaluation of hepatic fibrosis was determined by a semi-quantitative method to assess the degree of histologic injury, applying the following scores^[10,11]: 0, absence of fibrosis; 1, perivenular and/or pericellular fibrosis; 2, septal fibrosis; 3, bridging fibrosis (incomplete cirrhosis); 4, complete cirrhosis.

Immunohistochemical examination for estrogen receptor- α

Liver tissue sections were mounted on slides, deparaffinized in xylene, and rehydrated in alcohol. Estrogen receptor- α (ER α) was assessed and semi-quantitated by immunohistochemistry using a commercial antibody against ER α (Boster, Wuhan, China) followed by DAB detection. For each sample, ten random fields were evaluated for positively stained cells. The results were expressed as the percentage of positive cells to the total number of cells counted.

In situ hybridization for estrogen receptor mRNA of liver tissue

In situ hybridization kit was purchased from Boster Biological

Technology Limited Company (Wuhan, China, No. MK1069 α). In situ hybridization was performed according to the manufacturer's instructions. Briefly, the paraffin embedded serial sections (thickness of 4 μ m) were dried at 80 °C, and their paraffin was removed by xylene and rehydrated with graded ethanol. The sections were acidified in HCl for 30 min, and blocked in 3 mL of 300 mL/L H₂O₂ for 10 min before digestion in proteinase K for 30 min, and then dehydrated with graded ethanol. After prehybridization at 37-40 °C for 2 h, the labeled cDNA probes of ER α were denatured in hybridization buffer at 95 °C for 10 min, then at -20 °C for 10 min, then added into tissues prehybridized at 37 °C overnight. Sections were washed in turn with 2 \times SSC, 1 \times SSC, 0.2 \times SSC, and Buffer I, blocking water was added at room temperature for 20 min, and then mouse anti-digoxin serum at 37 °C for 60 min, biotinylated goat anti-mouse serum at 37 °C for 30 min, SABC at 37 °C for 30 min, finally DAB was added to be stained. After several times of washing, the sections were counterstained with hematoxylin, dehydrated with ethanol, rinsed in xylene and mounted with gum for microscopic examination and photography. For each sample, ten random fields were evaluated for positively stained cells. The results were expressed as the percentage of positive cells to the total number of cells counted.

Statistical analysis

Data were presented as $\bar{x} \pm s$ unless otherwise indicated. Mann-Whitney *u* test for nonparametric and unpaired values, Student's *t*-test or Fisher's exact test was used as appropriate. Results were considered significant when $P < 0.05$.

RESULTS

Estimation of serum indicators and hepatic nitric oxide synthase

At the end of a 8-week experimental period, 5 rats died because of infection at the site of injection and hepatic crack due to improper handling. It was evident that CCl₄ produced a marked increase in the activities of serum ALT and AST in both ovariectomy and sham ovariectomy rats. The extent of increase was lower in sham ovariectomy group than in ovariectomy group, but without statistical significance ($P > 0.05$). CCl₄ plus estradiol in both ovariectomy and sham ovariectomy groups showed a significant decrease in enzyme levels. However, they were still higher than those of control groups. The enzyme levels in the ovariectomy and estradiol treatment groups were similar to those in control group. The levels of serum NO₂⁻/NO₃⁻ and hepatic NOS activity increased significantly in both ovariectomy and sham ovariectomy rats when CCl₄ was injected, especially in estradiol treatment groups (Table 1). Ovariectomy itself had no influence on the above parameters.

Table 1 Serum ALT, AST, NO₂⁻/NO₃⁻ and hepatic NOS activity ($\bar{x} \pm s$)

Group	<i>n</i>	ALT (nkat/L)	AST (nkat/L)	NO ₂ ⁻ /NO ₃ ⁻ (μ mol/L)	NOS (KU/g)
Control	10	35.8 \pm 7.9	64.5 \pm 20.8	21.8 \pm 13.7	0.65 \pm 0.08
Ovx	10	31.6 \pm 6.5	66.4 \pm 18.3	19.3 \pm 11.2	0.54 \pm 0.33
Ovx+E	9	38.5 \pm 11.2	68.4 \pm 21.2	84.8 \pm 24.9 ^{ac}	2.57 \pm 1.06 ^{ac}
CCl ₄	9	540 \pm 252 ^a	631 \pm 268 ^a	55.3 \pm 23.1 ^a	1.65 \pm 0.46 ^a
CCl ₄ +Ovx	10	658 \pm 220 ^a	697 \pm 240 ^a	53.7 \pm 17.1 ^a	1.73 \pm 0.71 ^a
CCl ₄ +E	8	314 \pm 163 ^c	302 \pm 153 ^c	87.5 \pm 23.6 ^c	2.68 \pm 1.17 ^c
CCl ₄ +Ovx+E	9	311 \pm 146 ^c	321 \pm 121 ^c	93.3 \pm 24.2 ^c	2.49 \pm 1.20 ^c

^a $P < 0.05$, vs control; ^c $P < 0.05$, vs CCl₄.

Histopathological changes

The control livers showed a normal lobular architecture with central veins and radiating hepatic cords. Prolonged administration of CCl₄ caused severe pathological damages such as fat accumulation, inflammation, necrosis, and collagen deposition, especially in ovariectomy group. Administration of estradiol reduced the accumulation of hepatic collagen, decreased centrolobular necrotic areas as well as inflammatory reaction in rats subjected to CCl₄. Semi-quantitative hepatic collagen staging scores are shown in Table 2.

Table 2 Effects of ovariectomy and estradiol on histological scores of CCl₄-induced hepatic fibrosis

Group	n	Hepatic fibrosis scores				
		-	+	++	+++	++++
Control	10	10	0	0	0	0
Ovx	10	10	0	0	0	0
Ovx+E	9	9	0	0	0	0
CCl ₄	9	0	2	2	3	1
CCl ₄ +Ovx ^a	10	0	0	2	5	3
CCl ₄ +E ^a	8	0	4	2	1	0
CCl ₄ +Ovx+E ^a	9	0	5	2	2	0

^aP<0.05, vs control.

Immunohistochemical staining and *in situ* hybridization for estrogen receptor- α

By immunohistochemical detection, the positive signal of ER α as brown particles was scattered or diffused only in cytoplasm other than in nuclei of parenchymal (hepatocytes) and non-parenchymal hepatic cells, especially near the hepatic centrolobular and periportal areas. The positive signal of *in situ* hybridization for ER α mRNA also showed brown particles, and distributed in cytoplasm and partly in nuclei (Figure 1).

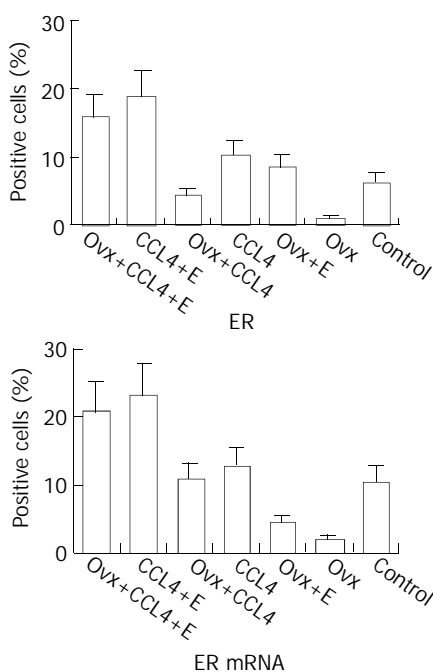


Figure 1 ER α and ER α mRNA in female rat liver.

It showed that livers of female rats contained ER, and ovariectomy decreased ER level and ER mRNA expression significantly ($P<0.05$). Treatment with estradiol at a high dose restored the liver ER and ER mRNA levels. CCl₄ administration

in control and ovariectomized groups was associated with an increase in ER level and ER mRNA expression, but the difference was not significant in control group ($P>0.05$). Hepatic ER and ER mRNA concentrations were elevated significantly after treatment with estradiol in CCl₄ induced fibrotic rats ($P<0.05$, Figures 2 and 3).

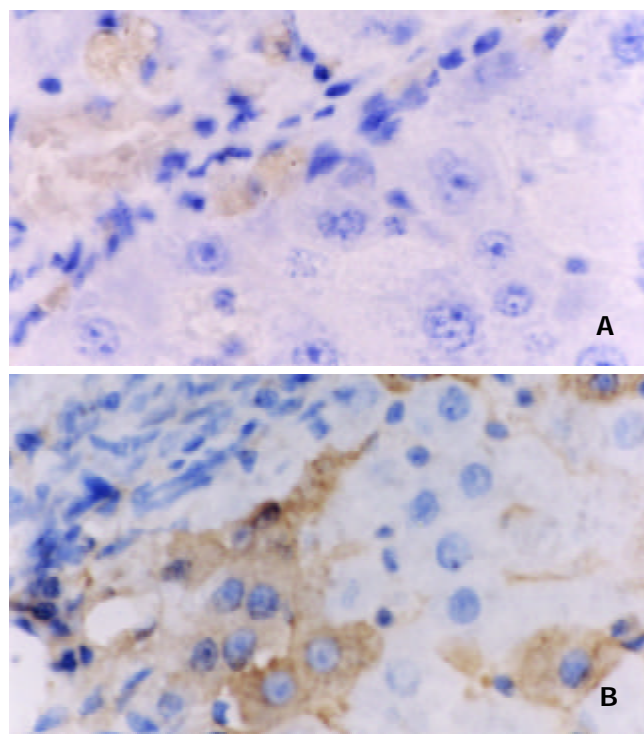


Figure 2 Positive signal of ER in female rat liver (Immunohistochemistry staining PAP method, magnification $\times 400$). 2A: CCl₄ group, 2B: Estradiol treatment group shows increased ER expression compared with 2A.

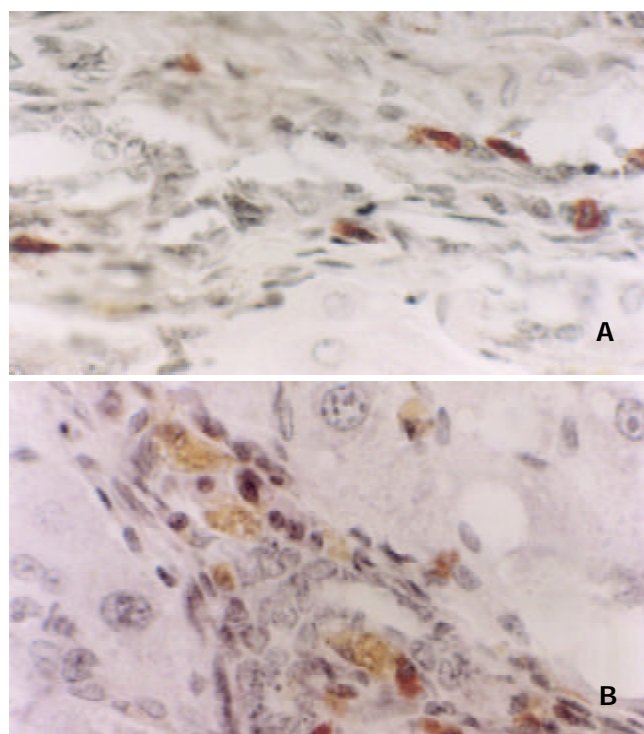


Figure 3 Positive signal of ER mRNA in female rat liver (*in situ* hybridization staining, SP method, magnification $\times 400$). 3A: CCl₄ group, 3B: Estradiol treatment group shows increased ER mRNA expression compared with 3A.

DISCUSSION

Hormone receptors are generally down regulated by high concentrations of their own ligands. This also seems to be the case with ER in reproductive tissues such as the uterus, ovaries, and mammary glands where estrogens are involved in cell growth and differentiation^[12]. In the liver, however, ER has an entirely different function and the hepatic responses to estrogens appear to require high concentrations of estrogens. Some data indicated^[9] that treatment with a low (physiological) dose of estradiol could increase ER and ER mRNA in livers of male rats. But the regulation of hepatic ER and ER mRNA in female rats by estrogen has been reported differently^[13,14]. The majority of studies concerning estrogenic effects have been performed in ovariectomized female rats. Some data showed^[15] that hepatic sinusoidal endothelial cell and Kupffer cell in the livers of female rats contained ER, and they were decreased by ovariectomy. Long-term treatment of 17 β -estradiol elevated the level of ER in hepatic sinusoidal endothelial cell and Kupffer cell in ovariectomized rats. On the other hand, ovariectomy has also been reported to increase ER level and decrease ER mRNA level in hepatocytes from female rats^[12]. This is somewhat divergent to what was seen in this study, where as ovariectomy decreased ER level and ER mRNA expression in parenchymal and non-parenchymal hepatic cells of female rats, and treatment with estradiol at a high dose restored their levels. These observations confirmed a reported increase in hepatic ER mRNA after estrogen treatment in ovariectomized female rats^[16]. An explanation for the mechanism whereby hepatic ER was increased is difficult based on our limited observations. It is possible that the effect of estrogen-treatment on ER levels in ovariectomized female rats was affected indirectly through the pituitary, or by increased hepatic growth hormone receptors. Treatment with 17 β -estradiol in combination with growth hormone and dexamethasone was reported to increase ER levels to eightfold, while estradiol treatment alone had a minimal influence on them in cultured hepatocytes from female rats^[12]. This may suggest that the regulation of hepatic ER is under a more complex control involving other factors.

It has been shown^[17] that prolonged alcohol abuse induced a marked increase in ER levels in livers of both male and female patients, especially in patients who had histological evidence of acute liver damage (alcoholic hepatitis). As we know, CCl₄-induced hepatitis and fibrosis shared several characteristics with human hepatitis and fibrosis of different etiologies^[18-24]. In this study, prolonged administration of CCl₄ induced increases in hepatic ER and ER mRNA expression in female rats, especially in ovariectomized group. The increase extent of ER and ER mRNA was correlated histologically with inflammation, fat accumulation, necrosis, activities of serum ALT and AST, and hepatic collagen disposition. As it is impossible to provide a detailed explanation of the regulation of hepatic ER in normal female rats, we can not establish whether the increase in ER is due CCl₄ administration in our study. Further investigations are thus required to clarify this point. Within these limitations, our data indicate that prolonged CCl₄ administration can affect ER levels and ER mRNA expression in female rat livers.

In our study, hepatic ER and ER mRNA concentrations were significantly elevated after treatment with estradiol in CCl₄-induced fibrotic rats, and the elevation of ER was correlated with a marked decrease in hepatic damage and fibrosis. It suggested that estradiol might suppress hepatic fibrosis by a receptor mechanism. This finding has not been reported previously^[25,26] but is in line with the experimental data obtained from cultured hepatic sinusoidal endothelial cells in rats. In the experiment^[27], ER was demonstrated in hepatic sinusoidal endothelial cells, and estrogen increased NOS activity and upregulated NO production in the cells through

an ER-mediated system, and then regulated the hepatic sinusoidal microcirculation. It has been found that in the liver, NO is produced by hepatic sinusoidal endothelial cells, Kupffer cells, hepatic stellate cells and hepatocytes^[28-32], and NO is synthesized by NOS from L-arginine as a substrate^[33,34]. It was observed that endogenous NO could protect the liver from lipid peroxidation, damage, and fibrosis^[35]. In the present study, estradiol treatment led to a paralleled increase in ER with serum NO and hepatic NOS activity in fibrotic rats. These findings suggest that in liver fibrosis, estrogen may promote NO synthesis through hepatic ER, resulting in improvements of liver damage and fibrosis in rats.

The liver has been found to be extremely sensitive to the action of sex hormones^[4,26], estrogen-dependent regulation of hepatic function could occur through ER present in the liver^[7]. We demonstrated that administration of estradiol elevated ER levels in hepatic fibrotic rats, and ER was distributed in parenchymal (hepatocytes) and non-parenchymal hepatic cells, especially near the hepatic centrolobular and periportal areas where non-parenchymal cells were mainly located. Although we could not identify the exact location of ER in hepatic cells in the present study, we know that the high affinity ER in Kupffer cells of rat liver could exhibit the same characteristics as that presented in hepatocytes^[15]. Therefore, estrogen may modulate Kupffer cell function. Kupffer cells upon stimulation, could produce mediators such as TNF, IL-6 and IL-10, and therefore playing a central role in the regulation of CCl₄-induced liver injury and fibrotic progression^[17,36-42].

As is generally believed that the expression of specific genes and cell responses to steroid hormones are related to the amount of receptors, the increase in hepatic ER and its mRNA as described in this paper may be part of the molecular mechanisms underlying the suppressive effect of estradiol on liver fibrosis induced by CCl₄ administration.

REFERENCES

- 1 **Becker U**, Deis A, Sorensen TI, Gronbaek M, Borch-Johnsen K, Muller CF, Schnohr P, Jensen G. Prediction of risk of liver disease by alcohol intake, sex, and age: a prospective population study. *Hepatology* 1996; **23**: 1025-1029
- 2 **Pinzani M**, Romanelli RG, Magli S. Progression of fibrosis in chronic liver diseases: time to tally the score. *J Hepatol* 2001; **34**: 764-767
- 3 **Yan JC**, Ma JY, Pan BR, Ma LS. Study of hepatitis B in China. *Shijie Huaren Xiaohua Zazhi* 2001; **9**: 611-616
- 4 **Xu JW**, Gong J, Chang XM, Luo JY, Dong L, Hao ZM, Jia A, Xu GP. Estrogen reduces CCl₄-induced liver fibrosis in rats. *World J Gastroenterol* 2002; **8**: 883-887
- 5 **Tan E**, Gurjar MV, Sharma RV, Bhalla RC. Estrogen receptor- α gene transfer into bovine aortic endothelial cells induces eNOS gene expression and inhibits cell migration. *Cardiovasc Res* 1999; **43**: 788-797
- 6 **Kwan G**, Neugarten J, Sherman M, Ding Q, Fotadar U, Lei J, Silbiger S. Effect of sex hormones on mesangial cell proliferation and collagen synthesis. *Kidney Int* 1996; **50**: 1173-1179
- 7 **Porter LE**, Elm MS, Van Thiel DH, Dugas MC, Eagon PK. Characterization and quantitation of human hepatic estrogen receptor. *Gastroenterology* 1983; **84**: 704-712
- 8 **Kuiper GG**, Carlsson B, Grandien K, Enmark E, Haggblad J, Nilsson S, Gustafsson JA. Comparison of the ligand binding specificity and transcript tissue distribution of estrogen receptor α and β . *Endocrinology* 1997; **138**: 863-870
- 9 **Koritnik DR**, Koshy A, Hoversland RC. 17 β -estradiol treatment increases the levels of estrogen receptor and its mRNA in male rat liver. *Steroids* 1995; **60**: 519-529
- 10 **George J**, Rao KR, Stern R, Chandrakasan G. Dimethylnitrosamine-induced liver injury in rats: the early deposition of collagen. *Toxicology* 2001; **156**: 129-138
- 11 **Pilette C**, Rousselet MC, Bedossa P, Chappard D, Oberti F, Rifflet H, Maiga MY, Gallois Y, Cales P. Histopathological evaluation

- of liver fibrosis: quantitative image analysis vs Semi-quantitative scores. Comparison with serum markers. *J Hepatol* 1998; **28**: 439-446
- 12 **Stavreus-Evers AC**, Feyschuss B, Eriksson HA. Hormonal regulation of the estrogen receptor in primary cultures of hepatocytes from female rats. *Steroids* 1997; **62**: 647-654
- 13 **Stavreus-Evers A**, Parini P, Freyschuss B, Elger W, Reddersen G, Sahlin L, Eriksson H. Estrogenic influence on the regulation of hepatic estrogen receptor- α and serum level of angiotensinogen in female rats. *J Steroid Biochem Mol Biol* 2001; **78**: 83-88
- 14 **Ignatenko LL**, Mataradze GD, Rozen VB. Endocrine mechanisms for the formation of sex-related differences in hepatic estrogen receptor content and their significance for the realization of an estrogen effect on angiotensinogen blood level in rats. *Hepatology* 1992; **15**: 1092-1098
- 15 **Vickers AE**, Lucier GW. Estrogen receptor levels and occupancy in hepatic sinusoidal endothelial and Kupffer cells are enhanced by initiation with diethylnitrosamine and promotion with 17 α -ethynylestradiol in rats. *Carcinogenesis* 1996; **17**: 1235-1242
- 16 **Shupnik MA**, Gordon MS, Chin WW. Tissue-specific regulation of rat estrogen receptor mRNAs. *Mol Endocrinol* 1989; **3**: 660-665
- 17 **Colantoni A**, Emanuele MA, Kovacs EJ, Villa E, Van Thiel DH. Hepatic estrogen receptors and alcohol intake. *Mol Cell Endocrinol* 2002; **193**: 101-104
- 18 **Du WD**, Zhang YE, Zhai WR, Zhou XM. Dynamic changes of type I, III and IV collagen synthesis and distribution of collagen-producing cells in carbon tetrachloride induced rat liver fibrosis. *World J Gastroenterol* 1999; **5**: 397-403
- 19 **Wu CH**. Fibrodynamics-elucidation of the mechanisms and sites of liver fibrogenesis. *World J Gastroenterol* 1999; **5**: 388-390
- 20 **Liu HL**, Li XH, Wang DY, Yang SP. Matrix metalloproteinase-2 and tissue inhibitor of metalloproteinase -1 expression in fibrotic rat liver. *World J Gastroenterol* 2000; **6**: 881-884
- 21 **Wei HS**, Li DG, Lu HM, Zhan YT, Wang ZR, Huang X, Zhang J, Cheng JL, Xu QF. Effects of AT1 receptor antagonist, losartan, on rat hepatic fibrosis induced by CCl₄. *World J Gastroenterol* 2000; **6**: 540-545
- 22 **Wang JY**, Zhang QS, Guo JS, Hu MY. Effects of glycyrrhetic acid on collagen metabolism of hepatic stellate cells at different stages of liver fibrosis in rats. *World J Gastroenterol* 2001; **7**: 115-119
- 23 **Zhang YT**, Chang XM, Li X, Li HL. Effects of spironolactone on expression of type I/III collagen proteins in rat hepatic fibrosis. *Shijie Huaren Xiaohua Zazhi* 2001; **9**: 1120-1124
- 24 **Wang LT**, Zhang B, Chen JJ. Effect of anti-fibrosis compound on collagen expression of hepatic cells in experimental liver fibrosis of rats. *World J Gastroenterol* 2000; **6**: 877-880
- 25 **Shimizu I**, Mizobuchi Y, Yasuda M, Shiba M, Ma YR, Horie T, Liu F, Ito S. Inhibitory effect of oestradiol on activation of rat hepatic stellate cells *in vivo* and *in vitro*. *Gut* 1999; **44**: 127-136
- 26 **Liu Y**, Shimizu I, Omoya T, Ito S, Gu XS, Zuo J. Protective effect of estradiol on hepatocytic oxidation damage. *World J Gastroenterol* 2002; **8**: 363-366
- 27 **Sakamoto M**, Uen T, Nakamura T, Hashimoto O, Sakata R, Kin M, Ogata R, Kawaguchi T, Torimura T, Sata M. Estrogen upregulates nitric oxide synthase expression in cultured rat hepatic sinusoidal endothelial cells. *J Hepatol* 2001; **34**: 858-864
- 28 **Huang YQ**, Zhang DZ, Mo JZ, Li RR, Xiao SD. Nitric oxide concentration of esophageal tissues and hemodynamics in cirrhotic rats. *Xin Xiaohuabingxue Zazhi* 1997; **5**: 558-559
- 29 **Yang CJ**, Zhen CE, Yao XX. Study on relationship between plasma NO and sex hormones in patients with hepatic cirrhosis. *Huaren Xiaohua Zazhi* 1998; **6**: 976-978
- 30 **Huang YQ**, Xiao SD, Zhang DZ, Mo J. Nitric oxide synthase distribution in esophageal mucosa and hemodynamic changes in rats with cirrhosis. *World J Gastroenterol* 1999; **5**: 213-216
- 31 **Qin JM**, Zhang YD. Intestinal expressions of eNOSmRNA and iNOSmRNA in rats with acute liver failure. *World J Gastroenterol* 2001; **7**: 652-656
- 32 **Wang X**, Zhong YX, Zhang ZY, Lu J, Lan M, Miao JY, Guo XG, Shi YQ, Ding J, Wu KC, Pan BR, Fan DM. Effect of L-NAME on nitric oxide and gastrointestinal motility alterations in cirrhotic rats. *World J Gastroenterol* 2002; **8**: 328-332
- 33 **Zhou JF**, Cai D, Zhu YG, Yang JL, Peng CH, Yu YH. A study on relationship of nitric oxide, oxidation, peroxidation, lipoperoxidation with chronic chole-cystitis. *World J Gastroenterol* 2000; **6**: 501-507
- 34 **Pei WF**, Xu GS, Sun Y, Zhu SL, Zhang DQ. Protective effect of electroacupuncture and moxibustion on gastric mucosal damage and its relation with nitric oxide in rats. *World J Gastroenterol* 2000; **6**: 424-427
- 35 **Muriel P**. Nitric oxide protection of rat liver from lipid peroxidation, collagen accumulation, and liver damage induced by carbon tetrachloride. *Biochem Pharmacol* 1998; **56**: 773-779
- 36 **Li D**, Zhang LJ, Chen ZX, Huang YH, Whang XZ. Effects of TNF α , IL-6 and IL-10 on the development of experimental rat liver fibrosis. *Shijie Huaren Xiaohua Zazhi* 2001; **9**: 1242-1245
- 37 **Jian HQ**, Zhang XL. The mechanisms of hepatic fibrosis. *Shijie Huaren Xiaohua Zazhi* 2000; **8**: 687-689
- 38 **Weng HL**, Cai WM, Liu RH. Animal experiment and clinical study of effect of gamma-interferon on hepatic fibrosis. *World J Gastroenterol* 2001; **7**: 42-48
- 39 **Dai WJ**, Jiang HC. Advances in gene therapy of liver cirrhosis: a review. *World J Gastroenterol* 2001; **7**: 1-8
- 40 **Tang NH**, Chen YL, Wang XQ, Li XJ, Yin FZ, Wang XZ. Construction of IL-2 gene-modified human hepatocyte and its cultivation with microcarrier. *World J Gastroenterol* 2003; **9**: 79-83
- 41 **Li D**, Wang XZ. Relationship of liver fibrosis and TNF α , IL-6 and IL-10. *Shijie Huaren Xiaohua Zazhi* 2001; **9**: 808-810
- 42 **Parola M**, Robino G. Oxidative stress-related molecules and liver fibrosis. *J Hepatol* 2001; **35**: 297-306

Edited by Zhu LH and Wang XL

Expression of liver insulin-like growth factor 1 gene and its serum level in rats with diabetes

Jian-Bo Li, Cheng-Ya Wang, Jia-Wei Chen, Zhen-Qing Feng, Hong-Tai Ma

Jian-Bo Li, Jia-Wei Chen, Department of Endocrinology, First Affiliated Hospital of Nanjing Medical University, Nanjing 210029, Jiangsu Province, China

Cheng-Ya Wang, Molecular Laboratory, First Affiliated Hospital of Nanjing Medical University, Nanjing 210029, Jiangsu Province, China

Zhen-Qing Feng, Hong-Tai Ma, Department of Pathology, Nanjing Medical University, Nanjing 210029, Jiangsu Province, China

Supported by the National Natural Science Foundation of China, No. 39770355

Correspondence to: Dr. Jian-Bo Li, Department of Endocrinology, First Affiliated Hospital of Nanjing Medical University, Nanjing 210029, Jiangsu Province, China. ljbjlx18@yahoo.com.cn

Telephone: +86-25-3718836-6983 **Fax:** +86-25-3724440

Received: 2003-06-04 **Accepted:** 2003-08-16

Abstract

AIM: To explore the effect of diabetic duration and blood glucose level on insulin like growth factor 1 (IGF-1) gene expression and serum IGF-1 level.

METHODS: Diabetes was induced into Sprague Dawley rats by alloxan and then the rats were subdivided into different groups with varying blood glucose level and diabetic duration. The parameters were measured as follows: IGF-1 mRNA by reverse transcriptase- polymerase chain reaction (RT-PCR), IGF-1 peptide and serum IGF-1 concentration by enzyme-linked immunosorbent assay (ELISA).

RESULTS: During early diabetic stage (week 2), in comparison with normal control group (NC), IGF-1 mRNA (1.17 ± 0.069 vs 0.79 ± 0.048 , $P < 0.001$; 1.17 ± 0.069 vs 0.53 ± 0.023 , $P < 0.0005$, respectively), IGF-1 peptide contents [(196.66 ± 14.9) ng·mg⁻¹ vs (128.2 ± 11.25) ng·mg⁻¹, $P < 0.0005$; (196.66 ± 14.9) ng·mg⁻¹ vs (74.43 ± 5.33) ng·mg⁻¹, $P < 0.0001$, respectively] were reduced in liver tissues of diabetic rats. The IGF-1 gene downregulation varied with glucose control level of the diabetic state, and deteriorated gradually further with duration of diabetes. By month 6, hepatic tissue IGF-1 mRNA was 0.71 ± 0.024 vs 1.12 ± 0.056 , $P < 0.001$; 0.47 ± 0.021 vs 1.12 ± 0.056 , $P < 0.0005$, respectively. IGF-1 peptide was (114.35 ± 8.09) ng·mg⁻¹ vs (202.05 ± 15.73) ng·mg⁻¹, $P < 0.0005$; (64.58 ± 3.89) ng·mg⁻¹ vs (202.05 ± 15.73) ng·mg⁻¹, $P < 0.0001$ respectively. Serum IGF-1 was also lowered in diabetic group with poor control of blood glucose. On week 2, serum IGF-1 concentrations were (371.0 ± 12.5) ng·mg⁻¹ vs (511.2 ± 24.7) ng·mg⁻¹, $P < 0.0005$, (223.2 ± 9.39) ng·mg⁻¹ vs (511.2 ± 24.7) ng·mg⁻¹, $P < 0.0001$ respectively. By month 6, (349.6 ± 18.62) ng·mg⁻¹ vs (520.7 ± 26.32) ng·mg⁻¹, $P < 0.0005$, (188.5 ± 17.35) vs (520.7 ± 26.32) ng·mg⁻¹, $P < 0.0001$, respectively. Serum IGF-1 peptide change was significantly correlated with that in liver tissue ($r = 0.99$, $P < 0.001$). Furthermore, No difference was found in the above parameters between diabetic rats with euglycemia and non-diabetic control group.

CONCLUSION: The influence of diabetic status on IGF-1

gene expression in liver tissues is started from early diabetic stage, causing down regulation of IGF-1 expression, and progresses with the severity and duration of diabetic state. Accordingly serum IGF-1 level decreases. This might indicate that liver tissue IGF-1 gene expression is greatly affected in diabetes, thus contributing to reduction of serum IGF-1 level.

Li JB, Wang CY, Chen JW, Feng ZQ, Ma HT. Expression of liver insulin-like growth factor 1 gene and its serum level in rats with diabetes. *World J Gastroenterol* 2004; 10(2): 255-259

<http://www.wjgnet.com/1007-9327/10/255.asp>

INTRODUCTION

Insulin like growth factor-1 (IGF-1) is widely present in tissues of mammalian animals and has a number of bioactivities including regulation of metabolism and enhancement of growth and development of tissues^[1-4]. Recently its research has attracted much attention. IGF-1 may probably be involved in metabolic abnormality and complications associated with diabetes. Liver might be the main source of circulating IGF-1^[1,5]. Recent studies have shown that there was early reduction in hepatic tissue IGF-1 gene expression in experimental diabetes^[6]. However, further investigation on it is lacking. Upon this basis, we further explored the effect of chronic diabetic status on liver tissue IGF-1 gene expression and IGF-1 concentration in the circulation and hoped to help elucidating the pathogenesis of diabetes related disorder of metabolism and complications and lay a basis for premise of intervention.

MATERIALS AND METHODS

Diabetic animal model

Randomly selected Sprague Dawley rats, weighing 180-200 g, were injected *ip*, with alloxan saline solutions at a dose of 240 mg·g⁻¹ body weight. Rats in non-diabetic normal control group (NC group, $n=28$) were injected *ip*, with an equivalent volume of saline solution^[7]. After 48 hours, blood samples were collected. Diabetic model was established in the rats injected with alloxan, whose blood glucose concentration was >20 mmol·L⁻¹ (diabetic group, $n=90$). The mean glucose concentration of the NC group was 5.14 ± 0.91 mmol·L⁻¹. The diabetic group was reassigned into 3 subgroups ($n=30$ for each group): ID-1 group [(4.93 ± 0.72) - (4.88 ± 0.67) mmol·L⁻¹], ID-2 group [(11.4 ± 0.56) - (10.86 ± 0.94) mmol·L⁻¹] and ID-3 group [(18.34 ± 1.03) - (17.50 ± 1.05) mmol·L⁻¹] with sixteen rats in each group based on glucose level regulated by pork regular insulin combined with protamine zinc insulin (2:1) injected subcutaneously. Both blood glucose level and aminofructose level were regularly measured.

Measurement of liver tissue IGF-1 mRNA contents

After rats were anaesthetized, 1 g liver tissue of the rats was taken. The total RNAs from the tissues were extracted by one-step method^[8,9]. Both quantity and purity of the RNA were determined with the 752 spectrophotometer. Through reverse

transcription polymerase chain reaction (RT-PCR), tissue IGF-1 mRNA was semi-quantitated. The RT-PCR kit was provided by Promega Company (USA) and rat β -actin was used as an internal standard^[8]. According to IGF-1 gene sequence, we designed RT-PCR IGF-1 upstream/downstream primer sequences 5' CTTTGC GGGGCTGAGCTGGT 3', 5' CTT CAGCGAGCAGTACA 3', respectively. All the primers were synthesized by Shanghai BioEngineer Company. The following was optimal reaction condition: reverse transcription at 48 °C for 45 min, denaturation of RNA/DNA hybrid and inactivation of reverse transcriptase at 94 °C for 2 min. PCR for 40 cycles, denaturation at 94 °C for 30 s, annealing at 60 °C for 1 min, extension at 68 °C for 2 min, final extension at 68 °C for 7 min. RT-PCR was performed on the Perkin Elmer (USA). The RT-PCR bands were 184 bp IGF-1 cDNA and 357 bp β -actin cDNA, respectively. Electrophoresis was carried out on 2% agarose gel containing ethidium bromide and semi-quantitated on the Gel DOC 1000 densitometry (Bio-RAD, USA). IGF-1 mRNA contents were calculated and expressed as cDNA relative densitometric units (ratio of IGF-1 cDNA/ β -actin).

Measurement of liver tissue IGF-1 peptide contents

One gram liver tissue was excised from each rat, then frozen in liquid nitrogen and homogenized in a mortar. The homogenates were extracted with 1 mmol·L⁻¹ acetic acid (precooled) and centrifuged. The supernatants were collected, then mixed with 0.05 mmol·L⁻¹ Tris·HCl (PH 7.8) to neutralization and finally stored under -70 °C for future use^[10]. An aliquot of the samples treated as above was taken to measure both total protein content by Brodford method and IGF-1 peptide concentration by enzyme linked immunosorbent assay (ELISA, Diagnostic Systems Laboratory, Inc.). DG-3022 type A was used to measure IGF-1 concentration with a maximum absorbance of 450 nm. IGF-1 tissue content was calculated and expressed as IGF-1 ng·mg⁻¹ total protein.

Measurement of serum IGF-1 peptide concentration

Serum samples from rat heart blood were frozen immediately for future analysis. The samples were pre-treated before assessment of IGF-1 peptide serum concentration (ng·ml⁻¹) with the methods used in ELISA^[11].

Statistical analysis

Data values were presented as $\bar{x}\pm s$. Significance of difference between groups was analyzed by one-way analysis of variance, nonparametric *t'* pair test, Wilcoxon test and χ^2 test. *P*<0.05 was considered statistically significant.

RESULTS

Blood glucose metabolic parameters

At the end of experiment, ID-1 group and NC group had no difference in glucose level, amino fructose level, and body weight. Both blood glucose level and fructose level were significantly higher in ID-2 group and especially in ID-3 group when compared with NC group (*P*<0.0001). Significant differences were also found in the above parameters between ID-2 and ID-3 groups (*P*<0.0001). Within each group, there was no significant difference in aminofructose level (Table 1).

Effects of diabetes on tissue IGF-1 gene expression

Two weeks after diabetic model was established, the liver tissue IGF-1 mRNA contents (IGF-1 cDNA/ β -actin cDNA) were decreased in both ID-2 group (*P*<0.001) and ID-3 group (*P*<0.0005) with a drop of 31% and 53% respectively. They were further decreased with progression of diabetes. On month 6, in comparison with NC group, obvious differences were shown in ID-2 group (*P*<0.0005) and ID-3 group (*P*<0.0001) with a drop of 36% and 59%. Between the two diabetic groups with poor diabetic control, ID-3 group had a significantly lower IGF-1 level than ID-2 group. The drop was 5% and 6% at week 2. Between group ID-1 and NC group, there was no significant difference (Table 2, Figure 1).

The change in tissue IGF-1 peptide content (IGF-1 peptide ng·mg⁻¹ total protein) nearly paralleled that in mRNA content. At the 2nd week, compared with NC group, ID-2 group (*P*<0.0005) and ID-3 group (*P*<0.005) showed a decrease of 32%, 62%, respectively. Both were further decreased over the time course, with a drop of 34% and 65% by the end of the 6th month (*P*<0.0001). A drop of 2% and 3% was found at week 2. ID-3 group had a significantly lower IGF-1 level than ID-2 group (*P*<0.001). There was no significant difference between ID-1 and NC groups (Table 2).

Table 1 Glucose metabolic parameters during the experiment

Group	Duration (month)	<i>n</i>	Initial weight (g)	Weight (g)	Blood (mmol·L ⁻¹)	Aminofructose (mmol·L ⁻¹)
NC	0.5	5	198.41±9.76	249.33±16.02	5.14±0.91	0.82±0.07
	2	5	202.53±17.67	351.20±18.23	5.3±0.44	0.85±0.08
	3	6	200.06±13.03	402.05±37.10	4.91±0.26	0.81±0.09
	6	5	199.65±15.22	544.54±30.41	5.21±0.47	0.85±0.05
ID-1	0.5	5	196.25±14.22	254.31±20.97	4.93±0.72	0.79±0.05
	2	4	202.34±19.12	345.75±23.48	5.10±0.62	0.84±0.08
	3	5	196.42±11.41	411.31±47.37	4.88±0.67	0.78±0.06
	6	6	198.68±12.64	538.52±31.62	4.94±0.58	0.84±0.07
ID-2	0.5	5	192.00±5.70	217.00±9.64 ^a	11.4±0.56 ^c	1.02±0.14 ^c
	2	5	199.00±16.73	241.00±16.44 ^c	10.94±1.08 ^c	1.00±0.29 ^c
	3	6	198.66±14.36	256.83±14.98 ^c	10.86±0.94 ^c	0.98±0.08 ^c
	6	5	201.37±14.11	266.24±13.53 ^c	12.13±0.63 ^c	1.10±0.14 ^c
ID-3	0.5	5	208.60±13.08	205.75±15.34 ^b	18.34±1.03 ^{ce}	1.20±0.12 ^{ce}
	2	5	198.60±16.66	192.80±13.35 ^{cd}	17.48±0.62 ^{ce}	1.18±0.21 ^{ce}
	3	5	211.50±11.37	204.8±11.03 ^{ce}	17.50±1.05 ^{ce}	1.21±0.19 ^{ce}
	6	6	204.35±12.34	185.22±14.36 ^{ee}	16.89±0.95 ^{ce}	1.2±0.34 ^{ee}

Data expressed as mean \pm SD. NC, normal control group; ID-1,-2,-3, insulin treatment group. vs NC, ^a*P*<0.0025, ^b*P*<0.001, ^c*P*<0.0001; vs ID-2 (for the same period), ^d*P*<0.001, ^e*P*<0.0001.

Table 2 Liver tissue IGF-1mRNA ,peptide contents and IGF-1serum concentration

Group	Duration (month)	n	Liver tissue mRNA contents*	Liver tissue IGF-1 peptide (ng·mg ⁻¹)**	Serum IGF-1 (ng·ml ⁻¹)
NC	0.5	5	1.15±0.09	196.66±14.9	511.2±24.7
	2	5	1.17±0.069	198.13±15.25	544.6±22.4
	3	6	1.12±0.056	202.05±15.73	525±30.2
	6	5	1.14±0.066	197.11±12.55	520.7±26.32
ID-1	0.5	5	1.20±0.064	196.7±17.4	536±18.1
	2	4	1.21±0.054	204.1±16.5	540.5±32.5
	3	5	1.18±0.047	200.42±14.9	520.2±14.4
	6	6	1.22±0.044	199.38±16.56	536.54±25.14
ID-2	0.5	5	0.79±0.048 ^b	128.2±11.25 ^c	371.0±12.5 ^c
	2	5	0.74±0.028 ^b	121.3±7.27 ^c	366.4±16.0 ^c
	3	6	0.71±0.024 ^{bh}	114.35±8.09 ^{ci}	353.5±22.4 ^{ce}
	6	5	0.68±0.035 ^{bh}	110.38±10.57 ^{ci}	349.6±18.62 ^{ci}
ID-3	0.5	5	0.53±0.023 ^{cf}	74.43±5.33 ^{df}	223.2±9.39 ^{dc}
	2	5	0.49±0.016 ^{cf}	67.4±6.07 ^{df}	205.6±12.7 ^{dc}
	3	5	0.47±0.02 ^{dgi}	64.58±3.89 ^{dgi}	196.4±15.67 ^{dgi}
	6	6	0.44±0.08 ^{dgi}	62.91±4.32 ^{dgi}	188.5±17.35 ^{dgi}

Data expressed as mean ±SD. *IGF-1relative mRNA contents: IGF-1 cDNA/β-actin cDNA, **tissue IGF-1peptide content: IGF-1 ng·mg⁻¹ total protein. ID-1,-2,-3 vs NC (for the same period): ^bP<0.001, ^cP<0.0005, ^dP<0.0001; vs ID-2 group (for the same period): ^eP<0.025, ^fP<0.0025, ^gP<0.001; vs ID-2 (week 2): ^hP<0.05, ⁱP<0.01; vs ID-3 (week 2): ^jP<0.01.

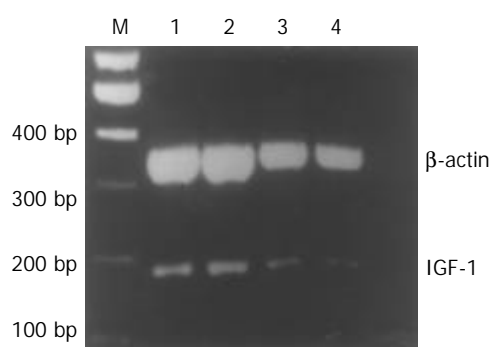


Figure 1 At month 6 of the experiment, liver tissue IGF-1 cDNA/β-actin mRNA RT-PCR product electrophoresis. (1: Control group, 2: ID-1 group, 3: ID-2 group, 4: ID-3 group).

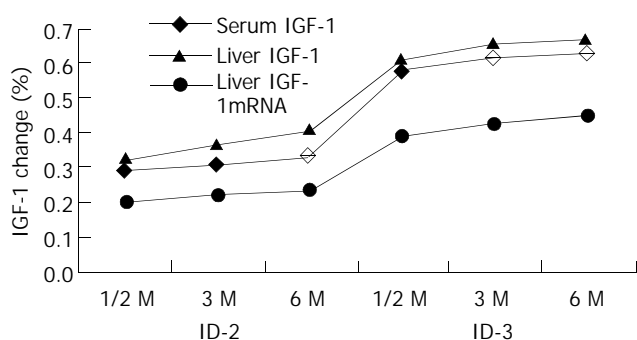


Figure 2 The trend of change in serum IGF-1, liver IGF-1 and mRNA over time course of DM ($r_1=0.99$, $P_1<0.001$; $r_2=0.966$, $P_2<0.001$).

Serum IGF-1 concentration

At week 2, in comparison with NC group, ID-2 and ID-3 groups showed a significant decrease in serum IGF-1 level: 371.0 ± 12.5 ng·mg⁻¹, $P<0.0005$ and 223.2 ± 9.39 ng·mg⁻¹, $P<0.0001$, a drop of 29% and 57%. By the sixth month, serum IGF-1 level was further lowered in both ID-2 and ID-3 groups [349.6 ± 18.62 ng·mg⁻¹, $P<0.0005$; 188.5 ± 17.35 ng·mg⁻¹, $P<0.0001$, respectively], with a fall of 33% and 63%. A drop of 4% and 6% was found at week 2. ID-3 group had a significantly

lower IGF-1 level than ID-2 group ($P<0.001$). There was no significant difference between ID-1 and NC groups.

Relationship between changes in liver IGF-1 mRNA, peptide and serum IGF-1 level

Correlation analysis showed that the trend of serum IGF-1 change was consistent with that occurred in liver IGF-1 peptide ($r_1=0.99$, $P_1<0.001$), and IGF-1mRNA ($r_2=0.99$, $P_2<0.001$) over the time course of diabetes (Figure 2).

DISCUSSION

The study made a preliminary exploration of the effect of chronic diabetic status (e.g. long duration and different glucose levels) on the hepatic IGF-1 gene expression and IGF-1 concentration of circulation.

Insulin like growth factors (IGFs) have similar structures and functions like those of insulin, and can be divided into IGF-1 and IGF-2, the latter of which exerts its biological action on embryonic development and growth. The action of IGF-1 peaks around puberty period and decreases gradually with aging. IGF-1, a single polypeptide with 70 amino acids, was widely expressed in mammal tissues^[1,2]. *In situ* hybridization and immunohistochemical techniques have proven the presence of IGF-1 gene expression (IGF-1 mRNA and peptide) in hepatic cells^[5]. The liver was found to have the highest concentration among all tissues and was probably the main source of circulating IGF-1^[1,5,12], which exert its effect by binding to specific receptors on target cells in endocrine pattern. Human IGF-1 gene is on the long arm of chromosome 12, spanning a minimum of 90 kb which contains 6 exons. Exons 1 and 2 encode 5' untranslated region and amino residue terminal end of IGF-1 peptide, 5' end of Exon 3 encodes carboxyl terminal end of IGF-1 signal peptide. The remaining exon 3 and the main part of exon 4 encode mature IGF-1 peptide including B, C, A, D domains. The 5' end of the remaining exons 4, 5 and 6 encodes signal peptide and 3' untranslated region. Human exon 5 contains stop codon. Gene transcription initiates at exon 1 or 2, varying with tissue specificity. Growth hormone (GH) might affect initiation activity of exon 1 and/or exon 2 to regulate liver IGF-1 gene expression. Insulin may directly regulate liver IGF-1 expression or indirectly by increasing the

number of GH receptors on hepatic cells. Nutritional state and corticosteroid hormones have been found in factors influencing IGF-1 gene expression^[1,5].

In our study, liver tissue IGF-1 gene expression was significantly downregulated in rats with poorly controlled blood glucose (ID-3 and ID-2 groups), as compared to that in rats with normally controlled blood glucose (ID-1 group). Among them, the rats with a higher blood glucose (ID-3) showed more abnormal IGF-1 than those with a relatively low blood glucose (ID-2), the severity of which varied with levels of blood glucose. We continued the observation of the rats with the same level of blood glucose for 6 months after 2 weeks and found that the liver tissue IGF-1 gene expression was gradually decreased with the time course in the rats with hyperglycemia, especially severe hyperglycemia. This showed its association with the progression of diabetes, but to a lower degree. It may indicate the effect of chronic diabetic state on IGF-1 gene expression is less significant than that of the severity of blood glucose. However, the discrepancy in IGF-1 drop rate between the two conditions may reflect a fraction of other tissue's contribution to the circulating IGF-1.

Our study, using RT-PCR technique, demonstrated the early reduction in IGF-1 mRNA contents in liver tissues of alloxan-induced diabetic rats, which was consistent with the previous studies using Northern blot and RT-PCR^[5,6]. However, Veronica MC and Goya *et al* did not study the changes in liver tissue IGF-1 protein and effect of different blood glucose level and duration. We furthermore observed the effect of chronic duration and different severity of hyperglycemia on hepatic IGF-1 gene expressions. In our study, liver tissue IGF-1 gene expression was significantly downregulated in the rats with poorly controlled blood glucose (ID-3 and ID-2 groups), as compared with the rats with normally controlled blood glucose (ID-1 group). Among them, the rats with a higher blood glucose (ID-3) showed more abnormal IGF-1 than those with a relatively low blood glucose (ID-2), the severity of the abnormality varied with the level of blood glucose. We continued the observation of rats with the same level of blood glucose for 6 months after 2 weeks and found that liver tissue IGF-1 gene expression continued to go down gradually with the time course in rats with hyperglycemia, especially severe hyperglycemia. This showed its association with the progression of diabetes, but to a lesser degree. It may indicate the effect of chronic state on IGF-1 gene expression is less significant than severity of hyperglycemia. We are the first to find this. We also found that at translation level, hepatic IGF-1 peptide changed in similar extent as that of mRNA content, indicating the same effect of diabetic status on different translational level. We also demonstrated that serum IGF-1 concentration had a parallel change of hepatic tissue IGF-1. Thus further evidence was provided that the liver might remain to be the main endocrine source of IGF-1 in experimental diabetes. However, the discrepancy in IGF-1 drop rate between the two conditions might reflect a fraction of other tissue's contribution to the circulating IGF-1. The IGF-1 down-regulation was prevented when hyperglycemia was corrected by subcutaneous injection of exogenous insulin, suggesting insulin might be a major regulator of IGF-1 gene expression during diabetes and exclude the possible direct influence of alloxan on IGF-1 gene expression.

Diabetes could result in down-regulation of gene expression, the major factors of which might be insulin secretion deficiency and/or its resistance. Some studies showed that tissue IGF-1 gene expression might be affected by systemic or local factors or both in diabetes, i.e. decrease of GH receptors in target cells and its binding affinity^[13], and by reduced or absent pulsatile pattern secretion of GH, metabolic abnormality of insulin like growth factor binding proteins (IGFBPs)^[6,14], negative nitrogen balance^[15,16] *etc.* All these may probably lead to a decline of

IGF-1. However, the deficiency of insulin or insulin resistance might be the main cause of IGF-1 gene downregulation^[1,17]. In diabetes, IGF-1 in most tissues were down regulated at different degrees, varying with specific tissues^[1,5,18,19]. In the liver it was down regulated^[1,6]. Insulin that corrects hyperglycemia can correct the abnormal IGF-1 gene expression. Our study further supported it. It is known that IGF-1 transcription started at exons 1 and 2 regulated by different initiators and mRNA products that varied in length and affluence with tissue specificity^[1,5,18]. The exact mechanism of insulin controlling IGF-1 gene expression remains to be elucidated.

We successfully established the animal model and found that the hepatic tissue IGF-1 gene expression was down regulated in the diabetic rats, the severity of which depended on glucose level and duration of diabetes. Accordingly, circulating IGF-1 was also decreased. The model established in our experiment is expected to mimic human diabetic status which will help us to interpret the role of IGF-1 in diabetic state. Diabetes can lead to a fall in IGF-1 of endocrine origin. IGF-1 it been found that has a number of bioactivities including mediating action of growth hormone, increasing glucose taken by tissues, inhibiting hepatic glycogenesis, improving insulin sensitivity, decreasing oxidation of lipid, lowering free fatty acids, increasing nucleotide synthesis, proliferation and differentiation of cells^[20-25]. These researches would inevitably help understand the molecular pathogenesis of disturbances of glucose, lipid, protein metabolism associated with diabetes, diabetic peripheral neuropathy and diabetic foot^[4,26-28] and probably might provide the premise of future molecular therapeutic intervention^[29,30].

REFERENCES

- 1 **Pankov YA.** Growth hormone and a partial mediator of its biological action, insulin-like growth factor I. *Biochemistry* 1999; **64**: 1-7
- 2 **Thraikill KM.** Insulin-like growth factor-I in diabetes mellitus: its physiology, metabolic effects, and potential clinical utility. *Diabetes Technol Ther* 2000; **2**: 69-80
- 3 **Cusi K, DeFronzo R.** Recombinant human insulin-like growth factor I treatment for 1 week improves metabolic control in type 2 diabetes by ameliorating hepatic and muscle insulin resistance. *J Clin Endocrinol Metab* 2000; **85**: 3077-3084
- 4 **Zhuang HX, Wuarin L, Fei ZJ, Ishii DN.** Insulin-like growth factor (IGF) gene expression is reduced in neural tissues and liver from rats with non-insulin-dependent diabetes mellitus, and IGF treatment ameliorates diabetic neuropathy. *J Pharmacol Exp Ther* 1997; **283**: 366-374
- 5 **Catanese VM, Scivolino PJ, Lango MN.** Discordant, organ-specific regulation of insulin-like growth factor-1 messenger ribonucleic acid in insulin-deficient diabetes in rats. *Endocrinology* 1993; **132**: 496-503
- 6 **Goya L, Rivero F, Martin MA, Alvarez C, Ramos S, de la Puente A, Pascual-Leone AM.** Liver mRNA expression of IGF-I and IGFBPs in adult undernourished diabetic rats. *Life Sci* 1999; **64**: 2255-2271
- 7 **Okada M, Shibuya M, Yamamoto E, Murakami Y.** Effect of diabetes on vitamin B6 requirement in experimental animals. *Diabetes Obes Metab* 1999; **1**: 221-225
- 8 **Onoue H, Maeyama K, Nomura S, Kasugai T, Tei H, Kim HM, Watanabe T, Kitamura Y.** Absence of immature mast cells in the skin of Ws/Ws rats with a small deletion at tyrosine kinase domain of the c-kit gene. *Am J Pathol* 1993; **142**: 1001-1007
- 9 **Wang P, Li N, Li JS, Li WQ.** The role of endotoxin, TNF-alpha, and IL-6 in inducing the state of growth hormone insensitivity. *World J Gastroenterol* 2002; **8**: 531-536
- 10 **Stiles AD, Sosenko IR, D' Ercole AJ, Smith BT.** Relation of kidney tissue somatomedin-C/insulin-like growth factor I to postnephrectomy renal growth in the rat. *Endocrinology* 1985; **117**: 2397-2401
- 11 **Assy N, Paizi M, Gaitini D, Baruch Y, Spira G.** Clinical implication of VEGF serum levels in cirrhotic patients with or without

- portal hypertension. *World J Gastroenterol* 1999; **5**: 296-300
- 12 **Sjogren K**, Jansson JO, Isaksson OG, Ohlsson C. A transgenic model to determine the physiological role of liver-derived insulin-like growth factor I. *Minerva Endocrinol* 2002; **27**: 299-311
 - 13 **Landau D**, Segev Y, Eshet R, Flyvbjerg A, Phillip M. Changes in the growth hormone-IGF-I axis in non-obese diabetic mice. *Int J Exp Diabetes Res* 2000; **1**: 9-18
 - 14 **Kobayashi K**, Amemiya S, Kobayashi K, Sawanobori E, Mochizuki M, Ishihara T, Higashida K, Miura M, Nakazawa S. The involvement of growth hormone-binding protein in altered GH-IGF axis in IDDM. *Endocr J* 1999; **46**(Suppl): S67-69
 - 15 **Heo YR**, Kang CW, Cha YS. L-Carnitine changes the levels of insulin-like growth factors (IGFs) and IGF binding proteins in streptozotocin-induced diabetic rat. *J Nutr Sci Vitaminol* 2001; **47**: 329-334
 - 16 **McCarty MF**. Hepatic monitoring of essential amino acid availability may regulate IGF-I activity, thermogenesis, and fatty acid oxidation/synthesis. *Med Hypotheses* 2001; **56**: 220-224
 - 17 **Kaytor EN**, Zhu JL, Pao CI, Phillips LS. Physiological concentrations of insulin promote binding of nuclear proteins to the insulin-like growth factor I gene. *Endocrinology* 2001; **142**: 1041-1049
 - 18 **Butler AA**, LeRoith D. Minireview: tissue-specific versus generalized gene targeting of the *igf1* and *igf1r* genes and their roles in insulin-like growth factor physiology. *Endocrinology* 2001; **142**: 1685-1688
 - 19 **Duan J**, Zhang HY, Adkins SD, Ren BH, Norby FL, Zhang X, Benoit JN, Epstein PN, Ren J. Impaired cardiac function and IGF-I response in myocytes from calmodulin-diabetic mice: role of Akt and RhoA. *Am J Physiol Endocrinol Metab* 2003; **284**: E366-376
 - 20 **Scharf JG**, Ramadori G, Dombrowski F. Analysis of the IGF axis in preneoplastic hepatic foci and hepatocellular neoplasms developing after low-number pancreatic islet transplantation into the livers of streptozotocin diabetic rats. *Lab Invest* 2000; **80**: 1399-1411
 - 21 **Cusi K**, DeFronzo R. Recombinant human insulin-like growth factor I treatment for 1 week improves metabolic control in type 2 diabetes by ameliorating hepatic and muscle insulin resistance. *J Clin Endocrinol Metab* 2000; **85**: 3077-3084
 - 22 **Butler ST**, Marr AL, Pelton SH, Radcliff RP, Lucy MC, Butler WR. Insulin restores GH responsiveness during lactation-induced negative energy balance in dairy cattle: effects on expression of IGF-I and GH receptor 1A. *J Endocrinol* 2003; **176**: 205-217
 - 23 **Sjogren K**, Sheng M, Moverare S, Liu JL, Wallenius K, Tornell J, Isaksson O, Jansson JO, Mohan S, Ohlsson C. Effects of liver-derived insulin-like growth factor I on bone metabolism in mice. *J Bone Miner Res* 2002; **17**: 1977-1987
 - 24 **Price JA**, Kovach SJ, Johnson T, Koniaris LG, Cahill PA, Sitzmann JV, McKillop IH. Insulin-like growth factor I is a comitogen for hepatocyte growth factor in a rat model of hepatocellular carcinoma. *Hepatology* 2002; **36**: 1089-1097
 - 25 **Reinmuth N**, Fan F, Liu W, Parikh AA, Stoeltzing O, Jung YD, Bucana CD, Radinsky R, Gallick GE, Ellis LM. Impact of insulin-like growth factor receptor-I function on angiogenesis, growth, and metastasis of colon cancer. *Lab Invest* 2002; **82**: 1377-1389
 - 26 **Busiguina S**, Fernandez AM, Barrios V. Neurodegeneration is associated to changes in serum insulin-like growth factors. *Neurobiol Dis* 2000; **7**(6 Pt B): 657-665
 - 27 **Pierson CR**, Zhang W, Murakawa Y, Sima AA. Early gene responses of trophic factors in nerve regeneration differ in experimental type 1 and type 2 diabetic polyneuropathies. *J Neuropathol Exp Neurol* 2002; **61**: 857-871
 - 28 **Li J**, Wang C, Chen J, Li X, Feng Z, Ma H. The role of insulin-like growth factor-I gene expression abnormality in pathogenesis of diabetic peripheral neuropathy. *Zhonghua Neike Zazhi* 2001; **40**: 93-97
 - 29 **Savage MO**, Camacho-Hubner C, Dunger DB, Ranke MB, Ross RJ, Rosenfeld RG. Is there a medical need to explore the clinical use of insulin-like growth factor I? *Growth Horm IGF Res* 2001; **11** (Suppl A): S65-69
 - 30 **Torrado J**, Carrascosa C. Pharmacological characteristics of parenteral IGF-I administration. *Curr Pharm Biotechnol* 2003; **4**: 123-140

Edited by Wang XL

Long term persistence of T cell memory to HBsAg after hepatitis B vaccination

Ru-Xiang Wang, Greet J. Boland, Jan van Hattum, Gijsbert C. de Gast

Ru-Xiang Wang, Shenyang Center for Disease Control and Prevention, Shenyang 110031, Liaoning Province, China

Greet J. Boland, Jan van Hattum, Department of Gastroenterology, University Hospital Utrecht, the Netherlands

Gijsbert C. de Gast, Netherlands Cancer Institute, Amsterdam, the Netherlands

Correspondence to: Dr. Ru-Xiang Wang, Shenyang Center for Disease Control and Prevention, 37 Qishan Zhong Lu, Huanggu District, Shenyang 110031, Liaoning Province China. rxwtxh@pub.sy.ln.cn

Telephone: +86-24-86853243 **Fax:** +86-24-86863778

Received: 2003-04-12 **Accepted:** 2003-10-11

Abstract

AIM: To determine if the T cell memory to HBsAg can persist for a long time after hepatitis B (HB) vaccination.

METHODS: Thirty one vaccine recipients who were healthcare workers (18 females and 13 males aged 34-58 years) from Utrecht University Hospital, Netherlands, and had previously received a standard course of vaccination for hepatitis B were investigated and another 9 unvaccinated healthy volunteers from the same hospital were used as the control. Blood samples were taken just before the experiment to test serum anti-HBs levels and the subjects were classified into different groups according to their serum titers of anti-HBs and vaccination history. Their peripheral blood mononuclear cells (PBMC) were isolated from freshly heparinized venous blood and the proliferative response of T lymphocytes to the recombinant hepatitis B surface antigen (HBsAg) was investigated.

RESULTS: Positive serum anti-HBs was found in 61.3% (19/31) vaccine recipients and a significant *in vitro* lymphocyte proliferative response to recombinant HBsAg was observed in all the vaccinees with positive anti-HBs. Serum anti-HBs level ≤ 10 IU/L was found in 38.7% (12/31) subjects. In this study, we specially focused on lymphocyte proliferative response to recombinant HBsAg in those vaccine recipients with serum anti-HBsAg less than 10 IU/L. Most of them had received a standard course of vaccination about 10 years before. T lymphocyte proliferative response was found positive in 7 of the 12 vaccine recipients. These results confirmed that HBsAg-specific memory T cells remained detectable in the circulation for a long time after vaccination, even when serum anti-HBs level had been undetectable.

CONCLUSION: The T cell memory to HBsAg can persist for at least 10 years after HB vaccination. Further booster injection is not necessary in healthy responders to HB vaccine.

Wang RX, Boland GJ, van Hattum J, de Gast GC. Long term persistence of T cell memory to HBsAg after hepatitis B vaccination. *World J Gastroenterol* 2004; 10(2): 260-263
<http://www.wjgnet.com/1007-9327/10/260.asp>

INTRODUCTION

Since the introduction of hepatitis B vaccination in the early 1980s, many epidemiological studies have been done to determine the efficacy of the vaccine in eliciting protective immunity against HBV infection. The antibody response to HB vaccine has been found occurring in more than 90% of the healthy vaccinees^[1-15]. Kinetic studies showed serum anti-HBs levels decreased with time following vaccination^[5,9,14,16]. Several demographic and behavioral factors have been found to be associated with a lower rate of antibody response to hepatitis B vaccine^[17,18]. In a considerable percentage of vaccinated persons the anti-HBs level was expected to drop to below 10 IU/L after 5-10 years^[5,19,20]. The decline seemed to be proportional to the antibody titer originally obtained^[15,21]. The necessity of implementing booster injections for those with their anti-HBs levels less than 10 IU/L has remained to be determined^[13,16,20,22,23].

A correlation between *in vivo* antibody production and *in vitro* T cell proliferative response following immunization with HBsAg vaccine has been reported^[24,25]. In previous studies we demonstrated that the B cell memory to HBsAg persisted for a long time after HB vaccination^[26]. The purpose of this study was to determine whether the HBsAg-specific T lymphocyte memory could persist for a long time after HB vaccination especially in vaccine recipients whose serum anti-HBs level was less than 10 IU/L in an attempt to determine the optimal policy of booster vaccination.

MATERIALS AND METHODS

Lymphocytes donor

Forty healthy healthcare personnel from Utrecht University Hospital, the Netherlands participated in the study. Of them, 31 subjects (18 females and 13 males aged 34-58 years) had previously received a standard course of hepatitis B vaccination of 10 or 20 μ g HB vaccine from Merck Sharp & Dohme, West Point, PA, USA (MSD) or Smith Kline and Beecham (SKB, Rixensart, Belgium) at 0, 1, and 6 months about 10 years before. Another 9 unvaccinated healthy volunteers (5 females and 4 males aged 29-57 years) from the same hospital functioned as the control.

Reagents

Recombinant HBsAg free of preservatives was a gift from Merck Sharp & Dohme, West Point, PA, USA. Hepatitis B vaccine used *in vivo* in the study was HB-Vax (MSD). Anti-HBs levels were measured in the study by means of Ausab EIA test (Abbott, Chicago, IL, USA).

Study protocol

The serum from all the volunteers was tested for HBV markers and the subjects were classified into four groups according to their serum titers of anti-HBs and vaccination history. Group I, unvaccinated ($n=9$); group II, vaccinated and with anti-HBs ≤ 10 IU/L ($n=12$); group III, vaccinated and with anti-HBs 10-100 IU/L ($n=6$); group IV vaccinated and with anti-HBs greater than 100 IU/L ($n=13$). The unvaccinated healthy

Table 1 Lymphocyte proliferation to HBsAg in controls and vaccine recipients

Group	<i>n</i>	anti-HBs Titer (IU/L)	Net count (mean)	T cell proliferation positive	ConA stimulation (mean ± SD)	Tetanus + diphtheria (mean ± SD)
1	9	unvaccinated	252 ^a	0/9 (0%)	61 000±29 058	19 075±13 688
2	12	≤10	2 810 ^{a, b}	7/12 (58%)	55 203±25 071	10 651±7 533
3	6	11-100	4 718 ^b	6/6 (100%)	35 273±33 140	19 448±16 171
4	13	>100	12 167	13/13	40 668±20 695	21 266±17 025

net count = mean cpm of medium, ^a*P*-value of statistical comparison of net counts of group II (anti-HBs ≤10 IU/L) with group I (unvaccinated control): *P*=0.0093, ^b*P*-value of statistical comparison of group II with group III + group IV (anti-HBs >10 IU/L): *P*=0.0022 (Mann-Whitney).

volunteers had no evidence of natural HBV infection (negative in the detection of serum HBsAg, anti-HBc or anti-HBs). Blood from all the subjects was collected, serum was tested for anti-HBs levels and peripheral mononuclear cells (PBMCs) were used for lymphocyte proliferation. All the subjects from whom blood was drawn gave their written informed consent for the study. This study was approved by the Medical Ethical Committee of Utrecht Hospital, the Netherlands, under No 92/82.

Cell culture and proliferation assays

PBMCs were isolated from freshly heparinized venous blood by Ficoll-Hypaque density gradient centrifugation. Blood samples were taken just before the experiment.

PBMCs were suspended in RPMI 1640 culture medium supplemented with 10% heat-inactivated pooled human AB serum (Red Cross Blood Bank, Utrecht, the Netherlands), 25 mM HEPES, 2 mmol/L L-glutamine, 50 U/ml penicillin and 50 µg/ml streptomycin. PBMCs (4×10⁵ cells/well) from each sample were prepared in 96-well U-bottom plates and stimulated with different doses of HBsAg (10 ng/mL, 30 ng/mL, 100 ng/mL, 300 ng/mL and 1.0 µg/ml) for 7 days at 37 °C in 95% humidified air with 5% CO₂. Concanavalin A (Con A) at 240 µg/ml, tetanus toxoid and diphtheria toxoid at 3.3 µg/ml served as each sample's positive control for lymphocyte proliferation. Negative control cultures were made by incubating cells in medium alone. During the final 18 h incubation, the cells were pulsed with 1.0 µCi of (³H)-thymidine per well. Sixteen to twenty hours after the cultures were harvested onto glass filters using a multichannel cell harvester the incorporated (³H)-thymidine was measured by liquid scintillation counting. Since there were individual variations in the concentration of maximal stimulation and 300 ng/mL and 1.0 µg/ml of HBsAg gave the maximal stimulation and the least variability in the triplicates, we chose the maximal stimulation at the concentration of 300 ng/mL and 1.0 µg/ml of HBsAg as the optimal result for each subject. Results were expressed as net counts (the value of (³H)-thymidine incorporation of HBsAg stimulation culture minus the value of (³H)-thymidine incorporation of medium). A net count was considered positive if the value of (³H)-thymidine incorporation was higher than the average in the unvaccinated control group + 2 SD.

Statistical method

ANOVA and Mann-Whitney *U*-test were used to compare the results between the different groups and the different concentrations.

RESULTS

HBsAg-induced *in vitro* proliferative response in vaccinated groups

The lymphocyte proliferation correlated with serum antibody levels. The highest proliferative response was observed in those vaccinated with serum anti-HBs greater than 100 IU/L (Table 1).

The difference of proliferative responses between those with serum anti-HBs levels ≤10 IU/L and those with serum anti-HBs level >10 IU/L was statistically significant (*P*=0.0022). The PBMCs from the unvaccinated control group did not respond to HBsAg (in comparison with those with serum anti-HBs levels ≤10 IU/L, *P*=0.0093). As shown in Figure 1, neither the proliferative response to diphtheria and tetanus toxoid, nor the response to mitogen ConA did differ significantly between groups I-IV.

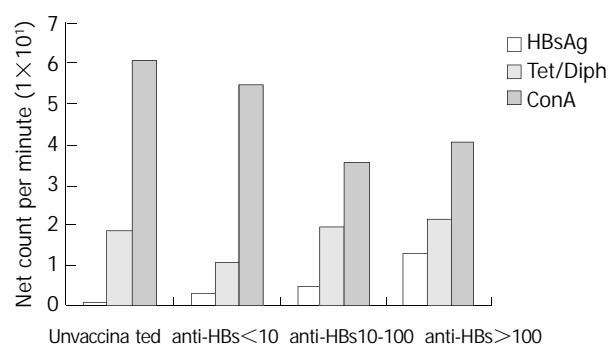


Figure 1 T cell proliferation to HBsAg, ConA and Tet/diph toxoid. The lymphocyte proliferation correlates with serum anti-HBs levels. Neither the proliferative response to diphtheria and tetanus toxoid nor to the mitogen ConA did differ significantly between groups I-IV.

Table 2 Lymphocyte proliferation to HBsAg in vaccine recipients with anti-HBs serum levels ≤10 IU/L

Donor	Sex	Time from vacc. to testing (years)	Time of vaccination	Serum anti-HBs (IU/L)	Net count
1	F	12	1983	4	304
2	F	11	1984	9	2 387 ^a
3	M	12	1983	0	2 853 ^a
4	F	8	1987	0	6 147 ^a
5	F	3	1992	9	11 729 ^a
6	F	9	1986	9	1 769 ^a
7	F	11	1984	0	1 346 ^a
8	M	11	1984	0	2 587 ^a
9	M	7	1988	10	254
10	M	12	1983	2	620
11	F	8	1987	6	475
12	M	11	1984	10	73

^aIf the net count of a subject was more than the net count of unvaccinated control group + 2 SD, it was considered positive. Abbreviation: F = female, M = male.

Lymphocyte proliferative response in vaccine recipients with serum anti-HBs less than 10 IU/L

A positive lymphocyte proliferative response was observed in 7 of the 12 subjects with serum anti-HBs less than 10 IU/L.

Compared with other groups (with anti-HBs >10 IU/L), the mean proliferative response was lower. There was no correlation between the presence of low anti-HBs titer (4-10 IU/L) or the absence of anti-HBs (≤ 2 IU/L) with the proliferative response, nor with the time from vaccination to testing (Table 2).

DISCUSSION

The humoral immune response to hepatitis B after vaccination has been studied systematically. However, duration and the quality of long term protection from HB infection in healthy vaccinees remain a matter of discussion^[1-8]. Especially the T cell response to hepatitis B vaccine has not been fully characterized. Several studies were performed to detect the lymphocyte proliferative response *in vitro* with purified HBsAg, recombinant HBsAg, preS1, preS2 and peptides of HBsAg, but results were not consistent^[26-29]. The immune response to HBsAg *in vitro* was difficult to detect and might not be detected in all vaccinated individuals^[27]. T cell responses *in vitro* after vaccination in individuals responding to vaccination were significantly diminished after 12 weeks, a time when the antibody response was still vigorous^[30]. It has been suggested that there were many variables such as geometry of the wells, the quality of culture media and in particular that of the added serum that influenced the assay results. In addition, the number of cultured PMBCs and duration of the culture might be important^[24]. In our previous experiments, we tested the influence of variables such as cell density, culture time and dose of antigen for lymphocyte proliferation. We observed that 1.0 $\mu\text{g/ml}$ HBsAg, 4×10^5 cells/well, use of human AB⁺ serum and 6 days of culture achieved optimal results. These results confirmed the assay conditions described by G. Leroux-Roels^[8].

To our knowledge, few reports have elucidated the long term efficacy of hepatitis B vaccination on T- cell immunity. In the past, a few groups have induced HBsAg-specific lymphocyte proliferative response in culture of fresh PBMCs from the individuals who were just vaccinated with hepatitis B vaccine or received a booster dose during the experiment^[24,30,31]. In our study 31 healthy persons (healthcare personnel) volunteered to give blood to test the specific response to hepatitis B. All of them were vaccinated several years ago. Our data showed that a lymphocyte proliferative response to HBsAg should be detected *in vitro* in all the vaccine recipients with positive anti-HBs. This result further confirms that *in vivo* humoral and *in vitro* cellular immune responses to HBsAg are closely correlated. In addition, we found that the HB vaccine has the capacity to stimulate the cellular immune response *in vitro*.

However, the most interesting group in our study was the vaccine recipients with serum anti-HBs levels less than 10 IU/L. We observed positive lymphocyte proliferative responses in 7 of the 12 subjects, although the maximal proliferation was lower than that in vaccine recipients with positive serum anti-HBs. We previously reported that an immunological B cell memory to hepatitis B after a vaccination existed in healthcare personnel though serum anti-HBs titers were decreased with time or not measurable in some cases^[32]. The long term efficacy of hepatitis B vaccination was also investigated in China and it was found that the protective efficacy of hepatitis B vaccination was still existed with a low risk of becoming a carrier and a low serum level of neutralizing antibody even at the time of 12 years after vaccination^[9]. These findings suggest that immunity can persist for a long time after vaccination even when the serum antibody levels are below 10 IU/L. It is therefore possible that the T cell immune response plays an important role in protecting against hepatitis B virus infection and becoming a carrier in the absence of antibodies, either directly

or indirectly by providing help to produce antibodies.

Our group previously showed a sensitive *in vitro* method for the study of B cell memory to HBsAg^[33]. A good correlation between *in vitro* mitogen induced IgG anti-HBs spots and immune memory after a booster dose of HB vaccination was observed in naturally infected subjects and vaccine recipients. Our results that 58% of the HB vaccine recipients with anti-HBs ≤ 10 IU/L have kept lymphocyte proliferative responses many years after vaccination could confirm that HB vaccine not only induces humoral immunity but also cell-mediated immunity and that T cell memory often persists longer than serum anti-HBs titers.

We conclude that T cell memory to HBsAg can be demonstrated by lymphocyte proliferation many years after HB vaccination, even in the majority of persons with serum anti-HBs ≤ 10 IU/L. Booster vaccination in those persons is probably not necessary as T cell memory is still existed, which means that the protective antibodies will reappear rapidly or that effector cytotoxic T cells can rapidly eliminate virus infected hepatocytes after exposure to HBV. Our results are of practical value because of high prevalence of hepatitis B in Asia, especially in China.

REFERENCES

- 1 **Liao SS**, Li RC, Li H, Yang JY, Zeng XJ, Gong J, Wang SS, Li YP, Zhang KL. Long-term efficacy of plasma-derived hepatitis B vaccine among Chinese children: a 12-year follow-up study. *World J Gastroenterol* 1999; **5**: 165-166
- 2 **Li H**, Li RC, Liao SS, Yang JY, Zeng XJ, Wang SS. Persistence of hepatitis B vaccine immune protection and response to hepatitis B booster immunization. *World J Gastroenterol* 1998; **4**: 493-496
- 3 **Kojouharova M**, Teoharov P, Bahtchevanova T, Maeva I, Eginlian A, Deneva M. Safety and immunogenicity of a yeast-derived recombinant hepatitis B vaccine in Bulgarian newborns. *Infection* 2001; **29**: 342-344
- 4 **Rendi-Wagner P**, Kundi M, Stemberger H, Wiedermann G, Holzmann H, Hofer M, Wiesinger K, Kollaritsch H. Antibody-response to three recombinant hepatitis B vaccines: comparative evaluation of multicenter travel-clinic based experience. *Vaccine* 2001; **19**: 2055-2060
- 5 **Ozaki T**, Mochizuki H, Ichikawa Y, Fukuzawa Y, Yoshida S, Morimoto M. Persistence of hepatitis B surface antibody levels after vaccination with a recombinant hepatitis B vaccine: a 3-year follow-up study. *J Oral Sci* 2000; **42**: 147-150
- 6 **Jain A**, Mathur US, Jandwani P, Gupta RK, Kumar V, Kar P. A multicentric evaluation of recombinant DNA hepatitis B vaccine of Cuban origin. *Trop Gastroenterol* 2000; **21**: 14-17
- 7 **Al-Faleh FZ**, Al-Jeffri M, Ramia S, Al-Rashed R, Arif M, Rezeig M, Al-Toraif I, Bakhsh M, Mishkhas A, Makki O, Al-Freih H, Mirdad S, AlJuma A, Yasin T, Al-Swailem A, Ayoola A. Seroepidemiology of hepatitis B virus infection in Saudi children 8 years after a mass hepatitis B vaccination programme. *J Infect* 1999; **38**: 167-170
- 8 **Li H**, Li RC, Liao SS, Gong J, Zeng XJ, Li YP. Long-term effectiveness of infancy low-dose hepatitis B vaccine immunization in Zhuang minority Area in China. *World J Gastroenterol* 1999; **5**: 122-124
- 9 **Liu HB**, Meng ZD, Ma JC, Han CQ, Zhang YL, Xing ZC, Zhang YW, Liu YZ, Cao HL. A 12-year cohort study on the efficacy of plasma-derived hepatitis B vaccine in rural newborns. *World J Gastroenterol* 2000; **6**: 381-383
- 10 **Li H**, Wang L, Wang SS, Gong J, Zeng XJ, Li RC, Nong Y, Huang YK, Chen XR, Huang ZN. Research on optimal immunization strategies for hepatitis B in different endemic areas in China. *World J Gastroenterol* 2000; **6**: 392-394
- 11 **Zeng XJ**, Yang GH, Liao SS, Chen AP, Tan J, Huang ZJ, Li H. Survey of coverage, strategy and cost of hepatitis B vaccination in rural and urban areas of China. *World J Gastroenterol* 1999; **5**: 320-323
- 12 **Shokri F**, Jafarzadeh A. High seroprotection rate induced by low doses of a recombinant hepatitis B vaccine in healthy Iranian neonates. *Vaccine* 2001; **19**: 4544-4548
- 13 **Trivello R**, Chiaramonte M, Ngatchu T, Baldo V, Majori S,

- Moschen ME, Simoncello I, Renzulli G, Naccarato R. Persistence of anti-HBs antibodies in health care personnel vaccinated with plasma-derived hepatitis B vaccine and response to recombinant DNA HB booster vaccine. *Vaccine* 1995; **13**: 139-141
- 14 **Whittle HC**, Maine N, Pikington J, Mendy M, Fortuin M, Bunn J, Allison L, Howard C, Hall A. Long-term efficacy of continuing hepatitis B vaccination in infancy in two Gambian villages. *Lancet* 1995; **345**: 1089-1092
- 15 **Jilg W**, Schmidt M, Deinhardt F. Decline of anti-HBs after hepatitis B vaccination and timing of revaccination. *Lancet* 1990; **335**: 173-174
- 16 **Wismans PJ**, Van Hattum J, Mudde GC, Endeman HJ, Poel J, de Gast GC. Is booster injection with hepatitis B vaccination necessary in healthy responders? A study of the immune response. *J Hepatol* 1988; **1**: 1-5
- 17 **Wood RC**, MacDonald KL, White KE, Hedberg CW, Hanson M, Osterholm MT. Risk factors for lack of detectable antibody following hepatitis B vaccination of Minnesota health care workers. *JAMA* 1993; **270**: 2935-2939
- 18 **Roome AJ**, Walsh SJ, Cartter ML, Hadler JL. Hepatitis B vaccine responsiveness in the Connecticut public safety personnel. *JAMA* 1993; **270**: 2931-2934
- 19 **Watson B**, West DJ, Chilkatowsky A, Piercy S, Ioli VA. Persistence of immunologic memory for 13 years in recipients of a recombinant hepatitis B vaccine. *Vaccine* 2001; **19**: 3164-3168
- 20 **Wistrom J**, Ahlm C, Lundberg S, Settergren B, Tarnvik A. Booster vaccination with recombinant hepatitis B vaccine four years after priming with one single dose. *Vaccine* 1999; **17**: 2162-2165
- 21 **Banatvala J**, Van Damme P, Oehen S. Lifelong protection against hepatitis B: the role of vaccine immunogenicity in immune memory. *Vaccine* 2000; **19**: 877-885
- 22 **Garcia Llop L**, Asensi Alcoverro A, Coll Mas P, Ramada Benedito MA, Grafia Juan C. Anti-HBs titers after a vaccination program in children and adolescents. Should a booster dose be given? *An Esp Pediatr* 2001; **54**: 32-37
- 23 **Huang LM**, Chiang BL, Lee CY, Lee PI, Chi WK, Chang MH. Long-term response to hepatitis B vaccination and response to booster in children born to mothers with hepatitis B e antigen. *Hepatology* 1999; **29**: 954-959
- 24 **Leroux-Roels G**, Van Hecke E, Michielsens W, Voet P, Hauser P, Petre J. Correlation between *in vivo* humoral and *in vitro* cellular immune responses following immunization with hepatitis B surface antigen (HBsAg) vaccines. *Vaccine* 1994; **12**: 812-815
- 25 **Are booster immunisations needed for lifelong hepatitis B immunity?** European Consensus Group on Hepatitis B Immunity. *Lancet* 2000; **355**: 561-565
- 26 **De Gast GC**, Houwen B, Nieweg HO. Specific lymphocyte stimulation by purified heat-inactivated hepatitis B antigen. *Br Med J* 1973; **4**: 707-709
- 27 **Ferman A**, Cayzer CJ, Cooksley WG. HBsAg-induced antigen-specific T and B lymphocyte response in chronic hepatitis B virus carriers and immune individuals. *Clin Exp Immunol* 1989; **76**: 222-226
- 28 **Ferrari G**, Penna A, Bertoletti A, Cavalli A, Valli A, Schianchi C, Fiaccadori F. The preS1 antigen of hepatitis B virus is highly immunogenic at T cell level in man. *J Clin Invest* 1989; **84**: 1314-1319
- 29 **Cupps TR**, Tibbles J, Hurmi WM, Miller WJ, Ellis RW, Milich D, Wetter N. *In vitro* T cell immune responses to the PreS2 antigen of the hepatitis B virus envelope protein in PreS2+S vaccine recipients. *J Immunol* 1993; **151**: 3353-3360
- 30 **Deulofeut H**, Iglesias A, Mikeal N, Bing DH, Awdeh Z, Yunis J, Marcus-Bagley D, Kruskall MS, Alper CA, Yunis EJ. Cellular recognition and HLA restriction of a midsequence HBsAg peptide in hepatitis B vaccinated individuals. *Mol Immunol* 1993; **30**: 941-948
- 31 **Degrassi A**, Mariani E, Honorati MC, Roda P, Miniero R, Capelli M, Faccini A. Cellular response and anti-HBs synthesis *in vitro* after vaccination with yeast-derived recombinant hepatitis B vaccine. *Vaccine* 1992; **10**: 617-621
- 32 **Wismans PJ**, van Hattum J, de Gast GC, Bouter KP, Diepersloot RJ, Maikoe T, Mudde GC. A prospective study of *in vitro* anti-HBs producing B cells (spot-ELISA) following primary and supplementary vaccination with a recombinant hepatitis B vaccine in insulin dependent diabetic patients and matched controls. *J Med Virol* 1991; **35**: 216-222
- 33 **Wismans PJ**, van Hattum J, de Gast GC, Endeman HJ, Poel J, Stolk B, Maikoe T, Mudde GC. The spot-ELISA: a sensitive *in vitro* method to study the immune response to hepatitis B surface antigen. *Clin Exp Immunol* 1989; **78**: 75-79

Establishment of transgenic mice carrying gene encoding human zinc finger protein 191

Jian-Zhong Li, Xia Chen, Hua Yang, Shui-Liang Wang, Xue-Lian Gong, Hao Feng, Bao-Yu Guo, Long Yu, Zhu-Gang Wang, Ji-Liang Fu

Jian-Zhong Li, Hua Yang, Shui-Liang Wang, Ji-Liang Fu, Department of Medical Genetics, Second Military Medical University, Shanghai 200433, China

Zhu-Gang Wang, Ji-Liang Fu, Shanghai Nanfang Research Center for Biomodel Organism, Shanghai 201203, China

Long Yu, Genetics Institute, Fudan University, Shanghai 200433, China

Jian-Zhong Li, Xue-Lian Gong, Hao Feng, Bao-Yu Guo, Department of Biochemical Pharmacy, Second Military Medical University, Shanghai 200433, China

Xia Chen, Shanghai Research Center of Biotechnology, Chinese Academy of Sciences, Shanghai 200233, China

Supported by the National Natural Science Foundation of China, No.39830360

Correspondence to: Professor Ji-Liang Fu, Department of Medical Genetics, Second Military Medical University, 800 Xiangyin Road, Shanghai 200433, China. jlfu@guomai.sh.cn

Telephone: +86-21-25070027 **Fax:** +86-21-25070027

Received: 2003-06-16 **Accepted:** 2003-07-24

Wang ZG, Fu JL. Establishment of transgenic mice carrying gene encoding human zinc finger protein 191. *World J Gastroenterol* 2004; 10(2): 264-267

<http://www.wjgnet.com/1007-9327/10/264.asp>

INTRODUCTION

Transcriptional regulation is controlled through interactions between DNA and protein complex, the latter contains transcription factors with highly conserved protein motifs. The most well known motifs are helix-turn-helix, helix-loop-helix, and zinc finger. During cell differentiation and development, each of these domains is involved in the binding of transcription factors to their cognate DNA recognition sites, resulting in specific activation or repression of gene expression^[1].

Zinc finger gene family belongs to one of the largest human gene families and plays an important role in the regulation of transcription. This large family may be divided into many subfamilies such as Cys₂/His₂ type, glucocorticoid receptor, ring finger, GATA-1 type, GAL4 type, and LIM family^[2-4]. In the Cys₂/His₂ type of zinc finger genes, there is a highly conserved consensus sequence TGEKPYX (X representing any amino acid) between adjacent zinc finger motifs. The zinc finger proteins containing this specific structure are named Krüppel-like zinc finger proteins because the structure was first found in *Drosophila* Krüppel protein^[1].

ZNF191 is a putative transcription factor belonging to Krüppel-like zinc finger gene family. It contains four Cys₂/His₂ zinc fingers in its C-terminus, and one SCAN box element (also known as LeR domain for leucine-rich) in its N-terminus^[5-7]. Biochemical binding studies showed SCAN as a selective heterologous and homologous oligomerization domain^[7,8]. Tissue mRNA analysis showed that ZNF191 gene was ubiquitously expressed^[5,9]. ZNF191 can specifically bind to the TCAT repeats (*HUMTH01*) in the first intron of the human tyrosine hydroxylase (*TH*) gene. *HUMTH01* may regulate transcription of *TH* gene, which encodes the rate-limiting enzyme in the synthesis of catecholamines^[9-11]. The disturbances of catecholaminergic neurotransmission have been implicated in neuropsychiatric and cardiovascular diseases^[12-17]. These studies suggested that ZNF191 might be relevant to these diseases. Analysis of amino acid sequence of ZNF191 showed 94% identity with the murine sequence of ZF-12^[18]. Mouse ZF-12 gene likely represents the murine counterpart of human ZNF191. ZF-12 also contains four zinc finger motifs of the Cys₂/His₂ type and one SCAN box. ZF-12 mRNA is expressed during embryonic development and in different organs in adult^[19]. ZF-12 may play an important role in cartilage differentiation and basic cellular processes^[19].

To facilitate the functional studies of ZNF191, we established transgenic mice carrying ZNF191 gene. Four transgenic mice were identified by PCR and Southern blot, and used as founders to establish transgenic mouse lineages. The results of F1 identification with PCR showed that ZNF191 gene could be transmitted stably. RT-PCR analysis demonstrated that ZNF191 gene was expressed in multiple tissues of transgenic mice.

Abstract

AIM: Human zinc finger protein 191 (ZNF191) was cloned and characterized as a Krüppel-like transcription factor, which might be relevant to many diseases such as liver cancer, neuropsychiatric and cardiovascular diseases. Although progress has been made recently, the biological function of ZNF191 remains largely unidentified. The aim of this study was to establish a ZNF 191 transgenic mouse model, which would promote the functional study of ZNF191.

METHODS: Transgene fragments were microinjected into fertilized eggs of mice. The manipulated embryos were transferred into the oviducts of pseudo-pregnant female mice. The offsprings were identified by PCR and Southern blot analysis. ZNF 191 gene expression was analyzed by RT-PCR. Transgenic founder mice were used to establish transgenic mouse lineages. The first generation (F1) and the second generation (F2) mice were identified by PCR analysis. Ten-week transgenic mice were used for pathological examination.

RESULTS: Four mice were identified as carrying copies of ZNF191 gene. The results of RT-PCR showed that ZNF 191 gene was expressed in the liver, testis and brain in one of the transgenic mouse lineages. Genetic analysis of transgenic mice demonstrated that ZNF 191 gene was integrated into the chromosome at a single site and could be transmitted stably. Pathological analysis showed that the expression of ZNF 191 did not cause obvious pathological changes in multiple tissues of transgenic mice.

CONCLUSION: ZNF 191 transgenic mouse model would facilitate the investigation of biological functions of ZNF191 *in vivo*.

Li JZ, Chen X, Yang H, Wang SL, Gong XL, Feng H, Guo BY, Yu L,

Pathological analysis results demonstrated that over-expression of ZNF191 did not cause obvious pathological changes in multiple tissues of the transgenic mice.

MATERIALS AND METHODS

Plasmid

pcDNA3-ZNF191 containing full length ZNF191 cDNA under control of CMV promoter.

Animals

C57, CBA mice were maintained by Shanghai Nanfang Research Center for Biomodel Organism. Transgenic mice were raised and bred in the Laboratory Animal Centre of Second Military Medical University, Shanghai.

Generation of transgenic mice

The 6.5 kb linearized pcDNA3-ZNF191 was purified from agarose gel with QIAGEN gel extraction kit (Qiagen), adjusted to a final concentration of 2 µg/ml in TE buffer and used as DNA solution in microinjection. The first generation (F1) female hybrids of C57 and CBA mice were hormonally superovulated and mated with F1 male hybrids. The next morning fertilized one-cell eggs were collected from the oviduct. The eggs were microinjected with the DNA solution under a microscope. The injected fertilized eggs were transplanted into the oviduct of pseudo-pregnant F1 hybrids of C57 and CBA mice.

Identification of transgenic mice

Founder (G0) mice were identified by PCR and Southern blotting analysis. For PCR analysis, genomic DNA was extracted from tails, and amplified using pcDNA3-ZNF191 primers (P1: 5' -ATGCGGTGGGCTCTATG-3' ; P2: 5' -CGGCTTCCATCCGAGTA-3') which produced a 1 353 bp fragment from mice carrying the transgene. For Southern blotting analysis, genomic DNA was digested overnight with *HindIII* and subjected to electrophoresis in a 0.7% agarose gel and transferred to nylon membrane (Millipore Co., Ltd). Hybridization was performed under stringent conditions with a random-primed (α -³²P)-labeled ZNF191 cDNA probe.

Expression of transgene

One of the transgenic mouse lineages was used to study the expression of transgene. Total RNA was isolated from tissues with TRIzol reagent (Invitrogen), according to the manufacturer's instructions. After digestion of the RNA with DNase I (RNase free), first strand cDNA was synthesized by reverse transcription (Promega). RT-PCR reactions were performed using primers (P3:5' -GTACTAGTAGAAGACATGGT-3' , P4:5' -CGCACACAAAAGAACAATCT-3') for ZNF191 cDNA, which produced a 394 bp fragment. PCR reactions were performed 35 cycles at 95 °C for 45 s, at 55 °C for 1 min, and at 72 °C for 1 min. The PCR products were electrophoresed on 1.2% agarose gel.

Transmission of transgene

To study transmission of the transgene in mice, transgenic founder mice were mated with normal C57 mice to produce the first generation (F1) which was identified by PCR analysis using primers P1/P2. F1 mice of the same founder carrying the transgene were mated between brother and sister mice to produce the second generation (F2). F2 mice were also identified by PCR analysis.

Histological examination

Various organs were dissected from the 10 weeks old mice and fixed in 10% formalin. Sections were obtained from

paraffin-embedded tissue samples, stained with H&E, and examined under a microscope and photographed. Pathological analysis was carried out in the Department of Pathology, Changhai Hospital of Second Military Medical University, Shanghai.

RESULTS

Establishment of ZNF191 transgenic mice

The transgene fragment containing full length ZNF191 cDNA was microinjected into the male pronuclei of 582 fertilized oocytes of F1 hybrids between C57 and CBA mice. The injected eggs were implanted into the oviducts of 27 pseudo-pregnant foster mothers, of which 15 mice became pregnant and gave birth to 81 offsprings. Four offsprings were identified to carry ZNF191 cDNA by PCR and Southern blotting analysis (Figures 1 and 2). The ratio of transgene integration was 4.9% by PCR and Southern blotting analysis.

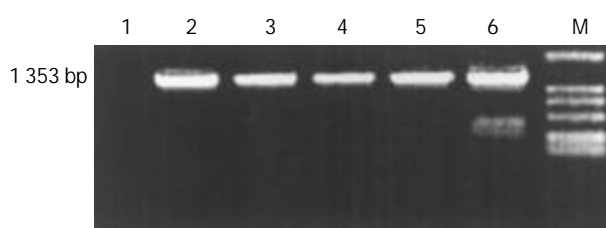


Figure 1 PCR results in transgenic mice. M: DL-2000 Marker, 1: Negative control (wild type mouse), 2-5: Transgenic founder mice, 6: Positive control (pcDNA3-ZNF191).

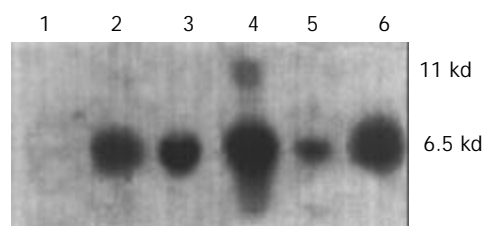


Figure 2 Results of genomic DNA Southern blotting analysis in transgenic mice. 1: Negative control (wild type mouse), 2-5: Transgenic founder mice, 6: Positive control (pcDNA3-ZNF191).

ZNF191 transgene expression in multiple tissues of transgenic mice

The transgene was driven by CMV promoter. To study whether it could be expressed in multiple tissues of transgenic mice, we analysed the tissue expression profile of ZNF191 transgene by RT-PCR. The results (Figure 3) showed that ZNF191 transgene was expressed in the liver, testis and brain.

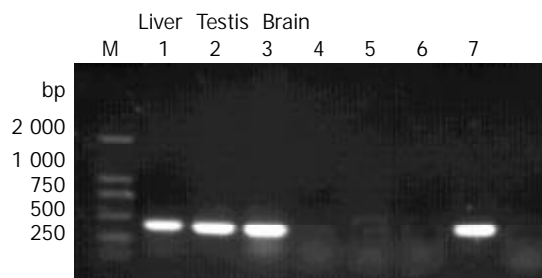


Figure 3 RT-PCR results in transgene expression. M: DL-2000 Marker, 1-3: Transgenic mice tissues, 4-5: Negative control (non-reverse transcribed RNA), 6:C57 mouse liver, 7: Positive control (pcDNA3-ZNF191).

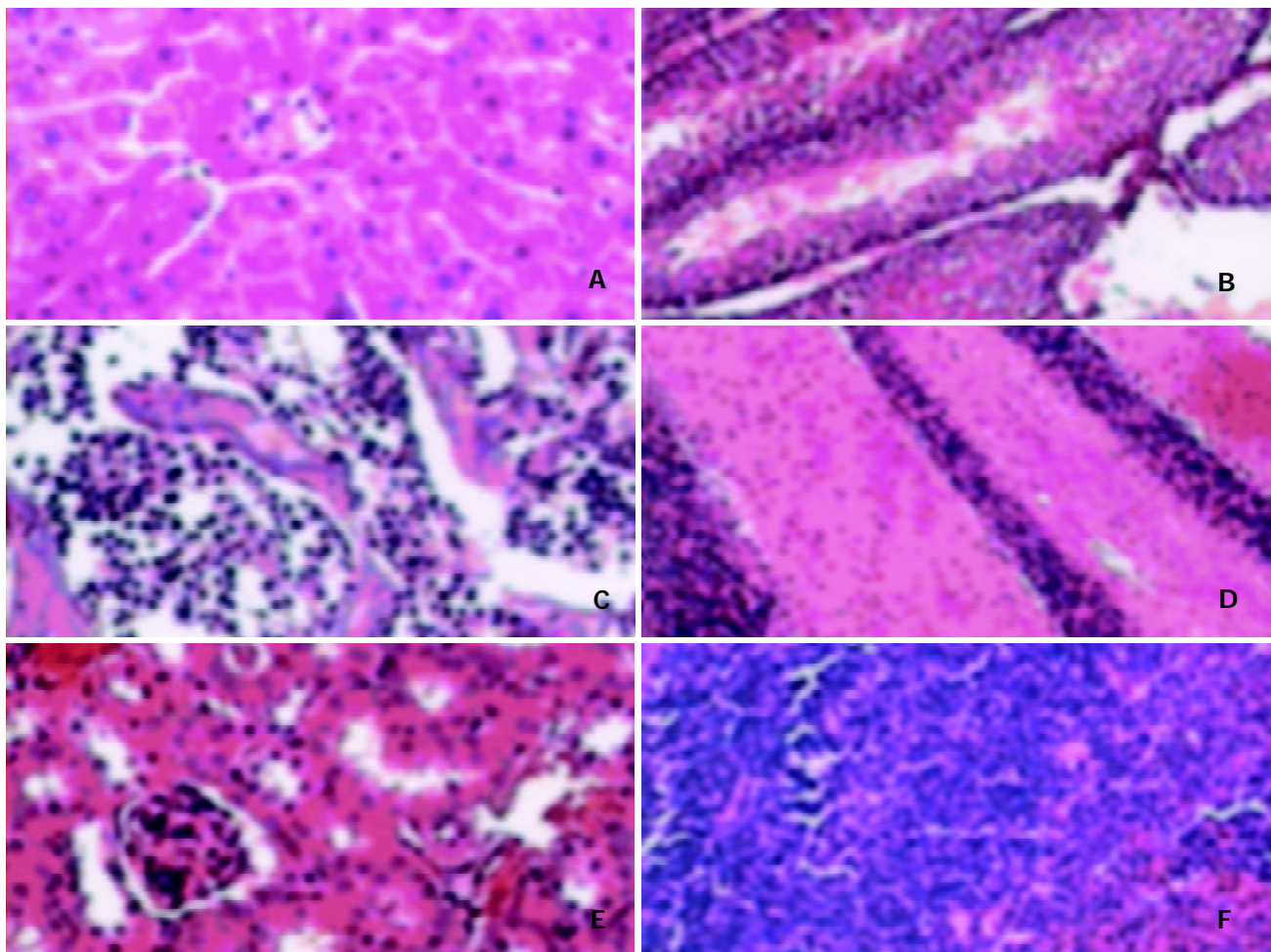


Figure 4 Morphology of tissues of transgenic mouse. A: Liver, B: Testis, C: Marrow, D: Brain, E: Kidney, F: Spleen.

Genetics of transgenic mice

To establish transgenic mouse lineages, the founder mice were mated to C57 mice to produce F1 mice. Among the 43 mice of first generation, 19 were identified as carrying *ZNF191* cDNA transgene by PCR analysis. The ratio of transgene transmission was 44.2%. F1 mice from the same founder were mated with each other to produce F2 mice. Sixty-one out of 86 F2 mice were *ZNF191* transgenic mice, with a transgene transmission ratio of 71%. These results showed that the inheritance of *ZNF191* transgene was in accordance with Mendel's laws, and the transgene was integrated into the chromosome at a single site and could be transmitted stably.

Pathological analysis of tissues

Pathological analysis was carried out to see whether the expression of *ZNF191* transgene would cause any pathological changes in tissues of the transgenic mice. The results (Figure 4) showed there were no obvious pathological changes in the tissues examined. Therefore, so far as the tissues examined, the expression of exogenous *ZNF191* did not cause any pathological consequences in the transgenic mice.

DISCUSSION

Cys₂/His₂ type zinc finger gene family is one of the largest gene families, and each member has repeated zinc finger motifs containing a finger-like structure, in which two cysteines and two histidines could covalently bind to one zinc ion^[20]. It is estimated that in this huge family, about one third of the members are *Krüppel*-like genes as characterized by the presence of highly conserved connecting sequences "TGEKPYX" between

adjacent zinc finger motifs. Substantial evidences indicate that *Krüppel* proteins are important players in many physiological processes as transcriptional regulators. *Krüppel*-like zinc finger genes are key transcriptional repressors in the development of *Drosophila*. In mammalian animals and human, these genes have been found involved in embryo development and carcinogenesis. For example, *KLF6* was reported as a tumor suppressor gene in prostate cancer^[21-23]. Gut-enriched *Krüppel*-like factor (GKLF) was expressed abundantly in epithelial cells of gastrointestinal tract, and deregulation of GKLF was linked to several types of cancer^[24-27].

ZNF191 gene is a novel member of the *Krüppel*-like zinc finger gene family. It was previously cloned from bone marrow and promyelocytic leukemia cell line NB4 using homologous PCR amplification with primers based on conserved sequences of the *Krüppel*-like family of transcription factors^[5]. This first identification suggested that *ZNF191* played a role in hematopoiesis. *ZNF191* has been found to contain a SCAN domain mediating selective protein oligomerization^[6-8]. *ZNF191* specifically binds to *HUMTH01* *in vitro*. The microsatellite *HUMTH01*, located at the first intron of tyrosine hydroxylase (*TH*) gene, is characterized by a TCAT repeated motif and has been used in genetic studies of neuropsychiatric and cardiovascular diseases, in which disturbances of catecholaminergic neurotransmission were implicated^[10-17]. Allelic variations of *HUMTH01* had a quantitative silencing effect on *TH* gene expression *in vitro*, and correlated with quantitative and qualitative changes in the binding by *ZNF191*^[9]. Since TCAT repeated sequence is widespread throughout the genome, this phenomenon might be relevant to the quantitative expression of several genes implicated in complex genetic traits, both

normal and pathological^[28-31]. These studies suggested that ZNF191 might be relevant to neuropsychiatric and cardiovascular diseases. It is vital to have a transgenic or knock-out animal model for the study of the biological role of ZNF191. So far, the attempt to produce ZNF191 transgenic and knock-out mice has not been reported. To our knowledge, we have generated the first transgenic mice carrying ZNF191 transgene and ZF-12^{+/-} mice (to be reported in another paper).

In *in vivo* situation, ZNF191 transcript was found in various organs^[5,9]. Moreover, ZNF191 expression was significantly up-regulated in liver cancer (personal communication), suggesting that ZNF191 might be relevant to hepatocellular carcinogenesis. In this study, ZNF191 transgene was expressed in multiple tissues, which are capable of expressing endogenous ZF-12 *in vivo*. Therefore, the ZNF191 transgenic mouse we generated would be an invaluable animal model not only for the investigation of ZNF191 functions in hepatic tissues, but also in other tissues, which may ultimately reveal the undefined biological functions of ZNF191.

Given that ZNF191 has important biological functions and is relevant to many diseases, it is somewhat unexpected that no pathological changes occurred in the ten-week transgenic mice with ZNF191 over-expression. It is possible that overexpression of exogenous ZNF191 may trigger a negative feedback response to the expression of endogenous ZF-12. It remains to be determined whether the expression of endogenous ZF-12 would change in cells overexpressing exogenous ZNF191. On the other hand, liver cancer, neuropsychiatric and cardiovascular diseases involve many factors and usually have a long incubation time before any pathological phenotypes can be observed. So, it is necessary to continue the investigation into possible pathological changes in a long term follow-up.

In conclusion, we reported here the successful generation of a transgenic mouse model expressing ZNF191 gene. Future studies should focus on the physiological and pathological changes in this mouse model using powerful analytic methods such as microarray comparisons of gene expression profiles among normal, transgenic, ZF-12^{+/-} and ZF-12^{-/-} mice.

REFERENCES

- Klug A, Schwabe JW. Protein motifs 5. Zinc fingers. *FASEB J* 1995; **9**: 597-604
- Borden KL, Freemont PS. The RING finger domain: a recent example of a sequence-structure family. *Curr Opin Struct Biol* 1996; **6**: 395-401
- Hammarstrom A, Berndt KD, Sillard R, Adermann K, Otting G. Solution structure of a naturally-occurring zinc-peptide complex demonstrates that the N-terminal zinc-binding module of the Lasp-1 LIM domain is an independent folding unit. *Biochemistry* 1996; **35**: 12723-12732
- Barlow PN, Luisi B, Milner A, Elliott M, Everett R. Structure of the C3HC4 domain by 1H-nuclear magnetic resonance spectroscopy. A new structural class of zinc-finger. *J Mol Biol* 1994; **237**: 201-211
- Han ZG, Zhang QH, Ye M, Kan LX, Gu BW, He KL, Shi SL, Zhou J, Fu G, Mao M, Chen SJ, Yu L, Chen Z. Molecular cloning of six novel Kruppel-like zinc finger genes from hematopoietic cells and identification of a novel transregulatory domain KRNB. *J Biol Chem* 1999; **274**: 35741-35748
- Collins T, Stone JR, Williams AJ. All in the family: the BTB/POZ, KRAB, and SCAN domains. *Mol Cell Biol* 2001; **21**: 3609-3615
- Stone JR, Maki JL, Blacklow SC, Collins T. The SCAN domain of ZNF174 is a dimer. *J Biol Chem* 2002; **277**: 5448-5452
- Schumacher C, Wang H, Honer C, Ding W, Koehn J, Lawrence Q, Coulis CM, Wang LL, Ballinger D, Bowen BR, Wanger S. The SCAN domain mediates selective oligomerization. *J Biol Chem* 2000; **275**: 17173-17179
- Albanese V, Biguet NF, Kiefer H, Bayard E, Mallet J, Meloni R. Quantitative effects on gene silencing by allelic variation at a tetranucleotide microsatellite. *Hum Mol Genet* 2001; **10**: 1785-1792
- Meloni R, Albanese V, Ravssard P, Treihou F, Mallet J. A tetranucleotide polymorphic microsatellite, located in the first intron of the tyrosine hydroxylase gene, acts as a transcription regulatory element *in vitro*. *Hum Mol Genet* 1998; **7**: 423-428
- Mallet J. The TiPS/TINS lecture. Catecholamines: from gene regulation to neuropsychiatric disorders. *Trends Pharmacol Sci* 1996; **17**: 129-135
- Sharma P, Hingorani A, Jia H, Ashby M, Hopper R, Clayton D, Brown MJ. Positive association of tyrosine hydroxylase microsatellite marker to essential hypertension. *Hypertension* 1998; **32**: 676-682
- Meloni R, Leboyer M, Bellivier F, Barbe B, Samolyk D, Allilaire JF, Mallet J. Association of manic-depressive illness with tyrosine hydroxylase microsatellite marker. *Lancet* 1995; **345**: 932
- Perez de Castro I, Santos J, Torres P, Visedo G, Saiz-Ruiz J, Llinares C, Fernandez-Piqueras J. A weak association between TH and DRD2 genes and bipolar affective disorder in a Spanish sample. *J Med Genet* 1995; **32**: 131-134
- Serretti A, Macchiardi F, Verga M, Cusin C, Pedrini S, Smeraldi E. Tyrosine hydroxylase gene associated with depressive symptomatology in mood disorder. *Am J Med Genet* 1998; **81**: 127-130
- Meloni R, Laurent C, Campion D, Ben Hadjali B, Thibaut F, Dollfus S, Petit M, Samolyk D, Martinez M, Poirier MF, Mallet J. A rare allele of a microsatellite located in the tyrosine hydroxylase gene found in schizophrenic patients. *C R Acad Sci III* 1995; **318**: 803-809
- Wei J, Ramchand CN, Hemmings GP. Possible association of catecholamine turnover with the polymorphic (TCAT)_n repeat in the first intron of the human tyrosine hydroxylase gene. *Life Sci* 1997; **61**: 1341-1347
- Li JZ, Chen X, Wang SL, Sun X, Zhang YZ, Yu L, Fu JL. Cloning, genomic organization and promoter activity of the mouse zinc finger protein gene ZF-12. *Yichuan Xuebao* 2003; **30**: 311-316
- Prost JF, Negre D, Cornet-Javaux F, Cortay JC, Cozzone AJ, Herbage D, Mallein-Gerin F. Isolation, cloning, and expression of a new murine zinc finger encoding gene. *Biochim Biophys Acta* 1999; **1447**: 278-283
- Jacobs GH. Determination of the base recognition positions of zinc fingers from sequence analysis. *EMBO J* 1992; **11**: 4507-4517
- Chen C, Hyytinen ER, Sun X, Helin HJ, Koivisto PA, Frierson HF Jr, Vessella RL, Dong JT. Deletion, mutation, and loss of expression of KLF6 in human prostate cancer. *Am J Pathol* 2003; **162**: 1349-1354
- Narla G, Heath KE, Reeves HL, Li D, Giono LE, Kimmelman AC, Glucksman MJ, Narla J, Eng FJ, Chan AM, Ferrari AC, Martignetti JA, Friedman SL. KLF6, a candidate tumor suppressor gene mutated in prostate cancer. *Science* 2001; **294**: 2563-2566
- Narla G, Friedman SL, Martignetti JA. Kruppel cripples prostate cancer: KLF6 progress and prospects. *Am J Pathol* 2003; **162**: 1047-1052
- Stone CD, Chen ZY, Tseng CC. Gut-enriched Kruppel-like factor regulates colonic cell growth through APC/beta-catenin pathway. *FEBS Lett* 2002; **530**: 147-152
- Wang N, Liu ZH, Ding F, Wang XQ, Zhou CN, Wu M. Down-regulation of gut-enriched Kruppel-like factor expression in esophageal cancer. *World J Gastroenterol* 2002; **8**: 966-970
- Chen ZY, Shie JL, Tseng CC. Gut-enriched Kruppel-like factor represses ornithine decarboxylase gene expression and functions as checkpoint regulator in colonic cancer cells. *J Biol Chem* 2002; **277**: 46831-46839
- Katz JP, Perreault N, Goldstein BG, Lee CS, Labosky PA, Yang VW, Kaestner KH. The zinc-finger transcription factor Klf4 is required for terminal differentiation of goblet cells in the colon. *Development* 2002; **129**: 2619-2628
- Meloni R, Biguet NF, Mallet J. Post-genomic era and gene discovery for psychiatric diseases: there is a new art of the trade? The example of the HUMTH01 microsatellite in the Tyrosine Hydroxylase gene. *Mol Neurobiol* 2002; **26**: 389-403
- Schadt EE, Monks SA, Drake TA, Luskis AJ, Che N, Colinayo V, Ruff TG, Milligan SB, Lamb JR, Cavet G, Linsley PS, Mao M, Stoughton RB, Friend SH. Genetics of gene expression surveyed in maize, mouse and man. *Nature* 2003; **422**: 297-302
- Mackay TF. The genetic architecture of quantitative traits. *Annu Rev Genet* 2001; **35**: 303-339
- Reif A, Lesch KP. Toward a molecular architecture of personality. *Behav Brain Res* 2003; **139**: 1-20

Effects of depression on parameters of cell-mediated immunity in patients with digestive tract cancers

Ke-Jun Nan, Yong-Chang Wei, Fu-Ling Zhou, Chun-Li Li, Chen-Guang Sui, Ling-Yun Hui, Cheng-Ge Gao

Ke-Jun Nan, Yong-Chang Wei, Fu-Ling Zhou, Chun-Li Li, Chen-Guang Sui, Department of Medical Oncology, First Hospital of Xi'an Jiaotong University, Xi'an 710061, Shaanxi Province, China
Ling-Yun Hui, Research Center of Medical Laboratory, First Hospital of Xi'an Jiaotong University, Xi'an 710061, Shaanxi Province, China
Cheng-Ge Gao, Department of Psychology, First Hospital of Xi'an Jiaotong University, Xi'an 710061, Shaanxi Province, China
Supported by the Natural Science Foundation of Shaanxi Province, No. 99SM50

Correspondence to: Dr. Ke-Jun Nan, Department of Medical Oncology, First Hospital of Xi'an Jiaotong University, Xi'an 710061, Shaanxi Province, China. alisantra0351@sina.com

Telephone: +86-29-3705937 **Fax:** +86-29-5324086

Received: 2003-03-12 **Accepted:** 2003-04-14

CONCLUSION: Depression occurs with a high incidence in patients with cancers of the digestive tract, which probably is not the sole factor leading to the impairment of immunological functions in these cases. However, comprehensive measures including psychological support should be taken in order to improve the immunological function, quality of life and clinical prognosis of these patients.

Nan KJ, Wei YC, Zhou FL, Li CL, Sui CG, Hui LY, Gao CG. Effects of depression on parameters of cell-mediated immunity in patients with digestive tract cancers. *World J Gastroenterol* 2004; 10(2): 268-272

<http://www.wjgnet.com/1007-9327/10/268.asp>

Abstract

AIM: To evaluate the effects of depression on parameters of cell-mediated immunity in patients with cancers of the digestive tract.

METHODS: One hundred and eight adult patients of both sexes with cancers of the digestive tract admitted between March 2001 and February 2002 in the Department of Medical Oncology, First Affiliated Hospital of Xi'an Jiaotong University were randomly enrolled in the study. The Zung self-rating depression scale (SDS), Zung self-rating anxiety scale (SAS), numeric rating scale (NRS) and social support rating scale (SSRS) were employed to evaluate the degree of depression and their contributing factors. In terms of their SDS index scores, the patients were categorized into depression group (SDS \geq 50) and non-depression group (SDS < 50). Immunological parameters such as T-lymphocyte subsets and natural killer (NK) cell activities in peripheral blood were determined and compared between the two groups of patients.

RESULTS: The SDS index was from 33.8 to 66.2 in the 108 cases, 50% of these patients had a SDS index more than 50. Similarly, the SAS index of all the patients ranged from 35.0 to 62.0 and 46.3% of the cases had a SAS index above 50. Cubic curve estimation showed that the depression was positively correlated with anxiety and negatively with social support. Furthermore, the depression correlated with the tumor type, which manifested in a descending order as stomach, gallbladder, pancreas, intestine, esophagus, duodenum and rectum, according to their correlativity. Stepwise regression analysis suggested that hyposexuality, dispiritment, agitation, palpitation, low CD₅₆ and anxiety were the significant factors contributing to depression. More severe anxiety (49.7 \pm 7.5 vs 45.3 \pm 6.9, P <0.05), pain (6.5 \pm 2.8 vs 4.6 \pm 3.2, P <0.05), poor social support (6.8 \pm 2.0 vs 7.6 \pm 2.1, P <0.05), as well as decline of lymphocyte count (0.33 \pm 0.09 vs 0.39 \pm 0.07, P <0.05) and CD₅₆ (0.26 \pm 0.11 vs 0.29 \pm 0.11, P <0.05) were noted in the depression group compared with those of the non-depression patients. However, fewer obvious changes in CD₄/CD₈ ratio and other immunological parameters were found between the two groups.

INTRODUCTION

Cancers of the digestive tract continue to be one of the most common malignancies in human worldwide^[1-14], in which gastric, esophageal, colorectal and liver cancers are among the top ten malignant tumors in China and account for 63% of total cancer mortality^[11]. Depressive symptoms such as pervasive senses of hopeless, helpless, valueless, despair, guilty, punishment and self-deprecatory thinking are often found in cancer patients. When severely enough, it may cause negative effects on the antitumor therapy, immunological function, prognosis, as well as the quality of life^[15,16]. However, up to the present, much attention has been paid to the effects of depression on patients with several kinds of malignancies^[17-20] except that of the digestive tract. Besides, despite mounting evidence that psychiatric depression heightens risk for cancerous morbidity and mortality, little is known about the detailed mechanisms responsible for this association, which is no doubt of importance in the improvement of therapy for cancer patients.

In the present study, we therefore investigated the effects of depression on cell-mediated immunity and its contributing factors in 108 patients with cancers of the digestive tract by SDS^[21] and other questionnaires, as well as immunological parameters including T-lymphocyte subsets and natural killer (NK) cell activities in peripheral blood, in an attempt to provide evidence for the necessities of psychological therapy of these cancer patients.

MATERIALS AND METHODS

Patients

One hundred and eight adult patients of both sexes with cancers of the digestive tract including 24 esophageal, 36 gastric, 4 duodenal, 4 gallbladder, 4 pancreatic, 28 colonic and 8 rectal cancer cases admitted between March 2001 and February 2002 in the Department of Medical Oncology, First Affiliated Hospital of Xi'an Jiaotong University were randomly enrolled in the study. The medical records of these patients were reviewed by investigators and their characteristics such as the family history of cancer and main symptoms were abstracted. Subjects with a history of abnormal mentality or cognitive disorders were excluded from the investigation. All the cancer cases were finally verified by histopathological examinations

and clinically diagnosed as stage I in 14, stage II in 34, stage III in 28 and stage IV in 32 according to TNM classification and the Union International Center of Cancer (UICC) system. The average disease course of the patients was 14 ± 11 months and the average age was 58 ± 9 years with the education background of 7 being graduated from primary school, 25 from junior high school and 76 from senior high school or above. Their performance status (PS) was defined by Eastern Cooperative Oncology Group (ECOG) and social information such as marital and employment status was obtained through an interview. The patients were categorized into depression group and non-depression group in terms of their SDS index scores. The study protocol was in accordance with the guideline for clinical research and approved by the Ethical and Research Committee of the hospital.

Psychological measurements

Zung self-rating depression scale (SDS) The Zung SDS system harbors 20 items of self-evaluation measurements for depressive symptoms^[21]. In the study, the patients were asked to rate each of the items regarding how they felt during the preceding week by a 4-point Likert scale with the 4 representing the most unfavorable response. After the scores of 10 reversely-graded items were adjusted in line with that of the sequentially-scored items, a raw score that was turned out from the total value of 20 items was further converted into a depression-judging variable termed as SDS index, based on which the cases were categorized into 2 levels of psychological conditions. Level 1, SDS index below 50, was considered not significant psychopathologically. Level 2, SDS index equal to or above 50, was suggested the presence of depression. It was not meant for SDS index to offer a strict diagnostic guideline but rather denote levels of depression in symptomatology that might be of clinical significance. Overall, the SDS index was shown to be relatively valid with a high internal consistency that was exhibited by an alpha coefficient of 0.84^[22].

Zung Self-rating anxiety scale (SAS) Just like Zung SDS system, Zung SAS also has 20 items to be scored with the 4-point Likert scale except that there are 5 reversely-scored items, in which the 4 represents the most unfavorable response^[23]. After the scores of 5 reversely-graded items were adjusted in line with that of the sequentially-scored items, a raw score that was turned out from the total value of 20 items was further converted into an anxiety-judging variable termed as SAS index, based on which the cases were categorized into 2 levels of psychological conditions. Level 1, SAS index below 50, was considered not significant psychopathologically. Level 2, SAS index equal to or above 50, was suggested the presence of anxiety.

Numeric rating scale (NRS) NRS consisting of four questions covering pain, nausea, insomnia and appetite was evaluated by using a 0-10 scale, with 0 meaning without symptoms and 10 indicating the situation being as bad as imagined, which was found to be a simple and valid pain measurement in some disease states^[24]. In this study, the patients were asked to circle the number that best described the symptom at its worst during a one-week period.

Social support rating scale (SSRS) SSRS was employed to evaluate the levels of objective, subjective and total social support, as well as the utility of this support^[25].

Study protocols

Two days before the investigation, each item for the psychological measurements was explained by specialized doctors in order to make the patients understand and complete the questionnaires correctly by themselves in a quiet condition to exclude any possible influence. If it could not be completed by the patients for some reasons as sickness or poor education, family members or

physicians in charge were prescribed to do it instead.

On the experimental day, 3.5 ml of peripheral blood was drawn from each patient and anticoagulated by ethylenediaminetetraacetic acid (EDTA), in which 50 μ l of blood was quantified with the Sysmes KX-21 blood counter (Japan) for the measurement of white blood cells, erythrocytes, thrombocytes, and fractions of lymphocytes, granulocytes and monocytes. The other 3.0 ml of blood sample was used to determine natural killer cells (CD₅₆) and T lymphocyte subsets with the EPICS ELITE flow cytometer (American) by individuals blinded to the clinical data of the patients in our immunology laboratory.

Statistical analysis

Experimental data were expressed as $\bar{x} \pm s$. Comparisons between experimental groups were performed by *t*-test to examine the variables with normal distribution and by Mann-Whitney *U* test to assess the other kinds of numerical values. Demographic variables were analyzed by descriptive statistics to evaluate the clinical and sociodemographic characteristics of the studied samples. Curve estimation, stepwise multiple or univariate linear regression and Pearson correlations were adopted to assess the correlation of depression with its possible contributing factors. A *P* value less than 0.05 was considered statistically significant. All statistical procedures were performed with statistical package of SPSS for social science (2000).

RESULTS

Incidence of depression in cancer patients

Questionnaires answered by the enrolled patients were correctly filled in according to the experimental protocol. The scores of SDS 4 grade evaluation are listed in Table 1. In the present study, SDS index was approximately a normal distribution in the 108 cases, ranging from 33.8 to 66.2 and averaging at 50.4 ± 8.8 . Fifty percent of the patients had a SDS index score more than 50. Similarly, SAS index of all the patients ranged from 35.0 to 62.0 and averaged at 46.9 ± 7.7 , 46.3% of the cases had a SAS index score above 50, 29.6% of the enrolled patients had scores above 50 simultaneously for both SDS and SAS indexes. The social support score was between 28 and 56 and averaged at 43.8 ± 7.2 . Curve estimation showed that the depression was positively correlated with anxiety and negatively with social support. Furthermore, the depression correlated with the tumor type, which manifested in a descending order as stomach, gallbladder, pancreas, intestine, esophagus, duodenum and rectum, according to their correlativity.

Factors contributing to depression

Many factors were associated with depression such as cancer pain, anxiety, poor economic status, tumor type, anorexia (X5: I eat as much as I used to), hyposexuality (X6: I enjoy looking at, talking to and being with attractive men/women), dispiritment (X1: I feel downhearted, blue and sad), agitation (X13: I am restless and can not keep still), palpitation (X9: My heart beats faster than usual), fatigue without apparent reasons (X10: I get tired for no reason), CD₅₆₊, *etc.* However, step-wise regression analysis suggested that hyposexuality, dispiritment, agitation, palpitation, CD₅₆ and anxiety were the significant factors contributing to depression (Table 2).

Effects of depression on cell-mediated immunity

More severe anxiety and poor social support were noted in the depression group compared with those of the non-depression patients. As for the parameter changes of cell-mediated immunity in peripheral blood, an increase of granulocyte count and a decline in T-lymphocyte subsets (CD₃, CD₄ and CD₈), erythrocyte and monocyte counts were observed in depression cases, but did not reach a significant level. Lymphocyte count

Table 1 SDS 4 grading of depressive manifestations in patients with gut cancers

Item	Factors	$\bar{x}\pm s$	Grade			
			1	2	3	4
X1	I feel downhearted, blue and sad	1.9±0.8	34	50	18	6
X2	Morning is when I feel best	2.6±1.1	18	42	18	30
X3	I have crying spells or feel like it	1.5±0.9	75	14	14	5
X4	I have trouble sleeping through the night	2.1±1.0	42	22	34	10
X5	I eat as much as I used to	2.6±1.0	22	22	46	18
X6	I enjoy looking at, talking to, and being with attractive men/women	2.6±1.1	25	26	26	31
X7	I notice that I am losing weight	2.4±1.0	18	46	22	22
X8	I have trouble with constipation	2.2±1.1	38	30	22	18
X9	My heart beats faster than usual	1.3±0.6	76	16	8	8
X10	I get tired for no reason	2.3±1.1	34	30	22	22
X11	My mind is as clear as it used to be	1.8±0.9	50	30	22	6
X12	I find it easy to do the things I used to do	2.3±0.9	22	42	30	14
X13	I am restless and can't keep still	1.6±0.9	62	22	18	6
X14	I feel hopeful about the future	2.2±0.9	30	30	42	6
X15	I am more irritable than usual	1.7±1.0	58	26	14	10
X16	I find it easy to make decisions	2.3±1.1	34	26	26	22
X17	I feel that I am useful and needed	1.9±1.0	42	42	10	14
X18	My life is pretty full	1.8±0.8	38	50	14	6
X19	I feel that others would be better off if I were dead	1.4±0.7	70	30	2	6
X20	I still enjoy the things I used to do	2.2±1.0	30	42	18	18

Table 2 Multivariate analysis of contributing factors of depression with step-wise regression

Variable	Unstandardized coefficients (B)	Standardized coefficients (β)	t	P value	Pearson correlation
X1 ^a	4.47	0.36	19 193 329	0.00	0.64
X6 ^a	4.13	0.51	19 076 980	0.00	-0.80
X9 ^a	0.97	0.07	3 266 595.5	0.00	0.65
X13 ^a	1.78	0.15	4 232 747.7	0.00	0.08
Anxiety ^a	6.04E-02	0.06	3 691 620.2	0.00	0.32
CD ₅₆ ^a	-2.33	-0.10	-28 074 903	0.00	-0.18

^aP<0.05 vs nondepression group.

and CD₅₆ were significantly decreased in the depression group compared with those of the non-depression patients ($P<0.05$) as shown in Table 3. However, fewer changes in CD₄/CD₈ ratio and other immunological parameters were found between the two groups.

Table 3 Multiple factors between depression and nondepression groups ($\bar{x}\pm s$)

Parameters	Depressive state	Non-depressive state	P
Anxiety	49.7±7.5 ^b	45.3±6.9	0.003
Pain	6.5±2.8 ^a	4.6±3.2	0.025
Social support	44.0±6.8	44.6±7.7	0.670
Objective support	11.9±3.0	12.5±3.0	0.360
Subjective support	24.8±3.8	24.5±4.4	0.630
Utilization of support	6.8±2.0 ^a	7.6±2.1	0.043
Cells in peripheral blood			
Erythrocyte (10 ¹² /L)	3.4±1.2	3.8±1.8	0.460
Lymphocyte (0.00)	0.33±0.09 ^a	0.39±0.87	0.032
Granulocyte (0.00)	0.61±0.12	0.56±0.88	0.240
Monocyte (0.00)	0.04±0.01	0.06±0.05	0.900
Thrombocyte (10 ⁹ /L)	137.5±12.5 ^a	167.7±43.2	0.020
T lymphocyte subsets			
CD ₃ (0.00)	0.53±0.11	0.59±0.11	0.070
CD ₄ (0.00)	0.27±0.07	0.30±0.11	0.440
CD ₈ (0.00)	0.32±0.10	0.35±0.10	0.240
Natural killer			
CD ₅₆ (0.00)	0.26±0.11 ^a	0.29±0.11	0.041

^aP<0.05, ^bP<0.01, vs nondepression group.

DISCUSSION

Depression is a psychotic or neurotic condition characterized by inability to concentrate, insomnia, and feelings of extreme sadness, dejection and hopelessness, which commonly occur in cancer patients. It has been estimated that the incidence of severe depression in these patients is about 3%-50% depending on tumor site, stage, assessment methods, and a lot of other contributing factors, with an average overall incidence of approximately 20%^[18,26,27]. However, depression remains an often unrecognized source of suffering among cancer patients, which is partially because of the lack of recognition by clinical physicians. Under such circumstances, particularly when the depression was confused with symptoms resulted from the underlying disease, clinicians were usually inclined to dismiss even severe depression on the assumption that these "symptoms" are understandable^[27]. In fact, untreated depression in these patients might cause more frequent clinic visits, higher medical costs, longer hospital stay, as well as noncompliance with therapeutic measures, poor quality of life, bad prognosis, and even accidental death^[20,28-32].

In the present study, we investigated the effects of depression on the parameters of cell-mediated immunity and its contributing factors in patients with cancers of the digestive tract. To our knowledge, it is one of the few clinical reports in recent years concerning depression in patients with digestive tract cancers. It was revealed that depression occurred in 50% of the cases, which was higher than the average total incidence among all tumor patients. Besides, there was also a higher percentage of cases with both SDS and SAS scores equal to or more than 50 in our study, accounting for 29.6% of the investigated patients. The exact reason for these has not yet been fully elucidated, it

is probably because the gut function relates so closely to people's daily life that a malignant disorder in the digestive tract might affect the psychological status of patients more easily compared with tumors of the other sites.

Lots of factors are closely related to the depression of cancer patients including physiological, immunological and psychosocial impacts. Although this correlation has been established as a whole in tumor cases^[33,34], however, little is known about the contributing factors to the depression in patients with cancer of the digestive tract according to the new bio-psycho-social model. Our study revealed that despite many factors such as cancer pain, poor economic status, tumor type, anorexia (X5), fatigue without apparent reasons (X10) might play a role, hyposexuality (X6), dispiritment (X1), agitation (X13), palpitation (X9), CD₅₆ and anxiety were the significant factors contributing to the depression of these patients by stepwise regression analysis.

Impairment of immunologic functions has been noted to be one of the major negative effects exerted by depression in cancer patients^[35]. Some immunological parameters such as T lymphocyte subsets and natural killer (NK) cells have been believed to be the major effectual mechanism against tumors^[36-43]. For instance, the growth of malignancies was inhibited by activated tumor-specific T cells^[44,45] and the depressed activity of NK cells was probably related to tumor enlargement and dissemination^[46]. Papadopoulos and his associates^[42] reported that the depletion of cytotoxic T cell (CD₈₊) and NK cell (CD₅₆₊) in advanced papillary ovarian cancer might in part explain the poor clinical outcomes of those patients. However, in our study, although significantly reduced NK cells (CD₅₆) and thrombocyte count were found in the depressive patients, T lymphocyte subset, CD₄/CD₈ ratio and other immunological parameters did not exhibit significant alterations between the two groups, suggesting that depression was probably not a necessarily factor leading to impairment of immune functions in patients with cancers of the digestive tract.

In summary, our study reveals that the incidence of depression is as high as 50% in patients with cancers of the digestive tract. Hyposexuality, dispiritment, agitation, palpitation, low CD₅₆ and anxiety are the significant factors contributing to the depression. Although significantly reduced NK cells (CD₅₆) and thrombocyte count are found in the depressive patients, T lymphocyte subset, CD₄/CD₈ ratio and other immunological parameters do not exhibit significant alterations between the depressive and non-depressive patients. Comprehensive measures including psycho-logical support therefore should be taken in order to improve their immunological functions, quality of life and clinical prognosis of cancer patients.

REFERENCES

- Newnham A**, Quinn MJ, Babb P, Kang JY, Majeed A. Trends in oesophageal and gastric cancer incidence, mortality and survival in England and Wales 1971-1998/1999. *Aliment Pharmacol Ther* 2003; **17**: 655-664
- Shibuya K**, Mathers CD, Boschi-Pinto C, Lopez AD, Murray CJ. Global and regional estimates of cancer mortality and incidence by site: II. Results for the global burden of disease 2000. *BMC Cancer* 2002; **2**: 37
- Ke L**. Mortality and incidence trends from esophagus cancer in selected geographic areas of China circa 1970-1990. *Int J Cancer* 2002; **102**: 271-274
- Le Vu B**, de Vathaire F, de Vathaire CC, Paofaite J, Roda L, Soubiran G, Lhoumeau F, Laudon F. Cancer incidence in French Polynesia 1985-1995. *Trop Med Int Health* 2000; **5**: 722-731
- Mohandas KM**, Jagannath P. Epidemiology of digestive tract cancers in India. VI. Projected burden in the new millennium and the need for primary prevention. *Indian J Gastroenterol* 2000; **19**: 74-78
- Zhang YL**, Zhang ZS, Wu BP, Zhou DY. Early diagnosis for colorectal cancer in China. *World J Gastroenterol* 2002; **8**: 21-25
- Shen ZY**, Shen WY, Chen MH, Shen J, Cai WJ, Yi Z. Nitric oxide and calcium ions in apoptotic esophageal carcinoma cells induced by arsenite. *World J Gastroenterol* 2002; **8**: 40-43
- Gu ZP**, Wang YI, Li JG, Zhou YA. VEGF165 antisense RNA suppresses oncogenic properties of human esophageal squamous cell carcinoma. *World J Gastroenterol* 2002; **8**: 44-48
- Chen K**, Cai J, Liu XY, Ma XY, Yao KY, Zheng S. Nested case-control study on the risk factors of colorectal cancer. *World J Gastroenterol* 2003; **9**: 99-103
- Tsukuma H**, Ajiki W, Oshima A. Time-trends in cancer incidence and mortality in Japan. *Gan To Kagaku Ryoho* 2001; **28**: 137-141
- Sun X**, Mu R, Zhou Y, Dai X, Qiao Y, Zhang S, Huangfu X, Sun J, Li L, Lu F. 1990-1992 mortality of stomach cancer in China. *Zhonghua Zhongliu Zazhi* 2002; **24**: 4-8
- Zhang S**, Li L, Lu F. Mortality of primary liver cancer in China from 1990 through 1992. *Zhonghua Zhongliu Zazhi* 1999; **21**: 245-249
- Zheng S**, Liu XY, Ding KF, Wang LB, Qiu PL, Ding XF, Shen YZ, Shen GF, Sun QR, Li WD, Dong Q, Zhang SZ. Reduction of the incidence and mortality of rectal cancer by polypectomy: a prospective cohort study in Haining County. *World J Gastroenterol* 2002; **8**: 488-492
- Wan J**, Zhang ZQ, Zhu C, Wang MW, Zhao DH, Fu YH, Zhang JP, Wang YH, Wu BY. Colonoscopic screening and follow-up for colorectal cancer in the elderly. *World J Gastroenterol* 2002; **8**: 267-269
- Murr C**, Widner B, Sperner-Unterweger B, Ledochowski M, Schubert C, Fuchs D. Immune reaction links disease progression in cancer patients with depression. *Med Hypotheses* 2000; **55**: 137-140
- Skarstein J**, Aass N, Fossa SD, Skovlund E, Dahl AA. Anxiety and depression in cancer patients: relation between the Hospital Anxiety and Depression Scale and the European Organization for Research and Treatment of Cancer Core Quality of Life Questionnaire. *J Psychosom Res* 2000; **49**: 27-34
- Sarna L**, Padilla G, Holmes C, Tashkin D, Brecht ML, Evangelista L. Quality of life of long-term survivors of non-small-cell lung cancer. *J Clin Oncol* 2002; **20**: 2920-2929
- Hopwood P**, Stephens RJ. Depression in patients with lung cancer: prevalence and risk factors derived from quality-of-life data. *J Clin Oncol* 2000; **18**: 893-903
- Gallagher J**, Parle M, Cairns D. Appraisal and psychological distress six months after diagnosis of breast cancer. *Br J Health Psychol* 2002; **7**(Part 3): 365-376
- Hjerl K**, Andersen EW, Keiding N, Mouridsen HT, Mortensen PB, Jorgensen T. Depression as a prognostic factor for breast cancer mortality. *Psychosomatics* 2003; **44**: 24-30
- Passik SD**, Lundberg JC, Rosenfeld B, Kirsh KL, Donaghy K, Theobald D, Lundberg E, Dugan W. Factor analysis of the Zung Self-Rating Depression Scale in a large ambulatory oncology sample. *Psychosomatics* 2000; **41**: 121-127
- Dugan W**, McDonald MV, Passik SD, Rosenfeld BD, Theobald D, Edgerton S. Use of the Zung Self-Rating Depression Scale in cancer patients: feasibility as a screening tool. *Psychooncology* 1998; **7**: 483-493
- Zung WW**. A rating instrument for anxiety disorders. *Psychosomatics* 1971; **12**: 371-379
- Paice JA**, Cohen FL. Validity of a verbally administered numeric rating scale to measure cancer pain intensity. *Cancer Nurs* 1997; **20**: 88-93
- Hu MY**, Zhou CJ, Xiao SY. Psychological health level and related psychosocial factors of nurses in Changsha. *Zhonghua Huli Zazhi* 1997; **32**: 192-195
- Chochinov HM**. Depression in cancer patients. *Lancet Oncol* 2001; **2**: 499-505
- Goldman LS**, Nielsen NH, Champion HC. Awareness, diagnosis, and treatment of depression. *J Gen Intern Med* 1999; **14**: 569-580
- DiMatteo MR**, Lepper HS, Croghan TW. Depression is a risk factor for noncompliance with medical treatment: meta-analysis of the effects of anxiety and depression on patient adherence. *Arch Intern Med* 2000; **160**: 2101-2107
- Watson M**, Haviland JS, Greer S, Davidson J, Bliss JM. Influence of psychological response on survival in breast cancer: a population-based cohort study. *Lancet* 1999; **354**: 1331-1336

- 30 **Breitbart W**, Rosenfeld B, Pessin H, Kaim M, Funesti-Esch J, Galiotta M, Nelson CJ, Brescia R. Depression, hopelessness, and desire for hastened death in terminally ill patients with cancer. *JAMA* 2000; **284**: 2907-2911
- 31 **Akechi T**, Okamura H, Nishiwaki Y, Uchitomi Y. Predictive factors for suicidal ideation in patients with unresectable lung carcinoma. *Cancer* 2002; **95**: 1085-1093
- 32 **Nie J**, Liu S, Di L. Cancer pain and its influence on cancer patients' quality of life. *Zhonghua Zhongliu Zazhi* 2000; **22**: 432-434
- 33 **Lissoni P**, Cangemi P, Pirato D, Roselli MG, Rovelli F, Brivio F, Malugani F, Maestroni GJ, Conti A, Laudon M, Malysheva O, Gianni L. A review on cancer-psycho-spiritual status interactions. *Neuroendocrinol Lett* 2001; **22**: 175-180
- 34 **Schussler G**, Schubert C. The influence of psychosocial factors on the immune system (psychoneuroimmunology) and their role for the incidence and progression of cancer. *Z Psychosom Med Psychother* 2001; **47**: 6-41
- 35 **Mafune K**, Tanaka Y. Influence of multimodality therapy on the cellular immunity of patients with esophageal cancer. *Ann Surg Oncol* 2000; **7**: 609-616
- 36 **Dhodapkar MV**, Young JW, Chapman PB, Cox WI, Fonteneau JF, Amigorena S, Houghton AN, Steinman RM, Bhardwaj N. Paucity of functional T-cell memory to melanoma antigens in healthy donors and melanoma patients. *Clin Cancer Res* 2000; **6**: 4831-4838
- 37 **Ochsenbein AF**, Sierro S, Odermatt B, Pericin M, Karrer U, Hermans J, Hemmi S, Hengartner H, Zinkernagel RM. Roles of tumour localization, second signals and cross priming in cytotoxic T-cell induction. *Nature* 2001; **411**: 1058-1064
- 38 **Marzo AL**, Kinnear BF, Lake RA, Frelinger JJ, Collins EJ, Robinson BW, Scott B. Tumor-specific CD₄⁺ T cells have a major "post-licensing" role in CTL mediated anti-tumor immunity. *J Immunol* 2000; **165**: 6047-6055
- 39 **Ferreira C**, Barthlott T, Garcia S, Zamoyska R, Stockinger B. Differential survival of naive CD₄ and CD₈ T cells. *J Immunol* 2000; **165**: 3689-3694
- 40 **Echchakir H**, Bagot M, Dorothee G, Martinvalet D, LeGouvello S, Bousmell L, Chouaib S, Bensussan A, Mami-Chouaib F. Cutaneous T cell lymphoma reactive CD₄⁺ cytotoxic T lymphocyte clones display a Th1 cytokine profile and use a fas-independent pathway for specific tumor cell lysis. *J Invest Dermatol* 2000; **115**: 74-80
- 41 **Wolf AM**, Wolf D, Steurer M, Gastl G, Gunsilius E, Grubeck-Loebenstein B. Increase of Regulatory T Cells in the Peripheral Blood of Cancer Patients. *Clin Cancer Res* 2003; **9**: 606-612
- 42 **Papadopoulos N**, Kotini A, Cheva A, Jivannakis T, Manavis J, Alexiadis G, Lambropoulou M, Vavetsis S, Tamiolakis D. Gains and losses of CD₈, CD₂₀ and CD₅₆ expression in tumor stroma-infiltrating lymphocytes compared with tumor-associated lymphocytes from ascitic fluid and lymphocytes from tumor draining lymph nodes in serous papillary ovarian carcinoma patients. *Eur J Gynaecol Oncol* 2002; **23**: 533-536
- 43 **Zhai SH**, Liu JB, Zhu P, Wang YH. CD₅₄, CD₈₀, CD₈₆ and HLA-ABC expressions in liver cirrhosis and hepatocarcinoma. *Shijie Huaren Xiaohua Zazhi* 2000; **8**: 292-295
- 44 **Pardoll D**. T cells take aim at cancer. *Proc Natl Acad Sci U S A* 2002; **99**: 15840-15842
- 45 **Dudley ME**, Wunderlich JR, Robbins PF, Yang JC, Hwu P, Schwartzentruber DJ, Topalian SL, Sherry R, Restifo NP, Hubicki AM, Robinson MR, Raffeld M, Duray P, Seipp CA, Rogers-Freezer L, Morton KE, Mavroukakis SA, White DE, Rosenberg SA. Cancer regression and autoimmunity in patients after clonal repopulation with antitumor lymphocytes. *Science* 2002; **298**: 850-854
- 46 **Takeuchi H**, Maehara Y, Tokunaga E, Koga T, Kakeji Y, Sugimachi K. Prognostic significance of natural killer cell activity in patients with gastric carcinoma: a multivariate analysis. *Am J Gastroenterol* 2001; **96**: 574-578

Edited by Zhu LH and Wang XL

Estimating medical costs of gastroenterological diseases

Li-Fang Chou

Li-Fang Chou, Department of Public Finance, National Chengchi University, Taipei, Taiwan, China

Correspondence to: Professor Li-Fang Chou, Department of Public Finance, National Chengchi University, 64, Sec. 2, Chih-Nan Road, Taipei 11623, Taiwan, China. lifang@nccu.edu.tw

Telephone: +886-2-29387310 **Fax:** +886-2-29390074

Received: 2003-06-05 **Accepted:** 2003-08-02

Abstract

AIM: To estimate the direct medical costs of gastroenterological diseases within the universal health insurance program among the population of local residents in Taiwan.

METHODS: The data sources were the first 4 cohort datasets of 200 000 people from the National Health Insurance Research Database in Taipei. The ambulatory, inpatient and pharmacy claims of the cohort in 2001 were analyzed. Besides prevalence and medical costs of diseases, both amount and costs of utilization in procedures and drugs were calculated.

RESULTS: Of the cohort with 183 976 eligible people, 44.2% had ever a gastroenterological diagnosis during the year. The age group 20-39 years had the lowest prevalence rate (39.2%) while the elderly had the highest (58.4%). The prevalence rate was higher in women than in men (48.5% vs. 40.0%). Totally, 30.4% of 14 888 inpatients had ever a gastroenterological diagnosis at discharge and 18.8% of 51 359 patients at clinics of traditional Chinese medicine had such a diagnosis there. If only the principal diagnosis on each claim was considered, 16.2% of admissions, 8.0% of outpatient visits, and 10.1% of the total medical costs (8 469 909 US dollars/83 830 239 US dollars) were attributed to gastroenterological diseases. On average, 46.0 US dollars per insured person in a year were spent in treating gastroenterological diseases. Diagnostic procedures related to gastroenterological diseases accounted for 24.2% of the costs for all diagnostic procedures and 2.3% of the total medical costs. Therapeutic procedures related to gastroenterological diseases accounted for 4.5% of the costs for all therapeutic procedures and 1.3% of the total medical costs. Drugs related to gastroenterological diseases accounted for 7.3% of the costs for all drugs and 1.9% of the total medical costs.

CONCLUSION: Gastroenterological diseases are prevalent among the population of local residents in Taiwan, accounting for a tenth of the total medical costs. Further investigations are needed to differentiate costs in screening, ruling out, confirming, and treating.

Chou LF. Estimating medical costs of gastroenterological diseases. *World J Gastroenterol* 2004; 10(2): 273-278
<http://www.wjgnet.com/1007-9327/10/273.asp>

INTRODUCTION

The cost analysis of disease management is essential for health policymaking in resource allocation and medical manpower

planning^[1-8]. Among all medical specialties, gastroenterology has played a major role because of disease prevalence and advanced technology^[9-12]. While the literature about economic assessments in gastroenterology dealt mainly with cost-effectiveness of single pharmaceuticals, diagnostic measures or therapeutic interventions^[13-23], analyses of the entire specialty are relatively scarce. One of the reasons might be that the complete utilization data of the total population or a representative sample are not easily available. The more decisive reason is the lack of a standardized analysis framework and operational measures.

The aim of this study was to estimate the direct medical costs of gastroenterological diseases among the population of local residents in Taiwan. Besides the diagnosis-based approach, the costs would also be sorted by diagnostic procedure, therapeutic procedure, and drug. The strength of this study was to use the complete claim data of a representative cohort of 200 000 people within the universal health insurance program in Taiwan. Not only the nominal costs of gastroenterological diseases but also their relative ratio in total medical costs could be measured.

MATERIALS AND METHODS

Data sources

The data of the first 4 cohort datasets (R01-R04) in 2001 from the National Health Insurance Research Database (NHIRD; <http://www.nhri.org.tw/nhird/>) in Taipei were used for the analysis. The NHIRD owned all claims in electronic form from the national health insurance (NHI) program that has started in 1995 and covered nearly all inhabitants in Taiwan (21 653 555 beneficiaries at the end of 2001)^[24]. The NHIRD has retrieved dozens of datasets publicly available for researchers. For each cohort dataset, the NHIRD at first randomly sampled 50 000 people from 23 753 407 people who had ever been insured from March 1, 1995 to December 31, 2000. Then, all insurance claims belonging to these people were drawn to make up one specific cohort dataset.

A cohort dataset included one registration file of the insured people and 6 files of original claim data: inpatient expenditures by admissions, details of inpatient orders, ambulatory care expenditures by visits, details of ambulatory care orders, expenditures for prescriptions dispensed at contracted pharmacies, and details of prescriptions dispensed at contracted pharmacies. The structure of the insurance claim files had been described in details on the NHIRD web site and in other published literature^[25-28].

Among the 4 cohort datasets in 2001, there were totally 183 976 eligible people, 22 746 admissions, 1 241 760 inpatient prescription items, 2 607 646 visits (including 234 598 visits for traditional Chinese medicine), 11 765 537 outpatient prescription items, 127 008 dispensed prescriptions at pharmacies, and 513 231 dispensed prescription items at pharmacies. The ambulatory sector included medical care services at clinics of Western medicine, traditional Chinese medicine, and dentistry, and pharmaceutical services at pharmacies. Because the separation of prescribing and dispensing was not yet thoroughly executed in Taiwan, relatively few outpatient prescriptions had been dispensed at independent pharmacies.

Besides, the fee schedule of 4 837 medical service items and the list of 21 146 approved drug items of Western medicine in Taiwan were downloaded from the web site of the Bureau of National Health Insurance (<http://www.nhi.gov.tw/>, accessed January 12, 2002). Each drug of different brand, strength and form had an official unique identifier for claims. The BNHI also offered a list of ATC codes (the Anatomical Therapeutic Chemical classification system, version 2000)^[29] for each drug item.

Study design

The costs of gastroenterological diseases were estimated in 4 dimensions: diagnosis, diagnostic procedure, therapeutic procedure, and drug. The reason for separate approaches was that on the one hand an admission or a visit with a gastroenterological diagnosis might contain service items not related to the gastroenterological diagnosis, and on the other hand a procedure or drug for gastroenterological diseases might not be associated with any gastroenterological diagnosis on the claim because of the coding error or limitation (5 diagnosis fields on an admission claim and 3 on a visit claim).

The age-sex prevalence of patients having any gastroenterological diagnosis during the year was at first calculated. All 5 diagnoses on an admission record and all 3 diagnoses on a visit record were taken into account. Then, medical costs of visits and admissions because of gastroenterological diseases as the principal diagnosis were calculated and stratified by major disease category.

The definition and categorization of gastroenterological diseases were based on the scheme of the Clinical Classifications Software (CCS for ICD-9-CM) developed by the Agency for Healthcare Research and Quality (AHRQ) of the U.S. Department of Health and Human Services^[30]. The single-level diagnosis CCS aggregated illnesses and conditions of over 12 000 diagnosis codes within the International Classification of Diseases, 9th Revision, Clinical Modification (ICD-9-CM) into 259 mutually exclusive categories. The single-level CSS categories 6, 12-18, 120, 135, 138-155, 214, 250, and 251 were deemed as gastroenterological diseases. Some codes such as benign neoplasm, injury, and screening that were dispersedly included in other CSS categories were also identified as gastroenterological diseases.

The fee schedule of the NHI included mainly consultation and rehabilitation fees, charges for diagnostic procedures (*e.g.* laboratory tests and radiological examinations), therapeutic procedures (*e.g.* general treatments, radiological interventions and surgeries) and materials, and case payments based on diagnosis-related groups. Among 1 470 items of diagnostic procedures and 2 435 items of therapeutic procedures, 132 and 338 items were related to gastroenterological diseases respectively.

Drugs for treating gastroenterological diseases in the current study included all drug items of the groups A02 (antacids, drugs for treatment of peptic ulcer and flatulence), A03 (antispasmodic and anticholinergic agents and propulsives), A04 (antiemetics and anti-nauseants), A05 (bile and liver therapy), A06 (laxatives), A07 (antidiarrheals, intestinal anti-inflammatory/anti-infective agents), A09 (digestives, including enzymes), C05A (antihemorrhoidals for topical use), P01A (agents against amoebiasis and other protozoal diseases), and P02 (anthelmintics) in the ATC classification system. The items in the group J07BC (hepatitis vaccines) were not included because they were not reimbursable within the NHI. A total of 2 269 drug items for treating gastroenterological diseases had been registered in Taiwan since 1995. Some drugs might be no more available on the market or not reimbursable by the insurance during the study period.

In describing utilization and costs of diagnostic procedures, therapeutic procedures, and drugs related to gastroenterological diseases, the number of recipients, the number of orders, and the total costs were calculated and stratified either by individual item of procedures or by group of drugs at the ATC 3rd and 4th levels. The original monetary values in unit of New Taiwan dollars were converted into U.S. currency based on the average exchange rate in 2001 (1 U.S. dollar [USD]=33.8003 New Taiwan dollars) according to the Central Bank of China in Taiwan (<http://www.cbc.gov.tw/>, accessed 6 February 2003).

Statistical analysis

The database software of Microsoft SQL Server 2000 was used for data linkage and processing. The regular statistics were displayed.

RESULTS

General information of the cohort

Among the 200 000-person cohort, only 183 976 people were still insured in 2001. There were more men than women (92 566 vs 91 394), and the status of sex was unknown in 16 persons (Table 1). The mean age of the eligible people was 33.9 (SD 20.3) years.

Table 1 Age-sex specific prevalence of gastroenterological diseases among cohorts ($n=183\ 976$) in 2001

Age group in year	No. of patients			Prevalence in percent		
	All	Female	Male	All	Female	Male
Sampling cohort^a						
<20	51 029	24 644	26 384			
20-39	63 800	32 115	31 670			
40-59	45 432	23 061	22 371			
>=60	23 715	11 574	12 141			
Total	183 976	91 394	92 566			
Patients with any gastroenterological diagnosis at both inpatient and ambulatory sectors^{b,c}						
<20	22 006	10 728	11 277	43.1	43.5	42.7
20-39	25 035	14 988	10 044	39.2	46.7	31.7
40-59	20 412	11 497	8 915	44.9	49.9	39.9
>=60	13 845	7 090	6 755	58.4	61.3	55.6
Total	81 298	44 303	36 991	44.2	48.5	40.0
Patients with any gastroenterological diagnosis at inpatient sector						
<20	947	388	559	1.9	1.6	2.1
20-39	792	301	491	1.2	0.9	1.6
40-59	1 056	431	625	2.3	1.9	2.8
>=60	1 738	737	1 001	7.3	6.4	8.2
Total	4 533	1 857	2 676	2.5	2.0	2.9
Patients with any gastroenterological diagnosis at ambulatory sector^d						
<20	21 931	10 698	11 232	43.0	43.4	42.6
20-39	24 932	14 955	9 974	39.1	46.6	31.5
40-59	20 310	11 459	8 851	44.7	49.7	39.6
>=60	13 643	6 996	6 647	57.5	60.4	54.7
Total	80 816	44 108	3 6704	43.9	48.3	39.7
Patients with any gastroenterological diagnosis at clinics of traditional Chinese medicine						
<20	1 833	1 005	828	3.6	4.1	3.1
20-39	3 608	2 259	1 349	5.7	7.0	4.3
40-59	2 892	1 687	1 205	6.4	7.3	5.4
>=60	1 310	731	579	5.5	6.3	4.8
Total	9 643	5 682	3 961	5.2	6.2	4.3

^aThose born after January 1, 2001 were not included in the cohort. The status of sex was unknown in 16 persons. ^b Patients with gastroenterological diseases included 4 persons of

unknown sex. All diagnoses of a patient during the year were taken into account, not confined to principal diagnosis at each admission or visit. The ambulatory sector included physician offices, hospital outpatient departments, and emergency departments of Western medicine, dentistry, and traditional Chinese medicine.

The medical care benefits of these people in 2001 totaled 83 830 239 USD, of which 26 443 645 USD (31.5%) was claimed at the inpatient sector and 57 386 595 USD (68.5%) at the ambulatory sector. The clinics of traditional Chinese medicine and independent pharmacies only accounted for 4.2% (3 499 397 USD) and 0.8% (677 908 USD) of the total costs respectively.

The utilization and costs of all kinds of procedures and drugs among the cohort were as following: 1 119 629 orders of diagnostic procedures summing to 7 858 087 USD (9.4% of the total costs), 774 340 orders of therapeutic procedures with 23 582 229 USD (28.1% of the total costs), and 8 683 664 prescribed or dispensed items of drugs with 21 193 285 USD (25.3% of the total costs).

Age-sex specific prevalence of gastroenterological diseases

Table 1 also displays the number of patients with any gastroenterological diagnosis in 2001 and their prevalence among the eligible cohort, stratified by age group, sex, and setting. Totally, 44.2% of the insured people had at least one gastroenterological diagnosis. The age group 20-39 years had the lowest prevalence rate while the elderly had the highest. The prevalence rate was higher in women than in men (48.5% vs 40.0%). But, men had a slightly higher prevalence rate (2.9%) at the inpatient sector than women (2.0%). During the year, 14 888 patients were admitted to hospitals. In other words, 30.4% of inpatients had ever a gastroenterological diagnosis at discharge. Physicians of traditional Chinese medicine made gastroenterological diagnoses in 9 643 patients, i.e. in 5.2% of the entire cohort and in 18.8% of the 51 359 patients having visited the clinics of traditional Chinese medicine during 2001.

Prevalence and costs of gastroenterological diseases by major disease category

Table 2 shows the aggregate costs of visits and admissions due to gastroenterological diseases. The analysis took account of the principal diagnosis into consideration on each claim only, the results were stratified by major disease category, and the numbers of affected patients were also calculated. Totally, 67 073 patients (36.5% of the cohort) were involved and medical care costs in value of 8 469 909 USD (10.1% of the total medical costs) were consumed. On average, 46.0 USD per insured person in a year was spent in treating gastroenterological diseases.

Besides, 16.2% ($n=3\ 676$) of all admissions, 8.0% ($n=209\ 254$) of all visits, and 10.4% ($n=24\ 429$) of all visits to traditional Chinese medicine during 2001 were primarily attributed to gastroenterological causes. While the largest patient group was noninfectious gastroenteritis (9.6% of the cohort), followed by other gastrointestinal disorders (8.7%), abdominal pain (7.7%), gastritis and duodenitis (7.7%), and other disorders of stomach and duodenum (4.2%), the top 5 diagnosis groups with higher total charges were gastroduodenal ulcer (10.6% of the costs related to gastroenterological diseases/1.1% of the total medical costs), other liver diseases (6.7%/0.7%), other gastrointestinal disorders (6.7%/0.7%), hepatitis (6.5%/0.7%), and biliary tract disease (6.0%/0.6%).

Utilization and costs of diagnostic procedures related to gastroenterological diseases

Among the cohort during 2001, 36 004 (19.6%) patients utilized 210 156 (18.8%) diagnostic procedures related to gastroenterological diseases with costs of 1 900 752 USD (24.2%

of the costs for all diagnostic procedures and 2.3% of the total medical costs). The computer tomography with 3 fee items took almost a two-fifth share of the costs for GI-related diagnostic procedures. The other two items with higher costs were abdominal sonography (18.4% of the costs for GI-related diagnostic procedures) and upper GI panendoscopy (13.0%). But, the most common procedures belonged to biochemical tests of blood: glutamic-pyruvic transaminase (GPT) with 47 523 orders and glutamic-oxalacetic transaminase (GOT) with 45 653 orders. Nearly a seventh of the cohort received these two tests (Table 3).

Table 2 Prevalence and costs of gastroenterological diseases among cohorts ($n=183\ 976$) in 2001 by major disease category, according to principal diagnosis only

CSS ^a code	Single-level CCS diagnosis categories	Patients		Total cost	
		No.	Mean age (SD)	US \$	%
6	Hepatitis	6 356	44.3 (16.1)	547 599	6.5%
12	Cancer of esophagus	67	47.4 (22.3)	193 853	2.3%
13	Cancer of stomach	110	64.0 (15.0)	207 765	2.5%
14	Cancer of colon	230	63.2 (14.3)	308 903	3.6%
15	Cancer of rectum and anus	180	65.9 (12.8)	328 540	3.9%
16	Cancer of liver and intrahepatic bile duct	242	60.5 (14.4)	448 114	5.3%
17	Cancer of pancreas	30	67.9 (13.4)	148 490	1.8%
18	Cancer of other GI organs, peritoneum	40	67.5 (11.5)	70 893	0.8%
120	Hemorrhoids	2 110	45.6 (17.1)	236 477	2.8%
135	Intestinal infection	7 727	25.3 (22.2)	175 479	2.1%
138	Esophageal disorders	967	46.9 (20.9)	145 264	1.7%
139	Gastroduodenal ulcer (except hemorrhage)	6 214	48.1 (18.5)	898 028	10.6%
140	Gastritis and duodenitis	14 112	36.7 (21.9)	348 621	4.1%
141	Other disorders of stomach and duodenum	7 736	38.7 (23.1)	285 697	3.4%
142	Appendicitis and other appendiceal conditions	362	33.1 (18.8)	217 212	2.6%
143	Abdominal hernia	515	35.6 (27.9)	228 586	2.7%
144	Regional enteritis and ulcerative colitis	1 406	31.4 (22.5)	29 259	0.3%
145	Intestinal obstruction without hernia	543	39.4 (29.3)	112 282	1.3%
146	Diverticulosis and diverticulitis	45	58.2 (20.9)	29 713	0.4%
147	Anal and rectal conditions	366	41.8 (21.4)	87 506	1.0%
148	Peritonitis and intestinal abscess	72	49.5 (21.5)	54 941	0.6%
149	Biliary tract disease	1 000	54.2 (17.5)	509 960	6.0%
150	Liver disease, alcohol-related	156	48.5 (12.3)	39 179	0.5%
151	Other liver diseases	2 102	47.7 (16.9)	569 503	6.7%
152	Pancreatic disorders (not diabetes)	157	50.0 (17.0)	116 327	1.4%
153	Gastrointestinal hemorrhage	1 385	52.4 (20.2)	442 493	5.2%
154	Noninfectious gastroenteritis	17 717	28.9 (21.9)	401 586	4.7%
155	Other gastrointestinal disorders	16 080	36.7 (22.6)	563 336	6.7%
214	Digestive congenital anomalies	84	31.2 (22.2)	15 785	0.2%
250	Nausea and vomiting	926	25.5 (24.3)	19 924	0.2%
251	Abdominal pain	14 113	34.4 (20.1)	404 085	4.8%
-	Others	997	37.6 (23.1)	284 509	3.4%
	Total	67 073	34.8 (21.8)	8 469 909	100.0%

^aCCS: Clinical Classifications Software by the Agency for Healthcare Research and Quality (AHRQ), Rockville, MD, USA.

Table 3 Utilization and costs of diagnostic procedures related to gastroenterological diseases among cohorts ($n=183\ 976$) in 2001: top 20 by total cost

Item of diagnostic procedures ^a	No. of patients	No. of orders	Total cost		
			US \$	%	Cum.%
Whole body computer tomography (without contrast)	2 541	3 092	374 106	19.7%	19.7%
Abdominal sonography	11 132	15 730	349 690	18.4%	38.1%
Whole body computer tomography (with/without contrast)	1 644	2 106	320 943	16.9%	55.0%
Upper GI panendoscopy	4 693	5 606	247 458	13.0%	68.0%
Serum GPT	25 427	47 523	69 765	3.7%	71.7%
Serum GOT	24 265	45 653	67 676	3.6%	75.2%
Whole body computer tomography (with contrast)	337	437	59 522	3.1%	78.3%
Colon fiberoscopy	730	780	50 698	2.7%	81.0%
Double-contrast study of lower GI series	421	432	29 421	1.5%	82.6%
AFP (RIA)	1 461	2 408	28 361	1.5%	84.1%
AFP (EIA)	2 363	3 570	20 865	1.1%	85.2%
Plain abdomen X-ray	2 338	2 856	18 498	1.0%	86.1%
Serum bilirubin, total	6 345	12 553	18 307	1.0%	87.1%
HbsAg (EIA)	3 678	3 999	17 237	0.9%	88.0%
Serum albumin	6 989	14 638	15 522	0.8%	88.8%
CEA (EIA)	856	1 308	15 293	0.8%	89.6%
Alkaline phosphatase	5 686	10 091	14 159	0.7%	90.4%
Upper GI series	296	315	13 347	0.7%	91.1%
CEA (RIA)	647	1 127	13 344	0.7%	91.8%
Sigmoid fiberoscopy	311	327	11 620	0.6%	92.4%
Others			144 922	7.6%	100.0%
Total ^b	36 004	210 156	1 900 752	100.0%	

^aMagnet resonance imaging (MRI) was excluded from analysis because the fee schedule of the National Health Insurance did not differentiate MRI for abdomen from MRI for other body parts. ^bNumbers might not add to totals because of rounding.

Table 4 Utilization and costs of therapeutic procedures (treatment and surgery) related to gastroenterological diseases among cohorts ($n=183\ 976$) in 2001

Item of therapeutic procedure	No. of patients	No. of orders	Total cost		
			US \$	%	Cum.%
Nasal feeding	917	28 352	167 762	15.7%	15.7%
Repair of inguinal hernia (without bowel resection)	322	359	94 046	8.8%	24.5%
Appendectomy	226	226	74 145	7.0%	31.5%
Laparoscopic cholecystectomy	83	84	68 081	6.4%	37.9%
Hemorrhoidectomy, internal & external	198	199	59 994	5.6%	43.5%
Trans-arterial embolization (T.A.E.)	65	96	57 634	5.4%	48.9%
Insertion of nasogastric tube	1 745	5 370	25 609	2.4%	51.3%
Heat probe during endoscopy	162	185	21 893	2.1%	53.4%
Cholecystectomy	58	58	18 485	1.7%	55.1%
Endoscopic papillectomy	31	32	17 893	1.7%	56.8%
Colonoscopic polypectomy	153	157	17 140	1.6%	58.4%
Internal hemorrhoid ligation	216	356	16 795	1.6%	60.0%
Gastric decompression	900	3 712	16 473	1.5%	61.5%
Percutaneous transhepatic cholangiography drainage (PTCD)	38	54	15 735	1.5%	63.0%
Choledocholithotomy with T-tube drainage	28	28	15 282	1.4%	64.4%
Radical gastrectomy	14	14	15 061	1.4%	65.8%
Radical proctectomy	11	11	14 723	1.4%	67.2%
Radical hemicolectomy with ascending colon anastomosis	23	23	13 973	1.3%	68.5%
Restorative proctectomy with colo-anal anastomosis	11	11	13 948	1.3%	69.8%
Vagotomy and pyloroplasty	20	20	13 911	1.3%	71.1%
Others			307 915	28.9%	100.0%
Total ^a	8 349	60 245	1 066 497	100.0%	

^aNumbers might not add to totals because of rounding.

Table 5 Utilization and costs of drugs related to gastroenterological diseases among cohorts ($n=183\ 976$) in 2001, by the fourth level of ATC classification system

ATC code	Drug group name	No. of patients	No. of orders	Total cost		
				US \$	%	Cum. %
A02BA	H ₂ -receptor antagonists	26 690	85 228	269 851	17.4%	17.4%
A02BC	Proton pump inhibitors	2 223	7 100	219 823	14.2%	31.6%
A02AF	Antacids with antiflatulents	98 197	385 623	156 244	10.1%	41.6%
A05BA	Liver therapy	3 234	12 990	113 482	7.3%	49.0%
A02AD	Combinations and complexes of aluminium, calcium and magnesium compounds	83 569	305 357	108 399	7.0%	55.9%
A03FA	Propulsives	46 418	140 278	108 006	7.0%	62.9%
A02AB	Aluminium compounds	20 845	50 850	71 820	4.6%	67.5%
A06AB	Contact laxatives	8 775	37 266	59 022	3.8%	71.3%
A02AG	Antacids with antispasmodics	53 966	160 086	52 394	3.4%	74.7%
A06AC	Bulk producers	2 327	5 851	47 848	3.1%	77.8%
A09AA	Enzyme preparations	15 041	37 149	35 754	2.3%	80.1%
A03AA	Synthetic anticholinergics, esters with tertiary amino group	19 071	43 779	28 953	1.9%	82.0%
A07EC	Aminosalicic acid and similar agents	248	1 504	24 494	1.6%	83.6%
A03AX	Other synthetic anticholinergic agents	2 264	4 110	22 682	1.5%	85.0%
A04AA	Serotonin (5HT ₃) antagonists	108	375	22 612	1.5%	86.5%
A02DA	Antiflatulents	38 126	97 683	16 448	1.1%	87.5%
A03AB	Synthetic anticholinergics, quaternary ammonium compounds	8 413	15 312	16 205	1.0%	88.6%
A03BB	Belladonna alkaloids, semisynthetic, quaternary ammonium compounds	20 940	39 494	15 415	1.0%	89.6%
A06AD	Osmotically acting laxatives	513	1 485	15 401	1.0%	90.6%
A05AA	Bile acid preparations	409	1 580	15 064	1.0%	91.5%
-	Others			131 330	8.5%	100.0%
	Total ^a	149 062	1719 500	1 551 250	100.0%	

^aNumbers might not add to totals because of rounding.

Utilization and costs of therapeutic procedures related to gastroenterological diseases

Among the cohort during 2001, 8 349 (4.5%) patients utilized 60 245 (7.8%) therapeutic procedures related to gastroenterological diseases with costs of 1 066 497 USD (4.5% of the costs for all therapeutic procedures and 1.3% of the total medical costs). The most common general treatments were nasal feeding, insertion of nasogastric tube, and gastric decompression. The most common surgeries were hernioplasty, appendectomy, cholecystectomy, hemorrhoidectomy, and trans-arterial embolization. The utilization of surgeries was far less frequent than that of general treatments (Table 4).

Utilization and costs of drugs related to gastroenterological diseases

Over four-fifths of the cohort received drugs for treating gastroenterological diseases in value of 1 551 250 USD (7.3% of the costs for all drugs and 1.9% of the total medical costs). The most popular drugs were antacids (ATC group A02A) prescribed to 141 185 (76.7%) patients, drugs for treatment of peptic ulcer (A02B) with 29 181 (15.9%) recipients had the largest (33.1%) share of drug costs related to gastroenterological diseases. Table 5 gives a breakdown of the utilization into the fourth level of ATC classification. Despite fewer recipients, proton pump inhibitors (A02BC) were the second in aggregate cost only to H₂-receptor antagonists (A02BA). Another noteworthy fact was that drugs for liver therapy were prescribed to 7.1% of the cohort.

DISCUSSION

The current study offered concrete and considerable details about prevalence and costs of gastroenterological diseases among the population of local residents in Taiwan. The major findings were as the following: 44.2% of the insured people had ever a gastroenterological diagnosis during the study year. 16.2% of admissions, 8.0% of outpatient visits, and 10.1% of the total medical costs were attributed to gastroenterological diseases as principal diagnoses. GI-related diagnostic procedures accounted for 24.2% of costs for all diagnostic procedures and 2.3% of the total medical costs. GI-related therapeutic procedures accounted for 4.5% of costs for all therapeutic procedures and 1.3% of the total medical costs. GI-related drugs accounted for 7.3% of costs for all drugs and 1.9% of the total medical costs.

The current study focused only on the direct medical costs within the health insurance system. Those services beyond the insurance coverage were not taken into analysis. Although the NHI in Taiwan reimbursed visits and drugs at clinics of traditional Chinese medicine, the popular utilization of various kinds of folklore medicine by the Chinese people remained yet unknown.

The feature of the current study was to estimate costs of gastroenterological diseases from 4 dimensions. The reason of adopting such an approach was mentioned in the subsection of study design. It was initially difficult to define diagnoses related to gastroenterological diseases. If directly the ninth chapter (diseases of the digestive system) of ICD-9-CM was chosen, not only the scope of dentistry would be included, but also it would miss some GI-related infections, neoplasms, injuries, symptoms and signs coded in other chapters. The analysis did not proceed from the specialties of gastroenterologists and general surgeons either, because it might include breast, thyroid diseases and others then. Besides, other specialists and general practitioners might take care of gastroenterological diseases, too. Consequently, the current study followed a popular and public grouping system (CSS for ICD-9-CM) from the U.S.A.

to facilitate international comparisons in the future.

The other dimensions of the current study had limitations, too. With respect to diagnostic procedures, some tests, *e.g.* serum albumin, were not specific to diagnosing gastroenterological diseases. Besides, some tests, *e.g.* serum GOT, GPT, and bilirubin, almost belonged to screening routines on admission, so their utilization could not reflect the prevalence of diseases. Magnetic resonance imaging (MRI) as a popular and expensive procedure was absent in the analysis because the fee schedule of the NHI did not differentiate MRI for abdomen from MRI for other body parts.

With respect to therapeutic procedures, general treatments such as nasal feeding and insertion of nasogastric tube might not be directly related to gastroenterological diseases. In case payments based on diagnosis-related groups, the reimbursement per admission was fixed no matter whether the actual service items aggregately cost more. Because of the discrepancy between nominal and real values, costs of procedures within case payments, *i.e.* hernioplasty, appendectomy, cholecystectomy, and hemorrhoidectomy, might not be estimated accurately.

Drugs for treating gastroenterological diseases in the current study did not include antineoplastic and immunomodulating agents because these drugs were not specific in indications. Antivirals such as lamivudine or ribavirin were not included in the analysis either because they had been not yet reimbursed by the NHI in Taiwan. Although physicians of traditional Chinese medicine also used ICD-9-CM on claims, the lack of a corresponding classification for traditional Chinese drugs limited the analysis. Furthermore, the widespread use of antacids might be a unique phenomenon that reflected the habit of Chinese physicians in co-prescribing antacids^[25].

Finally, it cannot be denied that the diagnoses on insurance claims serve primarily for administrative purposes. They are rather tentative diagnoses than definite ones. Only in combination with conventional epidemiological surveys or data verification, the costs of screening, ruling out, confirming, and treating can be further differentiated.

ACKNOWLEDGMENTS

This study was based in part on data from the National Health Insurance Research Database provided by the Bureau of National Health Insurance, Department of Public Health and managed by National Health Research Institutes in Taiwan. The interpretation and conclusions contained herein do not represent those of Bureau of National Health Insurance, Department of Public Health or National Health Research Institutes. Besides, the author thanks Dr. med. Tzeng-Ji Chen for the professional advice.

REFERENCES

- 1 A primer on outcomes research for the gastroenterologist: report of the American Gastroenterology Association task force on outcomes research. *Gastroenterology* 1995; **109**: 302-306
- 2 **Bodger K**, Daly MJ, Heatley RV, Williams DR. Clinical economics review: gastroenterology. *Aliment Pharmacol Ther* 1996; **10**: 55-60
- 3 **Provenzale D**, Lipscomb J. A reader's guide to economic analysis in the GI literature. *Am J Gastroenterol* 1996; **91**: 2461-2470
- 4 **Hoffman C**, Rice D, Sung HY. Persons with chronic conditions. Their prevalence and costs. *JAMA* 1996; **276**: 1473-1479
- 5 **Provenzale D**. Economic considerations for the hepatologist. *Hepatology* 1999; **29**(Suppl 1): 13S-17S
- 6 **Glick HA**, Polsky D. Analytic approaches for the evaluation of costs. *Hepatology* 1999; **29**(Suppl 1): 18S-22S
- 7 **Sandler RS**, Everhart JE, Donowitz M, Adams E, Cronin K, Goodman C, Gemmen E, Shah S, Avdic A, Rubin R. The burden of selected digestive diseases in the United States. *Gastroenterology* 2002; **122**: 1500-1511

- 8 **Marshall JK**, Cawdron R, Yamamura DL, Ganguli S, Lad R, O'Brien BJ. Use and misuse of cost-effectiveness terminology in the gastroenterology literature: a systematic review. *Am J Gastroenterol* 2002; **97**: 172-179
- 9 OECD Health Data 2001. Paris: *OECD (Organisation for Economic Co-operation and Development)* 2001
- 10 **Drossman DA**, Li Z, Andruzzi E, Temple RD, Talley NJ, Thompson WG, Whitehead WE, Janssens J, Funch-Jensen P, Corazziari E, Richter JE, Koch GG. U.S. householder survey of functional gastrointestinal disorders. Prevalence, sociodemography, and health impact. *Dig Dis Sci* 1993; **38**: 1569-1580
- 11 **Sonnenberg A**, Everhart JE. Health impact of peptic ulcer in the United States. *Am J Gastroenterol* 1997; **92**: 614-620
- 12 **Westbrook JI**. Trends in the utilization of diagnostic upper GI endoscopy in New South Wales, Australia, 1988 to 1998. *Gastrointest Endosc* 2002; **55**: 847-853
- 13 **Bloom BS**, Fox NA, Jacobs J. Patterns of care and expenditures by California Medicaid for peptic ulcer and other acid-related diseases. *J Clin Gastroenterol* 1989; **11**: 615-620
- 14 **Talley NJ**, Gabriel SE, Harmsen WS, Zinsmeister AR, Evans RW. Medical costs in community subjects with irritable bowel syndrome. *Gastroenterology* 1995; **109**: 1736-1741
- 15 **Segal R**, Russell WL, Ben-Joseph R, Mansheim B. Cost of acid peptic disorders in a managed-care organization. *Clin Ther* 1996; **18**: 319-333
- 16 **Greenberg PD**, Koch J, Cello JP. Clinical utility and cost effectiveness of *Helicobacter pylori* testing for patients with duodenal and gastric ulcers. *Am J Gastroenterol* 1996; **91**: 228-232
- 17 **Jönsson B**, Karlsson G. Economic evaluation in gastrointestinal disease. *Scand J Gastroenterol Suppl* 1996; **220**: 44-51
- 18 **Taylor JL**, Zagari M, Murphy K, Freston JW. Pharmacoeconomic comparison of treatments for the eradication of *Helicobacter pylori*. *Arch Intern Med* 1997; **157**: 87-97
- 19 **Levin TR**, Schmittiel JA, Kunz K, Henning JM, Henke CJ, Colby CJ, Selby JV. Costs of acid-related disorders to a health maintenance organization. *Am J Med* 1997; **103**: 520-528
- 20 **Levin TR**, Schmittiel JA, Henning JM, Kunz K, Henke CJ, Colby CJ, Selby JV. A cost analysis of a *Helicobacter pylori* eradication strategy in a large health maintenance organization. *Am J Gastroenterol* 1998; **93**: 743-747
- 21 **Moayyedi P**, Soo S, Deeks J, Forman D, Mason J, Innes M, Delaney B. Systematic review and economic evaluation of *Helicobacter pylori* eradication treatment for non-ulcer dyspepsia. Dyspepsia Review Group. *BMJ* 2000; **321**: 659-664
- 22 **Westbrook JI**, Duggan AE, McIntosh JH. Prescriptions for anti-ulcer drugs in Australia: volume, trends, and costs. *BMJ* 2001; **323**: 1338-1339
- 23 **van Hout BA**, Klok RM, Brouwers JR, Postma MJ. A pharmacoeconomic comparison of the efficacy and costs of pantoprazole and omeprazole for the treatment of peptic ulcer or gastroesophageal reflux disease in the Netherlands. *Clin Ther* 2003; **25**: 635-646
- 24 **Bureau of National Health Insurance**. 2001 National Health Insurance Annual Statistical Report. Taipei: *Bureau of National Health Insurance* 2002
- 25 **Liu JY**, Chen TJ, Hwang SJ. Concomitant prescription of non-steroidal anti-inflammatory drugs and antacids in the outpatient setting of a medical center in Taiwan: a prescription database study. *Eur J Clin Pharmacol* 2001; **57**: 505-508
- 26 **Chen TJ**, Chou LF, Hwang SJ. Trends in prescribing proton pump inhibitors in Taiwan: 1997-2000. *Int J Clin Pharmacol Ther* 2003; **41**: 207-212
- 27 **Chen TJ**, Chou LF, Hwang SJ. Prevalence of anti-ulcer drug use in a Chinese cohort. *World J Gastroenterol* 2003; **9**: 1365-1369
- 28 **Chen TJ**, Chou LF, Hwang SJ. Utilization of hepatoprotectants within the National Health Insurance in Taiwan. *J Gastroenterol Hepatol* 2003; **18**: 868-872
- 29 Guidelines for ATC Classification and DDD Assignment, 3rd ed. Oslo: *WHO Collaborating Centre for Drug Statistics Methodology* 2000
- 30 Clinical Classifications Software (ICD-9-CM) Summary and Download. Summary and Downloading Information. January 2003. Agency for Health Care Policy and Research, Rockville, MD. Available from: URL: <http://www.ahrq.gov/data/hcup/ccs.htm>

Edited by Wang XL

Expression of *bcl-2* family of genes during resection induced liver regeneration: Comparison between hepatectomized and sham groups

Kamil Can Akcali, Aydin Dalgic, Ahmet Ucar, Khemaais Ben Haj, Dilek Guvenc

Kamil Can Akcali, Ahmet Ucar, Khemaais Ben Haj, Department of Molecular Biology and Genetics, Bilkent University, Ankara, Turkey, 06800

Dilek Guvenc, Department of Mathematics, Bilkent University, Ankara, Turkey, 06800

Aydin Dalgic, Department of Surgery, Gazi University Medical School, Ankara, Turkey, 06510

Supported by Bilkent University Faculty Development Grant and Bilkent University Research Grant

Correspondence to: Dr. Kamil Can Akcali, Department of Molecular Biology and Genetics, Bilkent University, Bilkent, Ankara, Turkey, 06800. akcali@fen.bilkent.edu.tr

Telephone: +90-312-2902418 **Fax:** +90-312-2665097

Received: 2003-09-06 **Accepted:** 2003-10-12

Abstract

AIM: During liver regeneration cellular proliferation and apoptosis result in tissue remodeling to restore normal hepatic mass and structure. Main regulators of the apoptotic machinery are the Bcl-2 family proteins but their roles are not well defined throughout the liver regeneration. We aimed to analyze the expression levels of *bcl-2* gene family members during resection induced liver regeneration.

METHODS: We performed semi-quantitative RT-PCR to examine the expression level of *bak*, *bax*, *bcl-2* and *bcl-x_L* in the 70% hepatectomized rat livers during the whole regeneration process and compared to that of the sham and normal groups.

RESULTS: The expression of *bak* and *bax* were decreased whereas *bcl-2* and *bcl-x_L* were increased in hepatectomized animals compared to normal liver at most time points. We also reported for the first time that sham group of animals had statistically significant higher expression of *bak* and *bax* compared to hepatectomized animals. In addition, the area under the curve (AUC) values of these genes were more in sham groups than the hepatectomized groups.

CONCLUSION: We conclude that the expressional changes of *bak*, *bax*, *bcl-2* and *bcl-x_L* genes were altered not only due to regeneration, but also due to the effects of surgical operations.

Akcali KC, Dalgic A, Ucar A, Ben Haj K, Guvenc D. Expression of *bcl-2* family of genes during resection induced liver regeneration: Comparison between hepatectomized and sham groups. *World J Gastroenterol* 2004; 10(2): 279-283

<http://www.wjgnet.com/1007-9327/10/279.asp>

INTRODUCTION

Liver regeneration is a complex physiological response that takes place after the loss of hepatocytes caused by toxic or

viral injury or secondary to liver resection^[1,2]. During regeneration, series of reactions take place to maintain the homeostasis and virtually all of the surviving hepatocytes undergo mitosis^[3]. Experimentally partial hepatectomy (PH) has been a useful model to study the cellular mechanisms of hepatic regeneration.

Post-hepatectomy-induced proliferative response led to full restoration of the hepatic mass in rats in 14 days^[4,5]. Several converging lines of evidence from recent works have established that growth factors and cytokines including hepatocyte growth factor (HGF), tumor necrosis factor- α (TNF- α), interleukin-6 (IL-6), epidermal growth factor (EGF), transforming growth factor- α (TGF- α), fibroblast growth factor (FGF), vascular endothelial growth factor (VEGF), transforming growth factor- β 1 (TGF- β 1) and hormones such as insulin, glucagon, sex hormones, thyroid hormone, norepinephrine, nitric oxide and vasopressin are important components of liver regeneration^[5-9]. Multiple signaling pathways are then activated by these components^[10,11].

During liver regeneration, apoptosis occurs as a response to eliminate the defective cells that appear due to rapid cellular divisions after PH, resulting in fine-tuning of the liver size and tissue remodeling^[5,12-14]. Therefore, control of apoptosis plays a crucial role in liver regeneration. Among the regulators of apoptosis, the Bcl-2 family of proteins determines the life-or-death of a cell by controlling the releases of mitochondrial apoptogenic factors, cytochrome C and apoptosis inducing factors (AIF), which activate the downstream executional phases, including the activation of the caspases^[15,16]. Bcl-2 family of genes consists of both pro- and anti-apoptotic genes and by forming dimers, they exert their function^[17]. Since Bcl-2 family of proteins is the most important and critical regulators of apoptosis^[18], they should be tightly regulated during regeneration in a time-dependent manner. Existing data suggests the involvement of these proteins in regeneration process during the initial stages of this process^[19-23]. These studies investigated the expression of these genes during the first four days after hepatectomy, however the expression pattern of the Bcl-2 family members were not examined throughout the regeneration process. Therefore, the purpose of the present study was to quantitate the expression levels of some members of *bcl-2* family of genes (*bcl-2*, *bcl-x_L*, *bax*, *bak*) by using semi-quantitative RT-PCR within a time spectrum that extended to 14 days after hepatectomy, which was needed for the completion of the regeneration process. We also compared the expression levels of these genes with the levels of the corresponding sham group of animals. For this purpose, we used the "area under the curve" method as used in pharmacodynamic studies and other liver injury and stress models.

MATERIALS AND METHODS

Animals

Nine weeks old and 200-250 grams male Sprague-Dawley rats were used. They were housed under controlled environmental

conditions (22 °C) with a 12-hour light and 12 hour dark cycle in the animal holding facility of Bilkent University, Turkey. All the animals received care according to the criteria outlined in the "Guide for Care and Use of Laboratory Animals" prepared by the National Academy of Science and this study protocol complied with Bilkent University's guidelines on humane care and use of laboratory animals.

Experimental groups, partial hepatectomy and sham groups

Three randomly selected three animals were used for each time point. After injecting Ketamine (Ketalar, Park Davis) subcutaneously at a dose of 30 mg/kg, liver resections consisting of 70% of the liver mass were performed in PH group^[24]. Sham group of animals underwent the same per operative anesthesia with the PH group. All the surgical operations were done the same as PH, but the liver lobes were not resected. All the operations were performed between 8:00 AM and 12:00 PM to minimize diurnal effects. After the completion of the procedure, the animals were placed under a lamp to prevent the hypothermy and then put into cages (one animal per cage) with continuous supply of food and water. The animals in the PH and corresponding sham groups were sacrificed at 0.5, 2, 8, 18, 36 hours, 3 days, 7 days and 14 days after the operation. The group of animals in which no surgery was performed, as used as normal liver group and mentioned time "0" in quantitated graphs. After sacrificing the animal by cervical dislocation, the remnant liver lobes were excised and washed in DMEM medium, then immediately frozen in liquid nitrogen.

Total RNA isolation and reverse transcription

The RNAs were isolated from all the liver samples using Tripure solution (Roche- Boehringer, Mannheim) according to the manufacturer's protocol. The integrity of the isolated RNA samples was determined by denaturing- (formaldehyde-) agarose gel electrophoresis. The cDNA samples were synthesized from the total RNA samples with the RevertAid First Strand cDNA Synthesis Kit (MBI Fermentas) by using the manufacturer's protocol.

Primer design and semi-quantitative PCR

We designed primers for *bcl-2*, *bcl-x_L* and *bax* by using the cDNA sequences of rat homologues of these genes (GenBank accession numbers of rat homologues of *bcl-2* is NM_016993, *bcl-x_L* is U34963, and *bax* is S76511). In the case of *bak*, the cDNA sequences of mouse (Y13231) and human (U23765) were aligned by Blast (NCBI), and primers were chosen from the longest conserved regions by selecting the mouse sequences in the regions of mismatches. As a housekeeping gene, we used *cyclophilin*, and primers were designed by using the rat cDNA sequence (GenBank accession number: M19533). The primer pairs used for each gene were as follows: *cyclophilin*: GGAAGGTGAAAGAAGGCAT and GAGAGCAGAG ATTACAGGGT; *bcl-2*: CCTGGCATCTTCTCCTTC and TGCTGACCTCACTTGTGG; *bcl-x_L*: TCAATGGCAACC CTTCTG and ATCCGACTACCAATACCTG; *bax*: ACGCATCCACCAAGAAGC and GAAGTCCAGAGTC CAGCC; *bak*: CCGGAATTCCAGGACACAGAGGA and CCAAGCTTGCCCAACAGAACCAC.

In all the reactions, the negative control group was done by using ddH₂O instead of cDNA. For each gene, we determined the cycle number of PCR reactions in which the PCR reaction was not saturated. Based on this, we used the following PCR conditions: The initial denaturation step was at 95 °C, followed by 18 (*cyclophilin*), 33 (*bcl-2*), 37 (*bcl-x_L*), 28 (*bax*), 29 (*bak*) cycles of denaturation for 30 seconds at 95 °C, annealing for 30 seconds at either 55 °C (*cyclophilin*, *bcl-2*, *bak*) or 52 °C

(*bcl-x_L*), or 60 °C (*bax*), and extension for 30 seconds at 72 °C. A final extension at 72 °C for 10 minutes was applied to all the reactions and the PCR products were electrophoresed on a 1.2% agarose gel. Each PCR reaction was replicated three times. The quantitated values for the expression of *bcl-2* family members were normalized with the quantitated values for the *cyclophilin* for each sample respectively by comparing with the expression level of *cyclophilin* in normal liver. The normalized values were then analyzed using Multi-Analyst software and the graphs were drawn.

Calculation of AUC

Area under the curve (AUC) calculations was performed as shown by Tygstrup *et al*^[25]. Results of the expression levels of the *bcl-2* family genes by RT-PCR are given as mean ± SEM. As a measure of the change in expression level during the experimental period, the area of the expression level/time curve (AUC: cDNA level x time) was calculated as the sum of the area of the intervals between the samplings for PH and sham groups. Since the time intervals were different, in order to standardize the calculations, we used hour as the unit of X-axis i.e. between 7 days and 14 days, we multiplied with 168 (24x7) to calculate the area under the curve. To determine the hourly changes at the AUC, we divided the AUC values by the hour difference between each two-time points; i.e. between 2 and 8 hour groups, AUC value was calculated and divided by 6.

Statistical tests

For each group of three animals the mean expression level was calculated at the given time points. The means of PH and sham groups were compared using Mann-Whitney test. Since sham group animals seemed to have higher levels of expression of these genes than the hepatectomized animals, one-sided significance level (*P* value) of 0.05 was used. The null hypothesis of no difference between the expression of *bax*, *bak*, *bcl-2*, and *bcl-x_L* in PH and sham groups was tested versus the research hypothesis that PH group had lower level of expression than the sham group.

RESULTS

Since the transcriptional control of *bcl-2* gene family has been known to be important, we performed semi-quantitative RT-PCR to examine the changes in the expression levels of the transcripts of *bcl-2*, *bcl-x_L*, *bax* and *bak* in the livers of rats that were subjected to either 70% PH, or sham operation at different time points (Figures 1-4). In all the experiments, the expression at "time 0" was the quantitated expression of each gene in normal livers and accepted as "1" in order to make a comparison with the subsequent time groups.

Expression pattern of pro-apoptotic genes

Two hours after hepatectomy, in 70% PH groups, we observed that the transcript level of *bak* was decreased by twofold compared with that in normal liver (Figure 1, "time 0"). Although *bak* expression levels reached the levels observed in normal liver at 8 hours and 7 days, *bak* was expressed less in comparison with that in the normal liver at other time points (Figure 1, solid circles). On the other hand, in sham group of animals, the expression of *bak* mRNA was higher than that in the normal liver and hepatectomized group at every time point (Figure 1, open circles). The expression of *bak* was significantly higher in sham group than in PH group (*P*<0.001).

Another pro-apoptotic gene, *bax* mRNA expression, like *bak*, was increased at 0.5 hour after hepatectomy and then decreased to below the level in normal liver by 2 hours (Figure 2, solid circles). During the 14-day period except the increase

at 8 hours after hepatectomy, *bax* expression showed a steady pattern and by 14 days after hepatectomy, it reached almost the expression level of the normal liver (Figure 2, solid circles). The expression of *bax* in sham group did not show any sharp changes and unlike *bak*, it remained close to the levels of normal liver by 14 days (Figure 2, open circles). The test results revealed that the expression of *bax* was significantly higher in sham group than in PH group ($P < 0.05$).

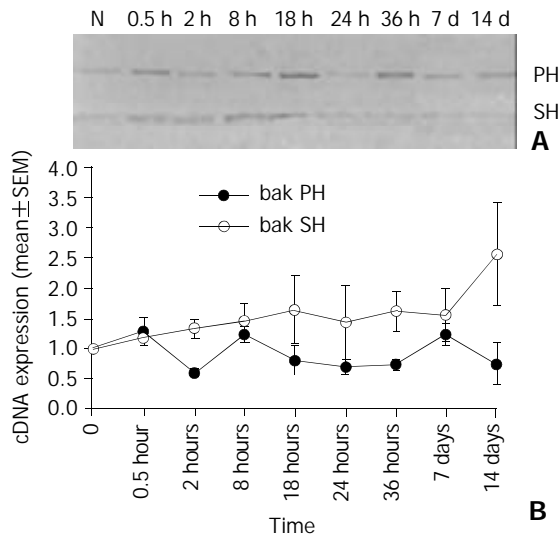


Figure 1 A: The expression of *bak* in 70% hepatectomized (PH) and sham (SH) groups shown in 1.2% agarose gel. B: The quantitated expression of *bak* in 70% PH (—●—) or sham (—○—) groups. Results were expressed as mean \pm SEM of triplicate animals with $n=3$ rats per time point. The expressions were quantitated with the expression of *cyclophilin* for each sample and analyzed using the Multi-Analyst software. The expression at “time 0” denoted the quantitated expression of *bak* in normal liver and was accepted as “1”. In comparison among the mean values at each time point, it was revealed that the means for *bak* in PH group were significantly less than those in SH group ($P < 0.001$ Mann Whitney U test).

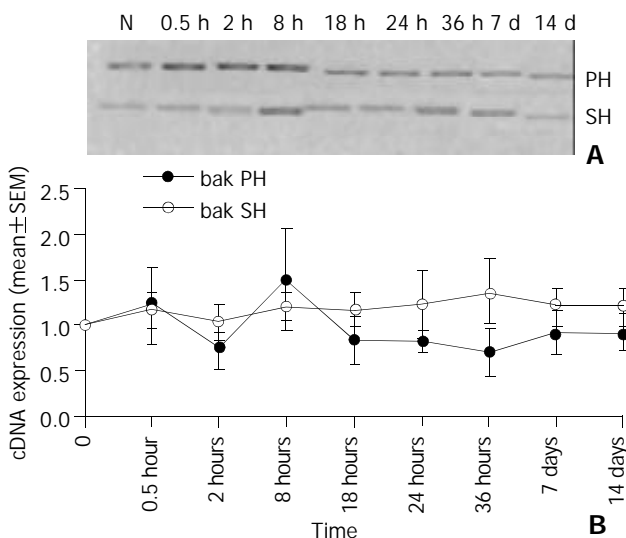


Figure 2 A: The expression of *bax* in 70% hepatectomized (PH) and sham (SH) groups shown in 1.2% agarose gel. B: The quantitated expression of *bax* in 70% PH (—●—) or sham (—○—) groups. Results were expressed as mean \pm SEM of triplicate animals with $n=3$ rats per time point. The expressions were quantitated with the expression of *cyclophilin* for each sample and analyzed using the Multi-Analyst software. The expression at “time 0” denoted the quantitated expression of *bax* in normal liver and was accepted as “1”. In comparison among the mean values at

each time point, it was revealed that the *bax* values in PH group were less than those in SH group (one-tailed $P < 0.05$, Mann Whitney U test).

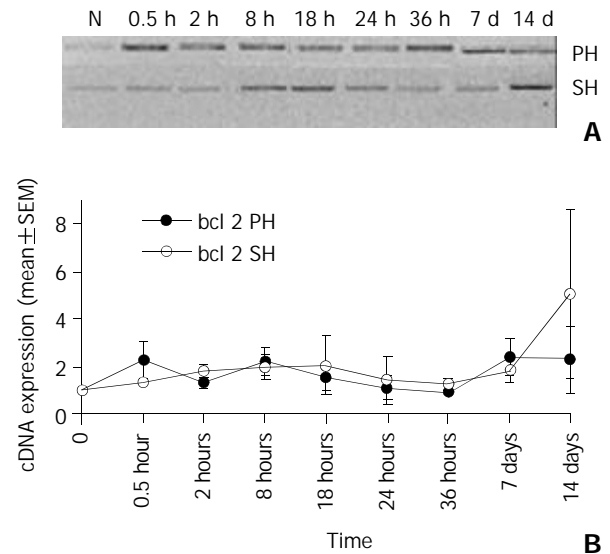


Figure 3 A: The expression of *bcl-2* in 70% hepatectomized (PH) and sham (SH) groups shown in 1.2% agarose gel. B: The quantitated expression of *bcl-2* in 70% PH (—●—) or sham (—○—) groups. Results were expressed as mean \pm SEM of triplicate animals with $n=3$ rats per time point. The expressions were quantitated with the expression of *cyclophilin* for each sample and analyzed using the Multi-Analyst software. The expression at “time 0” denoted the quantitated expression of *bcl-2* in normal liver and was accepted as “1”. Comparing the mean values at each time point, we found no difference in *bcl-2* values between PH and SH group.

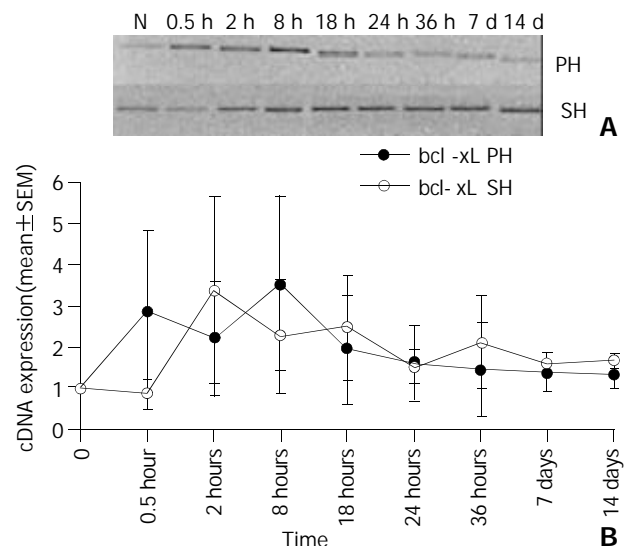


Figure 4 A: The expression of *bcl-x_L* in 70% hepatectomized (PH) and sham (SH) groups shown in 1.2% agarose gel. B: The quantitated expression of *bcl-x_L* in 70% PH (—●—) or sham (—○—) groups. Results were expressed as mean \pm SEM of triplicate animals with $n=3$ rats per time point. The expressions were quantitated with the expression of *cyclophilin* for each sample and analyzed using the Multi-Analyst software. The expression at “time 0” denoted the quantitated expression of *bcl-x_L* in normal liver and was accepted as “1”. Comparing the mean values at each time points, no difference in *bcl-x_L* values between PH and SH groups was found.

Expression pattern of anti-apoptotic genes

Amongst the anti-apoptotic members of *bcl-2* gene family, *bcl-*

2 mRNA expression did not decrease to below the level in normal liver both in PH and sham groups. Its level was increased 0.5 hour after hepatectomy and peaked at 8 hours and 7 days after hepatectomy, more than 2-fold that of the normal liver (Figure 3, solid circles). In the sham group of animals, the expression of this gene also increased by 0.5 hour after surgery and then followed a steady level until day 14. The expression of *bcl-2* in PH and sham group showed a similar pattern except at 14 day. At this time point, *bcl-2* expression was more than two-fold in sham group compared to PH group (Figure 3, open circles).

The expression of another anti-apoptotic gene *bcl-x_L* showed more than 3-fold increase by 8 hours after hepatectomy whereas at the same time interval, the sham group had almost two-fold increase compared to normal liver. The amount of *bcl-x_L* expression decreased afterwards both in PH and sham group (Figure 4). However, in both groups, the expression level was always above the levels in normal liver at all time points.

AUC calculation

In order to better compare the expression levels of *bak*, *bax*, *bcl-2* and *bcl-x_L* during the whole regeneration process, we calculated the AUC values for partially hepatectomized and sham groups, i.e.; the area between the lines connecting cDNA levels of different time and zero. It is important to emphasize that AUC is an arbitrary value but provides a comparison between the total expression of these genes in PH and sham groups. The AUC values for PH and sham groups for each gene analyzed are shown in Table 1. AUC values of all the genes were higher in sham group compared with those in the PH group. Interestingly however, the difference was more obvious for pro-apoptotic genes (*bak* and *bax*) than for anti-apoptotic genes (*bcl-2* and *bcl-x_L*). We detected an 87% and 64% increase in expression levels of pro-apoptotic genes (*bak* and *bax* respectively) in sham group compared to PH group, whereas, this difference was 25% in *bcl-2* and 21% in *bcl-x_L*.

Since the time intervals ranged from 0.5 hour to 7 days, we calculated hourly changes of AUC values in our experiments for each of *bcl-2* family of genes in hepatectomized and sham group of animals. We measured AUC value for each time group and divided this value by the hours of that particular group (Table 2). The values for *bak* and *bax* were found to be significantly higher in sham group than in hepatectomized group ($P < 0.05$). No significant difference was found for *bcl-2* and *bcl-x_L* values.

Table 1 AUC of cDNA expression for members of the *bcl-2* family of genes

	AUC (70% PH)	AUC (SH)	Change
<i>bak</i>	324	609	87%
<i>bax</i>	245	402	64%
<i>bcl-2</i>	666	837	25%
<i>bcl-x_L</i>	494	601	21%

Table 2 Hourly changes of AUC values for the members of the *bcl-2* family of genes

	<i>bak</i> PH ^a	<i>bak</i> SH ^a	<i>bax</i> PH ^a	<i>bax</i> SH ^a	<i>bcl-2</i> PH	<i>bcl-2</i> SH	<i>bcl-x_L</i> PH	<i>bcl-x_L</i> SH
0.5-2 h	0.94	1.25	1.12	2.36	1.81	1.56	2.53	2.13
2-8 h	0.91	1.37	0.8	1.12	1.76	1.88	2.86	2.82
8-18 h	1.01	1.5	1.15	1.19	1.86	2	2.73	2.36
18-24 h	0.75	1.53	0.8	1.19	1.33	1.73	1.78	1.99
24-36 h	0.7	1.52	0.75	1.03	1	1.28	1.53	1.82
36-168 h	0.97	1.58	0.45	1.29	1.65	1.53	1.41	1.87
168-33 6h	0.98	2.1	0.9	1.2	2.35	3.42	1.37	1.64

^a $P < 0.05$ vs the expression of *bak* and *bax* was significantly higher in sham group than that in the hepatectomized group.

DISCUSSION

During liver regeneration, apoptosis allows hepatocytes to die without provoking a potentially harmful inflammatory response. The harmony amongst these complex biological responses is crucial since abnormal regeneration may result in fulminant liver failure, cirrhosis and primary liver cancers^[26]. Since programmed cell death is a major component of hepatic regeneration mechanism, and the *bcl-2* family members are the main regulators of this cellular death pathway, we concentrated on the expression level of these genes throughout the regeneration of liver induced by partial hepatectomy. For all of the members of this family, it has been shown that the transcriptional activation or suppression is critical^[27,28]. Existing data in literature suggests the involvement of these genes in regeneration process however, the expression of these genes has been shown for only 4 days after hepatectomy^[19-23]. Liver regeneration is a long lasting event but there have been no studies regarding the expression of these genes during the later stages of liver regeneration. Since apoptosis is a homeostatic mechanism, the expression of the genes that regulate apoptosis should be important during the whole regeneration process. Therefore, in this study, we quantitated the expression levels of *bak*, *bax*, *bcl-2* and *bcl-x_L* up to 14 days post-hepatectomy, which is the time needed for the completion of regeneration process. In addition, we also examined the expression of these genes in corresponding sham group of animals.

Our data regarding the expression of *bak*, *bax* and *bcl-x_L* during early stages of regeneration (within the first four days) were consistent with previous studies^[19-23]. However contradictory data have been published about the expression of *bcl-2* in normal liver prior to hepatectomy. It has been reported that by using Northern blot Tzung *et al*^[29] did not find any *bcl-2* expression, whereas Kren *et al*^[21] did. Similar to our results Masson *et al*^[22] also found a basal expression of *bcl-2* by using RT-PCR. Since the source of *bcl-2* is non-parenchymal cells, a more sensitive method such as RT-PCR is a better choice of analyzing its expression.

According to our results, the expression levels of *bax* and *bak* in PH group were lower than those in the normal liver except 0.5 and 8 hours after 70% hepatectomy. On the other hand, the anti-apoptotic genes, *bcl-2* and *bcl-x_L* had higher expression levels than those in the normal liver at most of the time points. Amongst them, the expression of *bcl-x_L* in hepatectomized animals was higher than that of normal liver at all the time points. We observed an overall decrease in the pro-apoptotic genes (*bax* and *bak*) and an increase in the anti-apoptotic genes (*bcl-2* and *bcl-x_L*) expression compared to that in normal liver. Recently, Locker *et al* has also shown increased antiapoptotic regulators and down-regulated proapoptotic regulators by using microarray technology during liver regeneration in mouse^[30]. Thus, the increase in the ratio of anti- vs. pro-apoptotic gene expression was in favor of survival of the liver tissue throughout the regeneration process.

In our study, we also compared the total expression of these

genes between sham and partially hepatectomized groups by calculating AUC as used by Tygstrup *et al*^[25]. In their study AUC calculation was used to show and compare the mRNA profiles of a set of liver function related and repair related genes in different liver injury and stress models. By comparing AUC values, they have shown that the expressions of several genes related to liver function were reduced^[25]. By calculating AUC values, we found an interesting phenomenon that had not been reported in previous studies. The AUC values of all the *bcl-2* family of genes were higher in sham group than that of PH group, suggesting the overall expression levels of apoptotic regulator genes in sham group were increased more than those in the hepatectomized group. Since the sham group of animals had undergone the same period of anesthesia and were sacrificed at the same time, the effect of circadian rhythms on the expression of these genes could be ruled out. In addition, when we measured the hourly changes of the expression of these genes, we found an increase in all the genes that we studied in the sham group compared to PH group except for the first 18 hours in *bcl-x_L*. The increase in the case of *bak* and *bax* were statistically significant. This indicated that the expressions of *bak* and *bax* were up regulated in sham group compared to those in hepatectomized group. Therefore, many of the previous findings of expressional changes in transcript levels of *bcl-2*, *bcl-x_L*, *bax* and *bak* might be due to not only regeneration, but also the effects of surgical operations.

The reduction in the expression of proapoptotic *bak* and *bax* in PH group compared to sham group may be related to the enhanced effects of some growth factors on liver proliferation to prevent apoptosis and to ensure the survival of the tissue. It has also been reported that the majority of the rats that had undergone PH, later developed tumors in their remnant liver^[31]. Therefore it is tempting to speculate that decreased expression of proapoptotic genes might be responsible for this outcome. However, the cause for the reduction in the expression of anti-apoptotic *bcl-2* family of genes in PH group compared to sham group has been unclear. In the case of *bcl-2*, since it is expressed exclusively by non-parenchymal cells and especially cholangiocytes, removal of a large portion of the liver might be the explanation for this reduction. Thus, it could be speculated that upon removal of a large portion of the tissue, the liver conferred priority to the expression of vitally most important genes.

REFERENCES

- 1 **Sell S.** Is there a liver stem cell? *Cancer Res* 1990; **50**: 3811-3815
- 2 **Fausto N.** Hepatology- A Textbook of Liver Disease, 2nd ed., Philadelphia: Saunders 1990: 49-64
- 3 **Fausto N,** Webber EM. Liver Regeneration In: Arias IM, Boyer JL, Fausto N, Jakoby WB, Schachter DA, Shafritz DA, eds. The Liver: Biology and Pathobiology. New York: Raven 1994: 1059-1084
- 4 **Fausto N,** Thomson NL, Braun L. Cell separation: Methods and selected applications. Orlando: Academic Press 1986: 45-75
- 5 **Fausto N.** Liver regeneration. *J Hepatol* 2000; **32**(1 Suppl): 19-31
- 6 **Bucher NLR.** Liver regeneration then and now In: Jirtle RL, ed. Liver regeneration and carcinogenesis, Molecular and Cellular Mechanisms. San Diego: Academic Press 1995: 1-25
- 7 **Michalopoulos G,** Defrances M. Liver regeneration. *Science* 1997; **276**: 60-66
- 8 **Xia M,** Xue SB, Xu CS. Shedding of TNFR1 in regenerative liver can be induced with TNF alpha and PMA. *World J Gastroenterol* 2002; **8**: 1129-1133
- 9 **Li YC,** Xu CS, Zhu WL, Li WQ. Isolation and analysis of a novel gene over-expressed during liver regeneration. *World J Gastroenterol* 2003; **9**: 1282-1286
- 10 **Brenner DA.** Signal transduction during liver regeneration. *J Gastroenterol Hepatol* 1998; **13**: S93-95
- 11 **Stolz DB,** Mars WM, Petersen BE, Kim TH, Michalopoulos GK. Growth factor signal transduction immediately after two-thirds partial hepatectomy in the rat. *Cancer Res* 1999; **59**: 3954-3960
- 12 **Fan G,** Kren BT, Steer CJ. Regulation of apoptosis associated genes in the regenerating liver. *Semin Liver Dis* 1998; **18**: 123-140
- 13 **Kren BT,** Trembley JH, Fan G, Steer CJ. Molecular regulation of liver regeneration. *Ann N Y Acad Sci* 1997; **831**: 361-381
- 14 **Sakamoto T,** Liu Z, Murase N, Ezure T, Yokomuro S, Poli V, Demetris AJ. Mitosis and apoptosis in the liver of interleukin-6-deficient mice after partial hepatectomy. *Hepatology* 1999; **29**: 403-411
- 15 **Martinou JC,** Green DR. Breaking the mitochondrial barrier. *Nat Rev Mol Cell Biol* 2001; **2**: 63-67
- 16 **Zamzami N,** Kroemer G. The mitochondrion in apoptosis: how Pandora's box opens. *Nat Rev Mol Cell Biol* 2001; **2**: 67-71
- 17 **Adams JM,** Cory S. The Bcl-2 protein family: Arbiters of cell survival. *Science* 1998; **281**: 1322-1326
- 18 **Cory S,** Adams JM. The Bcl-2 family: regulators of the cellular life-or-death switch. *Nat Rev Cancer* 2002; **2**: 647-656
- 19 **Kamimukai N,** Togo S, Hasegawa S, Kubota T, Kurosawa H, Li XK, Suzuki S, Shimada H. Expression of Bcl-2 family reduces apoptotic hepatocytes after excessive hepatectomy. *Eur Surg Res* 2001; **33**: 8-15
- 20 **Taira K,** Hiroyasu S, Shiraishi M, Muto Y, Koji T. Role of the Fas system in liver regeneration after a partial hepatectomy in rats. *Eur Surg Res* 2001; **33**: 334-341
- 21 **Kren BT,** Trembley JH, Krajewski J, Behren TW, Reed JC, Steer CJ. Modulation of apoptosis-associated genes *bcl-2*, *bcl-x*, and *bax* during rat liver regeneration. *Cell Growth Differ* 1996; **7**: 1633-1642
- 22 **Masson S,** Scotte M, Garnier S, Francois A, Hiron M, Teniere P, Fallu J, Salier JP, Daveau M. Differential expression of apoptosis-associated genes post-hepatectomy in cirrhotic vs normal rats. *Apoptosis* 2000; **5**: 173-179
- 23 **Karavias DD,** Tsamandas AC, Tepetes K, Kritikos N, Kourelis T, Ravazoula P, Vagenas K, Siasos N, Mirra N, Bonikos DS. BCL-2 and BAX expression and cell proliferation, after partial hepatectomy with and without ischemia, on cholestatic liver in rats: an experimental study. *J Surg Res* 2003; **110**: 399-408
- 24 **Wang X,** Parsson H, Anderson R, Soltesz V, Johansson K, Bengmark S. Bacterial translocation, intestinal ultrastructure and cell membrane permeability early after major liver resection in the rat. *Br J Surg* 1994; **81**: 579-584
- 25 **Tygstrup N,** Bangert K, Ott P, Bisgaard HC. Messenger RNA profiles in liver injury and stress: A comparison of lethal and nonlethal rat models. *Biochem Biophys Res Comm* 2002; **290**: 518-525
- 26 **Diehl AM.** Liver generation. *Front Biosci* 2002; **7**: e301-314
- 27 **Gross A,** McDonnell JM, Korsmeyer SJ. Bcl-2 family members and the mitochondria in apoptosis. *Genes Dev* 1999; **13**: 1899-1911
- 28 **Tsujimoto Y,** Shimizu S. Bcl-2 family: Life-or-death switch. *FEBS Lett* 2000; **466**: 6-10
- 29 **Tzung SP,** Fausto N, Hockenberry DM. Expression of Bcl-2 family during liver regeneration and identification of *bcl-x* as a delayed early response gene. *Am J Pathol* 1997; **150**: 1985-1995
- 30 **Locker J,** Tian J, Carver R, Concas D, Cossu C, Ledda-Columbano GM, Columbano A. A common set of immediate-early response genes in liver regeneration and hyperplasia. *Hepatology* 2003; **38**: 314-325
- 31 **Picardo A,** Karpoff HM, Ng B, Lee J, Brennan MF, Fong Y. Partial hepatectomy accelerates local tumor growth: potential roles of local cytokine activation. *Surgery* 1998; **124**: 57-64

Complications of stent placement for benign stricture of gastrointestinal tract

Ying-Sheng Cheng, Ming-Hua Li, Wei-Xiong Chen, Ni-Wei Chen, Qi-Xin Zhuang, Ke-Zhong Shang

Ying-Sheng Cheng, Ming-Hua Li, Qi-Xin Zhuang, Ke-Zhong Shang, Department of Radiology, Sixth People's Hospital, Shanghai Jiaotong University, Shanghai 200233, China

Wei-Xiong Chen, Ni-Wei Chen, Department of Gastroenterology, Sixth People's Hospital, Shanghai Jiaotong University, Shanghai 200233, China

Supported by the National Key Medical Research and Development Program of China during the 9th Five-year Plan Period, No.96-907-03-04; Shanghai Nature Science Funds, No.02Z1314073; Shanghai Medical Development Funds, No.00419

Correspondence to: Dr. Ying-Sheng Cheng, Department of Radiology, Sixth People's Hospital, Shanghai Jiaotong University, Shanghai 200233, China. chengys@sh163.net

Telephone: +86-21-64368920 **Fax:** +86-21-64701361

Received: 2003-05-13 **Accepted:** 2003-06-02

Abstract

AIM: To observe the frequent complications of stent placement for stricture of the gastrointestinal tract and to find proper treatment.

METHODS: A total number of 140 stents were inserted in 138 patients with benign stricture of the gastrointestinal tract. The procedure was completed under fluoroscopy in all of the patients.

RESULTS: Stents were successfully placed in all the 138 patients. Pains occurred in 23 patients (16.7%), slight or dull pains were found in 21 patients and severe chest pain in 2 respectively. For the former type of pain, the patients received only analgesia or even no treatment, while peridural anesthetics was conducted for the latter condition. Reflux occurred in 16 of these patients (11.6%) after stent placement. It was managed by common antireflux procedures. Gastrointestinal bleeding occurred in 13 patients (9.4%), and was treated by hemostat. Restenosis of the gastrointestinal tract occurred in 8 patients (5.8%), and was apparently associated with hyperplasia of granulation tissue. In 2 patients, the second stent was placed under X-ray guidance. The granulation tissue was removed by cauterization through hot-node therapy under gastroscope guidance in 3 patients, and surgical reconstruction was performed in another 3 patients. Stent migration occurred in 5 patients (3.6%), and were extracted with the aid of a gastroscope. Food-bolus obstruction was encountered in 2 patients (1.4%) and was treated by endoscope removal. No perforation occurred in all patients.

CONCLUSION: Frequent complications after stent placement for benign stricture of the gastrointestinal tract include pain, reflux, bleeding, restenosis, stent migration and food-bolus obstruction. They can be treated by drugs, the second stent placement or gastroscopic procedures depend on the specific condition.

Cheng YS, Li MH, Chen WX, Chen NW, Zhuang QX, Shang KZ. Complications of stent placement for benign stricture of gastrointestinal tract. *World J Gastroenterol* 2004; 10(2): 284-286 <http://www.wjgnet.com/1007-9327/10/284.asp>

INTRODUCTION

Stricture of the gastrointestinal tract is a common complication associated with various diseases of the gastrointestinal tract. Previously, such conditions were treated surgically in most patients. Operational difficulties and increased expense have limited its application. The recently established non-vascular stent technology could provide a new approach for such patients^[1]. The procedure has been proved to be effective, but it has various complications^[2-5]. Since 1994, we have placed gastrointestinal stents for benign stricture in 138 patients. Various complications were encountered and treated effectively.

MATERIALS AND METHODS

Materials

Our cohort comprised 138 patients (81 males, 57 females; ages, 18 to 82 years, mean 53.6 years) with benign stricture of gastrointestinal tract. All patients were examined by endoscopy or gastrointestinal barium radiography. Among the 138 patients, 8 had simple sclerosis stricture after radiation therapy for esophageal carcinoma, 86 had achalasia, 36 had esophageal and esophago-gastric anastomosis stricture (complicated with anastomosis fistula in 2), 4 had gastro-duodenal anastomosis stricture, and 4 had esophageal chemical corrosive stricture. All the patients had dysphagia, frequent vomiting, and/or dysphoria before stent placement. The follow-up lasted for 1 week to 8 years.

Methods

Stents were placed in all of the 138 patients under X-ray guidance. For the patients with serious stricture, a probe or saccule was used repeatedly to expand the lesion before stent placement. A total of 140 stents were placed, with two stents at the same site in 2 patients.

RESULTS

Various complications encountered are listed in Table 1.

Table 1 Complications of stent placement for benign stricture of gastrointestinal tract

Type of complication	Patients (n)	Incidence (%)
Pain	23	16.7
Slight or mild	21	15.2
Severe	2	1.5
Reflux	16	11.6
Bleeding	13	9.4
Restonsis	8	5.8
Stent migration	5	3.6
Food-bolus obstruction	2	1.4

Complications were treated according to the specific conditions in each patient. Slight or mild pains ($n=21$) that did not affect work and rest were not treated ($n=12$) and that affecting work and rest were treated with analgesics ($n=9$). For the 2 patients who had severe pain, an analgesic was first

used. This was not effective, peridural anesthesia was conducted and the pain disappeared within 2 days. Sixteen patients had gastro-esophageal or duodenum-gastro biliary regurgitation. Thirteen patients who had gastro-esophageal reflux after stent placement in cardiac achalasia were treated with antacid agent (omeprazole), gastric mucosa protectant (sucralfate) and dynamic medicine (domperidone) for 2 weeks or longer. Administration of medicines was reduced or suspended when symptoms palliated. Thirteen patients exhibited bleeding after stent placement. The bleeding disappeared 2 weeks after venous injection of adrenobazonum. Recurrence of the stricture was observed after stent placement in 8 patients. The second stent was placed in 2 patients under X-ray guidance. Hyperplasia of granulation tissue was cauterized by hot-node therapy in 3 patients under gastroscopie and surgically reconstructed in 3 patients. Stent migration was encountered in 5 patients, and the stent was extracted with the aid of a gastroscopie. Two patients had food-bolus obstruction. It was removed under gastroscopie guidance. No perforation occurred in this series.

DISCUSSION

Complications were frequently encountered after stent placement in benign stricture of gastrointestinal tract^[1-3]. The application of this approach would be hampered if these complications were not well treated. The occurrence of complications was related to the material and structure of stents and skill of the operator. It was also associated with the region and nature of pathological changes and physiques of the patients^[4-6]. However, treatment of the complications remains difficult.

Pain is one of the common complications after stent placement in benign stricture of gastrointestinal tract, and it usually disappears within 2-4 weeks. The causes of pain are diverse. In terms of stent-related reasons, one is the resulted physical expansion, the other is that pain occurs more frequently in patients with severe lesions. Pain is also closely associated with sites of the lesions. The upper part of the esophagus is sensitive to pain, and mucosa erosion occurs more frequently in lower part due to reflux, resulting in a burning sensation. A stent with a diameter of 16 mm was used for patients with serious stricture, stricture at the upper or lower part of the esophagus. This reduced the pain markedly. Severe pain occurred in 2 patients after stent placement. When omeprazole was suspended, a severe chest pain was complained by the patients 3 days later. Treatment with dolantin was not satisfactory, and venous injection of omeprazole and peridural anesthesia were used for 2 days to relieve the pain. In terms of pain after stent placement, the incidence (16.7%) was slightly higher than those reported previously^[7-26]. This may be attributable to the types of lesions and size of the stents. In our series, all patients had benign stricture and large diameter stents were used.

Reflux was mostly associated with pathological changes at the lower part of the esophagus. Expansion by the stents often caused disruption of the lower sphincter of esophagus, resulting in reflux. This problem could cause reflux esophagitis. After stent placement in cardiac achalasia, both reflux and bleeding occurred in three patients and disappeared after treatment with antacid agent, hemostat, and antireflux agent. The incidence of reflux esophagitis (11.6%) in our patients was similar to those previously reported (10-50%). The incidence of bleeding (9.4%) was also similar to those described by other authors^[27-34].

Restenosis of the gastrointestinal tract is a thorny problem after stent placement. Benign restenosis is primarily caused by hyperplasia of granulation tissue, this was particularly true, while uncovered stents were used. We adopted one of the procedures for the restenosis including placement of the second stent, or cauterization through hot-node therapy or surgical reconstruction. However, in some patients covered stents could

not be used for anatomical and pathological reasons, such as the ampullary region (open end of the choledochus) or the descending part of the duodenum. Covered stents could easily cause obstructive jaundice, and uncovered stents were used in such patients. The incidence of restenosis in our series (5.8%) was among the range as reported by other authors (3-20%)^[35-38].

Stent migration was a complication that occurred within one to four weeks in most patients after stent placement in the gastrointestinal tract. In a few patients it occurred 3 months after stent placement. Typically, this occurred most frequently in patients with covered stents. The displaced stents were extracted under gastroscopie guidance. The incidence of stent displacement in our series (3.6%) was in the range as reported previously (0-12.5%)^[39-42].

The incidence of food-bolus obstruction reported in other countries ranged from 7% to 20%^[11], while it was 1.4% in our series. After stent placement, we provided the patients with a fluid or semi-fluid diet at the early stage, a small amount each time and several times a day. Patient compliance with this advice could explain, at least partially, the low incidence of food-bolus obstruction in our series. When this complication occurred, food-bolus could be removed under gastroscopie. Perforation in the gastrointestinal tract was rare^[43-46]. If happened, a second covered stent should be placed or surgery should be conducted immediately.

In patients with malignant pathological changes, stent placement in the gastrointestinal tract was very useful for improving their quality of life. For patients with benign strictures, however, caution was required when placing a stent, especially when it was intended to be permanent. Recoverable stents and biologically degradable stents can be expected to overcome the difficulties and prevent restenosis. This would also reduce the incidence of stent-related complications.

REFERENCES

- 1 **Wong VS**, Garvey CJ, Morris AI. Splitting of the polyethylene coverings as a previously unrecognized complication of oesophageal metallic covered stent (Gianturco-Rosch) inserted for malignant stricture. *Endoscopy* 1998; **30**: 557
- 2 **Boulis NM**, Armstrong WS, Chandler WF, Orringer MB. Epidural abscess: a delayed complication of esophageal stenting for benign stricture. *Ann Thorac Surg* 1999; **68**: 568-570
- 3 **Mayoral W**, Fleischer D, Salcedo J, Roy P, Al-Kawas F, Benjamin S. Nonmalignant obstruction is a common problem with metal stents in the treatment of esophageal cancer. *Gastrointest Endosc* 2000; **51**: 556-559
- 4 **Mauro MA**, Koehler RE, Baron TH. Advances in gastrointestinal intervention: the treatment of gastroduodenal and colorectal obstructions with metallic stents. *Radiology* 2000; **215**: 659-669
- 5 **Wang MQ**, Sze DY, Wang ZP, Wang ZQ, Gao YA, Dake MD. Delayed complications after esophageal stent placement for treatment of malignant esophageal obstructions and esophagorespiratory fistulas. *J Vasc Interv Radiol* 2001; **12**: 465-474
- 6 **Power C**, Rynne M, O'Gorman T, Maguire D, McAnena OJ. An unusual complication following intubation of a benign oesophageal stricture. *Endoscopy* 2001; **33**: 642
- 7 **Rajjman I**, Siddique I, Ajani J, Lynch P. Palliation of malignant dysphagia and fistulae with coated expandable metal stents: experience with 101 patients. *Gastrointest Endosc* 1998; **48**: 172-179
- 8 **Laasch HU**, Nicholson DA, Kay CL, Attwood S, Bancewicz J. The clinical effectiveness of the Gianturco oesophageal stent in malignant oesophageal obstruction. *Clin Radiol* 1998; **53**: 666-672
- 9 **Karras PJ**, Barawi M, Webb B, Michalos A. Squamous cell papillomatosis of esophagus following placement of a self-expanding metal stent. *Dig Dis Sci* 1999; **44**: 457-461
- 10 **Park HS**, Do YS, Suh SW, Choo SW, Lim HK, Kim SH, Shim YM, Park KC, Choo IW. Upper gastrointestinal tract malignant obstruction: initial results of palliation with a flexible covered stent. *Radiology* 1999; **210**: 865-870
- 11 **Pron G**, Common A, Simons M, Ho CS. Interventional radiology

- and the use of metal stents in nonvascular clinical practice: a systematic overview. *J Vasc Interv Radiol* 1999; **10**: 613-628
- 12 **Morgan R**, Adam A. The radiologist's view of expandable metallic stents for malignant esophageal obstruction. *Gastrointest Endosc Clin N Am* 1999; **9**: 431-435
- 13 **Camunez F**, Echenagusia A, Simo G, Turegano F, Vazquez J, Barreiro-Meiro I. Malignant colorectal obstruction treated by means of self-expanding metallic stents: effectiveness before surgery and in palliation. *Radiology* 2000; **216**: 492-497
- 14 **Law WL**, Chu KW, Ho JW, Tung HM, Law SY, Chu KM. Self-expanding metallic stent in the treatment of colonic obstruction caused by advanced malignancies. *Dis Colon Rectum* 2000; **43**: 1522-1527
- 15 **Gomez Herrero H**, Paul Diaz L, Pinto Pabon I, Lobato Fernandez R. Placement of a colonic stent by percutaneous colostomy in a case of malignant stenosis. *Cardiovasc Intervent Radiol* 2001; **24**: 67-69
- 16 **Tominaga K**, Yoshida M, Maetani I, Sakai Y. Expandable metal stent placement in the treatment of a malignant anastomotic stricture of the transverse colon. *Gastrointest Endosc* 2001; **53**: 524-527
- 17 **Maetani I**, Ukita T, Inone H, Yoshida M, Igarashi Y, Sakai Y. Knitted nitinol stent insertion for various intestinal stenoses with a modified delivery system. *Gastrointest Endosc* 2001; **54**: 364-367
- 18 **Mao AW**, Gao ZD, Xu JY, Yang RJ, Xiao XS, Jiang TH, Jiang WJ. Treatment of malignant digestive tract obstruction by combined intraluminal stent installation and intra-arterial drug infusion. *World J Gastroenterol* 2001; **7**: 587-592
- 19 **Adler DG**, Baron TH, Geels W, Morgan DE, Monkemuller KE. Placement of PEG tubes through previously placed self-expanding esophageal metal stents. *Gastrointest Endosc* 2001; **54**: 237-241
- 20 **Razzaq R**, Laasch HU, England R, Marriott A, Martin D. Expandable metal stents for the palliation of malignant gastroduodenal obstruction. *Cardiovasc Intervent Radiol* 2001; **24**: 313-318
- 21 **McGrath JP**, Browne M, Riordan C, Ravi N, Reynolds JV. Expandable metal stents in the palliation of malignant dysphagia and oesophageal-respiratory fistulae. *Ir Med J* 2001; **94**: 270-272
- 22 **Decker P**, Lippler J, Decker D, Hirner A. Use of the Polyflex stent in the palliative therapy of esophageal carcinoma: results in 14 cases and review of the literature. *Surg Endosc* 2001; **15**: 1444-1447
- 23 **Aviv RI**, Shyamalan G, Watkinson A, Tibballs J, Ogunbaye G. Radiological palliation of malignant colonic obstruction. *Clin Radiol* 2002; **57**: 347-351
- 24 **Martinez-Santos C**, Lobato RF, Fradejas JM, Pinto I, Ortega-Deballon P, Moreno-Azcoita M. Self-expandable stent before elective surgery vs emergency surgery for the treatment of malignant colorectal obstructions: comparison of primary anastomosis and morbidity rates. *Dis Colon Rectum* 2002; **45**: 401-406
- 25 **Sanchez W**, Baron TH. Palliative colonic stent placement. *Gastrointest Endosc* 2002; **56**: 735
- 26 **Zhong J**, Wu Y, Xu Z, Liu X, Xu B, Zhai Z. Treatment of medium and late stage esophageal carcinoma with combined endoscopic metal stenting and radiotherapy. *Chin Med J* 2003; **116**: 24-28
- 27 **Keymling M**. Colorectal stenting. *Endoscopy* 2003; **35**: 234-238
- 28 **May A**, Ell C. Palliative treatment of malignant esophagorespiratory fistulas with Gianturco-Z stents. A prospective clinical trial and review of the literature on covered metal stents. *Am J Gastroenterol* 1998; **93**: 532-535
- 29 **Bastos I**, Gomes D, Gregorio C, Baranda J, Gouveia H, Donato A, de Freitas D. An unusual foreign body in the rectum. *Hepatogastroenterology* 1998; **45**: 1587-1588
- 30 **Davies N**, Thomas HG, Eyre-Brook IA. Palliation of dysphagia from inoperable oesophageal carcinoma using Atkinson tubes or self-expanding metal stents. *Ann R Coll Surg Engl* 1998; **80**: 394-397
- 31 **Conio M**, Caroli-Bosc F, Demarquay JF, Sorbi D, Maes B, Delmont J, Dumas R. Self-expanding metal stents in the palliation of neoplasms of the cervical esophagus. *Hepatogastroenterology* 1999; **46**: 272-277
- 32 **Sandha GS**, Marcon NE. Expandable metal stents for benign esophageal obstruction. *Gastrointest Endosc Clin N Am* 1999; **9**: 437-446
- 33 **Paul L**, Pinto I, Gomez H, Fernandez-Lobato R, Moyano E. Metallic stents in the treatment of benign diseases of the colon: preliminary experience in 10 cases. *Radiology* 2002; **223**: 715-722
- 34 **Lee A**, Forbes K. Esophageal stents may interfere with the swallowing reflex: an illustrative case history. *J Pain Symptom Manage* 1998; **16**: 254-258
- 35 **McManus K**, Khan I, McGuigan J. Self-expanding oesophageal stents: strategies for re-intervention. *Endoscopy* 2001; **33**: 601-604
- 36 **Kaneko K**, Ito H, Konishi K, Kurahashi T, Katagiri A, Katayose K, Kitahara T, Ohtsu A, Mitamura K. Implantation of self-expanding metallic stent for patients with malignant stricture after failure of definitive chemoradiotherapy for T3 or T4 esophageal squamous cell carcinomas. *Hepatogastroenterology* 2002; **49**: 699-705
- 37 **Nemoto K**, Takai Y, Ogawa Y, Kakuto Y, Ariga H, Matsushita H, Wada H, Yamada S. Fatal hemorrhage in irradiated esophageal cancer patients. *Acta Oncol* 1998; **37**: 259-262
- 38 **Kennedy C**, Steger A. Fatal hemorrhage in stented esophageal carcinoma: tumor necrosis of the aorta. *Cardiovasc Intervent Radiol* 2001; **24**: 443-444
- 39 **Sen S**, Balaratnam N, Wood LA, Allison MC. Buckling of redundant expansile stent distal to an oesophageal cancer: endoscopic management. *Endoscopy* 1998; **30**: 422-424
- 40 **Von Schonfeld J**. Endoscopic retrieval of a broken and migrated esophageal metal stent. *Z Gastroenterol* 2000; **38**: 795-798
- 41 **De Palma GD**, Iovino P, Catanzano C. Distally migrated esophageal self-expanding metal stents: wait and see or remove? *Gastrointest Endosc* 2001; **53**: 96-98
- 42 **Di Fiore F**, Lecleire S, Antonietti M, Savoye G, Savoye-Collet C, Herve S, Roque I, Hochain P, Ben Soussan E. Spontaneous passage of a dislocated esophageal metal stent: report of two cases. *Endoscopy* 2003; **35**: 223-225
- 43 **Banerjee A**, Rao KS, Nachiappan M. Intrathoracic oesophageal perforations following bougienage: a protocol for management. *Aust N Z J Surg* 1989; **59**: 563-566
- 44 **Pajarinen J**, Ristkari SK, Mokka RE. A report of three cases with an oesophageal perforation treated with a coated self-expanding stent. *Ann Chir Gynaecol* 1999; **88**: 332-334
- 45 **Kim HC**, Han JK, Kim TK, Do KH, Kim HB, Park JH, Choi BI. Duodenal perforation as a delayed complication of placement of an esophageal stent. *J Vasc Interv Radiol* 2000; **11**: 902-904
- 46 **Sarmiento RI**, Lee DW, Wong SK, Chan AC, Chung SC. Mesenteric perforation of an obstructing sigmoid colon tumor after endoluminal stent insertion. *Endoscopy* 2003; **35**: 94

Edited by Wang XL

Long-term outcome of esophageal myotomy for achalasia

Jun-Feng Liu, Jun Zhang, Zi-Qiang Tian, Qi-Zhang Wang, Bao-Qing Li, Fu-Shun Wang, Fu-Min Cao, Yue-Feng Zhang, Yong Li, Zhao Fan, Jian-Jing Han, Hui Liu

Jun-Feng Liu, Zi-Qiang Tian, Qi-Zhang Wang, Bao-Qing Li, Fu-Shun Wang, Fu-Min Cao, Yue-Feng Zhang, Yong Li, Zhao Fan, Jian-Jing Han, Hui Liu, Department of Thoracic Surgery, Fourth Hospital, Hebei Medical University, Shijiazhuang 050011, Hebei Province, China

Jun Zhang, Department of Surgery, Shenzhou City Hospital, Shenzhou 052860, Hebei Province, China

Correspondence to: Jun-Feng Liu, Department of Thoracic Surgery, Fourth Hospital, Hebei Medical University, 12 Jiankang Road, Shijiazhuang 050011, Hebei Province, China. liujf@heinfo.net

Telephone: +86-311-6033941 **Fax:** +86-311-6077634

Received: 2003-06-21 **Accepted:** 2003-07-24

Abstract

AIM: Modified Heller's myotomy is still the first choice for achalasia and the assessment of surgical outcomes is usually made based on the subjective sensation of patients. This study was to objectively assess the long-term outcomes of esophageal myotomy for achalasia using esophageal manometry, 24-hour pH monitoring, esophageal scintigraphy and fiberoptic esophagoscopy.

METHODS: From February 1979 to October 2000, 176 patients with achalasia underwent modified Heller's myotomy, including esophageal myotomy alone in 146 patients, myotomy in combination with Gallone or Dor antireflux procedure in 22 and 8 patients, respectively. Clinical score, pressure of the lower esophageal sphincter (LES), esophageal clearance rate and gastroesophageal reflux were determined before and 1 to 22 years after surgery.

RESULTS: After a median follow-up of 14 years, 84.5% of patients had a good or excellent relief of symptoms, and clinical scores as well as resting pressures of the esophageal body and LES were reduced compared with preoperative values ($P < 0.001$). However, there was no significant difference in DeMeester score between pre- and postoperative patients ($P = 0.51$). Esophageal transit was improved in postoperative patients, but still slower than that in normal controls. The incidence of gastroesophageal reflux in patients who underwent esophageal myotomy alone was 63.6% compared to 27.3% in those who underwent myotomy and antireflux procedure ($P = 0.087$). Three (1.7%) patients were complicated with esophageal cancer after surgery.

CONCLUSION: Esophageal myotomy for achalasia can reduce the resting pressures of the esophageal body and LES and improve esophageal transit and dysphagia. Myotomy in combination with antireflux procedure can prevent gastroesophageal reflux to a certain extent, but further randomized studies should be carried out to demonstrate its efficacy.

Liu JF, Zhang J, Tian ZQ, Wang QZ, Li BQ, Wang FS, Cao FM, Zhang YF, Li Y, Fan Z, Han JJ, Liu H. Long-term outcome of esophageal myotomy for achalasia. *World J Gastroenterol* 2004; 10(1): 287-291

<http://www.wjgnet.com/1007-9327/10/287.asp>

INTRODUCTION

Achalasia is an esophageal motility disorder characterized by failure of lower esophageal sphincter (LES) to relax with swallowing and by the absence of esophageal peristalsis. Up to now, surgical treatment is still the first choice for the disease although dilatation and medication have been reported extensively^[1-5]. Because pathophysiological changes of achalasia could not be rectified by any measures, the treatment usually aims at the reduction of LES pressure in order to increase esophageal transit and relieve dysphagia^[6].

The outcomes of myotomy for achalasia have been assessed usually according to the subjective sensation of patients in other studies^[7], which lack objective criteria. Until now, there have been no reports about the objective evaluation on long-term outcomes of Heller's myotomy for achalasia in a large group of patients in China. The aim of this study was to objectively evaluate the long-term outcomes of Heller's myotomy for achalasia by 24-hour pH monitoring, esophageal manometry, esophageal scintigraphy and esophagoscopy.

MATERIALS AND METHODS

General materials

From February 1979 to October 2000, 176 patients underwent modified Heller's myotomy for achalasia at the Department of Thoracic Surgery, Fourth Hospital, Hebei Medical University. There were 78 men and 98 women, ranging from 8 to 62 years (mean 32.9 years). All patients (100%) had varying extent of dysphagia for a mean of 4.8 years (range 2 months to 37 years) before operation. One hundred and thirteen (64.2%) patients had vomiting, 54 (30.7%) regurgitation at night, 8 (4.5%) chest pain or substernal discomfort and 2 (1.1%) heartburn. Symptoms were evaluated by a clinical scoring system proposed by Eckardt *et al*^[8], in which a sum of the individual scores of three major symptoms including dysphagia, heartburn and chest pain was calculated. Each of these symptoms was graded as followings: 0, absent; 1, occasional; 2 daily; 3, with each meal. Therefore, the highest score was 9.

Pre-operative examination

Before surgery, esophagography was performed for all patients, esophagoscopy (Olympus GIF 100) for 114, esophageal manometry (Synectics Medical, Stockholm, Sweden) for 50, 24-hour esophageal pH monitoring (Synectics Medical, Stockholm, Sweden) for 12, esophageal scintigraphy as previously described^[9] for 12 patients and 12 normal subjects as controls. Existence of gastroesophageal reflux was defined if a DeMeester score was more than 14.72 by 24-hour esophageal pH monitoring.

Surgery

Myotomy was performed from 5 cm above the esophagogastric junction to 1.5 cm distal to the esophagogastric junction for all of the 176 patients. As an antireflux procedure, Gallone operation^[10] was added for 22 patients and Dor operation^[11] for 8 patients. Thus, 146 patients underwent esophageal myotomy only, and 30 patients underwent combined esophageal myotomy and antireflux procedure in the present study.

Follow-up study

Fifty-eight patients were followed up from 1 year to 22 years after surgery, with a median follow-up of 14 years. The patients were inquired for dysphagia, heartburn and chest pain. Clinical scores were calculated according to Eckardt *et al*^[8] and compared with preoperative values. According to the method described by Devaney *et al*^[12], the efficacy of operation was graded as excellent (completely asymptomatic), good (mild symptoms requiring no treatment), fair (symptoms requiring occasional treatment such as dilatation or anti-diarrhea medication), and poor (symptoms requiring regular treatment). Postoperatively, esophageal manometry was performed for 30 patients, 24-hour pH monitoring for 22, esophageal scintigraphy for 42, and esophagoscopy for 15.

Statistical analysis

Data on clinical scores, resting pressures of the esophageal body and LES, and DeMeester scores were expressed as mean±SD, and analysed with Student's *t* test. The incidence of gastroesophageal reflux and esophagitis was assessed with Chi-square test. Statistical analyses were performed using a SPSS 10.0 software package, and the differences were considered as significant if $P < 0.05$.

RESULTS

In the present study, 84.5% (49/58) of patients had a good or excellent relief of dysphagia after a median follow-up of 14 years. Table 1 shows pre- and post-operative clinical scores, resting pressures of the esophageal body and LES, and DeMeester scores. Clinical scores and resting pressures of the esophageal body and LES were significantly reduced after Heller's myotomy ($P < 0.001$). After a long-term follow-up study, both clinical scores and LES pressures still remained lower than preoperative values, but had a trend of elevation

with the lapse of postoperative time (Figures 1 and 2). There were no significant differences in DeMeester score between pre- and post-operative patients ($P = 0.512$). DeMeester scores were above normal value in 33.3% (4/12) of preoperative patients, and in 45.5% (10/22) of postoperative patients ($P = 0.717$). In contrast, esophagitis was detected with esophagoscopy in 21.9% (25/114) of the patients before surgery and in 46.7% (7/15) after surgery ($P = 0.054$). Compared with preoperative patients, the esophageal clearance rate was improved in postoperative patients, but did not reach normal until the fifth minute after swallowing of isotope-labeled semi-liquid food (Table 2).

In group of esophageal myotomy with anti-reflux procedure, clinical scores were similar to those in group of esophageal myotomy alone ($P = 0.27$). Also, there was no significant difference in objective parameters including LES resting pressure and DeMeester score between the 2 groups ($P > 0.05$) (Table 3). Twenty-four-hour esophageal pH monitoring showed that the incidence of gastroesophageal reflux in patients undergoing esophageal myotomy with anti-reflux procedure was 27.3% (3/11) compared to 63.6% (7/11) in those undergoing esophageal myotomy only ($P = 0.087$).

Four patients were found to have varying extents of resumption of esophageal peristalsis by esophageal manometry at 20 months, 7, 15 and 20 years after esophageal myotomy, respectively (Figure 3). Three (1.7%) patients underwent re-operation, of whom 2 underwent myotomy again at 1 year and 4 years after surgery respectively for severe dysphagia due to scar formation around abdominal segment of the esophagus, and the remaining 1 underwent resection of the lower third of the esophagus at the third postoperative year due to repeated bleeding resulted from gastroesophageal reflux. Squamous cell carcinoma occurred in 3 (1.7%) patients at 6, 17 and 18 years after Heller's myotomy, respectively, and esophagectomy was performed for these patients.

Table 1 Objective and subjective parameters from patients with achalasia before and after Heller's myotomy

	Before surgery		After surgery		<i>t</i>	<i>P</i>
	<i>n</i>	mean±SD	<i>n</i>	mean±SD		
Clinical score	176	4.11±0.93	58	1.84±1.26	14.66	0.000
RP of the LES (cm H ₂ O)	50	31.14±10.54	30	18.05±8.90	5.76	0.000
RP of the EB (cm H ₂ O)	50	13.66±5.49	30	4.96±4.86	7.15	0.000
DeMeester score	12	33.87±54.2	22	49.75±73.4	0.663	0.512

RP=resting pressure, EB=esophageal body.

Table 2 Esophageal clearance rates for pre- and post-myotomy patients and normal controls (mean±SD%)

<i>n</i>	Times after isotope labeled semi-liquid meal intaken				
	5 th second	1 st minute	2 nd minute	5 th minute	
Normal controls	12	91.7±1.4	92.5±1.9	92.8±2.1	93.0±2.5
Pre-myotomy pts	12	7.5±2.1 ^a	40.4±28.2 ^a	45.5±30.1 ^a	50.5±35.5 ^a
Post-myotomy pts	42	33.7±8.8 ^b	80.2±19.1 ^c	85.4±12.2 ^c	94.4±5.1

^a $P < 0.01$ vs normal controls and post-myotomy patients, ^b $P < 0.01$ vs normal controls, ^c $P < 0.05$ vs normal controls.

Table 3 Subjective and objective parameters from patients who underwent Heller's myotomy alone and in combination with antireflux procedure

	Heller alone		Heller+antireflux		<i>t</i>	<i>P</i>
	<i>n</i>	mean±SD	<i>n</i>	mean±SD		
Clinical score	47	1.79±1.19	11	2.27±1.62	1.11	0.27
LES RP(cm H ₂ O)	25	18.4±9.80	5	16.6±3.23	0.44	0.66
DeMeester score	11	44.4±38.5	11	55.1±29.3	0.34	0.74

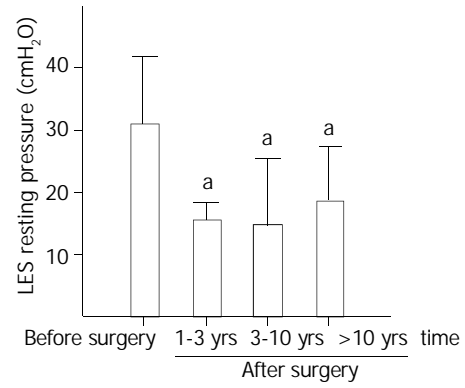
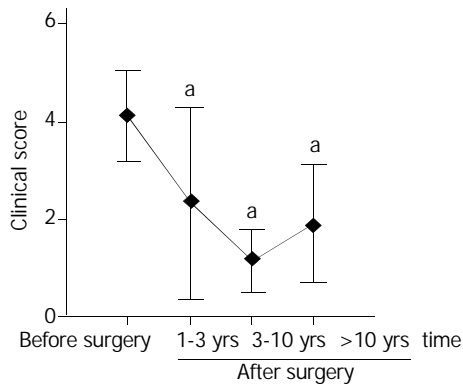


Figure 1 Clinical scores before and at various intervals after Heller's myotomy. Data were expressed as mean±SD. ^a*P*<0.001 vs before surgery.

Figure 2 Lower esophageal sphincter (LES) pressure before and at various times after Heller's myotomy. Data were expressed as mean±SD. ^a*P*<0.001 vs before surgery.

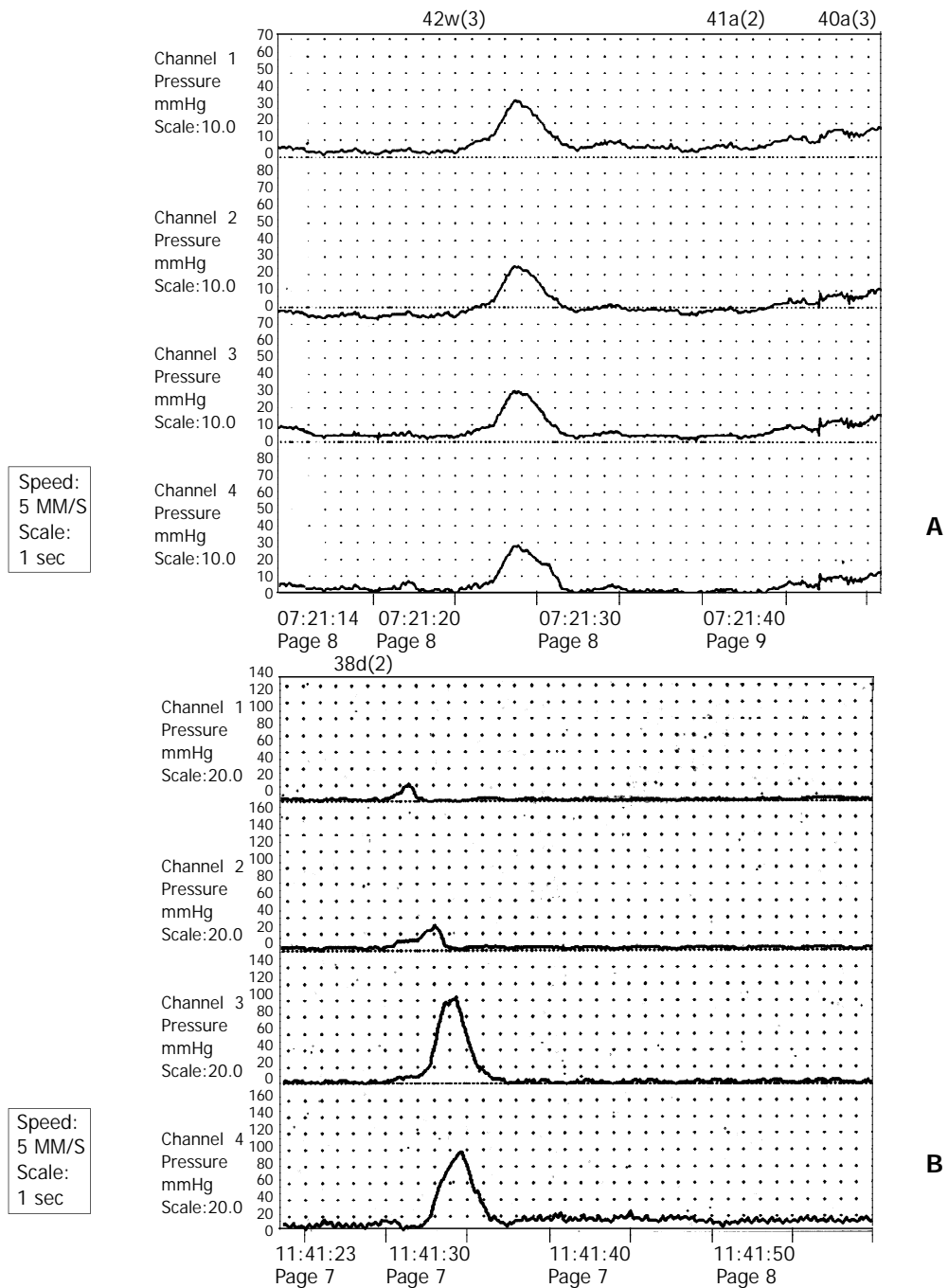


Figure 3 Esophageal manometric tracings obtained from a 29-y female patient with achalasia before and after Heller's myotomy. A, Preoperative manometry showed simultaneous contractions of the esophagus, suggestive of no pulsive peristalsis. B, Esophageal manometry revealed peristaltic contractions seven years after Heller's myotomy.

DISCUSSION

Achalasia is an uncommon disease. Although there are no epidemiological data in China, its incidence is one per 100 000 population in Western countries^[13-16]. The major pathophysiological changes of achalasia are aperistalsis of the smooth muscle portion of the esophagus and absent or incomplete relaxation of LES with swallowing. Neuroanatomic data suggest ganglion cell is degenerated in the esophageal myenteric plexus. Although the cause of achalasia is unknown, it has been hypothesized to be related to class II HLA antigen DQw1^[16], and herpes zoster^[17] or measles virus infections^[18]. The finding of antimyenteric neuron antibodies in achalasia patients has shown it is an autoimmune pathogenesis^[19].

In general, aperistalsis of the esophagus in achalasia patients is not reversible after esophageal myotomy. For this reason, its treatment usually aims at the reduction of LES resting pressure. In the currently used methods, medication and dilation have been found to have a certain efficacy, but the duration of dysphagia relief was short^[20,21]. Thus, up to now, myotomy has been the first choice for achalasia. In the present study, both LES resting pressure and clinical score were significantly decreased after Heller's myotomy, and 84.5% of patients had a good or excellent relief of dysphagia. This figure was consistent with other reports^[22,23]. Furthermore, the relief of clinical symptoms was permanent after Heller's myotomy in the present study. In contrast, the effective relief of symptoms has been reported to present in only 15%-30% of patients one year after intra-sphincter injection of botulinum toxin^[3,24], and in 50% of patients one year after pneumatic dilatation^[3].

Our results of esophageal manometry showed that resting pressure of the esophageal body was also decreased along with the drop of LES pressure after esophageal myotomy. This may be resulted from the reduction or disappearance of intra-esophageal content after Heller's myotomy. Generally, aperistaltic esophagus could not become peristaltic after Heller's myotomy. However, we found that aperistaltic esophagus resumed peristalsis in 4 patients at 20 months, 7, 15 and 20 years after surgery, respectively. In these patients, the mean time of dysphagia was 1.1 years (range 2 months to 8 years) before surgery, which was shorter than that in the entire group (4.8 years), and there were 2 patients with moderate dilation of the esophagus and 2 with mild dilation. Although the reason is unknown, this finding indicates that it is potential for a few achalasia patients to resume their esophageal peristalsis after Heller's myotomy. Chen and colleagues^[25] found that the return of peristalsis was seen mainly in patients with a short clinical evolution, and a little esophageal dilation with preserved contractile capacity. Therefore, we suggest that Heller's myotomy should be performed as early as possible once achalasia is diagnosed.

In the present study, DeMeester scores had no significant changes after Heller's myotomy compared with preoperative values. It was reported that gastroesophageal reflux seldom occurred in patients with achalasia before Heller's myotomy, and the reasons for higher DeMeester scores in aperistaltic esophagus were due to the increase of lactic acid resulted from fermentation of retained food in the esophagus^[26,27]. In the present study, 24-hour esophageal pH monitoring showed that DeMeester scores were above the normal level in 33.3% of patients before surgery, which is higher than the incidence in normal populations. After Heller's myotomy, gastroesophageal reflux may occur because of the destruction of anti-reflux barrier. Our results also showed that the overall incidence of gastroesophageal reflux was 45.5% in patients undergoing Heller's myotomy. In the literature, the corresponding figure was 25% in those who had undergone esophageal myotomy in combination with anti-reflux procedure^[28].

In the present study, 3 (1.7%) patients developed squamous cell carcinoma, while the reported incidence varied between

1.7% and 20%^[22,29]. Ribeiro *et al*^[30] indicated that chronic irritation of the esophagus appeared to participate in the process of carcinogenesis in patients with achalasia. Although esophageal emptying has been significantly improved after Heller's myotomy, it could not reach normal level because of the aperistaltic esophagus. For this reason, epithelial hyperplasia of the esophagus caused by chronic irritation before surgery may develop into cancer after surgery. Thus, the incidence of squamous cell carcinoma in achalasia patients who have undergone Heller's myotomy is still higher than that in normal population. For this reason, esophagoscopy should be performed for achalasia patients before surgery and at postoperative follow-up to rule out cancer.

It has been a controversy whether an anti-reflux procedure should be performed with Heller's myotomy^[31]. In the present study, the postoperative incidence of gastroesophageal reflux in patients who underwent Heller's myotomy in combination with antireflux procedure was 27.3% compared to 63.6% in those undergoing Heller's myotomy only. In addition, esophagitis was found in 46.7% of patients at postoperative follow-up, and most of them might be resulted from gastroesophageal reflux. However, there were no significant differences in DeMeester and clinical scores between Heller's myotomy only and myotomy in combination with antireflux procedure. Esophageal bleeding resulted from gastroesophageal reflux occurred in one patient who underwent myotomy alone and severe dysphagia occurred in 2 patients who underwent myotomy in combination with anti-reflux procedure due to scar formation around the abdominal segment of the esophagus. Therefore, there is no overwhelming evidence to indicate myotomy in combination with anti-reflux procedure is better than myotomy only for achalasia, and a large number of patients should be studied randomly before the dispute is settled. In our experience, partial rather than total fundoplication should be performed with myotomy because aperistaltic esophagus has a poor emptying ability, and total fundoplication hinders esophageal transit more severely than partial fundoplication does.

Up to now, modified Heller's myotomy is still the best choice for achalasia because of its high rate of symptom relief and permanent efficacy. Heller's myotomy in combination with antireflux procedure could stop gastroesophageal reflux to a certain extent, but a large number of patients should be studied randomly to further demonstrate its efficacy.

REFERENCES

- 1 **Anselmino M**, Perdakis G, Hinder RA, Polishuk PV, Wilson P, Terry JD, Lanspa SJ. Heller myotomy is superior to dilatation for the treatment of early achalasia. *Arch Surg* 1997; **132**: 233-240
- 2 **Katz PO**, Gilbert J, Castell DO. Pneumatic dilatation is effective long-term treatment for achalasia. *Dig Dis Sci* 1998; **43**: 1973-1977
- 3 **Mikaeli J**, Fazel A, Montazeri G, Yaghoobi M, Malekzadeh R. Randomized controlled trial comparing botulinum toxin injection to pneumatic dilatation for the treatment of achalasia. *Aliment Pharmacol Ther* 2001; **15**: 1389-1396
- 4 **Cuilliere C**, Ducrotte P, Zerbib F, Metman EH, de Looze D, Guillemot F, Hudziak H, Lamouliatte H, Grimaud JC, Ropert A, Dapigny M, Bost R, Lemann M, Bigard Denis P, Auget JL, Galmiche JP, Bruley des Varannes S. Achalasia: outcome of patients treated with intrasphincteric injection of botulinum toxin. *Gut* 1997; **41**: 87-92
- 5 **Pasricha PJ**, Ravich WJ, Hendrix TR, Sostre S, Jones B, Kalloo AN. Treatment of achalasia with intrasphincteric injection of botulinum toxin: A pilot trial. *Ann Intern Med* 1994; **121**: 590-591
- 6 **Spieess AE**, Kahrilas PJ. Treating achalasia: from whalebone to laparoscope. *JAMA* 1998; **280**: 638-642
- 7 **Torbey CF**, Achkar E, Rice TW, Baker M, Richter JE. Long-term outcome of achalasia treatment: the need for closer follow-up. *J Clin Gastroenterol* 1999; **28**: 125-130
- 8 **Eckardt VF**, Aigner C, Bernhardt G. Predictors of outcome in patients with achalasia treated by pneumatic dilation. *Gastroen-*

- terology* 1992; **103**: 1732-1738
- 9 **Liu JF**, Wang QZ, Li WQ, Li BQ, Wang FS, Cao FM, Tian ZQ, Zhang YF. Esophageal scintigraphy to quantitate esophageal transit of the achalasia patients after Heller's myotomy. *Zhonghua Heyixue Zazhi* 1995; **15**: 228-229
 - 10 **Gallone L**, Peri G, Galliera M. Proximal gastric vagotomy and anterior fundoplication as complementary procedures to Heller's operation for achalasia. *Surg Gynecol Obstet* 1982; **155**: 337-341
 - 11 **Bonavina L**, Nosadini A, Bardini R, Baessato M, Peracchia A. Primary treatment of esophageal achalasia. Long-term results of myotomy and Dor fundoplication. *Arch Surg* 1992; **127**: 222-226
 - 12 **Devaney EJ**, Lannettoni MD, Orringer MB, Marshall B. Esophagectomy for achalasia: patient selection and clinical experience. *An Thorac Surg* 2001; **72**: 854-858
 - 13 **Mayberry JF**, Atkinson M. Studies of incidence and prevalence of achalasia in the Nottingham area. *Q J Med* 1985; **56**: 451-456
 - 14 **Earlham RJ**, Ellis FH Jr, Nobrega FT. Achalasia of the esophagus in a small urban community. *May Clin Proc* 1969; **44**: 478-483
 - 15 **Howard PJ**, Maher L, Pryde A, Cameron EW, Heading RC. Five year prospective study of the incidence, clinical features, and diagnosis of achalasia in Edinburgh. *Gut* 1992; **33**: 1011-1015
 - 16 **Wong RK**, Maydonovitch CL, Metz SJ, Baker JR Jr. Significant DQw1 association in achalasia. *Dig Dis Sci* 1989; **34**: 349-352
 - 17 **Robertson CS**, Martin BA, Atkinson M. Varicella-zoster virus DNA in the oesophageal myenteric plexus in achalasia. *Gut* 1993; **34**: 299-302
 - 18 **Jones DB**, Mayberry JF, Rhodes J, Munro J. Preliminary report of an association between measles virus and achalasia. *J Clin Pathol* 1983; **36**: 655-657
 - 19 **Verne GN**, Sallustio JE, Eaker EY. Anti-myenteric neuronal antibodies in patients with achalasia: A prospective study. *Dig Dis Sci* 1997; **42**: 307-313
 - 20 **Gelfond M**, Rozen P, Gilat T. Isosorbide dinitrate and nifedipine treatment of achalasia: a clinical, manometric and radionuclide evaluation. *Gastroenterology* 1982; **83**: 963-969
 - 21 **Traube M**, Hongo M, Magyar L, McCallum RW. Effects of nifedipine in achalasia and in patients with high-amplitude peristaltic esophageal contractions. *JAMA* 1984; **252**: 1733-1736
 - 22 **Shai SE**, Chen CY, Hsu CP, Hsia JY, Yang SS. Transthoracic oesophagomyotomy in the treatment of achalasia-a 15-year experience. *Scand Cardiovasc J* 1999; **33**: 333-336
 - 23 **Ionescu NG**, Pereni O, Maghiar A, Ionescu C, Ionescu S, Maghiar T. Oesophageal: Surgical consideration in the management of achalasia. *Br J Surg* 1995; **82**: 105
 - 24 **Bassotti G**, Annese V. Review article: Pharmacological options in achalasia. *Aliment Pharmacol Ther* 1999; **13**: 1391-1396
 - 25 **Chen LQ**, Chughtai T, Sideris L, Nastos D, Taillefer R, Ferraro P, Duranceau A. Long-term effects of myotomy and partial fundoplication for esophageal achalasia. *Dis Esophagus* 2002; **15**: 171-179
 - 26 **Spechler SJ**, Souza RF, Rosenberg SJ, Ruben RA, Goyal RK. Heartburn in patients with achalasia. *Gut* 1995; **37**: 305-308
 - 27 **Smart HL**, Mayberry JF, Atkinson M. Achalasia following gastro-oesophageal reflux. *J R Soc Med* 1986; **79**: 71-73
 - 28 **Ponce J**, Juan M, Garrigues V, Pascual S, Berenguer J. Efficacy and safety of cardiomyotomy in patients with achalasia after failure of pneumatic dilatation. *Dig Dis Sci* 1999; **44**: 2277-2282
 - 29 **Sandler RS**, Nyren O, Ekblom A, Eisen GM, Yuen J, Josefsson S. The risk of esophageal cancer in patients with achalasia: A population-based study. *JAMA* 1995; **274**: 1359-1362
 - 30 **Ribeiro U Jr**, Posner MC, Safatle-Ribeiro AV, Reynolds JC. Risk factors for squamous cell carcinoma of the oesophagus. *Br J Surg* 1996; **83**: 1174-1185
 - 31 **Cosentini E**, Berlakovich G, Zacherl J, Stacher-Janotta G, Merio R, Wenzl E, Bergmann H, Stacher G. Achalasia. Results of myotomy and antireflux operation after failed dilatations. *Arch Surg* 1997; **132**: 143-147

Edited by Wang XL and Proofread by Zhu LH

Expression of COX-2 proteins in gastric mucosal lesions

Lian-Zhen Yu, Heng-Jun Gao, Jian-Feng Bai, Gu Sun, Han-Lin Zhao, Liang Sun, Kun Miu, Zhi-Quan Zhao

Lian-Zhen Yu, Heng-Jun Gao, Liang Sun, Kun Miu, Zhi-Quan Zhao, Department of Gastroenterology, the First Affiliated Hospital of Nanjing Medical University, Nanjing 210029, Jiangsu Province, China

Jian-Feng Bai, Gu Sun, Han-Lin Zhao, Department of General Surgery, the First Affiliated Hospital of Nanjing Medical University, Nanjing 210029, Jiangsu Province, China

Supported by the Natural Science Fund of the Educational Committee of Jiangsu Province, No.125FA9608 and Fund of Nanjing Medical University for Outstanding Young Faculty

Correspondence to: Heng-Jun Gao, Department of Gastroenterology, the First Affiliated Hospital of Nanjing Medical University, Nanjing 210029, Jiangsu Province, China

Received: 2003-04-02 **Accepted:** 2003-05-17

Abstract

AIM: To investigate the expression of COX-2 proteins in gastric mucosal lesions and to assess the relationship between COX-2 expression and type, pathologic stage, differentiation, or lymph node metastasis in gastric cancer and the relationship between COX-2 expression and *H pylori* infection in gastric mucosal lesions.

METHODS: Thirty patients with gastric carcinoma underwent surgical resection. Samples were taken from tumor site and paracancerous tissues, and ABC immunohistochemical staining was used to detect the expression of COX-2 proteins. *H pylori* was determined by rapid urea test combined with pathological staining/¹⁴C urea breath test.

RESULTS: The positive rate and staining intensity of mutant COX-2 gene expression in gastric cancer were significantly higher than those in paracancerous tissues (66.7% vs 26.7%) ($P < 0.01$, $P < 0.001$). There was a significant correlation between COX-2 and pathologic stage or lymph node metastasis type of gastric carcinoma (76.0% vs 20.0%, 79.2% vs 16.7%) ($P < 0.05$). No correlation was found between COX-2 expression and type or grade of differentiation ($P > 0.05$). COX-2 expression of intestinal metaplasia (IM) or dysplasia (DYS) with positive *H pylori* was significantly higher than that with negative *H pylori* (50.6% vs 18.1%, 60.0% vs 33.3%) ($P < 0.05$).

CONCLUSION: COX-2 overexpression was found in a large proportion of gastric cancer tissues compared with matched non-cancerous tissues and was significantly associated with advanced tumor stage and lymph node metastasis. Overexpression of COX-2 plays an important role in tumor progression of gastric cancer. COX-2 may also play a role in the early development/promotion of gastric carcinoma and is associated with *H pylori* infection.

Yu LZ, Gao HJ, Bai JF, Sun G, Zhao HL, Sun L, Miu K, Zhao ZQ. Expression of COX-2 proteins in gastric mucosal lesions. *World J Gastroenterol* 2004; 10(2): 292-294
<http://www.wjgnet.com/1007-9327/10/292.asp>

INTRODUCTION

Recently, a number of researches show that COX-2 was expressed at a very high level in gastrointestinal tumors. However, we know less about COX-2 expression in gastric cancer, especially the relationship between COX-2 overexpression and typing, degree, differentiation, lymphonic metastasis of gastric cancer. In this paper, we investigated the expression of COX-2 proteins in gastric mucosal lesions and assessed the relationship between COX-2 expression and the type, pathologic stage, differentiation, or lymph node metastasis in gastric cancer and the relationship between expression of COX-2 and *H pylori* infection in gastric mucosal lesions.

MATERIALS AND METHODS

Materials

Tissue samples were acquired from 30 patients with gastric cancer diagnosed between April 1996 and March 1998 in our hospital, including a piece of tumor tissue and a piece of paracancerous tissue obtained from the surgery. Samples were then fixed quickly into formalin solution at pH 7.0, embedded in paraffin and cut into slices (4 μ m thick). Slides were used for HE staining and ABC immunohistochemical staining, the latter was used to detect the expression of COX-2 proteins. *H pylori* was determined by rapid urea test combined with pathological staining/¹⁴C urea breath test.

Methods

ABC immunohistochemical staining Polyclone antibody against COX-2 was obtained from Gene Company Limited, ABC immunohistochemical kits and DAB substrate solution were from Vector Laboratories Inc, USA. Slides were treated with 0.01 mol/L citric acid buffer to recover the antigen activity, and developed with routine ABC immunohistochemical staining at an antibody concentration of 1:50, and the second antibody with labeled biotin at 1:200. The negative control was used with PBS buffer replacing the polyclone antibody, and positive control was also set up with a tissue sample with a known positive reaction. The criteria for positive reactions were as follows: positive staining of COX-2 protein located within cytosol, but without stain in the nucleus, being pale yellow to deep pale yellow, even pale red. In evaluation of the positive activity, the positive cell number and reaction level were two useful parameters. When over 10% cells were dyed, it could be considered as a positive expression, and the positive reaction levels were shown as weakly positive (+), moderately positive (++) and strongly positive (+++).

Statistics

Statistical analysis system (SAS) software package was used for χ^2 test, and rank sum test for the degree of group data.

RESULTS

COX-2 expression in gastric cancer tissue and paracancerous tissue

The positive rate and intensity of COX-2 expression in gastric cancer tissue were all significantly higher than those in paracancerous tissues ($P < 0.01$, $P < 0.001$, Table 1).

Table 2 COX-2 expression in gastric mucosa with *H pylori* infection, n (%)

	CG (n=30)		IM (n=19)		DYS (n=11)		GC (n=30)	
	Hp+	Hp -	Hp+	Hp -	Hp +	Hp -	Hp +	Hp -
n	25	5	9	11	5	6	11	19
COX-2	2(8.0%)	1(0%)	5(50.6%) ^a	2(18.1%)	3(60.0%) ^a	2(33.3%)	8(72.7%)	12(63.5%)

^aP<0.05, IM or DYS (*H pylori* positive) vs IM or DYS (*H pylori* negative).

Table 1 COX-2 expression in gastric cancer and paracancerous tissues

	Number	COX-2 expression intensity ^b				Positive rate ^d n (%)
		-	+	++	+++	
Gastric cancer	30	10	4	8	8	20 (66.7)
Paracancerous tissue	30	22	6	2	0	8 (26.7)

^bP<0.001 gastric cancer vs paracancerous tissue; ^dP<0.01 gastric cancer vs paracancerous tissue.

COX-2 expression in gastric mucosa with *H pylori* infection

COX-2 expression of IM or DYS with positive *H pylori* was significantly higher than that with negative *H pylori* ($P<0.05$), (Table 2).

Relationship between COX-2 expression and type, pathologic stage, differentiation, or lymph node metastasis of gastric cancer

The relationship between COX-2 expression and type, pathologic stage, differentiation, or lymph node metastasis of gastric cancer is shown in Table 3. COX-2 positive expression in gastric cancer tissue at the developing stage (76.0%) was significantly higher than that at the early stage (20.0%) ($P<0.05$). The positive rate in gastric cancer with lymph node metastasis (79.2%) was significantly higher than that without lymph node metastasis (16.7%) ($P<0.05$). But the COX-2 positive expression in intestinal gastric cancer (66.7%) was the same as that in gastric type of gastric cancer (66.7%). The positive rate in gastric cancer with low or no differentiation (80%) was not higher than that with high or moderate differentiation (57.1%) ($P>0.05$), (Table 3).

Table 3 COX-2 expression in gastric cancer tissues

Groups	Number	COX-2 n (%)
Type		
Intestinal type	24	16 (66.7)
Gastric type	6	4 (66.7)
Stage		
Early stage	5	1 (20.0)
Developing	25	19 (76.0) ^a
Differentiation (Intestinal type)		
High and moderate	14	8 (57.1)
Low and no differentiation	10	8 (80.0)
Lymph node metastasis		
Without metastasis	6	1 (16.7)
With metastasis	24	19 (79.2) ^a

^aP<0.05, developing stage vs early stage; metastasis vs no metastasis.

DISCUSSION

New COX isozyme-COX-2, is not expressed in normal tissues, but expressed at a high level in inflammatory tissues. It has

been shown in animal studies that COX-2 expression can enhance PGE2 production, which induces cell proliferation and bcl-2 expression. These can destroy the balance between proliferation and apoptosis and induce tumors. More and more studies have shown that COX-2 could express at a high level in human colorectal tumor^[1-5] and other gastrointestinal tumors^[6-8]. COX-2 overexpression was found in well-differentiated epidermoid carcinoma of the esophagus. Ratnasinghe^[9] studied the COX-2 expression in epidermoid carcinoma of the esophagus and found that COX-2 expressed at a high level in well-differentiated tissues, at a low positive level in the normal esophagus, and negative in poorly-differentiated tissues. Hao^[10] found COX-2 protein expressed at a high level in adenocarcinoma and adenoma of colon, compared with normal mucosal tissues. COX-2 mRNA expressed in tumor tissues at a significantly higher level than that in normal tissues. There was neither a relationship between COX-2 protein expression and proliferation degree or volume of adenoma, nor a relationship between COX-2 expression and tumor differentiation, Duke's stage as well as lymph node metastasis ($P>0.05$). Interestingly, COX-2 expressed in the tissues near adenocarcinoma or adenoma at a higher level than in normal mucosal tissues ($P<0.0001$), but lower than that in adenocarcinoma or adenoma itself ($P<0.001$, $P<10^5$).

It has been found that the positive rate of COX-2 expression in gastric cancer tissue was 60%-70%^[6-8]. Ratnasinghe^[6] found that COX-2 expressed positively in 36% cardia adenocarcinoma and 60% gastric body adenocarcinoma in his research on 19 patients with cardia adenocarcinoma and 15 patients with gastric body adenocarcinoma. COX-2 overexpression was found in most of gastric body adenocarcinoma and some cardia adenocarcinoma tissues. It is necessary to further confirm the status of COX-2 expression in gastric cancer tissues, especially the characteristics of COX-2 overexpression related to typing, degree, differentiation and lymph node metastasis^[11-15]. We studied the COX-2 expression at gene and protein levels in tissues with gastric mucosal lesion, and explored the relationship between COX-2 expression and gastric carcinoma and *H pylori* infection at pathological and pathophysiological levels.

Our study based on 30 tissue samples with gastric cancer as well as paracancerous tissues showed that COX-2 protein expressed at a high level in tumor tissues, which was significantly higher than that in paracarcinoma tissues ($P<0.01$), and also significantly higher in tumor tissues ($P<0.01$). COX-2 positive expression in gastric cancer tissues at the developing stage was significantly higher than that at early stage, the positive rate in gastric cancer with lymph node metastasis was significantly higher than that without lymph node metastasis ($P<0.05$), but the COX-2 positive expression in intestine type of gastric cancer was the same as that in gastric type of gastric cancer. The positive rate in gastric cancer with low or no differentiation was not higher than that with high or moderate differentiation ($P>0.05$). Our results were similar to those of foreign investigators^[7,8]. In conclusion, abnormal expression of COX-2 protein was related to the progress of gastric carcinoma as well as lymph node metastasis, while it was not significantly related to the type of gastric cancer and degree of pathological differentiation^[13,15].

We also found that COX-2 expression in tissues with *H pylori* positive intestinal metastasis or dysplasia was significantly higher than that in tissues with *H pylori* negative infection. *H pylori* could induce acute and chronic inflammation of gastric mucosa, and the production of cell factors such as IL-8 and IL-1 β , and the secondary high COX-2 expression which caused gastric mucosal lesions. *H pylori* infection could also induce gastric mucosal cell proliferation by COX-2 expression. COX-2 gene expression was one of the related factors mediating the progress from gastritis with *H pylori* infection to pre-carcinoma lesions even gastric carcinoma^[16,17]. Based on this study, treatment of *H pylori* infection and special COX-2 inhibitor could be useful for the prevention of gastric carcinoma^[18].

REFERENCES

- Eberhart CE**, Coffey RJ, Radhika A, Giardiello FM, Ferrenbach S, DuBois RN. Up-regulation of cyclooxygenase-2 gene expression in human colorectal adenomas and adenocarcinomas. *Gastroenterology* 1994; **107**: 1183-1188
- Sano H**, Kawahito Y, Wilder RL, Hashiramoto A, Mukai S, Asai K, Kimura S, Kato H, Kondo M, Hla T. Expression of cyclooxygenase-1 and -2 in human colorectal cancer. *Cancer Res* 1995; **55**: 3785-3789
- Reddy BS**, Rao CV, Seibert K. Evaluation of cyclooxygenase-2 inhibitor for potential chemopreventive properties in colon carcinogenesis. *Cancer Res* 1996; **56**: 4566-4569
- Tsuji M**, Kawano S, DuBios RN. Cyclooxygenase-2 expression in human colon cancer cells increases metastatic potential. *Proc Natl Acad Sci U S A* 1997; **94**: 3336-3340
- Watson AJ**. Chemopreventive effects of NSAIDs against colorectal cancer: regulation of apoptosis and mitosis by COX-1 and COX-2. *Histol Histopathol* 1998; **13**: 591-597
- Ratnasinghe D**, Tangrea JA, Roth MJ, Dawsey SM, Anver M, Kasprzak BA, Hu N, Wang QH, Taylor PR. Expression of cyclooxygenase-2 in human adenocarcinomas of the gastric cardia and corpus. *Oncol Rep* 1999; **6**: 965-968
- Murata H**, Kawano S, Tsuji S, Tsuji M, Sawaoka H, Kimura Y, Shiozaki H, Hori M. Cyclooxygenase-2 overexpression enhances lymphatic invasion and metastasis in human gastric carcinoma. *Am J Gastroenterol* 1999; **94**: 451-455
- Yamamoto H**, Itoh F, Fukushima H, Hinoda Y, Imai K. Overexpression of cyclooxygenase-2 protein is less frequent in gastric cancers with microsatellite instability. *Int J Cancer* 1999; **84**: 400-403
- Ratnasinghe D**, Tangrea J, Roth MJ, Dawsey S, Hu N, Anver M, Wang QH, Taylor PR. Expression of cyclooxygenase-2 in human squamous cell carcinoma of the esophagus; an immunohistochemical survey. *Anticancer Res* 1999; **19**(1A): 171-174
- Hao X**, Bishop AE, Wallace M, Wang H, Willcocks TC, Maclouf J, Polak JM, Knight S, Talbot IC. Early expression of cyclooxygenase-2 during sporadic colorectal carcinogenesis. *J Pathol* 1999; **187**: 295-301
- Ristimaki A**, Honkanen N, Jankala H, Sipponen P, Harkonen M. Expression of cyclooxygenase-2 in human gastric carcinoma. *Cancer Res* 1997; **57**: 1276-1280
- Sawaoka H**, Kawano S, Tsuji S, Tsujii M, Murata H, Hori M. Effects of NSAIDs on proliferation of gastric cancer cells *in vitro*: possible implication of cyclooxygenase-2 in cancer development. *J Clin Gastroenterol* 1998; **27**(Suppl 1): S47-52
- Saukkonen K**, Nieminen O, van Rees B, Vilkkii S, Harkonen M, Juhola M, Mecklin JP, Sipponen P, Ristimaki A. Expression of cyclooxygenase-2 in dysplasia of the stomach and in intestinal-type gastric adenocarcinoma. *Clin Cancer Res* 2001; **7**: 1923-1931
- Van Rees BP**, Saukkonen K, Ristimaki A, Polkowski W, Tytgat GN, Drilenburg P, Offerhaus GJ. Cyclooxygenase-2 expression during carcinogenesis in the human stomach. *J Pathol* 2002; **196**: 171-179
- Yamagata R**, Shimoyama T, Fukuda S, Yoshimura T, Tanaka M, Munakata A. Cyclooxygenase-2 expression is increased in early intestinal-type gastric cancer and gastric mucosa with intestinal metaplasia. *Eur J Gastroenterol Hepatol* 2002; **14**: 359-363
- Walker MM**. Cyclooxygenase-2 expression in early gastric cancer, intestinal metaplasia and *Helicobacter pylori* infection. *Eur J Gastroenterol Hepatol* 2002; **14**: 347-349
- Wambura C**, Aoyama N, Shirasaka D, Sakai T, Ikemura T, Sakashita M, Maekawa S, Kuroda K, Inoue T, Ebara S, Miyamoto M, Kasuga M. Effect of *Helicobacter pylori*-induced cyclooxygenase-2 on gastric epithelial cell kinetics: implication for gastric carcinogenesis. *Helicobacter* 2002; **7**: 129-138
- Sung JJ**, Leung WK, Go MY, To KF, Cheng AS, Ng EK, Chan FK. Cyclooxygenase-2 expression in *Helicobacter pylori*-associated premalignant and malignant gastric lesions. *Am J Pathol* 2000; **157**: 729-735

Edited by Ma JY and Wang XL

Effects of *zhaoyangwan* on chronic hepatitis B and posthepatic cirrhosis

Cui-Ping Zhang, Zi-Bin Tian, Xi-Shuang Liu, Qing-Xi Zhao, Jun Wu, Yong-Xin Liang

Cui-Ping Zhang, Zi-Bin Tian, Xi-Shuang Liu, Qing-Xi Zhao, Jun Wu, Yong-Xin Liang, Department of Gastroenterology, the Affiliated Hospital of Qingdao Medical College, Qingdao University, Qingdao, 266003, Shandong Province, China

Supported by the Natural Science Foundation of Shandong Province, No.1999CA1CKB3

Correspondence to: Dr. Cui-Ping Zhang, Department of Gastroenterology, the Affiliated Hospital of Qingdao Medical College, Qingdao University, Qingdao 266003, Shandong Province, China. tianzbsun@public.qd.sd.cn
Telephone: +86-532-2911304

Received: 2003-05-13 **Accepted:** 2003-06-02

Abstract

AIM: To study the therapeutic effects of *zhaoyangwan* (ZYW) on chronic hepatitis B and hepatic cirrhosis and the anti-virus, anti-fibrosis and immunoregulatory mechanisms of ZYW.

METHODS: Fifty cases of chronic hepatitis B and posthepatic cirrhosis with positive serum HBsAg, HBeAg, anti-Hbc and HBV-DNA were divided randomly and single-blindly into the treatment group (treated with ZYW) and the control group (treated with interferon). After 3 month treatment, the effects of the treatment group and the control group were evaluated.

RESULTS: The serum ALT normalization was 83.3%(30/36) in the treatment group and 85.7%(12/14) in the control group, with no significant difference ($\chi^2=0.043$, $P>0.05$). After the course, the negative expression rates of the serum HBV-DNA and HBeAg were 44.4%(16/36) and 50%(18/36) in the treatment group, and 50%(7/14) and 50%(7/14) in the control group, respectively, with no significant difference ($\chi^2=0.125$, $\chi^2=0.00$, both $P>0.05$). Negative HBsAg and positive HBsAb appeared in 4 cases of the treatment group and 1 case of the control group. Serum anti-HBc turned negative in 6 cases of the treatment group and 1 case of the control group, respectively. After the ZYW treatment, serum CD₃⁺, CD₄⁺, CD₈⁺, CD₄⁺/CD₈⁺ and NK cell activation were significantly increased. Only serum CD₃⁺ and NK cell activation were significantly increased in the control group with a significant difference between the two groups. The serum C₄, C_{1q}, C₃, B and C₉ were significantly increased in the treatment group. In the control group only the serum C₄ was increased. The concentration of serum interferon had no change after treatment with ZYW, while it was significantly increased in the control group after treatment with interferon. The ultrastructure of the liver restored, which helped effectively to reduce the degeneration and necrosis of hepatic cells, infiltration of inflammatory cells and hepatic cirrhosis.

CONCLUSION: ZYW is a pure Chinese herbal medicine. It can exert potent therapeutic effects on chronic hepatitis B and posthepatic cirrhosis. ZYW has similar therapeutic effects to those of interferon. It is cheap and easily administered with no obvious side-effects. It can be widely used in clinical practice.

Zhang CP, Tian ZB, Liu XS, Zhao QX, Wu J, Liang YX. Effects of *zhaoyangwan* on chronic hepatitis B and posthepatic cirrhosis. *World J Gastroenterol* 2004; 10(2): 295-298

<http://www.wjgnet.com/1007-9327/10/295.asp>

INTRODUCTION

HBV is highly prevalent in China. HBsAg-positive rate is 8-10% among young adults, some of them may develop chronic hepatitis B (CHB), with poor liver function and positive HBeAg and HBV-DNA. Therefore, it is urgent to improve the immunity of CHB patients to make the virus unable to replicate so as to reduce the damage to the liver and to slow down the progress of CHB to fibrosis and cancer. Anti-virus treatment is the key point^[1-7], and great attention has been paid to it. However, no specific therapy has been found. The use of interferon and lamivudine is clinically limited because they are expensive and the patients are easy to relapse^[8-14]. An urgent issue of top priority is how to treat CHB and other virus infection with traditional Chinese medicine according to syndrome differentiation. Insufficiency of experience and the complexity of the drug ingredients result in the lack of objective parameters. This study used the proprietary Chinese medicine of *zhaoyangwan* (Morning Sun Pill) invented by Professor Jiang Tingdong. Interferon was used as controls. Fifty patients with hepatitis B were observed for the changes in liver function, cellular immunity function, NK cell activity, serum complement, serum marker of HBV, HBV-DNA, ultrastructure of the liver and serum interferon before and after treatment with ZYW to investigate the mechanisms of the anti-virus, anti-fibrosis activity in the liver and immuno-regulatory of traditional Chinese medicine and to provide theoretic basis for the treatment of chronic hepatic diseases with Chinese herbs.

MATERIALS AND METHODS

Materials

The 50 patients were all HBsAg, HBeAg, Anti-HBc and HBV-DNA positive. Thirty-four were males and 16 females, aged 15 to 57 years, with an average of 38.5 years. They were classified according to the diagnostic criteria devised on the Beijing Conference of Infectious and Parasitic Diseases in 1995. Thirty-eight cases were CHB, 22 cases were post-hepatitis active hepatocirrhosis(in compensation). They had no such chronic diseases as other types of hepatitis, diabetes or tuberculosis.

Methods

The 50 patients were divided into *zhaoyangwan* (ZYW) group and interferon group (control group). The 36 patients in ZYW group took orally 2 packs of ZYW a day, one in the morning and one in the evening, for 3 months. The 14 patients in the control group were administered intramuscularly with α -interferon made by Changchun Bio-product Institute, 3 mU once every other day for 3 months. Vitamins might be added to the patients in both groups, but no other anti-virus, immuno-

regulatory or liver enzyme reduction drugs were used during the treatment. One therapeutic course lasted for 3 months. Serum marker of HBV, T-cell subgroup, NK cell activity, contents of serum complement, and level of serum interferon were examined before and after the treatment, respectively. The liver function was examined once a week. Liver puncture and electrodiaphanoscopy were performed for some patients to observe the ultrastructure of the liver before and after the treatment.

Assay methods

HBVDNA was assayed with PCR, T-cell sub-group with direct method of bacterial ring, NK cell activity with MTT colorimetry, serum complement with one-direction immunity diffusion, and serum interferon with ELISA, with reagent produced by Endogen of USA. The ultrastructure of the liver was observed under electrodiaphanoscope.

RESULTS

Changes of symptoms and signs before and after treatment

Changes of symptoms and signs in both groups before treatment (BT) and after treatment (AT) are compared in Table 1, which showed that the symptom disappearance rate (DR) of the treated group was similar to or higher than that of the control group, but the sign disappearance rate was lower, with no statistical significance.

Changes of liver function and serum markers before and after treatment

Serum glutamic-pyruvic transaminase (ALT) was evidently improved in both groups. The serum ALT returned to normal in 83.3% (30/36) of the treated group and 85.7% (12/14) of the control group. No significant difference was found between

both groups. ($\chi^2=0.043, P>0.05$). The negative conversion rate of HBVDNA and HBeAg in the treated group was 44.4% (16/36) and 50% (18/36), respectively, while in the control group, it was 50% (7/14) and 50% (7/14), respectively, with no significant difference ($\chi^2=0.123, \chi^2=0.00$, both $P>0.05$). HBsAg turned negative in 4 cases of the treated group and 1 case of the control group, and their HBsAb turned positive. Anti-HBc turned negative in 6 cases of the treated group and 2 cases of the control group.

Changes of T-cell sub-group and NK cell activity before and after the treatment

Serum CD3⁺, CD4⁺, CD8⁺, CD4⁺/CD8⁺ and NK cell activity were significantly increased in the ZYW treated group ($t=8.921-13.380$, all $P<0.001$), while in the control group, only CD3⁺ and NK cell activity were significantly increased ($t=7.473, 10.101, P<0.001$). The results of the two groups were significantly different after the treatment ($t=6.812-14.108$, all $P<0.001$), as shown in Table 2.

Changes of serum complement elements before and after treatment

The five serum complement elements, ie. C₄, C_{1q}, C₃, BF, and C₉, increased significantly compared with those before the treatment in the ZYW group ($t=4.437-24.330, P<0.001$), while in the control group, only C₄ increased ($t=5.044, P<0.001$). The results of the two groups were significantly different after the treatment ($t=3.972-12.910, P<0.001$), as shown in Table 3.

Changes of serum interferon concentration

The serum interferon concentration changed little in the ZYW group, while in the interferon group, it rose significantly. The results of the two groups were significantly different after treatment ($t=2.723, P<0.001$), as seen in Table 4.

Table 1 Improvement of symptoms and signs in both groups before and after treatment

Symptoms and signs	Treated group			Control group			χ^2	P
	BT	AT	DR(%)	BT	AT	DR(%)		
Fatigue	29	14	51.7	12	6	50	0.10	>0.05
Abdominal distension	31	9	71	13	5	61.5	0.375	>0.05
Nausea	12	7	41.7	8	6	25	0.586	>0.05
Anorexia	23	6	73.9	11	4	63.6	0.379	>0.05
Hepatic pain	17	10	41.2	7	5	28.6	0.336	>0.05
Sallow complexion	14	4	71.4	5	3	40	1.564	>0.05
Hepatomegaly	20	12	40	6	3	50	0.189	>0.05
Splenomegaly	9	7	22.2	4	3	25	0.012	>0.05
Percussion pain of liver	21	12	42.9	9	5	44.4	0.006	>0.05

Table 2 Changes of T-cell sub-group and NK cell activity before and after treatment (%)

	n	CD3 ⁺	CD4 ⁺	CD8 ⁺	CD4 ⁺ /CD8 ⁺	NK
Treated group BT	36	47.14±4.76	41.56±5.06	30.10±3.03	1.41±0.24	43.62±5.92
AT	36	57.81±5.83	54.81±5.64 ^{ab}	23.07±4.47 ^{ab}	2.49±0.72 ^{ab}	56.69±5.29 ^{ab}
Control group BT	14	39.93±5.00	28.38±3.40	23.38±3.40	1.40±0.18	40.36±5.90
AT	14	52.28±7.18 ^b	29.17±1.86	29.17±1.86	1.34±0.88	59.40±4.97 ^b

^aThe treated group vs control group after treatment, $P<0.001$, ^bResults after treatment vs those before treatment for both groups, $P<0.001$.

Table 3 Changes of 5 serum complement elements before and after treatment (mg/L)

	n	C ₄	C _{1q}	C ₃	BF	C ₉
Treated group BT	36	339.68±35.40	245.09±47.11	842.13±62.51	220.91±32.84	746.28±62.79
AT	36	529.48±42.49 ^b	349.32±35.01 ^b	1 114.05±218.22 ^b	279.71±52.86 ^b	819.31±103.17 ^b
Control group BT	14	331.84±42.63	240.08±25.32	838.54±44.32	219.56±25.08	715.06±77.58
AT	14	427.57±112.18 ^{ab}	238.35±23.59 ^a	843.89±50.32 ^a	225.08±26.85 ^a	732.08±51.12 ^a

^aThe treated group vs control group after treatment, $P<0.001$, ^bResults after treatment vs those before treatment for both groups, $P<0.001$.

Table 4 Changes of serum interferon concentration before and after treatment

	Case number	BT	AT	t	P
Treated group	13	156.25±17.62	155.93±19.76	0.046	>0.05
Control group	8	143.27±21.44	218.72±63.34	3.193	<0.05

After treatment, the serum interferon concentration of the two groups was significantly different ($t=2.723$, $P<0.05$).

Changes of hepatic ultrastructure

Degeneration, necrosis, cholestasis, fibrosis, and lysis of the organelles existed in different degrees in the liver cells before treatment, while after treatment, the necrotic cells of the liver resiled to a certain extent.

Side effects of ZYW

No evident side effects appeared in the ZYW group. Xerostomia and constipation appeared in one case and slight dizziness in another case, but they disappeared automatically with the continuous use of the pills. More side effects appeared in the interferon group, including influenza-like symptoms, symptoms of the digestive tract, sore and painful muscles. However, the patients continued taking their drugs after patient persuasion of the doctors.

DISCUSSION

Some studies indicated that ZYW had two-way immune modulation functions^[15]. It could improve the function of Kupffer cells of the liver and the activity of natural killer (NK) cells. It also could induce interferon to produce antiviral activity and turn HBeAg negative. We investigated the effects of ZYW on chronic hepatitis by random single-blind ways. The effects of three-month short-term therapy were good and the overall effectiveness was 83.3% (30/36). Some main symptoms such as fatigue, abdominal distension, nausea, anorexia were improved or disappeared after the treatment. The effects of the treatment group were better than those of the control group and were statistically significantly different. In most patients, the color of facial skin turned from dark and gloomy to bright red, with their vigor improved, hepatosplenomegaly improved, percussive pain of the liver region disappeared and state of general health apparently improved. Liver function tests turned normal in half of the patients including 6 patients with slight jaundice which completely disappeared, and serum bilirubin turned normal after the three-month therapy. In the control group, the rate of ALT normalization was 85.7% (12/14) with no statistical significance compared with the treatment group ($P>0.05$). ZYW has some antiviral activity. After the treatment, the rates of negative conversion of HBVDNA and HBeAg were 44.4% (16/36) and 50% (18/36) in the treatment group. There was no statistical significance compared with the control group, in which the rates were 50% (7/14) and 50% (7/14). The HBsAg of four patients in the treatment group and one patient in the control group turned from positive to negative and their HBsAb turned positive. The HBeAb of six patients in the treatment group and two patients in the control group turned negative. Therefore, ZYW has high antiviral activity and the effectiveness is similar to that of interferon. Because the treatment was short-termed, we did not investigate the incidence of recurrence. If the course of treatment is lasted for six months, it would have better efficiency.

Hepatitis B virus infection is the primary cause of viral hepatitis. Persistent existence of hepatitis B virus in the body is the primary cause of chronic hepatitis B^[16-19]. Hepatitis B virus infection leads to chronic hepatitis and persistent damage

to the liver function. Low antiviral immunity of the body and abnormal immunity modulation are also the primary cause of chronicity^[20-25]. Some studies have found that there are different degrees of low cellular immunity^[26,27], which represent deficient T cell immunity and decreased activity of NK cells in patients with chronic hepatitis B and liver cirrhosis. NK cells of the liver are important to antiviral immunity and against tumor metastasis^[28-31]. Kakimi *et al*^[32] injected lactate(activator of NK-T cell) into HBV-transgenic mouse and found that interferon- γ in the liver of the mouse increased, reproduction of HBV stopped and OK-T cells decreased. They believed that activated OK-T cells could activate NK cells, release lots of cytokines and prevent virus from reproducing. It indicates that NK cell is important in the process of erasing HBV. The results of our study showed that there were different levels of modulation disturbance of cellular immunity, such as elevation of CD3⁺, CD4⁺, CD8⁺ and decrease of CD4⁺/CD8⁺ and activity of NK cells in the patients of hepatitis B before ZYW treatment. After ZYW treatment, values of CD3⁺, CD4⁺, CD8⁺ and CD4⁺/CD8⁺ and activity of NK cells improved differently, indicating that ZYW can improve cellular immunity, especially the total amount of T lymphocyte and function of NK cells. It remains to be further studied whether it can be used as an activator of NK cells.

Besides, low cellular immunity, the level of blood complement decreased differently in patients with chronic hepatitis B. HBV antigen is highly compatible with liver cells. The complex of HBV-antibody-complement can damage the liver cells by activating the typical route as common complexes, or by adhering to the liver cells as half-antigen through the typical route of antibody-complement^[33]. Our study indicated that low serum complement was improved differently in patients with chronic hepatitis B after treatment with ZYW and interferon, especially in the ZYW treated group.

Interferon is a broad-spectrum antiviral protein and has some antiviral activity. It does not kill viruses directly but prevents viruses from replication by mediating RNA-dependent PKR or RHA-activated enzyme. Interferon can also improve phagocytosis of phagocytes and activity of T killer cells and NK cells^[29,34-36]. Our study indicated that the activity of NK cells was only slightly elevated in some patients and had no change in patients treated with interferon, indicating that the immuno-modulating function of interferon is not evident. Besides, it is difficult for interferon to be widely used due to its high price and poor tolerance in practice. So other medications which can modulate and improve immunity are suggested to be used in conjunction with interferon, which is mainly used for antiviral treatment.

Liver fibrosis is a pathologic process in which abnormal hyperplasia of fibro-connective tissue develops after inflammatory necrosis has occurred in the liver. The liver can worsen the inflammatory necrosis by cytokines or microcirculation in the liver. The activity of lesions in the liver means the activity of liver fibrosis. Some authors^[37] have suggested that drugs that can prevent or slow down liver fibrosis would cure most of chronic hepatitis. Thus, preventing or delaying liver fibrosis and treating viruses are two aspects of chronic hepatitis B therapy. Today drugs for anti-liver fibrosis are rare and the curative effect is not certain. Our study found that ultramicrocirculation in the liver and liver fibrosis were improved differently after ZYW treatment in patients with chronic hepatitis B and early-stage liver fibrosis. Since the case number was small, and it needs to be further studied.

Patina in ZYW is one of its characteristic ingredients that is different from other drugs in treating chronic hepatitis in practice. Modern medicine believes that copper is an important ingredient for blood-production in the body. Taking appropriate copper orally can improve retina cells and hemoglobin in the bone marrow and blood, and stimulate and repair the liver.

Copper combined with protein in the body produces copper-protein compounds which can restrain hepatitis viruses and induce the body to produce interferon. Our results indicated that the liver function and immunity index of the patients with chronic hepatitis B were differently improved after ZYW treatment and the rate of negative conversion of chronic hepatitis B markers was similar to that of interferon group. The level of serum interferon was elevated after ZYW treatment, but the difference was not statistically significant. Because our case number was small, this needs to be further investigated. We believe that ZYW has a good curative effect and fewer side-effects in treating chronic viral hepatitis. It is also cheap and can be easily taken. So it can be widely used in practice.

REFERENCES

- Guidotti LG**, Rochford R, Chung J, Shapiro M, Purcell R, Chisari FV. Viral clearance without destruction of infected cells during acute HBV infection. *Science* 1999; **284**: 825-829
- Suri D**, Schilling R, Lopes AR, Mullerova I, Colucci G, Williams R, Naoumov NV. Non-cytolytic inhibition of Hepatitis B virus replication in human hepatocytes. *J Hepatol* 2001; **35**: 790-797
- Lau GK**, Tsiang M, Hou J, Yuen S, Carman WF, Zhang L, Gibbs CS, Lam S. Combination therapy with Lamivudine and Famiciclovir for chronic hepatitis B infected Chinese patients: a viral dynamic study. *Hepatology* 2000; **32**: 394-399
- Shiratori Y**, Yoshida H, Omata M. Management of hepatocellular carcinoma: advances in diagnosis, treatment and prevention. *Expert Rev Anticancer Ther* 2001; **1**: 277-290
- Okuno M**, Kojima S, Moriwaki H. Chemoprevention of hepatocellular carcinoma: concept, progress and perspectives. *J Gastroenterol Hepatol* 2001; **16**: 1329-1335
- Merle P**, Zoulim F, Vitvitski L, Trepo C. The prophylaxis of hepatocellular carcinoma by interferon-alpha in virus-induced cirrhosis. *Gastroenterol Clin Biol* 2000; **24**: 1166-1176
- Hajnicka V**, Proost P, Kazar J, Fuchsberger N. Comparison of manganese superoxide dismutase precursor induction ability in human hepatoma cells with or without hepatitis B virus DNA insertion. *Acta Virol* 2000; **44**: 343-347
- Korba BE**, Cote P, Hornbuckle W, Schinazi R, Gangemi JD, Tennant BC, Gerin JL. Enhanced antiviral benefit of combination therapy with Lamivudine and alpha interferon against WHV replication in chronic carrier woodchucks. *Antivir Ther* 2000; **5**: 95-104
- Mutimer D**, Dowling D, Cane P, Ratcliffe D, Tang H, O' Donnell K, Shaw J, Elias E, Pillay D. Additive antiviral effects of Lamivudine and alpha interferon in chronic hepatitis B infection. *Antivir Ther* 2000; **5**: 273-277
- Han HL**, Lang ZW. Changes in serum and histology of patients with chronic hepatitis B after interferon alpha-2b treatment. *World J Gastroenterol* 2003; **9**: 117-121
- Yang SS**, Hsu CT, Hu JT, Lai YC, Wu CH. Lamivudine does not increase the efficacy of interferon in the treatment of mutant type chronic viral hepatitis B. *World J Gastroenterol* 2002; **8**: 868-871
- Terrault NA**. Combined interferon and lamivudine therapy: is this the treatment of choice for patients with chronic hepatitis B virus infection? *Hepatology* 2000; **32**: 675-677
- Tamam L**, Yerdelen D, Ozpoyraz N. Psychosis associated with interferon alfa therapy for chronic hepatitis B. *Ann Pharmacother* 2003; **37**: 384-387
- Jung MC**, Gruner N, Zachoval R, Schraut W, Gerlach T, Diepolder H, Schirren CA, Page M, Bailey J, Birtles E, Whitehead E, Trojan J, Zeuzem S, Pape GR. Immunological monitoring during therapeutic vaccination as a prerequisite for the design of new effective therapies: induction of a vaccine-specific CD4+ T-cell proliferative response in chronic hepatitis B carriers. *Vaccine* 2002; **4**: 3598-3612
- Zhaoyangwan study group**. The development of research on zaoyangwan. Beijing: *Military Medical Sciences Press* 1997: 1-201
- Rabe C**, Pilz T, Klostermann C, Berna M, Schild HH, Sauerbruch T, Caselmann WH. Clinical characteristics and outcome of a cohort of 101 patients with hepatocellular carcinoma. *World J Gastroenterol* 2001; **7**: 208-215
- Lan GK**. Hepatitis B infection in China. *Clin Liver Dis* 2001; **5**: 361-379
- Zhang DF**. To pursuit novel therapeutic approaches based on the mechanism of clearance of HBV infection. *Zhonghua Ganzangbing Zazhi* 2001; **9**: 196-202
- Protzer U**, Schaller H. Immune escape by hepatitis B viruses. *Virus Genes* 2000; **21**: 27-37
- Schalm SW**. Lamivudine-interferon combination therapy for chronic hepatitis B: further support but no conclusive evidence. *J Hepatol* 2001; **35**: 419-420
- Liu S**, Tan D, Li C. Specific cellular and humoral immune responses induced by intramuscular injection of DNA vaccine containing HBV HBsAg gene in mice. *Hunan Yike Daxue Xuebao* 1999; **24**: 313-315
- Koziel MJ**. What once was lost, now is found: restoration of hepatitis B-specific immunity after treatment of chronic hepatitis B. *Hepatology* 1999; **29**: 1331-1333
- Luers C**, Sudhop T, Speugler U, Berthold HK. Improvement of sarcoidosis under therapy with interferon-alpha 2b for chronic hepatitis B virus infection. *J Hepatol* 1999; **30**: 347
- Liaw YF**. Treatment of chronic hepatitis B: a need for consensus. *J Gastroenterol Hepatol* 1999; **14**: 1-2
- Zhang HY**, Lu H, Li XM, Duan HY. Therapeutic effect of alpha 1b interferon on patients with chronic hepatitis B: changes in serological fibrosis markers and histology. *Zhonghua Ganzangbing Zazhi* 2003; **11**: 117-118
- Sing GK**, Ladhams A, Arnold S, Parmar H, Chen X, Cooper J, Butterworth L, Stuart K, D' Arcy D, Cooksley WG. A longitudinal analysis of cytotoxic T lymphocyte precursor frequencies to the hepatitis B virus in chronically infected patients. *J Viral Hepat* 2001; **8**: 19-29
- Liu CJ**, Chen PJ, Lai MY, Kao JH, Jeng YM, Chen DS. Ribavirin and interferon is effective for hepatitis C virus clearance in hepatitis B and C dually infected patients. *Hepatology* 2003; **37**: 568-576
- Valiante NM**, D' Andrea A, Crotta S, Lechner F, Klennerman P, Nuti S, Wack A, Abrignani S. Life, activation and death of intrahepatic lymphocytes in chronic hepatitis C. *Immunol Rev* 2000; **174**: 77-89
- Schirren CA**, Jung MC, Gerlach JT, Worzfeld T, Baretton G, Mamin M, Hubert Gruener N, Houghton M, Pape GR. Liver-derived hepatitis C virus (HCV)-specific CD4(+)T cells recognize multiple HCV epitopes and produce interferon gamma. *Hepatology* 2000; **32**: 597-603
- Webster GJ**, Reignat S, Maini MK, Whalley SA, Ogg GS, King A, Brown D, Amlot PL, Williams R, Vergani D, Dusheiko GM, Bertolotti A. Incubation phase of acute hepatitis B in man: dynamic of cellular immune mechanisms. *Hepatology* 2000; **32**: 1117-1124
- Kakimi K**, Lane TE, Chisari FV, Guidotti LG. Cutting edge: Inhibition of hepatitis B virus replication by activated NK T cells does not require inflammatory cell recruitment to the liver. *J Immunol* 2001; **167**: 6701-6705
- Kakimi K**, Guidotti LG, Koezuka Y, Chisari FV. Natural killer T cell activation inhibits hepatitis B virus replication *in vivo*. *J Exp Med* 2000; **192**: 921-930
- Zhang CP**, Zhang DX, Shen LQ, Zhang ZG. The measurement and clinical significance of complement system in serum of patients with liver cirrhosis and cancer. *Linchuang Gandanbing Zazhi* 1993; **9**: 19-21
- Weng HL**, Cai WM, Liu RH. Animal experiment and clinical study of effect of gamma-interferon on hepatic fibrosis. *World J Gastroenterol* 2001; **7**: 42-48
- Xu KC**, Wei BH, Yao XX, Zhang WD. Recent therapy for chronic hepatitis B by combined transitional Chinese and Western medicine. *Shijie Huaren Xiaohua Zazhi* 1999; **7**: 970-974
- Yang LM**, Xu KC, Zhao YL, Wu ZR, Chen DF, Qin ZY, Zuo JS, Wei BH, Zhang WD. Clinic-pathological study on therapeutic efficacy of Qianggan capsule for hepatic fibrosis of chronic hepatitis B. *Weichang Bingxue Yu Ganbingxue Zazhi* 2001; **10**: 247-249
- Bongiovanni M**, Viberti L, Pecchioni C, Papotti M, Thonhofer R, Hans Popper H, Sapino A. Steroid hormone receptor in pleural solitary fibrous tumours and CD34+ progenitor stromal cells. *J Pathol* 2002; **198**: 252-257

Enhancement of migration and invasion of hepatoma cells via a Rho GTPase signaling pathway

De-Sheng Wang, Ke-Feng Dou, Kai-Zong Li, Zhen-Shun Song

De-Sheng Wang, Ke-Feng Dou, Kai-Zong Li, Zhen-Shun Song,
Department of Hepatobiliary Surgery, Xijing Hospital, Fourth Military
Medical University, Xi'an 710032, Shannxi Province, China

Correspondence to: De-Sheng Wang, MD., Department of Hepatobiliary
Surgery, Xijing Hospital, Fourth Military Medical University, Xi'an,
710032, Shannxi Province, China. wangdesh@163.com

Telephone: +86-29-3375259 **Fax:** +86-29-3375255

Received: 2003-08-05 **Accepted:** 2003-09-18

Abstract

AIM: Intrahepatic extension is the main cause of liver failure and death in hepatocellular carcinoma patients. The small GTPase Rho and one of its effector molecules ROCK regulate cytoskeleton and actomyosin contractility, and play a crucial role in cell adhesion and motility. We investigated the role of small GTPase Rho in biological behaviors of hepatocellular carcinoma to demonstrate the importance of Rho in cancer invasion and metastasis.

METHODS: Using Western blotting, we quantitated Rho protein expression in SMMC-7721 cells induced by Lysophosphatidic acid (LPA). Furthermore, we examined the role of Rho signaling in regulating the motile and invasive properties of tumor cells.

RESULTS: Rho protein expression was stimulated by LPA. Using the Rhotekin binding assay to assess Rho activation, we observed that the level of GTP-bound Rho was elevated transiently after the addition of LPA, and Y-27632 decreased the level of active Rho. LPA enhanced the motility of tumor cells and facilitated their invasion. Rho played an essential role in the migratory process, as evidenced by the inhibition of migration and motility of cancer cells by a specific inhibitor of ROCK, Y-27632.

CONCLUSION: The finding that invasiveness of hepatocellular carcinoma is facilitated by the Rho/Rho-kinase pathway is likely to be relevant to tumor progression and Y-27632 may be a new potential effective agent for the prevention of intrahepatic extension of human liver cancer.

Wang DS, Dou KF, Li KZ, Song ZS. Enhancement of migration and invasion of hepatoma cells via a Rho GTPase signaling pathway. *World J Gastroenterol* 2004; 10(2): 299-302
<http://www.wjgnet.com/1007-9327/10/299.asp>

INTRODUCTION

Hepatocellular carcinoma is one of the most common cancers worldwide, especially in Asia^[1]. It frequently shows early invasion into blood vessels together with intrahepatic extensions and later extrahepatic metastasis^[2]. A better understanding of the processes involved in the development of the metastasis might improve future prognosis by facilitating treatment strategies.

Tumor invasion is a complex biological process, during

which tumor cells detach from the primary tumor and infiltrate the surrounding tissue. This process requires loss of cell contacts between tumor cells, active cell migration, adhesion to the extracellular matrix and proteolytic degradation of the extracellular matrix^[3-5]. Rho, a member of the Ras family of small GTP-binding proteins, has a molecular weight of approximately 27 kDa and is located under the cell membrane, potentially functioning in signal transduction pathways^[6]. Small GTPase Rho protein is known to work as a molecular switch for the regulation of signal transduction of intracellular events related to cell motility, cytoskeletal dynamics, and tumor progression^[7,8]. In the present study, we hypothesized that Rho protein might be associated with the development of hepatocellular carcinoma.

Lysophosphatidic acid (LPA) is a product of phospholipid metabolism. Exogenous LPA binds to surface G protein-coupled receptors and its biological activities are mediated in part by the cytosolic small GTPase Rho^[9-11]. The motility of tumor cells could be regulated by the target of Rho, Rho-associated coiled-coil forming protein kinase (p160ROCK), through reorganization of the actin cytoskeleton^[12]. A recently described specific inhibitor of p160ROCK, the (+)-(R)-*trans*-4-(1-Aminoethyl)-N-(4-pyridyl) cyclohexanecarboxamide dihydrochloride (Y-27632), was reported to inhibit Rho-mediated cell migration as well as smooth muscle contraction both *in vivo* and *in vitro*^[13-15].

Given the recent interest in the participation of Rho in cell migration, we analyzed the role of Rho associated signal transduction pathways during the LPA-induced transmigration of human hepatocellular cells, and more importantly the activity of Rho regulated by LPA and inhibitor of p160ROCK.

MATERIALS AND METHODS

Cell lines and treatment

SMMC-7721 cell, originally isolated from a poorly differentiated hepatocellular carcinoma, was used in all experiments. SMMC-7721 cell was cultured in modified minimum essential medium (MEM) containing 2-fold concentrated amino acids and vitamins supplemented with 10% fetal calf serum (FCS) at 37 °C in a humidified atmosphere of 5% CO₂ in air. The cells were used within 15-20 passages after the initiation of cultures. Before each experiment, cells were cultured under serum-free conditions (in medium containing 0.1% bovine serum albumin) for 24 h.

Western blot analysis

Cells were starved in serum-free culture medium for 24 h and subsequently treated with LPA at 37 °C for various times. The cells were washed twice with PBS and lysed in ice-cold lysis buffer (20 mM Tris, pH 7.4, 150 mM NaCl, 1% Triton X-100, 1 mM EDTA, 1 mM EGTA, 2.5 mM sodium pyrophosphate, 1 mM glycerolphosphate, 1 mM sodium orthovanadate, 1 µg/ml leupeptin, and 1 mM phenylmethylsulfonyl fluoride). The extracts were centrifuged to remove cellular debris, and protein content of the supernatants was determined using the Bio-Rad protein assay reagent. Samples were resolved by SDS-polyacrylamide gel electrophoresis and transferred to

Hybond-P. The transferred samples were incubated with the anti-rho antibody indicated, and then incubated with HRP-conjugated IgG, and the immunoblotted proteins were visualized with ECL reagents.

Rho activation assay

A commercial pull-down assay (Rho activation assay kit, Upstate) was used to measure the effect of LPA and Y-27632 on Rho activity in SMMC-7721 cells. The cells were washed twice with modified MEM and incubated in fresh modified MEM without serum for 24 h, 25 μ M LPA with or without Y-27632 (25 μ mol/L) was added and the cell suspension was centrifuged at the indicated time after LPA addition, and then the cell pellet was lysed (lysis buffer, Upstate) and the activated Rho pull-down assay was performed according to the manufacturer's protocol. A protein assay was performed prior to beginning pull-down assay to equalize the total protein concentration of each treatment group. Positive and negative controls were also performed according to the manufacturer's protocol. Briefly, lysates of cells were preincubated with 100 μ M nonhydrolyzable GTP γ S (positive Rho activation) or 100 μ M GDP (negative Rho activation) prior to undergoing precipitation by the Rhotekin GTP-Rho binding domain.

Morphological changes by Rho-kinase pathway

The cells were cultured in serum-free culture medium, and the dishes were incubated for an additional period of 24 hours. LPA (5 μ mol/L) was then added to the dishes with or without different concentrations of Y-27632 (5, 25, 125 μ mol/L) and cultured for 1 hour. The cells were examined using a phase-contrast microscope.

Cell motility assay

Random motility was determined by using the gold-colloid assay^[16]. Gold colloid was layered onto glass coverslips and placed into 6-well plates. Cells were seeded onto the coverslips and allowed to adhere for 1 h at 37 °C in a CO₂ incubator (12 500 cells/3 ml in serum-free medium). To stimulate the cells, the serum-free medium was replaced with 5% FBS containing LPA (5 μ mol/L) with or without Y-27632 (25 μ mol/L) and allowed to incubate for 24 h at 37 °C. The medium was aspirated and the cells were fixed with 2% glutaraldehyde. The coverslips were then mounted onto glass microscope slides and areas of clearing in the gold colloid corresponding to phagokinetic cell tracks were counted.

Cell invasion assay

Chemotactic directional migration was evaluated using a modified Boyden chamber^[17,18]. In this invasion assay, tumor cells had to overcome a reconstituted basement membrane by a sequential process of proteolytic degradation of the substrate and active migration. Costar transwells (pore size 8 μ m) were coated with matrigel, dried at 37 °C in an atmosphere of 5% CO₂, and reconstituted with serum-free medium. Cells (3×10^4) were plated in the upper chamber in medium containing LPA with or without Y-27632 and allowed to migrate for 4.5 h. Nonmigrating cells were removed from the upper chamber with a cotton swab and migrating cells adherent to the underside of the filter were fixed and stained with Mayer's hematoxylin solution and counted with an ocular micrometer. All experiments were performed in triplicate, and at least 10 fields/filter were counted. Data were expressed as relative migration (number of cells/field) and represented as $\bar{x} \pm s$ of at least three independent experiments.

Statistical analysis

All data were expressed as $\bar{x} \pm s$. Statistical analysis was done

by statistical package of SPSS for window release 9.0. Differences between the mean were tested with the Mann-Whitney test. $P < 0.05$ was considered statistically significant.

RESULTS

Increase of Rho protein levels as a result of LPA treatment

Using Western blot analysis with Rho polyclonal antibody, we detected the changes of the level of Rho family protein in SMMC-7721 cell extracts. The protein level of Rho rapidly increased within 5 h and reached the nearly maximal level at 25 h after the treatment with LPA, with more than 2-fold increase over the untreated control value (Figure 1).

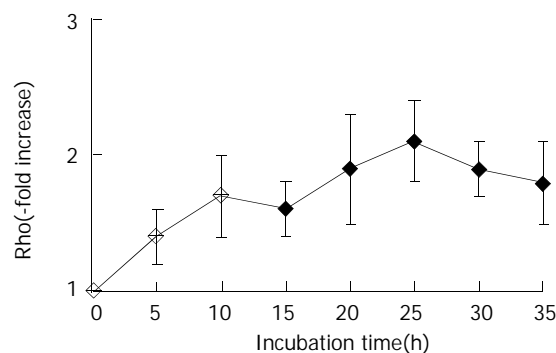


Figure 1 Changes in levels of Rho family protein in SMMC-7721 cells induced by LPA. The levels of Rho protein were analyzed by Western blot analysis. The data shown are expressed as $\bar{x} \pm s$ from three different experiments.

Inhibition of LPA-induced Rho activation by Y-27632

We measured the intracellular levels of the GTP-bound active form of Rho by the pull-down assay system^[19]. Activated GTP-Rho was precipitated by the Rho-binding domain of Rhotekin, a downstream Rho effector that specifically binds to only activated GTP-Rho^[20]. The level of GTP-bound Rho was elevated transiently after the addition of LPA and reached the peak level at 30 min after LPA addition, whereas Y-27632 decreased the level of active Rho. Since the total amount of Rho in each lysate was almost constant, Y-27632 inhibited Rho activation. This result was controlled by equalizing the harvested protein levels from each treatment with an appropriate dilution of buffer determined by a protein concentration assay prior to beginning the pull-down assay. A positive and negative control for active or inactive Rho was also performed in parallel. Lysates of cells were preincubated with nonhydrolyzable GTP γ S (positive Rho activation) or GDP (negative Rho activation) prior to undergoing precipitation by Rhotekin. Similar levels of active Rho were detected in cells grown on LPA and in cells incubated with GTP γ S. Thus, the result indicated that LPA might stimulate an increase in activated Rho and Y-27632 might inhibit the activation of Rho.

Morphological changes induced by Rho-kinase inhibitor and LPA

The effect of Y-27632 on morphologic changes induced by LPA in serum-starved SMMC-7721 cells was observed under a phase-contrast microscope. In serum starvation, cells formed relatively cohesive colonies, and after addition of LPA, they formed dissociated and scattered lamellipodial extensions at the cells' edges. Addition of Y-27632 at a concentration of 25 μ mol/L or more inhibited these LPA-induced morphologic changes, and SMMC-7721 cells remained cohesive with each other.

Inhibition of LPA-induced motility and invasion by Y-27632

To evaluate the effect of Rho-mediated cellular motility, we

assessed the treated cell line in colloidal-gold random motility assay. Cells were seeded onto glass coverslips overlaid with a gold colloid and stimulated with LPA to induce motility. Discernable and quantifiable tracks were left as the cells moved and phagocytized the gold colloid. As determined by the trypan blue dye exclusion assay, the reduction in cell motility was not caused by a decrease in the number of viable cells. At 24 h after stimulation, the cells treated with LPA were 2.2 fold more motile than their untreated counterparts ($P < 0.01$) and Y-27632 significantly suppressed the LPA-induced motility (Figure 2).

As shown in Figure 3, when the cells were tested for their ability to invade through a matrigel-coated filter in response to a chemoattractant, the LPA-treated cells were 2.3 fold more invasive than the untreated cells. Addition of Y-27632 at a concentration of 25 $\mu\text{mol/L}$ significantly inhibited the LPA-induced invasion ($P < 0.01$). Taken together, these data suggested that treatment of SMMC-7721 cells with Y-27632 could lead to the inhibition of LPA-mediated motility and invasion.

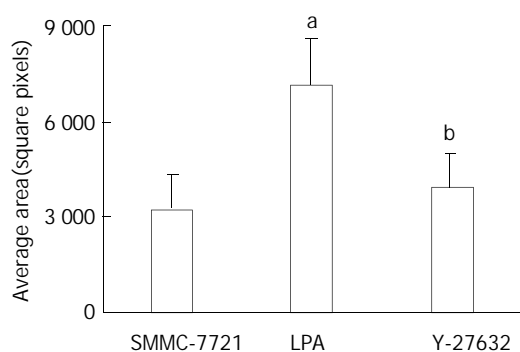


Figure 2 Tumor cell random motility determined by gold-colloid assay. Cells were seeded onto the coverslips and allowed to adhere for 1 h and then incubated in FBS containing LPA with or without Y-27632 for 24 h. The areas of clearing in the gold colloid corresponding to phagokinetic cell tracks were counted and represented as $\bar{x} \pm s$ from triplicate experiments. ^a $P < 0.01$ LPA treated cells vs SMMC-7721 control cells, ^b $P < 0.01$ Y-27632 treated cells vs LPA treated cells.

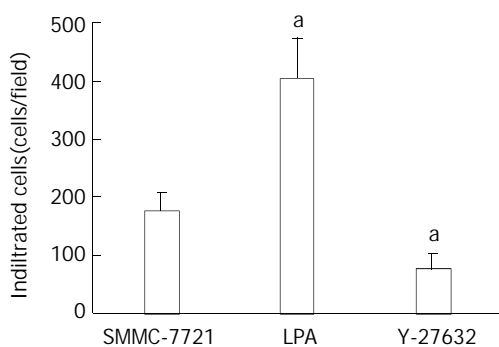


Figure 3 Inhibition of LPA-induced tumor cell invasion by Y-27632. Serum-starved cells were seeded onto porous filters. After incubation of the filters with Y-27632 in the presence of LPA 25 μM for 4.5 h to permit penetration of the cells, nonmigrating cells were removed from the upper chamber and migrating cells adherent to the underside of the filters were counted in a minimum of 10-high power fields. Data were expressed as relative migration (number of cells/field) and represented as $\bar{x} \pm s$ from triplicate experiments. ^a $P < 0.01$ relative to SMMC-7721 control cells.

DISCUSSION

Generally, metastasis has been found to be a multistep process, which includes detachment of cancer cells from primary tumor, migration, adhesion and invasion of cancer cells into the blood

or lymphatic vessels, extravasation out of the vessel, and finally, interactions with the target tissue and the formation of metastatic foci in distant organs^[21,22]. In spite of recent advances in diagnostic and therapeutic methods, the prognosis of HCC patients with intrahepatic metastasis was poor^[1]. Accordingly, analysis of the mechanism of the migration of cancer cells might lead to new strategies for preventing the progression of hepatocellular carcinoma. The molecular and cellular mechanisms of intrahepatic metastasis have not been fully understood, although cell motility mediated by Rho signaling pathway was recently shown to play a critical role in metastasis of various tumor cells.

Rho is a small GTPase that was found to play an essential role in a variety of cellular processes^[6,23]. The active GTP-bound form was involved in cytoskeletal responses to extracellular signaling pathways, resulting in the formation of stress fibres and focal adhesions^[24]. Other Rho effects included important roles in signaling pathways that control gene transcription, cell cycle regulation, apoptosis, and tumor progression^[25]. Rho proteins could oscillate between an active GTP-bound state and inactive GDP-bound state. The ratio between these two forms is regulated by two classes of proteins: GTPase-activating proteins (GAPs), which promote hydrolysis of GTP bound to the active form and accumulation of the inactive GDP-bound form, and guanine nucleotide exchange factors (GEFs), which promote the exchange of GDP for GTP and therefore induce accumulation of the activated GTP-bound form. In resting cells, inactive GDP-bound Rho proteins were found in the cytosol in complex with another class of regulatory proteins, nucleotide dissociation inhibitors (RhoGDIs). Upon activation, dissociation of RhoGDIs from the complex was required to enable interaction with GEFs and exchange of GDP for GTP^[26,27]. To exert their function, activated Rho proteins need to associate with the cell membrane and this in turn depends on their posttranslational modification.

It has been demonstrated that the role of Rho in inducing the invasion could be substituted for by one of its downstream effectors, the Rho-associated kinase (ROCK)^[28]. Invasion by tumor cells is a process composed of proteolytic degradation of extracellular matrix barriers and the migration of the cells through the modified region. Contraction of the actomyosin system is important for cell migration, and ROCK regulates the myosin light chain (MLC) phosphorylation by direct phosphorylation of MLC and by inactivation of myosine phosphatase, which was found to result in an increase in actomyosin-based contractility^[29,30]. Lysophosphatidic acid is a simple phospholipid that nonetheless has the properties of an extracellular growth factor, mediating diverse cellular responses through the activation of multiple signal transduction pathways. LPA could trigger actin-cytoskeletal events through Rho GTPases, thereby influencing transcellular migration^[31]. LPA could induce MLC phosphorylation through Rho activation, leading to the stimulation of cell contractility and motility of fibroblasts and cancer cells^[32].

Overexpression of Rho family members increases migration and invasion in various cell lines and culture models, this suggests that such an overexpression in carcinomas might profoundly affect metastatic potential *in vivo*^[33]. The result of Western blot showed that the level of activation of Rho was augmented by LPA. In our study, we extended this observation by providing the evidence that a specific inhibitor of Rho kinase, Y-27632, could inhibit LPA induced Rho activation by GTP-bound Rho pull-down assay. The Rho pathway through a G protein-coupled receptor appeared to be an important process of LPA-mediated signaling.

Y-27632 had an excellent selectivity to inhibit Rho-kinase as compared to other kinases, such as protein kinase C and myosin light-chain kinase in a cell-free system^[34]. Thus, Y-

27632 is a powerful tool to investigate the role of the Rho/Rho-kinase system, especially *in vivo*, although more potent Rho-kinase inhibitors have been synthesized^[35]. Y-27632 was reported to inhibit transcellular invasion and reduce the extent of local peritoneal metastases by MM1 rat hepatoma and also *in vivo* dissemination of prostate cancer cells^[36]. In the present study, Y-27632 blocked LPA-mediated SMMC-7721 cell transmonolayer invasion, suggesting the essential role of Rho-Rho kinase pathway in LPA-mediated cell migration. We also observed that Y-27632 induced morphological changes in SMMC-7721 cells, characterized by remaining relatively cohesive colonies, suggesting that Rho-kinase was necessary as a downstream effector of Rho for cell morphologies. Previous reports also demonstrated that Y-27632 inhibited LPA-induced morphologic changes in various cell lines *in vitro*.

As cell migration, invasion, cellular proliferation, and survival are advantageous to tumor cells for the formation of metastases, the finding that invasiveness of hepatocellular carcinoma is facilitated by the Rho/Rho-kinase pathway is likely to be relevant to tumor progression and the Rho/Rho-kinase may be useful as a prognostic indicator and also in the development of novel therapeutic strategies. Y-27632 may be a new potentially effective agent for the prevention of intrahepatic extension of human HCC.

REFERENCES

- Tang ZY**. Hepatocellular carcinoma—cause, treatment and metastasis. *World J Gastroenterol* 2001; **7**: 445-454
- Poon RT**, Fan ST, Ng IO, Wong J. Prognosis after hepatic resection for stage IVA hepatocellular carcinoma: a need for reclassification. *Ann Surg* 2003; **237**: 376-383
- Bartsch JE**, Staren ED, Appert HE. Adhesion and migration of extracellular matrix-stimulated breast cancer. *J Surg Res* 2003; **110**: 287-294
- Mareel M**, Leroy A. Clinical, cellular, and molecular aspects of cancer invasion. *Physiol Rev* 2003; **83**: 337-376
- Gupta MK**, Qin RY. Mechanism and its regulation of tumor-induced angiogenesis. *World J Gastroenterol* 2003; **9**: 1144-1155
- Wang P**, Bitar KN. Rho A regulates sustained smooth muscle contraction through cytoskeletal reorganization of HSP27. *Am J Physiol* 1998; **275**: G1454-G1462
- Nishimura Y**, Itoh K, Yoshioka K, Ikeda K, Himeno M. A role for small GTPase RhoA in regulating intracellular membrane traffic of lysosomes in invasive rat hepatoma cells. *Histochem J* 2002; **34**: 189-213
- Stice LL**, Forman LW, Hahn CS, Faller DV. Desensitization of the PDGFbeta receptor by modulation of the cytoskeleton: the role of p21(Ras) and Rho family GTPases. *Exp Cell Res* 2002; **275**: 17-30
- Wojciak-Stothard B**, Ridley AJ. Rho GTPases and the regulation of endothelial permeability. *Vascul Pharmacol* 2002; **39**: 187-199
- Hashimoto T**, Yamashita M, Ohata H, Momose K. Lysophosphatidic acid enhances *in vivo* infiltration and activation of guinea pig eosinophils and neutrophils via a Rho/Rho-associated protein kinase-mediated pathway. *J Pharmacol Sci* 2003; **91**: 8-14
- Sawada K**, Morishige K, Tahara M, Kawagishi R, Ikebuchi Y, Tasaka K, Murata Y. Alendronate inhibits lysophosphatidic acid-induced migration of human ovarian cancer cells by attenuating the activation of rho. *Cancer Res* 2002; **62**: 6015-6020
- Kawaguchi A**, Ohmori M, Harada K, Tsuruoka S, Sugimoto K, Fujimura A. The effect of a Rho kinase inhibitor Y-27632 on superoxide production, aggregation and adhesion in human polymorphonuclear leukocytes. *Eur J Pharmacol* 2000; **403**: 203-208
- Ai S**, Kuzuya M, Koike T, Asai T, Kanda S, Maeda K, Shibata T, Iguchi A. Rho-Rho kinase is involved in smooth muscle cell migration through myosin light chain phosphorylation-dependent and independent pathways. *Atherosclerosis* 2001; **155**: 321-327
- Itoh K**, Yoshioka K, Akedo H, Uehata M, Ishizaki T, Narumiya S. An essential part for Rho-associated kinase in the transcellular invasion of tumor cells. *Nat Med* 1999; **5**: 221-225
- Somlyo AV**, Bradshaw D, Ramos S, Murphy C, Myers CE, Somlyo AP. Rho-kinase inhibitor retards migration and *in vivo* dissemination of human prostate cancer cells. *Biochem Biophys Res Commun* 2000; **269**: 652-659
- Albrecht-Buehler G**. The phagokinetic tracks of 3T3 cells. *Cell* 1977; **11**: 395-404
- van Golen KL**, Risin S, Staroselsky A, Berger D, Tainsky MA, Pathak S, Price JE. Predominance of the metastatic phenotype in hybrids formed by fusion of mouse and human melanoma clones. *Clin Exp Metastasis* 1996; **14**: 95-106
- van Golen KL**, Bao L, DiVito MM, Wu Z, Prendergast GC, Merajver SD. Reversion of RhoC GTPase-induced inflammatory breast cancer phenotype by treatment with a farnesyl transferase inhibitor. *Mol Cancer Ther* 2002; **1**: 575-583
- Ren XD**, Kiosses WB, Schwartz MA. Regulation of the small GTP-binding protein Rho by cell adhesion and the cytoskeleton. *EMBO J* 1999; **18**: 578-585
- Wahl S**, Barth H, Ciossek T, Aktories K, Mueller BK. Ephrin-A5 induces collapse of growth cones by activating Rho and Rho kinase. *J Cell Biol* 2000; **149**: 263-270
- Qin LX**, Tang ZY. The prognostic molecular markers in hepatocellular carcinoma. *World J Gastroenterol* 2002; **8**: 385-392
- Bartsch JE**, Staren ED, Appert HE. Adhesion and migration of extracellular matrix-stimulated breast cancer. *J Surg Res* 2003; **110**: 287-294
- Matozaki T**, Nakanishi H, Takai Y. Small G-protein networks: their crosstalk and signal cascades. *Cell Signal* 2000; **12**: 515-524
- Greenberg DL**, Mize GJ, Takayama TK. Protease-activated receptor mediated RhoA signaling and cytoskeletal reorganization in LNCaP cells. *Biochemistry* 2003; **42**: 702-709
- Van Aelst L**, D' Souza-Schorey C. Rho GTPases and signaling networks. *Genes Dev* 1997; **11**: 2295-2322
- Zwartkruis FJ**, Bos JL. Ras and Rap1: two highly related small GTPases with distinct function. *Exp Cell Res* 1999; **253**: 157-165
- Geyer M**, Wittinghofer A. GEFs, GAPs, GDIs and effectors: taking a closer (3D) look at the regulation of Ras-related GTP-binding proteins. *Curr Opin Struct Biol* 1997; **7**: 786-792
- Riento K**, Ridley AJ. Rocks: multifunctional kinases in cell behaviour. *Nat Rev Mol Cell Biol* 2003; **4**: 446-456
- Chen BH**, Tzen JT, Bresnick AR, Chen HC. Roles of Rho-associated kinase and myosin light chain kinase in morphological and migratory defects of focal adhesion kinase-null cells. *J Biol Chem* 2002; **277**: 33857-33863
- Katoh K**, Kano Y, Amano M, Onishi H, Kaibuchi K, Fujiwara K. Rho-kinase-mediated contraction of isolated stress fibers. *J Cell Biol* 2001; **153**: 569-584
- Panetti TS**, Nowlen J, Mosher DF. Sphingosine-1-phosphate and lysophosphatidic acid stimulate endothelial cell migration. *Arterioscler Thromb Vasc Biol* 2000; **20**: 1013-1019
- Amano M**, Chihara K, Nakamura N, Fukata Y, Yano T, Shibata M, Ikebe M, Kaibuchi K. Myosin II activation promotes neurite retraction during the action of Rho and Rho-kinase. *Genes Cells* 1998; **3**: 177-188
- Steeg PS**. Metastasis suppressors alter the signal transduction of cancer cells. *Nat Rev Cancer* 2003; **3**: 55-63
- Feng J**, Ito M, Kureishi Y, Ichikawa K, Amano M, Isaka N, Okawa K, Iwamatsu A, Kaibuchi K, Hartshorne DJ, Nakano T. Rho-associated kinase of chicken gizzard smooth muscle. *J Biol Chem* 1999; **274**: 3744-3752
- Uehata M**, Ishizaki T, Satoh H, Ono T, Kawahara T, Morishita T, Tamakawa H, Yamagami K, Inui J, Maekawa M, Narumiya S. Calcium sensitization of smooth muscle mediated by a Rho-associated protein kinase in hypertension. *Nature* 1997; **389**: 990-994
- Somlyo AV**, Bradshaw D, Ramos S, Murphy C, Myers CE, Somlyo AP. Rho-kinase inhibitor retards migration and *in vivo* dissemination of human prostate cancer cells. *Biochem Biophys Res Commun* 2000; **269**: 652-659

Determination of chemical composition of gall bladder stones: Basis for treatment strategies in patients from Yaounde, Cameroon

Fru F. Angwafo III, Samuel Takongmo, Donald Griffith

Fru F. Angwafo III, Samuel Takongmo, Department of Surgery, Faculty of Medicine and Biomedical Sciences, The University of Yaounde I, Cameroon

Donald Griffith, Department of Urology, Baylor University, Houston, Texas, USA

Correspondence to: Fru F. Angwafo III, MD, Department of Surgery, Faculty of Medicine, The University of Yaounde I, PO Box 1364, Yaounde, Cameroon. asanji25@hotmail.com, fobuzshi@yahoo.com

Telephone: +237-7705749 **Fax:** +237-2315733

Received: 2003-06-04 **Accepted:** 2003-09-13

Abstract

AIM: Gallstone disease is increasing in sub-saharan Africa (SSA). In the west, the majority of stones can be dissolved with bile salts, since the major component is cholesterol. This medical therapy is expensive and not readily accessible to poor populations of SSA. It was therefore necessary to analyze the chemical composition of biliary stones in a group of patients, so as to make the case for introducing bile salt therapy in SSA.

METHODS: All patients with symptomatic gallstones were recruited in the study. All stones removed during cholecystectomy were sent to Houston for x-ray diffraction analysis. Data on age, sex, serum cholesterol, and the percentage by weight of cholesterol, calcium carbonate, and amorphous material in each stone was entered into a pre-established proforma. Frequencies of the major components of the stones were determined.

RESULTS: Sixteen women and ten men aged between 27 and 73 (mean 44.9) years provided stones for the study. The majority of patients (65.38%) had stones with less than 25% of cholesterol. Amorphous material made up more than 50% and 100% of stones from 16 (61.53%) and 9 (34.61%) patients respectively.

CONCLUSION: Cholesterol is present in small amounts in a minority of gallstones in Yaounde. Dissolution of gallstones with bile salts is unlikely to be successful.

Angwafo III FF, Takongmo S, Griffith D. Determination of chemical composition of gall bladder stones: Basis for treatment strategies in patients from Yaounde, Cameroon. *World J Gastroenterol* 2004; 10(2): 303-305

<http://www.wjgnet.com/1007-9327/10/303.asp>

INTRODUCTION

Biliary lithiasis has been a common disease in Europe and the USA for decades. Over half of the cases are asymptomatic, usually detected by an abdominal ultrasound^[1]. For a very long time, biliary stone disease was said to be rare in Sub-Saharan Africa (SSA). Archampong reported a 0.4% prevalence of all admissions in the Korle Bu Teaching Hospital in 1969 in Ghana^[2]. Today the prevalence of gallstone disease has increased considerably with the widespread use of ultrasonography^[3].

This increase has also been observed in African populations of Jamaica^[4] and SSA^[2,5].

Many studies to identify risk factors for biliary lithiasis in the West have focused on supersaturation of cholesterol in bile in the nucleation process, a critical step in the genesis of bile stones^[1,6]. The high concentration of cholesterol in gallstones has been the basis for the widespread use of bile acids, a nonsurgical treatment for the dissolution of gall bladder stones. These stones account for as much as 80% of Western stones^[6]. Unfortunately, gall bladder stone composition is heterogeneous, and differs within and without populations around the world^[3-8].

The increasing frequency of biliary stones in SSA, with its different epidemiological factors and diseases, prompted us to carry out a chemical analysis of gallstones. This study would demonstrate the role of cholesterol in our stones and therefore the necessity of using bile salts for gall stone dissolution in SSA.

MATERIALS AND METHODS

This was a cross-sectional study of a series of stones removed from patients at the University Hospital Center (UHC) of the University of Yaounde I from January 1, 1989 to December 31, 1998. All stones removed during surgery were placed on sterile gauze to air dry, transferred into a paper envelope bearing the name, age, and sex of the patient as well as the date. The first batch of stones from 19 patients was sent to the Urolithiasis laboratory in Houston, Texas in January 1996. A second collection of stones from 7 patients was sent to the same laboratory in May 1999.

All stone specimens were first examined for shape, size, and color. They were classified as cholesterol, black or brown pigmented stones, examined under a polarized microscope. The composition of the nidus, the internal and external shells was determined by X-ray diffraction as described previously^[9]. The percentage of cholesterol, calcium carbonate, and amorphous material such as black bilirubinate, black phosphate, glycoproteins and salts was determined. A descriptive analysis was done for stones from each patient. Patients who were able to pay for a serum cholesterol assay did so. Hemoglobin electrophoresis was not asked in this mainly adult population who did not give histories of sickle cell disease or crisis.

RESULTS

Patient population

There were 26 Cameroonian patients, all black Africans, aged between 27 and 73 years (mean 44.9 years). There were 16 women and 10 men, a 1.6 female to male sex ratio. The men were aged between 36 and 62 years whereas 6 women were less than 35 years (23.07%). All our patients resided in the city. They consumed mainly an African traditional diet made of local vegetarian menus mixed with imported processed Western items such as rice and wheat. The serum cholesterol level was normal in all 10 patients who did it.

Stone analyses

The percentage of cholesterol in the stones by weight is

depicted in Table 1. Seventeen patients (65.38%) had stones with less than 25% cholesterol. Of these, 11 (42.30%) had cholesterol free stones. Seven patients (26.92%) and 9 others (34.61%) had stones with 50% and 80% cholesterol content, respectively.

Calcium carbonate was detected in stones from 4 (15.38%) patients, three of whom were female. Two of these females had mixed stones containing cholesterol, calcium carbonate and amorphous material.

Table 2 shows the distribution of amorphous material by weight in these stones. Stones from 16 (61.53%) patients contained more than 50% amorphous material. The entire stone was made of amorphous material in 9 (34.61%) cases.

Table 1 Percent by weight of cholesterol in the gallstones from 26 patients

% by weight	Males	Females	Patient (%)
0	6	5	11 (42.30)
<25	1	5	6 (23.07)
> or =25 and <50	0	0	0
> or = 50 and <80	1	1	2 (7.69)
> or = 80 <100	0	4	4 (15.38)
100	2	1	3 (11.53)
	10	16	26 (100)

Table 2 Percent by weight of amorphous material in the gallstones from 26 patients

% by weight	Males	Females	Patient (%)
0	2	1	3 (11.53)
<25	0	5	5 (19.23)
> or = 25 and <50	1	1	2 (7.69)
> or = 50 and <80	1	0	1 (3.84)
> or = 80 and <100	0	6	6 (23.07)
100	6	3	9 (34.61)
	10	16	26 (100)

DISCUSSION

The results from this hospital-based nonrandomized study cannot be extrapolated to the community due to several limitations. In this group there were no children. Yet, it is known that children with hemolytic diseases develop cholesterol-poor, bilirubin-rich gallstones^[2]. Even in children without hemolytic disease, the composition of gallstones was different from those of adults in Leeds, England^[7]. Limitations to recruiting a potentially representative population of patients include poverty, in the absence of a financial scheme for health care coverage, ignorance and cultural factors that dissuade people from attending hospital services. Nonetheless, this pilot study permits us to raise the hypothesis that dissolution of gall bladder stones with bile salts is not a cost-effective alternative to surgical treatment.

A recent series of biliary lithiasis revealed a 4-fold increase of symptomatic gall bladder stone disease in Ghana from 1966-1999. This series also reported that the majority of Ghanaian stones were not cholesterol rich. Furthermore, cholesterol stones were more common in females and only 34% of their stones contained 75% or more of cholesterol by weight. They also showed that the external appearance of the stone was a poor predictor of its composition^[2]. This means that even in the poorer regions of the world, such as Sub-Saharan Africa, all attempts should be made to chemically analyze stones.

The treatment of gallstone diseases runs the gamut from bile salts dissolution, to fragmentation with laser^[10], pulverization with extracorporeal shock wave lithotripsy^[11], endoscopic

extraction, and classical surgery, whereas noninvasive medical therapy is appealing, bile acid therapy is only effective in some cholesterol gallstones. Bile acids are not effective in treating calcium bilirubinate or calcium carbonate/phosphate stones. It is therefore imperative that the composition of the stone be determined to tailor treatment for the individual patient^[12].

To determine stone composition, there are many possibilities offered by different technologies. On simple X-ray, radiologically undetectable stone calcification reduces the probability of dissolution and calcified structures appearing in stones during treatment are composed of calcium carbonate. A radio-opaque stone would suggest that medical therapy is unlikely to succeed. Stone composition is also determined on computed tomography. Results from polarizing microscopy of gall bladder bile suggest that the presence of cholesterol crystals is a sensitive measure of cholesterol and vaterite microspheruliths confirm presence of calcium carbonate in the gallstone^[13].

In the less technically developed areas the chemical composition of stones was determined from its external appearance. This has been shown to be inaccurate. Frequently the stones are homogenized and chemically analyzed. Our stones were analyzed with X-ray diffraction where cholesterol, calcium carbonate, and amorphous material were detected. The components of the amorphous material (bilirubine, glycerophosphates and bile salts) were not identifiable on X-ray diffraction. Infra-red spectroscopy and scanning electron microscopy were used to show that black and brown pigment gallstones differ in microstructure and micro-composition, suggesting that they form by different mechanisms. Black carbonate and brown stones layered structure suggests that stone growth is dependent on cyclical changes in biliary substances^[14]. This may explain the permissive or causal role endogenous hormones have in gallstone formation^[15]. Stone formation begins with nucleation where the interaction of pronucleators and antinucleators leads to formation of cholesterol crystals and these develop into gallstones^[6,16]. Hepatic cholesterol hypersecretion is associated with the increased unsaturated fatty acid proportion in biliary phospholipids and gallbladder mucin secretion, thereby causing rapid crystal nucleation^[17]. It is evident that gallstone disease has a multifactorial causation, including gall bladder infection,^[18] decreased gall bladder motility after surgery for obesity and/or weight loss^[19], ileal disease (Crohn's)^[20], hemolytic diseases^[2], familial hypercholesterolemia^[21], and metabolic defects in hepatic bilirubin glucuronidation^[22].

A shortcoming in our study is the absence of hemoglobin electrophoresis in a population where the prevalence of the sickle trait varies between 10% and 20% and that of the disease is about 1%^[2]. We did not explore many of the risk factors mentioned above largely due to technical and financial limitations. The absence of calcium in the stones of 22 (84.61%) patients correlates with a small number of gallstones detected on plain X-ray of the abdomen in our region. The extremely infrequent occurrence of pure cholesterol gallstones is a strong argument against the introduction of oral dissolution agents in SSA.

CONCLUSION

There is a corresponding variation in prevalence of cholesterol rich stones as a variation in composition of gallstones. This variation seems to be related to genes and the environment. Stone composition determines the therapeutic approaches in each locality. This pilot study suggests that oral bile salt dissolution therapy would not be effective in 70% of our patients. As populations in SSA undergo epidemiologic transition from infectious diseases to noncommunicable diseases, there will be increasing prevalence of biliary lithiasis.

REFERENCES

- 1 **Bartoli E**, Capron JP. Epidemiology and natural history of cholelithiasis. *Rev Prat* 2000; **50**: 2112-2116
- 2 **Darko R**, Archampong EQ, Qureshi Y, Muphy GM, Dowling RH. How often are Ghanaian gallbladder stones cholesterol-rich. *West Afr J Med* 2000; **19**: 64-70
- 3 **Kratzer W**, Mason RA, Kachele V. Prevalence of gallstones in sonographic surveys worldwide. *J Clin Ultrasound* 1999; **27**: 1-7
- 4 **Walker TM**, Hambleton IR, Serjeant GR. Gallstones in sickle cell disease: observations from the Jamaican cohort study. *J Pediatr* 2000; **136**: 80-85
- 5 **Akute OO**, Marinho AO, Kalejaiye AO, Sogo K. Prevalence of gallstones in a group of antenatal women in Ibadan. *Nigeria Afr J Med Sci* 1999; **3-4**: 159-161
- 6 **Kaloo AN**, Kanstevoev SV. Gallstones and biliary disease. *Prim Care* 2001; **28**: 591-606
- 7 **Stringer MD**, Taylor DR, Soloway RD. Gallstone composition: are children different? *J Pediatr* 2003; **142**: 435-440
- 8 **Kim MH**, Lim BC, Myung SJ, Lee SK, Ohor HC, Kim YT, Roe IH, Kim JH, Chung JB, Kim CD, Shim SC, Yun YB, Min YI, Yang US, Kang JK. Epidemiological study of Korean gallstone disease: a nationwide cooperative study. *Dig Dis Sci* 1999; **44**: 1674-1683
- 9 **Bassi N**, Aggio L, Ghio S, Meggiato T, Di Mario F, Del Favero G, Scalon P, Molin M, D' Amico D, Naccarato R. X-ray diffraction study of biliary calculi. Morphological and composition correlations of calculi. *G Clin Med* 1990; **71**: 331-335
- 10 **Shi W**, Vari S, Papaioannou T, Daykovsky L, Grundfest W. Biliary calculi fragmentation by a 308 mm excimer laser. *J Clin Laser Med Surg* 1991; **9**: 139-141
- 11 **Ertran A**. Treatment of gall stones by extracorporeal shock wave lithotripsy. *Am J Gastroenterol* 2002; **97**: 831-832
- 12 **Ros E**, Navarro S, Fernandez I, Reixach M, Ribo JM, Rodes J. Utility of biliary microscopy for the prediction of the chemical composition of gall stones and outcome of dissolution therapy with ursodexycolic acid. *Gastroenterology* 1986; **91**: 703-712
- 13 **Nakai K**, Tazuma S, Ochi H, Chayama K. Does bilirubin play a role in the pathogenesis of both cholesterol and pigment gallstone formation? Direct and indirect influences of bilirubin on bile lithogenicity. *Biochim Biophys Acta* 2001; **1534**: 78-84
- 14 **Kleiner O**, Ramesh J, Huleihel M, Cohen B, Kantarovich K, Levi C, Polyak B, Marks RS, Mordehai J, Cohen Z, Mordechai S. A comparative study of gallstones from children and adults using FTIR spectroscopy and fluorescence microscopy. *BMC Gastroenterol* 2002; **2**: 3-15
- 15 **Russo F**, Cavallini A, Messa C, Mangini V, Guerra V, D' Amato G, Misciagna G, Di Leo A. Endogenous sex hormones and cholesterol gallstones: a case-control study in an echographic survey of gallstones. *Am J Gastroenterol* 1993; **88**: 712-717
- 16 **Portincasa P**, Moschetta A, Calamita G, Margari A, Palasciano G. Pathobiology of cholesterol gallstone disease: from equilibrium ternary phase to agents preventing cholesterol crystallization and stone formation. *Curr Drug Targets Immune Endocr Metabol Disord* 2003; **3**: 67-81
- 17 **Hatsushika S**, Tasuma S, Kajiyama G. Nucleation time and fatty acid composition of lecithin in human gallbladder bile. *Scand J Gastroenterol* 1993; **28**: 131-136
- 18 **Stewart L**, Ponce R, Oesterk AL, Griffiss JM, Way LW. Pigment gallstones pathogenesis: slime production by biliary bacteria is more important than beta-glucuronidase production. *J Gastrointest Surg* 2000; **4**: 547-553
- 19 **Al-Jiffry BO**, Shaffer EA, Saccone GT, Downey P, Kow L, Toouli J. Changes in gall bladder motility and gall stone formation following laparoscopic banding for morbid obesity. *Can J Gastroenterol* 2003; **17**: 169-174
- 20 **Lapidus A**, Bangstad M, Astrom M, Muhrheck O. The prevalence of gallstones disease in a defined cohort of patient with Crohn's disease. *Am J Gastroenterol* 1999; **94**: 1130-1132
- 21 **Hoogerbrugge-vd LN**, de Rooy FW, Jansen H, van Blankenstein M. Effect of pravastatin on biliary lipid composition and bile acid synthesis on familial hypercholesterolemia. *Gut* 1990; **31**: 348-350
- 22 **Duvaldestin P**, Manu JL, Metreau JM, Arondel J, Preaux AM, Berthelot P. Possible role of defect in hepatic bilirubin glucuronidation in the initiation of cholesterol gallstones. *Gut* 1980; **21**: 650-655

Edited by Ma JY

Can HB vaccine yield a booster effect on individuals with positive serum anti-HBs and anti-HBc markers?

Ru-Xiang Wang, Ying Guo, Chang-Hong Yang, Yu Song, Juan Chen, Fu-Sheng Pang, Shao-Ping Lei, Xiao-Ming Jia, Jin-Ying Wen, Christina Y. Shi

Ru-Xiang Wang, Ying Guo, Yu Song, Juan Chen, Shenyang Center for Disease Control and Prevention, Shenyang 110031, Liaoning Province, China

Chang-Hong Yang, Dongling District Anti-epidemic Station, Dongling District, Shenyang 110015, Liaoning Province, China

Fu-Sheng Pang, Shao-Ping Lei, Liaoning Center for Disease Control and Prevention, Shenyang, 110003, Liaoning Province, China

Xiao-Ming Jia, No.2 Hospital of China Medical University, Shenyang 110004, Liaoning Province, China

Jin-Ying Wen, Shenyang 606 Hospital, Shenyang 110015, Liaoning Province, China

Christina Y. Shi, Vita-Tech Canada, 1345 Denison Street, Markham, Ontario, Canada L3R 5V2

Correspondence to: Dr. Ru-Xiang Wang, Shenyang Center for Disease Control and Prevention, 37 Qishanzhong Road, Huanggu District, Shenyang 110031, China. rxwtxh@pub.sy.ln.cn

Telephone: +86-24-86853243 **Fax:** +86-24-86863778

Received: 2003-04-12 **Accepted:** 2003-10-11

Abstract

AIM: To evaluate if HB vaccination can yield a booster effect on the anti-HBs level of those naturally acquired HBV positive markers.

METHODS: Sera were collected from 1399 newly enrolled university students aged between 18-20 years at the entrance medical examination in 2001. Forty-four students (28 males and 16 females) with positive serum anti-HBs and anti-HBc markers served as an observation group and another 44 students (24 males and 20 females) without any HBV markers as the control. HB vaccination was given to all the students without positive serum HBsAg according to 0, 1, 6 month regimen and the peripheral venous blood was sampled from those of both observation and control groups for anti-HBs detection one month after the second and third doses. Anti-HBs levels were measured by ELISA.

RESULTS: The seroconversion rate of anti-HBs in the control group was 100% after the second dose, but the geometric mean titers (GMTs) were low. The tendency of serum anti-HBs changes after the 3rd dose was completely different between the two groups. Although more than half of those with positive anti-HBs and anti-HBc showed a mild increase of anti-HBs levels after the 2nd boosting dose (mean anti-HBs level was 320:198 mIU), but the increase of serum anti-HBs titer was much smaller than that in the control group. The averages of their initial serum anti-HBs levels and the levels after the 2nd and 3rd doses were 198, 320 and 275 mIU respectively. All the subjects from the control group had an obvious increase in their serum anti-HBs levels which was nearly 4 times the baseline level (302:78 mIU).

CONCLUSION: HB vaccination can not enhance anti-HBs levels in those with positive serum anti-HBs and anti-HBc markers.

Wang RX, Guo Y, Yang CH, Song Y, Chen J, Pang FS, Lei SP, Jia

XM, Wen JY, Shi CY. Can HB vaccine yield a booster effect on individuals with positive serum anti-HBs and anti-HBc markers? *World J Gastroenterol* 2004; 10(2): 306-308

<http://www.wjgnet.com/1007-9327/10/306.asp>

INTRODUCTION

HB vaccination program has been well developed for neonates and younger adults in China. Nowadays, according to Chinese regulation all the newly enrolled university students are required to have their blood detected for HBsAg and those with negative HBsAg are eligible to receive HB vaccination. Since it has been well demonstrated that an additional dose can induce a booster effect on vaccinees' serum anti-HBs titers, it is natural for most people to get the idea that the more doses they get, the more benefits they will gain. Our previous survey in a group of university students showed that HBsAg carrier rate in those of the 18-20 age group was about 4-6% and when gained entrance to the university more than 50% students with positive serum anti-HBs or anti-HBc or both were vaccinated each year. Is it necessary to vaccinate the people with positive anti-HBc and anti-HBs markers? To answer this question, we followed up the newly enrolled students from a university to observe the changes of their serum anti-HBs titers after HB vaccination, especially those with positive serum anti-HBs and anti-HBc markers before. The changes of serum anti-HBs titers in students without any HBV markers before the vaccination were observed after HB vaccination as the experimental control. The results might be helpful for the establishment of a scientific, reasonable and economic vaccination program against HBV infection in the adult population.

MATERIALS AND METHODS

Reagents

Ten μ g of yeast recombinant HB vaccine (Lot No: 2990104-1) was produced in Kangtai Biological Pharmaceutical Company, China. ELISA kits of HBV markers were from Sino-American Biotechnology Company, Luoyang, China. ELISA kit of Measles antibody was provided by Institute of Virus, Chinese Center of Disease Control and Prevention, Beijing, China.

Subjects and vaccination methods

Forty-four students with positive serum anti-HBs and anti-HBc and 44 without any HB markers who experienced a regular medical examination in one college were selected to be investigated after vaccinated with HB vaccine according to 0, 1, 6 month scheme, in which the vaccine was intramuscularly injected into the deltoid muscle. All the subjects were also injected measles vaccine one week before the first dose of HB vaccination. An informed consent was given by each participant before the beginning of observation.

Determination of serum anti-HBs antibody

Serum anti-HBs antibody was measured respectively at one

month after the 2nd and 3rd doses of HB vaccine. The sera were randomly chosen from 35 subjects with positive anti-HBs and anti-HBc to measure the antibodies (IgG) to both measles and HBsAg according to the manufacturer's instructions. The resulting value was determined according to Holliger formula: $mIU=418 \times [EXP \times 0.9(S-N)/(P-N)-1]$ in the light of OD values. mIU of anti-HBs titers greater than 10 was considered as positive anti-HBs. *t* test was used to compare GMTs between groups and the difference was considered significant when $P < 0.05$.

Table 1 Comparison of booster effect on anti-HBs levels between two groups

No.	Anti-HBs (anti-HBc pos.)			Anti-HBs (anti-HBc neg.)		
	Before	After 2 nd dose	After 3 rd dose	No.	After 2 nd dose	After 3 rd dose
23338	161	578	362	22404	48	471
23306	266	293	163	13236	25	268
23310	406	295	293	13240	45	598
23304	168	417	337	24332	48	324
23116	44	86	76	24327	63	144
23140	30	37	43	24311	186	314
23139	372	456	344	24105	344	656
23129	309	459	225	17239	135	83
23105	145	451	461	17238	58	253
23119	162	269	252	17226	83	598
27138	592	387	533	17214	53	384
27128	406	494	449	23240	63	268
27130	341	272	199	23201	40	370
27103	182	148	145	23141	201	340
27137	53	328	211	23108	26	512
27001	326	424	269	17129	22	970
27109	99	122	116	17125	178	318
27133	573	373	316	17122	45	22
27120	151	420	207	17118	78	466
22222	115	438	588	17108	236	414
22225	442	417	338	17106	88	350
22214	283	293	466	17102	197	264
22206	176	282	208	13139	186	291
22205	547	275	377	13129	17	158
22201	183	193	158	13126	73	264
24120	128	558	393	13125	93	191
24107	239	356	257	13118	17	176
24140	35	426	409	13114	53	263
24141	212	275	231	13108	216	280
22138	392	534	659	13107	35	338
22130	660	643	504	13102	130	252
13214	247	331	244	13101	113	216
13223	491	315	176	14130	320	520
23235	106	232	199	14131	65	407
24137	108	472	280	14129	320	365
22202	61	205	253	18302	30	63
18238	244	302	303	18310	73	336
23322	422	463	503	16119	53	395
18223	333	314	389	16112	30	370
25122	355	315	286	16122	200	375
25139	206	361	337	16104	45	420
25129	116	391	303	16108	30	365
25121	38	119	204	16107	441	476
18220	65	507	506	16110	107	499
Total GMT	198	320	275	GMT	78	302

RESULTS

Anti-HBs titers before and after HB vaccination in those with positive anti-HBs and anti-HBc

The tendency of serum anti-HBs changes after the 3rd dose was completely different between the two groups. Although more than half of those with positive anti-HBs and anti-HBc markers showed a mild increase of serum anti-HBs titer after the 2nd booster dose, the increase of serum anti-HBs titer (mean anti-HBs level was 198:320 mIU) was much smaller than that in the control group, in which 100% subjects had an obvious increase in their serum anti-HBs levels which was nearly 4 times their baseline (302:78 mIU).

It was interesting to note that the serum anti-HBs levels did not change in most of the subjects with positive anti-HBs and anti-HBc markers after the 3rd dose. The mean serum anti-HBs level of the baseline, after the 2nd and 3rd doses was 198, 320 and 275 mIU (Table 1) respectively.

Effect of a boost dose on antibody titers of HBsAb and measles Ab

In order to confirm that all the subjects in this study had a normal immune competence, the serum antibodies to measles were detected in 35 subjects and an increased antibody level was observed in 91.4% (32/35) subjects after a booster dose. A comparison of antibody levels before and after a booster dose was made and the difference was statistically significant ($P < 0.05$, Table 2).

Table 2 Effect of a boost on antibody titers of HBsAb and measles Ab

Boost	A-HBsAb		B-HBsAb		C-HBsAb		MeaslesAb	
	No.	GMT	No.	GMT	No.	GMT	No.	GMT
Before	44	198	44	198	44	78	35	322
After	44	320	44	275	44	302	35	1 207

Comparison of anti-HBs induced by HB vaccination before and after a boost in HBV negative group, $P < 0.05$.

DISCUSSION

Hepatitis B vaccination has been implemented for 20 years, however, the disease remains a global problem^[1-4]. Although the safety and efficacy of HB vaccine have been well demonstrated^[5-16], few papers regarding the immune response of those with positive anti-HBs and anti-HBc to HB vaccination are available. In this study, we observed if a booster effect and a better protection against HBV infection could be obtained after HB vaccination in those with positive serum anti-HBs and anti-HBc markers.

It has been well demonstrated that the HB vaccine-induced antibody might gradually decline or was even undetectable some years after primary immunization^[17-20]. It is not clear if such persons could be protected against HB infection following exposure to HBV^[21]. Although some studies have proved that memory cells to HBsAg might exist in vaccinees for a long time even the serum anti-HBs was undetectable^[19,22,23]. Whether additional booster doses should be used has been under discussion^[17-20,23-25]. Considering the available data on measles vaccine, which showed that loss of detectable antibody following vaccination was correlated with the waning of immunity^[26], a booster HB vaccination might be necessary.

Our data revealed that the serum anti-HBs levels in the subjects with positive serum anti-HBs and anti-HBc markers did not significantly increase one month after the 2nd dose of HB vaccination. Although a mild increase was seen in some cases, the elevation of serum anti-HBs levels in the observatory

group was much less than that in the control in which 100% subjects had an obvious increase of serum anti-HBs levels that was nearly 4 times their baseline. After the 3rd dose, anti-HBs levels remained unchanged in most of the subjects with positive serum anti-HBs and anti-HBc markers compared with that in the control, in which a sharp increase of serum anti-HBs levels was observed after the 3rd dose. The phenomenon might be related to the following possibilities. First, the subjects with positive serum anti-HBs and anti-HBc markers before the vaccination might not be in a normal condition of immune competence during the observation period. In the present study, their increased response to measles after the booster dose was observed in 91.4% (32/35) subjects. Because measles vaccination has been well practiced in China and normally all the subjects have to be vaccinated in their early age, the increased immunological response could prove that the subjects had the normal immune competence. Second, the immune response to viruses can damage the host via the formation of immune complexes, or directly damage the infected cells. Thus, the poor response to the HB vaccine might probably relate to the damage caused by HBV before the vaccination.

HB vaccination program is implemented in children and adults in China. But the problem is that our current vaccination regimen is not completely suitable for adult vaccination. An appropriate vaccination program for the adult population has to be established to prevent the prevalence of HBV. Our results indicate that it is not necessary to vaccinate those with positive serum anti-HBs and anti-HBc because no significant increase of anti-HBs titers was observed after a standard HB vaccination. It suggests that the vaccine-induced anti-HBs can not be elevated in those infected with HBV naturally before the HB vaccination.

REFERENCES

- Cassidy WM.** Adolescent hepatitis B vaccination. *Minerva Pediatr* 2001; **53**: 559-566
- Kralj N,** Hofmann F, Michaelis M, Berthold H. Current hepatitis B epidemiology in Germany. *Gesundheitswesen* 1998; **60**: 450-455
- Bayas JM,** Bruguera M, Vilella A, Carbo JM, Vidal J, Navarro G, Nebot X, Prat A, Salleras L. Prevalence of hepatitis B and hepatitis A virus infection among health sciences students in Catalonia, Spain. *Med Clin* 1996; **107**: 281-284
- Bonanni P.** Universal hepatitis B immunization: infant, and infant plus adolescent immunization. *Vaccine* 1998; **16**(Suppl): S17-22
- Kojouharova M,** Teoharov P, Bahtchevanova T, Maeva I, Eginlian A, Deneva M. Safety and immunogenicity of a yeast-derived recombinant hepatitis B vaccine in Bulgarian newborns. *Infection* 2001; **29**: 342-344
- Liao SS,** Li RC, Li H, Yang JY, Zeng XJ, Gong J, Wang SS, Li YP, Zhang KL. Long-term efficacy of plasma-derived hepatitis B vaccine among Chinese children: a 12-year follow-up study. *World J Gastroenterol* 1999; **5**: 165-166
- Li H,** Li RC, Liao SS, Yang JY, Zeng XJ, Wang SS. Persistence of hepatitis B vaccine immune protection and response to hepatitis B booster immunization. *World J Gastroenterol* 1998; **4**: 493-496
- Rendi-Wagner P,** Kundi M, Stemberger H, Wiedermann G, Holzmann H, Hofer M, Wiesinger K, Kollaritsch H. Antibody-response to three recombinant hepatitis B vaccines: comparative evaluation of multicenter travel-clinic based experience. *Vaccine* 2001; **19**: 2055-2060
- Ozaki T,** Mochizuki H, Ichikawa Y, Fukuzawa Y, Yoshida S, Morimoto M. Persistence of hepatitis B surface antibody levels after vaccination with a recombinant hepatitis B vaccine: a 3-year follow-up study. *J Oral Sci* 2000; **42**: 147-150
- Jain A,** Mathur US, Jandwani P, Gupta RK, Kumar V, Kar P. A multicentric evaluation of recombinant DNA hepatitis B vaccine of Cuban origin. *Trop Gastroenterol* 2000; **21**: 14-17
- Al-Faleh FZ,** Al-Jeffri M, Ramia S, Al-Rashed R, Arif M, Rezeig M, Al-Toraif I, Bakhsh M, Mishkhas A, Makki O, Al-Freih H, Mirdad S, AlJuma A, Yasin T, Al-Swailem A, Ayoola A. Seroprevalence of hepatitis B virus infection in Saudi children 8 years after a mass hepatitis B vaccination programme. *J Infect* 1999; **38**: 167-170
- Li H,** Li RC, Liao SS, Gong J, Zeng XJ, Li YP. Long-term effectiveness of infancy low-dose hepatitis B vaccine immunization in Zhuang minority area in China. *World J Gastroenterol* 1999; **5**: 122-124
- Liu HB,** Meng ZD, Ma JC, Han CQ, Zhang YL, Xing ZC, Zhang YW, Liu YZ, Cao HL. A 12-year cohort study on the efficacy of plasma-derived hepatitis B vaccine in rural newborns. *World J Gastroenterol* 2000; **6**: 381-383
- Li H,** Wang L, Wang SS, Gong J, Zeng XJ, Li RC, Nong Y, Huang YK, Chen XR, Huang ZN. Research on optimal immunization strategies for hepatitis B in different endemic areas in China. *World J Gastroenterol* 2000; **6**: 392-394
- Zeng XJ,** Yang GH, Liao SS, Chen AP, Tan J, Huang ZJ, Li H. Survey of coverage, strategy and cost of hepatitis B vaccination in rural and urban areas of China. *World J Gastroenterol* 1999; **5**: 320-323
- Shokri F,** Jafarzadeh A. High seroprotection rate induced by low doses of a recombinant hepatitis B vaccine in healthy Iranian neonates. *Vaccine* 2001; **19**: 4544-4548
- Peces R,** Lares AS. Persistence of immunologic memory in long-term hemodialysis patients and healthcare workers given hepatitis B vaccine: role of a booster dose on antibody response. *Nephron* 2001; **89**: 172-176
- Li H,** Li R, Liao S, Yang J, Zeng X. Persistence of HB vaccine immune protection and response to hepatitis B booster immunization. *Zhongguo Yixue Kexueyuan Xuebao* 1998; **20**: 54-59
- Watson B,** West DJ, Chilkatowsky A, Piercy S, Ioli VA. Persistence of immunologic memory for 13 years in recipients of a recombinant hepatitis B vaccine. *Vaccine* 2001; **19**: 3164-3168
- Garcia Llop L,** Asensi Alcoverro A, Coll Mas P, Ramada Benedito MA, Grafia Juan C. Anti-HBs titers after a vaccination program in children and adolescents. Should a booster dose be given? *An Esp Pediatr* 2000; **54**: 32-37
- Wood RC,** MacDonald KL, White KE, Hedberg CW, Hanson M, Osterholm MT. Risk factors for lack of detectable antibody following B vaccination of Minnesota health care workers. *JAMA* 1993; **270**: 2935-2939
- Wismans PJ,** Van Hattum J, De Gast GC, Endeman HJ, Poel J, Stolk B, Maikoe T, Mudde GC. The spot-ELISA: a sensitive *in vitro* method to study the immune response to hepatitis B surface antigen. *Clin Exp Immunol* 1989; **78**: 75-78
- Trivello P,** Chiamonte M, Ngatchu T, Baldo V, Majori S, Moschen ME, Simoncello I, Renzulli G, Naccarato R. Persistence of anti-HBs antibodies in health care personnel vaccinated with plasma-derived hepatitis B vaccine and response to recombinant DNA HB booster vaccine. *Vaccine* 1995; **13**: 139-141
- Coursaget P,** Yvonnet B, Chotard J, Sarr M, Vincelot P, N' doye R, Diop-Mar I, Chiron JP. Seven-year study of hepatitis B vaccine efficacy in infants from an endemic area (Senegal). *Lancet* 1986; **15**: 1143-1144
- Hadler SC,** Francis DP, Maynard JE, Thompson SE, Judson EN, Echenberg DF, Ostrow DG, O' Malley PM, Penley KA, Altman NL. Long-term immunogenicity and efficacy of hepatitis B vaccine in homosexual men. *N Engl J Med* 1986; **315**: 209-215
- Center for Disease Control.** Measles prevention: recommendation of the Immunization Practices Advisory Committee. *MMWR Morb Mortal Wkly Rep* 1989; **38**: S-9